THE DEGRADATION OF GEL-SPUN POLY(β-HYDROXYBUTYRATE) FIBROUS MATRIX.

VOLUME I.

LESLIE JOHN RAY FOSTER

Doctor of Philosophy

THE UNIVERSITY OF ASTON IN BIRMINGHAM

August 1992

THESIS SUMMARY.

L.J.R. Foster. August 1992.

The Degradation Of Gel-spun Poly(β-hydroxybutyrate) Fibrous Matrix.

Poly(β-hydroxybutyrate), (PHB), is a biologically produced, biodegradable thermoplastic with commercial potential. In this work the qualitative and quantitative investigations of the structure and degradation of a previously unstudied, novel, fibrous form of PHB, were completed. This gel-spun PHB fibrous matrix, PHB(FM), which has a similar appearance to cotton wool, possesses a relatively complex structure which combines a large volume with a low mass and has potential for use as a wound scaffolding device.

As a result of the intrinsic problems presented by this novel structure, a new experimental procedure was developed to analyze the degradation of the PHB to its monomer hydroxybutyric acid, (HBA). This procedure was used in an accelerated degradation model which accurately monitored the degradation of the undegraded and degraded fractions of a fibrous matrix and the degradation of its PHB component. The *in vitro* degradation mechanism was also monitored using phase contrast and scanning electron microscopy, differential scanning calorimetry, fibre diameter distributions and Fourier infra-red photoacoustic spectroscopy. The accelerated degradation model was used to predict the degradation of the samples in the physiological model and this provided a clearer picture as to the samples potential biodegradation as medical implantation devices.

The degradation of the matrices was characterized by an initial penetration of the degradative medium and weakening of the fibre integrity due to cleavage of the ester linkages, this then led to the physical collapse of the fibres which increased the surface area to volume ratio of the sample and facilitated its degradation. Degradation in the later stages was reduced due to the experimental kinetics, compaction and degradation resistant material, most probably the highly crystalline regions of the PHB. The *in vitro* degradation of the PHB(FM) was influenced by blending with various polysaccharides, copolymerizing with poly(β-hydroxyvalerate), (PHV), and changes to the manufacturing process. The degradation was also determined to be faster than that of conventional melt processed PHB based samples.

It was concluded that the material factors such as processing, sample size and shape affected the degradation of PHB based samples with the major factor of sample surface area to volume ratio being of paramount importance in determining the degradation of a sample.

Keywords: **Biodegradation, Fibre, Hydroxybutyric Acid, Photoacoustic Spectroscopy, Blending.**

This thesis is dedicated to the courage of my mother and the memory of my father, *'lo que ha hecho el cabello beber'*

Vaya con Dios.

Acknowledgements

I am deeply indebted to Prof. B.J. Tighe for all his assistance and advice during my pleasurable years here and for providing the opportunity to do this PhD.as part of his prestigious research team.

I must also gratefully acknowledge the support of my fiancee Mechthild during the relatively long and stressful period of writing up. Similarly, the invaluable support of my parents and brother Miguel also deserve recognition.

Many thanks to Roger Howell for his help and assistance with the SEM, X-ray crystallography and numerous photographs. Steve Ludlow for his advice and immeasurable assistance in ensuring the prompt supply of equipment. Thanks also to Mr. Martin Burrell and Dr Linda Reeves for their advice and support. A special mention to Dr. Alan Amass for his interest and assistance.

I would also like to express my thanks to Brians research group for their help and friendship during my stay here. Although too numerous to mention, certain members warrant a special thanks. They are, in no particular order: Dr. Phil Corkhill and his lovely wife Dr. Helen Oxley, Dr. Valerie Franklin, Dr. Mohamed Yasin, Mr. Steven Tonge, Miss Helen Fitton and especially the lovely Miss Julie Patterson!

LIST OF CONTENTS.

Volume 1.

Chapter 2. Materials And Methods.

Volume 2.

LIST OF TABLES.

LIST OF FIGURES.

LIST OF PLATES.

LIST OF GRAPHS.

LIST OF ABBREVIATIONS.

DSC	Differential scanning calorimetry.
ΔHm.	Fusion enthalpy (J/g.).
FTIR-PAS	Fourier transform infra-red photoacoustic spectroscopy, sometimes referred to as 'PAS.'
HBA	Hydroxybutyric acid, sometimes referred to as 'monomer.'
mp.	Melting point (°C.).
Mwt.	Molecular weight.
Mwn.	Molecular weight number.
PHB	Poly(β-hydroxybutyrate).
PHV	Poly(β-hydroxyvalerate).
PHB(FM)TG	PHB fibrous matrix produced from technical grade polymer, sometimes referred to as the 'TG sample' or 'TG.'
PHB(FM)IP	PHB fibrous matrix produced from increased purity polymer, sometimes referred to as the 'IP sample' or 'IP'.
PCM	Phase contrast microscopy.
SEM	Scanning electron microscopy.
Tg.	Glass transition temperature. (°C.)
t_{10}	Time for 10% of initial dry weight of sample/PHB to be lost.
t_{50}	Time for 50% of initial dry weight of sample/PHB to be lost.

Chapter One.

Introduction.

1.0. General Introduction.

Medical implantation devices have been used for centuries.[1] The use of 'biodegradable' materials for surgical and medical implantation devices has the distinct advantage of preventing further trauma to the patient due to the lack of need for their explantation and this results in faster healing rates. Consequently, any materials possessing the properties of 'biodegradability' (and 'biocompatibility' to an appropriate extent) are likely to become commercially successful implantation devices. Such a material is poly(β-hydroxybutyrate) which has now been developed into a new and novel fibrous form combining a large volume and low mass. One intended use of this form is as a wound scaffolding device, designed to support and protect a wound against further damage whilst promoting healing by encouraging cellular growth on and within the device from the wound surface.

1.1. Surgical And Medical Implantation Devices.

The most common surgical fixation device is probably the surgical suture, its earliest use dates back to approximately 4000BC when linen and catgut were used by the ancient Egyptians for wound closure. Cotton sutures are first recorded in use by 600BC in India.[1] Other such materials include silk, plaited horse hair, leather strips and tree bark fibres,[2] whilst gold and silver wire sutures are recorded as being used in the sixteenth and nineteenth centuries respectively.[1] In the 1930's steel wire replaced the silver, being somewhat stronger and less brittle.[2,3] There was a rapid increase in the synthesis and production of new polymers in the 1940's, however, it was not until the 1960's that the

first synthetic biodegradable polymer; poly(glycolic acid), was used in suture manufacture.[4] Similarly, it is only comparatively recently that other such devices; staples, ligators, tape, screws, pins, plates,[5] surgical sutures[6,7] and drug delivery devices[8-13] have been readily available.

A medical implantation device must obviously fulfill a number of factors to be a success. These factors are briefly discussed in the following sections:

1.1.1. Biocompatibility.

The device must not produce an adverse reaction by the body, this is usually found as inflammation and migration of various leucocytes to the wound site. The biocompatibility of the device is influenced by the material, its processing and physical structure, and naturally changes during degradation. The issue of biocompatibility is a complex one, the work in this thesis is concerned with the *in vitro* degradation of the novel fibrous form and as such no further discussion is given here.

1.1.2. Biodegradability.

Holland *et al*[14] reviewed the various definitions of biodegradation and, as indicated by such authors, there is considerable confusion in the literature as to its exact definition. Taylor defined biodegradation as the breakdown of the polymeric materials by living organisms or their secretions.[15] This view is similar to those expressed by Potts,[16] Williams,[17] Griffin[18] and Kopet *et al.*[19] In contrast, Pitt *et al*[20] and Gilbert *et al*[21] define biodegradation as the simple hydrolytic breakdown of polymeric materials. Doi[22] defines it as the simple hydrolytic and enzymatically induced hydrolytic

degradation processes occurring in a polymer. Similarly, further definitions by Gilding,[23] Zaikov[24] and others all vary according to the particular work concerned. To complicate matters further, the terms 'bioerosion' and 'bioerodible' are widely used when dealing with drug release devices, as in the papers by Langer *et al*[25] and Heller.[26] Consequently, it is necessary to define each term in respect to the work in this thesis.

Biodegradation in this thesis is defined as the breakdown of polymeric material by a variety of physical and chemical processes present in the *in vitro* physiological and accelerated degradation models, (See Chapter 3), to the comparable extent that the partially degraded polymer could either be adsorbed into the body for storage, resynthesis etc. or effectively excreted. Bioerosion is considered as a physical process by which the polymer degrades.

Therefore, a biodegradable medical implantation device should degrade at a beneficial and predetermined rate, according to its function and the nature of the particular wound site for which it was designed.

1.1.3. Biocompatibility Of The Degradation Products.

The biocompatibility of the device (Sec. 1.1.1.) changes during degradation and the subsequent degradation products may be very different from the original polymer material. These products should, by the biodegradation definition, be readily utilized by the body or easily excreted. They should be:

a) Non-toxic

b) Non-immunogenic

c) Non-carcinogenic

d) Non-thrombogenic

Polymer degradation products can usually be eliminated by the kidneys, however, there is a renal cut-off point which is dependent upon the polymer nature and molecular weight.[27] Those degradation products utilized by the body have been referred to as 'bioresorpable' and have been documented for a number of polymers.[28-31]

1.1.4. Commercial Interests.

A medical device, besides satisfying the above factors in respect to implantation, must also be profitable in production. The polymer must be readily available, its production and device manufacture weighed financially against its cost and profit. The 'flexibility' of the material; its ability to undergo various manufacturing processes into different devices, must also be a commercial consideration, since their is a definite commercial concern and market for a suitable final product.

Thus, to fulfill a role as a medical implantation device a material must satisfy the above factors. Poly(β-hydroxybutyrate), commonly referred to as PHB, is such a material.

1.2. PHB As A Medical Implantation Device.

PHB (Fig. 1.1) was first isolated and characterized from the bacterium *Bacillus megaterium* in 1925 by Lemoigne at the Pasteur Institute in Paris.[32-34] Since then investigations have revealed its occurance in a large number of bacteria and fungi, including *Azobacter beijeinckii*,[35] *Rhodospirillum rubrum* and *Bacillus cereus*.[32]

Poly(-β-hydroxybutyrate) (PHB)

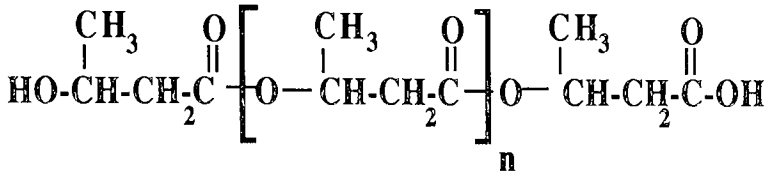

Poly(-β-hydroxyvalerate) (PHV)

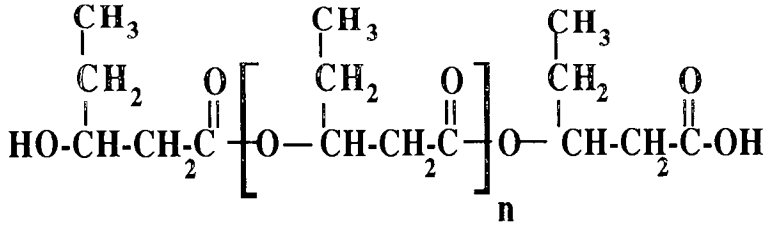

Poly(-γ-hydroxybutyrate) (P4HB)

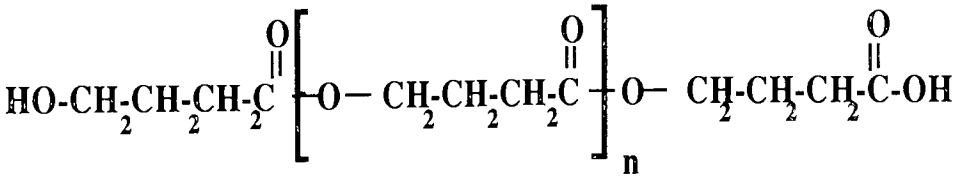

N.B.
The prefixes 3- (for β-) and 4- (for γ) are frequently and interchangeably used.

Figure: 1.1.
Structure Of Poly(hydroxybutyrate) And Its Copolymers.

The whitish PHB granules possessing diameters ranging from 0.3 to 1um. are readily observed in the cytoplasmic fluid and may account for 30 to 80% of the bacteriums dry cellular weight. PHB is accumulated by the bacteria and fungi when growth is limited by the depletion of an essential nutrient, and is utilized as a carbon and/or energy reserve or as a sink for any excess reducing equivalents, in a similar fashion as glycogen in mammalian blood.[63]

PHB isolated from bacterial cells is usually of a very high number average molecular weight, approximately 10^5 - 10^6, and of a high crystallinity, greater than 50%. Unlike other biological polymers such as proteins and polysaccharides, PHB is a thermoplastic with a melting temperature around 180°C. The physical properties of PHB have been discussed by Barham[36] and Doi.[37]

But how does PHB satisfy the essential factors for a medical implantation device?

1.2.1. Biocompatibility Of PHB.

Bonfield *et al*[38] and Doyle *et al*[39] have investigated the biocompatibility of injection moulded PHB plaques in the femurs of New Zealand white rabbits and reported a favourable bone tissue adaption response with no evidence of undesirable chronic inflammation after implantation periods of up to 12 months. Similarly, *in vivo* studies of PHB biocompatibility, in a variety of forms from monofilament fibres to microspheres by a number of authors, have also determined that no adverse reactions to the PHB implants occurred.[40-44]

The biocompatibility of the novel fibrous form of PHB studied in this thesis has been investigated in pigs by Chen,[45] who reported a good ingrowth of the granulation tissue into the PHB, accompanied by a mild foreign body reaction. However, this was most probably due to a 3% contamination by proteins and their breakdown products, lipids, lipopolysaccharides and a production solvent residue.[46]

Thus, PHB in various forms, including the new and novel form studied in this thesis, appears to be relatively biocompatible.

1.2.2. Biodegradability Of PHB.

The *in vivo* biodegradation of PHB in the form of microgranules and sheets has been investigated by Saito *et al*[42] with little degradation observed over a period of several months. Similarly, the *in vivo* biodegradation of PHB monofilament fibres by Miller and Williams[7,47] was also reported to be minimal over a 6 month period. However, it was also found that the susceptibility of the fibres to biodegrade was increased with gamma irradiation.

Miller and Williams[7,47] also studied the degradation of monofilament fibres *in vitro* under conditions of 37 ±1°C. temperature and pH 7.2, they concluded that little degradation of the PHB homopolymer was evident. The irradiated monofilament fibres lost all mechanical integrity after 7 days *in vivo* but altered very little after 14 days *in vitro*. Their results appeared to indicate that the mechanism for degradation of the irradiated fibres *in vivo* may be different than that *in vitro*, possibly as a result of enzymatic action. The *in vitro* degradation of melt spun monofilament fibres has also

been investigated by Kanesawa and Doi[48], who report no molecular weight loss until after 80 days under conditions of 37°C. temperature and pH 7.4. Other PHB based forms including melt-pressed discs and films,[39,42,49-54] injection moulded samples[49-57] and microspheres[58] have also been investigated.

Work by the Speciality Materials Research Group at Aston University has shown that the susceptibility of the PHB based samples to degradation is altered by copolymerization with poly(3-hydroxyvalerate) (PHV) (Fig. 1.1) and blending with polysaccharides and other compounds.[49-54] Similarly, work by Kunioka *et al*[59,60] has produced the copolymer of 3- and 4-hydroxybutyrate, P(3HB-4HB) using 4-hydroxybutyrate and butyric acids as the carbon source in the production fermentation process. The presence of the 4HB units in the PHB has been shown to accelerate the degradation by simple as well as enzymatic hydrolysis.[61,62]

Thus, the biodegradation of PHB is reported to be relatively slow, in a few cases this may be beneficial to the wound healing, but in most cases it is generally considered to be detrimental. However, the degradation of the PHB and its devices has the promising attribute in that it can be altered by various means, and therefore, would fulfill a number of possible roles as medical and surgical implantation devices.

1.2.3. Biocompatibility Of PHB Degradation Products.

PHB degrades to its monomer; β-hydroxybutyric acid[55] (HBA). HBA was first discovered in human urine by Minkowski[64] and Kutz[65] in 1884 and in the sera of diabetic patients, reported by Bondy *et al*[66] in 1949. HBA is a stable analyte normally

found in human sera with levels of around 0 to 4.39mgdl.$^{-1}$ in adults and 0.25 to 3.05mgdl.$^{-1}$ for children.[67]

HBA together with acetoacetate and acetone are collectively known as the ketone bodies, (Fig. 1.2), these are formed naturally from acetyl coenzyme-A (acetyl co-A) in the Krebs citric acid cycle in the liver mitochondria during fatty acid oxidation (Fig. 1.3). The acetoacetate and HBA are not oxidized by the liver but transported by the blood to the peripheral tissues, where the free acetoacetate is reversibly reduced by the mitochondrial enzyme β-hydroxybutyrate dehyrogenase to HBA, which then re-enters the citric acid cycle.[68] The ketone bodies formation is an overflow pathway diverting some of the acetyl co-A produced during fatty acid oxidation in the liver to other tissues. By this method the liver can distribute 'fuel' to the rest of the body. This pathway is particularly important during conditions of prolonged fasting or starvation, where the HBA can be utilized by the brain, in particular, as another energy source instead of glycogen.

Normally the concentrations of HBA and ketone bodies in human blood are rather low, however, in sufferers of diabetes mellitus these levels might become quite high and is responsible for the characteristic sweet acetone breath. This condition is known as ketoacidosis[69] and occurs when the formation of the ketone bodies by the liver exceeds their utilization by the peripheral tissues, their production is due to the failure of the tissues to use glucose from the blood. HBA and this method of energy distribution is also found in other mammals. Some bacteria and fungi also possess HBA and exhibit similar metabolic pathways using inter- and extracellular enzymes. The presence of HBA, the accumulation of PHB and their metabolism in various bacteria and fungi has been studied and reported by a number of authors.[70-76]

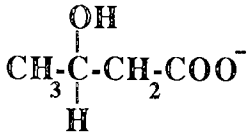

β -Hydroxybutyrate Anion.

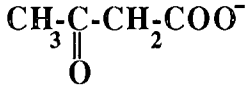

Acetoacetate Anion.

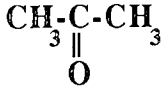

Acetone.

Figure 1.2.

Structure Of The Ketone Bodies.

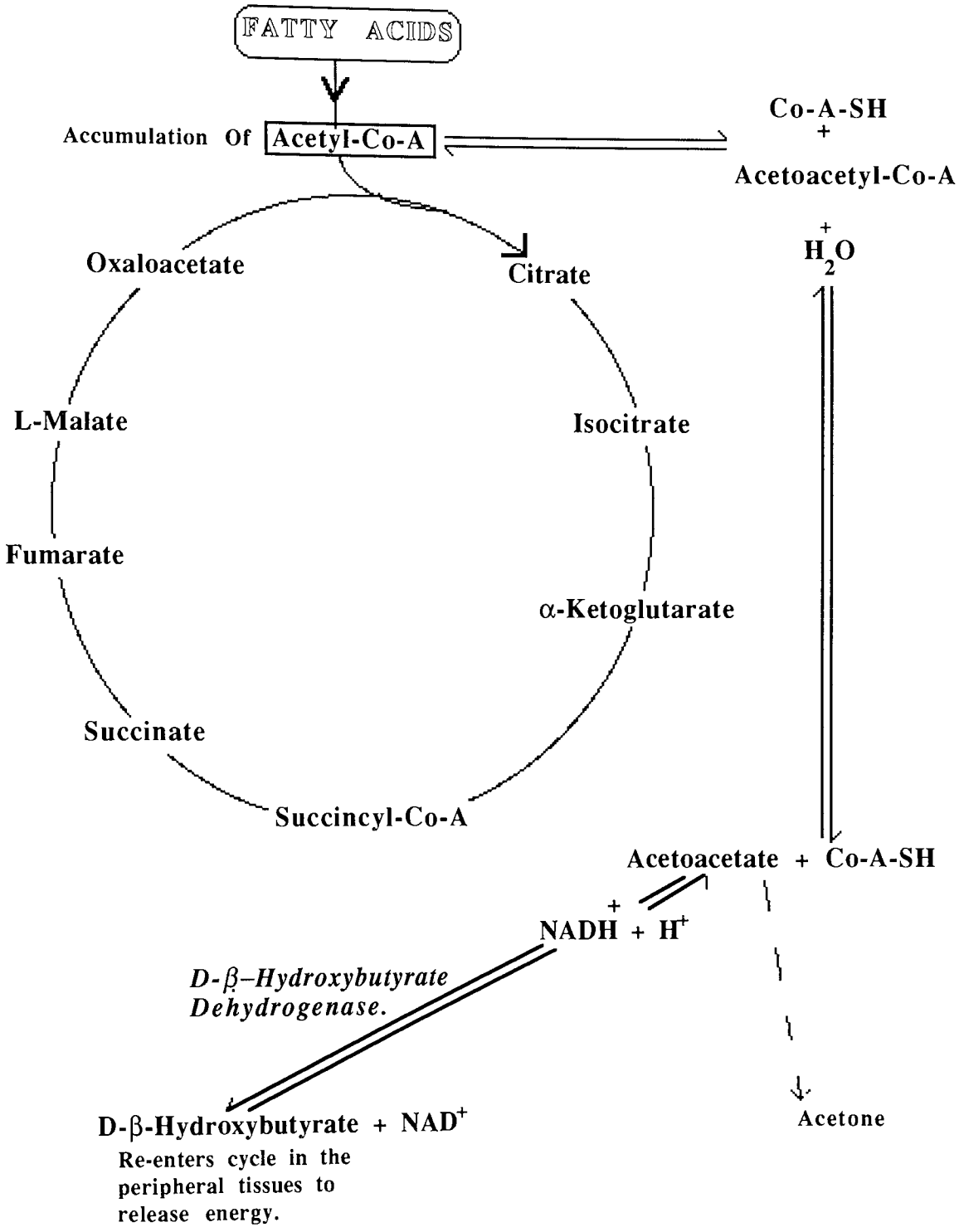

Figure 1.3.

The Krebs Citric Acid Cycle And The Formation Of Ketone Bodies In The Liver Mitochiondria.

In vivo studies in rats using radio labelled carbon 14 PHB granules showed that 86, 2.5 and 2.4% of the total radioactivity administered were distributed in the liver, spleen and lung respectively and the radioactivity gradually decreased during a 2 month period.[42]

Therefore, the monomeric degradation product of PHB; HBA, could be considered as biocompatible.

1.2.4. Commercial Interests.

The synthetic production of PHB by ICI and its subsidiary; Marlborough Biopolymers Ltd. has developed to the extent that it is readily and economically available for the product market.[77] It also has the distinct advantage over other convential thermoplastics in that there are no catalyst residues in the polymer and comparatively few impurities.[78]

As already discussed, the flexibility and adaptability of PHB is such that it has been processed into a variety of forms, copolymerized and blended. The physical aging of bacterial PHB has been investigated by Scandola *et al*[79] who reported that aging at room temperature caused an increase in the rigidity and resulted in an embrittlement of the material. P(3HB-3HV) is produced by ICI under the trade name Biopol.[77] Thus, the flexibility and availability of PHB appears to satisfy these commercial considerations.

Therefore, it can be concluded that PHB is a very promising polymer for use in the production of medical implantation devices, apparently satisfying all the necessary requirements.

1.3. PHB As A Wound Scaffolding Device.

A novel fibrous form of PHB has been produced with a possible use as a wound scaffolding device, such a device would be particularly useful for such difficult to heal wounds as bedsores or ulcers. The very nature of these wounds ensures comparatively long healing times, during which they are relatively prone to further damage. This novel fibrous form of PHB is intended to act as a 'scaffold', binding a fragile wound site over an extended period of time before being assimilated into the body. The concept is one of reepithelialisation progressing over the surface of the fibrous PHB implant, closing the wound whilst the temporary scaffold provides a framework for the laying down of a permanent dermal collagen architecture. Thus, the wound scaffolding device would prevent further damage and promote healing.

In vitro preliminary studies of the cellular reactions to this novel form, by Davies,[80] indicates that the device actually promotes cellular growth. A wound scaffolding device of this kind could be utilized in a wide variety of wounds, including dental and surgical applications, providing the biodegradation profiles were suitable.

1.4. Recent Commercial Developments.

In the last few years there has been increased interest in biodegradable plastics as a result of the increase in ecological awareness. Biopol has been utilized in a trial commercial production and sale in Germany of 'Wella' shampoo bottles, allegedly the first totally

biodegradable product; biodegradable contents in biodegradable packaging.[81] (Plate 1.1) Investigations into the biodegradation of these shampoo bottles in the environment have been reported by Bardkte *et al*[82] and Brandt and Püchner.[83] Bardkte *et al* reported approximately 18% weight loss of the shampoo bottle's initial weight after 9 weeks composting, after 15 weeks 80% of the bottle material could no longer be found. Brandt and Püchner investigated the biodegradation of the bottles under the comparatively unfavourable degradation conditions of low temperature, high pressure and no sunlight, at approximately 85m. depth in lake Lugano, Switzerland. From their results they estimate a bottle lifespan of around 10 years and thus it was concluded, that even under these 'hostile' conditions Biopol plastic articles were degraded.

A recent survey by Jewell and Krupp[84] of 12 commercially available, allegedly biodegradable plastics, revealed that only one could actually be classified as biodegradable! This was Biopol. In all the other cases a starch filler readily biodegraded but left a polyethylene component which remained intact even after 25 weeks in a bioreactor.

Thus, the use of PHB and Biopol in the commercial field has recently increased and it has been shown that such items are more 'eco-friendly' than their non-biodegradable counterparts, which are seriously damaging the environment. However, more recently a somewhat ecologically disturbing trend towards the use and marketing of 'recyclable' plastics has arisen; It is estimated that the U.S.A. produces around 158 million tonnes of municipal solid waste (MSW) per year, of this around 7% by weight (1984 figures) and 27% by volume are plastics. 80% of this waste is landfilled, 9% incinerated and 11%

Plate 1.1.

Recent Commercial Developments Involving PHB: Biopol Biodegradable Wella Shampoo Bottle.

recycled.[85] However, only 1% of the plastic waste is recycled whilst in other countries no recycling at all occurs!

1.5. General Conclusions.

PHB and Biopol have been readily investigated for their biodegradation in the macroenvironment of the earth and this has led to the development of several commercially available products. However, the studies of PHB in the microenvironment of the body system are comparatively more scarce, nevertheless these investigations tend to indicate that the PHB is relatively biocompatible.

Unfortunately, the biodegradation time of PHB within the mammalian body system is generally too long for the polymer to be useful in convential medical implantation devices. However, the biodegradation can be readily altered by changes in the processing, blending and copolymerizing. Therefore, it may be concluded that poly(β-hydroxybutyrate) is very promising as a material for the production of a variety of surgical and medical implantation devices. The complex structure of the novel fibrous form studied in this thesis combines a large volume with low mass and this is anticipated to facilitate in its degradation, so that the biodegradation would be more favourable compared to other convential PHB forms eg; melt processed discs and plaques.

1.6. Scope Of This Work.

The aim of this work was to investigate the *in vitro* degradation of the new and novel fibrous form of PHB, and to alter its degradation times to those considered more favourable for its intended use as a wound scaffolding device.

The novel fibrous form was of a relatively complex structure (See Chapter 3) compared to PHB based samples used in previous studies, and as such, the convential degradation monitoring methods using gravimetry were not suitable for this novel fibrous form which combines a large volume with a low mass and its structure changes substantially as part of the degradation process. Therefore a new technique for monitoring the degradation had to be developed. This technique was then utilized in the development of an *in vitro* accelerated degradation model which monitored both the degraded and undegraded fractions of the sample during degradation and investigated the physical and chemical changes of the undegraded or 'partially degraded' fractions.

Changes in the degradation rates of the novel form due to blending and copolymerizing the sample and by altering its processing were investigated utilizing the accelerated degradation model. The results obtained were then compared to those determined for the same samples in a physiological degradation model. Thus, providing a more accurate indication to the samples biodegradation as an implantation device.

Finally, the degradation of the novel form in the accelerated and physiological degradation models was compared to the degradation of some melt processed PHB based forms in the

same degradation models. This then would allow the theoretical comparison with a wide variety of other PHB samples from similar degradation models.

Therefore, it is anticipated that the work in this thesis will provide a new and accurate accelerated degradation model to monitor the changes in the degradation of any PHB based samples, whilst utilizing this model to investigate the degradative pathway, and its alteration, of this exciting new fibrous PHB form. Thus, it is hoped that the work in this thesis will eventually lead to the production of suitable biodegradable, biocompatible wound scaffolding devices, individually 'tailored' to suit various wound types and to fulfill a neglected niche in the medical field.

Chapter Two.

Materials And Methods.

2.0. General Introduction.

This chapter deals with the materials and methods involved in the work in this thesis and explains the degradation models utilized in monitoring the degradation of the PHB samples.

The accurate quantitative degradation of the novel fibrous form was difficult to determine due to its rather unique and complex structure, which combined a large volume with low mass and readily altered during, and as part of, the degradation process. As a result of these intrinsic problems, the degradation monitoring techniques previously utilized for the more convential PHB based forms were unsatisfactory for this novel form. Therefore, a new method of monitoring the degradation had to be developed. This involved the determination of the monomer (HBA) concentration during degradation, incorporating this into the measurement of both the degraded and undegraded fractions of the sample during degradation and the monitoring of both the sample and the PHB degradation.

An experimental procedure that takes into account the intrinsic problems presented by the novel structure of this material, was devised and is summarized in figure 2.1. This experimental pathway was then implemented for all the samples investigated and should be considered when reading this chapter.

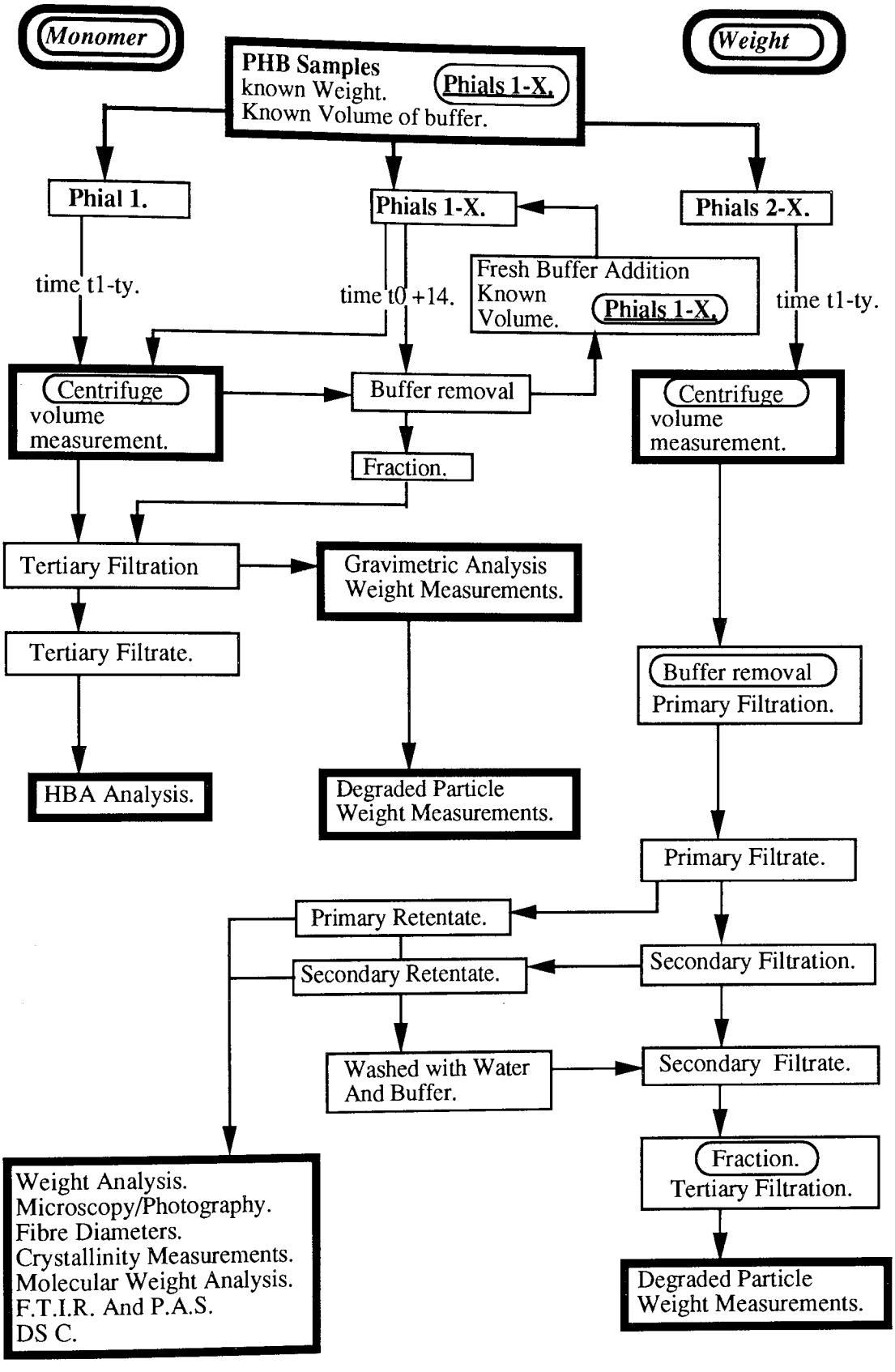

Figure 2.1.

Experimental Pathway For The Degradation Of PHB(FM) And PHB Based Samples.

2.1. Materials.

The homopolymer fibre samples and the co-blended/copolymer samples were supplied by ICI Biological Products. The polysaccharides and the compounds for buffer preparations were purchased from the Sigma Chemical Company, whilst the kits for the determination of the monomer β-hydroxybutyric acid were purchased from Sigma Diagnostics Ltd.

2.2. Analysis Of Degradation.

2.2.1. Optical Microscopy.

The undegraded and partially degraded samples were examined at low magnifications (x5-x25) using an Olympus CK2 phase contrast microscope. Photographic plates of the samples were obtained using the camera attachment.

2.2.2. Scanning Electron Microscopy. (SEM)

A small amount of the sample was mounted on a clean, dry, aluminium SEM stub of 12mm. diameter and 3mm. pin, using mounting agent. The stub surface was then gold coated under vacuum and the sample examined using a Cambridge 90 Stereoscan Electron Microscope. Photographic plates were obtained using the camera attachment and Pixie thermal imager. Other samples were examined after being dehydrated in a vacuum oven for approximately 24hrs. under conditions of 40°C. and a pressure of 460mm. mercury.

2.2.3. Fibre Diameter Determinations.

Using SEM (Sec. 2.2.2), samples were examined at a magnification range of x200 - x1K. Utilizing the separation lines facility of the microscope, the diameter of the fibres in focus were measured. A random sampling of 100 fibres from a minimum of 5 different sections of the stub were examined from each specimen. The fibre diameter distribution was measured as the percentage of fibres in the respective diameter ranges; 0-1, 1-2, 2-3, ...14-15 and 15+ microns.

2.2.4. X-Ray Crystallography.

Samples were placed between two clean, glass, microscope slides, these were compressed together using clamps and placed in an oven at 60°C. for a period of 24hrs. and then removed. Upon cooling, the upper glass slide was removed and the extreme edges of the compressed sample secured to the lower slide using Sellotape. The middle of the sample was then analyzed using a Phillips X-ray diffractometer (40Kv. & 20ma.).

The crystallinity of the samples was calculated from the diffracted intensity data in the range of 10 to 50°, according to the method of Fredericks *et al.*[86] A baseline was drawn through the two lowest points of the trace and the amorphous and crystalline regions estimated. The percentage crystallinity was then calculated using the following equation:

$$\% \text{ Crystallinity} = \frac{\text{Crystalline Area.}}{\text{Total Area.}} \times 100 \qquad \text{....(Equation 2.1.)}$$

2.2.5. Molecular Weight Analysis.

Molecular weight measurements of the PHB samples were performed by RAPRA

Technology Ltd., using gel permeation chromatography with chloroform as a solvent, polystyrene was used for calibration and the results were expressed as the 'polystyrene equivalent'.

2.2.6. Determination Of Degradation Conditions.

Three waterbaths were maintained at constant temperatures of 37.5, 50 and 70 ±0.2°C. Buffer solutions were made according to Dawson[87] for the following pH's:

1) pH 2.1; $Na_2HPO_4.12(H_2O)$/Citric Acid.(H_2O)

2) pH 7.4; $Na_2HPO_4.12(H_2O)/NaH_2PO_4.2(H_2O)$

3) pH 10.6; $Na_2CO_3.10(H_2O)/NaHCO_3$

PHB samples of approximately equal weight were placed in clear, glass phials with screw cap lids. The samples were handled using sterile gloves and forceps to prevent contamination. 20mls. of the respective buffer was added to each phial, so that samples with each of the different buffers were degraded at all of the temperatures. Controls of solid sample only and buffer solution only were also prepared. The phials were tightly closed and sealed using 'Nesco-film'. In some instances samples were photographed prior to and after placing them in the phials and during the degradation period.

2.2.7. Filtration And Gravimetric Analysis.

A 4.25 cm. diameter macroscopic filter disc and a 3 micron porosity Millipore disc were accurately weighed in a clear, plastic container to prevent contamination.

A glass phial containing the degraded sample and the degrading medium were filtered

under gentle pressure through the macroscopic disc in a clear buchner funnel attached to a filter tube (Primary filtration). The contents of the tube were then measured using a pippette and placed in a syringe attached to a swinnex disc holder containing the millipore filter. The contents were then filtered under gentle pressure (Secondary filtration). The initial glass phial was then washed with 10mls. of distilled water and filtered through the same discs into a separate container labelled accordingly. Thus, two containers were obtained:

1) Day 'X' — Known volume of buffer with particulate matter ideally below 3 microns in diameter and monomer in solution.

2) Day 'X' (Washings) — Known volume of distilled water with particulate matter ideally below 3 microns in diameter.

The filter discs were removed and replaced back in their containers. The discs with the sample retentates were then dried in a dessicator at 60°C. for 36hrs. Upon removal they were allowed to cool in the dessicator at room temperature for 15 minutes and weighed (dry weight) then left to stand in a dust free environment for 48hrs. and reweighed (standing weight.). All values were corrected by the use of controls. Weight losses were calculated using the equations below:

(Equation 2.2.)....

$$\% \text{ Change in standing weight} = \frac{\text{Standing Wt. - Initial Wt. (+/- Correction)}}{\text{Initial Sample Weight.}} \times 100$$

(Equation 2.3.)....

$$\% \text{ Change in dry weight} = \frac{\text{Dry Wt. - Initial Wt. (+/- Correction)}}{\text{Initial Sample Weight.}} \times 100$$

2.2.8. Particle Analysis.

2.2.8.1. Initial Study.

An initial study to determine the percentages, by weight, of those particles considered as degraded during the time periods was performed using a Malvern laser particle sizer with a 63mm. lens. The sample holder was filled with a known volume of buffer and sealed. The particles within the buffer were then analyzed and noted as the background value. Distilled water was used for the washings. A known volume of the sample filtrate was then added and the holder resealed. Mixing was achieved using a magnetic stirrer at a fixed setting. The differences in particle distribution were computed and displayed in tabulated and graphic form, within a range of 118 to 1.2 microns diameter. An approximate value was also given for particles 1.2 to 0.5 microns diameter. Using this data and density values for the sample, the percentage of particles with a diameter less than 3 microns was calculated. Particles below this size were considered as bioresorbable.[88]

2.2.8.2. Tertiary Filtration and Weight Analysis.

A 0.22 micron Millipore Millex filter unit was weighed (initial weight) and then used to filter the solution from the secondary filtration process in section 2.2.7. The unit was then dried in a dessicator at 60°C. for 36hrs. and reweighed (dry weight). The Millex filter was left to stand in a dust free environment for 24hrs. and then weighed again ('standing' or 'wet' weight). Millex units with buffer only were used as controls and from these a mean

percentage correction factor was calculated. This factor was then applied to the initial weight of the individual filter units and the percentage, by weight, of particles was calculated using the equations 2.2 and 2.3 in section 2.2.7.

2.2.9. β-Hydroxybutyric Acid (HBA) Measurements.

2.2.9.1. Monomer Determination.

A kit was obtained from Sigma Diagnostics to determine the concentration of β-hydroxybutyrate (HBA) in solution. Although the kit was originally designed for the determination of HBA in human sera and plasma, experiments carried out to determine the stability of the monomer HBA under the experimental degradation conditions concluded that the determination was accurate in the accelerated degradation model (Sec. 2.3.).

The samples were analyzed using a pair of matched quartz cuvets and a Unicam SP1800 ultra violet spectrophotometer, set at a wavelength of 340nm. with a constant temperature cuvet holder at 25°C.

3.0ml. of HBA reagent and 0.05ml. of hydroxybutyrate dehydrogenase solution (HBDH) were accurately pipetted into a glass phial. The phial was sealed and mixed by gentle rolling, then warmed in a constant temperature waterbath at 37°C. 0.05ml. of the filtrate from the tertiary filtration process was then added and the phial contents mixed by gentle inversion. The phial was then replaced in the bath and incubated for 10 minutes. The absorbance of the sample was determined within 30 minutes of removal. Between 3 and 8 phials were analyzed per filtrate and the mean determined.

The mean absorbance was then processed into the linear calibration equation and the monomer concentration calculated (Sec. 2.2.9.2.). The total amount of monomer present within the sample phial was calculated from the monomer concentration and the volume of the phial contents. Degradation samples having values greater than 80mgdl.$^{-1}$ were diluted with distilled water and reassayed.

Figure 2.2. illustrates the enzymatic reaction involved in the assay:

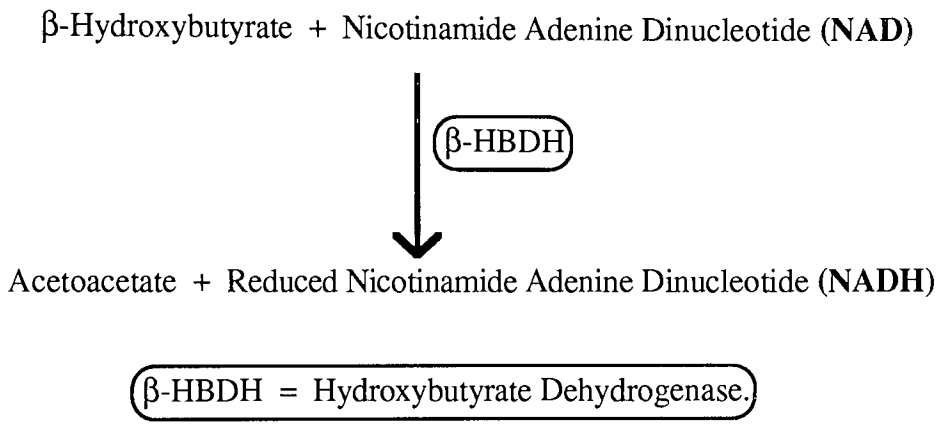

Figure 2.2.
Quantitative Enzymatic Assay Of β-Hydroxybutyrate.

The dehydrogenase (HBDH) catalyzes the oxidation of the monomer β-HBA to acetoacetate. During this oxidation an equimolar amount of nicotinamide dinucleotide (NAD) is correspondingly reduced (NADH). This absorbs light at 340nm. and therefore an increase in absorbance at this wavelength is directly proportional to the concentration of the monomer in the sample. This method has been extensively used to determine the concentration of HBA in human blood and sera as an indicator to diabetes and has been adapted for automation.[89-95]

2.2.9.2. Calibration

A series of phials were labelled 1-5, to each phial 3.0ml. of HBA reagent and 0.05ml. of

HBDH solution were added, mixed and warmed to 37°C. To phials 1-5 0.05ml. of distilled water and calibrator solution at concentrations of 10mg.dl.$^{-1}$, 25mg.dl.$^{-1}$, 50mg.dl.$^{-1}$ and 75mg.dl.$^{-1}$ were added respectively. The phials were then mixed, incubated for 10 minutes and the absorbances measured. This was repeated such that a mean absorbance of a minimum of 5 readings were calculated. Using these mean absorbances a calibration graph of absorbance against monomer concentration in mg.dl.$^{-1}$ was plotted. The graph was linear from 0 to 80mg.dl.$^{-1}$. Calibration was repeated at periodic intervals to ensure accuracy.

2.2.10 Differential Scanning Calorimetry. (DSC)

PHB samples weighing approximately 5-10mg. were analyzed in a Perkin Elmer 7500 Series differential scanning calorimeter. The samples were heated from 30 to 200°C. at a rate of 20°C.min.$^{-1}$, held at 200°C. for 1 minute before being cooled at 40°C.min.$^{-1}$ to -40°C., this temperature was then maintained for 4 minutes, the samples were then reheated at 10°C.min.$^{-1}$ to 30°C. The resultant heat flow curves were analyzed and the melting points (mp.), fusion enthalpies (ΔHm.) and glass transition temperatures (Tg.) determined.

Both the undegraded and partially degraded samples (Sec. 2.4.2.) were analyzed and a mean of at least 4 readings calculated.

2.2.11. Fourier Transform Infra-red Spectroscopy (FTIR) - Photoacoustic Spectroscopy.(PAS)

PHB samples of approximately 10mg. weight were placed in a MTEC Photoacoustic

model 200 attachment in a Nicolet 5200 fourier transform infra-red spectrophotometer and the samples analyzed using FTIR-PAS in a helium atmosphere. Both the undegraded and partially degraded samples were analyzed.

2.3. Stability Experiments.

2.3.1. Monomer Stability Under Accelerated And Physiological Conditions.

15mls. of buffer at a pH of 10.6 were placed in glass phials labelled low, med and high. 5mls. of HBA calibrator solutions at concentrations of 10mg.dl.$^{-1}$, 50mg.dl.$^{-1}$ and 75mg.dl.$^{-1}$ were added respectively and mixed by gentle inversion. The HBA determination procedure as described in section 2.2.9. was carried out using a series of 0.05mls from each of the phials as the samples and the mean absorbances of each phial determined, these values were considered as the initial readings. The phials were then closed using screw cap lids and sealed with 'Nesco-film', these were then placed in a water bath at a constant temperature of 70 ±0.2°C. At periodic intervals the phials were removed, allowed to cool by standing for 15 minutes, the volume measured and the absorbances determined. The percentage variations of these values from the initial readings was calculated and illustrated graphically against the time of the readings.

The same process was performed using a buffer of pH 7.4 and a temperature of 37.5 ±0.2°C. to determine the stability under physiological conditions.

2.3.2. Monomer Stability Under Accelerated Conditions In The Presence Of Polysaccharides.

15mls. of buffer at a pH of 10.6 were placed in glass phials labelled 1-4, 5mls. of HBA calibrator solution at a concentration of 50mg.dl.$^{-1}$ were added to each phial. To the individual phials a known weight of polysaccharide, approximately similar to that of the ideal percentage utilized in the co-blended samples, was added (Chapter 3).

The phials were mixed by gentle inversion and the absorbance of the monomer in each was determined. (2.2.9.) This was the initial value. The phials were then sealed and placed in a water bath at a temperature of 70 ±0.2°C. At periodic intervals the phials were removed, allowed to cool by standing for 15 minutes and the volume and mean absorbance of each phial was then determined. The variation in absorbance from the initial values was examined with time.

2.4. Degradation Experiments.

2.4.1. Monitoring Monomer Production.

Known weights of a sample were placed in labelled glass phials with screw sealing lids and 20mls. of buffer at a pH of 10.6 were added, the phials were closed and sealed using 'Nesco-film'. The contents were mixed by gentle inversion a number of times and the phials placed in a constant temperature waterbath at 70 ±0.2°C. At periodic intervals the phials were removed, allowed to cool and the monomer concentration analyzed.

After 14 days the phials were removed and allowed to cool. Centrifuging the phials at 3,500rpm. for 20 minutes accumulated most of the sample matter at the base of the phials without mechanical damage to the samples. The majority of the solutions were then removed and a known fraction filtered through the Millex filters (Tertiary filtration.). This filtrate was used to determine the amount of HBA present. 20mls. of freshly prepared buffer was then added to each phial, the phials sealed, their contents gently mixed and allowed to settle before replacing them into the waterbath. At termination of the experiment the phial contents were also filtered in the primary and secondary stages for weight analysis.

2.4.2. Monitoring Weight Loss.

A number of phials containing similar weights of the same PHB sample and the same volume of buffer (pH 10.6) were placed in a waterbath at 70°C. At periodic intervals a phial was removed, allowed to cool and then the contents were filtered through the primary and secondary discs. A known fraction of this filtrate was then filtered through the tertiary disc. The discs were analyzed gravimetrically and the processes described in section 2.2 and in the pathway; figure 2.1. were then carried out. At 14 day intervals the same procedure of buffer replacement, as detailed in section 2.4.1. above, was repeated. Gravimetric analysis of the samples in the physiological degradation model of pH 7.4 and temperature 37.5 ±0.2°C. was also carried out with buffer replacement every 28 days.

2.5. Other Experiments.

2.5.1. Introduction.

As is generally the case with all new materials, the investigative process contained a certain amount of 'trial and error'. A number of experiments were performed in an attempt to analyze this novel and 'difficult' form of PHB, and unfortunately failed. Two of these experiments deserve a mention, since the results are somewhat useful in understanding the nature of this novel form.

2.5.2. Surface Energy Measurements.

Samples were pressed between two glass slides, clamped and heated at 60°C. for 48hrs. The top slide was removed and a drop of distilled water placed on the sample. The contact angle formed on either side of the drop was measured directly using a goniometer eyepiece fitted to a cathometer. Unfortunately the drop was apparently suspended and this led to the conclusion that the samples were hydrophobic. The same samples were then placed in the accelerated degradation model for 5 minutes, removed and pressed whilst drying. After this treatment they were then tested again, the samples were then found to be hydrophilic, with the water drop being adsorbed too quickly to measure.

These results led to the conclusion, that in all the samples, a coating, most probably a solvent residue, was initially present.

2.5.3. Tensile Testing.

Attempts to directly measure the tensile properties of the sample using a Hounsfield

tensiometer failed. Attempts to indirectly measure the samples by mounting pressed samples in poly(HEMA) hydrogels also failed. Hydrogels of various thicknesses were investigated, however, the PHB samples prevented a complete hydrogel membrane formation. Qualitative examination of the sample revealed it to have considerable strength.

2.6. General Conclusions.

Thus, a combination of experimental procedures was determined to quantitatively monitor the degradation of the PHB samples by measuring the degraded and undegraded fractions of a sample. This method permitted a confirmation of the experimental accuracy (Ch:3). The undegraded, or 'partially degraded', fractions were then analyzed qualitatively and quantitatively, so that a more complete picture of the degradation was determined.

Two degradation models were designed; accelerated and physiological with conditions of pH 10.6 and temperature 70°C. and pH 7.4 and 37.5°C. respectively. Some of the experiments in chapters 3 and 4 were necessary to 'fine tune' these models, investigate the effects of the models on the sample degradation and to confirm their accuracy. However, before the degradation of the samples could be investigated it was necessary to examine the undegraded samples, as discussed in chapter 3.

Chapter Three.

Preliminary Studies.

3.0 Introduction.

Chapter three, 'preliminary studies', concerns the structure and physical properties of the undegraded novel fibrous form. This novel PHB form was produced from chloroform extraction using a gel spinning process (Marlborough Biopolymers Ltd.). Two forms were originally manufactured; one using the technical grade polymer (TG) and that from increasing the polymer purity (IP). The structure and properties of both these forms were investigated. The effects of altering the production solvent, blending the fibrous form with various polysaccharides and increasing their loading was also studied. These investigations were neccessary in that:

a) This is the first study of the novel and complex fibrous form. No other investigations had previously been carried out.

b) The results would provide an indication as to the suitability and potential of the novel form for a role as a wound scaffolding device.

c) The results were to be used as a baseline for the comparison with the degraded fibrous form samples from the accelerated and physiological degradation models.

The HBA stability experiments in this chapter were neccessary to determine the suitability of the monomer analysis method for monitoring the PHB degradation and to determine suitable time frameworks for the degradation models.

3.1. Structure And Physical Properties Of The Novel Fibrous Form.

3.1.0. General Introduction.

Optical and Scanning Electron microscopy was performed on the undegraded samples produced from technical grade and increased purity polymer (TG and IP) in order to determine the structure of the samples. The samples were also examined using X-ray crystallography, differential scanning calorimetry, molecular weight analysis and photoacoustic spectroscopy to provide a more detailed chemical analysis of the structures. These were necessary to permit structural comparisons with samples which had been treated and/or degraded.

3.1.1. PHB(FM) Technical Grade (TG) And Increased Purity (IP).

3.1.1.1 Observations And Comparisons Between The Undegraded Samples.

An initial investigation of the undegraded technical grade polymer novel form, produced from chloroform solvent extraction, revealed a dense fibrous mass, with a macrostructure and texture very similar to that of common cotton wool, (Plate 3.1). This has led to its name; PHB 'fibrous matrix' ie: PHB(FM), more familiarly called 'wool' because of this similarity. The PHB(FM) is referred to in this thesis as being produced from either the technical grade polymer; PHB(FM)TG or from the increased purity PHB; PHB(FM)IP.

Agglutinations were noted to occur quite commonly (Plate 3.2), although these were usually limited to a maximum of three fibres. These agglutinations were more common with the technical grade sample than with the increased purity sample, indicating that this factor was probably a function of the manufacturing process. Forking, in a variety of

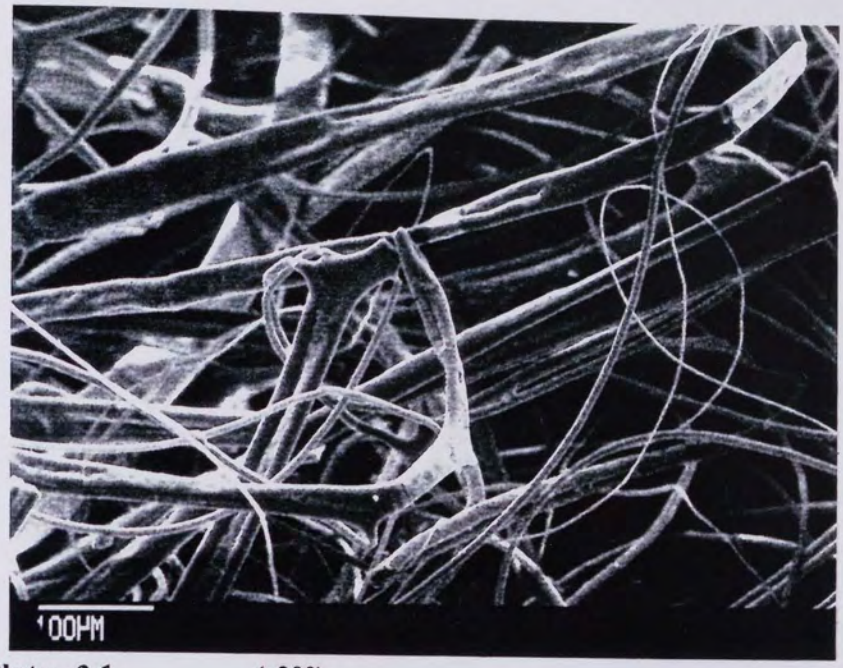

Plate 3.1. (x200)
SEM Illustrating The Fibrous Matrix Structure Of The Undegraded Poly(β-hydroxybutyrate) Fibrous Matrix Technical Grade Fibres.

Plate 3.2. (x1.59K)
PHB(FM)TG; Agglutination Of Three Fibres.

Plate 3.3. (x2.00K)
PHB(FM)TG; Forking Of Two Fibres.

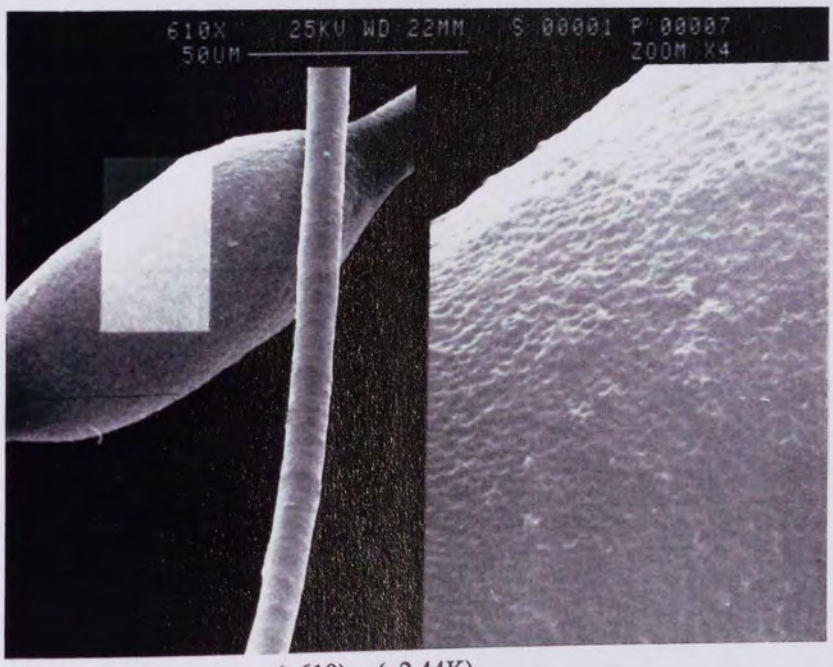

Plate 3.4. (x610) (x2.44K)
PHB(FM)TG; Terminal Bulbous Region And Surface Pores.

forms, also occurred (Plates 3.2 & 3.3). Although no multiple branching effect similar to that of a tree was noticed, some unusual variations were observed, (Plate 3.5). It was also noticed that in some fibres relatively large bulbous regions occurred. These were usually situated at the terminal ends of the fibres, (Plate 3.4).

A majority of the fibres were also noted to possess 'pits' or 'pores'. These were particularly prominent with those fibres having relatively large diameters. These 'pits' and 'pores' varied in size and apparent depth according to the fibre and appeared to be directly related to the fibre diameter. The difference in porosity between the TG and the IP fibres was quite noticeable, this was due to a change in the manufacturing processes which were implemented in order to improve the purity and reduce contaminants within the fibres and matrix.

Upon examination of the fibres using phase contrast microscopy, with water or trypan blue as a wetting medium, it was observed that a number of surface irregularities occurred in a small number of the fibres. These 'indentations' were also occasionally seen in some of the smaller diameter fibres and were probably structurally weak points predetermined by the manufacturing and handling processes. These were uncommon in the medium and larger diameter fibres, (Plates 3.6 & 3.7). In some instances these larger diameter fibres also possessed a number of comparatively large irregular regions, (Plates 3.4 & 3.5). These were also due to the manufacturing process.

A number of the fibres had hollow regions which contained 'pockets'. In some of the larger diameter fibres 'bubbles' were observed, these were possibly trapped solvent

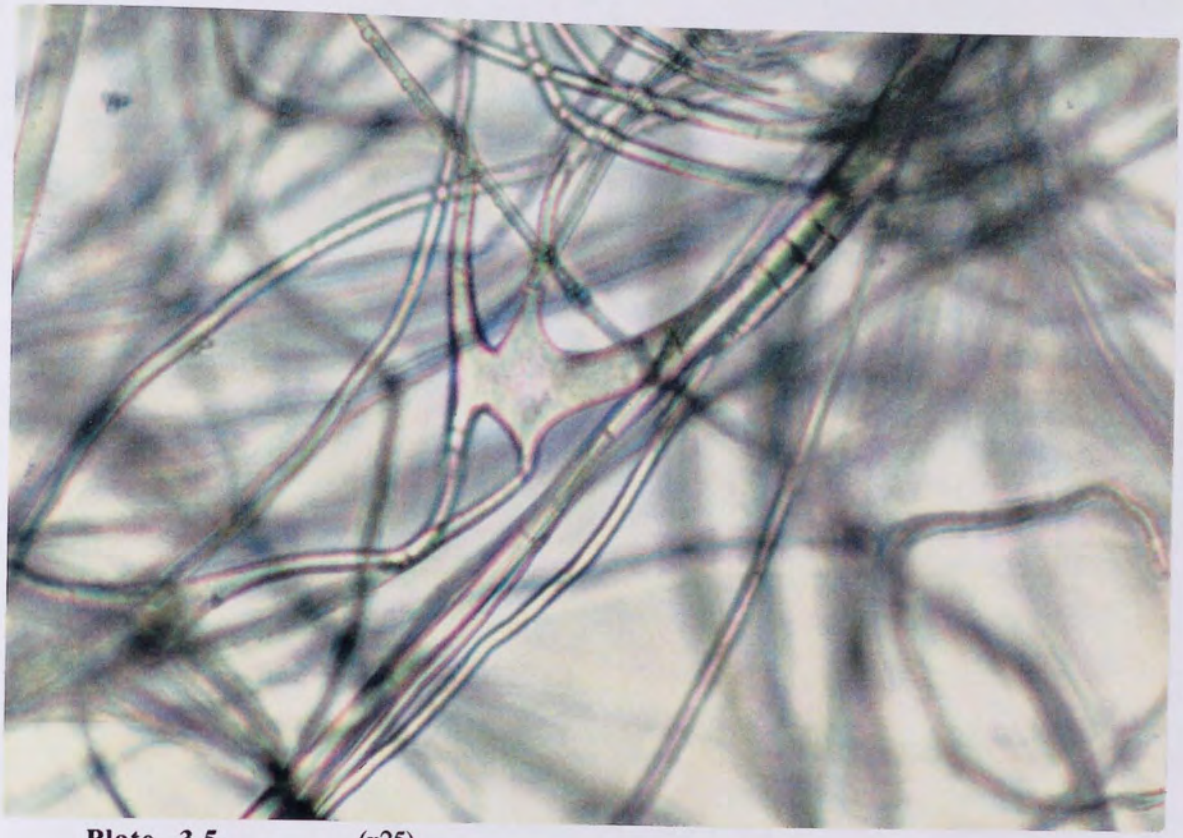

Plate 3.5. (x25)
Phase Contrast Photograph Of Undegraded PHB(FM)TG Using Water As A Wetting Medium, Illustrating The Comparatively Complex Structure.

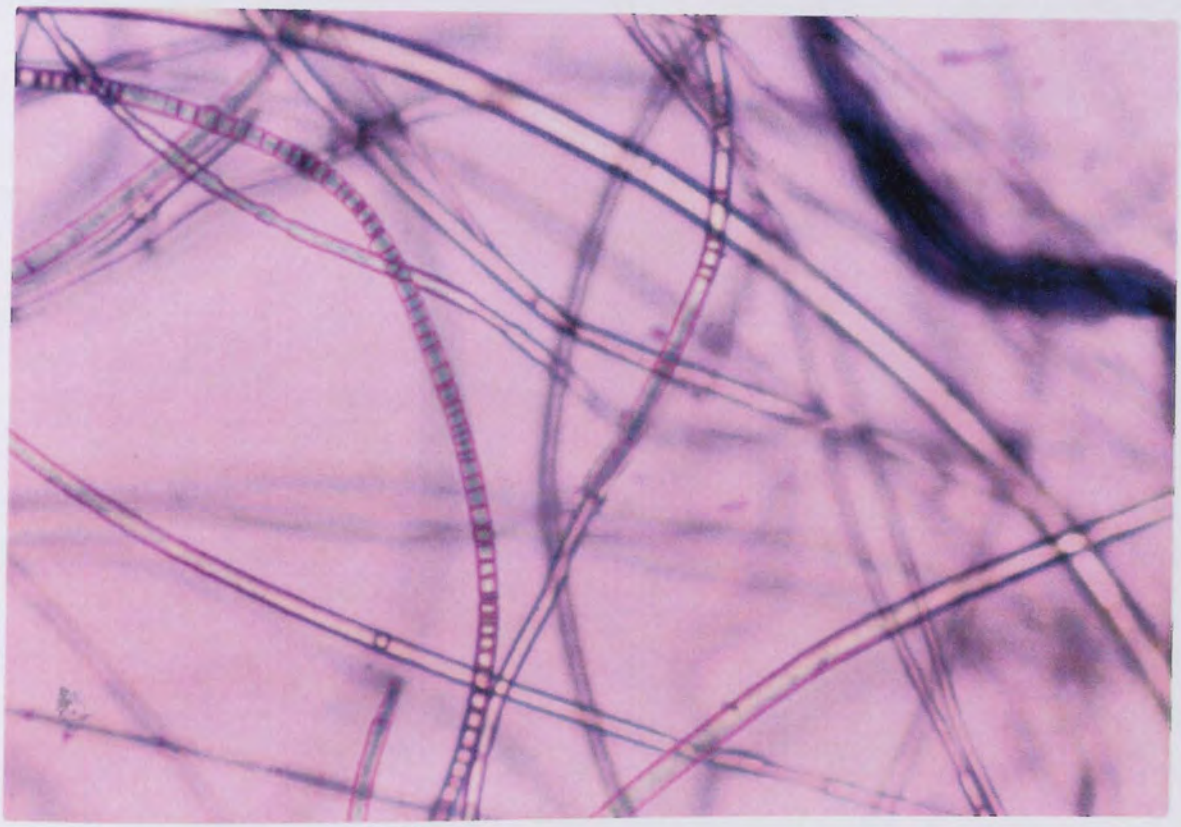

Plate 3.6. (x25)
Phase Contrast Photograph Of Undegraded PHB(FM)TG Using Trypan Blue As A Wetting Medium, Illustrating The 'Indentations' Commonly Observed In The Small Diameter Fibres.

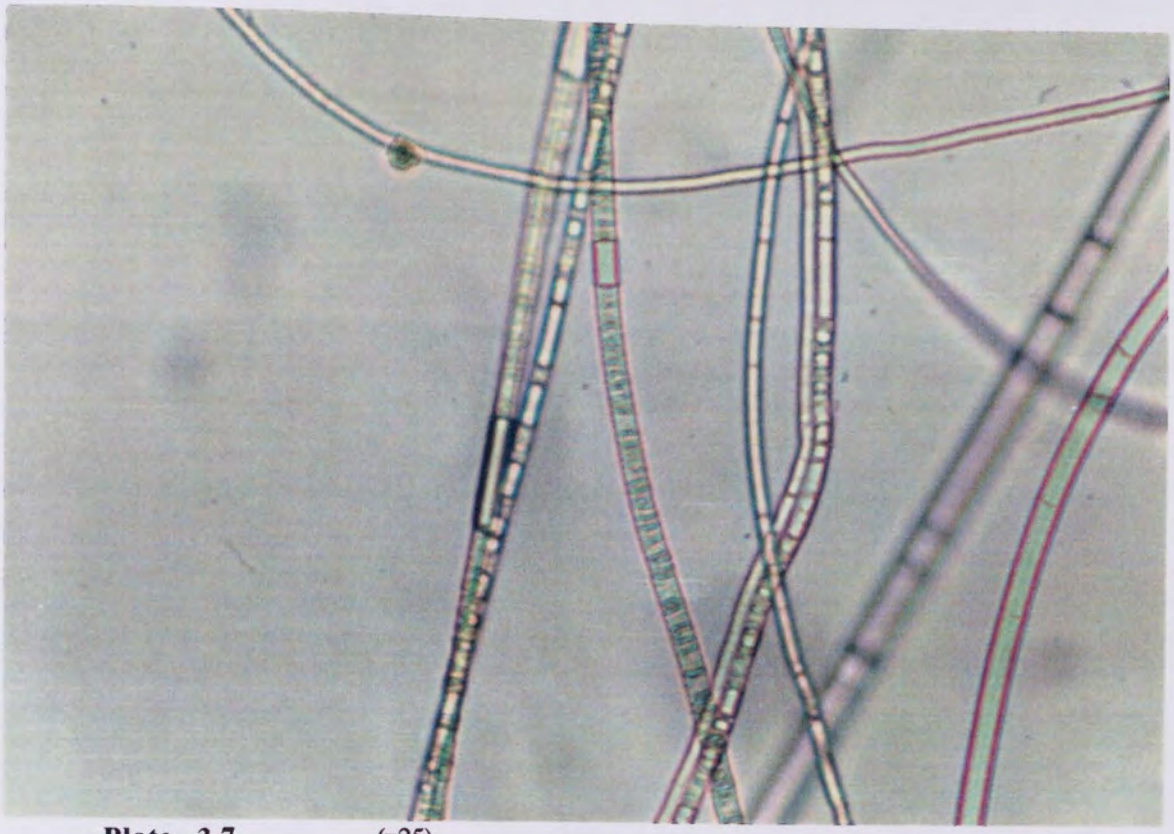

Plate 3.7. (x25)
PHB(FM)TG; Indentations And 'Bubbles' In The Small Diameter Fibres.

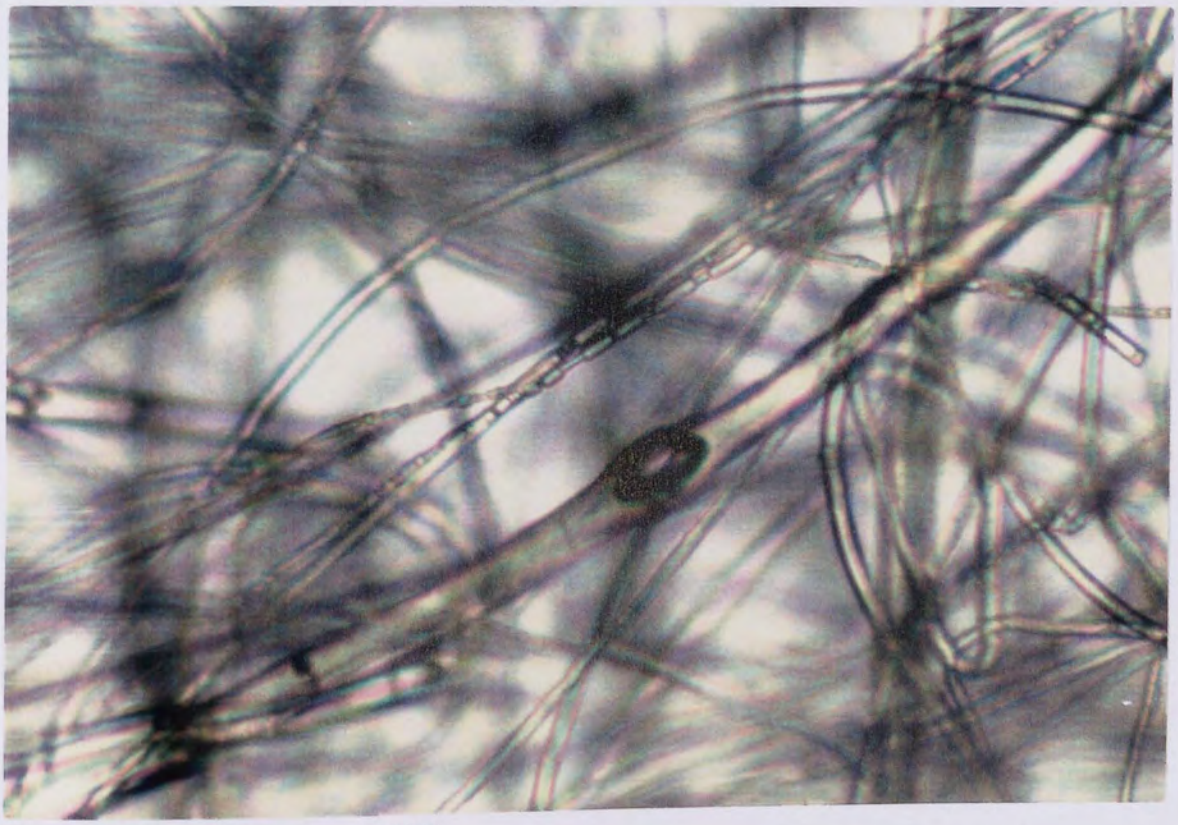

Plate 3.8. (x25)
PHB(FM)TG; Hollow Regions In The Smaller Diameter Fibres And Bubble In The Large Diameter Fibre.

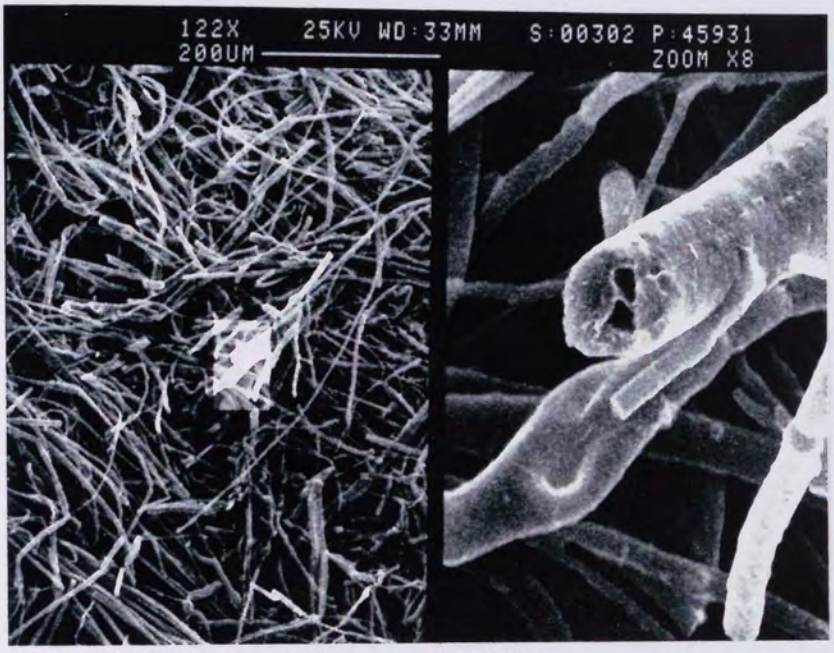

Plate 3.9. (x200) (x1.60K)

SEM Of PHB(FM)IP After 120 Days Degradation In The Physiological Degradation Model, Illustrating The Hollow Cavities After Mechanical Fracturing.

Plate 3.10. (x4.67K)

PHB(FM)IP After 120 Days Degradation In The Physiological Degradation Model, Illustrating The Hollow Cavities After Fracturing.

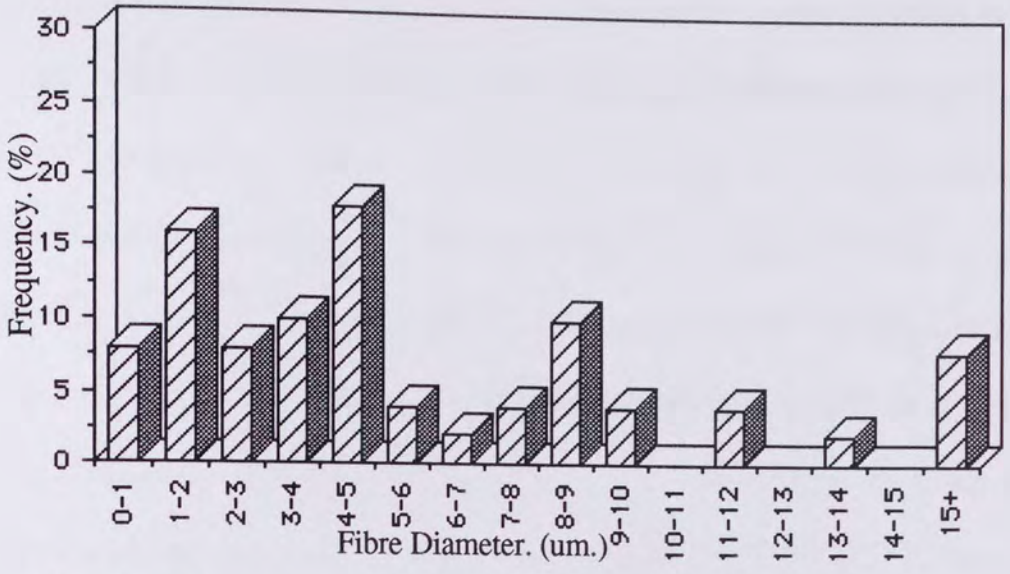

Graph 3.1.

Fibre Diameter Distribution For Fibres From The Undegraded PHB(FM) Produced Using Chloroform As A Solvent.

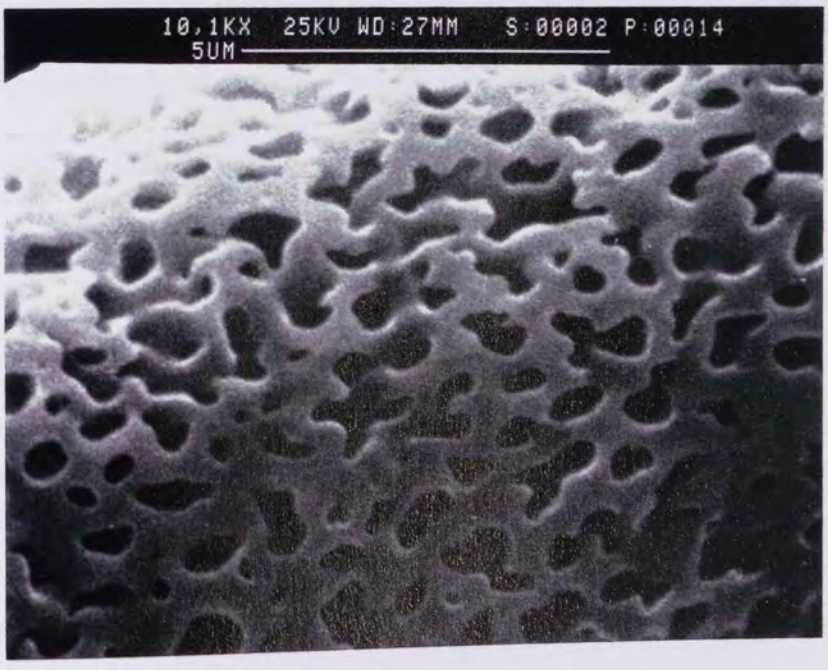

Plate 3.11. (x10.4K)

Undegraded PHB(FM) Produced Using Methylene Chloride As A Solvent, Illustrating The Porous Nature Of A Large Diameter Fibre.

vapour, (Plate 3.8). The bubbles moved within the fibre gradually rising to the higher regions and in some instances dissipated with time. This indicated that these fibres, besides being hollow in regions, had certain pores which were in direct contact with the hollow 'pocket' of the fibre. Thus, they effectively increased the surface area to volume ratio and were anticipated to facilitate the degradation process. It was also noted that a large proportion of these bubbles did not dissipate and consequently these pockets could be considered as effectively 'sealed' hollow regions. Some hollow regions or 'cavities' were also noted using scanning electron microscopy, (Plates 3.9 & 3.10). It is most likely that these cavities are also structurally weak points within the fibres.

The fibres consisted of a variety of diameters, the majority ranging from 0-16 microns (Graph 3.1). However, it was noticed that 7% of the fibrous matrix had relatively extremely large diameters up to 72 microns. Approximately 60% had diameters within a 0-5 micron range, with two noticeable peaks of 16 and 18% at 1-2 and 4-5 microns. The majority of fibres had non-uniform diameters within the same fibre. Increasing the purity of the fibres had apparently little effect on the fibre diameter distributions.

3.1.1.2. Physical Properties.

Thermal analysis of the technical grade and increased purity fibres revealed a small difference in the melting points, (mp.) 170 and 174°C. respectively, whilst the enthalpies of fusion (ΔHm) also illustrated a small difference of 74 and 79 J/g. Determination of the glass transition temperatures (Tg) was hampered by the small graphic changes involved, which meant utilizing the first order derivative, (Fig. 3.1 & 3.2). This then gave values of 0.3 and 5.2°C. for the technical grade and the increased purity fibres respectively.

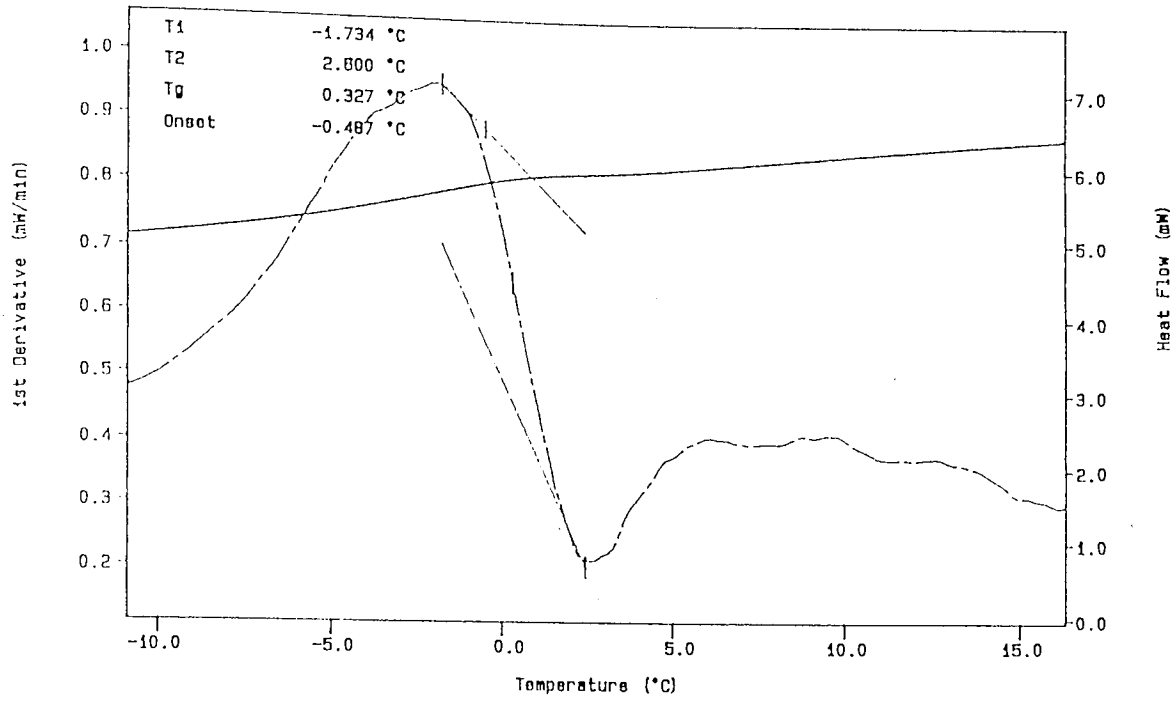

PHB(FM)TG

Figure 3.1.

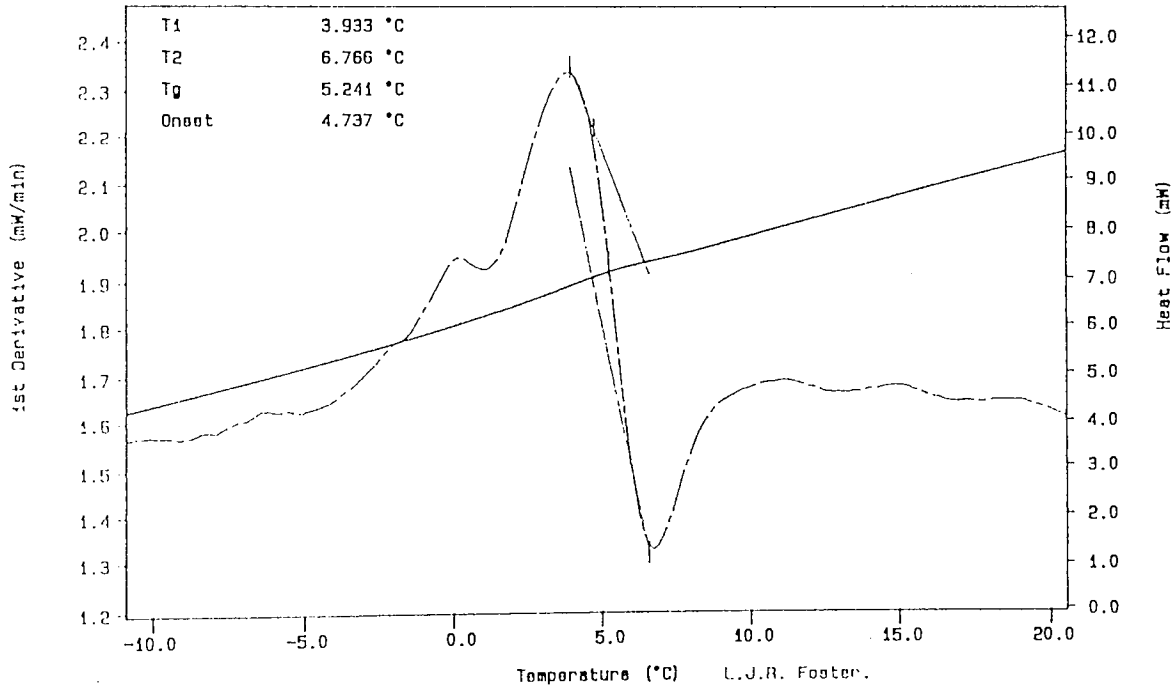

PHB(FM)IP

Figure 3.2.

Characterization Of Undegraded PHB(FM); DSC Curves For IP And TG Samples And The Need For The Derivative To DetermineThe Glass Transition Temperatures.

The Tg is effectively the main characteristic temperature of the amorphous solid and liquid states and an indicator of the bond polarity/mobility and also, therefore, the possible susceptibility of the samples to the degrading medium. The difficulty in determining the Tg. qualitatively indicated the high percentage crystallinity of the samples, whilst the fusion enthalpies also indicated a high degree of crystallinity for both samples. Similarly, X-ray crystallinity revealed the increased purity fibres to be highly crystalline with 73 ±3% and the technical grade fibres to be slightly more amorphous with a similar value of 70 ±3%.

Figure 3.3 illustrates a trace of the undegraded PHB(FM) technical grade (TG) sample utilizing photoacoustic spectroscopy which was particularly suited to the fibrous matrix sample, using a Nicolet 5200 Fourier Transform Infra-red Spectrometer, (FTIR). This trace was matched and found to be consistent with a PHB library trace from the Nicolet library.

The peak at 1048 $cm.^{-1}$ was probably due to the carbon-oxygen (C-O) bond stretching, which normally occurs within a range of 1040 to 1150 $cm.^{-1}$ Similarly, the strong waveband at 1284 $cm.^{-1}$ was probably due to the oxygen-hydrogen (O-H) bond bending, this occurred at the hydroxide terminal ends of the polymer chains. A minor sharp peak indicating either oxygen-hydrogen bond stretching in free hydrogen-oxygen bonds or more probably; water of crystallization, was also observed at approximately 3460 $cm.^{-1}$ Another weak water of crystallization band may also be present between 1615 and 1640 $cm.^{-1}$ and this may account for the slight 'shoulder' at the main peak of 1723 $cm.^{-1}$ in region A, (Fig. 3.3).

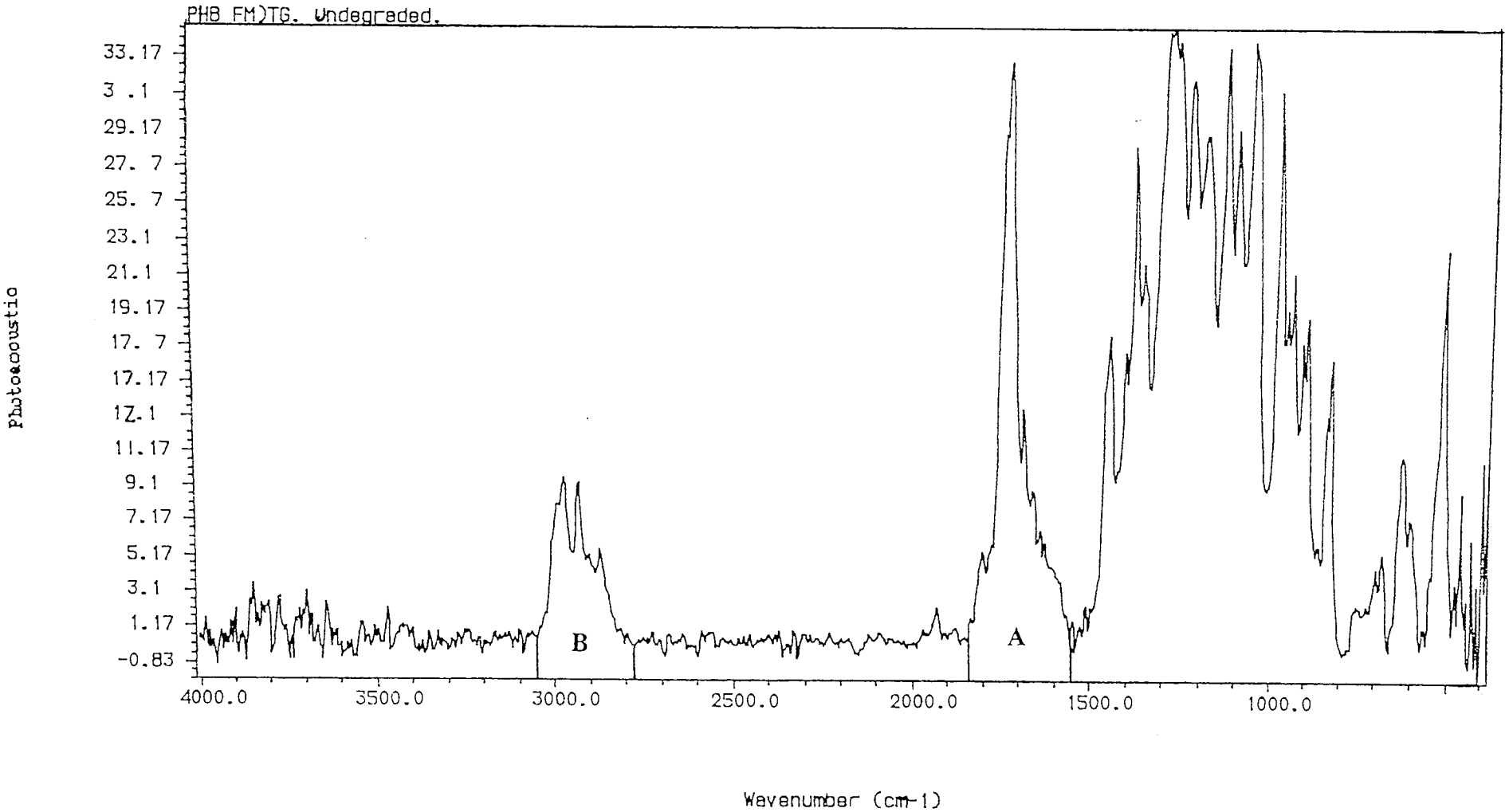

Figure 3.3.

Characterization Undegraded PHB(FM)TG; FTIR-Photoacoustic Spectrum.

Two main waveband groups occurred from the remaining spectrum above the fingerprint region, these were between approximately 1558 to 1864 $cm.^{-1}$ and 2822 to 3044$cm.^{-1}$ Identified as regions A and B respectively, (Fig. 3.3).

The main peak in region A was a sharp waveband at 1723 $cm.^{-1}$, this was the ester bond vibration. The normal frequency range for a saturated ester bond, in a dilute solution, is between 1735 and 1750 $cm.^{-1}$ However, this range was affected by the hydrogen bonding of the ester carbonyl group, responsible for the helical structure of the polymer chain, such that a shift to the lower frequency was observed. Similarly, a slightly lower value for the carbonyl stretching frequency occurs in the solid state when compared to the values of a dilute solution. [96] A number of shoulder peaks also existed in region A, the main ones of these were at frequencies 1688 and 1805 $cm.^{-1}$, the former could have been due to a ketone carbonyl, whilst the latter may have been a combination band or a result of contamination and/or solvent residue.

Region B was between 2822 and 3044 $cm.^{-1}$, the three noticeable peaks observed were of a much reduced intensity compared to those of region A and the majority of the wavebands in the fingerprint region. These peaks occurred at wavenumbers 2865, 2929 and 2972 $cm.^{-1}$ and were due to the saturated carbon-hydrogen (C-H) bonds. The sharp, relatively strong peaks at 2929 and 2972 $cm.^{-1}$ frequencies were most probably due to stretching of the $C\text{-}H_2$ and $C\text{-}H_3$ bonds, whilst the smaller, weaker peak at 2865 $cm.^{-1}$ was most probably due to the C-H stretching.

This trace was then compared to a trace obtained from a sample of the increased purity

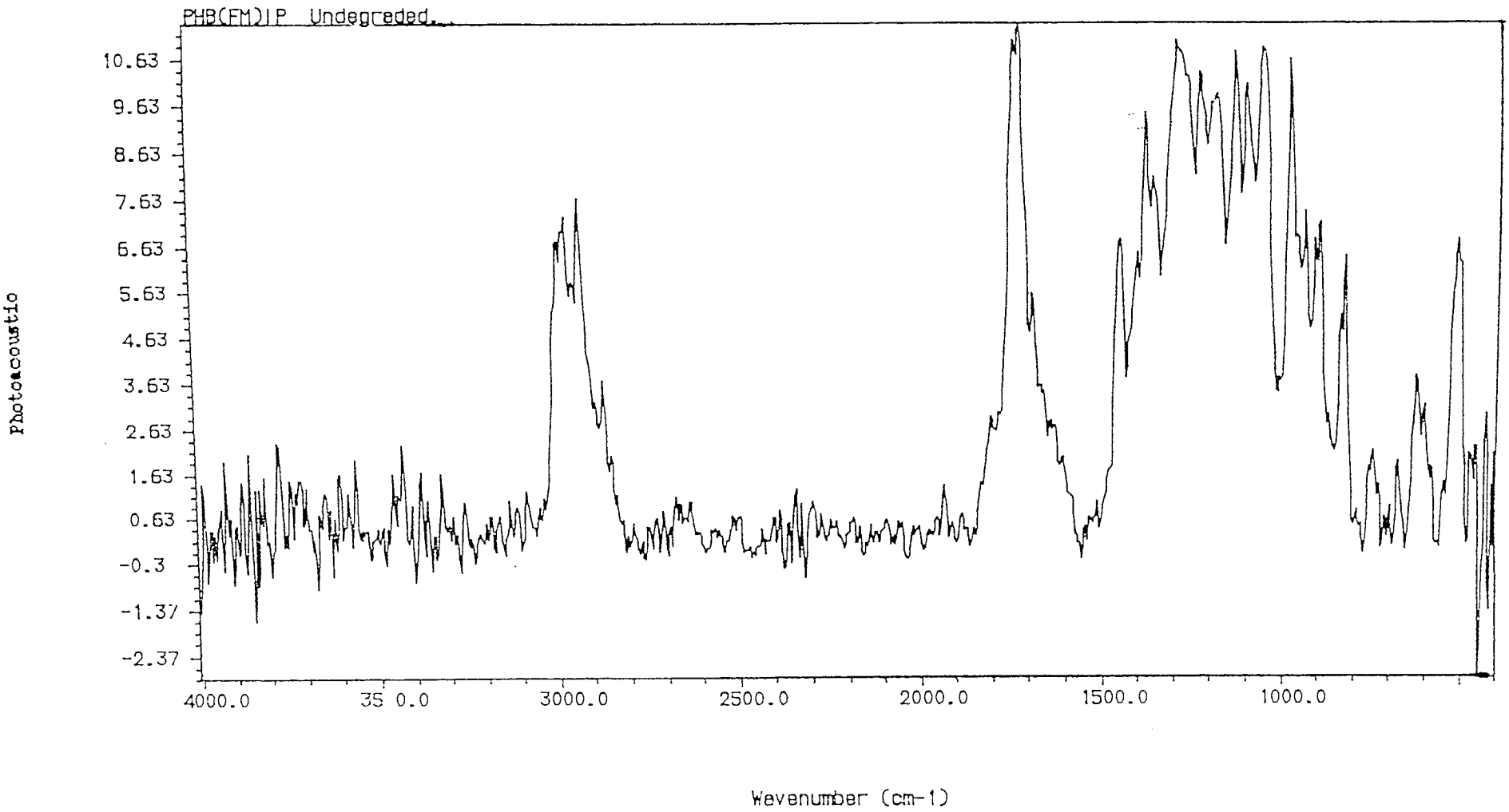

Figure 3.4.

Characterization Of Undegraded PHB(FM)IP; FTIR-Photoacoustic Spectrum.

(IP) PHB, (Fig. 3.4). As can be observed from figure 3.4, there was little difference between the two samples. This indicated that the purification process had apparently little effect on the chemical structure.

Similar to the PAS traces. the molecular weight data revealed little differences between the IP and TG samples, (Table 3.1). Although the repeat readings for the molecular weight were quite accurate, the reproducibility of the molecular weight numbers was not as consistent. Therefore, despite the apparently lower molecular weight and polydispersity of the TG sample compared to the IP, no conclusions could be drawn, except that similar to the other studies, little change in the samples due to the purity increase appeared to have occurred.

Sample:	Mwt.	Mwn.	Polydispersity.
PHB(FM)TG.	569,000	196,000	2.9
PHB(FM)IP.	587,000	179,000	3.3

Table 3.1.

Molecular Weight Data For Undegraded Homopolymer PHB(FM).

3.1.1.3. Conclusions.

Therefore, it was concluded that the technical grade fibres, due to the impurities introduced in the manufacturing process, were slightly more amorphous and somewhat less stable when compared to the fibres from the increased purity sample. Consequently the degradation rate of the PHB(FM)TG was anticipated to be comparatively faster.

3.1.2. The Effect Of Solvent On Structure.

SEM of the PHB(FM) samples produced from the following solvents were also examined:

a) 100% Methylene chloride.

b) 50/50% (w/w) Methylene chloride and chloroform.

It was observed that the fibres from the methylene chloride solvent produced pronounced, more noticeable pores in all the fibres examined when compared to those produced using chloroform as solvent, (Plates 3.11 & 3.12). However, those fibres manufactured from the 50/50% mixture were relatively smooth, (Plate 3.13).

Phase contrast microscopy of the fibres produced from 100% methylene chloride revealed noticeable differences from those of the chloroform solvent. Approximately 7% of the larger diameter fibres had a 'mosaic' appearance, (Plate 3.14), whilst the medium and smaller diameter fibres retained a similar appearance and structure to those of the chloroform solvent, (Plate 3.15). It was also noticed that there was a large reduction in the amount of pockets and hollow cavities. This lack of cavities coupled with the distinct pores present in the larger diameter fibres appears to indicate that the hollow regions were readily penetrated by the wetting medium.

Therefore, it was anticipated that the rate of degradation for the fibres produced using methylene chloride as a solvent would be faster than those manufactured from the chloroform. Thus, the degree and nature of the porosity of the fibres is a function of the

Plate 3.12. (x11.2K)
PHB(FM)Produced From Methylene Chloride Extraction, Illustrating The Heavily Porous Nature.

Plate 3.4. (x10.4K)
PHB(FM) Produced From Chloroform/Methylene Chloride Extraction, Illustrating A Smooth Fibre.

Plate 3.14. (x25)
PHB(FM) Produced From Methylene Chloride Extraction, Illustrating A 'Mosaic' Appearance In The Larger Diameter Fibres.

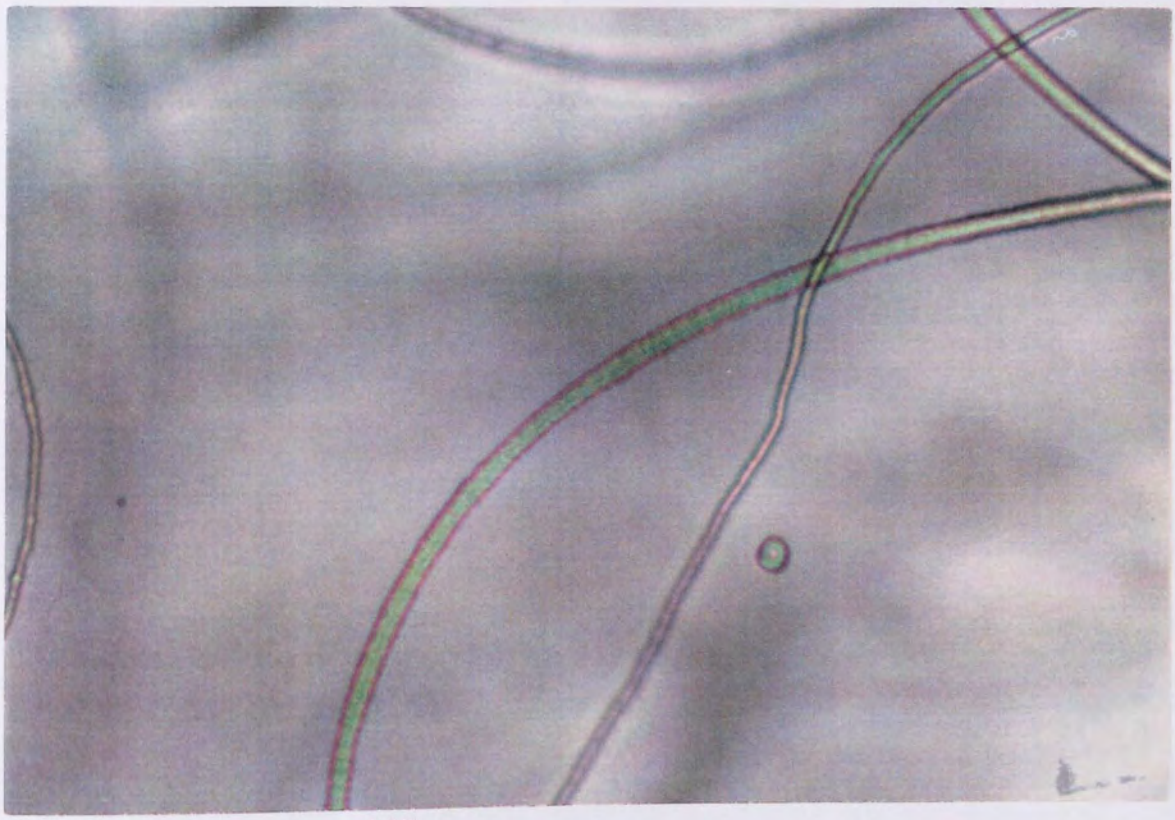

Plate 3.15. (x25)
PHB(FM) Produced From Methylene Chloride Solvent, Illustrating The Appearance Of The Medium And Small Diameter Fibres.

solvent and manufacturing process. Commercially the use of methylene chloride as a solvent is unfavourable, due to the comparatively greater expenditure and cost in heating, as a result of its higher vapour pressure. Consequently, manufacture of all subsequent fibres continued with the use of chloroform as the solvent.

3.1.3. The Effect Of Blending On Structure.

3.1.3.1 Observations And Comparisons.

A number of fibre samples were produced from PHB and various polysaccharides, as illustrated below;

1)	Glu-42.	PHB(FM) + 42% Glucose.
2)	L.Pec.9.	PHB(FM) + 9% Pectin.
3)	SA-7.	PHB(FM) + 7% Sodium Alginate.
4)	SA-30.	PHB(FM) + 30% Sodium Alginate.
5)	SCC-9.	PHB(FM) + 9% Sodium Carboxycellulose.
6)	Suc.-42.	PHB(FM) + 42% Sucrose.

These were examined utilizing the same techniques as for the undegraded PHB(FM)IP samples. The co-blended samples were then compared to the PHB(FM)IP.

The texture of the co-blended samples differed from that of the unblended matrix, with a greater roughness noticed. Granular regions were also felt in those samples possessing a high percentage polysaccharide loading. In some instances a slight 'stickiness' was noticed, where the fibres readily attached themselves to the handling instruments. This indicated a lack of strength and integrity in the whole matrix when compared to the PHB(FM)IP.

SEM of the co-blends revealed few structural differences when compared to the unblended samples. The most noticeable difference was an irregularity of the various pits and indentations within the fibres, (Plates 3.16 & 3.17). Two distinct types of fibres were observed from samples Glu-42. and SA-30., to varying extents. The more common fibres were similar to those observed in the unblended PHB(FM)IP sample, whilst a relatively large amount of finer, smooth fibres (Plate 3.18) were intermingled within the sample. Sample SCC-9. possessed a number of intra-fibrular bulbous regions, being somewhat smaller than the terminal bulbs of the homopolymer fibres, (Plate 3.19).

All samples when viewed using phase contrast microscopy, revealed differences to the unblended fibres. The fibres from PHB(FM)IP appeared comparatively smooth with a number of hollow indentations observed at the sights of the pockets, (Sec. 3.1.1.). However, the bubbles and pockets generally appeared much smaller in the co-blended samples SA-7. and SCC-9. where the percentage loading of the polysaccharides were small. (Plates 3.20 - 3.24) The fibres in these cases were relatively smooth, similar to those of the unblended matrix. In those samples possessing a higher percentage loading; Glu-42., Suc-42. and SA-30. the bubbles were observed to be more reduced and less noticeable, even in those large irregularities where they were previously observed in the PHB(FM)IP, (Plate 3.25). These fibres also appeared to be irregular and 'patched' in a mosaic style, (Plates 3.25 & 3.27).

These irregularities of the fibres from the co-blended samples, were anticipated to enhance the degradation rate by increasing the surface area to volume ratio of the sample in contact with the degrading medium. The comparative reduction of the pockets may be due to a

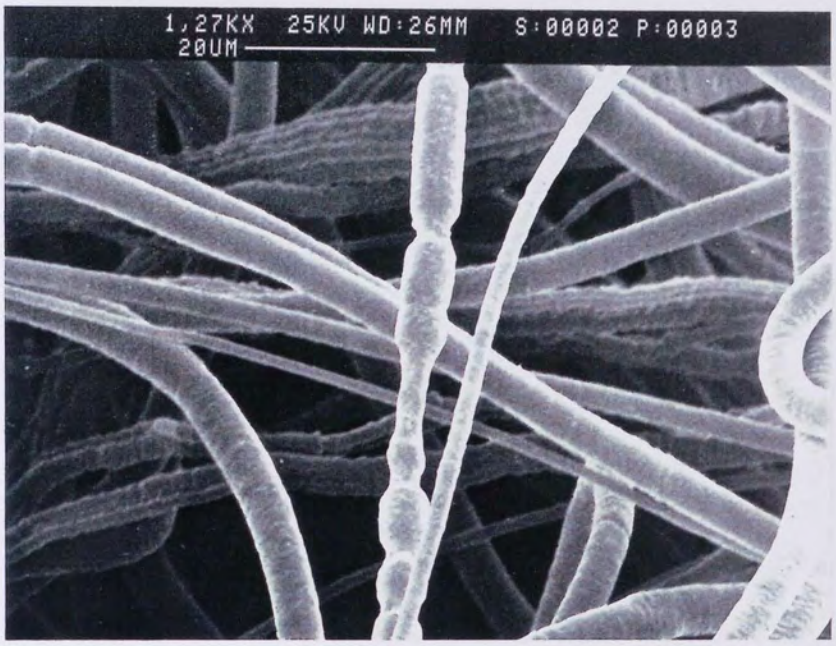

Plate 3.16. (x2.88K)
L.Pec.9.; PHB(FM)IP Blended With 9% Low Molecular Weight Pectin, Illustrating The Irregular Pits.

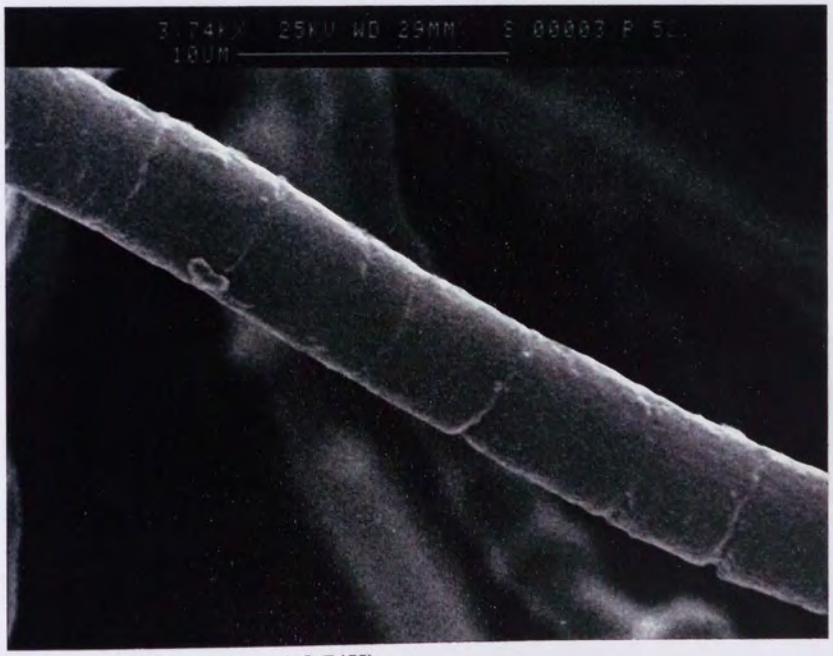

Plate 3.17. (x3.74K)
SA-30.; PHB(FM)IP Blended With 30% Sodium Alginate Illustrating A Comparatively Smooth Fibre With Indentations.

Plate 3.18. (x196)
SA-30.; Varying Fibre Diameters With The Presence Of Small 'Fine' Fibres.

Plate 3.19. (x220)
SCC-9.; PHB(FM)IP Blended With 9% Sodium Carboxycellulose, Illustrating The Intrafibrular Bulboous Regions.

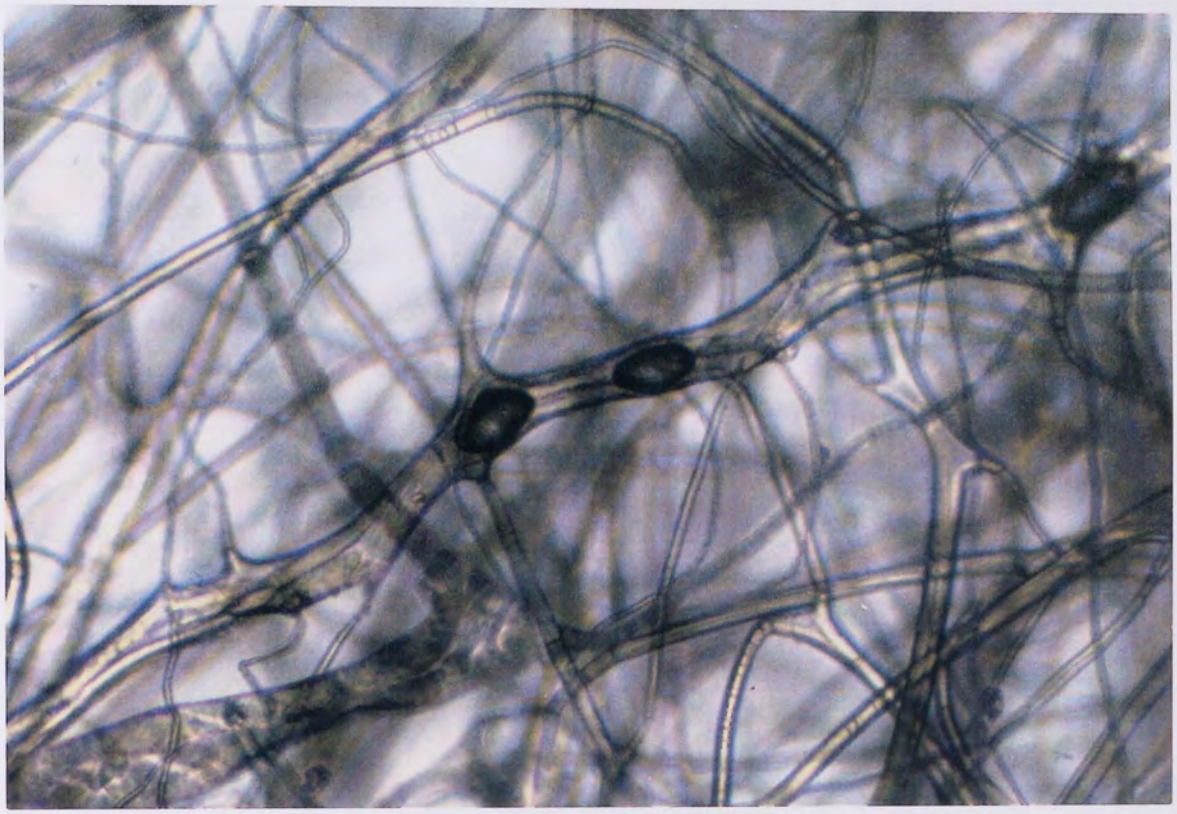

Plate 3.20. (x15)
SA-7.; PHB(FM)IP Blended With 7% Sodium Alginate, Illustrating The 'Bubbles' In The Hollow Regions Or 'Pockets'.

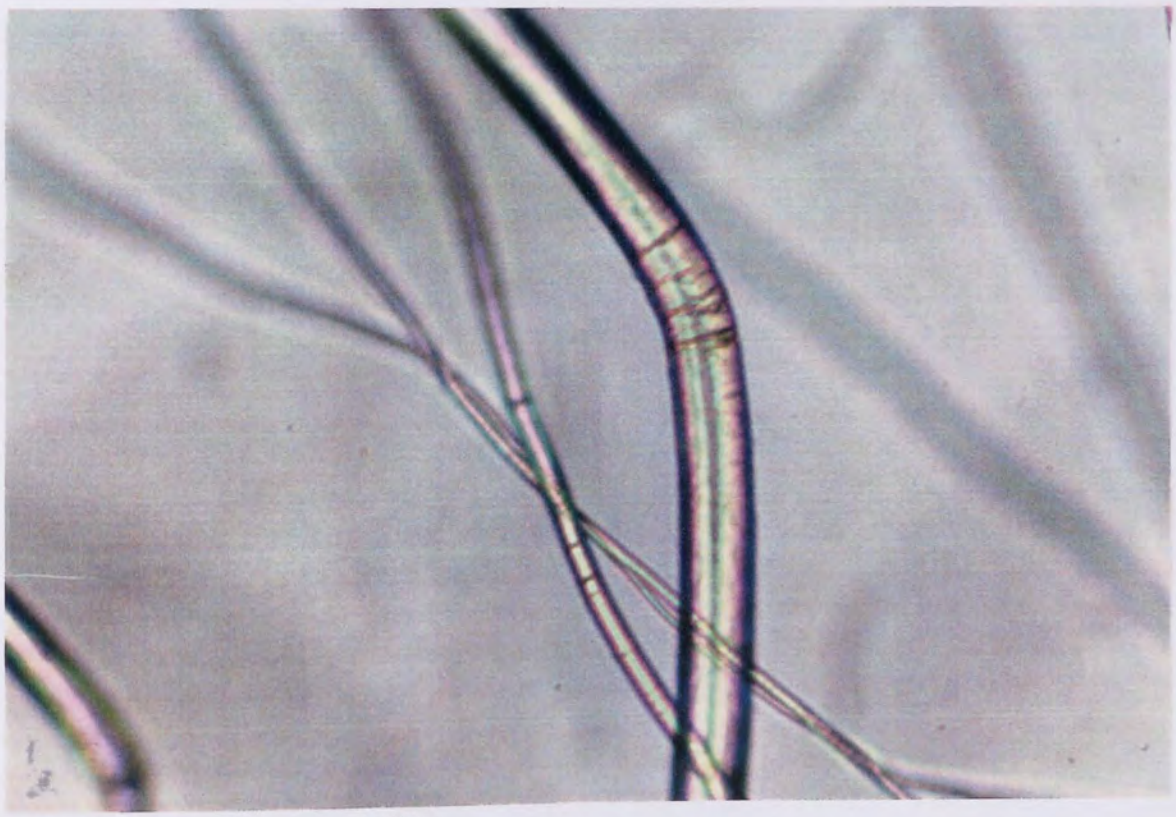

Plate 3.21. (x25)
SA-30.; The Absence Of Hollow Regions And Pockets In The Medium And Small Diameter Fibres.

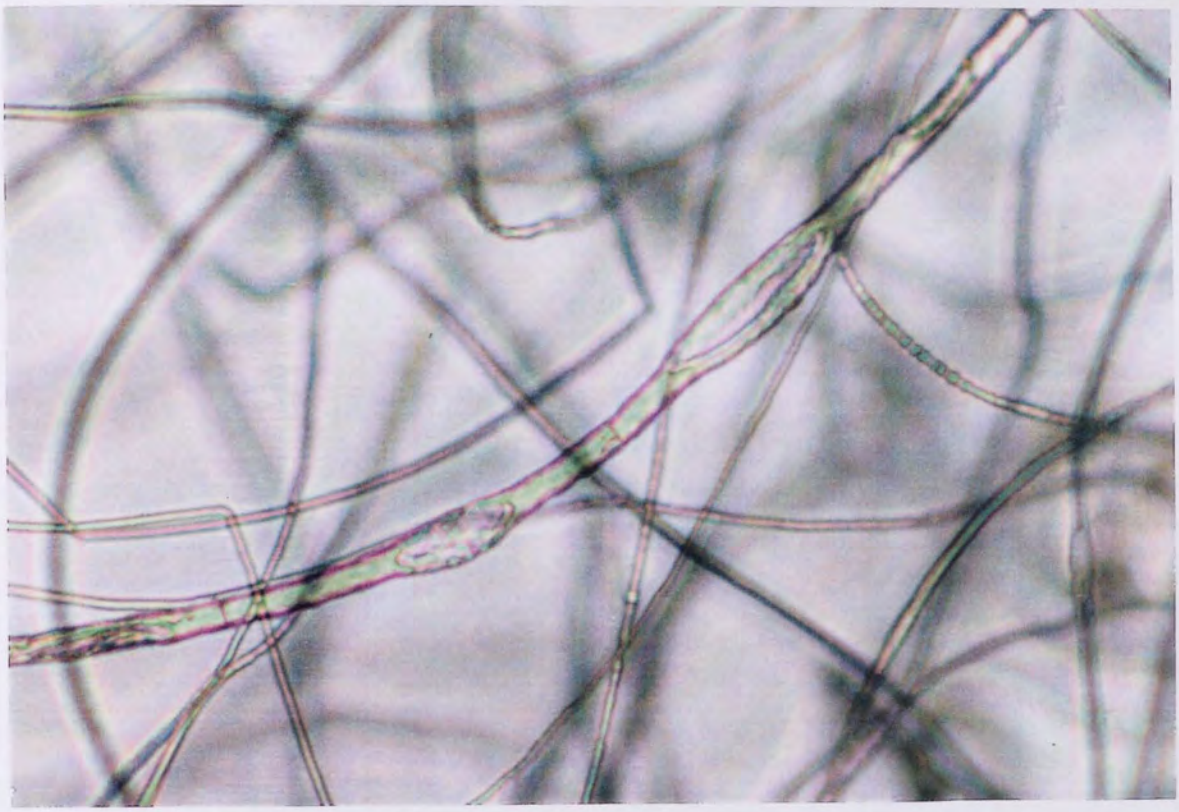

Plate 3.22. (x25)
SCC-9.; The Reduced Number Of Air Pockets And Bubbles Compared To The Unblended PHB(FM)IP.

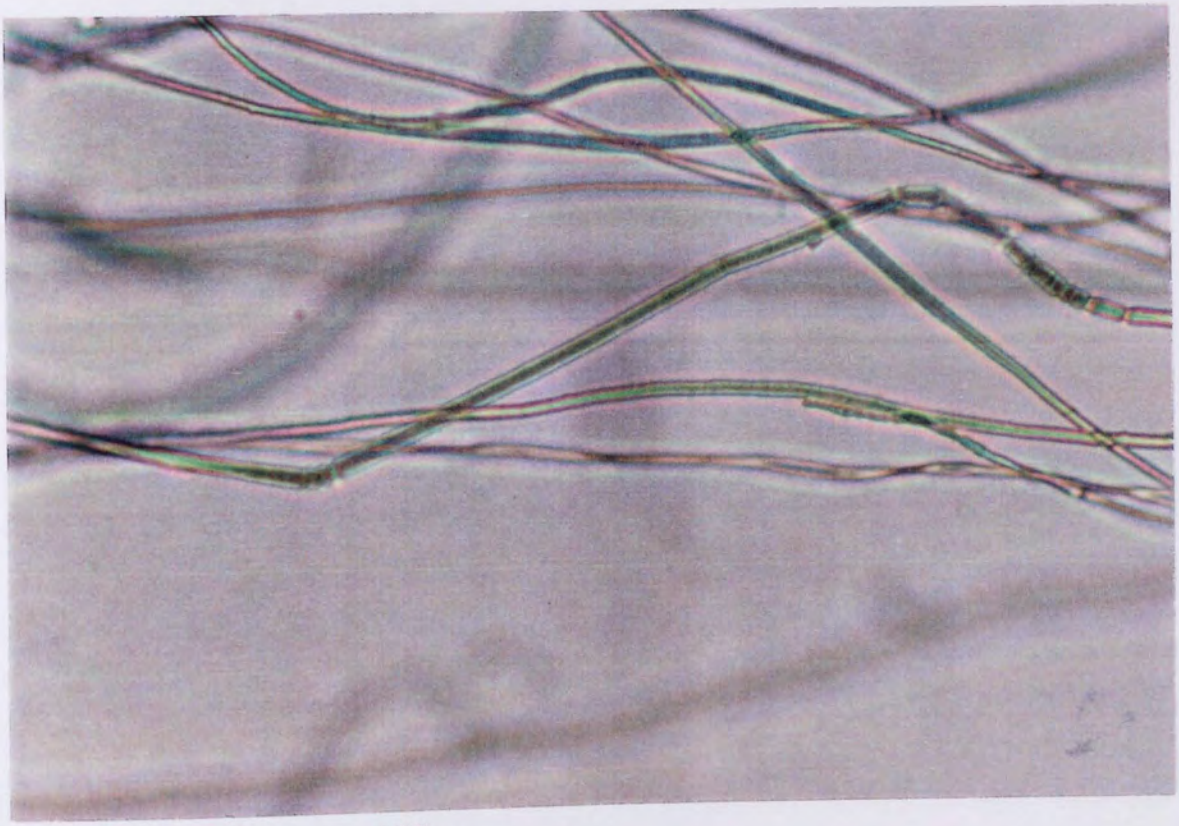

Plate 3.23. (x25)
SCC-9.; The Absence Of Bubbles And Hollow Cavities And The Comparatively Smooth Fibre Surfaces.

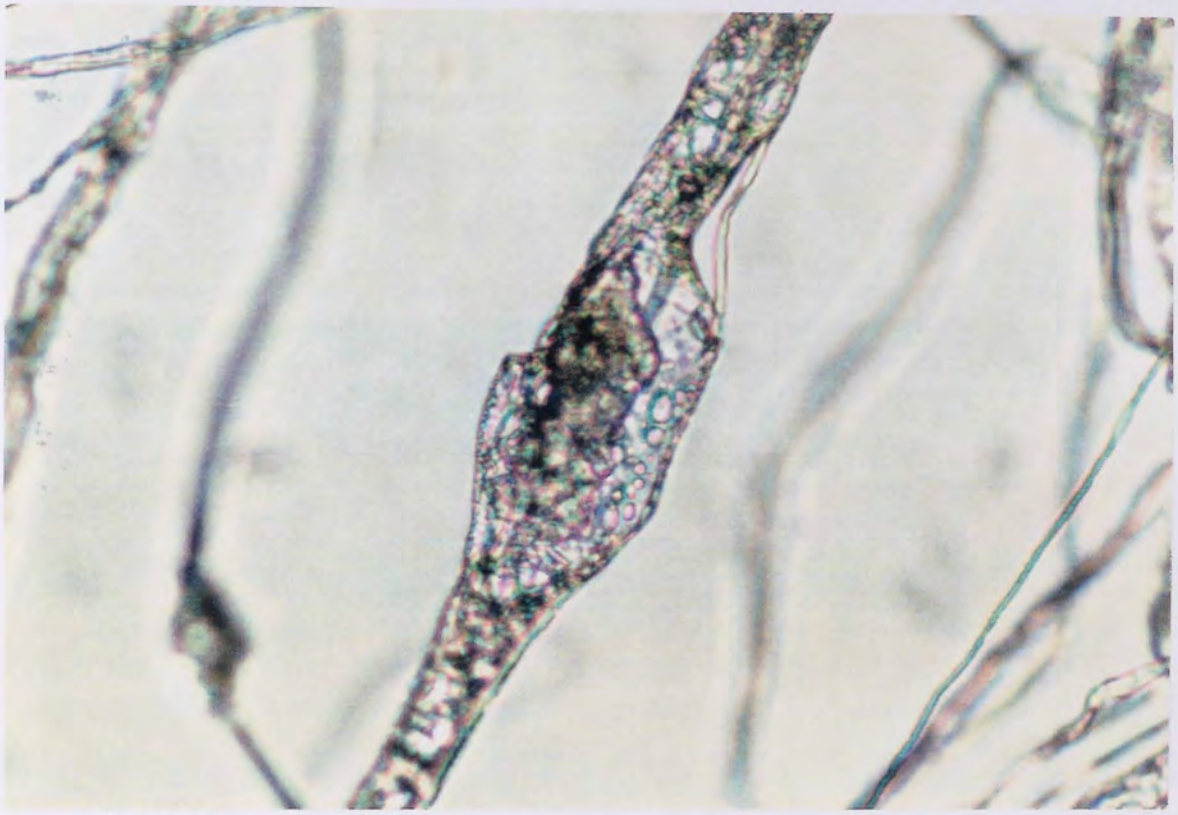

Plate 324. (x25)
SA-30.; The Hollow Cavities And Possible Sodium Alginate 'Filling' In A Large Irregular Region.

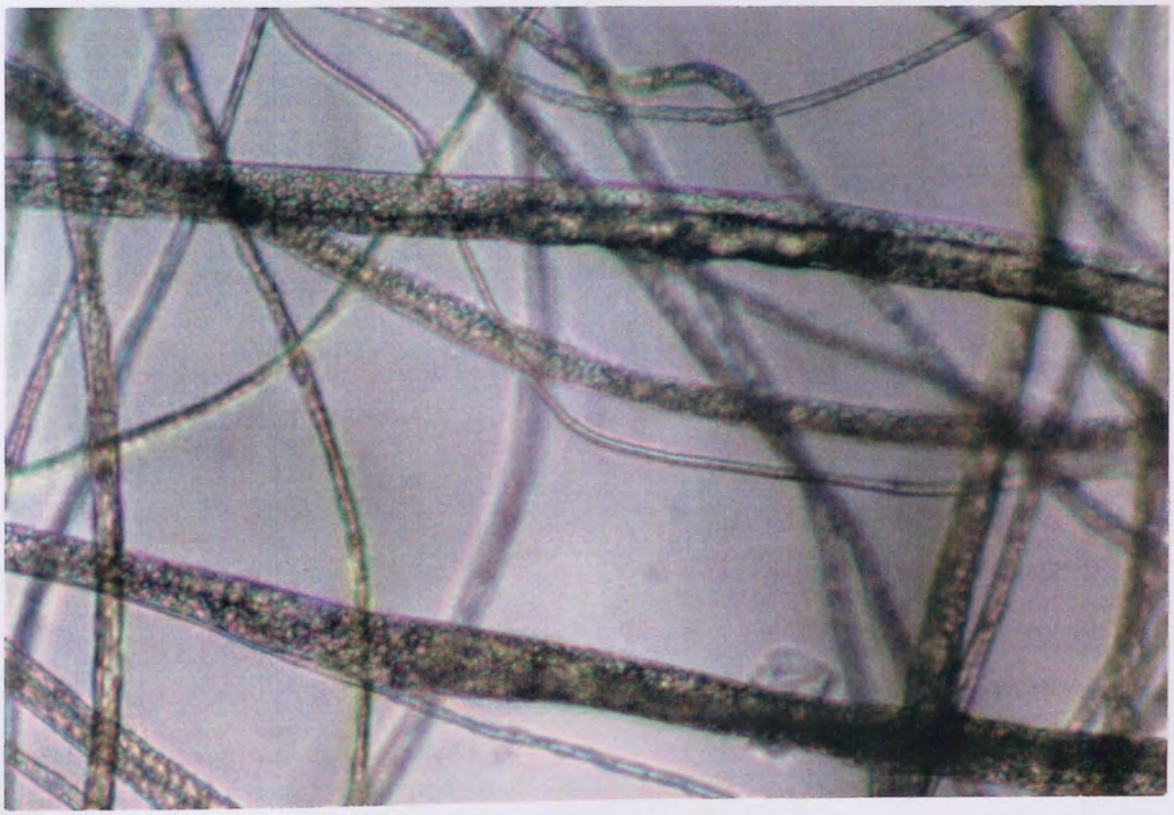

Plate 3.25. (x25)
Suc-42.; PHB(FM)IP Blended With 42% Sucrose, Illustrating The 'Mosaic' Appearance Of The Fibres.

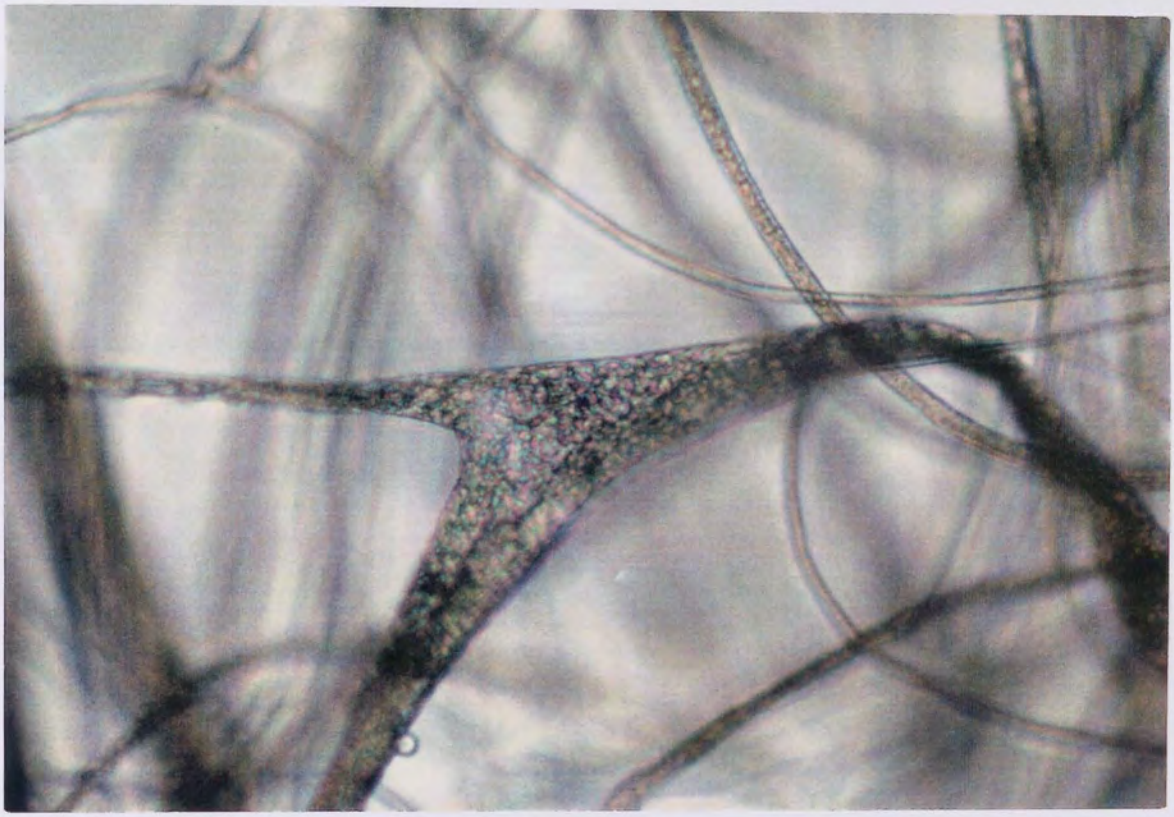

Plate 3.26. (x25)
Suc-42.; The 'Mosaic' Appearance Of A Large Irregular Region.

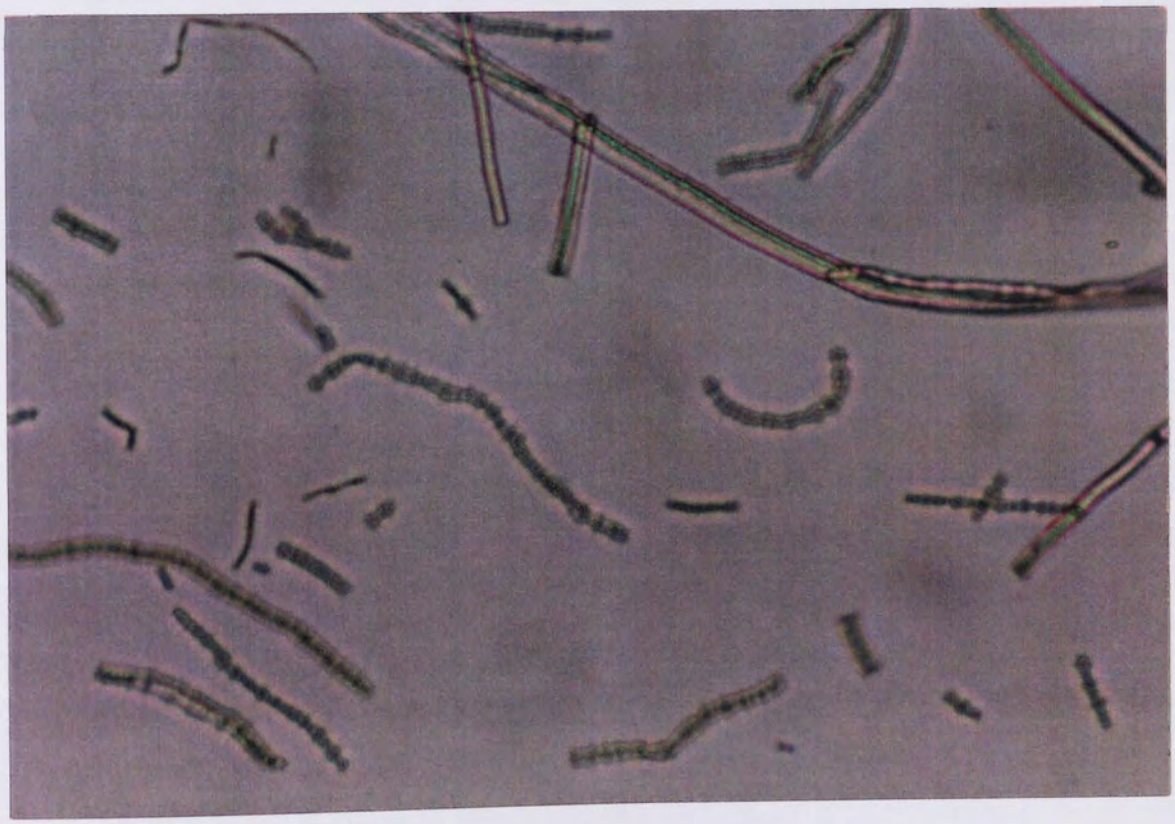

Plate 3.27. (x25)
PHB/5V.; PHB(FM)IP Copolymerized With 5% PHV, Illustrating The Irregular 'Banded' Appearance Of Some Of The Smaller Diameter Fibres.

number of factors; it is possible that the mosaic effect ensured that the hollow regions of the fibres were readily penetrated by the wetting medium and thus, under degradation conditions, would enhance the degradation rate by increasing the available surface area to volume ratio even further, whilst simultaneously providing structural weaknesses to facilitate a faster loss of fibre integrity. It may also be that the polysaccharides acted as 'fillers' and reduced the amount of hollow regions compared to the PHB(FM)IP fibres. The most likely explanation is that a combination of both internal wetting and hollow region filling occurred to varying degrees, due to the presence of the polysaccharides, with the extents being determined by the nature and loading of the polysaccharide.

Fibre diameter distributions of the samples were determined (Graphs 3.2 -3.5.). In each case a number of fibres with relatively large diameters were noted, similar to those of the unblended fibres. The pectin co-blend, L.Pec.9., had a main distribution of fibres with diameters between 1 and 10 microns, (Graph 3.2), whilst for the glucose sample the distribution was between 2 and 10 microns, with a small percentage of fibres around the 15 micron range, (Graph 3.3). The fibres from the sodium carboxycellulose sample, SCC-9., (Graph 3.4), had a narrow distribution between 0 and 7 microns, larger fibres were observed ranging from 9 to 16 microns diameter, but with approximately 6% frequency. However, blending the fibres with 7% sodium alginate, SA-7., (Graph 3.5), produced frequencies at all the fibre diameters between 1 and 16 microns, with the average at 5 to 6 microns. Increasing the percentage of the sodium alginate load to 30% had a marked effect on the the fibres; 10% of those sampled had a diameter between 13 and 16 microns, whilst a majority of approximately 86% possessed diameters between 0 to 6 microns, of these nearly half were between 1 and 2 microns. Thus, in this case,

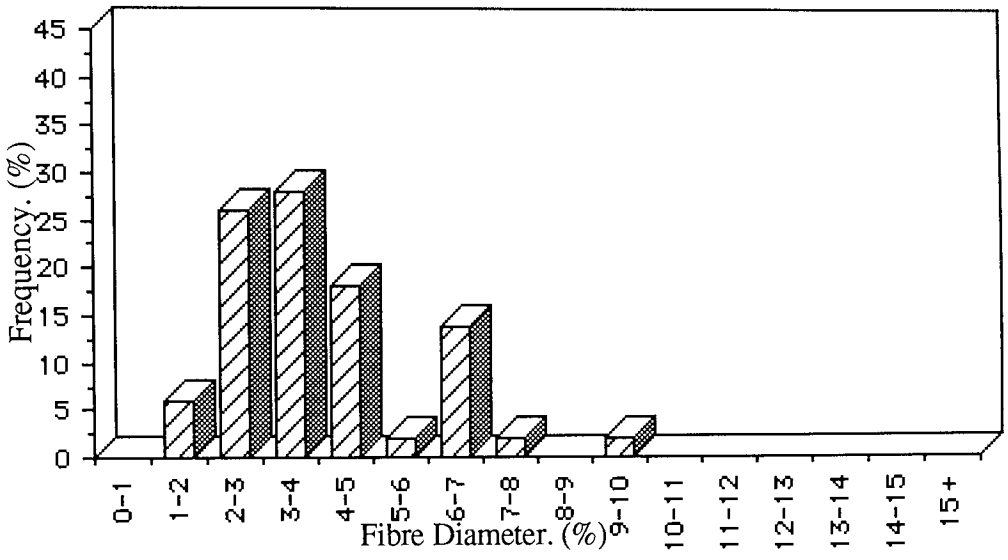

Graph 3.2.

Fibre Diameter Distribution For Fibres From Undegraded Pec-9.

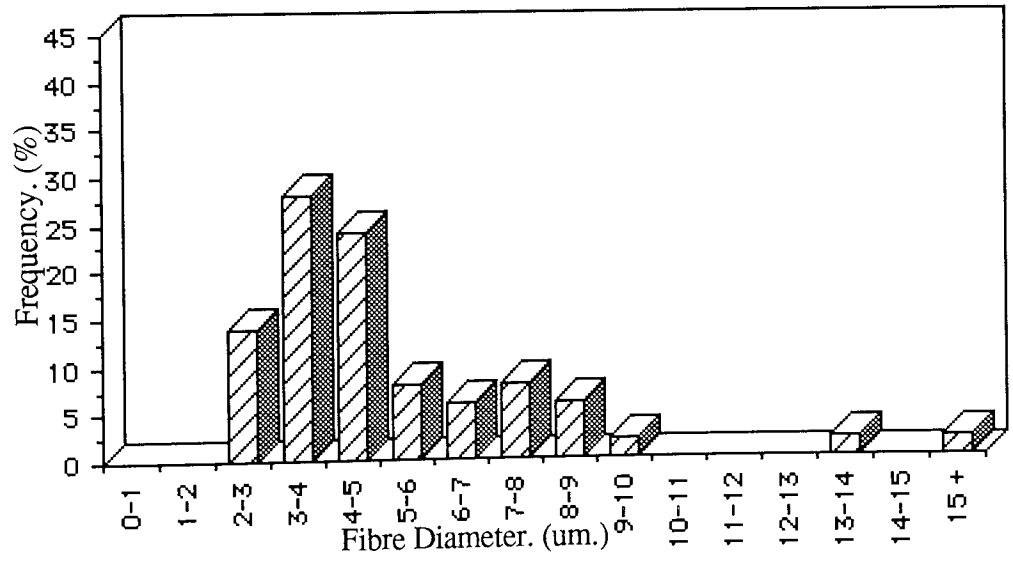

Graph 3.3.

Fibre Diameter Distribution For Fibres From Undegraded Glu-42.

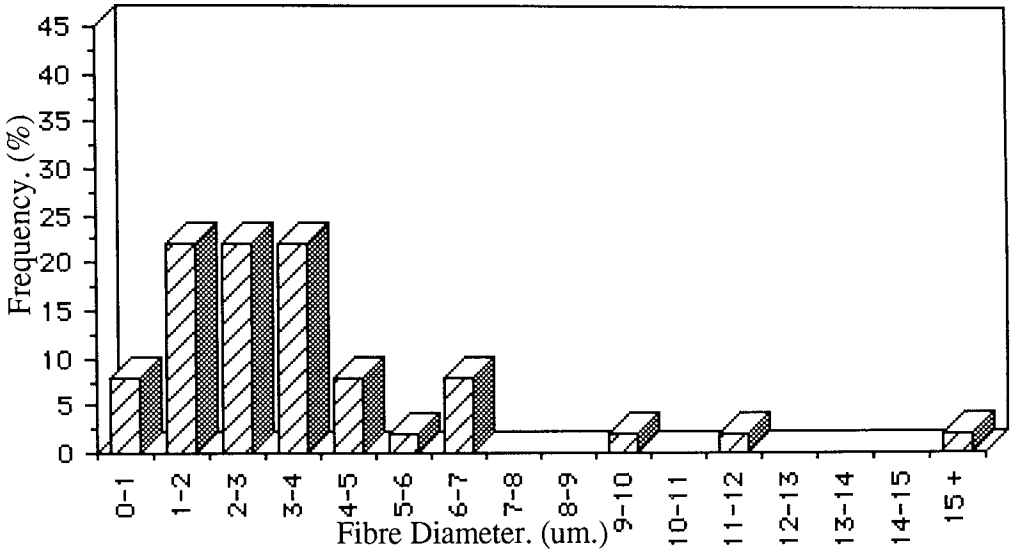

Graph 3.4.

Fibre Diameter Distribution For Fibres From Undegraded SCC-9.

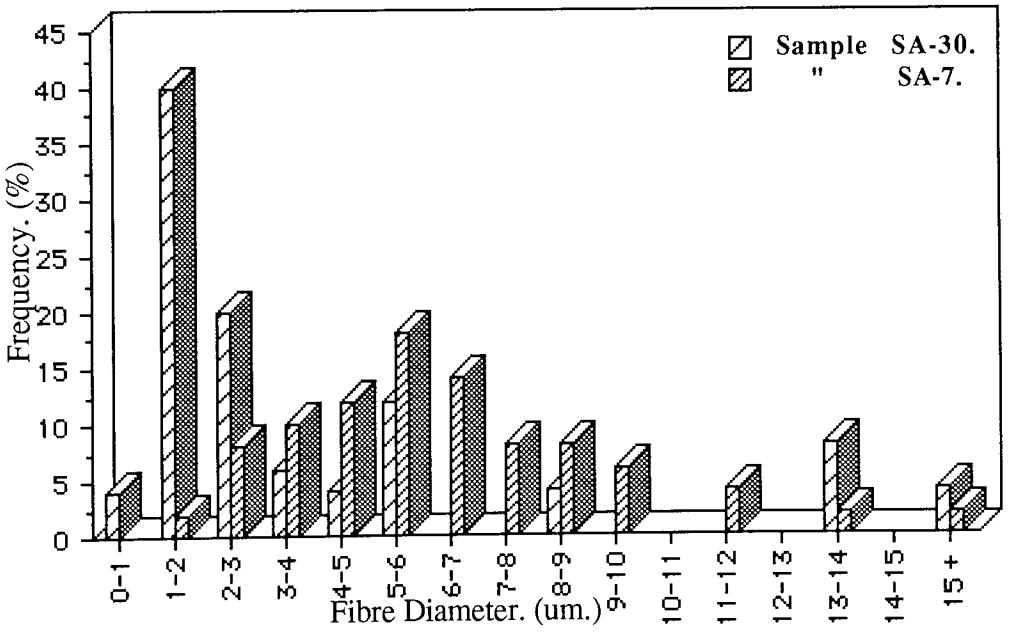

Graph 3.5.

Fibre Diameter Distributions For Fibres From Undegraded Samples SA-7. And SA-30.

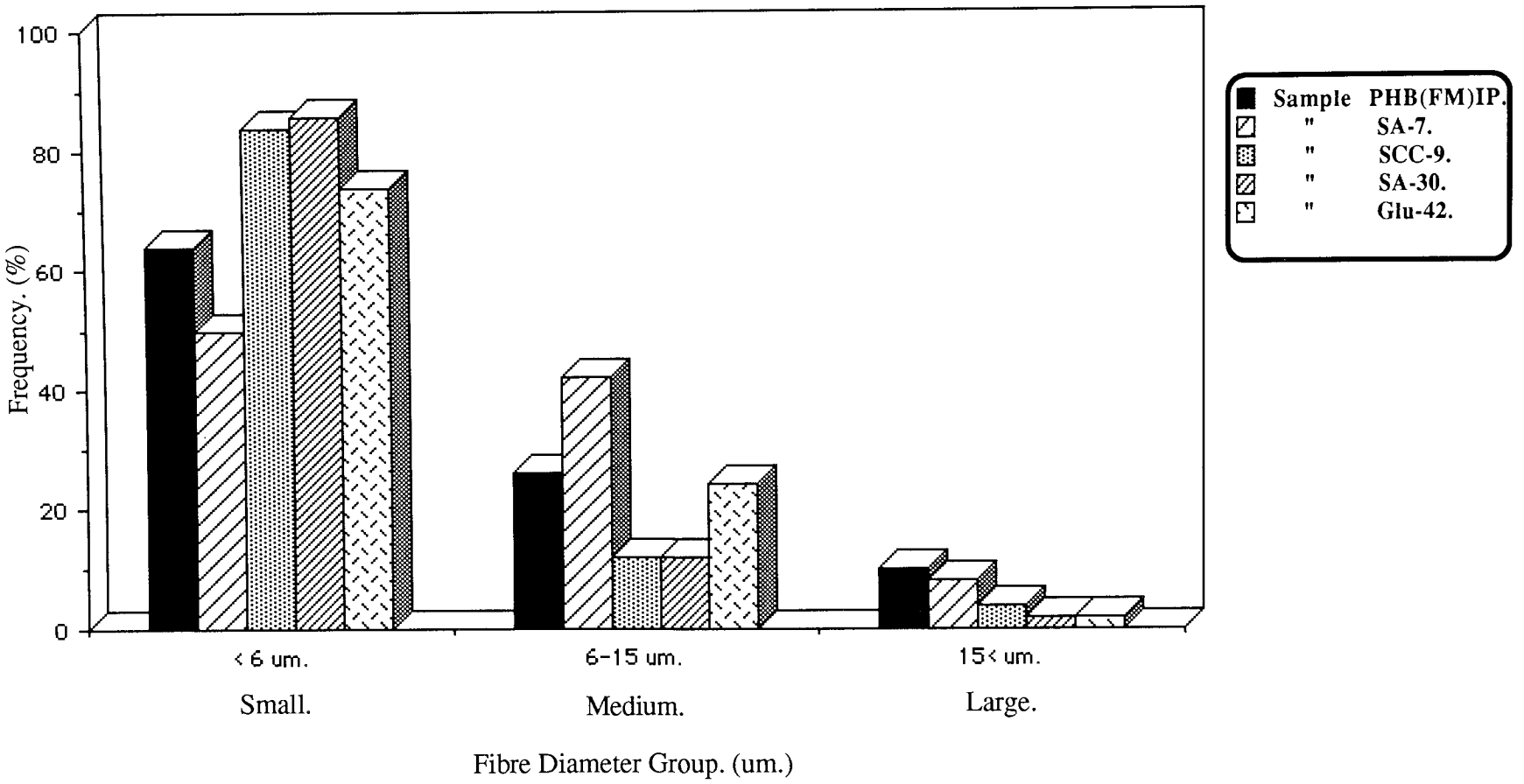

Graph 3.6.

General Fibre Diameter Distributions For The Undegraded Co-blends Compared To PHB(FM)IP.

increasing the loading of the polysaccharide had the effect of reducing the sample fibre diameters and increasing the frequency. This was noticed as the presence of two kinds of fibres, observed with those fibres possessing a higher polysaccharide loading.

Graph 3.6 summarizes the average distribution of the co-blended samples by grouping them into small, medium and large sizes for diameters <6, 6-15 and >15 microns respectively and compares them to that of the PHB(FM)IP. The changes in fibre diameter did not appear directly related to the percentage loading of the polysaccharide, since blending the PHB with 42% glucose, did not reduce the average diameter as much as 30% sodium alginate or the 9% sodium carboxycellulose. However, the changes in diameter for the 7% and 30% sodium alginate samples varied quite noticeably. This confirmed previous conclusions that the effects of blending the PHB were dependent upon both the polysaccharide nature and its percentage loading.

The effects of increasing the percentage loading of the pectin on the fibre structure was also examined, for the samples below;

1) L.Pec.9. PHB(FM)IP + 9% Low molecular weight pectin.
2) L.Pec.15. PHB(FM)IP + 15% " " " "
3) L.Pec.25.S. PHB(FM)IP + 25% " " " " (Start of run)
4) L.Pec.25.E. PHB(FM)IP + 25% " " " " (End of run)
5) H.Pec.10. PHB(FM)IP + 10% High molecular weight pectin.

Phase contrast and scanning electron microscopy of the samples revealed no differences when compared to the previous observations of the other co-blended samples. A more

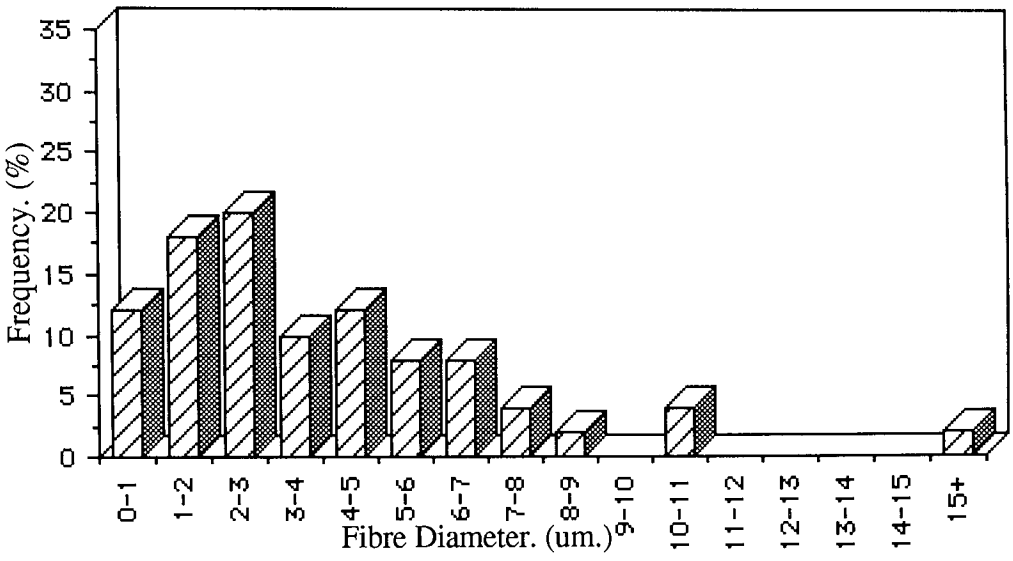

Graph 3.7.

Fibre Diameter Distribution For Fibres From Undegraded L.Pec.9.

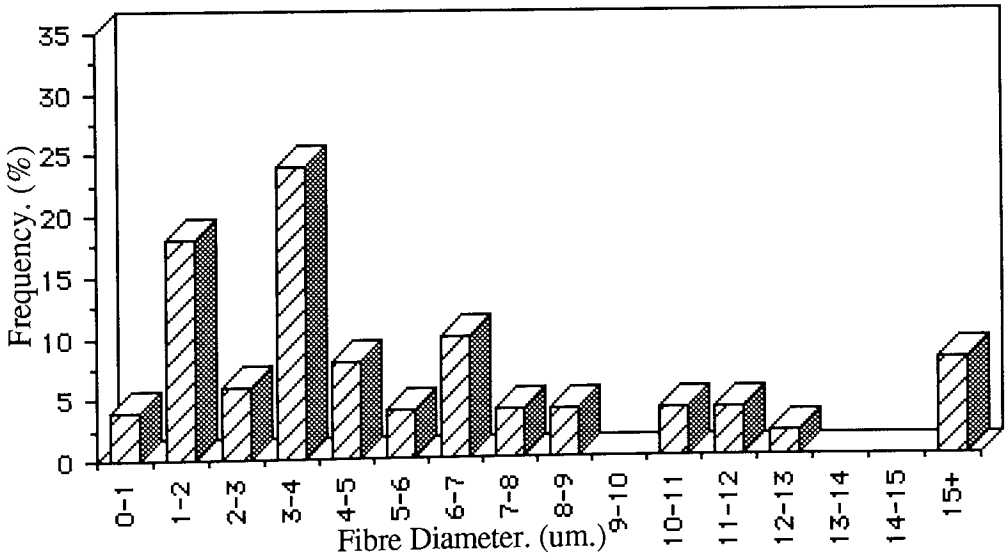

Graph 3.8.

Fibre Diameter Distribution For Fibres From Undegraded L.Pec.15.

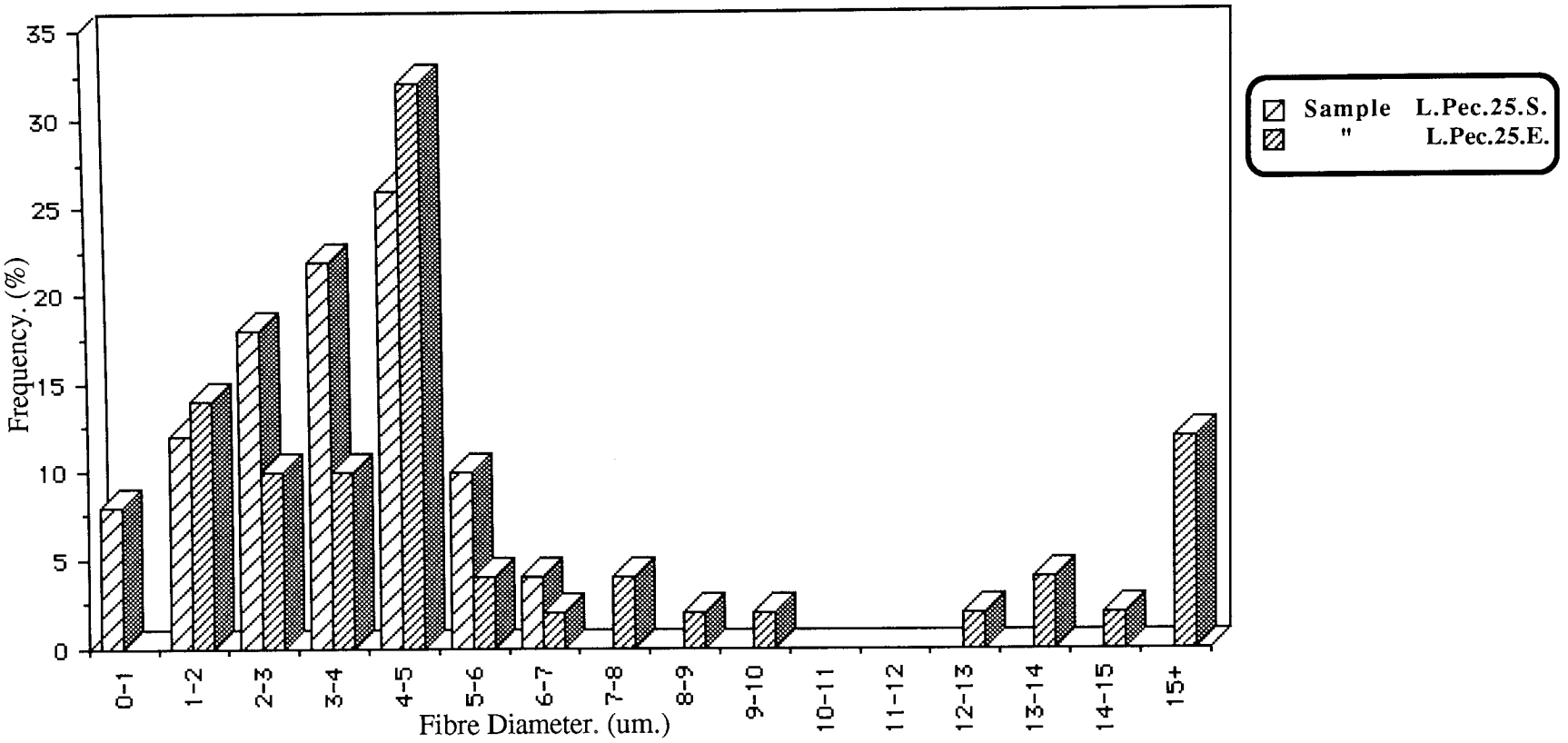

Graph 3.9.

Fibre Diameter Distributions For Fibres From Undegraded Samples L.Pec.25.S. And L.Pec.25.E.

noticeable change was that of the fibre diameters, (Graphs 3.7-3.10). Increasing the pectin loading from 9 to 25% had a noticeable increase in the percentage of fibres with diameters above 15 microns, from approximately 2 to 12%. Sample L.Pec.9. had a fibre diameter distribution of 93% between 0 and 9 microns, (Graph 3.7), whilst for samples L.Pec.15 and L.Pec.25.E. this was reduced to 78%. (Graphs 3.8 & 3.9) However, in the latter sample the fibres had a narrower distribution with a peak of 32% at 4-5 microns and shifted slightly to the higher diameter ranges compared to the former which presented a less general distribution with two main peaks of 18 and 24% at the 1-2 and 3-4 micron range. The large diameter distribution also differed for the two samples, with the L.Pec.15. fibres having a 10% frequency between 10 and 13 microns diameter and the L.Pec.25.E. sample having 8% at the 13 to 15 micron range. Thus, the entire distribution of the L.Pec.25.E. sample appeared to shift to the higher diameter range and increase its main peak. This sample was taken at the end of the manufacturing run, fibre samples from the start of the run (L.25.Pec.S.) also showed a noticeable difference, with all the fibres possessing diameters between 0 and 7 microns and a gradual rise from 7% to 26% between the 0 and 5 micron range. Graph 3.10 illustrates the differences in fibre diameter distribution between samples L.Pec.25.S. and L.Pec.25.E. in the medium and lower diameter ranges. This indicated that the blending efficiency with the pectin was not homogenous and this was anticipated to probably cause difficulties in the degradation studies.

Main distribution peaks occurred at diameters 2-3, 3-4 and 4-5 microns for the samples with 9, 15 and 25% loadings respectively, with gradually increasing frequencies. Therefore, increasing the percentage loading of the pectin co-blend had the apparent effect

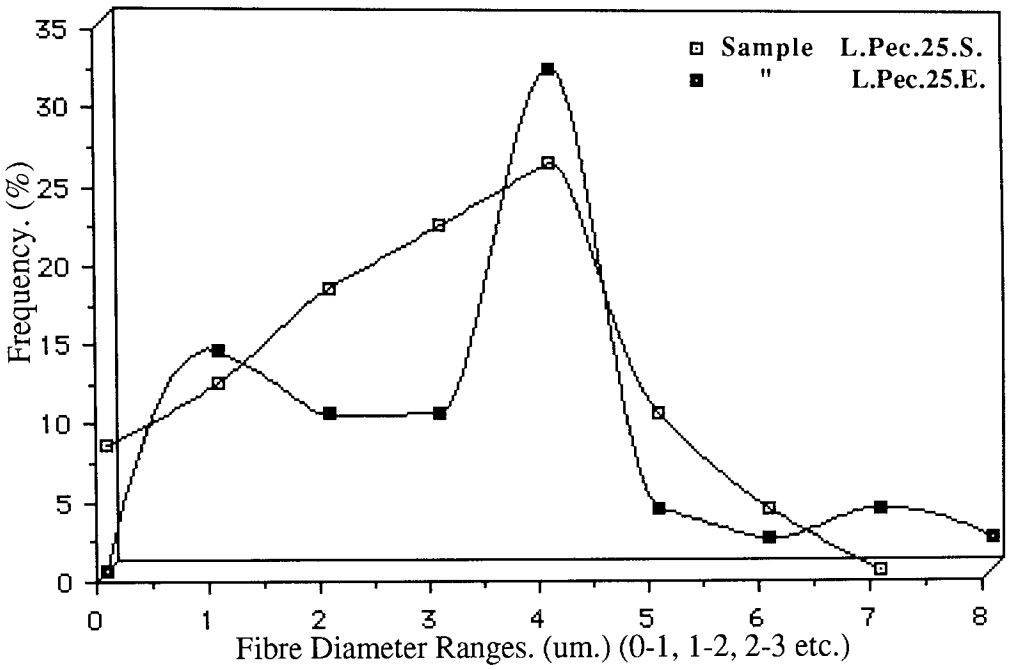

Graph 3.10.

Comparison Of The Small Fibre Diameter Distributions For Undegraded Samples L.Pec.25.S. And L.Pec.25.E.

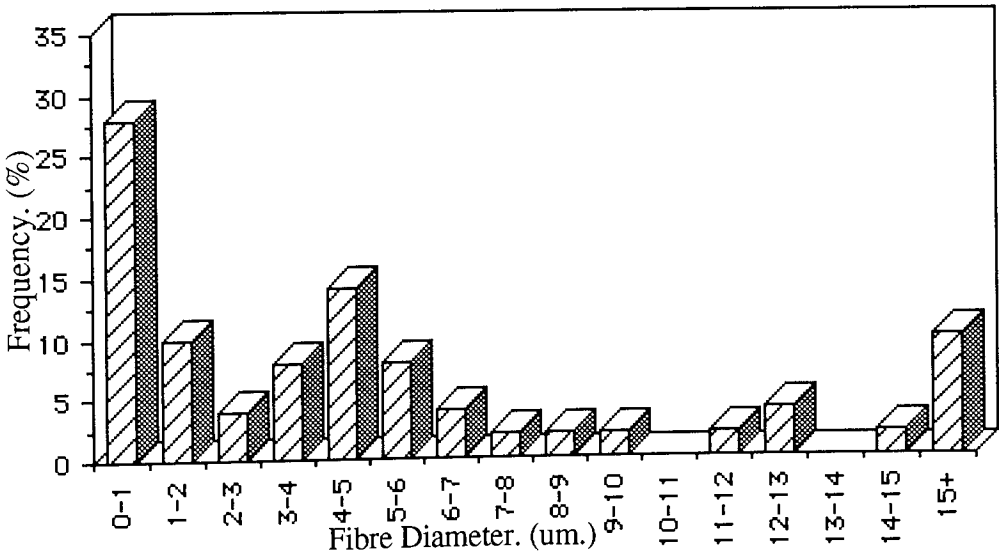

Graph 3.11.

Fibre Diameter Distribution For Fibres From Undegraded H.Pec.10.

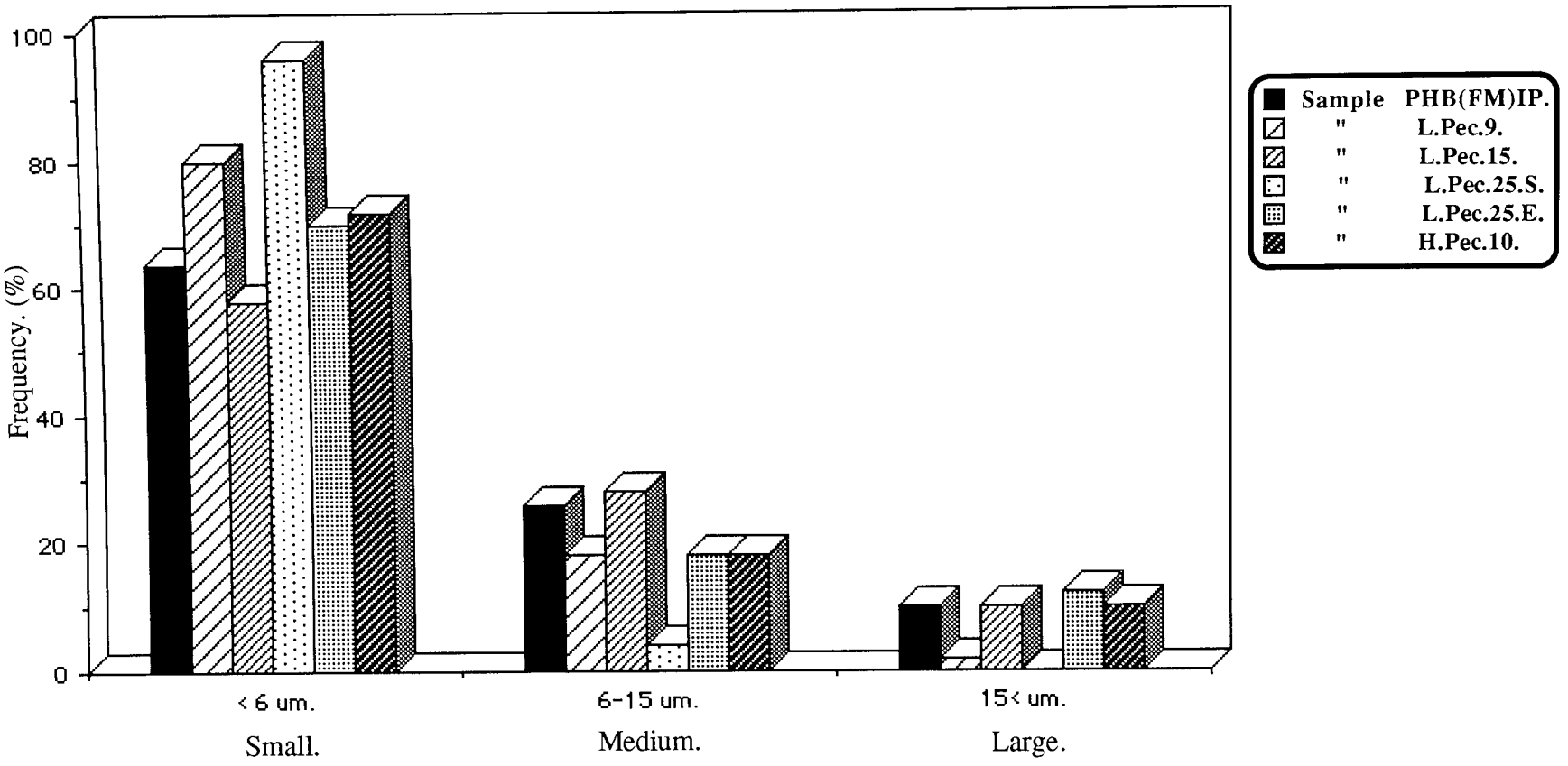

Graph 3.12.

General Fibre Diameter Distributions For The Pectin Co-blends Compared To PHB(FM)IP.

of shifting the diameter distribution to the higher diameter ranges and increasing the frequency.

Blending the PHB(FM) with 10% high molecular weight pectin (H.Pec.10.) had a comparatively greater effect on the fibre diameters than increasing the low molecular weight loading, (Graph 3.11). Comparing this sample to that of L.Pec.9. revealed a sharp difference despite similar loadings. Sample H.Pec.10. had a noticeable shift of its main distribution to the smaller diameter range when compared to those of sample L.Pec.9. Two main peaks occurred, a narrow distribution at the 0 to 3 micron range, with 26% between 0 and 1 microns diameter, and a wider peak from the 3 to 8 micron range, with 14% at 4 to 5 microns. However, an increase to 16% in the large-medium diameter range of 11 to 15+ microns was also noticed.

Graph 3.12 illustrates the general fibre distribution trends for the pectin samples according to the small, medium and large diameter groupings. It can be observed that the frequency distribution at the smaller diameters favoured the lower percentage loadings. ie; L.Pec.9 > L.Pec.15. > L.Pec.25.

Thus, it was concluded that the fibre diameter variation was dependent upon the particular blending agent, its molecular weight and its percentage loading. Although fibre diameter is anticipated to play an important part in determining the degradation rate of a sample, by their surface area to volume ratio, it cannot be concluded that the larger diameter fibres may degrade slower than the smaller ones, whilst this is more than likely for the unblended fibres, with the co-blended samples the crystallinity is an important affecting

factor. It is possible that some of these co-blended, larger diameter fibres contained higher proportions of the polysaccharides, possibly acting as fillers and are highly amorphous, or have a higher percentage of hollow cavities readily penetrated by the degrading medium, as was probably indicated from the phase contrast studies, (Plates 3.24 & 3.27), thus degrading more rapidly.

3.1.3.2 Physical Properties Of The Co-blended Samples.

The undegraded co-blended samples were also examined using X-ray crystallography, photoacoustic spectroscopy, (PAS) molecular weight and differential scanning calorimetry techniques. The DSC results were taken from a mean of five individual runs and the correlation between these was generally very good. The results obtained are listed in table 3.2.

From table 3.2 it can be observed that the melting points (mp.) of the co-blended samples varied from 171 to 176°C. Sample SA-30. had the same value as that of the PHB(FM)IP, with a melting point of 174°C. The other samples had slightly lower values with the exception of samples L.Pec.15. and L.Pec.25., which had slightly higher melting points. However, in all cases the percentage variation from the melting point of the undegraded PHB(FM)IP sample was within a range of only ±1.5%, this variation was within a 3% error range and consequently no conclusions could be drawn.

The glass transition temperatures (Tg.) were difficult to measure graphically and subsequently the first order derivatives had to be utilized. All the co-blended samples investigated exhibited Tg.s apparently slightly lower than that of the unblended increased

	Sample	Tg. (°C.)	mp.	ΔHm. (J/g.)	Polysaccharide. (%)	Crystallinity. (%)
	PHB(FM)TG.	5	174	79	0	73 +/-3
▣	PHB(FM)IP.	3	170	74	0	70 +/-3
	Suc-42.	n/d	171	43	42	45 +/-3
	SA-30.	0	174	60	30	58 +/-3
■	Pec-9.	2	172	76	9	57 +/-5
	SCC-9.	1	173	82	9	53 +/-3
	SA-7.	1	171	70	7	59 +/-4
	L.Pec.9.	2	172	76	9	57 +/-5
	L.Pec.15.	1	175	74	15	57 +/-5
◆	L.Pec.25.S.	3	175	61	25	55 +/-3
	L.Pec.25.E.	3	176	49	25	46 +/-3
	H.Pec.10.	1	172	67	10	53 +/-3

Table 3.2.

Characterization Of The Undegraded Samples: Differential Scanning Calorimetry (DSC) And X-Ray Crystallography Results.

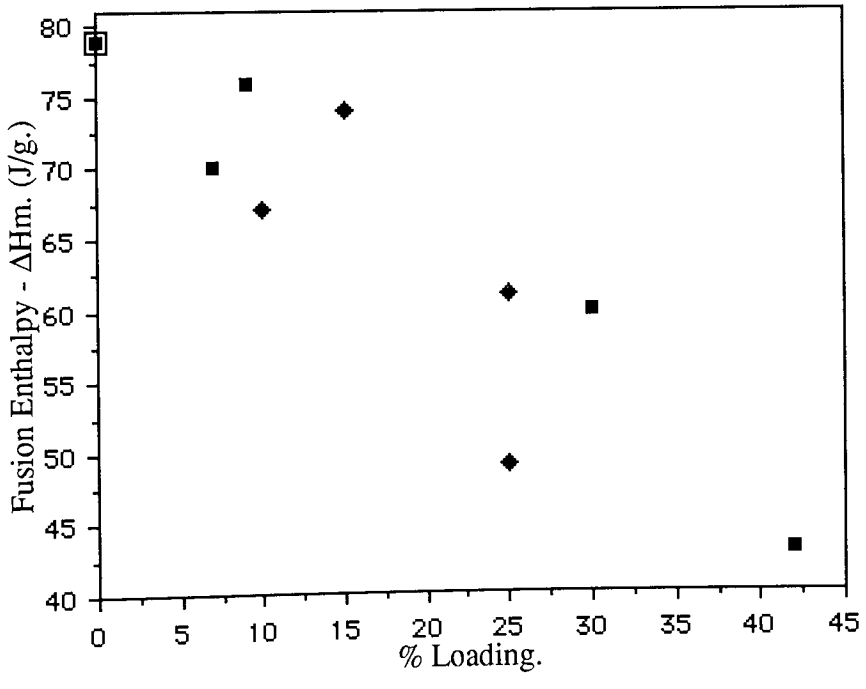

Graph 3.13.

Relationship Between Polysaccharide Loading And Fusion Enthalpy For The Undegraded Co-blends.

purity polymer matrix. However, due to the nature of the Tg. and its determination, these results were all within a reasonable error range. Thus it was concluded that the blending had little effect on the polymer structure. It was noticed, however, that the presence of the polysaccharides qualitatively reduced the integrity of the fibrous matrix and in the case of the pectin co-blends; increasing the percentage loading appeared to reduce the strength of the matrix and introduce the presence of increasing amounts of matted and granular regions.

The difficulty in determining the Tg.s indicated the high percentages of crystallinity for the samples examined. The percentage crystallinities were determined by X-ray crystallography. The more amorphous samples were Suc-42. and L.Pec.25.E. with values of 45 ±3% and 46 ±3% crystallinity respectively. In all cases, blending the PHB(FM)IP resulted in a reduction in the percentage crystallinity from 73% to a minimum of 45% for sample Suc-42. and a maximum of 59% for sample SA-7.

Graph 3.13 illustrates the relationship between the enthalpies of fusion and the percentage loading of the polysaccharides in the sample. It was determined that there was no conclusive change in the mp. or Tg. of the co-blended samples but a reduction in the enthalpy with increasing polysaccharide loading. It was also observed that sample L.Pec.25.E. had a lower enthalpy, 49J/g., than sample L.Pec.25.S., which had a fusion enthalpy of 61J/g. This difference was also reflected in the crystallinities: 46 and 55% respectively. It is possible, therefore, that sample L.Pec.25.E., probably due to the percentage loading and the manufacturing process, had either a higher molecular weight pectin than sample L.Pec.25.S. and/or possessed a larger proportion of the pectin.

The PAS traces obtained for the co-blended samples revealed no differences when compared to the homopolymer trace. Although some differences in the molecular weight data of the samples did occur, these were minimal and inconclusive, (Table 3.3).

3.1.3.3. Conclusions.

The examination of the undegraded samples lead to the conclusion that blending the PHB with various polysaccharides probably proceeded until a saturation point was attained, at which stage the fibres were no longer affected. Thus, the remaining polysaccharide was then observed as matted, granular regions. The blending did not affect the polymer structure but did affect the fibre/matrix structure.

Therefore, it was concluded that the nature of the co-blend played a primary role in affecting the structure of the fibrous matrix with the percentage loading probably being of less importance after an optimum loading was achieved.

3.1.4. The Effect Of Copolymerization On The PHB(FM)IP.

The PHB(FM)IP was manufactured with 5%, by weight, of its comonomer; poly(β-hydroxyvalerate), sample PHB/5V. Phase contrast observations were similar to the co-blended samples in that the fibres appeared to have a mosaic appearance. However, it was also observed that a number of the smaller diameter fibres exhibited irregular, 'banded' regions. (Plate 3.27) This banding was probably due to the comonomer presence.

SEM of the fibres revealed similar structures to the PHB(FM)IP, whilst a more noticeable change was observed in the fibre diameter distributions, (Graph 3.14). As can be

Sample	Mw.	Mn.	Polydispersity.
SA-7.	507,000	155,000	3.3
SA-30.	597,000	230,000	2.6
Scc-9.	595,000	208,000	2.9
Suc-42.	654,000	203,000	3.2
L.Pec.9.	548,000	179,000	3.1
L.Pec.15.	561,000	198,000	2.8
L.Pec.25.S.	568,000	203,000	2.8
L.Pec.25.E.	595,000	216,000	2.8
H.Pec.10.	578,000	176,000	3.3
PHB(FM)IP.	587,000	177,000	3.3

Table 3.3.

Characterization Of The Undegraded Co-blends; Molecular Weight Data.

Sample	PHB(FM)IP	PHB/5V.
Mw.	587,000	505,000
Mn.	177,000	179,000
Polydispersity.	3.3	2.8
mp. (°C.)	174	165
Tg. "	5.2	0.1
ΔHm. (J/g.)	79	57
Crystallinity. (%)	73 +/-3	44 +/-3

Table 3.4.

Characterization Of The Undegraded Homopolymer And Copolymer Samples; Molecular Weight, DSC And X-Ray Crystallography Data.

observed from graph 3.14, there was a large proportion of fibres sampled with diameters below 6 microns. ie; small diameters, (Approximately 52%). Main peaks occurred at 5-6 and 8-9 um. with frequencies of 16 and 12% respectively. Very small fibres at 0-1 and 1-2 um. diameters were readily noticeable with frequencies of 8 and 16%. No fibres were observed at the 2-3 um. range for the sample PHB/5V., whilst the homopolymer sample possessed a frequency of 8%. The distribution therefore was such that when the small, medium and large diameter group frequencies were considered, the large diameter frequencies for both samples were approximately the same. Changes in the medium and small diameters were readily observed. The PHB/5V. sample had 36% frequency for the medium diameter fibres compared to the 26% for the PHB(FM)IP sample. However, the homopolymer sample had a greater frequency, 64%, for the smaller diameter fibres compared to the PHB/5V., 52%. Therefore it was anticipated that the PHB(FM)IP would degrade more quickly than its copolymerized counterpart.

Table 3.4 illustrates the results of the physical properties investigations for the PHB/5V. sample and compares them to the PHB(FM)IP. From table 3.4 it can be observed that the copolymer presence greatly reduced the initial enthalpy, melting point and glass transition temperature. This indicated a comparatively less stable polymer and matrix. Similarly, the crystallinity also reduced considerably and this indicated a greater amorphous presence. The molecular weight was reduced from 587,000 to 505,000 whilst the molecular weight number remained approximately the same around 179,000.

It appeared therefore, that the presence of the comonomer reduced the number of long polymer chains and consequently the crystallinity of the fibres, such that the PHB/5V.

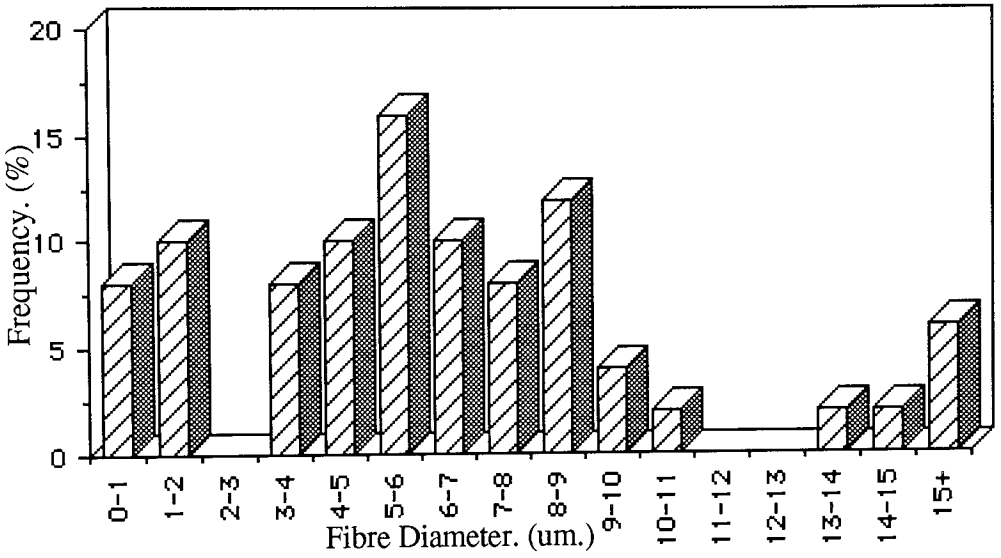

Graph 3.14.

Fibre Diameter Distribution For Fibres From Undegraded PHB/5V.

was apparently less stable and would therefore degrade quicker than the homopolymer sample. However, it may be that considering the fibre diameter distributions, the comonomer presence would facilitate the collapse of the matrix and certain fibres, but only by virtue of this collapse and the subsequent changes in surface area to volume ratio would the comonomer enhance the degradation of the PHB.

Thus, the presence of 5% PHV was observed to have an apparently greater effect on the physical properties of the fibrous matrix compared to the simple blending of the matrix with various polysaccharides in different percentage loadings.

3.2 Initial Study Of Degradation Conditions.

The degradation of PHB technical grade (TG) samples under varying conditions of pH and temperature were investigated. This experiment helped to determine the conditions and time periods involved in an accelerated degradation model.

It can be readily observed from the photographic record, (Plate 3.28), that degradation occurred with the rate increasing with temperature and a higher alkaline buffer. In phial 9 (pH 10.6 and 70°C.) the fibres apparently 'collapsed' within a day and exhibited an apparent loss of all mechanical structure by day 3. Similarly, fibres in phials 3 and 6, pH 10.6 and temperatures 37.5, 50°C. respectively, followed at periodic intervals, with total collapse at days 100 and 27 respectively. A similar trend occurred with those phials containing buffer pH 7.4, but total collapse did not occur until day 100 for those samples

Plate 3.28.

Photographic Record Of Qualitative Degradation Of PHB(FM)TG With Varying Temperature And Buffer Conditions.

at a temperature of 70°C., (phial 8). The fibre samples in the acidic buffer of pH 2.1 (phials 1, 4 and 7) essentially retained their structure at all the temperatures examined.

It can be concluded therefore, that the degradation of the fibres occurred by base hydrolysis, this is consistent with previous degradation studies using PHB.[49-54] Two degradation models were determined and utilized for further experiments; an accelerated model with conditions of 70°C. and pH 10.6 and a physiological model with conditions of 37.5°C. and pH 7.4, having similar hydrolytic conditions to those within the mammalian body.

3.3. Validation Of The Monomer Measurement Technique.

3.3.0. General Introduction.

The stability of the monomer in varying concentrations was examined under the accelerated and physiological degradation conditions. The effect of the polysaccharides on the monomer stability was also examined under accelerated conditions. These experiments determined the suitability of the monomer detection method to monitor the degradation of PHB and a maximum period of stability before the necessary replacement of the degrading solution, under the conditions utilized in the degradation models.

3.3.1. Stability Of The HBA Monomer Under Accelerated Conditions.

Graph 3.5 illustrates the absorbance variation from the initial for samples 1-Lo. to 3-Hi., containing HBA monomer in relatively low ($2.5mg.dl.^{-1}$), medium ($12.5mg.dl.^{-1}$) and

high (18.8mg.dl.$^{-1}$) concentrations respectively.

.

It can be observed from graph 3.5 that the stability of the monomer in the samples fluctuated quite noticeably. Both samples 1-Lo. and 2-Med. exhibited a variation of approximately ±3%, whilst sample 3-Hi. had a much greater variation with values of +8% and -6%, the absorbance generally increased and the negative value was most probably an error. This increase in variation in sample 3-Hi. corresponded to an apparent increase in the monomer concentration. However, this can be explained by the decrease in the volume of each phial, (Graph 3.6). Although the phials were closed with screw-sealing lids and sealed with 'nesco-film', after 21 days at a temperature of 70°C. the volume contents decreased by approximately 5mls. ie: nearly 45%. This loss was due to evaporation. Consequently, the experiment was repeated using simple distillation equipment and the distillate analysed. No absorbance was detected from the distillate, but higher absorbance values than the initial were determined for the distilling sample. Thus, it was concluded that the volume loss from each phial did not contain any of the HBA monomer. Therefore, this volume decrease caused a concentrating effect of the remaining monomer and this was detected as a corresponding rise in the absorbance when compared to the initial absorbance, ie; a positive variation.

Correcting the absorbance values for the concentrating effect had little effect on the graphic trend for samples 1-Lo. and 2-Med., (Graphs 3.17 & 3.18) which illustrated variations of approximately ±2.5% within a time limit of 2 weeks. These values were within an acceptable error range and consequently a time period of 14 days was adopted for the accelerated degradation model. The fluctuating nature of the variations indicated

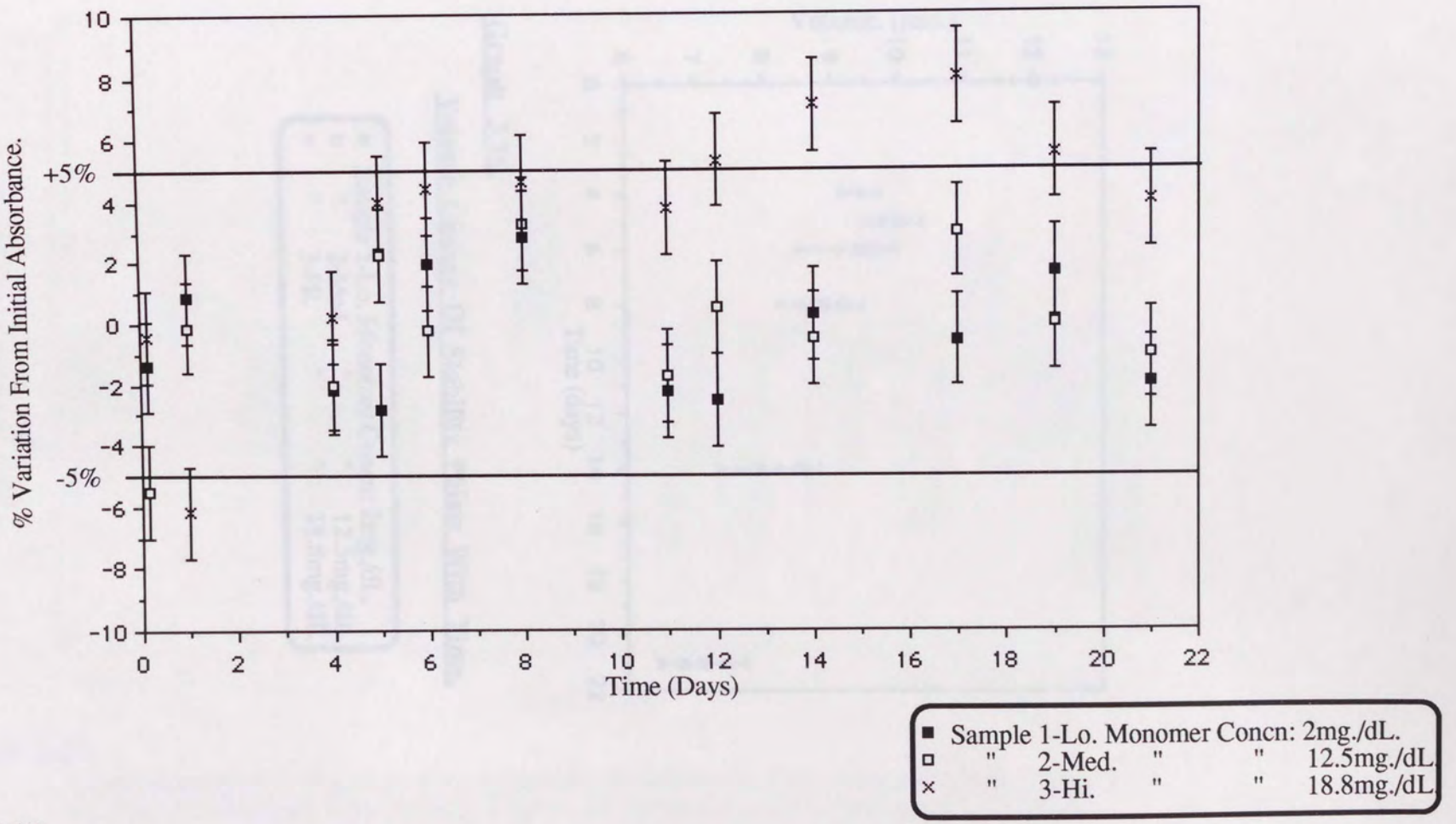

Graph 3.15.

Determination Of Experimental Accuracy,Stability Of Monomer With Time In The Accelerated Degradation Model, Monitored By The Percentage Variation From Initial Absorbance.

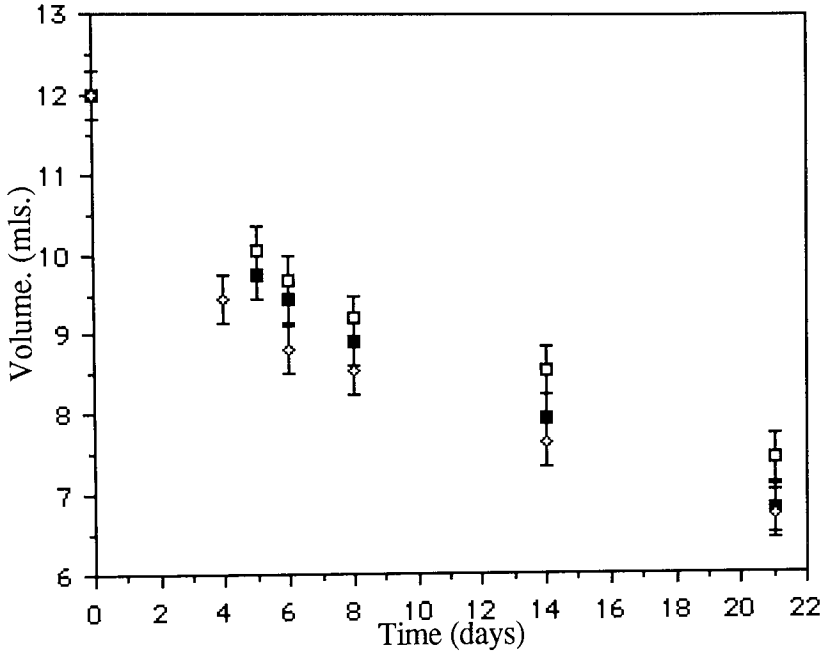

Graph 3.16.

Volume Change Of Stability Phials With Time.

■ Sample 1-Lo. Monomer Concn: 2mg./dL.
□ " 2-Med. " " 12.5mg./dL.
◇ " 3-Hi. " " 18.8mg./dL.

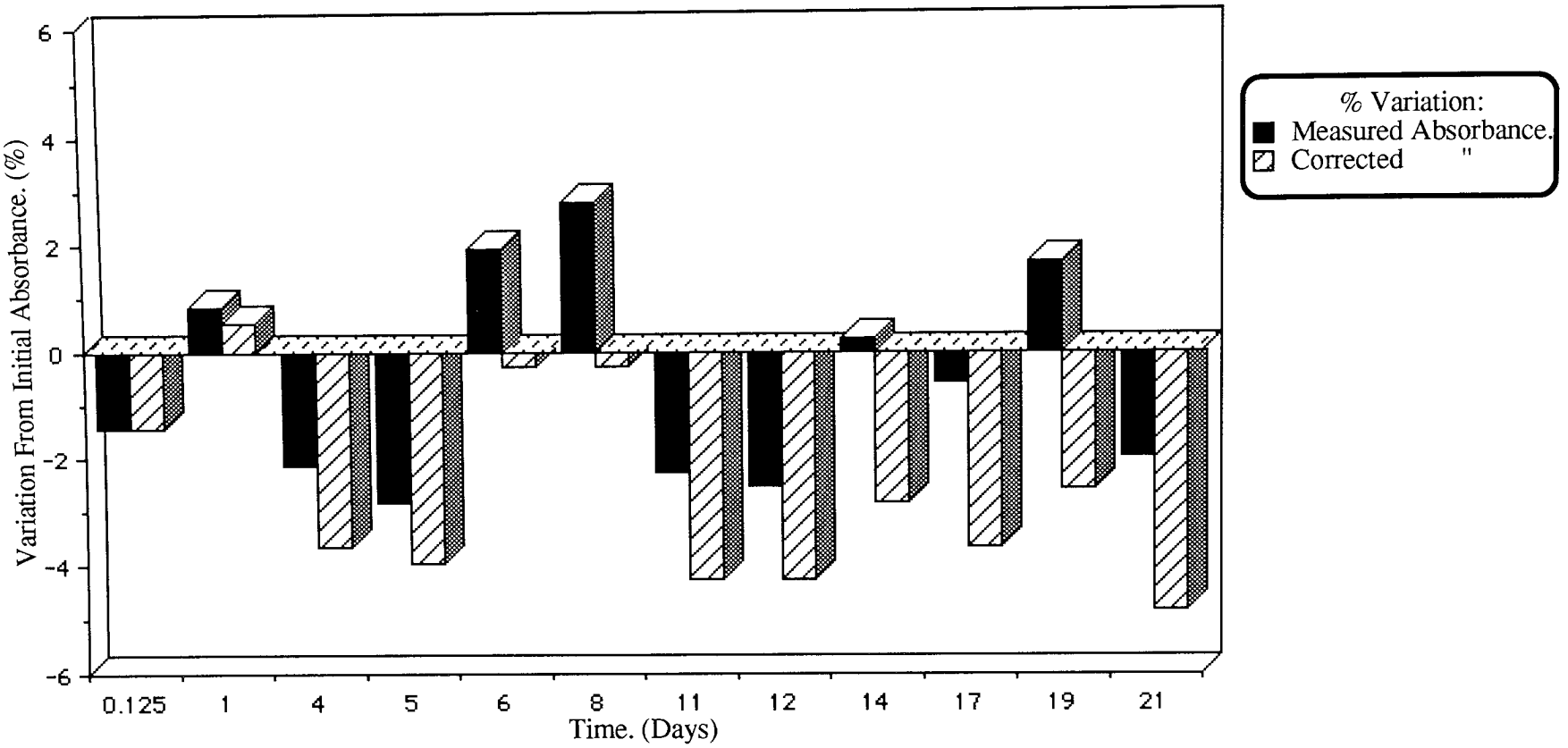

Graph 3.17.

Determination Of Experimental Accuracy; Stability Of The Monomer With Time In The Accelerated Degradation Model, Monitored By The Percentage Variation From The Initial Absorance. Sample 1-Lo. (2mg/dL.)

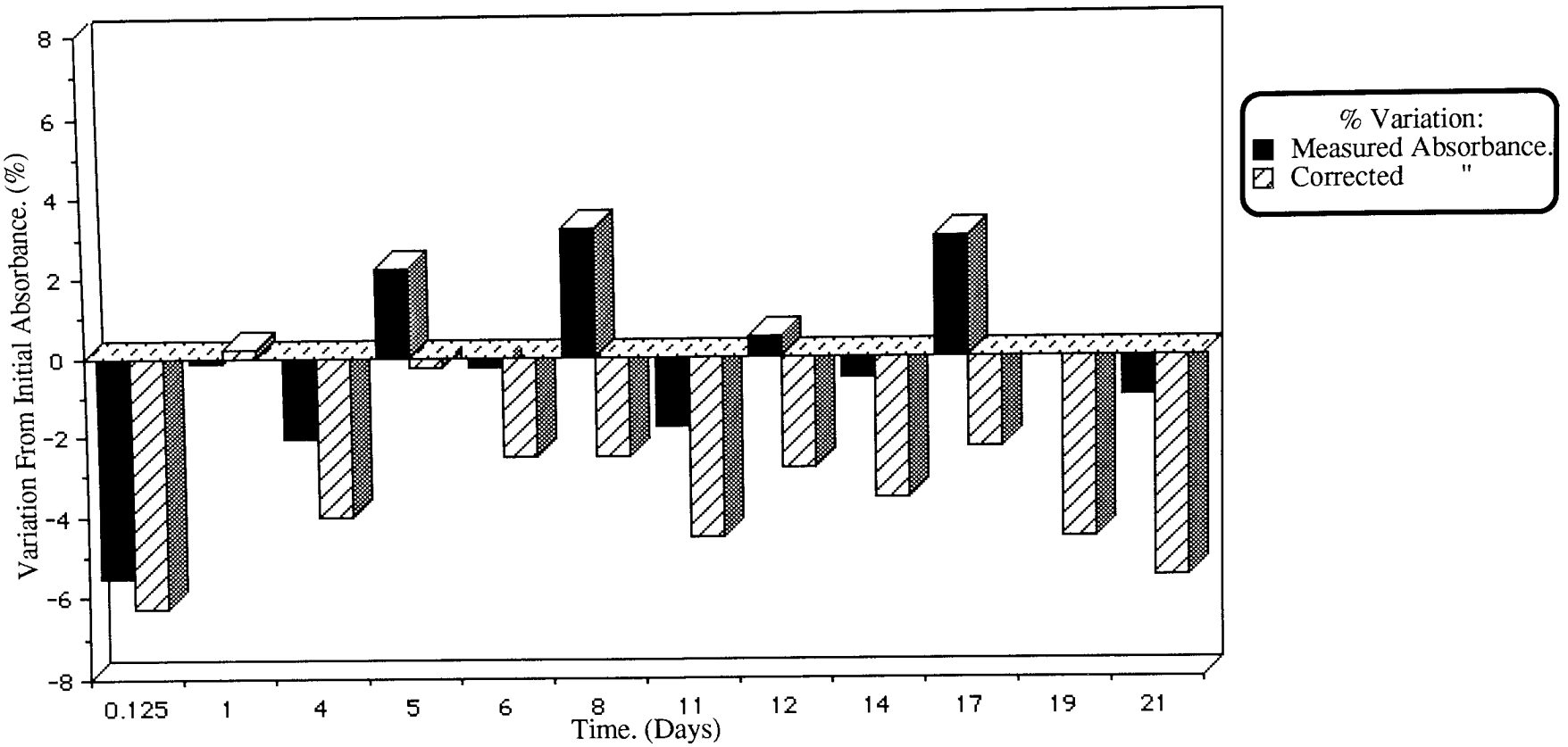

Graph 3.18.

Determination Of Experimental Accuracy; Stability Of The Monomer With Time In The Accelerated Degradation Model, Monitored By The Percentage Variation From The Initial Absorance. Sample 2-Med. (12.5mg/dL.)

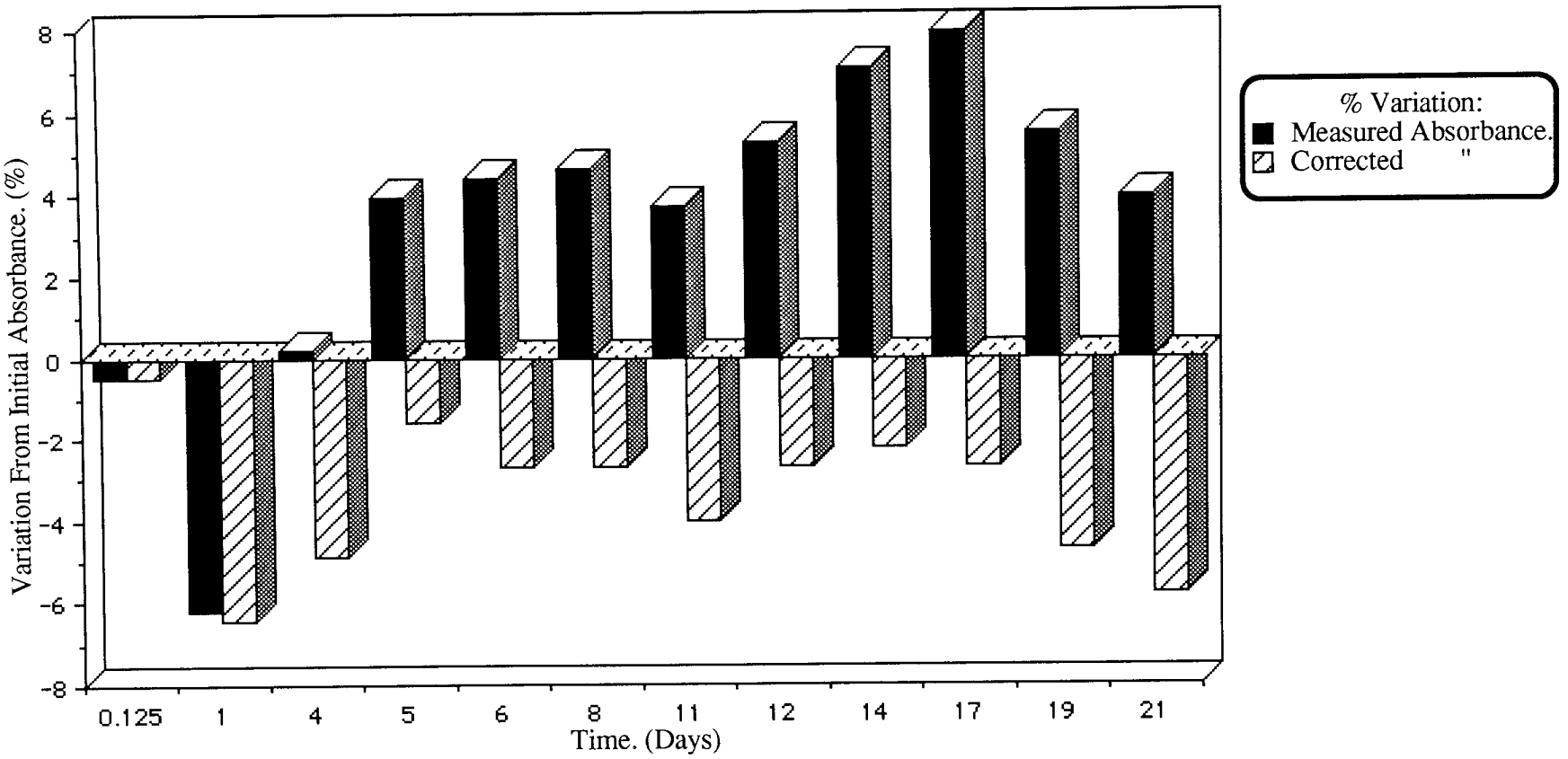

Graph 3.19.

Determination Of Experimental Accuracy; Stability Of The Monomer With Time In The Accelerated Degradation Model, Monitored By The Percentage Variation From The Initial Absorance, Sample 3-Hi, (18.8mg/dL.)

that these error ranges were not only due to stability changes, but also to procedural and human error.

The corrected absorbances for sample 3-Hi. illustrated a reversal of the uncorrected trend, (Graph 3.9). The error range for the uncorrected variations was altered to approximately ±3% for the corrected absorbance values, whilst within the 14 day period this was further reduced to ±2.5%.

Thus, it was concluded that a time period of 14 days was to be utilized in the accelerated degradation model, before solution removal and fresh buffer addition. The stability of the monomer during this period was suitable to provide an accurate measurement of the amount of HBA within a sample phial solution and thus, the amount of PHB degraded to monomer. A maximum variation of ±3% within the experimental procedure also ensured that the error of these measurements was satisfactory.

3.3.2. Stability Of The HBA With Polysaccharides Under Accelerated Conditions.

Graph 3.20 illustrates the percentage variation of the measured from the initial absorbances with time, for monomer solutions in a medium concentration ($12.5mg.dl.^{-1}$) with the presence of sucrose, pectin, sodium alginate and sodium carboxycellulose, under accelerated degradation conditions of pH 10.6 and temperature of 70°C. The polysaccharides were added to the buffer and monomer phials in a percentage, by weight, proportional to their ideal percentages within the co-blended samples. ie: 42% sucrose, 9% pectin, 30% sodium alginate and 9% sodium carboxycellulose.

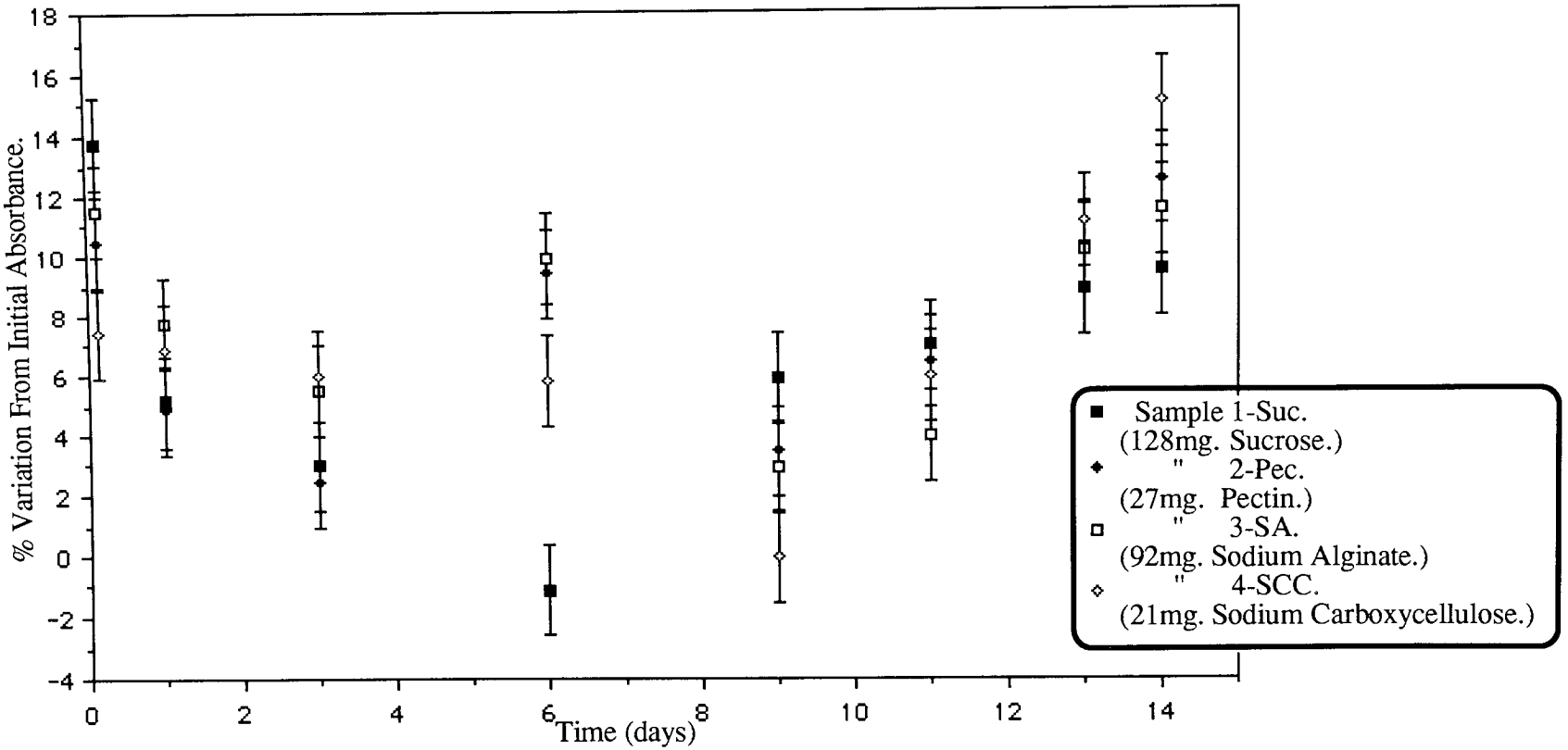

Graph 3.20.

Confirmation Of Experimental Accuracy; Stability Of Monomer With Time In The Accelerated Degradation Model In The Presence Of Polysaccharides, Monitored By Percentage Variation From The Initial Absorbance.

As can be observed from the graph 3.20, the absorbances of the samples in each phial fluctuated quite markedly from the initial absorbances. The percentage variation of sample 1-Suc (sucrose) and 4-SC (sodium carboxycellulose) increased dramatically after a period of only three hours to a value of approximately +14 and +7% respectively. The variation then gradually decreased until day 6 (-1%) and day 9 (0%) respectively, before gradually increasing once again. The absorbances of samples 2-Pec (pectin) and 3-SA (sodium alginate) followed a similar trend, however, at day 6 for both samples a large increase to approximately 10% was also noted.

Similar to section 3.3.1. volume fluctuations due to evaporation were also observed. However, in each case the volume increased initially and then decreased. These fluctuations were due to the presence of the polysaccharides, their volume displacement and gradual dissolution into the solution. Taking these volume fluctuations into account produced corrected absorbances and percentage variation values as illustrated in graphs 3.21 - 3.24. Thus, the corrected absorbances were greater than the actual measured values whilst the volumes were greater than the initials. As the volumes decreased below the initial volumes the corrected absorbances became less than the measured values.

Therefore, the initial increases in the percentage variations were due to the physical presence of the polysaccharide in the undissolved form. The particulate matter of the sodium alginate and pectin powders formed a suspension in the buffer solution and interfered with the absorbance values, by preventing the passage of light through the cuvet in the spectrophotometer during the analysis. In the pectin sample (2-Pec) this initial increase in absorbance decreased quite rapidly from +10% variation to +3% by day 3. The

sodium alginate sample (3-SA) however, maintained higher levels of +12% reduced to +5.5% by day 3. This was due to the initially greater amount of sodium alginate present when compared to the pectin; 30% and 9% respectively. The large variations observed at day 6 in each case, indicate that the gradual reductions observed between day 0.125 (3 hrs.) and day 3 were due, not only to the polysaccharides gradually dissolving into the buffer solution, but also to the settling of the particulate matter at the base of the phials. At day 6 this matter was disturbed by agitating the phial prior to the measurement process. Absorbances for both samples were measured prior to and after agitation at the termination of the experiment (day 14) and little difference was observed in each case, thus indicating that the dissolution was complete. From day 9 to 14 the measured absorbances gradually increased due to the evaporation effect and consequently the corrected variation values were within a ±2.5% error range.

A similar trend to 2-Pec. and 3-SA. was also noticed for samples 1-Suc. (sucrose) and 4-SC. (sodium carboxycellulose). These samples were initially in a crystalline form, the sucrose compound, although in a greater amount (42%), was present in the form of small crystals and these readily dissolved into the buffer. Thus, the originally high variation of +14% at day 0.125 (3 hrs.) quickly reduced to 5% and 3% by days 1 and 3 respectively. The sodium carboxycellulose compound was present in a larger crystalline form, but with a reduced amount of 9%, therefore, the percentage variation values at day 0.125 was +7% reduced to approximately 6.5, 5 and 4.5% at days 1, 3 and 6 respectively. Thus, the sucrose had an initially high percentage variation which was quickly reduced, whilst the sodium carboxycellulose did not dissolve as quickly and therefore had a comparatively smaller initial variation which did not reduce so rapidly.

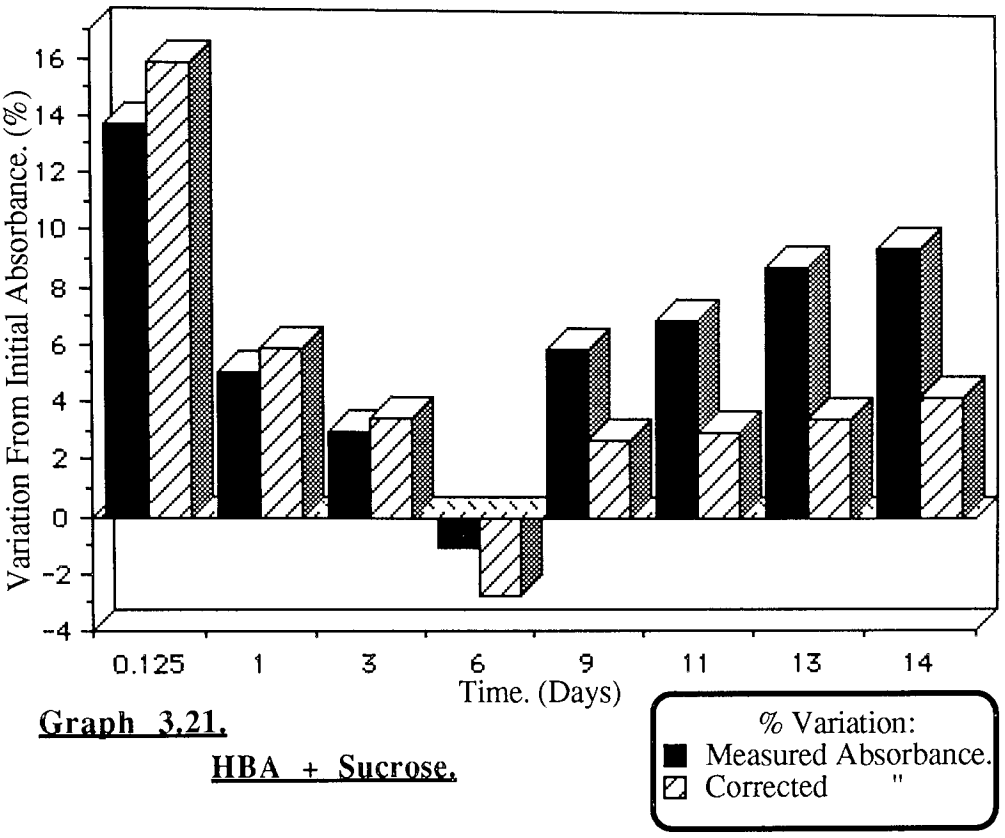

Graph 3.21.

HBA + Sucrose.

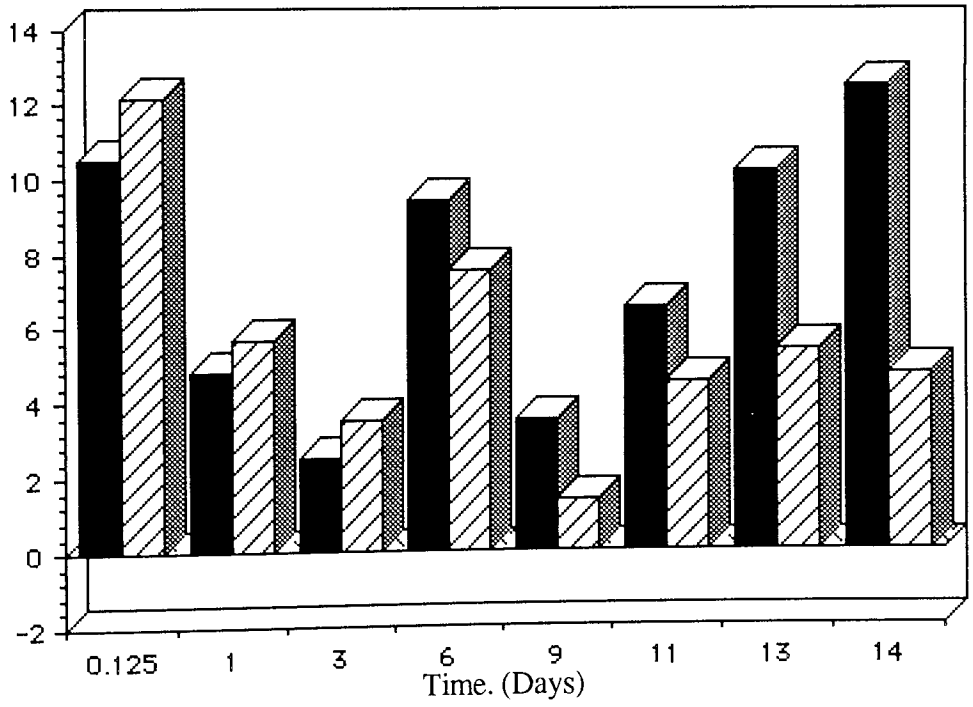

Graph 3.22.

HBA + Pectin.

Determination Of Experimental Accuracy: Stability Of The Monomer In The Presence Of The Polysaccharides In The Accelerated Degradation Model, Monitored By Percentage Variation From The Initial Absorbance.

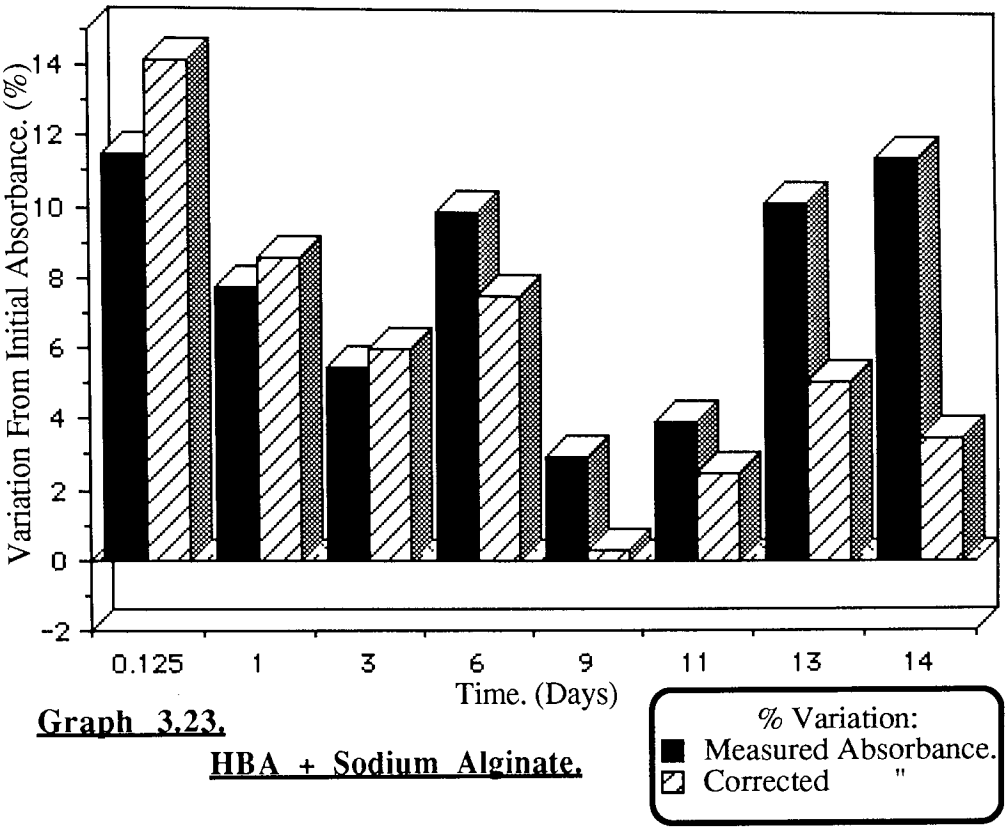

Graph 3.23.

HBA + Sodium Alginate.

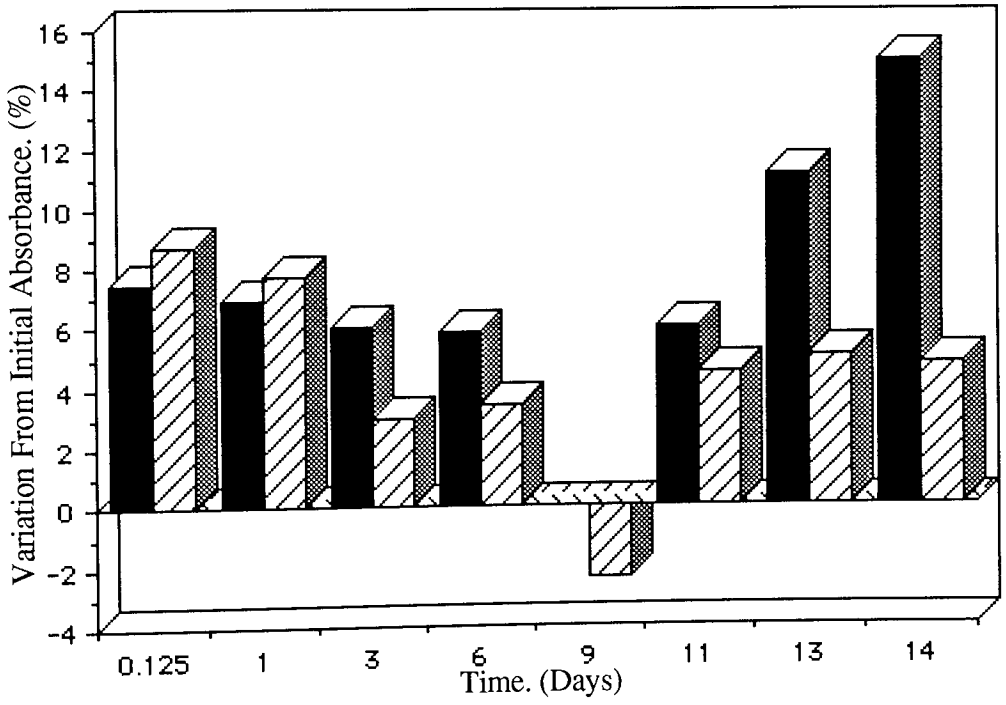

Graph 3.24.

HBA + Sodium Carboxycellulose.

Determination Of Experimental Accuracy; Stability Of The Monomer In The Presence Of The Polysaccharides In The Accelerated Degradation Model, Monitored By Percentage Variation From The Initial Absorbance.

In all the samples the stability of the monomer from around day 6, after the initial increases, was within a ±4% error range.

Thus, it was concluded that the polysaccharides initially interfered with the monomer determination process by action of their physical presence. This was observed until the polysaccharide had dissolved into the solution or settled at the base of the phial. However, under degradation conditions interference by the polysaccharides was considered unlikely since they would be blended within the fibre samples and therefore the rate of dissolution and particulate settlement would be altered. More importantly, the samples for HBA analysis would be prefiltered to remove any interfering particulate matter.

3.3.3. Stability Of The HBA Monomer Under Physiological Conditions.

The stability of the monomer in a medium concentration (12.5mg.dl.$^{-1}$) was examined under physiological conditions of pH 7.4 and temperature 37.5°C. The percentage variation of the measured absorbances from the initial were calculated and expressed as a function of time. The volume changes within the sample phial were also measured.

Graph 3.25 illustrates the changes in the percentage variation and the volume of the phial contents with time. As can be observed, there was little change in the volume of the solution, with an approximate decrease of 0.9 mls. (7.5%), the subsequent monomer concentrating effect therefore being of little importance. This volume loss could have been due to error and evaporation.

The percentage variation of the monomer rapidly decreased to approximately -20% by day

12 and then remained at this approximate value until termination at day 28. Assuming a 5% error margin, the stability of the monomer was limited to a period of two and a half days.

Thus it was concluded that the stability of the monomer under the physiological conditions was unsuitable as a means of degradation measurement. PHB is known to have an extremely slow degradation rate under physiological conditions[22,51] and therefore, it was anticipated that the monomer production would be very slow and thus prone to error within a reasonable time period. Consequently, the quantitative degradation of the PHB(FM) samples in the physiological degradation model was examined by gravimetric analysis.

3.3.4. Conclusions.

Therefore it was concluded from the stability studies that HBA analysis was suitable to measure the PHB degradation within a time period of 14 days for the accelerated degradation model. The presence of the polysaccharides would not interfere in the model due to pre-analysis filtering. The error margin was determined as ±3%.

Monomer analysis was not suitable in the physiological model, due to the lack of monomer stability and the anticipated slow monomer production during degradation of the PHB.

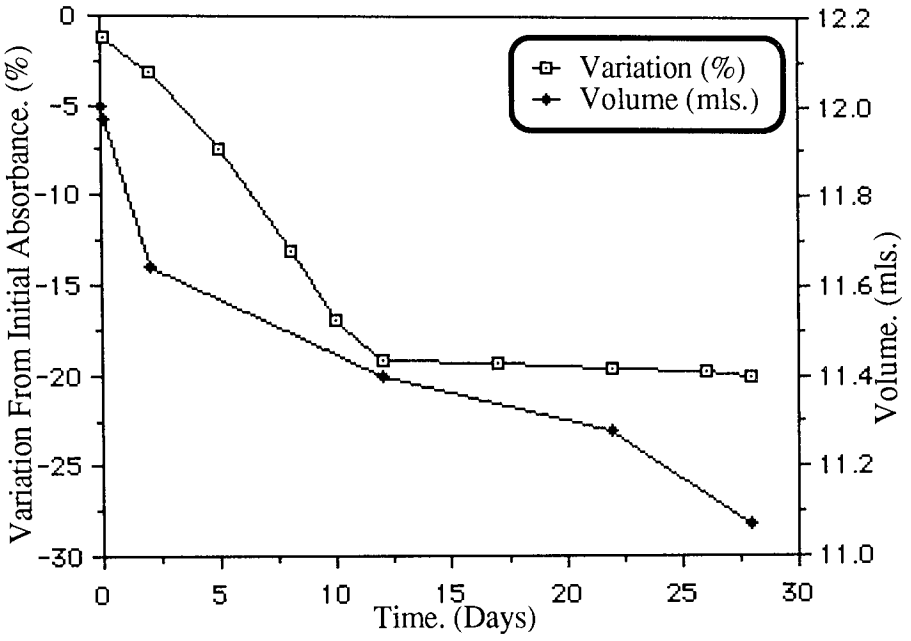

Graph 3.25.

Determination Of Experimental Accuracy; Volume Change And Monomer Stability With Time In The Physiological Variation Model, Monitored By Percentage Variation From Initial Absorbance.

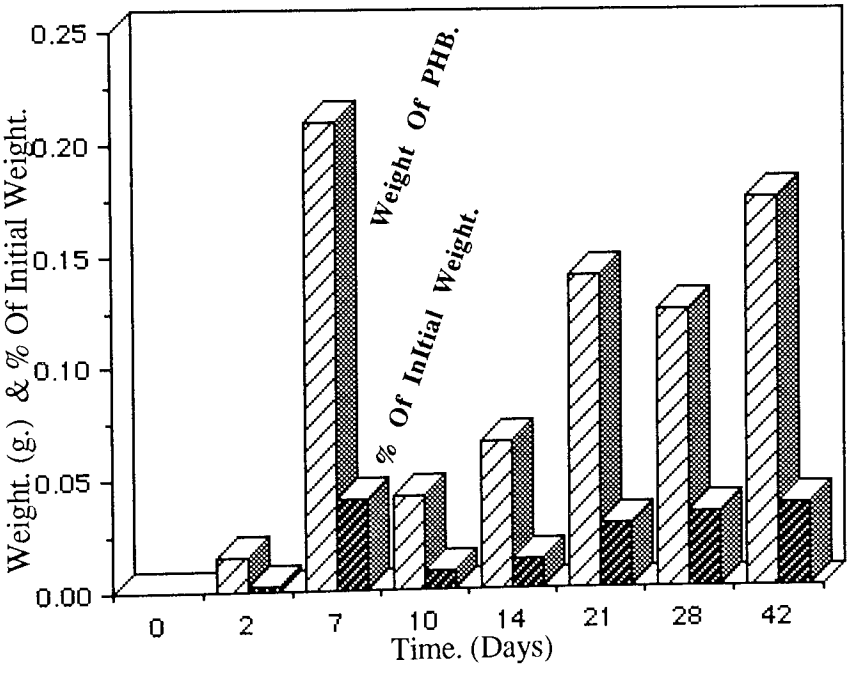

Graph 3.26.

Initial Study; Determination Of Degraded Particulate Matter With Time In The Accelerated Degradation Model, Moniotored By Gravimetry.

3.4 Initial Particulate Analysis.

Using the analysis process illustrated in Figure 2.1 and the accelerated degradation model determined in section 3.3, a PHB(FM) technical grade sample was degraded under accelerated conditions of pH 10.6 and temperature 70°C. and the values for particle analysis determined during degradation, using a Malvern particle mastersizer.

Particle analysis revealed a low percentage of bioresorbable particles, by initial sample weight, with only fractions of milligrams being detected. This was probably due to the method used, where values for particles 3 microns to 1 micron diameter and estimates to 0.5 microns were determined. The necessary use of approximately 10mls. of fresh buffer to obtain a background reading greatly diluted the addition of approximately 5mls. of the filtrate, consequently detection was complicated. It is also quite possible that additional degradation from the particles to the monomer occurred when placed in the sample holder, due to the presence of this buffer and the agitation by the mixer utilized in the experiment. The use of the buffer as a background was necessary to avoid a change in the refractive index of the sample when the filtrate was added. Similarly, distilled water was used for the washings.

Consequently graph 3.26 cannot be used as a measurement of the actual weights or percentages of particles involved in the degradation process, but it does reveal a qualitative trend. The production of degraded/bioresorbable particles gradually increased with time (day 7 sample was probably an error) and thus, it can be concluded that the degradation rate was not constant. Similarly, the filtering procedure before monomer analysis was

anticipated to remove the majority of the degraded particulate matter below 3um.

3.5. General Conclusions.

This chapter has dealt with the preliminary studies of the novel fibrous PHB form and investigated the conditions and methods of monitoring its degradation. This novel form was observed to possess a structure very similar to cotton wool and was called PHB fibrous matrix, PHB(FM) or 'wool'. This wool consisted of hollow and porous fibres of varying, non-uniform diameters which agglutinated and branched to form a complex fibrous mass. Terminal bulbous regions were also observed at some fibre ends. The fibres had a main distribution (60%) of diameters between 0 and 5 microns with the majority at two main peaks of 1-2 and 4-5um., whilst a small percentage of these fibres counted had diameters greater than 15 microns and up to approximately 72um.

It was determined that increasing the PHB purity, PHB(FM)IP, had apparently little effect on the matrix structure and only slightly increased the crystallinity and DSC results. Altering the production solvent had a more noticeable effect on the matrix structure with a number of fibres produced from methylene chloride extraction exhibiting a more heavily pitted and porous nature compared to those from the chloroform extraction, whilst those fibres produced from a 50/50 solvent mixture were comparatively smooth. Similarly, blending the PHB(FM)IP with various polysaccharides produced noticeable differences in the fibre diameter distributions and physical properties when compared to the homopolymer matrix. The extent of these changes were dependent upon the nature and

loading of the polysaccharide, generally, increasing the loading increased the diameters, however, the reverse effect was noticed for the blending with sodium alginate, samples SA-7. and SA-30. The penetration of the wetting medium into the hollow cavities of these blended large diameter fibres occurred more readily. Increasing the loading of low molecular weight pectin increased the number of large fibres with diameters greater than 15 microns, whilst the remaining diameter range was also shifted to the larger diameters. Blending was determined to be inefficient, with sample L.Pec.25.S. apparently possessing either a larger pectin load than its counterpart L.Pec.25.E. or a pectin of a comparatively greater molecular weight. Blending the PHB(FM)IP with high molecular weight pectin, H.Pec.10., produced a shift in the fibre diameter distribution towards the smaller diameters. The melting points, fusion enthalpies, glass transition temperatures and crystallinities of the co-blended samples were generally lower than that of the homopolymer sample. Copolymerizing with 5% poly(β-hydroxyvalerate), PHV, produced similar effects to the blending. It was also noticed that the blending and copolymerizing apparently reduced the initial matrix strength. The unusual, complex structure of the PHB fibrous matrix possessed a large surface area to volume ratio and this was anticipated to facilitate in its degradation.

The use of monomer measurement as a means of monitoring the PHB degradation was concluded as being accurate in the accelerated degradation model of conditions pH 10.6 and temperature 70°C. for a period of 14 days. However, the method was found to be unsuitable in the physiological degradation model, which possessed conditions of pH 7.4 and 37.5°C.

This chapter determined the structure and characterization of the undegraded 'wool' samples which were to be utilized as a baseline for the comparison with the degraded samples as studied in chapters 4 to 7. Further investigations and 'fine tuning' of the conditions in the degradation models were also studied in chapter 4 and the accuracy of utilizing monomer analysis in the degradation monitoring was confirmed in the degradation experiment.

Chapter Four.

The Degradation Of PHB(FM) In The Accelerated Degradation Model.

4.0 General Introduction.

This chapter concerns the degradation of the technical grade and increased purity PHB(FM) in the accelerated degradation model, (pH 10.6 & 70°C.). Degradation was monitored by gravimetric, particulate and monomer analysis. The partially degraded samples were analyzed by SEM, Optical microscopy, DSC, FTIR-PAS and molecular weight analysis. The effects of changing the initial sample weight and the manufacturing solvent on the matrix and PHB degradation were also investigated. The results of these experiments provided the reference to which the various effects of blending and copolymerizing the PHB(FM)IP on the degradation could be related.

4.1. The Effects Of Initial Sample Weight And Buffer Volume On The Degradation Of PHB(FM).

Samples of PHB(FM) technical grade (TG) possessing varying weights and volumes of buffer were degraded under accelerated conditions of pH 10.6 and temperature 70°C. This experiment was performed in order to investigate the relationship between the initial weights of the samples and the degradation rates they exhibit. The amount of undegraded sample was determined by gravimetric analysis at specific time periods. The percentage of undegraded sample was then calculated and presented as a function of time, (Graph 4.1).

It was observed that altering the initial weights of the samples, whilst maintaining the same conditions and buffer volume, 20mls. , produced noticeable differences in the

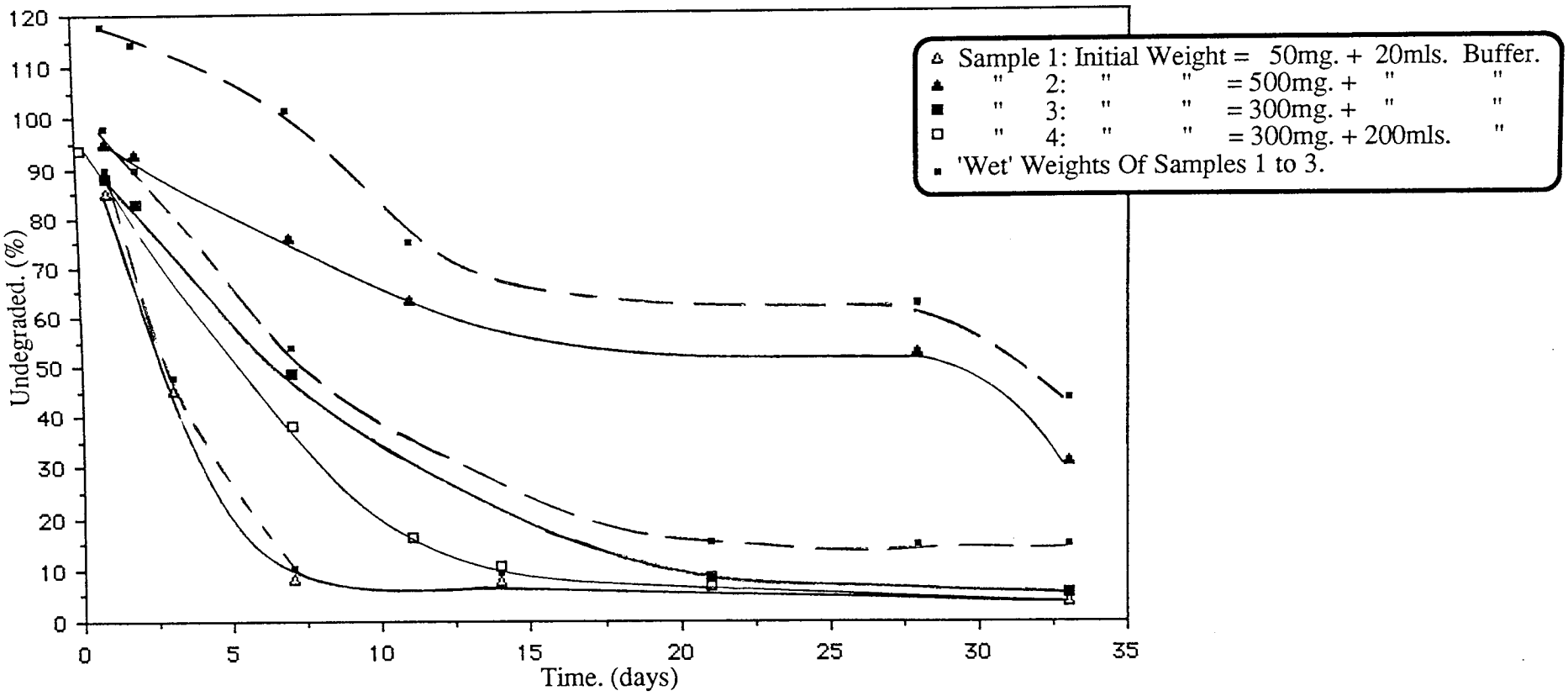

Graph 4.1.

Degradation Profiles Of PHB(FM)TG Samples With Different Initial Weights In The Accelerated Degradation Model, Monitored By Gravimetric Analysis.

degradation profiles.

In each sample the degradation profiles attained a final period of extremely slow degradation, so that the profiles were practically horizontal, (Graph 4.1). These periods occurred after a similar amount of degradation, approximately 92 to 95%, although the time periods involved in reaching this final stage increased with an increase in the initial sample weight. The final stage in the degradation profiles was attained when the fibrous matrix had collapsed and the remaining particulate matter deposited on the floor of the container. This then reduced the available surface area to volume ratio for the fibres available for degradation and therefore, the degradation rate was greatly reduced. (Sec. 4.2). Thus, it was concluded that increase in the initial sample weight effectively reduced the degradation rate of the sample in the degradation model.

Increasing the initial sample weight provided a greater fibre matrix integrity and consequently more pronounced 'step' stages were observed. Decreasing the initial weight caused a greater initial degradation rate until total collapse occurred in the final stage, such that the initial degradation step stages were less distinguished.

It was also noticed that those samples with larger initial weights exhibited greater differences between the dry and wet weights. This was as expected, since these samples had a greater weight of PHB and thus the increase was proportional.

Graph 4.2 illustrates the relationship between the initial sample weight and the overall degradation rate to the final stage, assuming linearity, for each of the degradation profiles.

Sample 4 had a larger degradation rate than sample 3, which had the same initial weight, 300mg., but a different buffer volume of 20mls., a factor of 10 less. This comparative increase in the degradation for sample 4 could have been due to an excess of buffer, however, if the initial weight to buffer volume ratio is considered, the rate was less than that of sample 1, which had a larger ratio. 0.0025g.:1ml. for sample 1, compared to 0.0015g.:1ml. for sample 4. Therefore, this indicates that the increase in the degradation rate of sample 4 compared to sample 3 was not solely due to the excess buffer, although it is possible that this excess of the buffer may increase the penetration of the degrading medium into the lower levels of the remaining particulate matter at the base of the phial and thus facilitate degradation. The other attributable factor to the increase in degradation for sample 4 was the container. A large glass sample container was utilized instead of the usual glass phials, the surface area at the base of the container was considerably larger than that of a phial and thus, as the fibrous matrix collapsed the particulate matter formed a less dense layer covering a larger accesible surface area at the base of the container when compared to its degradation in the phial, (Sample 3.). Consequently the degradation rate was greater.

A graph of the log. of the overall linear degradation rates to the final stages against the initial sample weight was plotted. This was done in order to provide a quantitative comparison between the degradation of the samples due to the changes in their initial PHB weights. The graph exhibited a linear relationship and thus, the equation expressing this line could be utilized for the co-blended samples to determine if any changes in degradation were due to the reduction in initial PHB weight. However, because of the possible differences in degradation between the TG and increased purity (IP) samples,

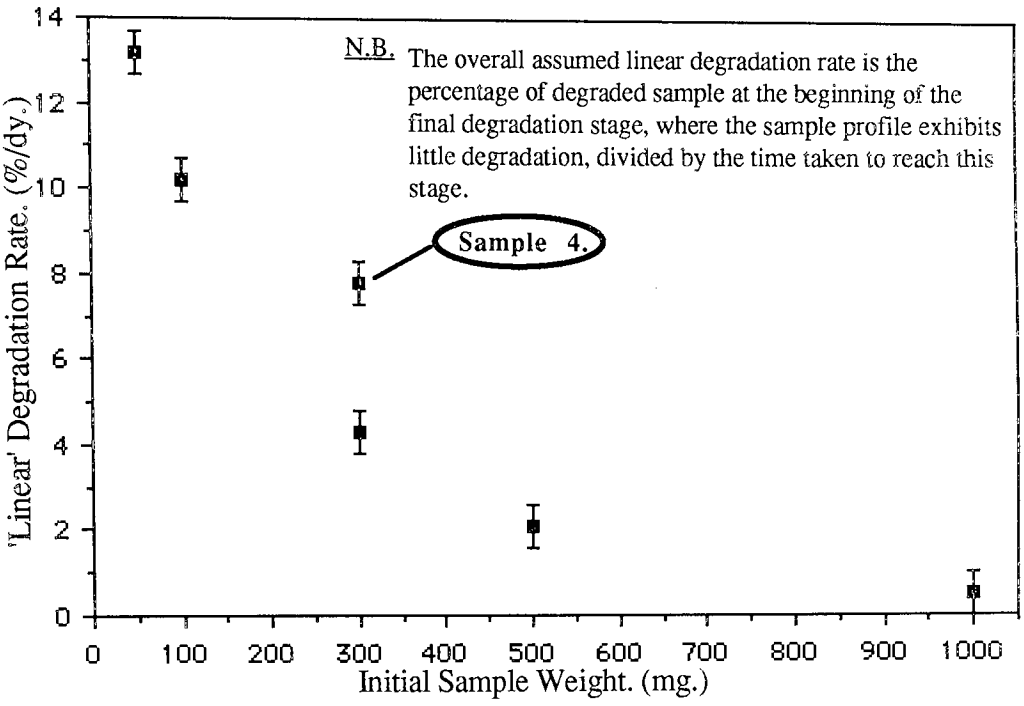

Graph 4.2.

Effect Of Initial PHB Weight On The Overall Linear Degradation Rate, Determined From Gravimetric Data, Graph 4.1, (Sec. 4.1)

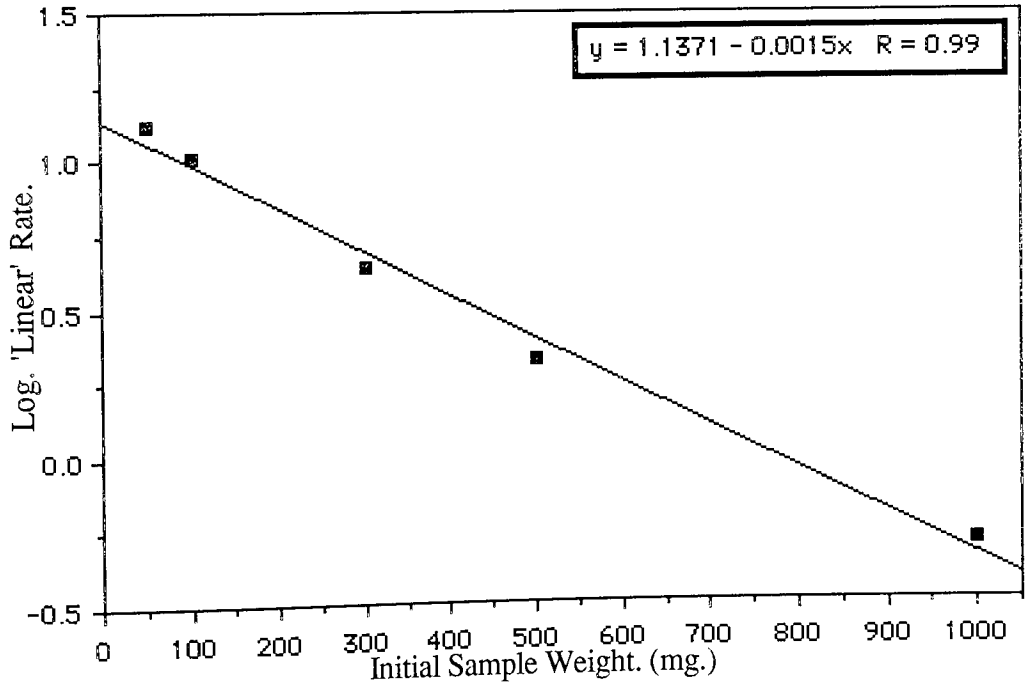

Graph 4.3.

Effect Of The Initial PHB Weight On The Overall Linear Degradation Rate, Determined From Gravimetric Data Of Graph 4.2.

these comparisons may only be utilized as approximations. Thus, it can be concluded that the degradation of the PHB(FM) is surface area to bulk related with the surface area constantly changing due to settling and compaction of the particulate matter throughout the degradation process. Should the process be performed with constant agitation the degradation rates should ideally be similar. Therefore, comparisons between the degradation of samples can only be quantitatively performed when the degradation conditions in each case are constant with respect to sample weight, temperature, pH, container and agitation during the process. Thus, graph 4.3 can only be utilized in the comparison of samples which have been degraded under these conditions.

It was concluded therefore, that the accelerated degradation model would utilize an initial sample weight of approximately 300 mg. and a buffer volume of 20 mls.

4.2. The Degradation Of PHB(FM)TG.

4.2.0 Introduction.

A number of samples of PHB(FM) technical grade (TG) with initial weights of 305mg. (±1.6%) were degraded under accelerated conditions of pH 10.6 and temperature 70 ±0.2°C. Individual samples were removed periodically, the contents were filtered and the percentage degradation determined by gravimetric analysis, according to the analysis procedure in figure 2.1, (Ch2). An individual sample was also removed periodically and the percentage degradation of the sample to the monomer determined by HBA analysis. This sample was utilized continuously until termination of the experiment at day 32, when

both HBA and gravimetric analysis were performed.

This experiment was carried out in order to determine the degradation profiles of the PHB(FM)TG, and to investigate the mechanism and nature of the degradation. The results could then be used to 'tailor' the degradation for specific scaffolding devices individually suitable to the relevent wound type. This could possibly be done by altering the production process, co-blending and copolymerizing. The degradation of the PHB(FM)TG formed a reference basis to which the degradation of the PHB(FM)IP samples were then compared.

4.2.1. Degradation Profiles.

Graphs 4.4 and 4.5 illustrate the degradation profiles for the PHB(FM)TG samples determined by gravimetric and monomer analysis respectively. Graph 4.6 reveals the measured partial and proportionately total ideal weights of the degraded particulate matter. Graph 4.7 is a measure of the percentage variation from the initial weights for the individual samples, since the undegraded and the degraded matter should ideally total 100%; the original weight. Graph 4.7 is therefore a confirmation of the experimental accuracy.

The percentage dry weight remaining (Graph 4.4) illustrates the amount of the undegraded material present, whilst the percentage remaining according to monomer analysis (Graph 4.5) is a measure of the amount degraded to the monomer, HBA. It can be observed by comparing graphs 4.4 and 4.5 that the difference between these two profiles gradually increased with time, this would appear to indicate an increasing error between the two

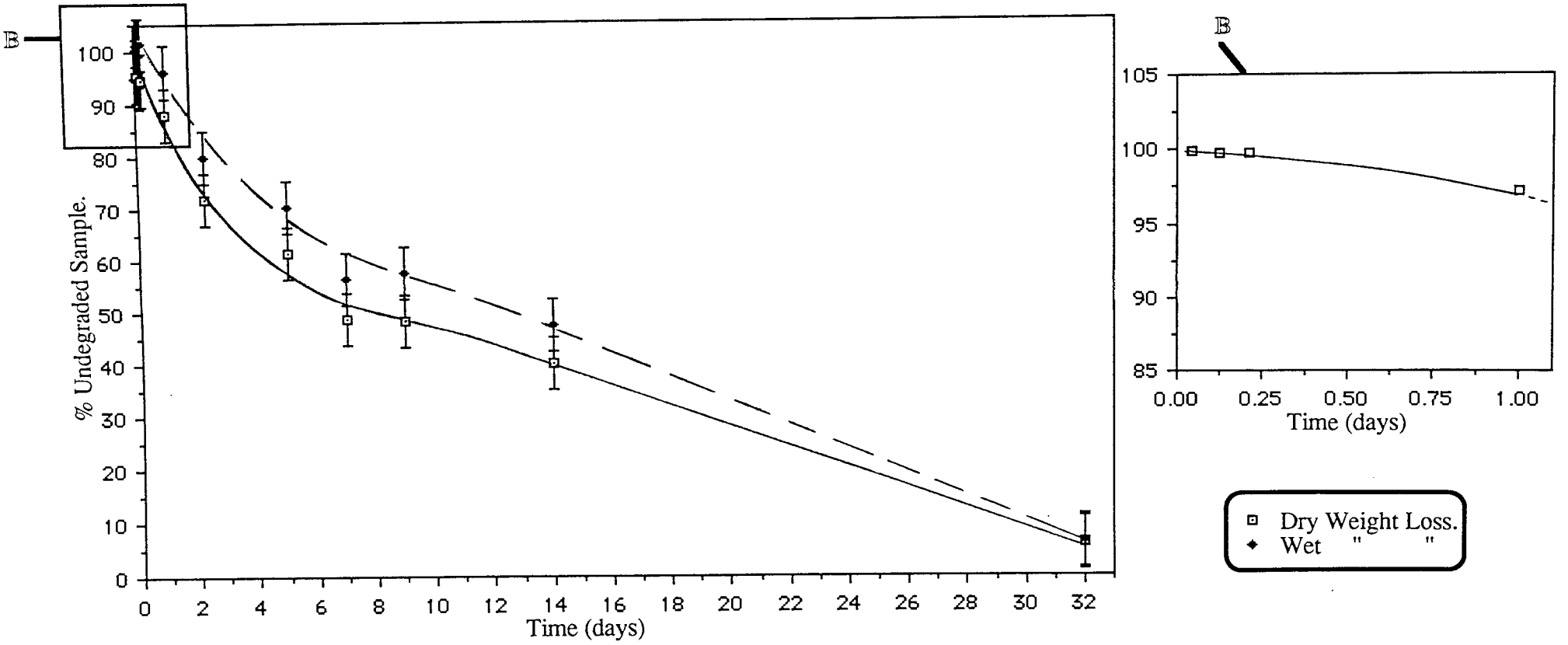

Graph 4.4.

Degradation Profile Of PHB(FM)TG. In The Accelerated Model, Monitored By Gravimetric Analysis.

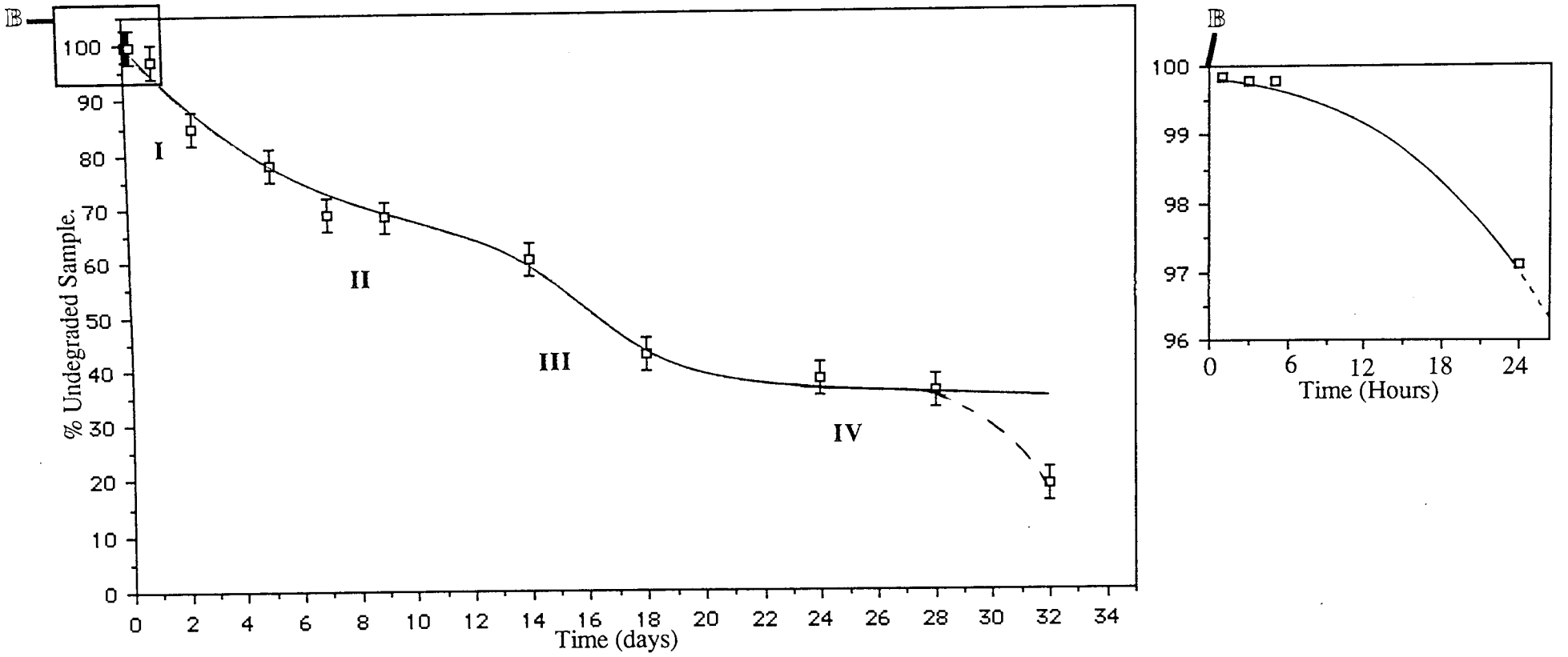

Graph 4.5.

Degradation Profile Of PHB(FM)TG In The Accelerated Model, Monitored By Monomer Analysis.

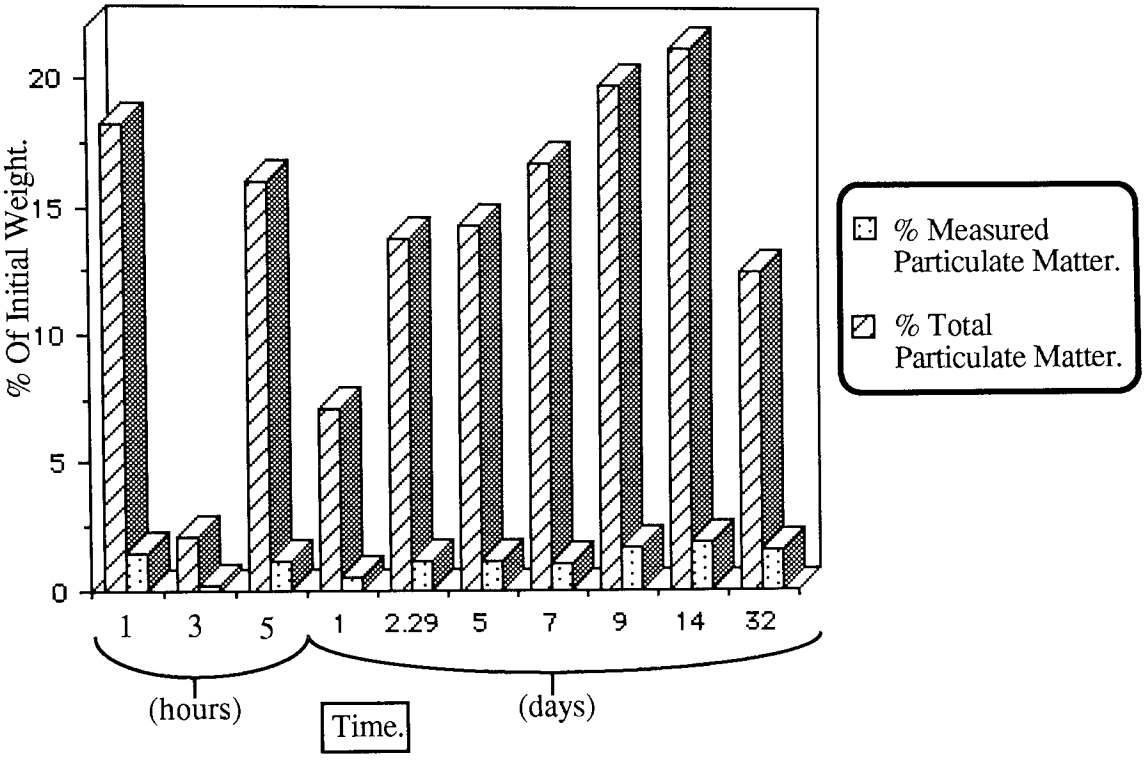

Graph 4.6.

Degraded Particulate Matter Production During PHB(FM)TG. Degradation.

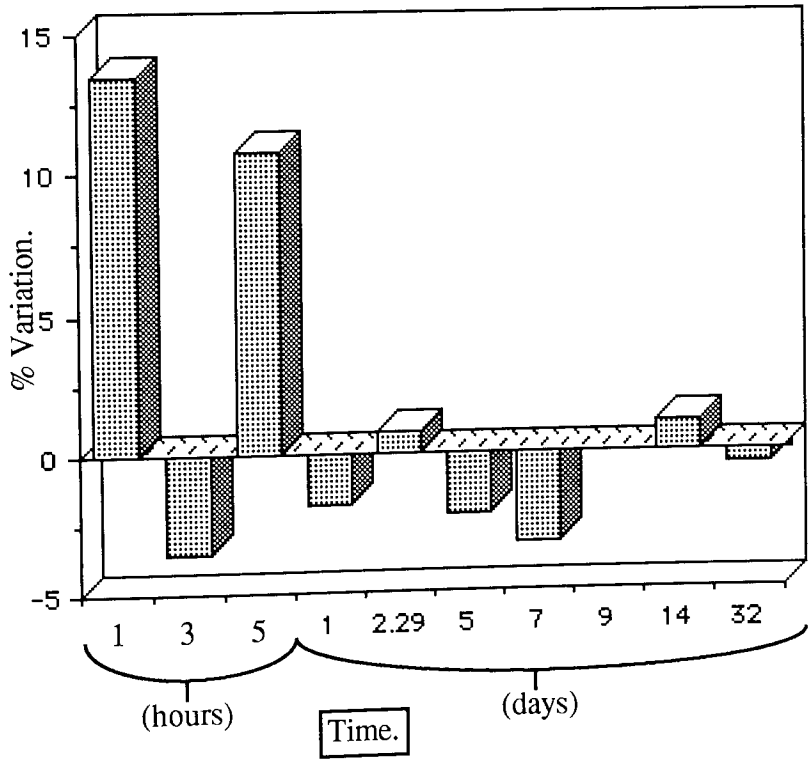

Graph 4.7.

Confirmation Of Experimental Accuracy. (% Error)

determination methods. Degraded particulate matter was also determined (Graph 4.6) and from these results the 'ideal' amounts of degraded matter present were calculated. Taking this proportionate 'ideal' amount into consideration, the percentage variations from the initial weights of the individual samples were then calculated: (Graph 4.7).

$$\left[\frac{\{\text{Undegraded Fraction} + \text{Degraded Fraction}\} \times 100}{\text{Initial Weight.}} \right] - 100\% = +/- \%\ \text{Variation.}$$

It was then observed that the variation during the course of the degradation experiment rarely exceeded a 5% error margin. The most noticeable exceptions to this were in the initial stages of the degradation; 1 and 7 hrs. These measurements were difficult to determine accurately since the particulate distribution within the medium was probably non-uniform and the small values involved ensured a high error due to the calculation procedure. Similarly, errors may have also been due to those particles not measured ie; below 0.2 microns, and contaminants which may have dissolved in the degrading medium but did not register in the monomer analysis. Apart from the error readings at 1 and 7 hours, it was observed that there was a gradual increase in the amount of degraded particulate matter, incorporating a slight 'step' stage between days 5 and 7. Thus, the gradually increasing difference observed between the two degradation profiles in graphs 4.4 and 4.5, was accounted for as this increase in the degraded particulate matter. Particulate matter was determined for the individual samples until day 14 and therefore, the percentage variation may also reflect the variation in the amounts of contaminants.

Comparing graphs 4.6 and 4.7 it was observed that the percentage variation was a

reflection of the values of the measured and ideal degraded particulate weights, indicating that the main sources of error were probably due to weight and volume measurements. The measured degraded particulate weight value was for a fraction of the total secondary filtrate, whilst the ideal was for the full volume, (Fig. 2.1). The fact that these variation calculations revealed an average of approximately ±2% indicated the accuracy and suitability of combining monomer and gravimetric analysis to measure both the undegraded and degraded fractions of the PHB(FM)TG samples. This was of particular interest when the co-blended samples were investigated in chapter 5.

The initial degradation studies between 1 to 6 hours, for both the monomer and weight loss profiles (Graphs 4.4B and 4.5B) were somewhat unreliable due to the errors involved in determining the comparatively small weights present. Generally, there was little degradation between 1 and 6 hours either by weight loss or monomer measurement. Although there was a noticeable difference of approximately 4-5% between the two analysis methods at the first reading of 1 hour. This was probably partially due to an initial loss of residual chloroform solvent coating the fibres, the ready collapse of some unstable fibres and the formation of degraded particles with a small amount of surface erosion to monomer.

The monomer analysis degradation profile was divided into 5 stages, 0-IV, (Graph 4.5). After the initial induction period at stage 0, where little degradation was observed, the concentration of HBA gradually increased during stage I between days 1 and 7 until approximately 31% degradation was measured. During this period it was observed that some fibres within the undegraded matrix lost their integrity and collapsed at the phial base to form a 'fibre fragment' mass. Some of these 'fibre fragments' were also trapped

within the matrix, from these and the fibres constituting the matrix itself, particulate matter formation and surface erosion to the monomer occurred. This increase in the surface area to volume ratio of the sample available to hydrolytic degradative action by the buffer medium, facilitated the degradation. The collapse of a proportion of these fibres may have been due to manufacture and handling induced structural weaknesses.

The 'step' stage II was observed between days 7 and 9 and occurred when the matrix had totally collapsed and formed a fibre fragment mass at the phial base. The compaction of this mass decreased the available surface area to volume ratio when compared to the matrix structure during stages 0-I, reduced the amount of degradation to monomer for a brief period. The step stage was also observed in graph 4.6 which showed similar values for degraded particulate matter at days 5 and 7. This displacement of the step stage to days 5 to 7 from days 7 to 9 in the monomer analysis profile reveals the progressive degradation of the matrix from fibre to fragments, to large particulate matter then to degraded particulate matter, eventually to the HBA oligomers and finally the monomer.

Following the step stage II, the degradation increased due to a greater amount of fragmentation to smaller fibre fragments and large particulate and degraded matter, this increased the surface area to volume ratio thus facilitating an increase in the degradation rate, so that an increase in monomer was determined in stage III until approximately 57% degradation around day 18.

At day 18 the degradation profile reached the terminal step stage IV, with a rate of approximately 0.7%dy.$^{-1}$ This was due to the degradation kinetics and a total collapse of

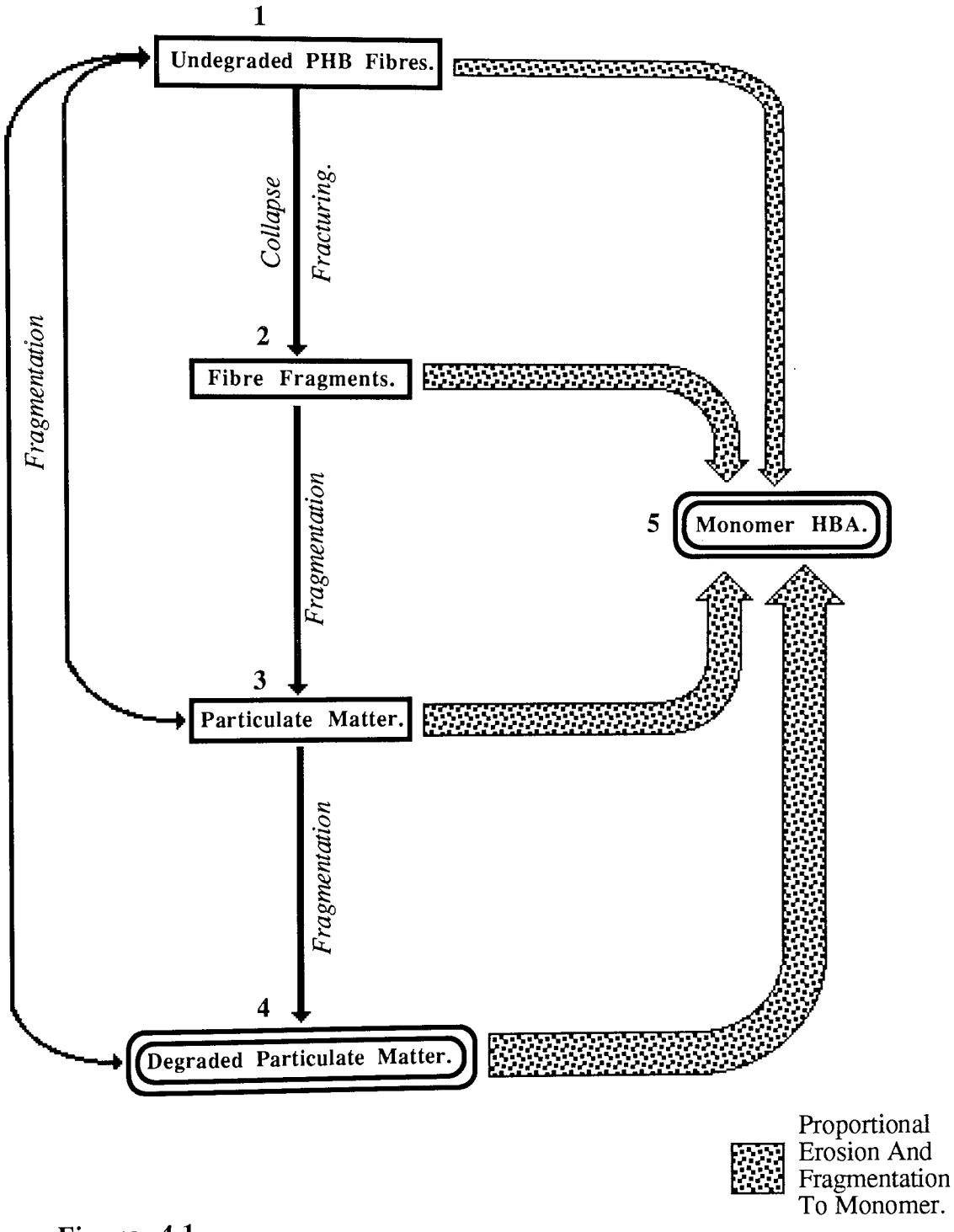

Figure 4.1.

Diagram Of Proposed Degradation Of PHB(FM)TG For Individual Fibres And Matrix

the fibre fragments to large particulate matter and their compaction at the phial base which reduced the available surface area to volume ratio. A final increase in the monomer production was detected at day 32, this was due to agitation of the phial during the final buffer changeover at day 28, which increased the surface area to volume ratio by displacement of the particles into the buffer medium and during settlement surface erosion and degradation to monomer rapidly occurred.

The weight loss profile exhibited similar stages but the degradation rates were slightly greater. These differences were due to the degraded particulate matter which were unaccounted for in the monomer analysis profile.

The residual dry weight profile was mirrored by the residual atmospheric equilibrated weight, ('wet' or 'standing' weight) indicating that the PHB adsorbed water from the atmosphere, with the weight of water proportional to the weight of PHB.

The difference between the monomer and the weight loss profiles, together with the observations of the matrix behaviour, (Graph 4.4), illustrated the progressive nature of the degradation mechanism, as proposed in figure 4.1. This degradative pathway occurred for individual fibres and as such all stages were present to varying extents during the course of the degradation when the matrix as a whole is considered, (Fig. 4.1).

4.2.2. Observations Of The Undegraded PHB(FM)TG During The Course Of Degradation.

The retentate samples of the filtered matrix from the degradation experiment were analyzed using phase contrast and scanning electron microscopy. It was also noticed during the mounting of these samples that the strength of the matrices were drastically reduced after the filtering and drying procedures, such that by day 2, the partially degraded fibrous mass readily crumbled into fine fibre pieces when gently handled with forceps. Therefore, the extent of fragmentation concerning those samples still maintaining some degree of matrix integrity before mounting could not be accurately determined, but only utilized as a comparative effect. The pre-mounted samples however, were found to be consistent with the degradative pathway derived from the degradation profiles, (Fig. 4.1).

Examination of the fibres from the sample degraded for 1 hour using phase contrast microscopy with water as a wetting medium, revealed the initial degradation of the matrix to be rather slow, with only a few fibres having collapsed to form smaller fibre fragments, whilst the matrix still maintained its integrity, (Plates 4.1 & 4.2). Fragmentation was rare, but observed in a few instances and this could have possibly been due to the mechanical damage caused by the drying and mounting procedures, (Plate 4.3). It was also noted that in some instances the fibre regions possessing cavities had bubbles which gradually reduced in size, probably due to the wetting medium entering via the pores. This occurred to a similar extent as those in the undegraded fibres. (Ch3). Some cavities also appeared to be structurally weak points and the bubbles provided internal pressure to facilitate the weakening of the fibre and its fragmentation at that point, (Plate 4.4).

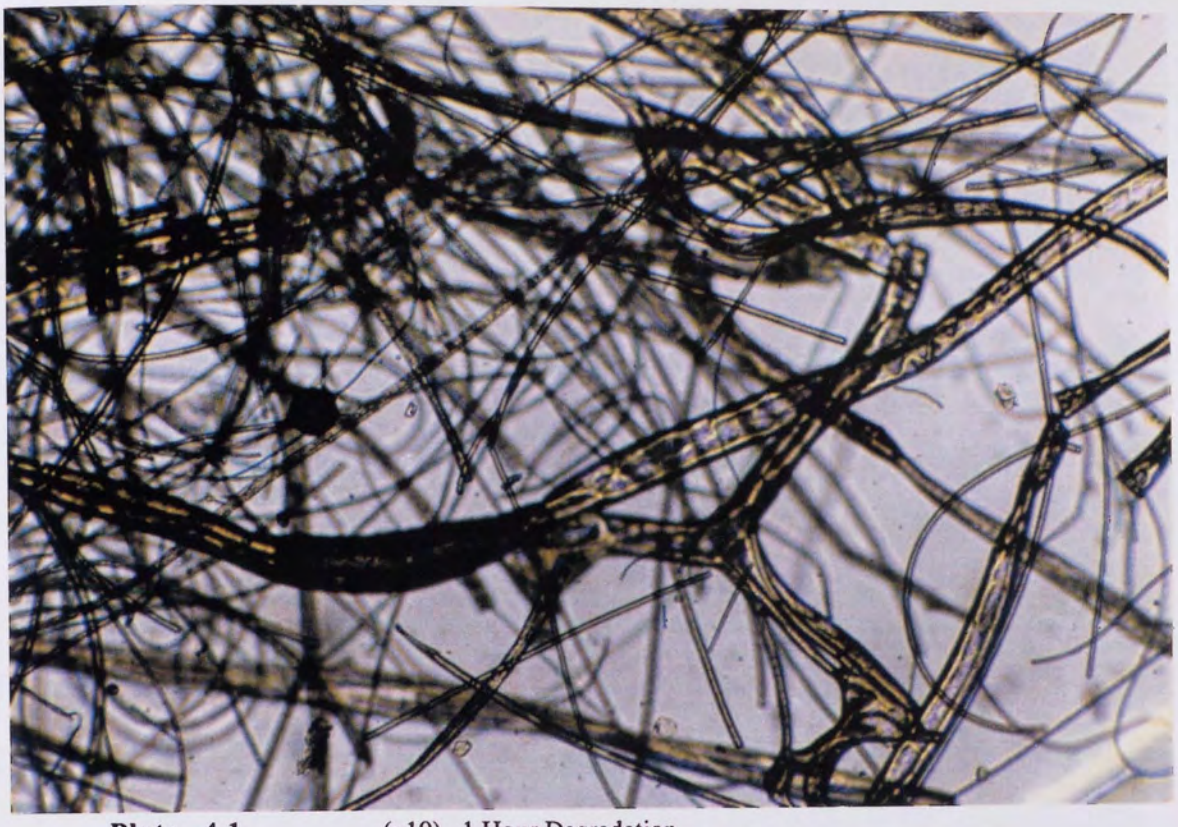

Plate 4.1. (x10) 1 Hour Degradation.
Partially Degraded PHB(FM)TG, Illustrating The Lack Of Fragmentation And Maintainance Of Matrix Integrity.

Plate 4.2. (x10) 1 Hour Degradation.
PHB(FM)TG; Illustrating The Comparatively Small Degree Of Fragmentation In The Initial Degradation Stage.

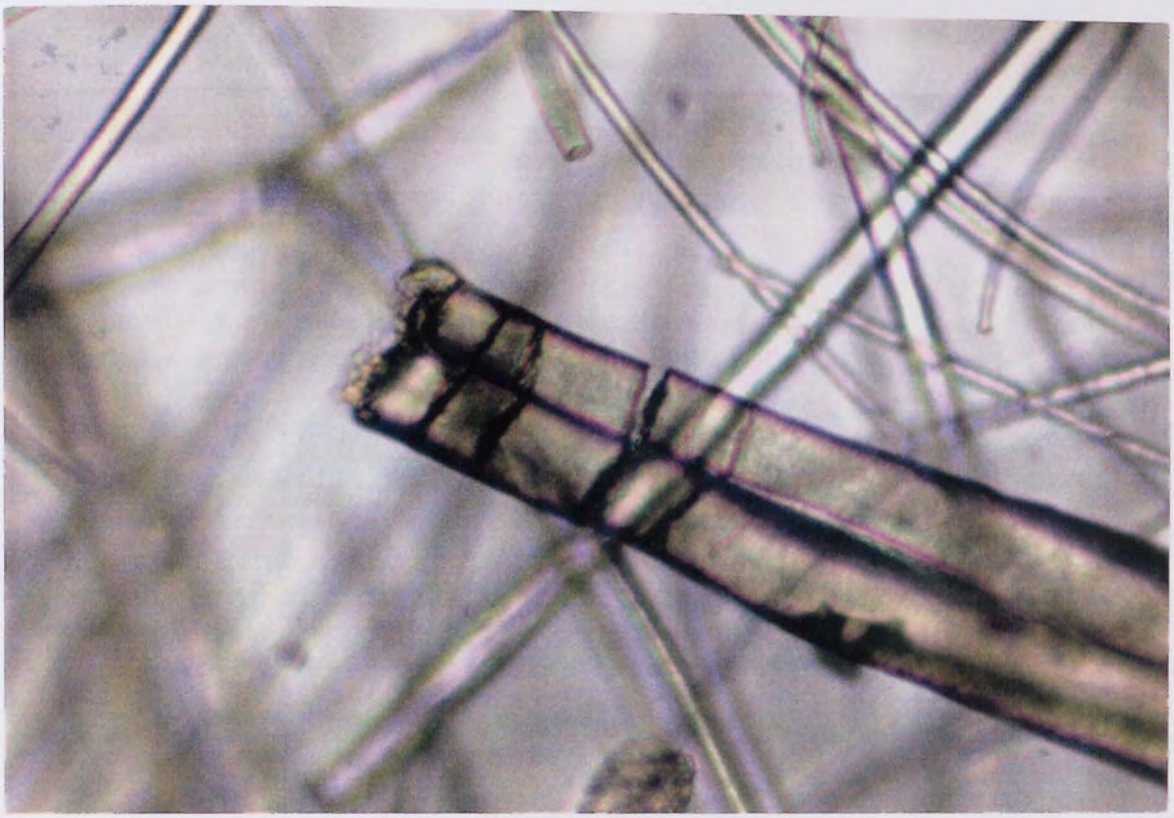

Plate 4.3. (x25) 1 Hour Degradation.
PHB(FM)TG; Illustrating The Fracturing In Some Medium Sized Fibres, Most Probably Due To The Filtering And Drying Procedures.

Plate 4.4. (x25) 1 Hour Degradation.
PHB(FM)TG; A Hollow Cavity With A Bubble Forming A Structurally Weak Point In The Fibre.

A large number of fibre pieces were observed for sample 3 hour, indicating that the collapse of the matrix was gradually progressing (Plate 4.5). This collapse appeared more noticeable in the larger diameter fibres and some of the smaller diameter, finer fibres, whilst the medium sized fibres appeared more resistant to mechanical breakdown and were still readily flexible. A larger proportion of fracturing occurred in the large diameter ranged fibres when compared to the 1 hour sample, (Plate 4.6). Fibres after 5 hours degradation appeared very similar to those from 3 hours. This slight change in the fibres between 3 and 5 hours degradation, yet the noticeable difference with the 1 hour sample, leads to the conclusion that a proportion of the larger and smaller diameter fibres were readily unstable as a result of manufacture and handling stresses. Therefore they collapsed within the first hour of hydrolytic action, whilst the remaining matrix was more resistant. Bubbles were still readily observed but these were somewhat reduced in size when compared to the cavity within the fibre, (Plate 4.7), indicating the gradual filling by the wetting medium of these cavities at a greater rate than observed for previous samples.

The fibres from sample 24 hours, 1 day degradation, readily collapsed upon handling with apparently all loss of mechanical integrity. A large amount of fibre fragments and large particulate matter were observed. However, the majority of pieces were still recognizable as fibrous, whilst comparatively large numbers of the fibres were observed to be relatively 'smooth', (Plate 4.8).

Some surface erosion was noticed in a number of fibre pieces after 2.29 days degradation, (2 days 7 hours). This was observed in varying degrees and did not appear directly related to the diameter size, (Plate 4.9), since other fibres of similar diameters were still relatively

Plate 4.5. (x10) 3 Hours Degradation.
PHB(FM)TG; Fragmentation And Gradual Collapse Of The Matrix.

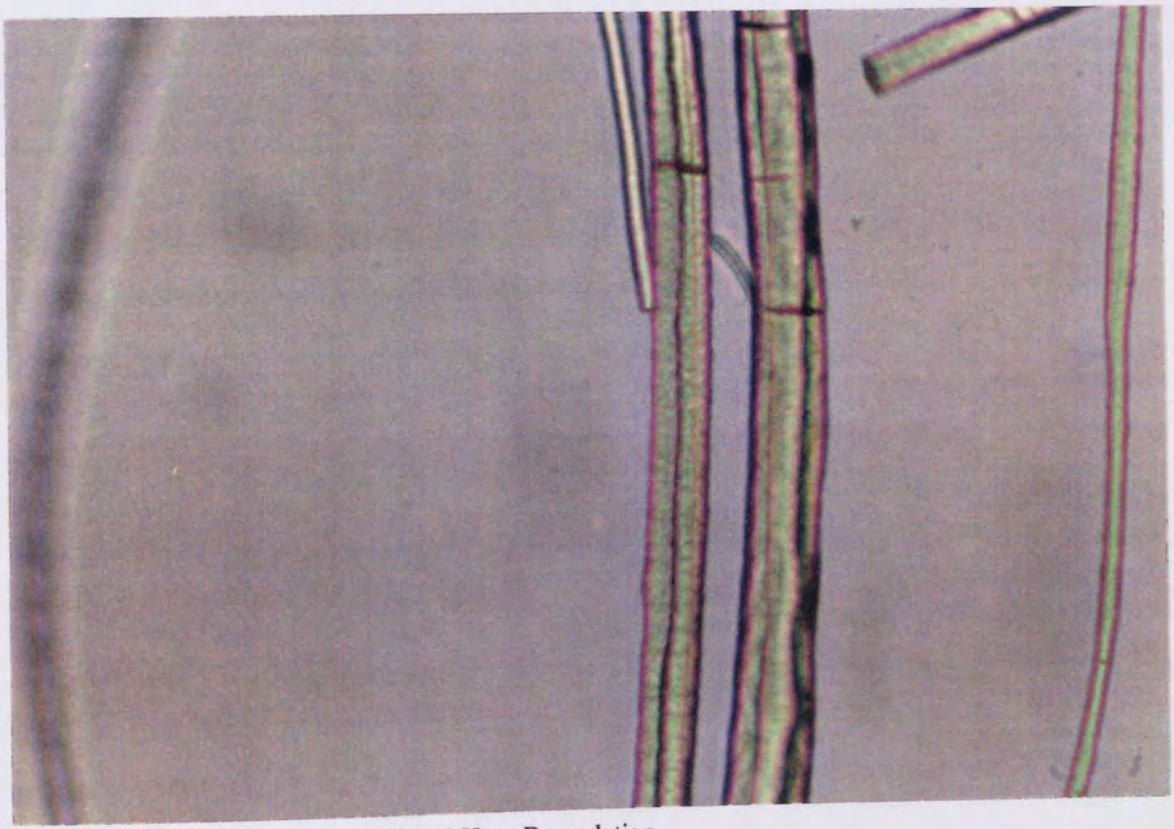

Plate 4.6. (x10) 1 Hour Degradation.
PHB(FM)TG; Hollow Regions In The Smaller Diameter Fibres And Bubble In The Large Diameter Fibre.

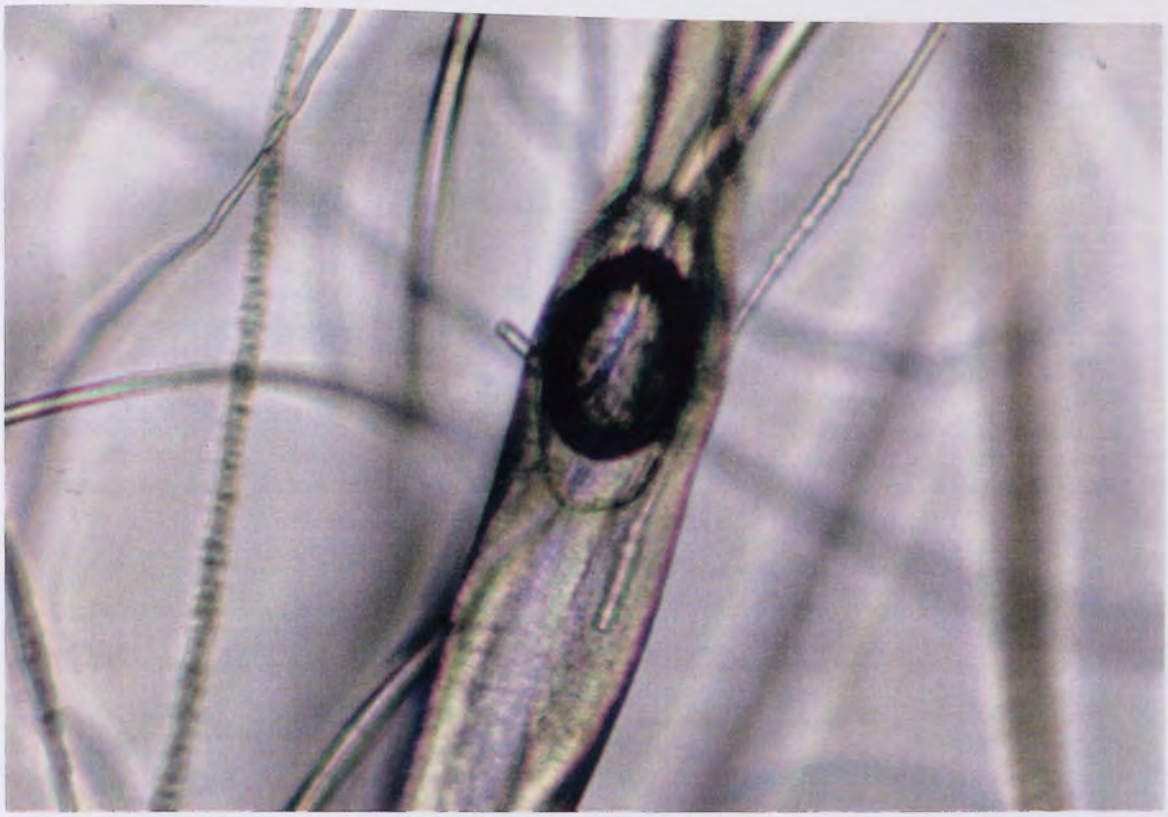

Plate 4.7. (x25) 5 Hours Degradation.
PHB(FM)TG; Gradual Reduction In Bubble Size, Indicating The Filling Of The Cavity With Degrading Medium.

Plate 4.8. (x10) 1 Day Degradation.
PHB(FM)TG; Hollow Regions In The Smaller Diameter Fibres And Bubble In The Large Diameter Fibre.

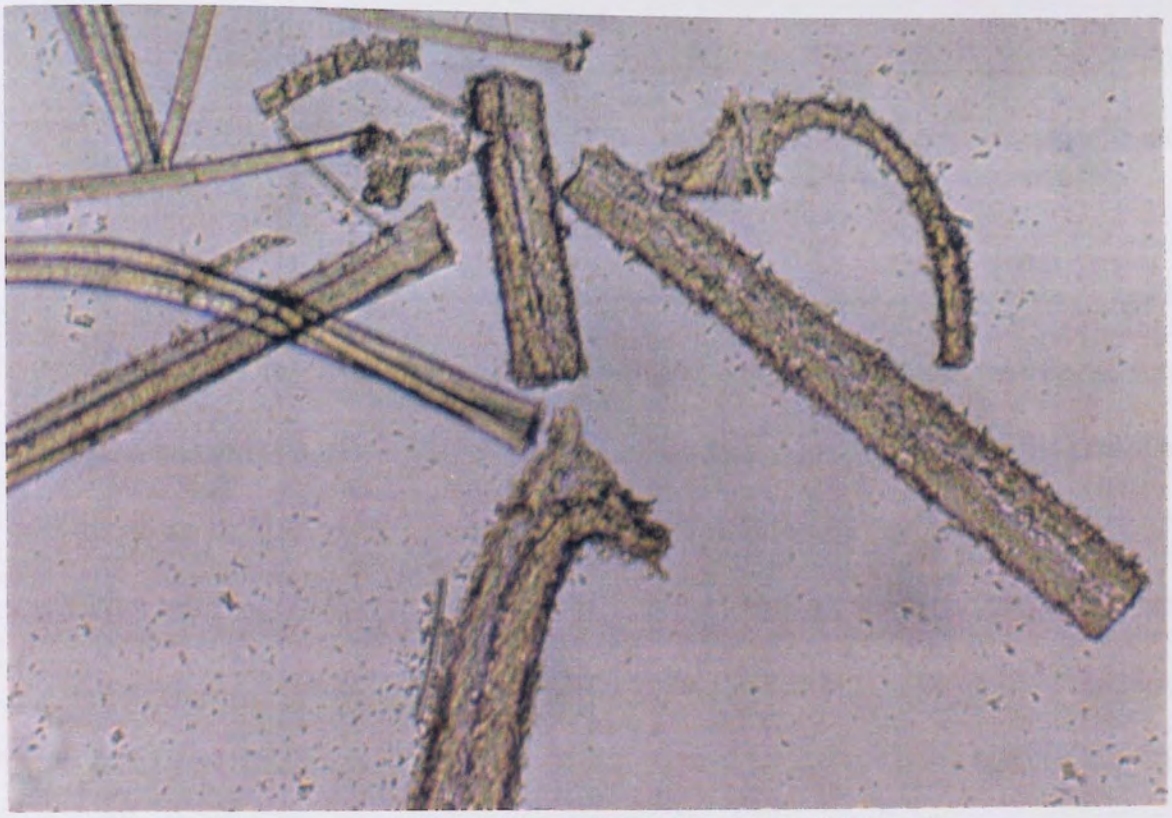

Plate 4.9. (x25) 2.29 Days Degradation (2 Days & 7 Hours).
PHB(FM)TG; Surface Erosion Of A Proportion Of Fibres.

Plate 4.10. (x10) 2.29 Days Degradation (2 Days & 7 Hours).
PHB(FM)TG; Fibre Specific Surface Erosion And A Proportion Of Unaffected, Comparatively Smooth Fibres.

'smooth' and undegraded, (Plate 4.10). Thus, it was concluded that those fibres with a large amount of pores were more susceptible to surface erosion and degradation than their smooth counterparts, due to their larger surface area to volume ratio, this behaviour may also be due to the presence of amorphous contaminants within the fibres. It is also possible that these porous fibres were similar to the unstable ones that readily collapsed during the early stages of the degradation experiment. However, the compaction effect may also have been responsible for some of these fibres being less eroded. A number of bubbles were still observed in some large diameter fibre fragments, (Plate 4.11). these tended to be rather small and further away from the fibre surface than the other bubbles in the more readily collapsible fibres, in these fracturing at the weakest point had occurred and released the bubble, (Plate 4.12).

At day 5, fragmentation of the fibres had readily occurred with a total collapse of the matrix during degradation and the formation of both large quantities of 'semi-fibrous' and large particulate material, (Plate 4.13), such that upon wetting, a dense cloudy mixture was noticed. Surface erosion had occurred in all fibres to a similar extent to that of sample fibres from day 2.29, (Plate 4.14).

The final noticeable stages of degradation were observed at day 7 where it was difficult to distinguish the fibrous remains. The undegraded material formed a dense, caked mat of PHB, after the filtering and drying processes. Multiple fragmentation in all directions was obvious within the fibre remains, (Plates 4.15 & 4.16). The samples obtained after 9, 14 and 32 days degradation were very similar and no noticeable differences except for an availability of material were observed.

Plate 4.11. (x15) 2.29 Days Degradation (2 Days & 7 Hours).
PHB(FM)TG; Hollow Cavity With Bubble.

Plate 4.12. (x25) 2.29 Days Degradation (2 Days & 7 Hours).
PHB(FM)TG; Hollow Cavity With Fracture And Absence Of Bubble.

Plate 4.13. (x10) 5 Days Degradation.
PHB(FM)TG; Loss Of Matrix Integrity And The Presence Of Particulate Matter.

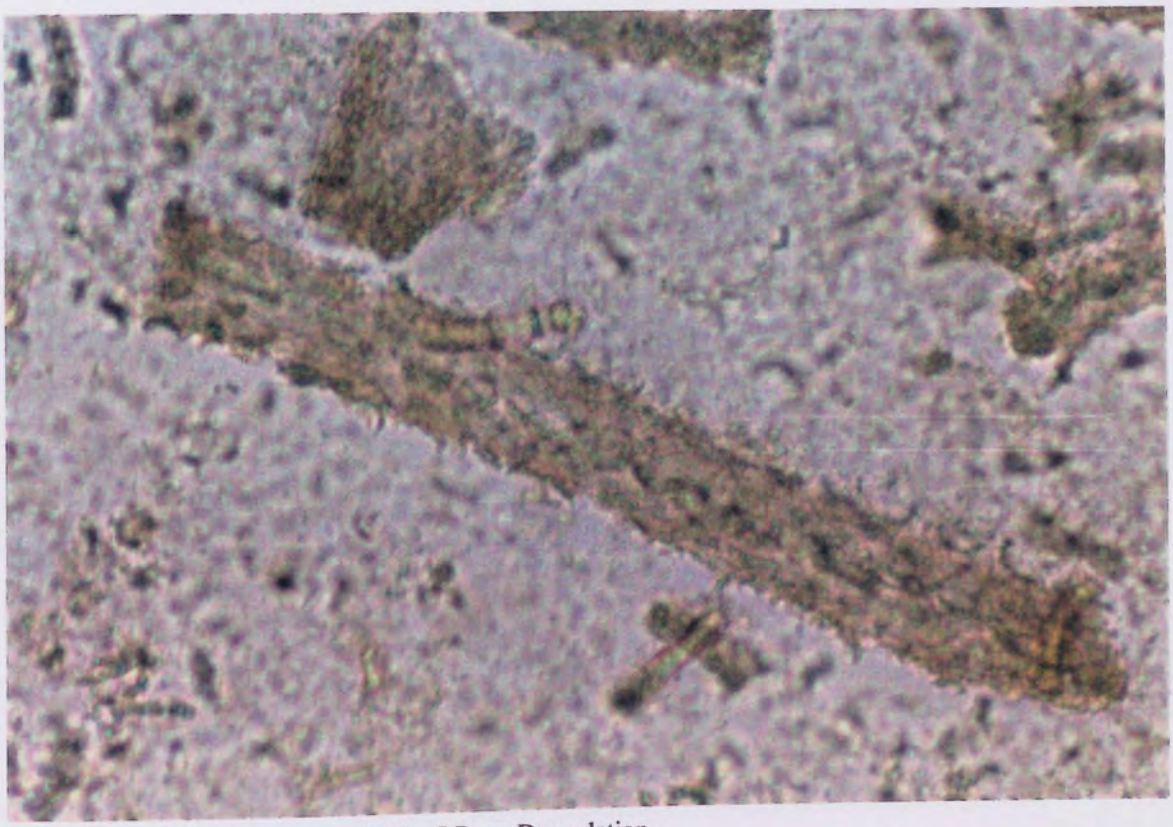

Plate 4.14. (x25) 5 Days Degradation.
PHB(FM)TG; Surface Erosion Observed At All Fibre Surfaces.

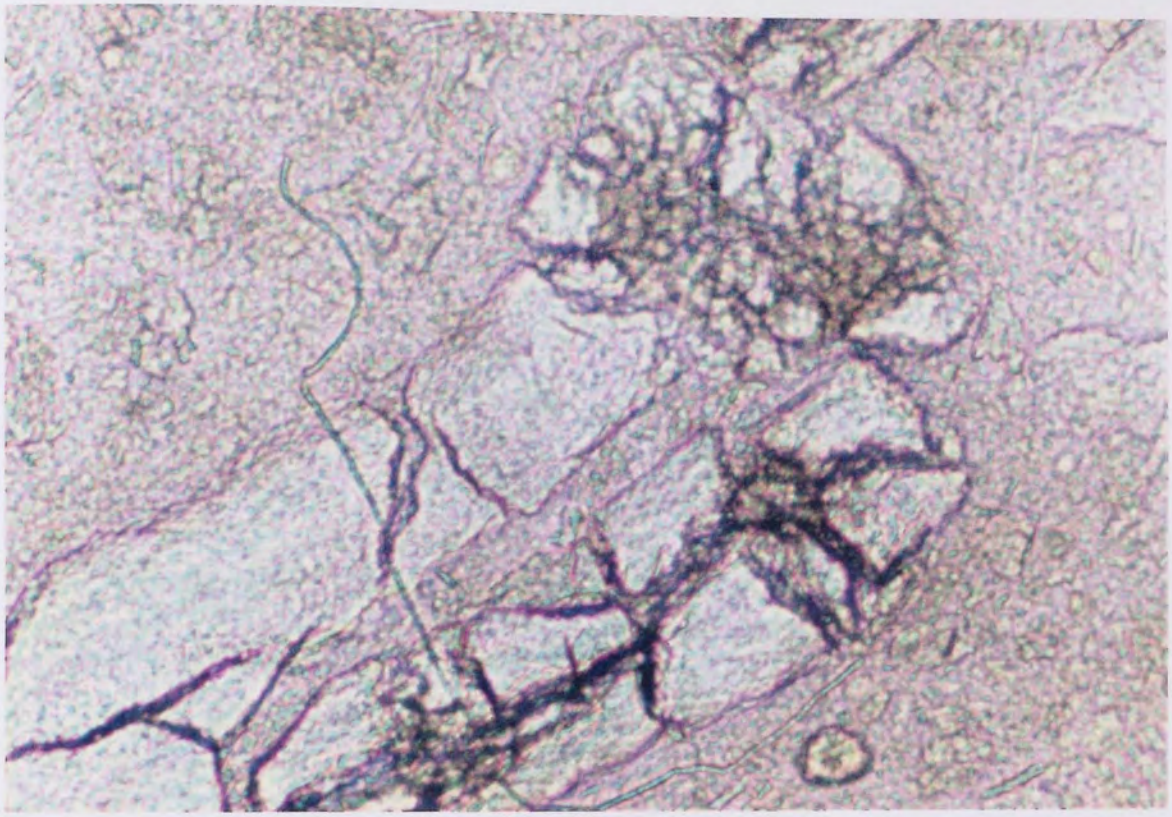

Plate 4.15. (x25) 7 Days Degradation.
PHB(FM)TG; Fibrous Remains With Multiple Fragmentation In All Plains Eventually Leading To The Formation Of Monomer.

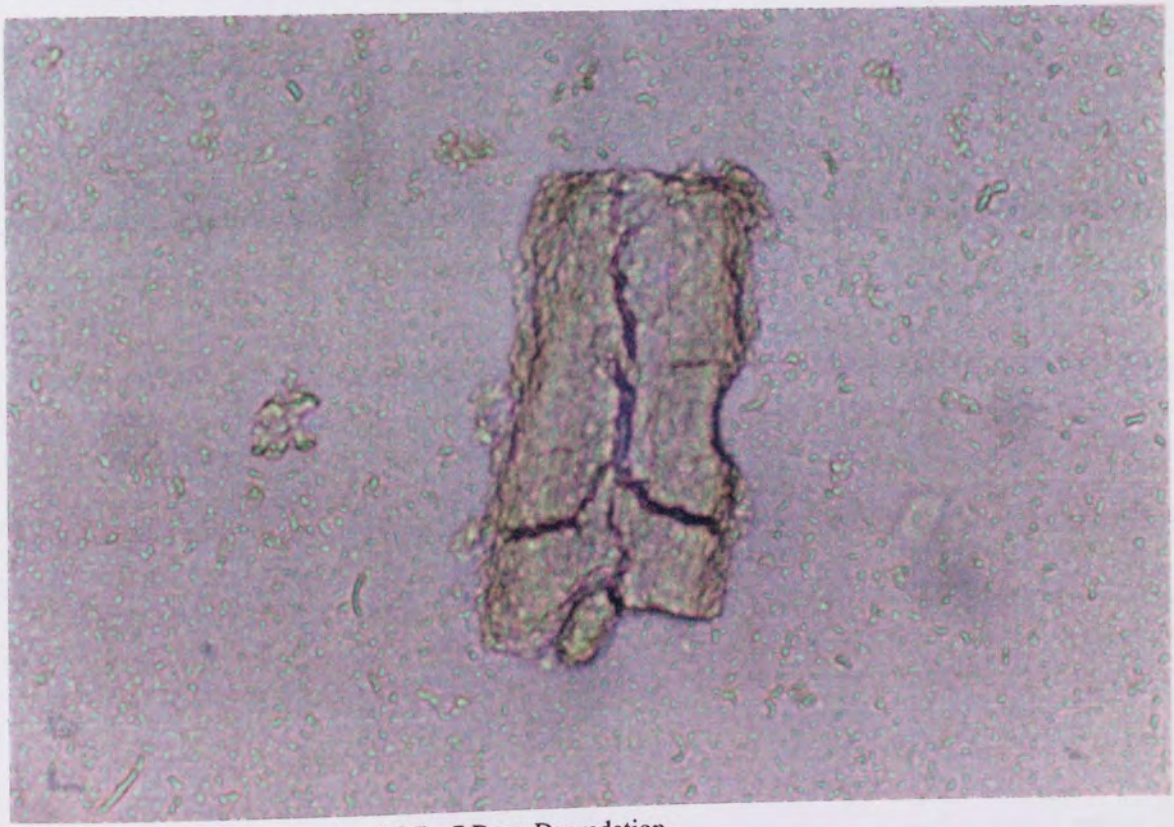

Plate 4.16. (x25) 7 Days Degradation.
PHB(FM)TG; Fibre Fragment With Multiple Fragmentation.

Similar to the phase contrast examinations, scanning electron microscopy of the fibre samples after 1 hour degradation revealed little change in the structure of the matrix, when compared to the undegraded sample. However, it was noticed in some instances that the larger diameter fibres had broken, this was most probably due to the mounting process. (Plate 4.17) It was also observed that fine crystalline structures were present on a large number of fibres, (Plates 4.17-4.18). These were probably crystals formed by the residual saline buffer which was trapped by the matrix during the filtration process and this confirms the error source of volume measurement for this sample and samples 3 and 5 hours, where similar structures were also observed, (Plate 4.19).

Fibre collapse had occurred by day 2.29 and some of the larger diameter fibre fragments had noticeable pores and rough surfaces, (Plate 4.20), whilst fragmentation of some of these revealed the hollow nature of certain regions and their structural weakness, (Plate 4.21). The fragmentation of the fibre pieces at day 5 observed with the phase contrast were similarly revealed using the SEM, (Plate 4.22). This fragmentation appeared to have occurred within all the diameter ranges and was not limited to the structurally weak points as previously observed, although the larger diameter fibre fragments did seemingly appear to be somewhat more susceptible. (Plate 4.23) Examination of the fibres from day 7 revealed a dense mass of particulate matter, with some of the more degradation resistant, larger diameter fibre pieces still being noticeable. Fracturing was observed to occur in all plains, with pitting and irregularities of the fibre surfaces, (Plate 4.24).

The most noticeable difference observed between the fibre samples using SEM was a change in the fibre diameter distribution. (Graphs 4.8-4.13). These changes were due to

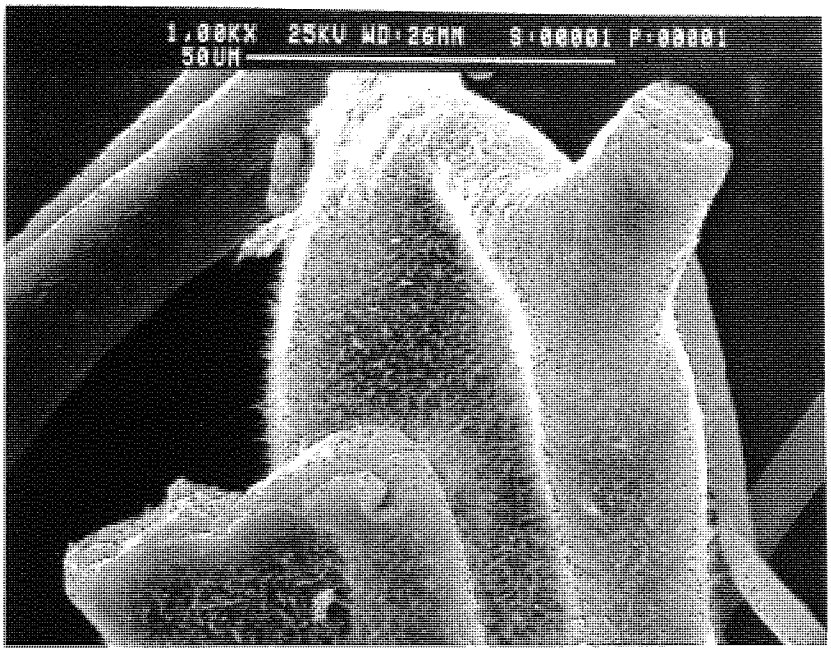

Plate 4.17. (x1.00K) 1 Hour Degradation.
PHB(FM)TG; Fibre Fragmentation And 'Furry' Surface.

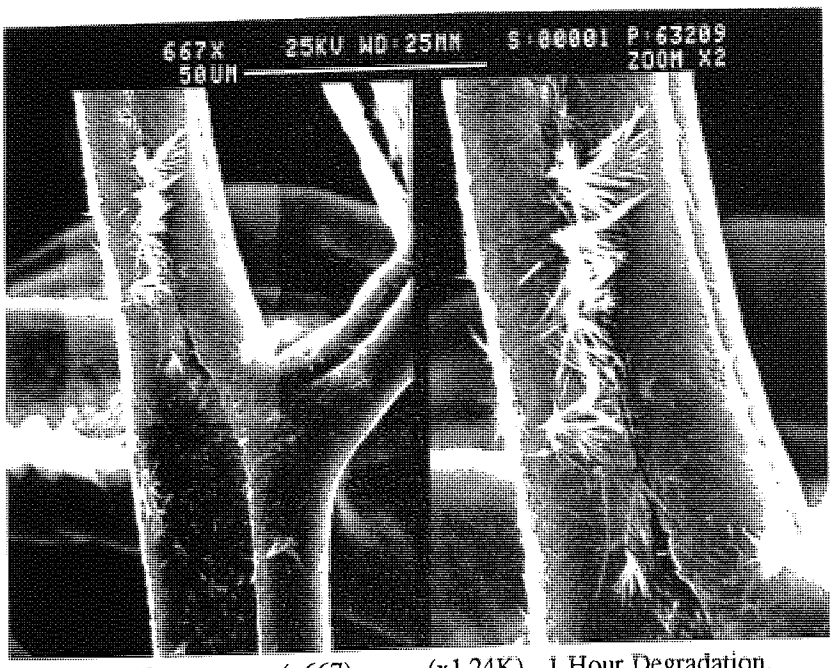

Plate 4.18. (x667) (x1.24K) 1 Hour Degradation.
PHB(FM)TG; Fibre Fork With Crystalline Formations Of 'Trapped' Dried Buffer Salts.

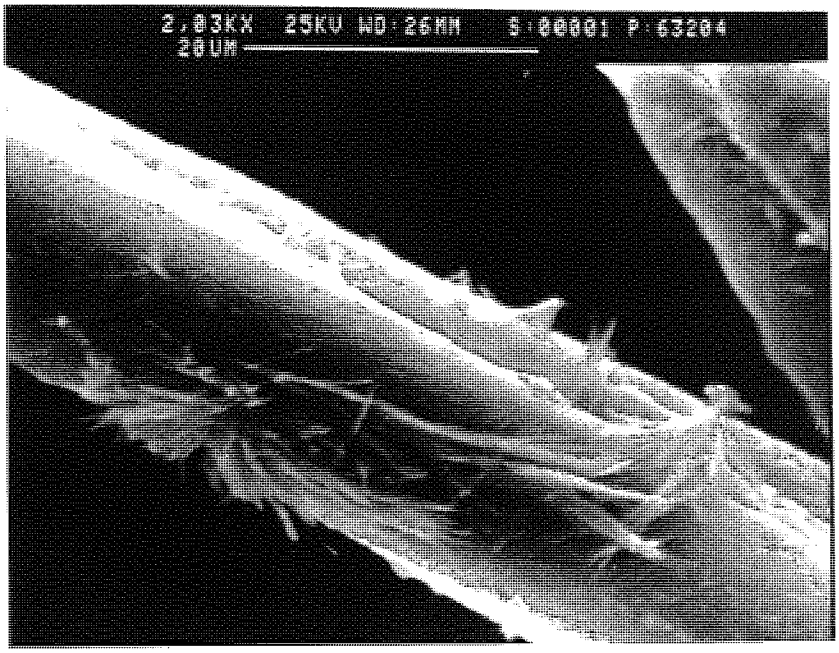

Plate 4.19. (x2.03K) 3 Hours Degradation.
PHB(FM)TG; Crystalline Formations Of Dried Buffer Salts Trapped By The Matrix.

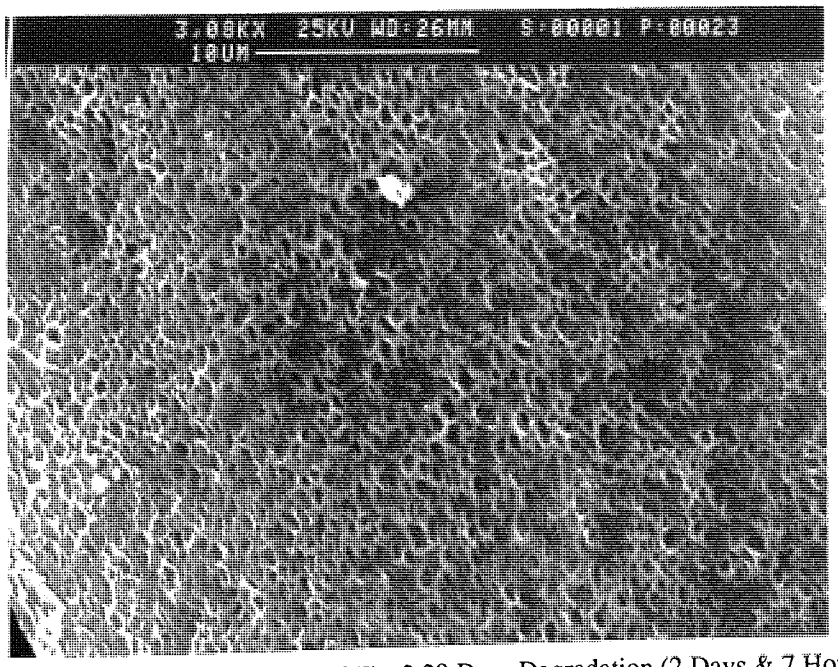

Plate 4.20. (x3.08K) 2.29 Days Degradation (2 Days & 7 Hours).
PHB(FM)TG; Large Diameter Fibre With A Heavily Porous Nature.

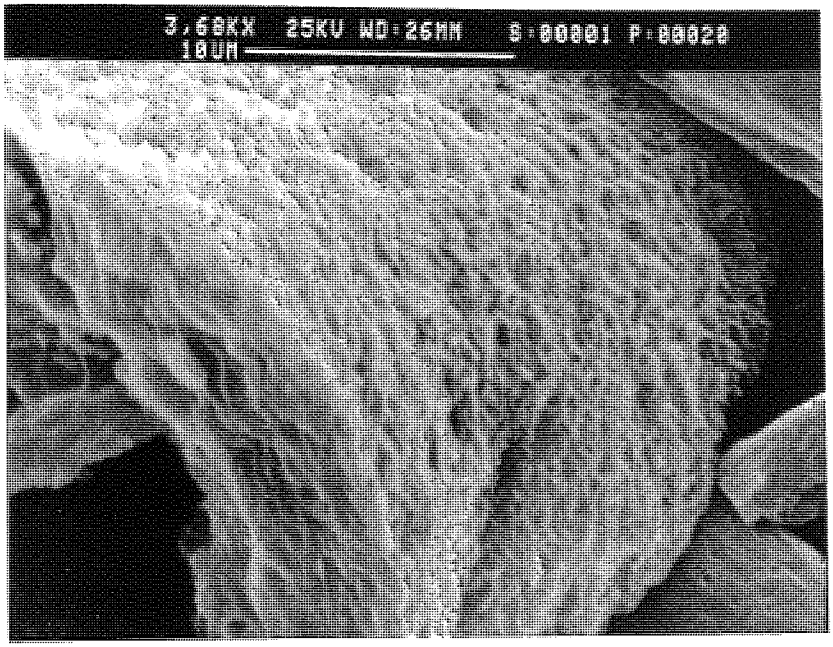

Plate 4.21. (x3.68K) 2.29 Days Degradation (2 Days & 7 Hours).
PHB(FM)TG; Pitted Surface Of Large Diameter Fibre Fragment, Illustrating A Hollow Region.

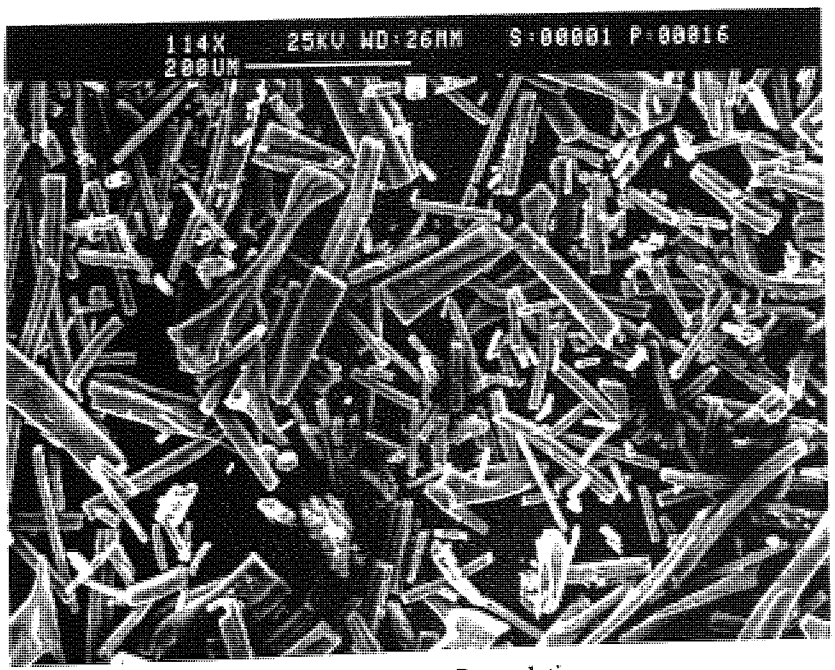

Plate 4.22. (x114) 5 Days Degradation.
PHB(FM)TG; Matrix Collapse And Fibre Fragmentation.

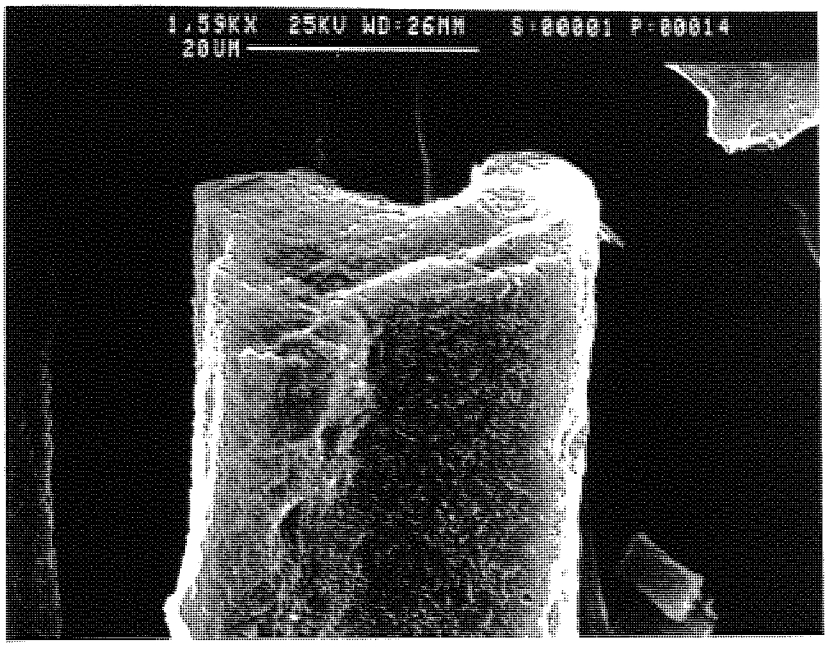

Plate 4.23. (x1.59K) 5 Days Degradation.
PHB(FM)TG; Fragment Of A Large Diameter Fibre With An Irregular And Pitted Surface

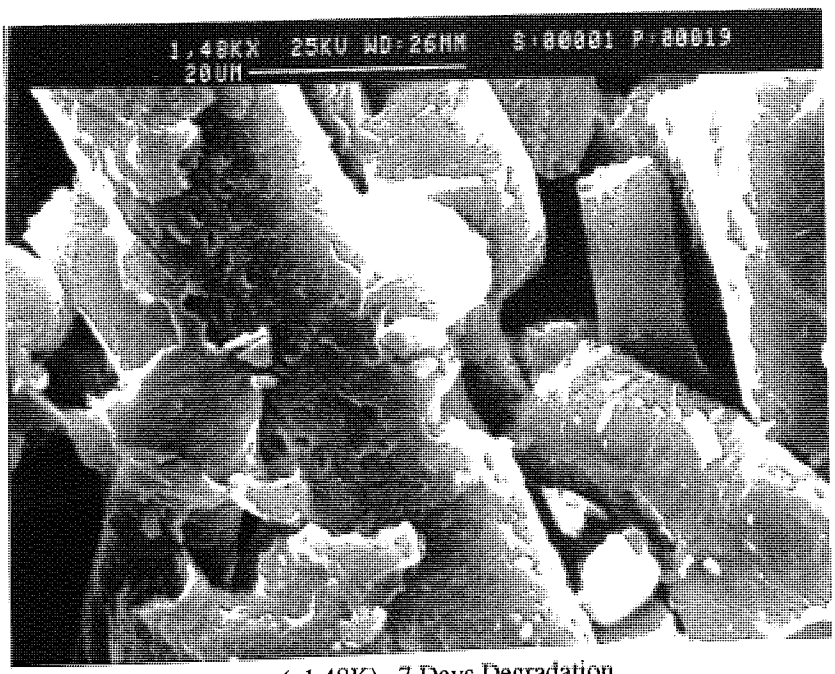

Plate 4.24. (x1.48K) 7 Days Degradation.
PHB(FM)TG; Multiple Fragmentation To Fibre Fragments And Large Particulate Matter.

surface erosion during degradation and fragmentation to the fibre fragments. The latter of which affected the count and therefore was an indication of the susceptibilty of the fibre diameter groups to fragmentation/degradation.

The distribution of diameters for fibres sampled after 1 hours degradation, (Graph 4.8), revealed a marked change from the distribution of the undegraded fibres, with a main peak of approximately 18% at 5-6 microns, whilst the undegraded fibres had main peaks at 1-2 and 4-5 um. Although the frequency of fibres with diameters greater than 15um. remained the same, an abscence of fibres at the 0-1 um. range was observed, when compared to the undegraded fibres which had a frequency of 8%. These very small diameter fibres probably fragmented into large particulate matter and gradually to the monomer. A reduction of the frequency at 1-2 um. was also noticed, thus there was an increase in the large diameter fibres. However, after 3 hours degradation (Graph 4.9) it was observed that the fibre distribution tended to form three peaks with approximately 16% frequencies for each diameter range; 4-5, 8-9 and 15+ microns, ie: small, medium and large diameters. A few of the larger diameter fibres (15+ um.) which readily fragmented within 3 hours of degradation were observed, this increased the distribution of these fibres from 8% at 1 hour to 16%, however, after this period fragmentation was more limited to the small and medium sized diameters, such that the distribution by 5 hours maintained a maximum peak at 4-5um. with a slightly reduced frequency of 14%, whilst the general distribution for the full range was more 'level', (Graph 4.10). These results indicated that the fragmentation occurred over the whole diameter range, but that a number of the larger diameter fibres were relatively more resistant to the degradation process at this stage.

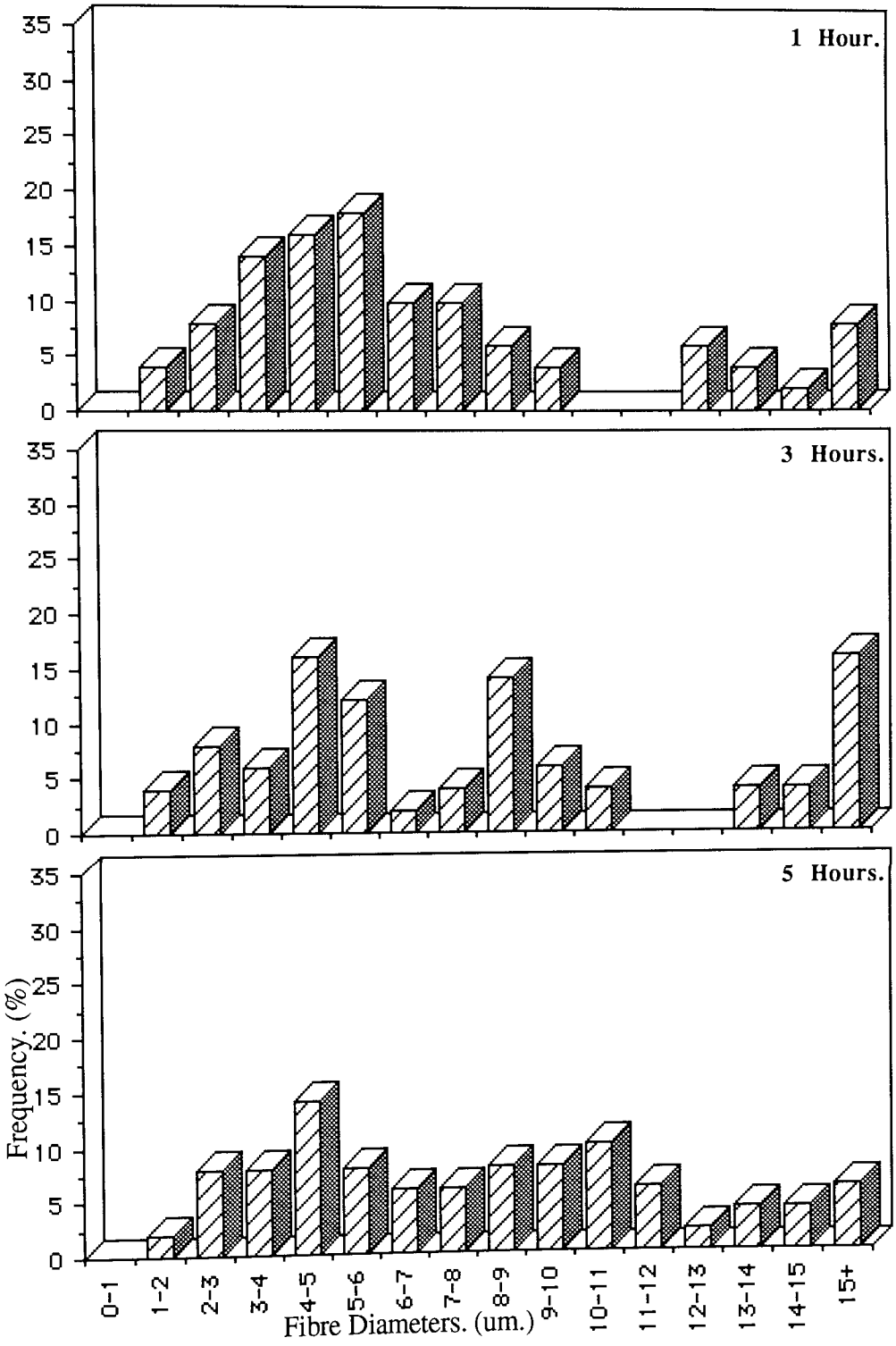

Graphs 4.8. To 4.10.

Fibre Diameter Distributions For Sample PHB(FM)TG During Degradation In The Accelerated Degradation Model.

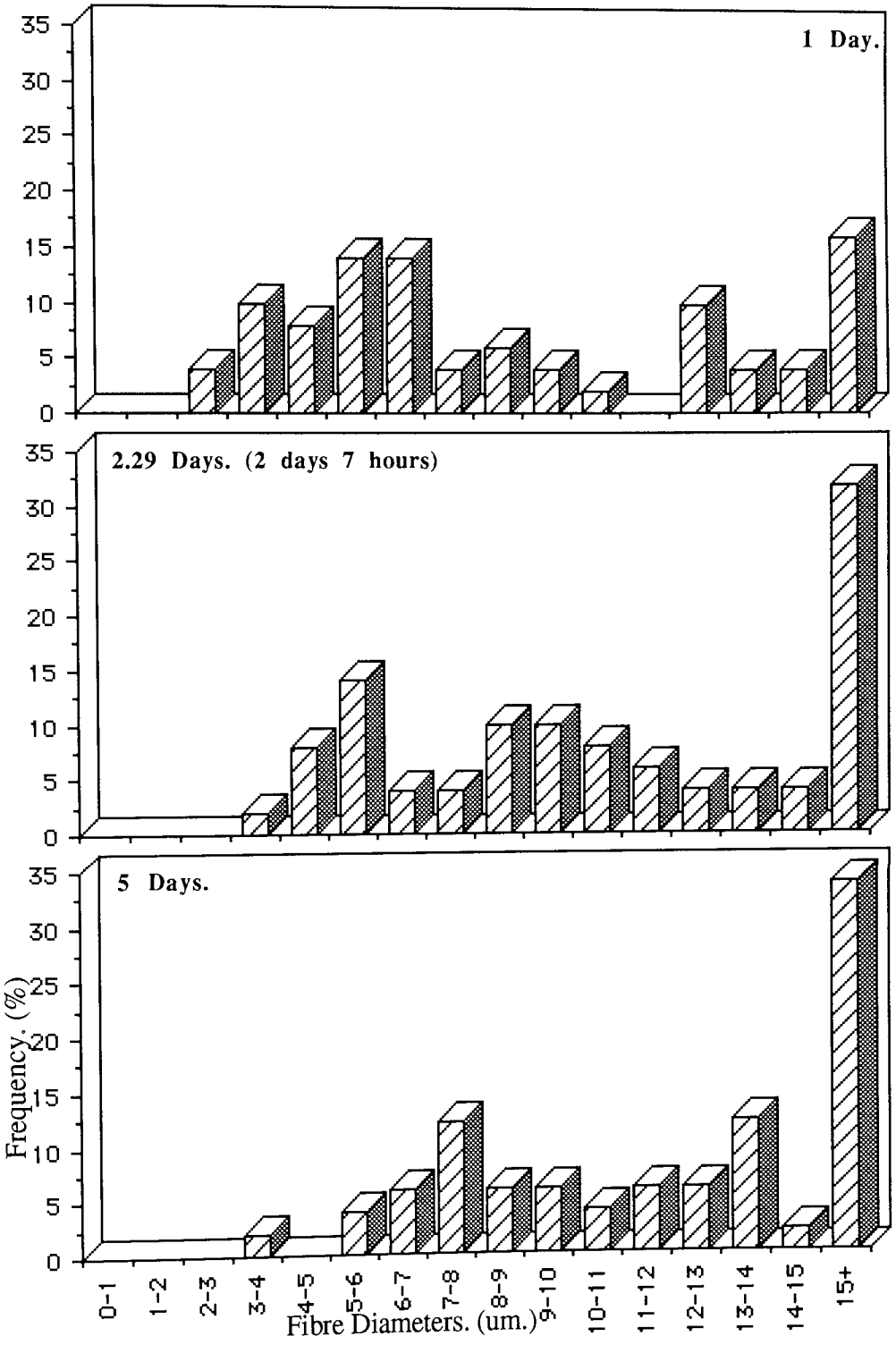

Graphs 4.11. To 4.13.

Fibre Diameter Distributions For Sample PHB(FM)TG During Degradation In The Accelerated Degradation Model.

Thus, in the initial stages of the degradation process (1-5 hrs) the proportion of fibres counted with diameters below 6 microns, ie: small diameter range, decreased with time from 64% in the undegraded sample to 60, 46 then 40% frequency, for 1, 3 and 5 hours degradation respectively. The medium diameter ranged fibres (6-15um.) correspondingly increased from 28% to 34, 45 and then 54%. The large diameter group (15+um.) had a periodic peak at 3 hours and then apparently decreased, this was probably a result of the counting procedure, whilst those fragmenting were a small proportion of unstable fibres.The reduction in the frequency of the smaller diameter fibres may also have been due to surface erosion to monomer and fragmentation to large particulate matter, the former was determined by HBA analysis to be of a low value, whilst the latter, although given credence by the weight loss profile, was not observed to any great extent using phase contrast and scanning electron microscopy. Consequently, it could be concluded that surface erosion and the formation of large undegraded and small degraded particulate matter were less responsible for the fibre diameter change, and therefore the degradation process in the initial stages, than the fragmentation of the fibres themselves.

The results of the fibre diameter distribution were separated into groups; small, medium and large diameters with values <6, 6-15 and >15um. respectively. These were then represented graphically, with the frequency versus time of degradation, (Graph 4.14).

From graph 4.14 and the phase contrast/SEM observations it was observed that within the initial stage the low diameter fibres decreased sharply in frequency whilst the medium sized fibres fractured and increased in number. Unstable large diameter fibres fractured within 3 hours and thus a frequency increase was observed, but this then decreased due to

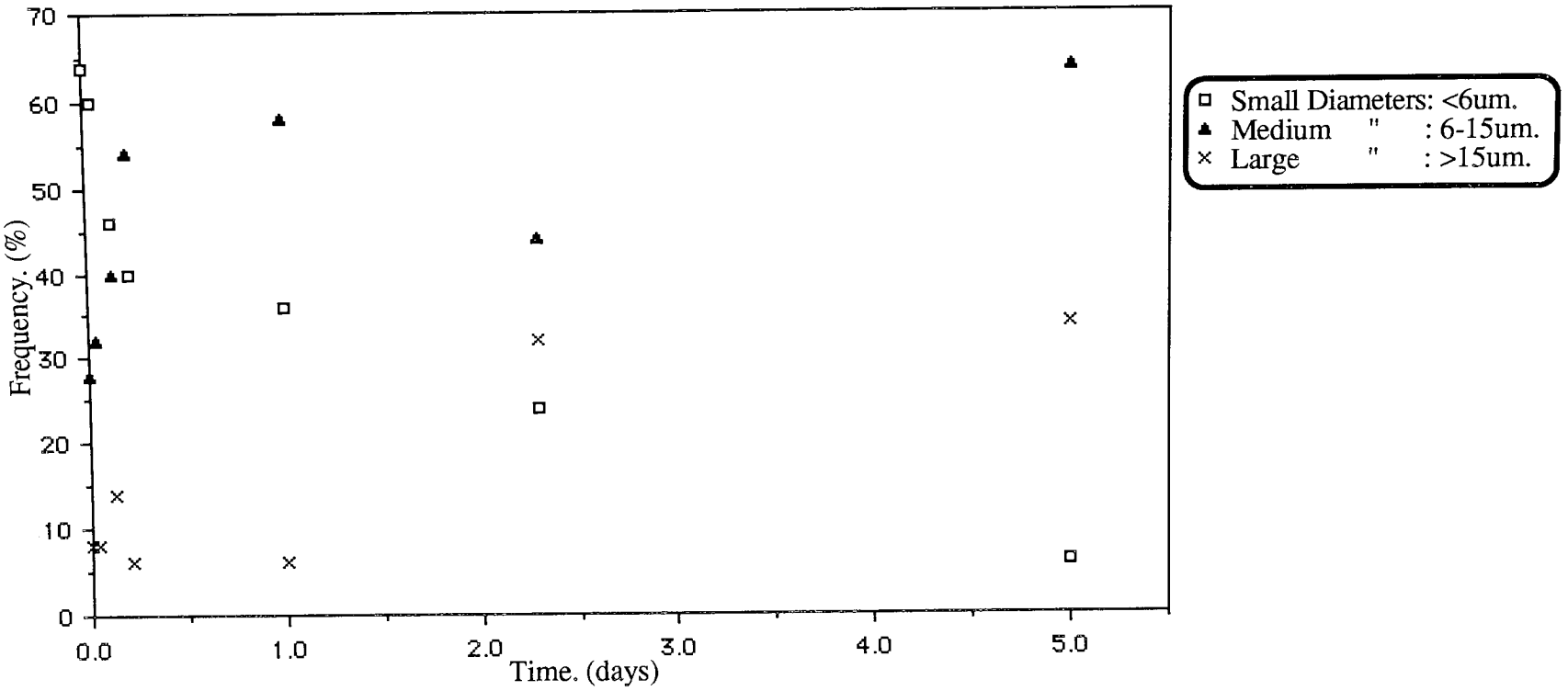

Graph 4.14.

General Fibre Diameter Distributions For Sample PHB(FM)TG, During Degradation In The Accelerated Degradation Model.

a larger proportion of medium diameter fibres and the degradation resistance of the remaining large diameter fibres and fibre fragments. In the later stages (Days 1-5) the small diameter fibre frequency continued to reduce, this was due to fragmentation forming large particulate and degraded matter which was uncountable. The fragmentation of the medium diameter fibres increased to a maximum by day 5, whilst the larger fibres also fragmented but at a slower rate than the smaller and medium sized fibres. The determination of the fibre diameter distributions for the samples between days 7 and 14 was impossible due to the lack of discernible fibre fragments and thus the matrix had finally degraded to a mixture of undegraded and degraded particulate matter, whilst surface erosion was observed at all surfaces, (Plate 4.14).

It was noticed that certain fibres from sample day 5 retentate were agglutinated, some of these were originally present in the undegraded sample, (Chapter 3), whilst a number of others could have been 'stuck' together by the degradation and mounting processes. In those instances where fibres of different diameters were agglutinated they were measured and counted as individual fibres. In other cases the fibres were classified as a single large diameter, these usually occurred with three fibres having essentially the same diameters of 12-14um. This naturally introduced a further error for consideration.

Thus, measurements of fibre diameter distribution provided a comparative quantitative indication to the degradative nature of the PHB(FM)TG and the relevent strengths and structural ability of the fibres themselves. This information was also facilitated by the qualitative observations obtained using SEM and phase contrast microscopy.

4.2.3. Characterization Of The Partially Degraded PHB(FM)TG Samples.

4.2.3.1 Differential Scanning Calorimetry (DSC) Studies.

The sample retentates were examined using differential scanning calorimetry. (DSC) A mean of a number of readings were obtained and the correlation between these were, apart from a few instances, considerably good.

The DSC traces were dependent upon the weight and packing of the sample in the holder, therefore the actual size of the curve acted only in a comparative means. Generally it was observed that the heat flow curves shifted to the lower temperatures during the course of the degradation process. It was also noticed that after 5 days degradation they tended to 'flatten' and occupy a greater temperature range, after this they then tended to form a more narrow distribution. This trend is illustrated in figure 4.2. This indicated a gradual decrease in the stability of the sample and the formation of different molecular weight material within the partially degraded matrix. Studies of the fibre samples during the initial stages of degradation were affected due to the presence of the buffer salts and other non-dissolved contaminants trapped within the matrix. (Sec. 4.1.2.).

Graph 4.16 illustrates the change in the melting points of the sample during the degradation. It can be observed that the melting points decreased sharply from 170°C. at day 0, undegraded, until 143°C. after 5 days degradation and then gradually to 135°C. at day 14, thus indicating a decrease in the stability of the matrix and its subsequent increased susceptibility to degradative action.

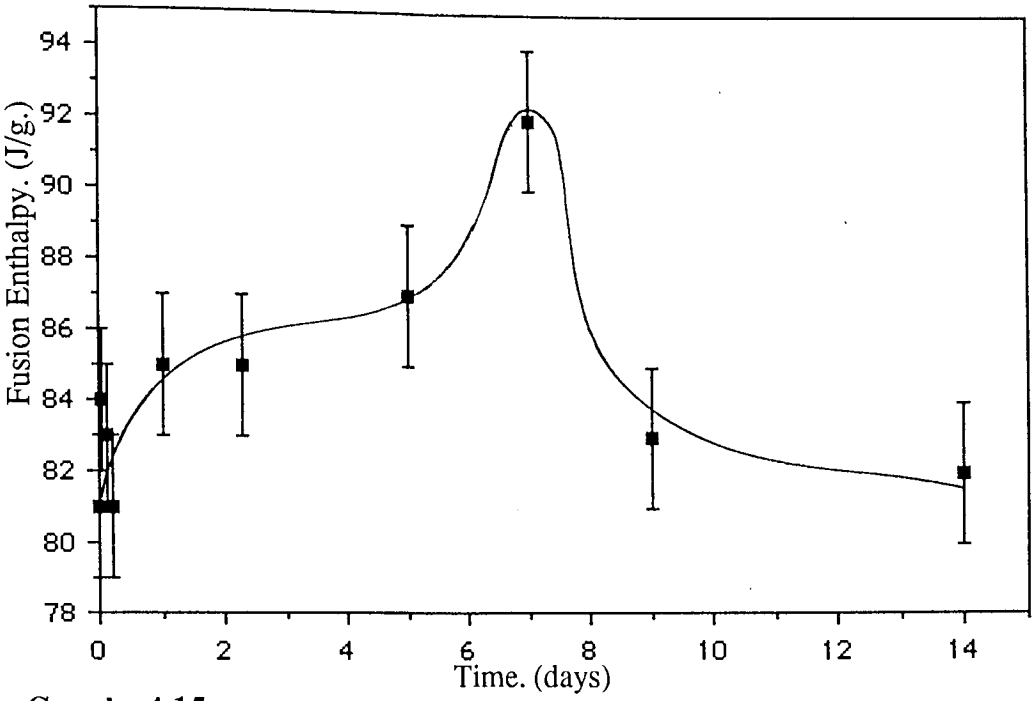

Graph 4.15.

Change In The Fusion Enthalpy Of Sample PHB(FM)TG During Degradation In The Accelerated Degradation Model.

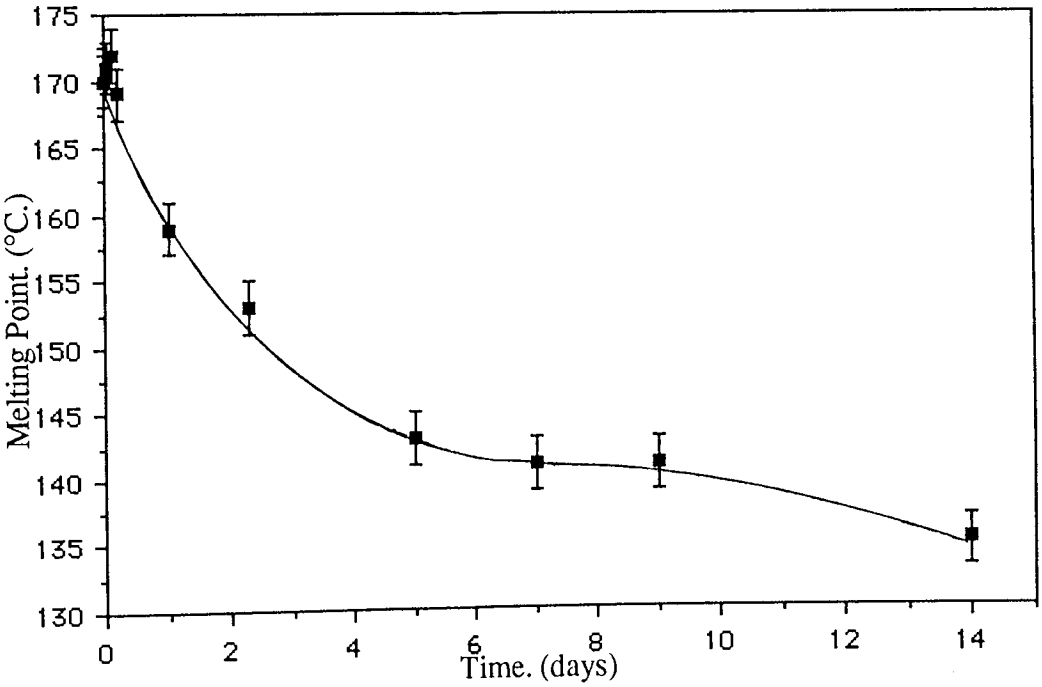

Graph 4.16.

Change In The Melting Point Of Sample PHB(FM)TG During Degradation In The Accelerated Degradation Model.

Graph 4.15 illustrates the fusion enthalpy of the sample during degradation, from this it was noticed that the fusion enthalpy rose rapidly from 74 to around 85Jg.$^{-1}$ at day 1 maintained this level until day 2.29 when it gradually rose to 92Jg.$^{-1}$ at day 7, before rapidly decreasing to 83Jg.$^{-1}$ and maintaining a similar level until day 14. The fusion enthalpy was utilized as a measure of the percentage crystallinity and thus the same trends were present, with a rise from 70% crystallinity in the undegraded sample to 80% at day 1 and maintaining this value until day 2.29 before rising to a maximum of 87% by day 7. This indicated that the amorphous parts of the matrix were probably present in two types; the readily available, possibly in the form of surface coating or non-fibrous material, which readily dissolved into the buffer medium within the initial stages of degradation, (Primary amorphous regions), and the more degradation resistant amorphous material, this was probably bound within the fibres and was not readily available for degradation either by a reduced available surface area due to location eg: shielding by crystalline PHB, or chemically more resistant, (Secondary amorphous regions). This amorphous material was gradually degraded and a corresponding collapse of the matrix was observed. (Sec. 4.1.2.). By day 7 maximum crystallinity was attained (87%) and after this the percentage crystallinity decreased dratically until 79 and 78% for days 9 and 14 respectively. This sudden decrease indicates that the previously crystalline matter was then degraded into more amorphous material, with a rapid collapse in crystallinity and fusion enthalpies between days 7 and 9.

The peak in crystallinity occurred at day 7, when the fibrous matrix had collapsed into large and small particulate matter with no diameters discernible and surface erosion was readily noticed in abundance. Similarly, this was the start of the stage II 'step'.

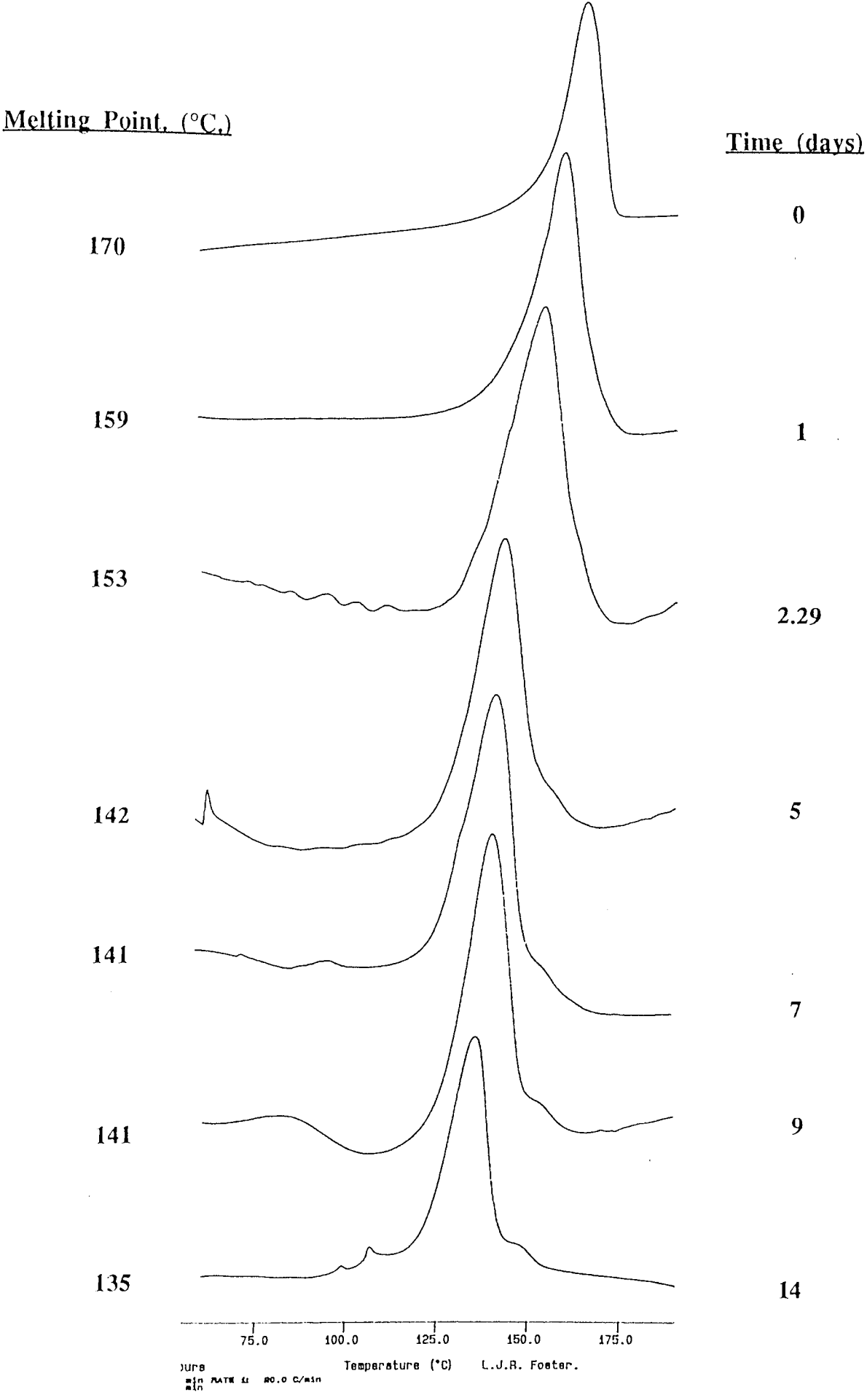

Figure 4.2

DSC Curves Illustrating The Change In PHB(FM)TG Melting Points During Degradation In The Accelerated Model.

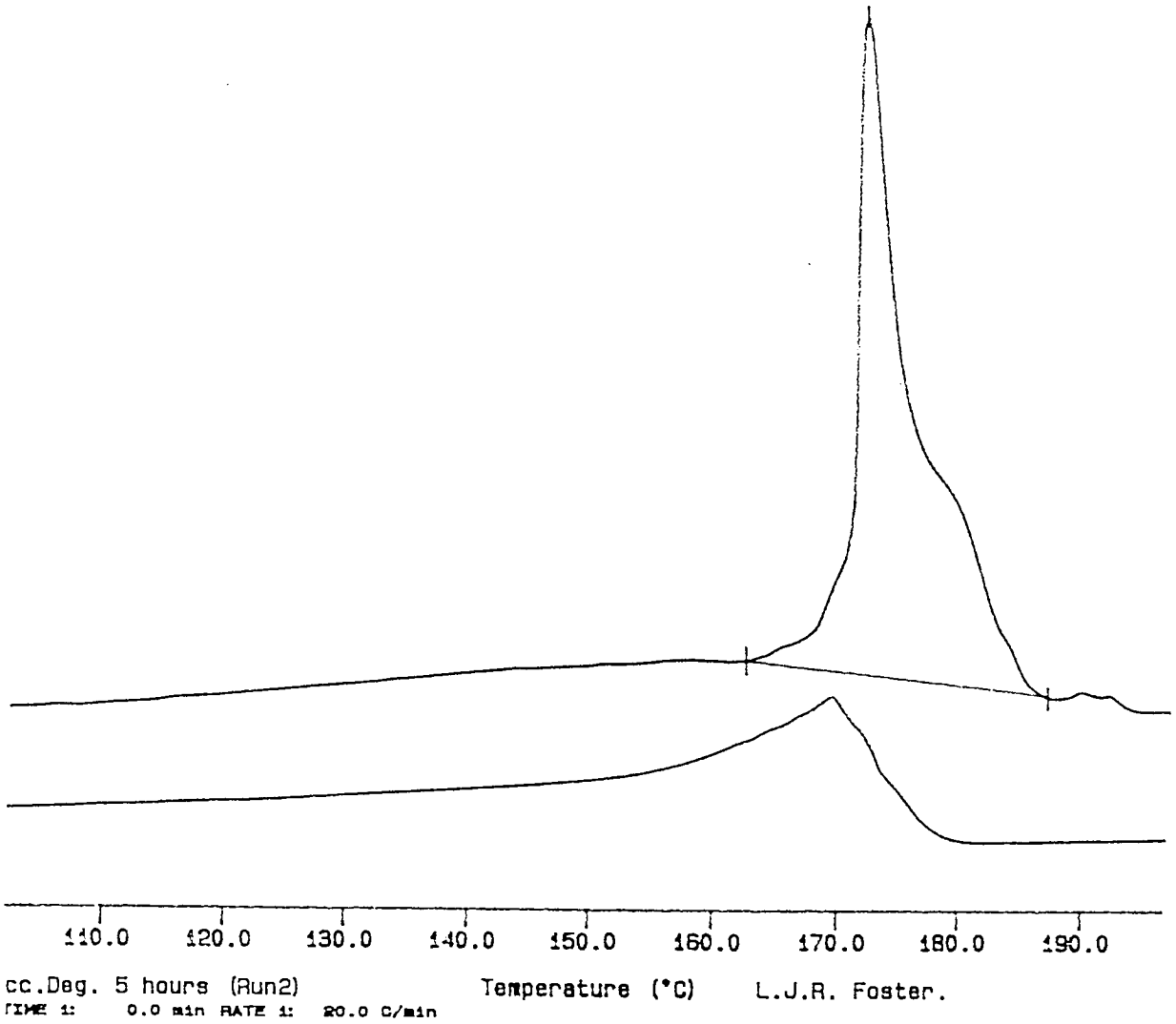

:Sample 1.

:Sample 2.

Figure 4.3.

DSC Curves Illustrating Sampling Difference For PHB(FM)TG. After 5Hrs. Degradation.

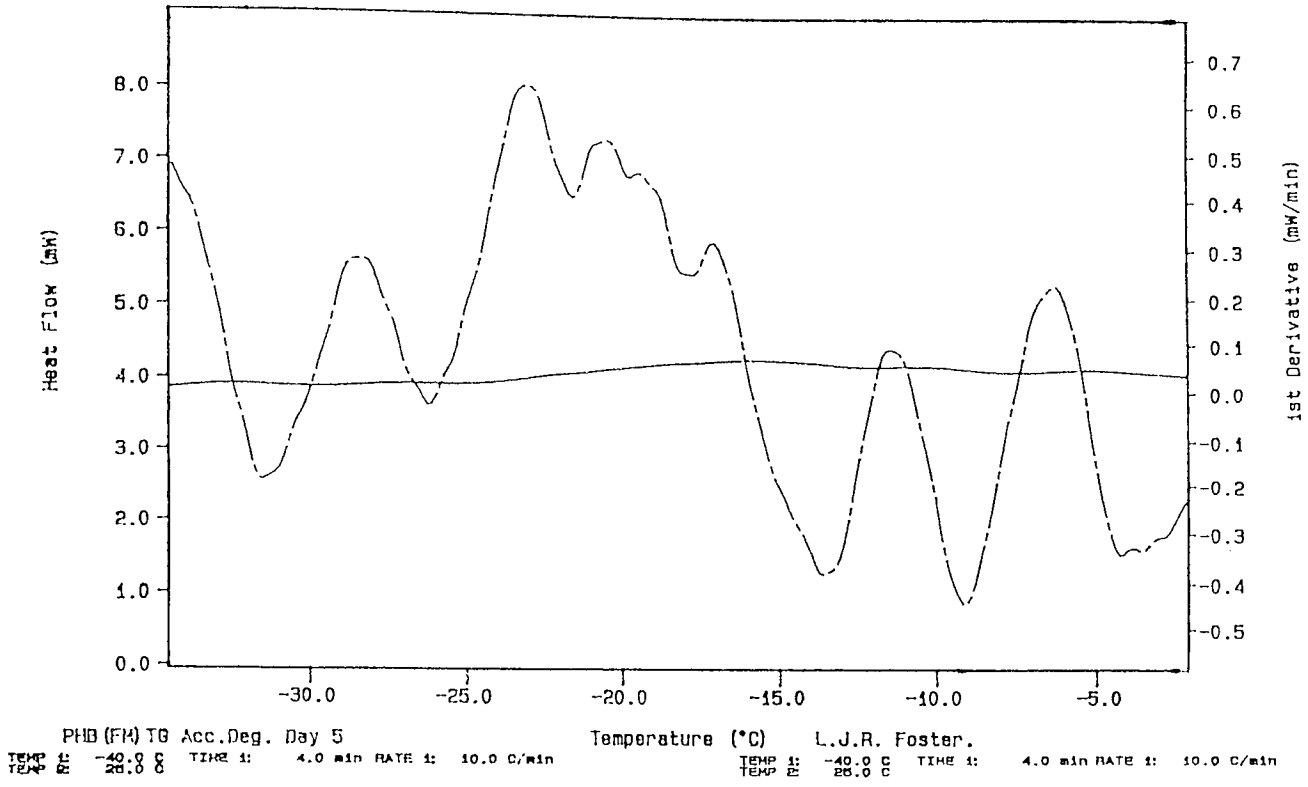

:5 Days Degradation.

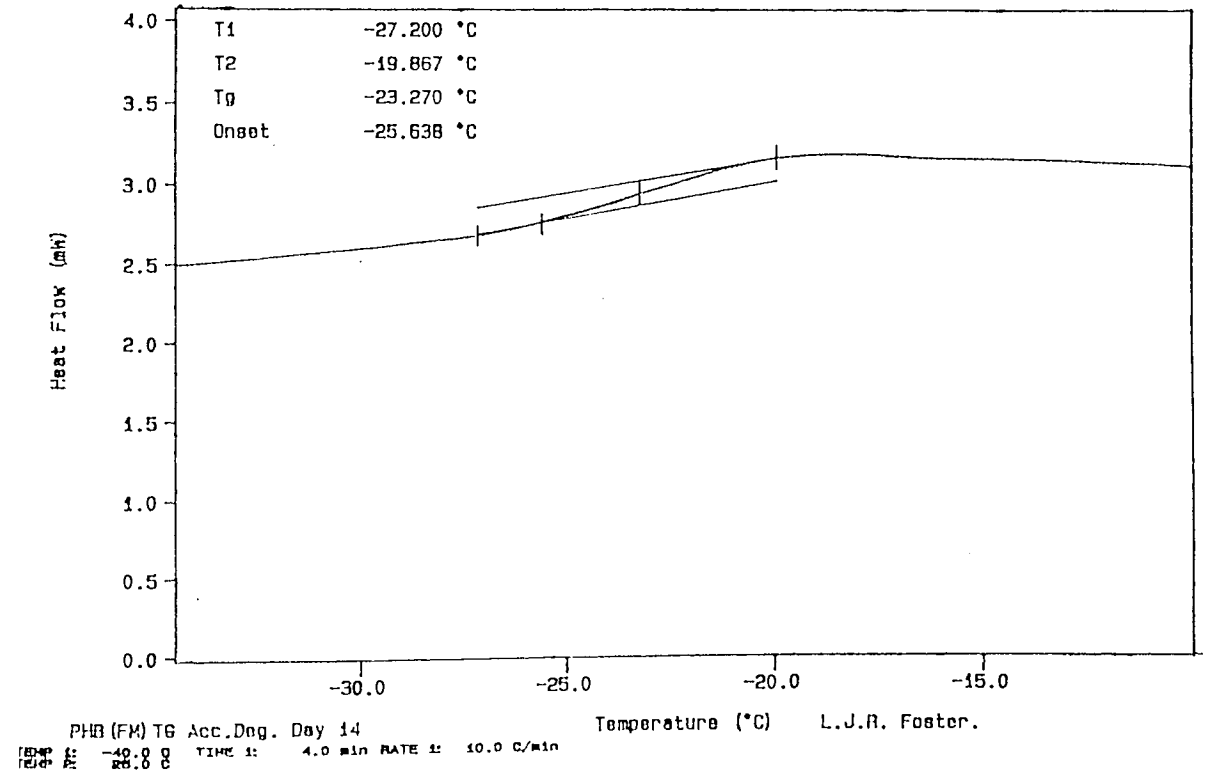

:14 Days Degradation.

Figure 4.4.

DSC Curves For PHB(FM)TG., Determination Of Glass Transition Temperatures.

It was observed that the repeat readings from fibres for sample 5 hours varied in their enthalpies and melting points. Although this variation could be due to error, the DSC traces obtained were greatly different, (Fig. 4.3). It was noticed that the location of the sample from the retentate caused this variation. Those traces from the upper regions of the matrix had a much 'flatter' curve occupying a large temperature region, thus indicating a large distribution of different molecular weight fractions. This was probably due to the partially degraded fibres and fibre fragments and particulate matter, trapped within the remaining matrix. The other samples were obtained from the base of the retentate, this was mainly the collapsed fibre fragments and produced a more prounounced narrow peak, (Fig. 4.3).

Thus, for sample 5 hours two distinct types of fibrous matter were determined; the more general matrix with its progressive degradation and the already collapsed fibre fragments which were not as degraded as the actual matrix. These were probably the large unstable fibres which had fragmented due to structural weaknesses possibly caused by a large percentage of amorphous material.

No glass transition temperatures (Tg.) were measurable for samples from 1 to 5 days degradation, even utilizing the first order derivative, (Fig. 4.4). This indicated that the previous amorphous material of the undegraded matrix had readily dissolved and thus the samples were considered to be highly crystalline, this was confirmed by the fusion enthalpy measurements. However, at day 14 the Tg. was readily observed and determined to be -23°C. This indicated the decrease in the percentage crystallinity and the degradation of the PHB, (Fig. 4.4).

4.2.3.2. Photoacoustic Spectroscopy (PAS) studies.

A comparison of the photoacoustic spectra obtained from the PHB(FM)TG sample during the course of the degradation revealed little difference in the absorption bands present, (Fig. 4.5). The undegraded sample possessed some small peaks in the waveband range 3400 to 3850 $cm.^{-1}$, which were not as conspiciously present in any of the partially degraded samples, even after only three hours in the degradative medium. These bands were probably due to contaminants and/or solvent residue which readily dissolved into the degrading solution.

The small free hydroxyl peak at 3460 $cm.^{-1}$ remained throughout the degradation process, this confirmed the previous conclusion that the 'undegraded' retentate samples retained water from the atmosphere proportional to the weight of PHB present. A small carbon dioxide peak was observed between 2,300 and 2,400 $cm.^{-1}$, for samples 3hrs., 1, 5 and 14 days degradation, this was due to a change in the gas flow during these sample readings.

The main difference observed between the traces was the gradual emergence of a peak at waveband 1568 $cm.^{-1}$, this was first noticed at day 2.29 (2 days 7 hours) and was retained at an apparently similar peak intensity until day 14; the termination of the experiment. This waveband was also observed in the undegraded and initial degradation stages until day 1 as a shoulder of the ester peak at 1728 $cm.^{-1}$ in region A. The differences between the partially degraded samples and the undegraded was highlighted by subtracting the former from the latter, (Fig. 4.6). These subtractions show the development of the peak at 1568 $cm.^{-1}$ more clearly and indicate its emergence at an earlier

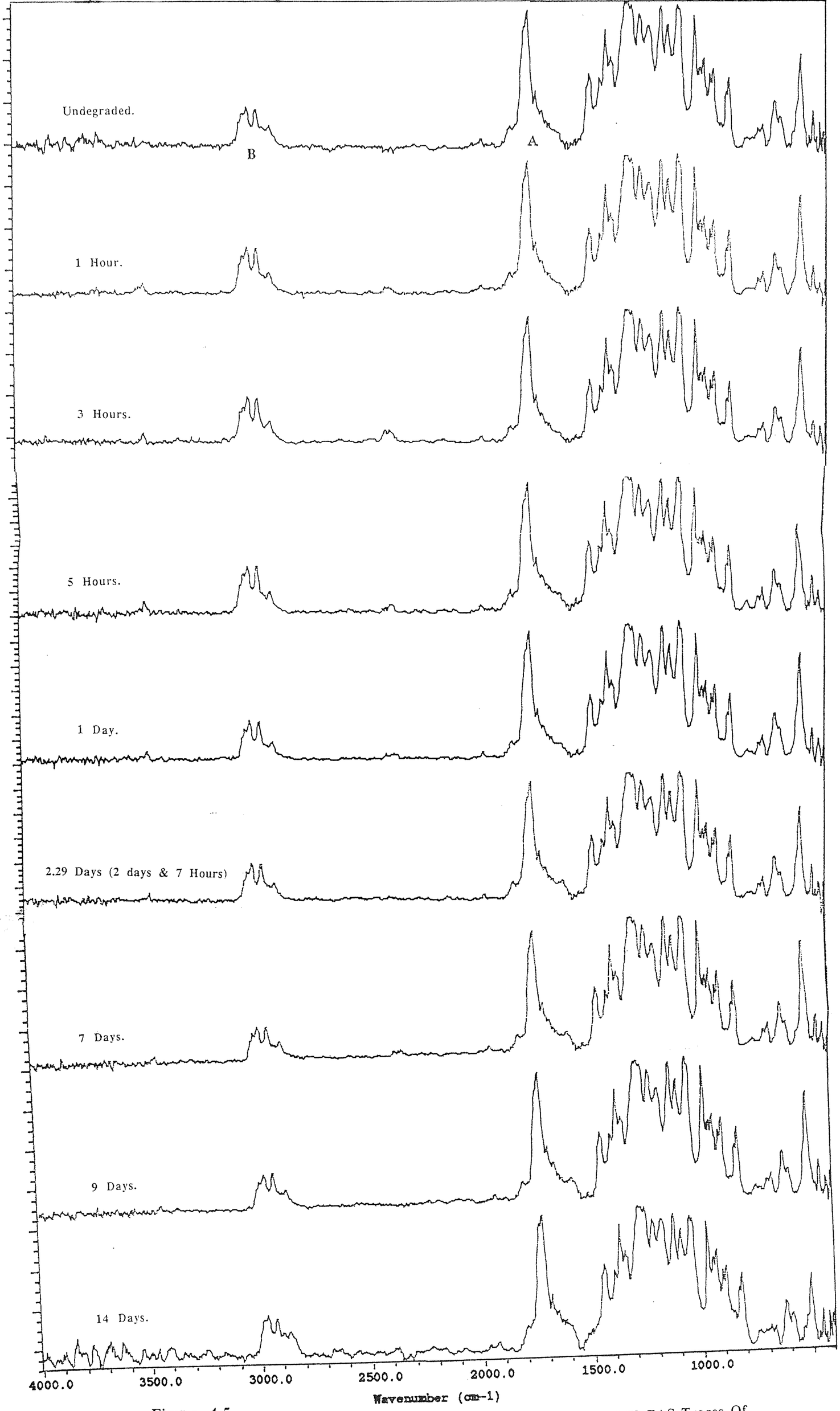

Figure 4.5.

Characterization Of Partially Degraded PHB(FM)TG; FTIR-PAS Traces Of PHB(FM)TG Samples During Degradation In The Accelerated Degradation Model.

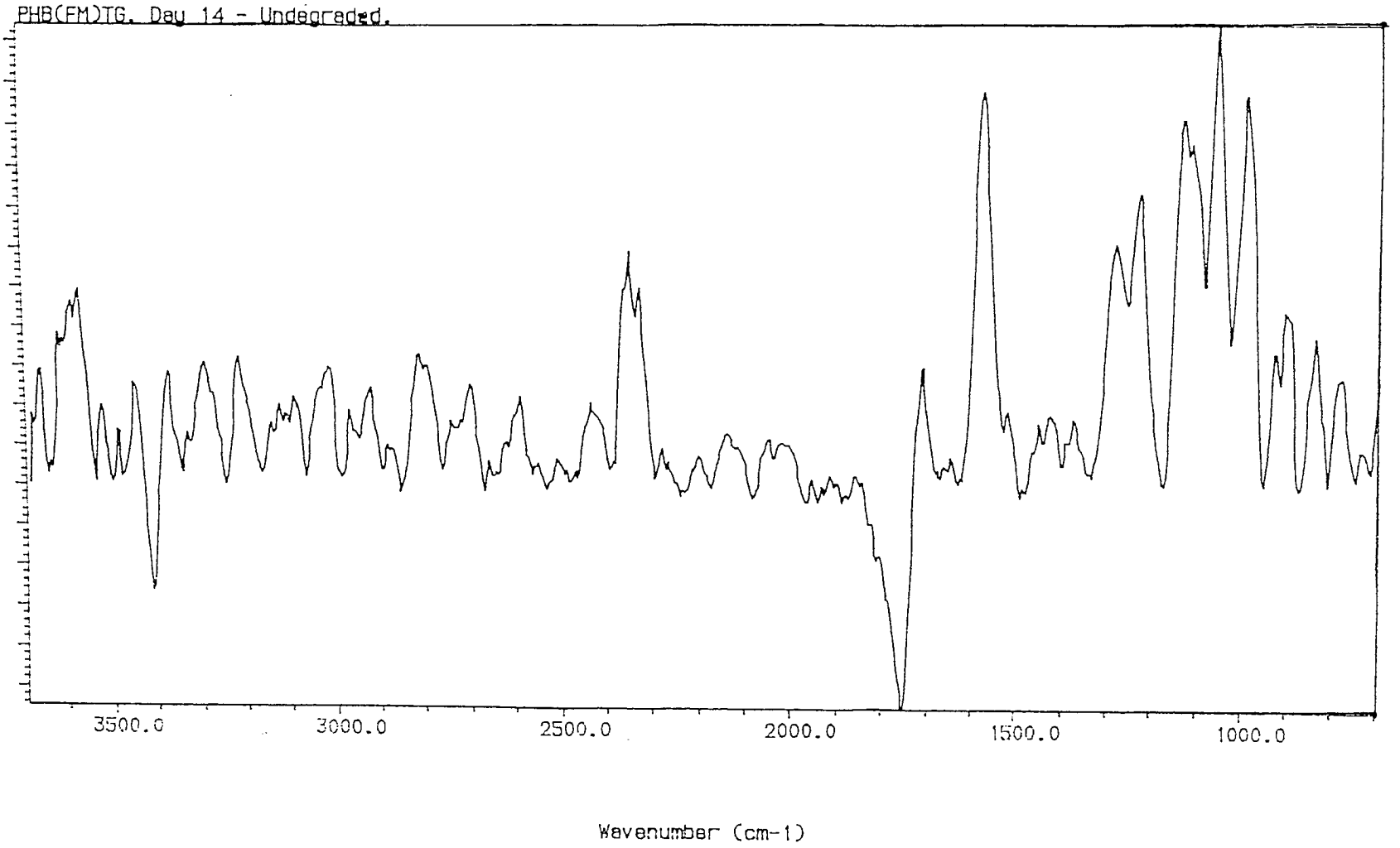

Figure 4.6.

FTIR-PAS Trace Difference Between Sample PHB(FM)TG After 14 Days Degradation In The Accelerated Degradation Model And The Undegraded PHB(FM)TG.

stage of 3 hours degradation and its increase to a sharper, larger peak until termination at day 14. This peak at 1568 $cm.^{-1}$ corresponds to a waveband indicating the gradual formation and proportional increase of carboxylate ions. These carboxylate ions were formed by the cleavage of the ester bond within the polymer chain during the degradation, by the action of base hydrolysis.

It was also noticed from figures 4.5 and 4.6, that the three sharp peaks in region B, 2822 to 3044 $cm.^{-1}$, gradually decreased during the course of degradation until they were approximately the same as in the undegraded sample. Therefore, the amount of carbon-hydrogen stretching energies for the saturated carbon-hydrogen bonds apparently increased within the initial degradation stages and then decreased. However, this is assuming that the sample amount was the same in each case. This assumption has justification, since a full sample holder would ensure that the laser penetration was similar in each reading, consequently the traces obtained could be theoretically considered as quantitative.[97] Unfortunately this was not the case, since the density of the partially degraded PHB in the sample holder and therefore the amount sampled effectively changed. Thus, it was concluded that the reduction in the height of the wavebands; 2865, 2929 and 2972 $cm.^{-1}$, was due to a proportional reduction of carbon-hydrogen bond energies in the sample during the degradation, after the initial degradation stage when an apparent increase was present probably due to a sampling difference.

Thus, it was concluded that the polymer chains were cleaved at the ester bond linkages, effectively reducing the waveband peak at 1728 $cm.^{-1}$, with the formation of carboxylate ion chain ends with a waveband at 1568 $cm.^{-1}$ and a carbonyl shift to 1768 $cm.^{-1}$.

The ester link breakages may have occurred at the ends of the polymer chains, thereby 'chopping' consecutive individual units off the chain and thus forming the monomer; β-hydroxybutyric acid. It is also possible that the breakages could have occurred at any ester linkage within the polymer chain and continuing until the monomer was formed and detected. A third option is that a combination of both terminal and random excission occurred. Due to the gradual increase in the rates of monomer production during the course of the degradation experiment, as observed in the degradation profile graph 4.5, it is most probable that random excission was the main form of chemical breakdown.

The breakages in the polymer chains produced a large quantity of shorter chains and effectively reduced the strength of the polymer. This accounted for the brittle and delicate nature of the sample matrix in the early stages of degradation, whilst by day 9, the breakdown of the polymer had occurred to such an extent that only a powdered mass with no matrix integrity whatsoever remained.

4.2.4. Conclusions.

The qualitative and quantitative examination of the PHB(FM)TG degradation determined the nature of the matrix and polymer degradation and this is summarized in figures 4.1, 4.7 and 4.8. Figure 4.7 illustrates the degradation of a single fibre, when the matrix as a whole is considered, all the stages may be found at any one time with a general progression from the undegraded to the degraded being more common. The experimental accuracy was also confirmed by the degradation experiment.

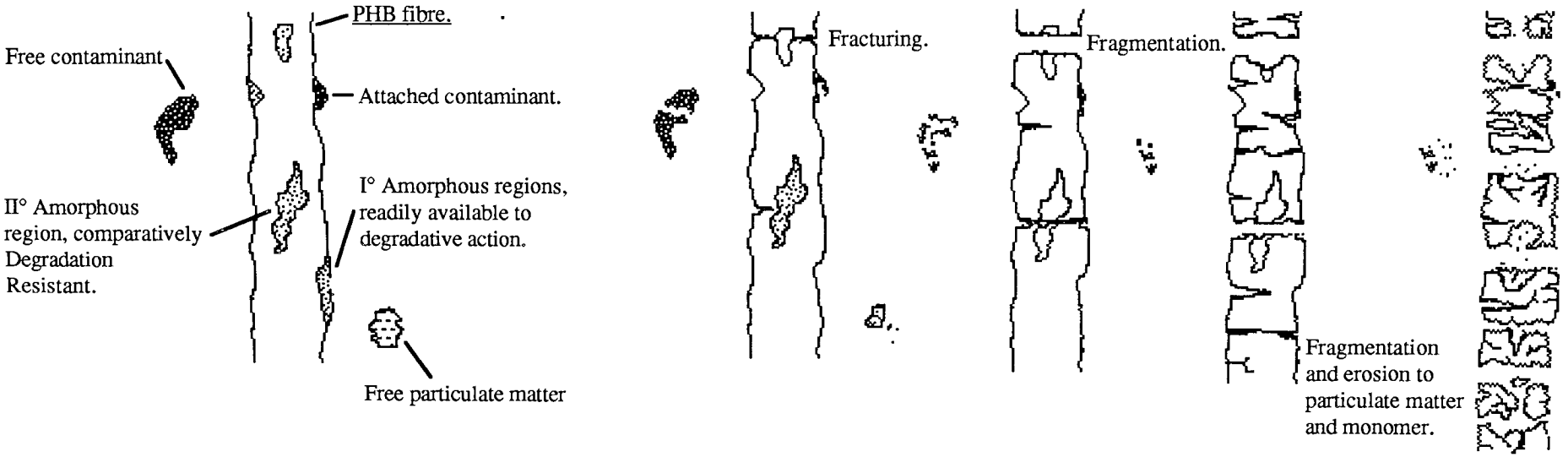

Undegraded PHB fibre, incorporating primary and secondary amorphous regions and contaminants. The matrix also includes particulate matter which may be PHB and /or contaminants, crystalline and/or amorphous. Free contaminants are also present.

Initial matrix degradation; Penetration of the degradative medium into the matrix dissolution of the primary amorphous regions and contamiants, erosion and fragmentation of the particulate matter and contaminants. Fracturing of the fibre, this occurs to different extents and is affected by manufacturing and handling induced stresses.

Continued degradation of contaminants, dissolution of secondary amorphous regions, increased fracturing and fragmentation to fibre fragments and particulate matter with erosion of the latter. Increase in crystallinity and fragility of the fibres.

Fibres readily fragment to small fibre fragments and to particulate matter, with erosion to monomer; HBA. The degradation Of crystalline PHB readily occurs. Contaminants may still be present.

Figure 4.7.

Diagrammatic Representation Of Proposed Fibre Degradation From PHB(FM)TG.

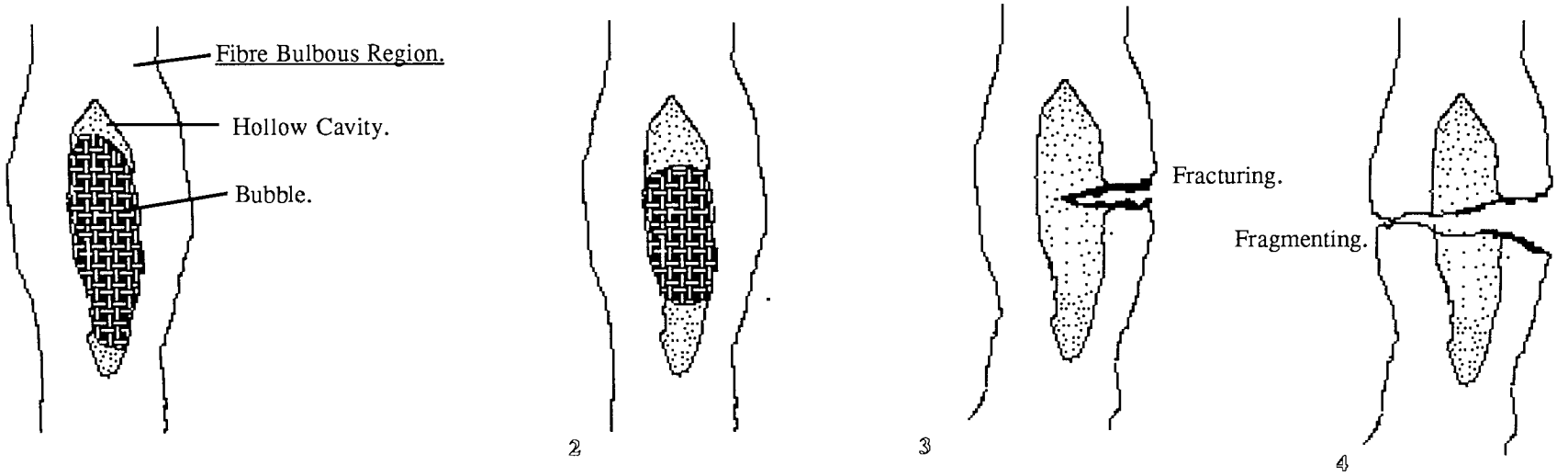

Bubble in hollow cavity, usually occurring in bulbous regions and large diameter fibres facilitates the flotation of the matrix in the degradative medium. The cavity is connected to the medium by porous regions. The porosity occurs to varying extents.

The bubble decreases in size due to penetration of the degradative medium via the pores with their gradual erosion.

The bubble is released, the pressure of the bubble in the cavity and the empty cavity are structurally weak points that readily fracture.

The structural weakness readily fragments with the possible release of particulate matter.

Figure 4.8.

Diagrammatic representation Of Proposed Fibre Degradation From PHB(FM)TG; Agglutinated And Forked Fibres, And Hollow Regions.

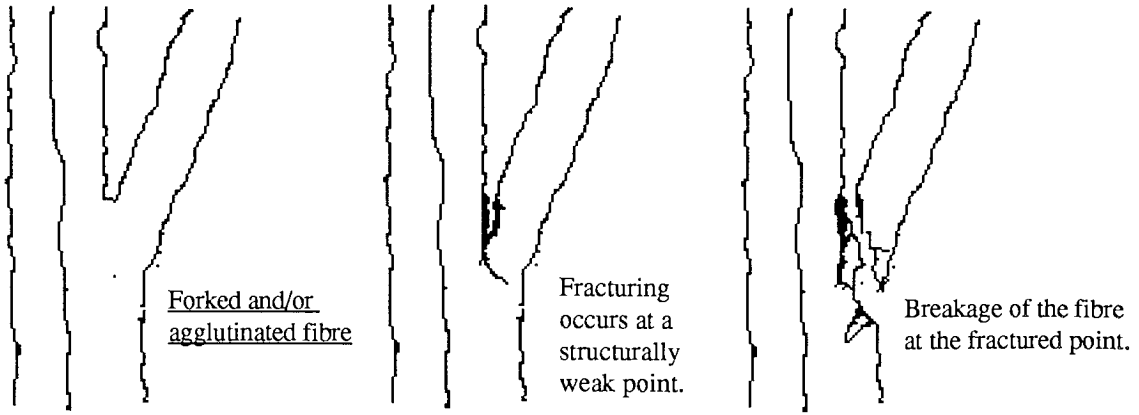

The TG matrix consisted of a proportion of unstable fibres in the small and large diameter ranges, the former continued to readily fragment until the eventual release of monomer, similarly, a proportion of the latter also did so. The remaining unstable large diameter fibres initially fragmented into fibre fragments which were then comparatively degradation resistant until complete matrix collapse occurred. The instability of these fibres was mainly introduced by manufacturing and handling.

Degradation occurred by the hydrolytic action of the buffer medium which randomly broke the ester linkages within the PHB, initially weakening the fibres by reducing the polymer chain lengths, which then led to the physical collapse and erosion.

Two types of amorphous regions were concluded as being present, the primary were readily available to initial degradation and were proportionately responsible for the monomer formation and weight loss in the first instances, (Stage 0). The secondary amorphous regions were present within the fibres and less available to degradation until later stages when they facilitated the matrix and fibre collapse, (Stage I).

4.3. PHB(FM)IP Degradation And Its Comparison To That Of PHB(FM)TG Degradation.

4.3.0 Introduction.

The Degradation of the PHB(FM) increased purity (IP) was investigated in the same manner as that of the technical grade matrix (TG) and the two experiments were run

simoultaneously. Therefore, the possibility of errors in the comparison of the two different types of matrices degradation, due to experimental variation, was considered to be minimal.

The degradation of the increased purity matrix was compared to that of the technical grade sample. (Sec.4.2.). The increased purity sample and its degradation was then utilized as a baseline for comparison with the co-blended matrix samples which also used the purified polymer PHB(FM).

4.3.1. Degradation Profiles.

Graph 4.17 illustrates the degradation profile for the PHB(FM)IP utilizing monomer measurement and particle analysis, whilst graph 4.18 illustrates the gravimetric analysis profile. From graph 4.17 it was observed that the degradation profile for the IP sample was generally similar to that of the TG. However, the profile was smoother and did not exhibit a step stage II. The PHB(FM)IP gradually degraded exhibiting a comparatively smooth curve compared to the TG degradation profile.

The terminal step stage began at day 18 for the TG sample after approximately 57% degradation to monomer. Assuming linearity, the overall degradation rate to this time was 3.2%.dy.$^{-1}$. The IP sample, however, had an earlier terminal stage at day 14 also after 57% degradation, a rate of 4.1%.dy.$^{-1}$. This indicated a faster degradation for the IP sample compared to the TG.

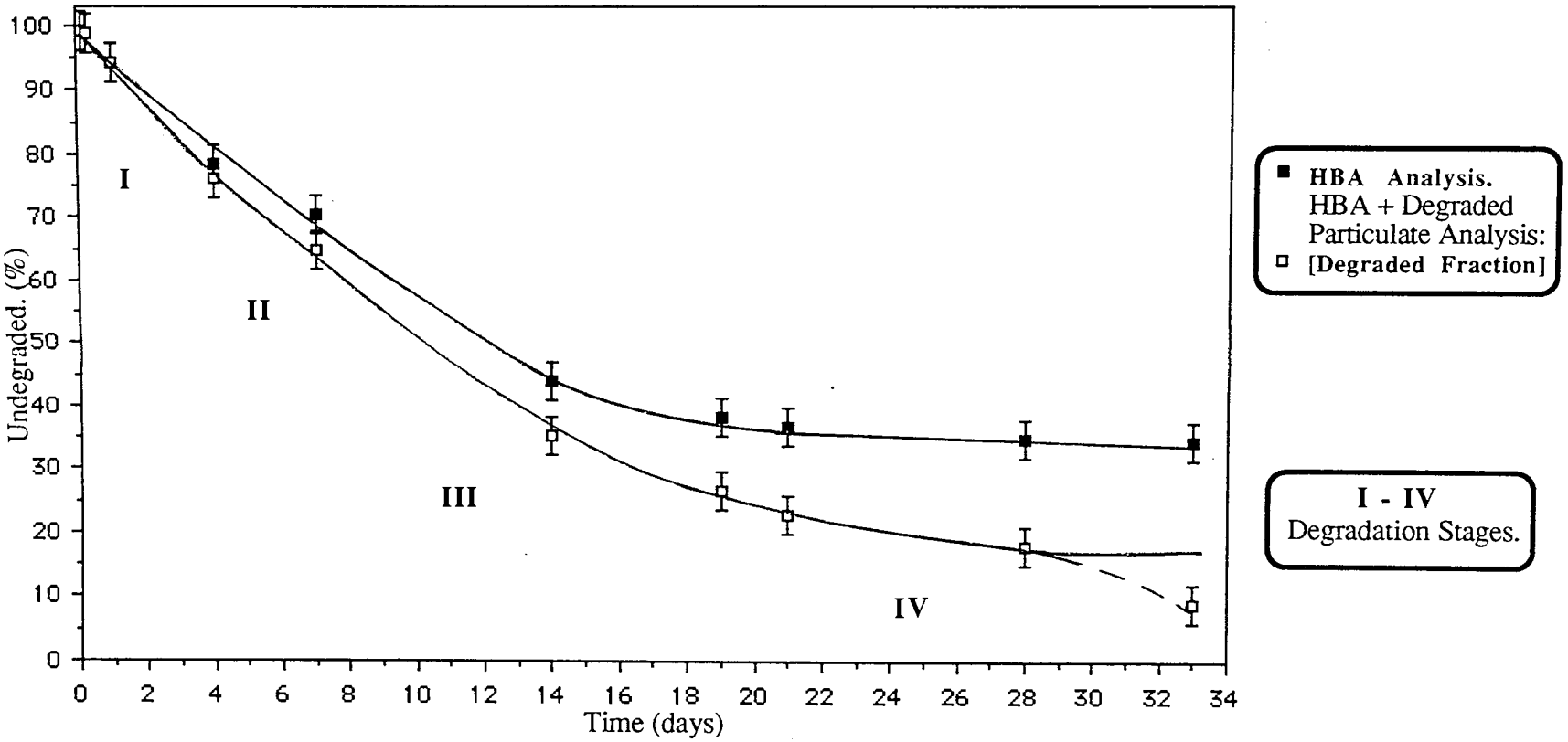

Graph 4.17.

Degradation Profile Of PHB(FM)IP, In The Accelerated Model, Monitored By Monomer And Particulate Analysis.

The IP fibres gradually degraded, such that total collapse and settlement occurred by day 14. The TG fibre fragments however, apparently retained some integrity until day 18, before the terminal step stage IV occurred. This tended to indicate that the TG matrix was more stable than the IP, in fact the amorphous regions and contaminants in the TG sample facilitated the initial collapse and settlement, such that the step stage II was observed. The proportionally greater collapse of the TG fibres compared to the IP fibres and their particle/fragment settlement and compaction at periods before the terminal step stage IV ensured that the TG fibres appeared to have a greater stability, when in fact the reverse was initially true. This was vindicated by the general observations of the phials during degradation.

A comparison of the gravimetric profiles for the TG and IP samples, graphs 4.4 and 4.18 respectively, also indicate that the reduced stability of the TG matrix facilitated its degradation in the initial stages. There was approximately 50% degradation by weight loss at day 7 for the TG samples, compared to about 39% degradation for the IP matrix.

The initial 4-5% weight difference between the monomer and gravimetric analysis in the undegraded and 1hr degraded TG sample (Graph 4.4) was not observed for the IP sample. This would appear to indicate that the solvent residue and contaminants in the TG matrix were comparatively greater, as anticipated. Their presence in the TG sample was confirmed by the characterization of both undegraded samples, (Ch.3), where impurities slightly reduced the DSC measurements compared to the IP.

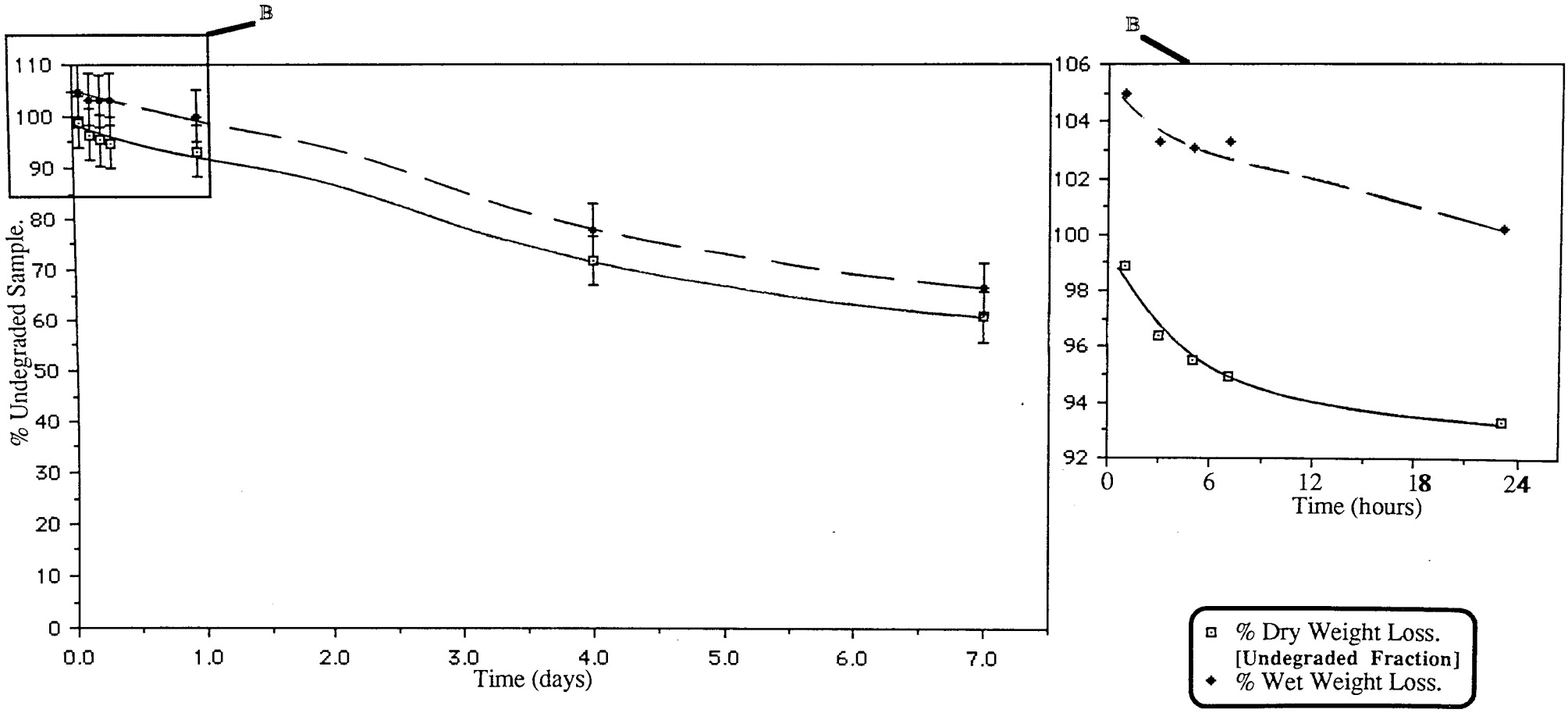

Graph 4.18.

Degradation Profile Of PHB(FM)IP, In The Accelerated Model, Monitored By Gravimetric Analysis.

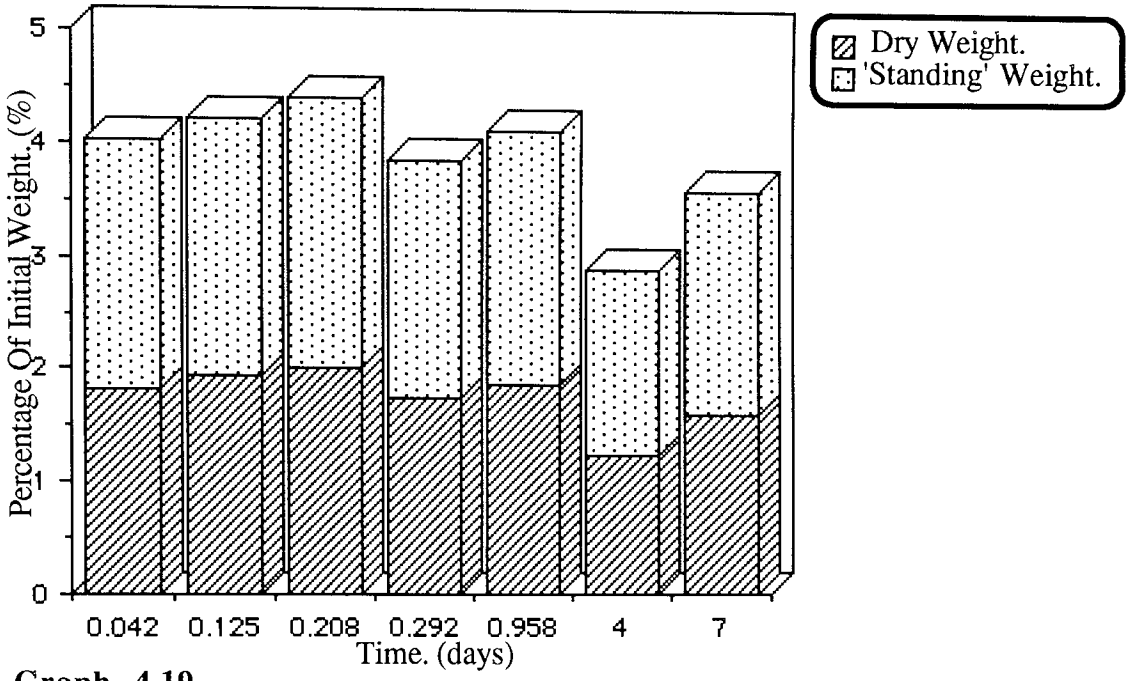

Graph 4.19.

Measured Degraded Particulate Matter For PHB(FM)IP During Degradation In The Accelerated Degradation Model.

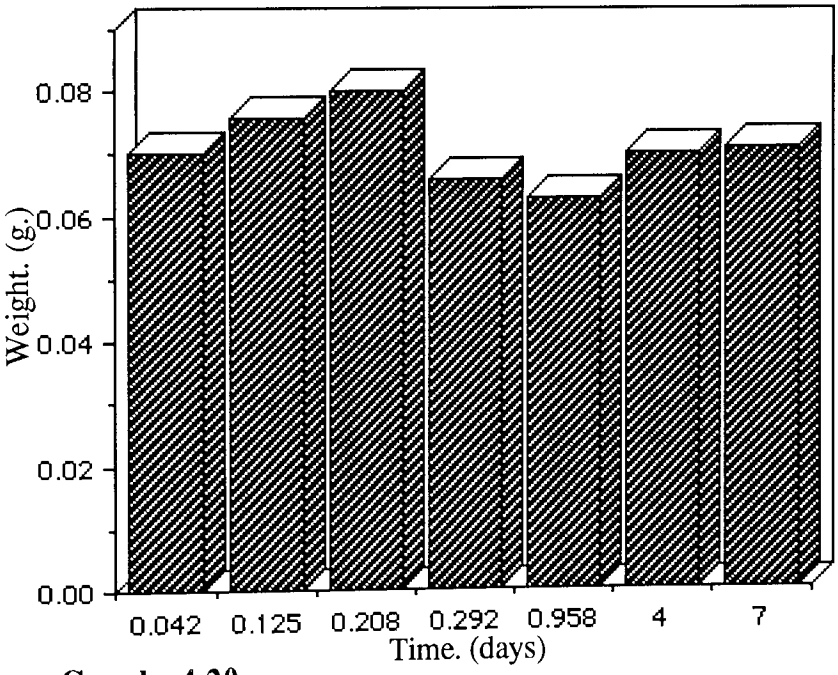

Graph 4.20.

Ideal Total Degraded Particulate Matter For PHB(FM)IP During Degradation In The Accelerated Degradation Model.

Degraded particulate matter was measured during degradation and observed to maintain a similar level throughout the first seven days, however, it then increased to a maximum at termination of the experiment at day 33, this was due to a reduction in the available surface area to volume ratio of the matrix and therefore a reduction in the degradation to monomer, which facilitated an accumulation of degraded particulate matter, (Graph 4.19 & 4.20).

Addition of the degraded particulate matter to the monomer degradation profile (The degraded fraction profile - graph 4.17) produced very little difference in the degradation curve until day 5. This indicated that all the degraded particulate matter was readily eroded to the monomer in the initial stages. During stage II the degraded particulate matter gradually increased until the terminal step stage IV. At day 21 (stage IV) the degradation to monomer was greatly reduced to a rate of approximately $0.2\%.dy.^{-1}$, whilst the degraded particulate matter increased, such that at day 33 approximately 65% of the matrix had degraded to monomer with a further 27% to degraded particulate matter. This indicated that the fibre fragments and undegraded particulate matter compaction greatly reduced the rate of degradation, so that the erosion to the monomer probably only occurred from the surface layer of the compacted matter, whilst in the lower regions fragmentation and erosion proceeded more slowly.

Thus, it can be concluded that the TG matrix was initially less stable than the IP matrix, whilst certain individual fibres were more stable. The TG matrix readily collapsed with a rapid degradation rate until the step stage II was attained. As a result of this initial collapse the available surface area to volume ratio in comparison to the IP matrix was reduced and

the IP sample then had a comparatively greater rate of degradation. The final step stage IV did not occur until day 18 for the TG matrix, whilst for the IP sample it occurred at day 14.

It was concluded therefore, that despite these differences in the IP and TG degradation the profiles were quite similar. The apparently faster degradation of the IP matrix compared to the TG was a result of the constraints of the degradation model and purification process.

4.3.2. Observations Of The Partially Degraded Increased Purity (IP) Fibres And Their Comparison To PHB(FM)TG.

As were concluded from the degradation profiles, the method of matrix breakdown and degradation was basically the same for both the TG and IP samples. This was further illustrated by the observations of the IP matrix during degradation using phase contrast and scanning electron microscopy and comparing them with those observed for the TG matrix.

The integrity of the TG and IP matrix samples appeared the same after 1, 3 and 5hrs degradation utilizing phase contrast microscopy, despite the initial 5% weight loss of the TG sample, (Plate 4.25). No cavities were observed and the fragmentation of the fibres appeared to be limited to the smaller diameters, (Plate 4.26). Similarly, after 23hrs degradation, multiple fragmentation was noticed, however, this may have been due to the handling of the brittle matrix after the drying procedure. Nevertheless, no real difference between the TG and IP samples were noticed, (Plate 4.27).

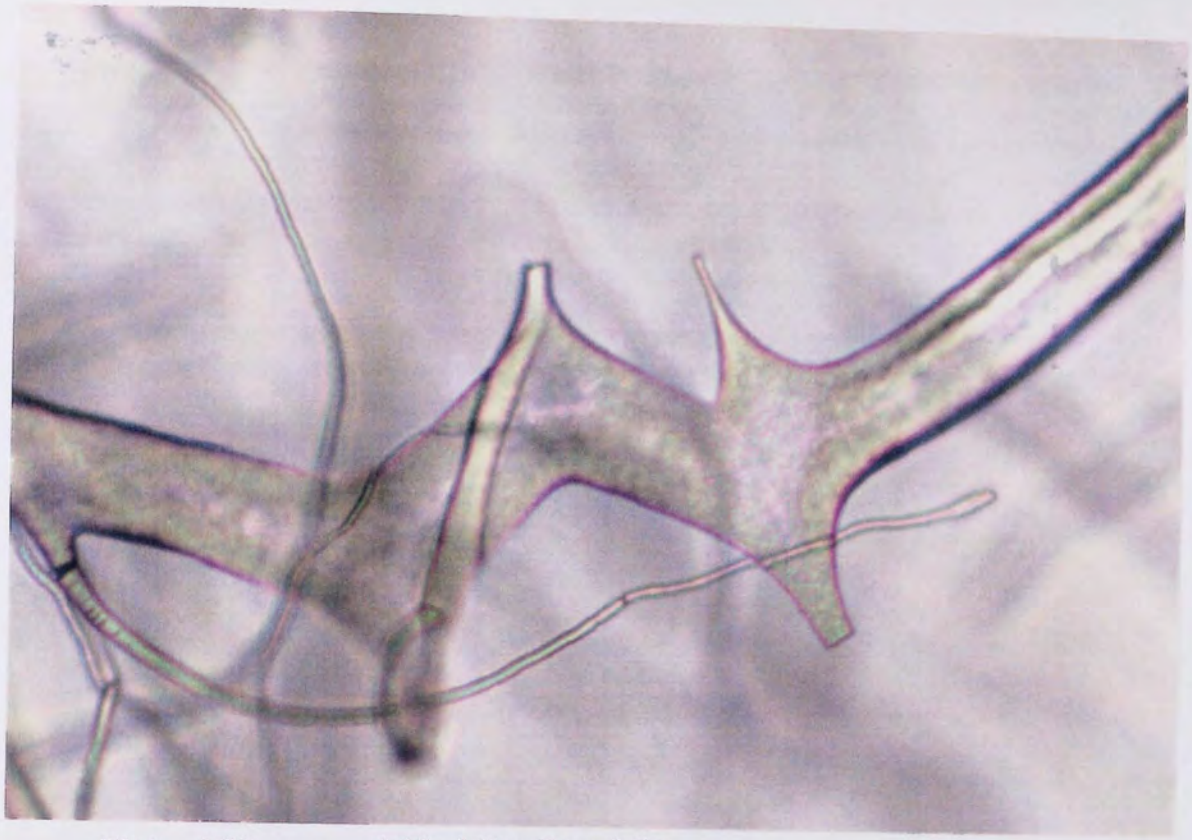

Plate 4.25. (x25) 1 Hour Degradation.
PHB(FM)IP; Matrix Integrity Still Present After 1 Hours Degradation With Some Fracturing Of The Smaller Unstable Fibres.

Plate 4.26. (x15) 5 Hours Degradation.
PHB(FM)IP; Fibre Fragmentation And Fracturing, Apparently More Limited To The Smaller Diameter Fibres.

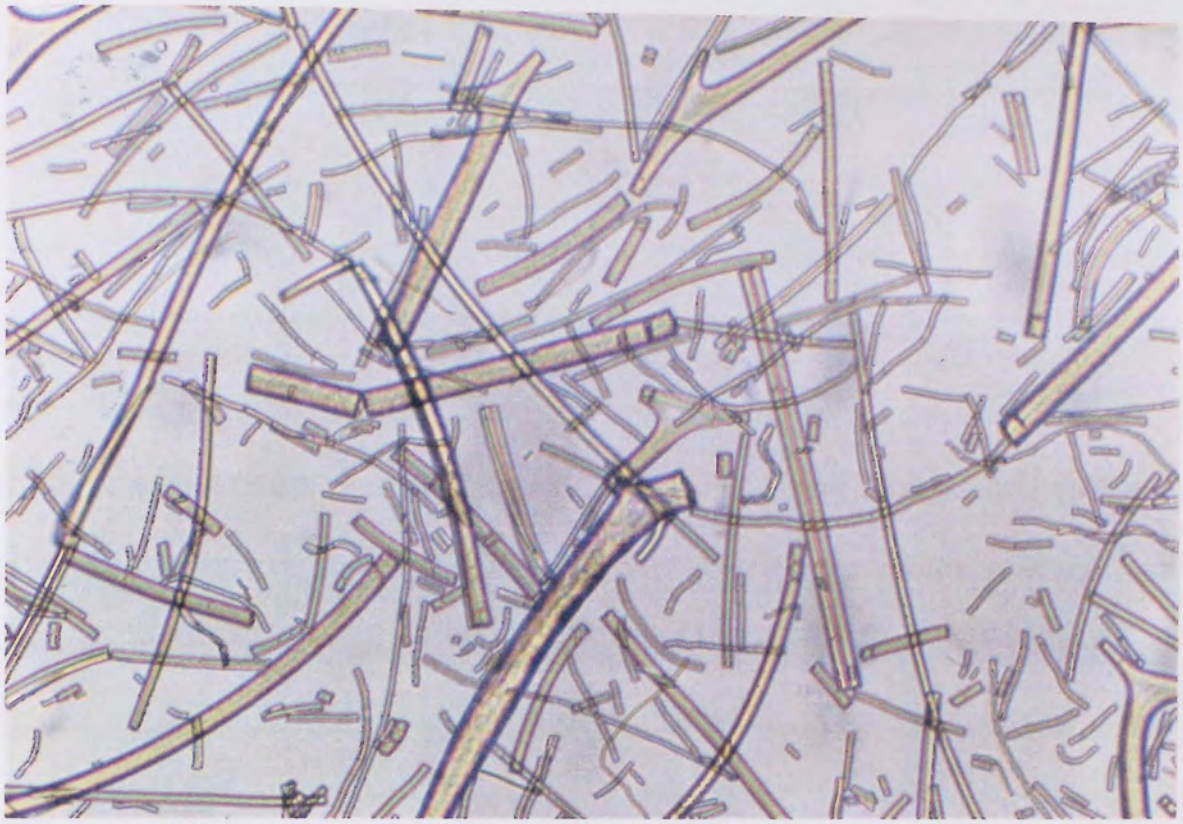

Plate 4.27. (x15) 23 Hours Degradation.
PHB(FM)IP; Multiple Fragmentation Of Matrix Similar To The Day 1 Degradation Observations For PHB(FM)TG.

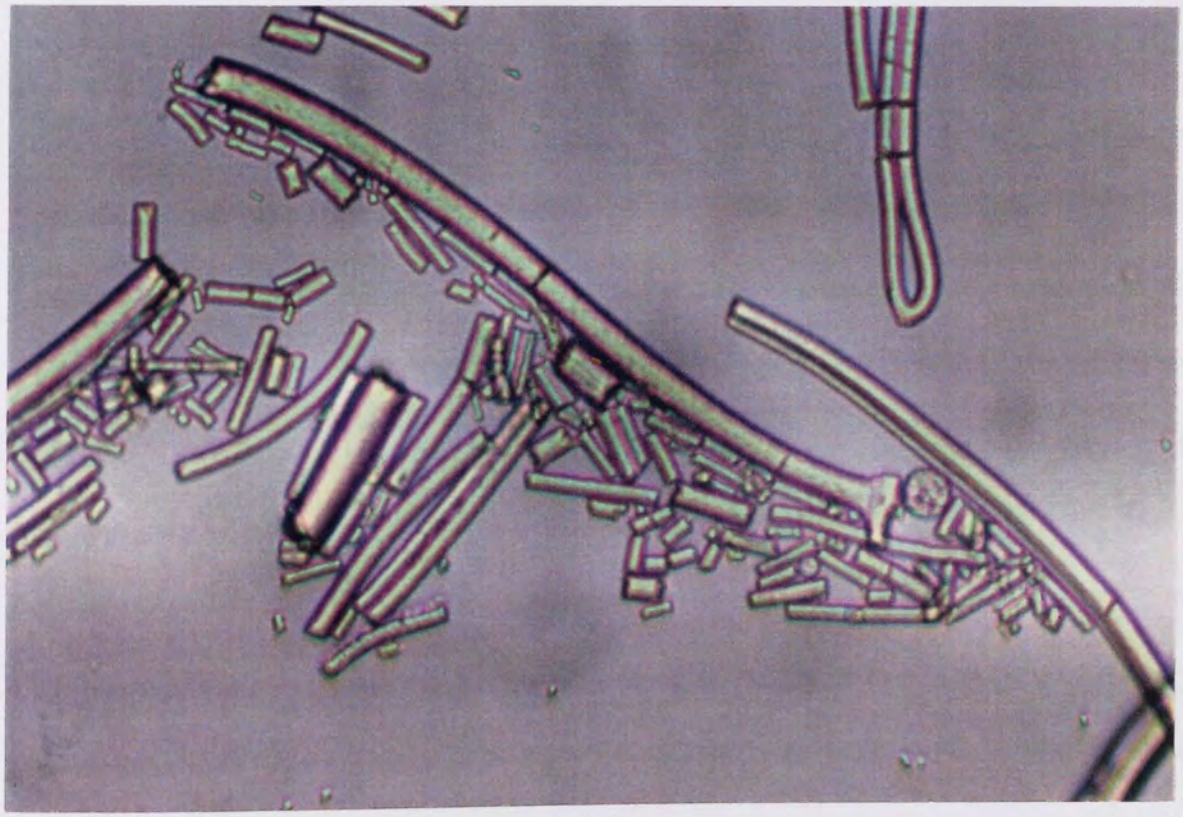

Plate 4.28. (x25) 4 Days Degradation.
PHB(FM)IP; Multiple Fragmentation And Fracturing Of Fibres.

It was observed in the TG matrix that some fibres had noticeable amounts of surface erosion by day 2.29, (Plates 4.10 & 4.11). No such erosion was present for the IP fibres even after four days degradation, whereas by day 5 the TG fibres had large amounts of surface erosion and the appearance of a powdered mass. This indicated that in the TG sample the contaminants and amorphous regions were also blended with the PHB and not simply mixed, therefore readily promoting surface erosion. However, large amounts of fragmentation in the IP fibres had occurred (Fig. 4.28) and fracturing was noticeable in a number of the larger diameter fibres, (Plate 4.29). This difference in the surface erosion indicated that the TG degradation occurred to an apparently greater extent in the initial stages than the IP fibres.

Day 7 degradation for the IP fibres illustrated a great difference from that of the TG fibres. The TG matrix had completely collapsed and surface erosion readily occurred to such an extent that it was difficult to distinguish the fibrous remains in those few pieces remaining, multiple fracturing in all plains occurred. (Plates 4.15 & 4.16. Sec.4.2). In the case of the IP sample, fragmentation of the fibres had occurred to a large extent but with no noticeable difference from the day 4 sample, although some slight surface erosion was observed, (Plate 4.30). However, fracturing occurred to a much larger extent in some fibre pieces when compared to day 4. This fracturing was dissimilar from that of the TG fibres in that the fractured regions appeared to be 'eaten away' (Plate 4.31) rather than a simple 'cracking' as in the TG sample. The large fracture regions observed in Plate 4.31 were not due to fibre pieces seperating but actual erosion of the polymer. Thus, the erosion of the IP fibres was less noticeable and therefore the fibres appeared to be more resistant than those of the TG.

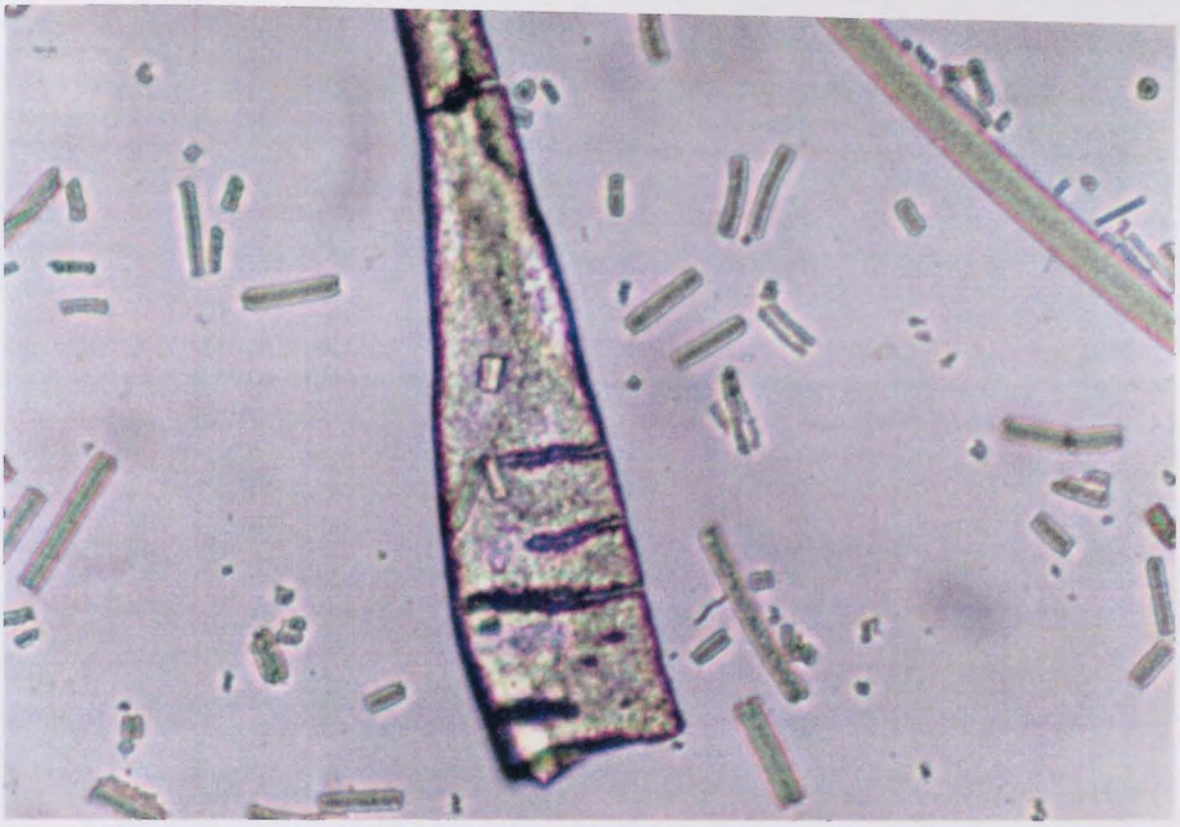

Plate 4.29. (x25) 4 Days Degradation.
PHB(FM)IP; Fracturing And Erosion In A Large Diameter Fibre Fragment, Fractures Appear 'Eaten Away'.

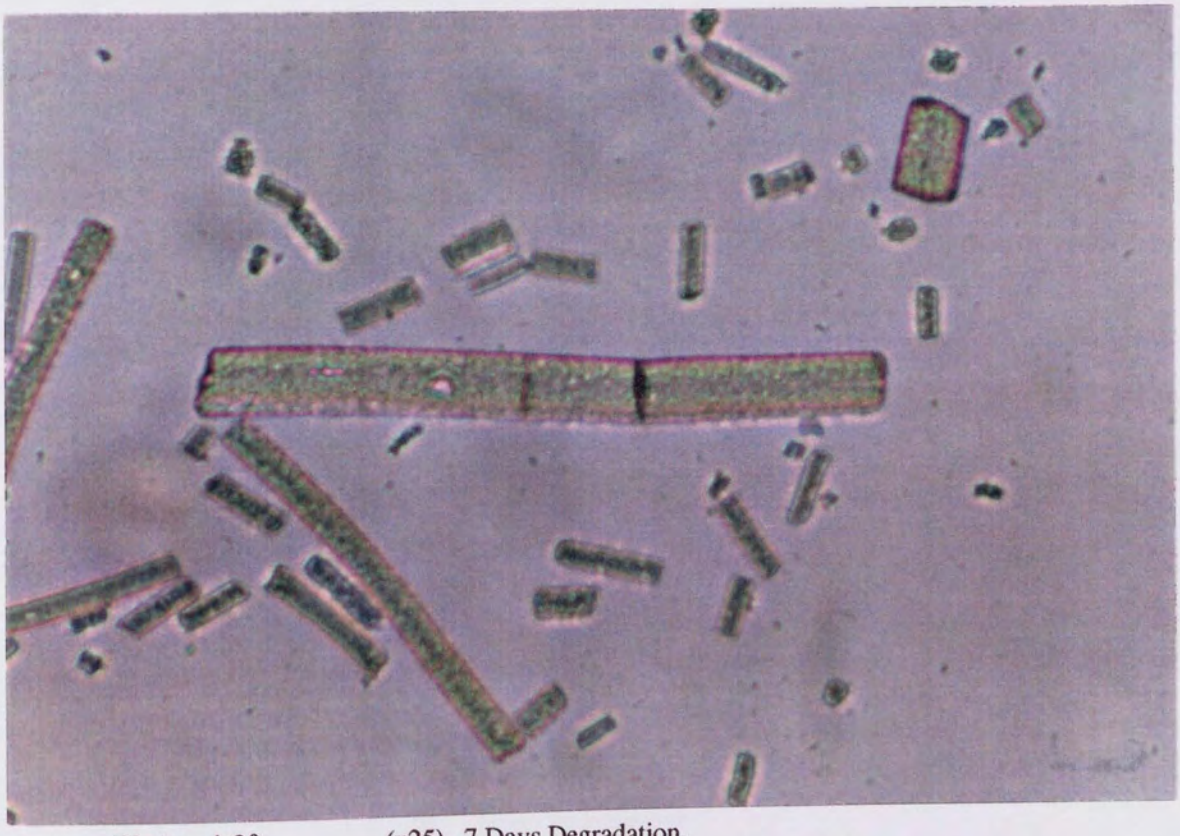

Plate 4.30. (x25) 7 Days Degradation.
PHB(FM)IP; Fracturing And Surface Erosion Of Fibre Fragments.

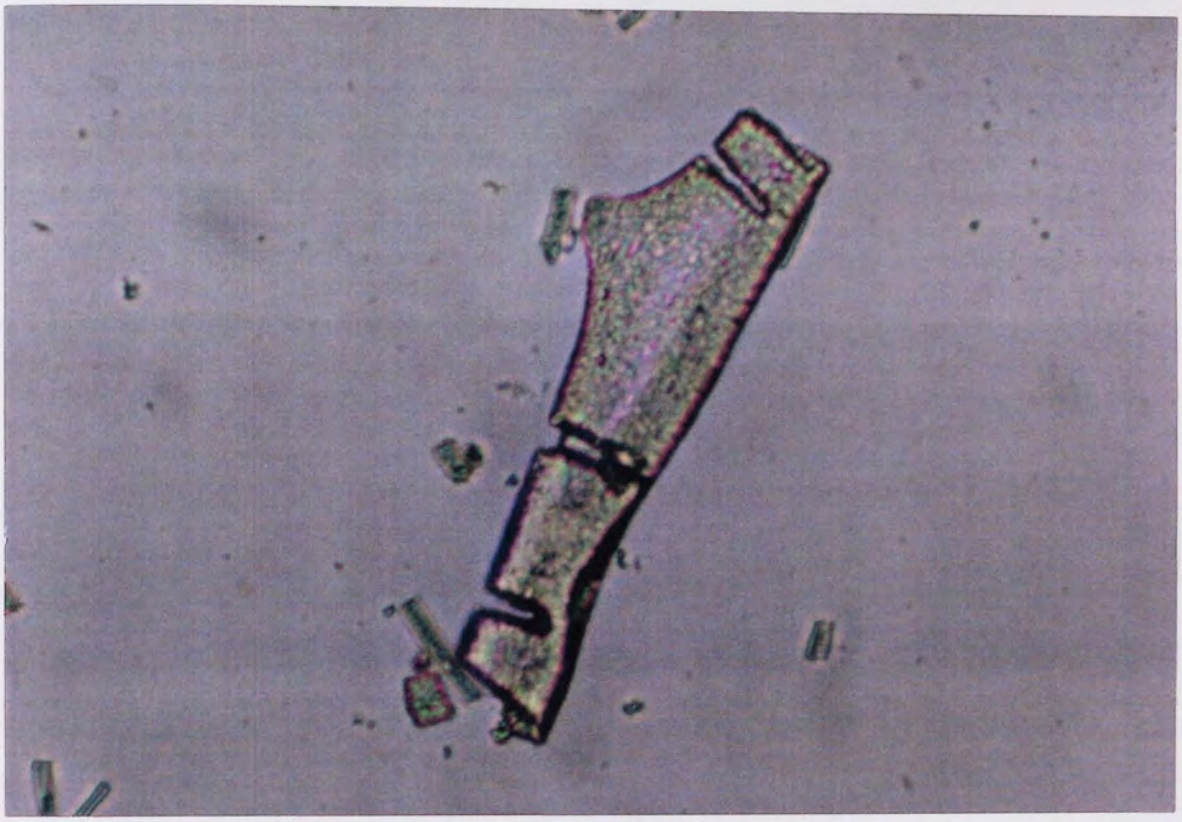

Plate 4.31. (x25) 7 Days Degradation.
PHB(FM)IP; Fracturing Of Fibre Fragment, With The Fracture Being Eroded.

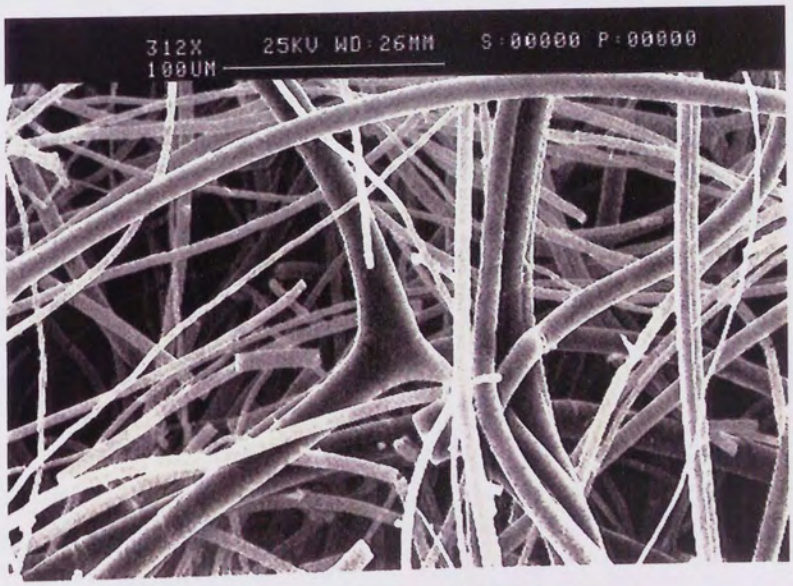

Plate 4.32. (x312) 3 Hours Degradation.
PHB(FM)IP; Matrix Integrity With Few Signs Of Degradation.

Scanning electron microscopy of the partially degraded samples revealed similar observations to those of the TG. The IP matrix integrity was still present after 3 hrs degradation, although some mechanical fracturing had occurred, (Plates 4.32 & 4.41). Small particulate matter was observed attached to a number of fibres, (Plate 4.42), but the crystalline structures readily noticeable in the TG samples were not present.

Scanning electron micrographs of the IP fibres from day 4 illustrated the highly pitted and porous nature of the larger diameter fibres, (Plate 4.35). Plate 4.36 illustrates the partially collapsed matrix and the hollow nature of some of the fibres. This hollow region probably occurred due to the presence and eventual release of a bubble.

The collapsed IP matrix after 7 days degradation was similar to that of the TG fibres, with multiple fragmentation to small fibre fragments, whilst the larger diameter fibre fragments also had multiple fractures. A dense mass of small fibre fragments was thus observed, (Plates 4.37 & 4.38).

Therefore the degradation of the IP matrix appeared similar to that of the TG matrix using scanning electron microscopy, however, noticeable differences were observed using phase contrast microscopy. From these observations it was concluded that the TG fibres apparently degraded more quickly than the IP fibres in the initial time periods.

The presence of an irregular shaped plastic mass from the phial base for the IP sample degradation was also noted. This mass consisted of a substantial weight considering the total weight remaining, but was also heavily porous, (Plates. 4.39 & 4.40). It is possible

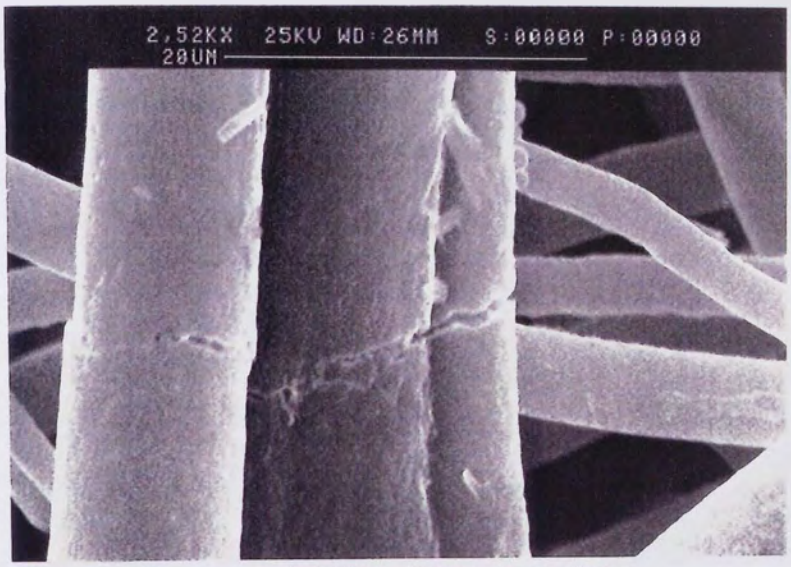

Plate 4.33. (x2.52K) 3 Hours Degradation.
PHB(FM)IP; Fracturing Of Fibres, Most Probably Due To SEM Drying And Mounting Procedures.

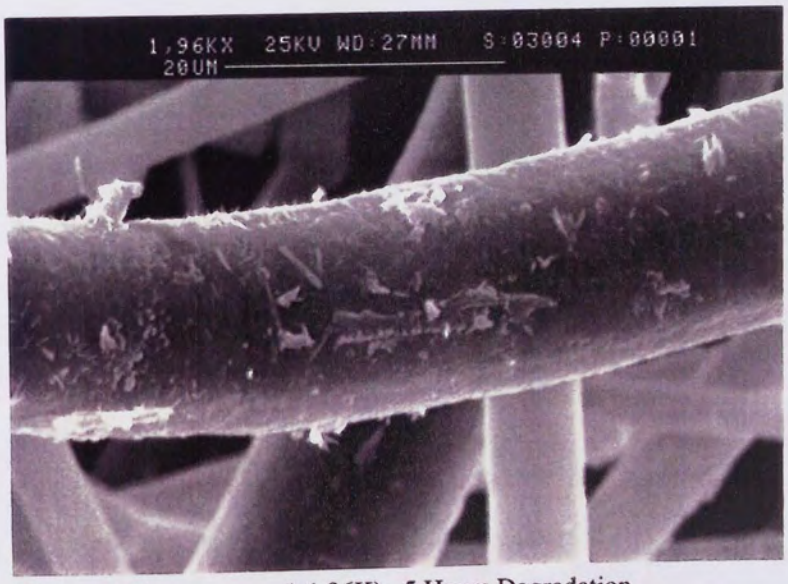

Plate 4.34. (x1.96K) 5 Hours Degradation.
PHB(FM)IP; Small Particulate Matter Attached To A Large Diameter Fibre.

Plate 4.35. (x1.83K) 4 Days Degradation.
PHB(FM)IP; Heavily Pitted And Porous Large Diameter Fibre With A Fragmented Smaller Diameter Fibre Revealing Its Hollow Nature.

Plate 4.36. (x706) 4 Days Degradation.
PHB(FM)IP; Collapsed Matrix And A Fibre Showing The Fragmentation At A Hollow Region Caused By The Release Of A Bubble.

Plate 4.37. (x292) 7 Days Degradation.
PHB(FM)IP; Dense Mass Of Small Fibre Fragments And Particulate Matter.

Plate 4.38. (x670) 7 Days Degradation.
PHB(FM)IP; Pitted Large Diameter Fibre And Particulate Matter.

that this mass was formed by the heat and compressive forces within the phial, forming a type of melt pressed plastic, whilst the impurities in the TG sample and its degradation may have prevented a similar formation.

Scanning electron microscopy of the mass (Plate 4.41) revealed its unusual structure to be heavily pitted and porous, (Plate 4.42), with an apparent crystalline formation, (Plate 4.43), whilst other regions tended to indicate its formation from collapsed fibre fragments, (Plate 4.44).

It is unsure to what extent the presence of this melt pressed mass would have altered the degradation profile, this would be dependent upon its surface area to volume ratio, which although heavily pitted and porous may still be reduced compared to the equivalent mass of fibre fragments at the same stage of degradation. This may also help to explain the lack of observed surface erosion for the IP mass, when compared to the TG sample.

Using scanning electron microscopy the changes in fibre diameter during degradation were determined, these were then related to the fibre diameter distributions of the TG matrix, (Graphs 4.21-4.27). In the initial degradation stages the distributions of the IP and TG matrices were generally similar in the lower diameter range, with a loss of fibres possessing diameters between 0 and 1 microns. However, unlike the TG fibres of the same degradation time period, the main peak occurred at 4-5 microns as in the undegraded sample, with a similar frequency of 18%. The other main peaks in the undegraded sample occurred at 8-9 and 15+ microns, these changed within one hour of degradation to a single peak of 11-12 microns, having a frequency of approximately 12%. Unlike the TG

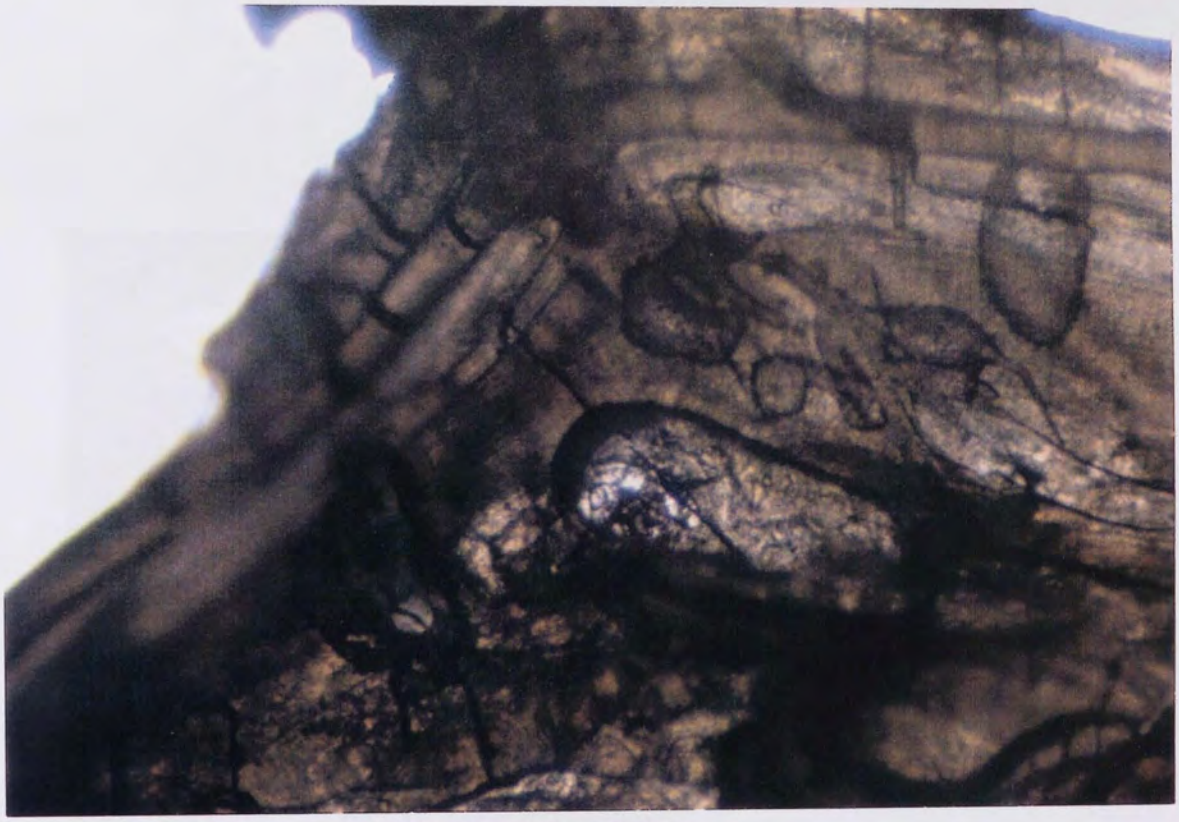

Plate 4.39. (x10) 33 Days Degradation.
PHB(FM)IP; Residual Melt Compressed PHB Mass At The Phial Base Showing A Noticeable Porous Nature.

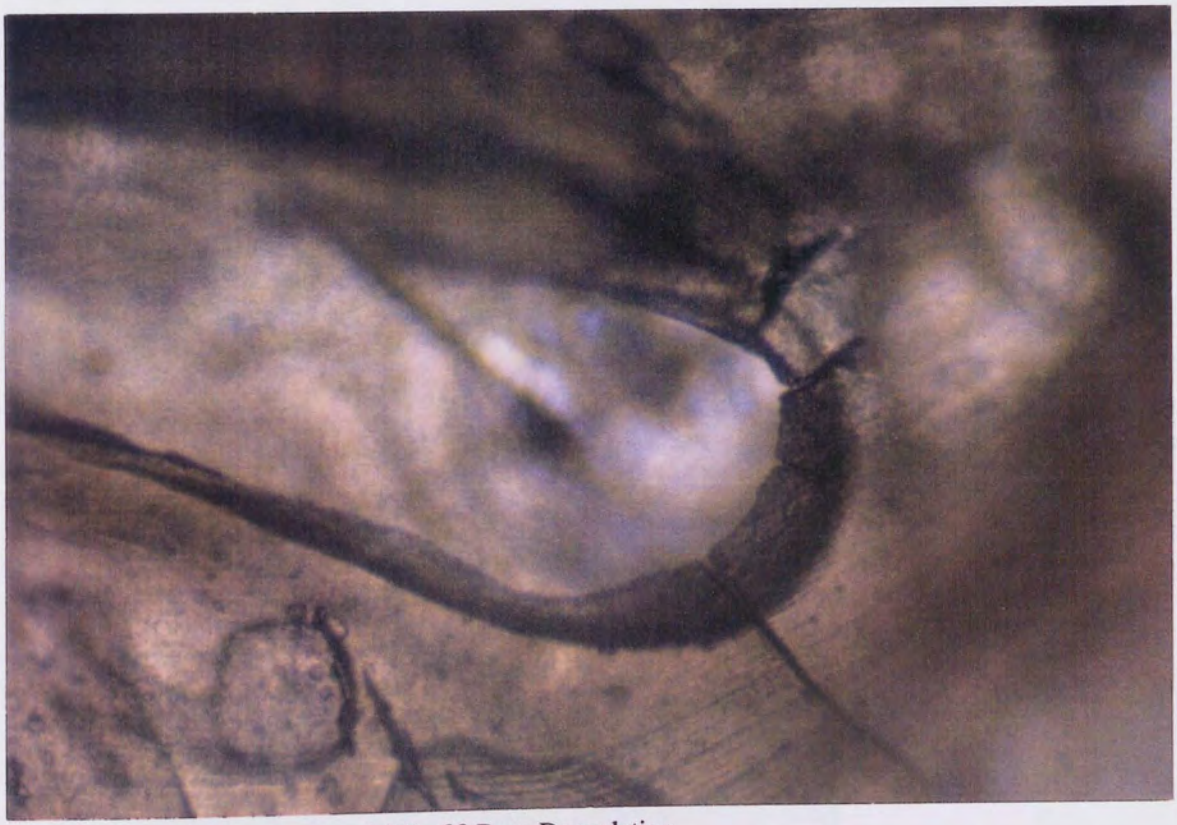

Plate 4.40. (x25) 33 Days Degradation.
PHB(FM)IP; Residual Melt Compressed Mass Illustrating A Large 'Pore'

Plate 4.41. (x17.2) 33 Days Degradation.
PHB(FM)IP; Residual Melt Compressed PHB Mass From The Phial Base.

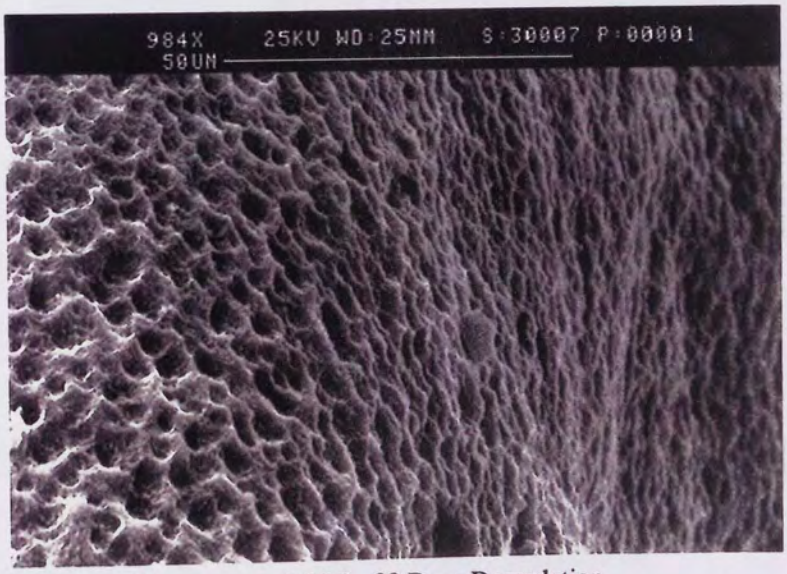

Plate 4.42. (x984) 33 Days Degradation.
PHB(FM)IP; Heavily Pitted And Porous Nature Of The Residual Melt Compressed PHB Mass.

Plate 4.43. (x118) 33 Days Degradation.
PHB(FM)IP; Section Of Melt Compressed PHB Mass, Illustrating Its Formation From The Collapsed PHB(FM)IP.

Plate 4.44. (x498) 33 Days Degradation.
PHB(FM)IP; Surface Of The Residual Mass Illustrating Its Origin From The Fibre Fragments.

fibres frequency distribution from the same time period, the peaks were much more irregular in the IP sample, with the main frequencies being in the smaller diameter range, 0-6 microns, (Graph 4.21). The distribution of the fibres for the TG sample after five hours degradation possessed fibres from all the diameter ranges except for the 0-1 micron range, whilst the IP fibres formed a much more irregular distribution with few fibres present in the medium diameter range, 6 to 15 microns. The 4-5 micron peak decreased to 10%, but the 3-4 and the 5-6um. ranges drastically increased to 22 and 18% frequency respectively.

Seperating the fibre distributions into small, medium and large diameter classifications, provided a somewhat clearer picture, (Graph 4.27). The smaller diameter distribution gradually rose within the initial degradation stages from 52 to 58% at 5hrs, before falling to 48% at 7hrs. This then increased in frequency until 66% of the fibres were in the small diameter range. Conversely the TG small fibre diameter frequency fell sharply during the initial stages and continued to decrease during the course of the degradation.

The medium and large diameter fibre frequencies gradually rose during degradation for the TG fibres, whilst in the case of the IP samples the medium diameters initially decreased from 40 to 24% at 5hrs, before sharply rising to 44% at 7hrs. This could be due to the medium diameter fibres having a larger proportion of amorphous material than the other diameters and readily collapsing to smaller diameters. Alternatively the smaller diameters readily collapsed, thus reducing the percentage of the medium diameter fibres. The latter was the most likely until 5hrs degradation, when a proportion of the medium diameter fibres, due to the amorphous regions, fragmented. These increased the frequency until a

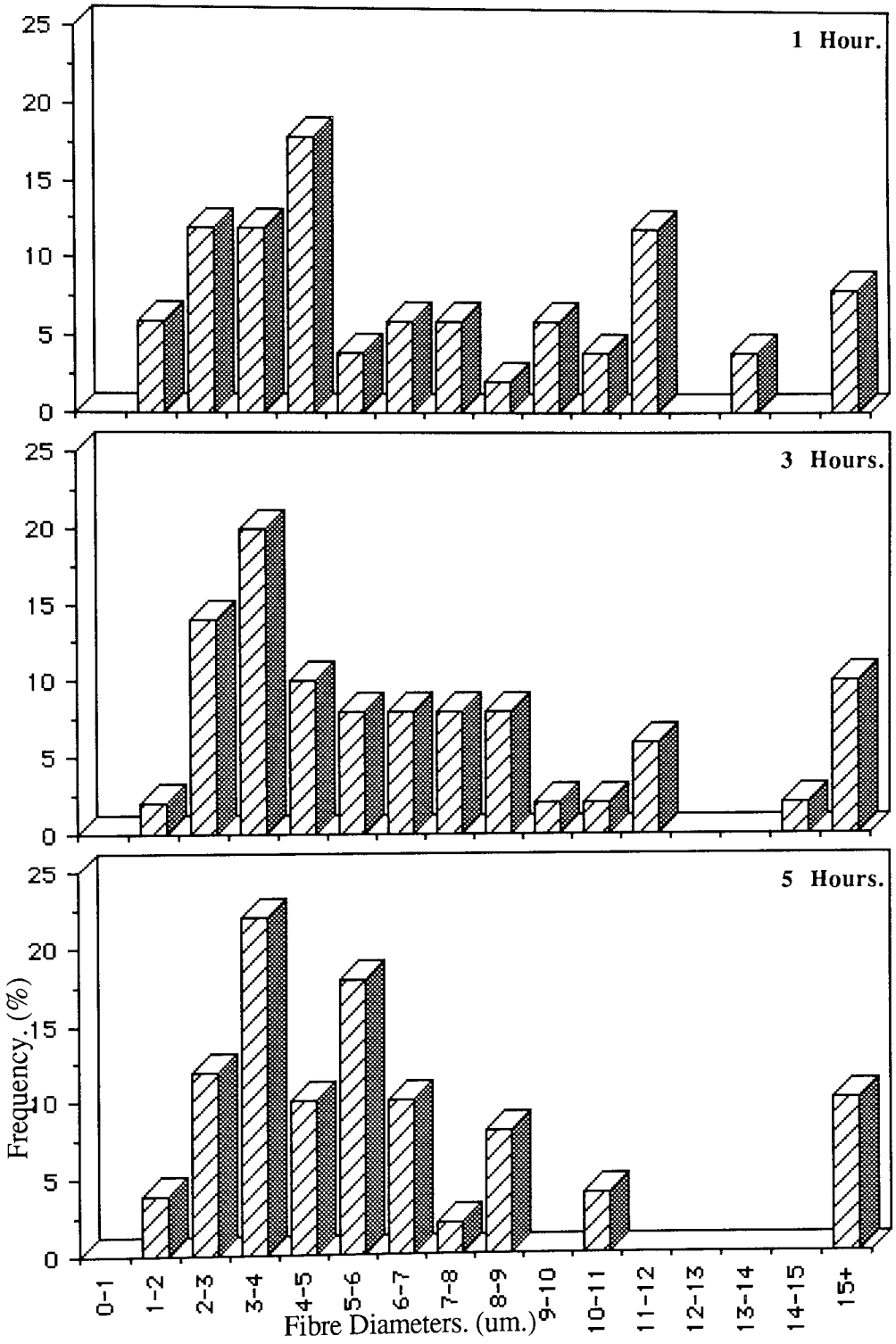

Graphs 4.21. To 4.23.

Fibre Diameter Distributions For PHB(FM)IP During Degradation In The Accelerated Degradation Model.

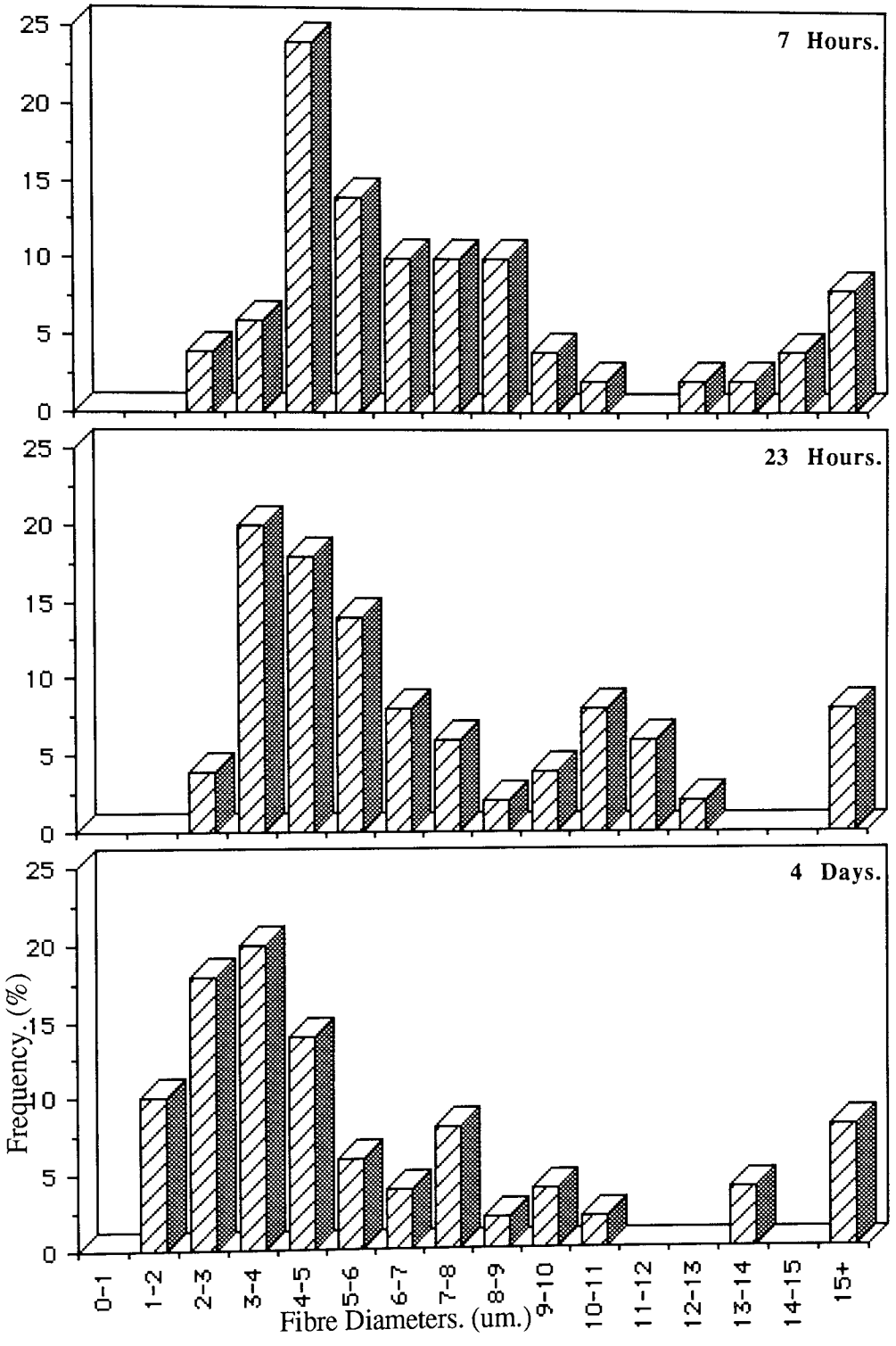

Graphs 4.24. To 4.26.

Fibre Diameter Distributions For PHB(FM)IP During Degradation In The Accelerated Degradation Model.

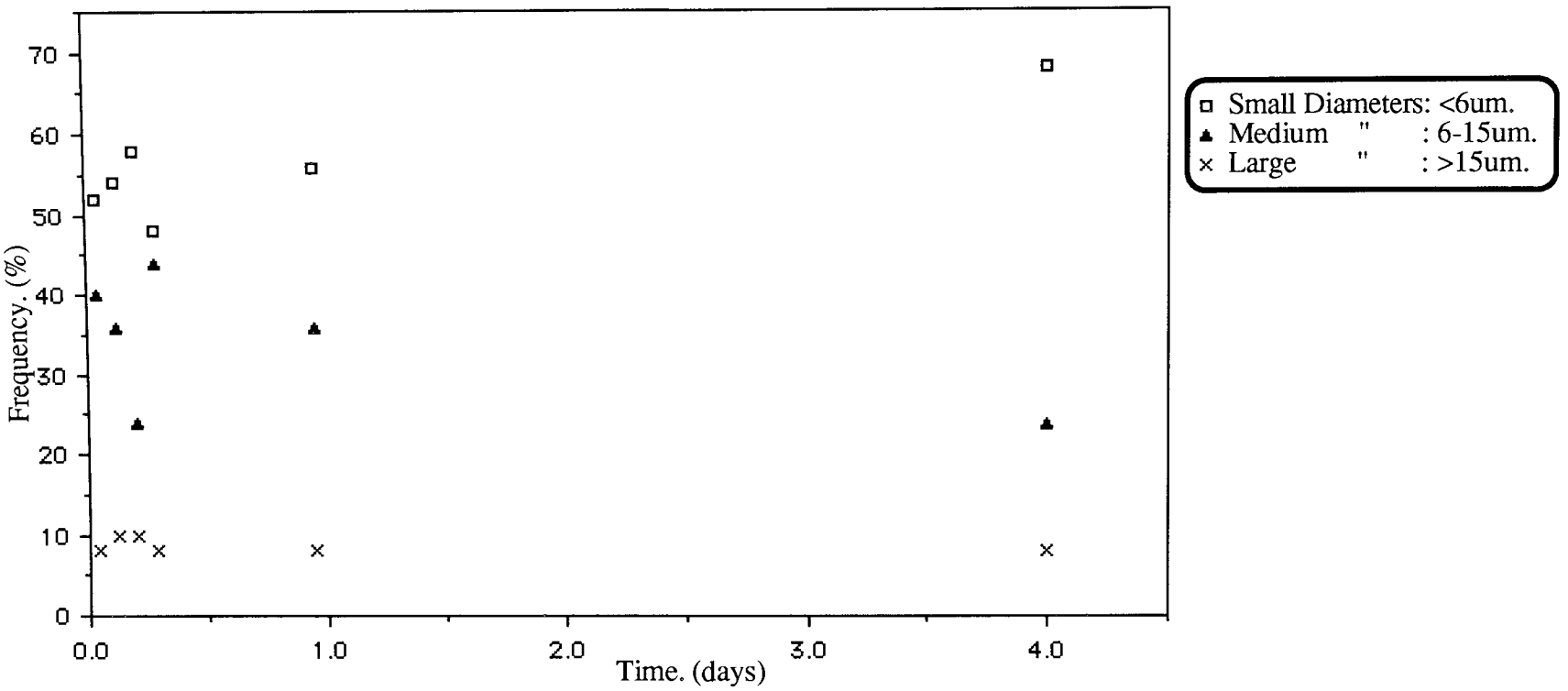

Graph 4.27.

General Fibre Diameter Distributions For Sample PHB(FM)IP. During Degradation In The Accelerated Degradation Model.

maximum of 44% at 7hrs was observed, with a corresponding decrease in the smaller diameter frequency. The number of fibres in the medium diameter range then gradually decreased to approximately 44% at day 4. The larger diameter distribution remained constant at 8 to 10 % frequency throughout the degradation experiment.

These results indicated that the larger diameter fibres were firmly resistant to degradation and maintained a similar percentage frequency throughout the experiment. The medium diameter frequency gradually decreased and this indicated that the main proportion of these fibres were also resistant to degradation by fragmentation in comparison to the smaller diameter fibres which readily fragmented and increased in proportion to the other fibres. This method of matrix breakdown in the primary stages of the degradation experiment contrasted with that of the TG samples, which had an increase in the medium and large diameter fibres due to a proportionately greater increase in fragmentation and the ready degradation to particulate matter and monomer of the smaller diameter fibres.

Thus, it was concluded that the TG matrix was more susceptible to collapse than the IP matrix. This would then provide a larger surface area to volume ratio and consequently the degradation rate would be greater than that of the IP sample in the initial stages. This was consistent with the degradation profiles obtained. The difference in the step stage between the samples indicates that the TG sample readily collapsed, whilst the IP sample gradually reduced matrix integrity. However, this initial rapid collapse in the TG matrix ensured a comparatively greater and faster reduction in the surface area to volume ratio, such that the degradation rate was reduced and the step stage formed.

4.3.3. Characterization Of The Partially Degraded PHB(FM)IP.

4.3.3.1 Differential Scanning Calorimetry (DSC) Studies.

The traces obtained using differential scanning calorimetry were initially similar to the TG curves, with the partially degraded fibres up to 7 hours degradation exhibiting interference, most possibly due to the buffer salts and contaminants. These fluctuations in the melting points (mp) and enthalpies (ΔHm) occurred until around day 1.

From graph 4.28 it can be observed that the fusion enthalpy gradually increased from 76Jg.$^{-1}$ at day 1 to a maximum of 98Jg.$^{-1}$ at day 4, before finally decreasing to 81Jg.$^{-1}$ at day 7. The enthalpy and percentage crystallinity increased after day 1 to form a peak at day 4, 98Jg.$^{-1}$. This peak corresponds to the TG peak at day 7 and both possessed a similar degree of crystallinity, 87 and 89 $\pm$3% for the TG and IP samples respectively. The time period difference tended to indicate that the undegraded IP sample had comparatively less available amorphous regions than the TG sample. This time difference of approximately three days was similar to the difference obtained in the onset of the terminal step stages in the monomer analysis degradation profiles; approximately 4 days. Similarly, the enthalpy peak occurred at the step stage in the TG sample degradation profiles.

The melting point for the TG fibres drastically decreased until day 4, however the melting point of the IP fibres gradually decreased indicating a more gradual reduction in stablity, whilst the minimum melting point at day 7 was approximately 159°C. for the IP fibres, the minimum for the TG was much less at approximately 136°C.

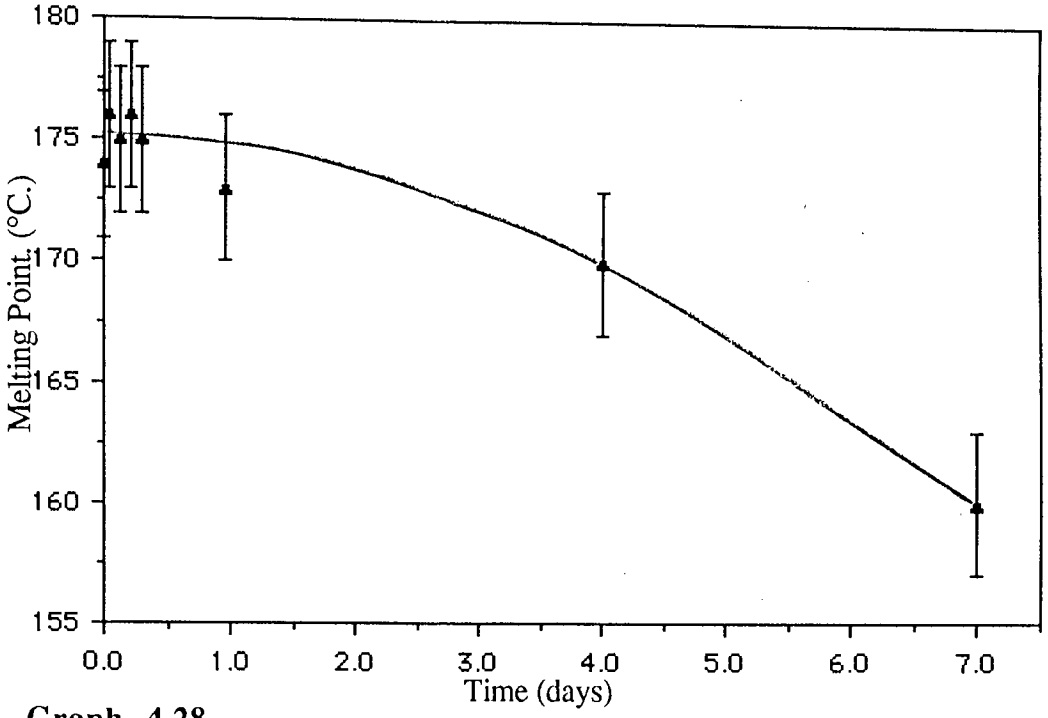

Graph 4.28.

Changes In Melting Point Of PHB(FM)IP, During Degradation In The Accelerated Model.

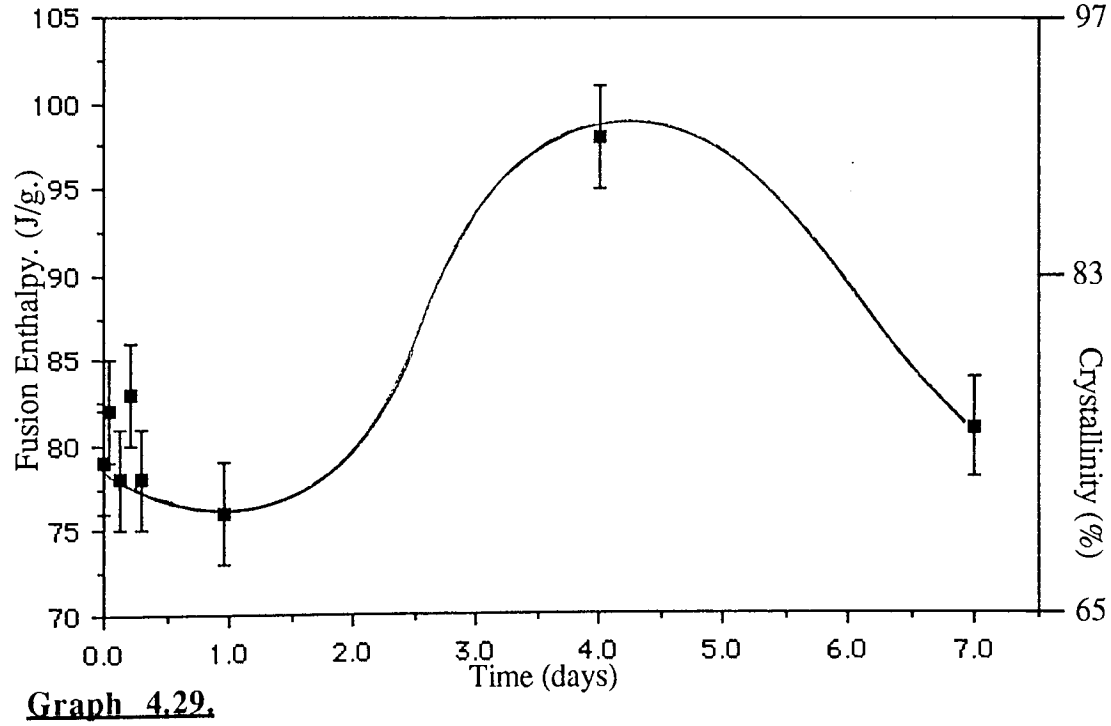

Graph 4.29.

Changes In The Fusion Enthalpy Of PHB(FM)IP, During Degradation In The Accelerated Model.

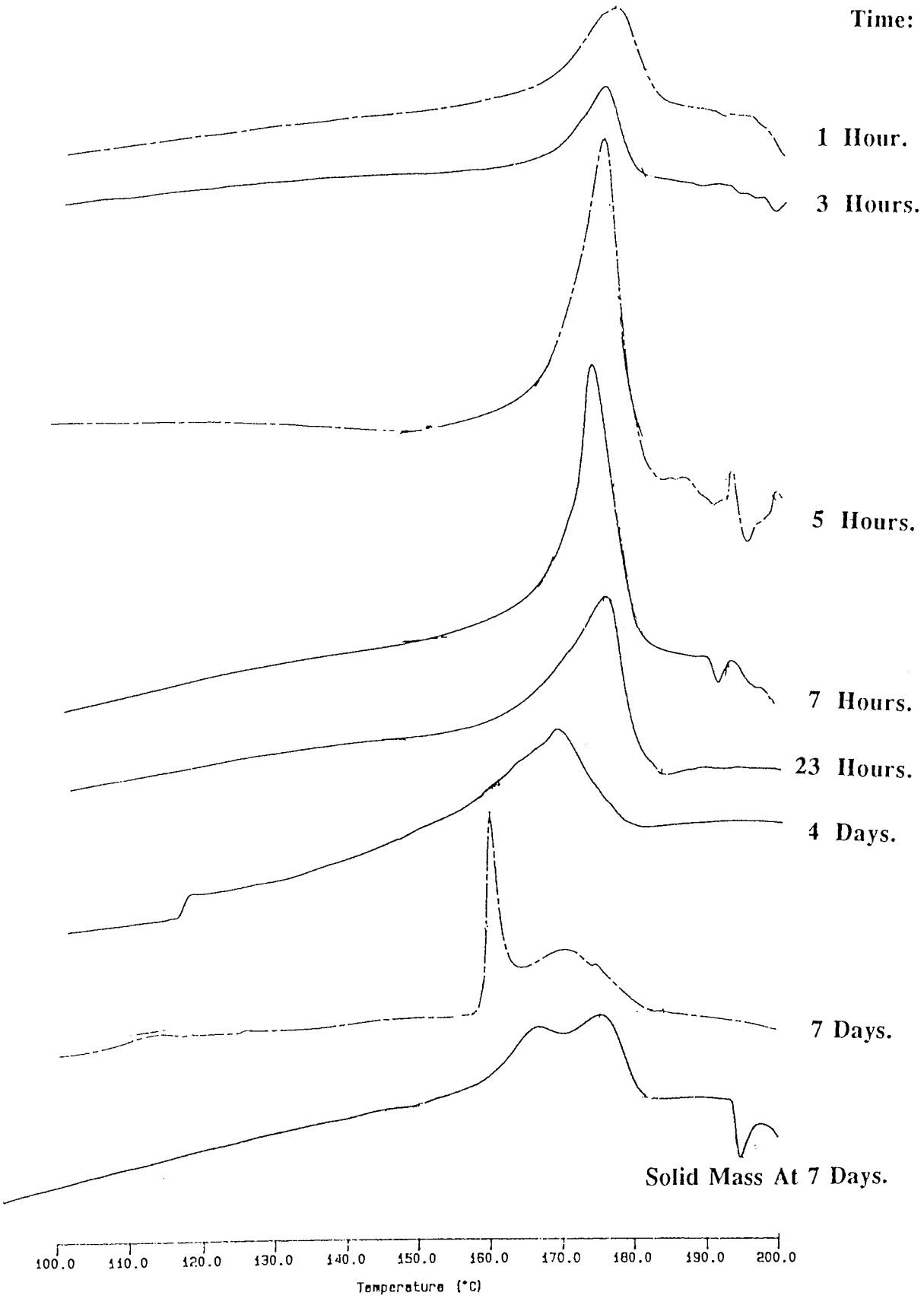

Figure 4.9.

Characterization Of PHB(FM)IP; Change In DSC Curves During Degradation In The Accelerated Degradation Model.

7 Days.

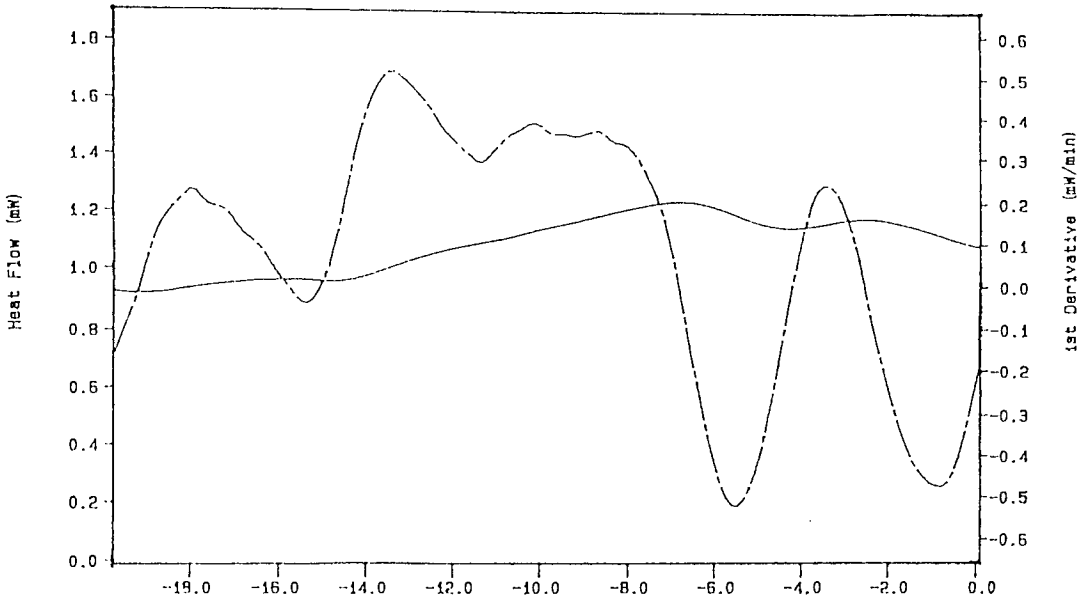

1 Hour.

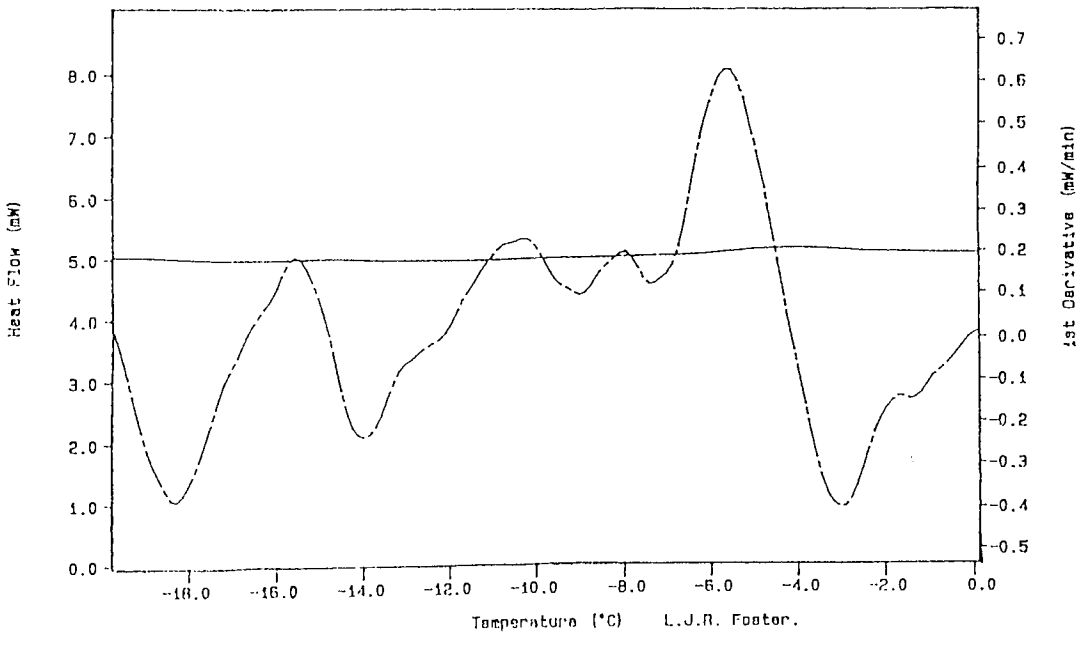

Figure 4.10.

Characterization Of PHB(FM)IP; DSC Curves Illustrating The Difficulty In Glass Transition Temperature Determination.

The DSC traces obtained were similar to the TG, (Fig. 4.9). However, there was the appearence of a slight shoulder towards the lower temperature range which gradually became more noticeable and thus a double 'hump' occurred. This also indicated a difference in the sampling with a proportion being comparatively more degraded.

The determination of the glass transition point (Tg) was also similar to that of the TG sample with no Tg's noticed even utilizing the first order derivative, (Fig. 4.10).

The solid plastic mass had a value of 177°C and a fusion enthalpy of approximately $77Jg.^{-1}$. The high melting point indicated a greater stability but the low enthalpy indicated a more amorphous material with a crystallinity of approximately 70 ±3%. These values were similar to the undegraded sample and therefore the plastic mass was most probably formed by those fibres which initially collapsed.

Thus, the DSC results confirmed that the TG sample was more degraded in the initial stages than the IP, although the purified PHB attained maximum crystallinity approximately 3 days before fibres from the PHB(FM)TG.

4.3.3.2. Photoacoustic Spectroscopy (PAS) Studies.

The initial undegraded sample of the PHB(FM)IP was practically identical to the trace obtained for the PHB(FM)TG. The traces obtained during degradation were also similar. A decrease in the waveband peaks for the two regions A and B were noted and the formation of a carboxylate ion peak at 1728 $cm.^{-1}$ was observed, together with the carbonyl shift, (Fig. 4.11).

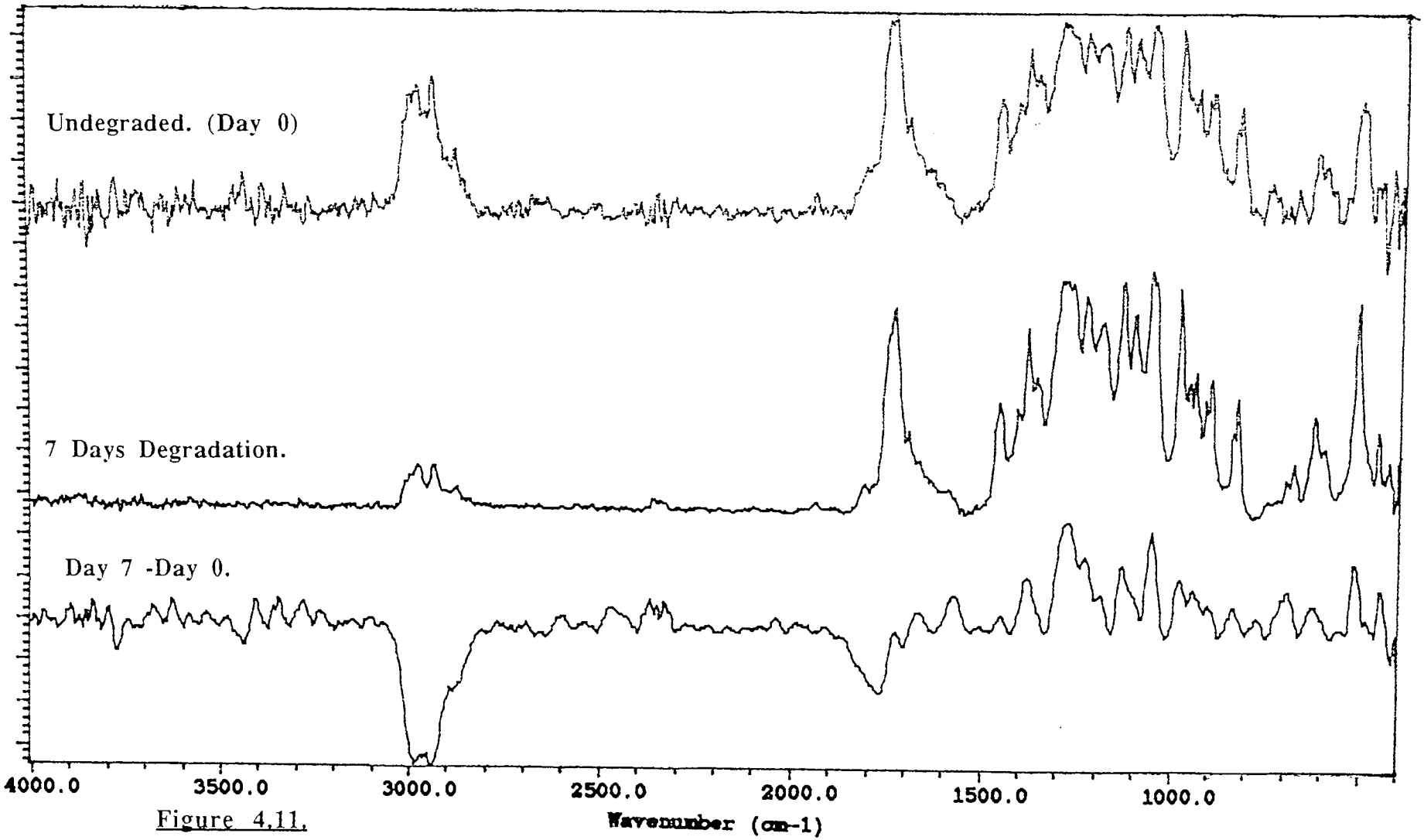

Figure 4.11.

Characterization Of PHB(FM)IP; FTIR-PAS Traces From The Undegraded PHB(FM)IP, Day 7 Degradation In The Accelerated Degradation Model And Their Difference.

The similarity of the PAS traces for the undegraded and partially degraded samples of the IP and TG matrices, indicated that there was little chemical difference between the two matrix types and the degradation mechanism was as anticipated.

4.3.4. Conclusions.

From the results obtained it was concluded that the increased purity polymer fibrous matrix was very similar to that of the technical grade matrix. Some of the impurities, solvent residue and a large proportion of the primary amorphous regions were removed during the purification process.

The increased purity matrix was generally more stable than that of the technical grade, with greater proportions of the latter collapsing more readily in the initial degradation stages, this then increased the surface area to volume ratio and facilitated the degradation, such that the initial degradation rate was greater than that of the increased purity. As the degradation progressed and fibre fragments settled and compacted at the phial base the rate was reduced, whilst the more gradual, slow collapse of the increased purity matrix ensured a more steady continuous degradation, so that the total percentage degradation for the increased purity sample was greater than that of the technical grade.

4.4. The Effects Of Different Solvents In The Production Process On The Degradation Of The Fibrous Matrix.

Samples of PHB(FM) increased purity grade (IP) with initial weights of 305mg. ±1.6% were gel-spun using the following solvents:

1)	Chloroform.	Sample Ch.
2)	Methylene Chloride.	" MC.
3)	50/50 Chloroform and Methylene Chloride.	" Ch/MC.

Samples of these were degraded under accelerated conditions of pH 10.6 and temperature 70 ±0.2°C. The amount of degradation was determined by monomer analysis.

It can be observed from graph 4.30 that the fibres produced using the chloroform solvent (Sample Ch.) had an initially slower degradation rate than those illustrated for the other solvents which possessed similar rates. There was approximately 45% degradation for the MC. and Ch/MC. samples at day 5 with only 21% for the Ch. sample. However, degradation proceeded in the Ch. sample whilst the step stages were observed for the other samples, such that by day 14 all three samples possessed approximately the same degradation to monomer, (55%).

The initial degradation in stage I for the MC. and Ch/MC. samples was probably due to the instabilities in the matrix introduced by the use of different solvents. At the start of stage III fragmentation in sample Ch/MC. exceeded that of MC., this was due to the 50/50 solvent balance which obviously facilitated the further breakdown of the fragments. Thus, sample Ch/MC., with fibres extracted from both chloroform and methylene chloride

solvents, appeared to exhibit the best degradation characteristics from both samples Ch. and MC., whilst surface erosion and fibre collapse had more noticeable effects on the initial degradation rates.

The final degradation stage IV began around day 28 for samples MC. and Ch/MC. But this occurred earlier for sample Ch., at approximately day 25. At stage IV, the degradation was such that the sample order was Ch/MC.>MC.>Ch. with values of approximately 91, 82 and 67% degradation to the monomer respectively. Assuming linearity to day 28, overall degradation rate values of 3.1, 2.7 and 2.3%dy.$^{-1}$ respectively were noted. Measuring these values at the beginning of stage IV in each case gave an alternative rate for sample Ch. of 2.6%dy.$^{-1}$, very similar to that of sample MC. but with less degradation actually measured.

Thus, it was concluded that within the accelerated degradation model, the fibrous matrix produced from the mixed solvents of chloroform and methylene chloride was comparatively more degraded than the matrices produced from the single solvent. The production of the PHB fibrous matrix utilizing methylene chloride solvent is less cost effective than those with chloroform, due to the higher vapour pressure required and consequently the greater expenditure in heating. Thus, production has continued using chloroform as a solvent. It would be interesting to note however, the effect of varying the percentages of the the two solvents on their matrix degradation profiles. Similarly the use of other solvents should also be explored, since solvent type has a noticeable effect on the degradation nature of the matrix produced. The PHB(FM) could therefore be 'tailored' for individual requirements determined by the wound type and severity etc.

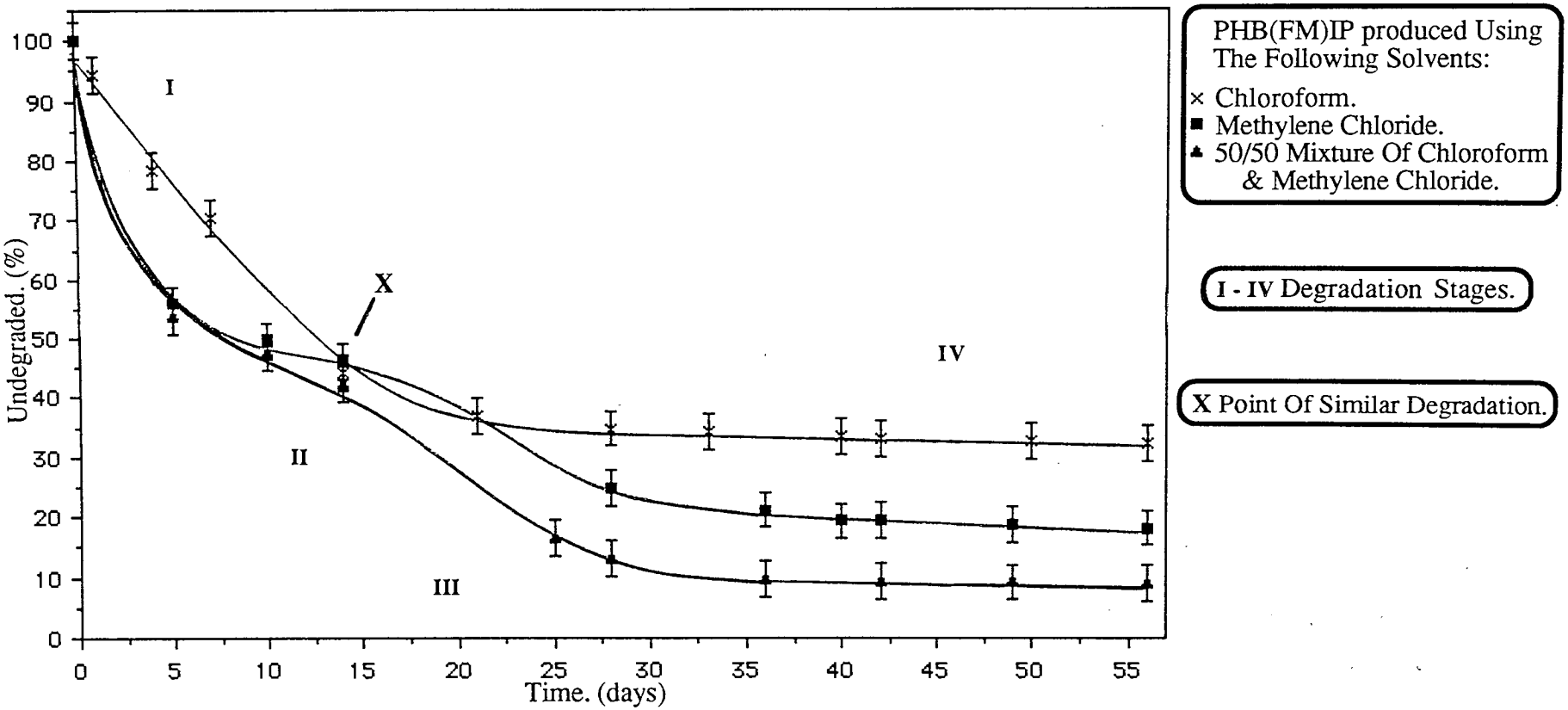

Graph 4.30.

The Affects Of Production Solvents On The Degradation Of PHB(FM)IP In The Accelerated Degradation Model.

4.5. The Effect Of Sample Agitation On The Degradation Profiles

Two samples of PHB(FM) increased purity grade (IP) with initial weights of 305mg. ±1.6% produced using chloroform as solvent were degraded under accelerated conditions of pH 10.6 and temperature 70 ±0.2°C. Sample 1-A. had continuous agitation in a vertical direction. This was performed in order to prevent settling of the particulate and fibre fragments at the base of the phial. The agitation was limited to this function and it was ensured that little mechanical breakdown of the matrix was incurred as a result of this motion. The degradation was determined by monomer analysis. Sample 2-NA. had no agitation.

Graph 4.31 illustrates the degradation profiles of the two samples. It can be observed that the degradation profiles for the two samples were similar in the initial stages until around day 6, where approximately 28% degradation was determined. After day 6 the degradation proceeded such that the terminal step stage IV was observed to start at day 14 for both samples, but with approximately 57% degradation for sample 2-NA. and about 78% for 1-A. (Table 4.1) This difference in the percentage degraded sample between 1-A. and 2-NA. was due to the degraded particulate analysis and agitation effect. It is interesting to note that in both cases the 'plateauing' of the degradation curve during stage IV occurred to a similar extent and at a similar time. The reduction in degradation rates during stage IV was practically identical for both samples, (Graph 4.31). In both cases, the limiting factor difference between the samples was the presence of the agitation for sample 1-A.

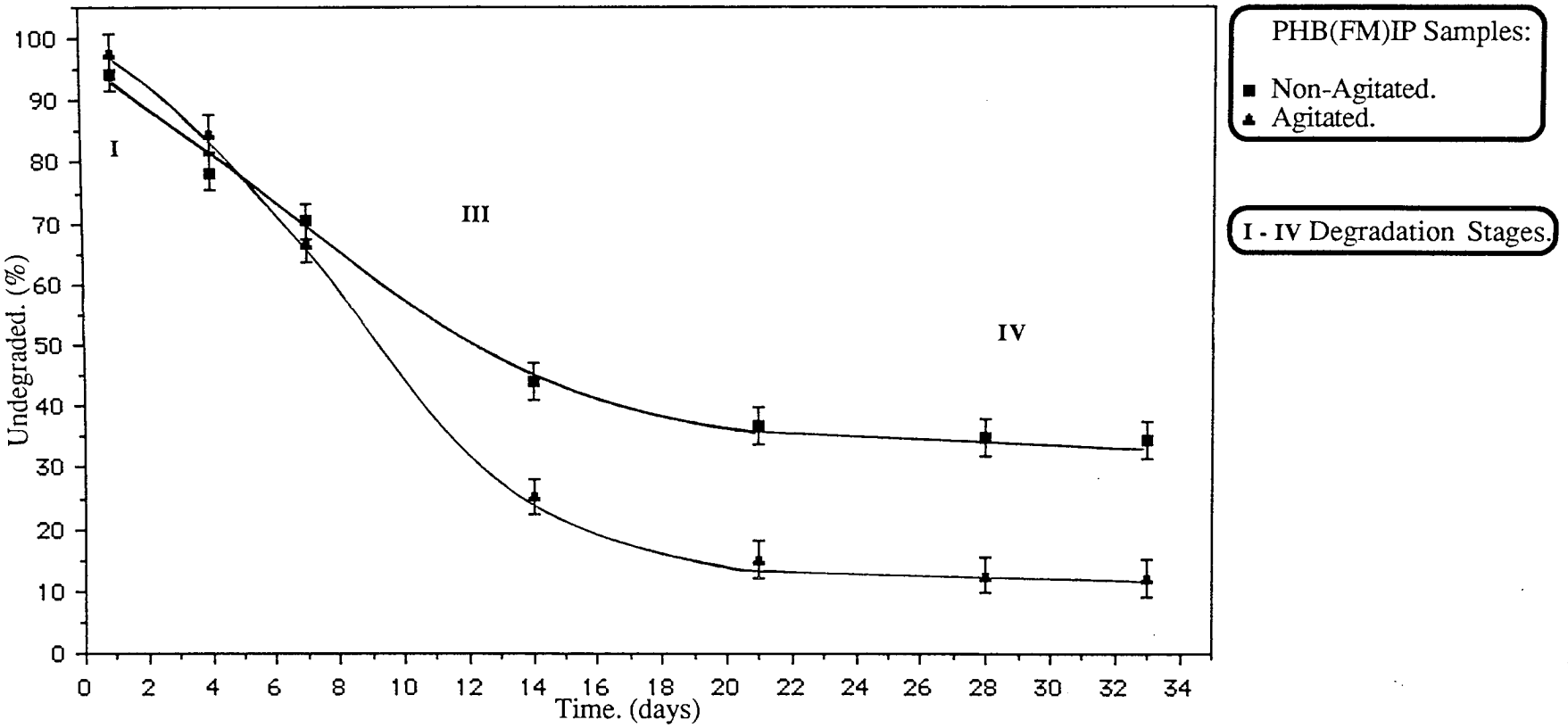

Graph 4.31.

The Affect Of Sample Agitation On The Degradation Profile Of PHB(FM)IP In The Accelerated Degradation Model, Monitored By Monomer Analysis.

Stage IV for sample 2-NA. was previously concluded as being due to degradation kinetics, degraded particulate matter and the compaction of particulate and fibre fragments at the phial base with a subsequent reduction in the available surface area to volume ratio of the sample. As a result of the agitation, stage IV for sample 1-A. was due to the degradation kinetics and degraded particulate matter. However, when the weight of undegraded material at termination of the experiment (day 33) was measured, there remained approximately 6 and 17% of the agitated and non-agitated samples respectively.

	Sample 1-A. (Agitated)	Sample 2-NA. (Non-agitated)
Degraded to monomer.	88%	65%
" " particulate.	6%	18%
Total Degraded.	**94%**	**83%**
Undegraded.	6%	17%

Table 4.1

Approximate Values Of Degraded And Undegraded Samples.

The difference between the undegraded material determined at termination for sample 2-NA. and the weight that had degraded to monomer for sample 1-A. was about 6%. This difference was due to the removal of the degraded particulate matter and soluble impurities. The remaining 6% of the 1-A. sample indicated that some other limiting factor was affecting the degradation and facilitating the formation of the terminal step. This was concluded as being degradation resistant matter, of which highly crystalline PHB formed a substantial proportion.

The difference between the undegraded matter and that degraded to monomer for sample 2-NA. was approximately 18%. This 18% difference was due to soluble contaminants and degraded particulate matter which were removed during the experiment and not retained by the filtration process at termination. Utilizing the difference determined for sample 1-A., it can be concluded that the agitation was responsible for approximately 11% of sample degradation that did not occur in sample 2-NA. Similarly, agitation was also responsible for the further degradation of approximately 12% of degraded particulate matter to monomer.

Therefore, it can be concluded that particulate/fibre fragment matter settlement and compaction and thus phial base surface area, was an important limiting factor in the sample degradation. Agitation removed this limiting factor and enhanced degradation of the PHB(FM)IP by approximately 11%. This occurred due to a maintainance of the optimum available surface area to volume ratio for the sample. Therefore, the terminal step stage IV of the non-agitated degradation profile was concluded as being caused by a number of limiting factors:

1) The kinetics of the degradation experiment.

2) Material settlement and compaction, this reduced the available surface area to volume ratio and as a result degradation was affected by the phial base size.

3) Degradation resistant material, impurities and mainly highly crystalline PHB.

4.6. General Conclusions.

This chapter has investigated and discussed the degradation of the technical grade and the increased purity polymer fibrous matrix, PHB(FM)TG and PHB(FM)IP, in the accelerated degradation model. The effects of initial sample weight and agitation in the model were also investigated and from these experiments it was concluded that the degradation models should incorporate the following factors:

a) 20mls of buffer.

b) An initial sample weight of 305mg. ±1.6%.

c) Minimum agitation of the samples.

The degradation of the PHB(FM)TG was discussed and related to the undegraded matrix. The monomer analysis degradation profile was characterized by a number of stages; there was an initial induction phase, stage 0, until approximately 6 hrs with little degradation observed. This was due to the collapse to particulate matter of a proportion of the structurally weaker fibres in the diameter range 0-1um., this particulate matter continued to fragment and this led to the stage I degradation which occurred until around day 7. Between days 7 and 9 there was a 'step' stage (II) with little degradation determined, this was due to fragmentation of the remaining matrix to fibre fragments and particulate matter and consequently, the stage II was not observed in the gravimetric analysis profile. Degradation to monomer progressed in stage III between days 9 and 18, at day 18 the 'terminal step' stage IV began with little or no further degradation exhibited. These degradation stages, and stage IV in particular, were determined as being affected by the following 'limiting factors':

a) The kinetics of the experiment.

b) Matter settlement and compaction (a reduction in the surface area to volume ratio).

c) Degradation resistant matter (impurities and highly crystalline PHB).

The degradation profiles confirmed that the experimental accuracy of measuring the undegraded (gravimetry) and degraded fractions (monomer + degraded particulate analysis) of the matrix during its degradation was within ±2%.

A number of small and large 'unstable' fibres were observed in approximate diameter ranges 0-2 and 15+um. respectively, their structural weaknesses were due to handling and manufacturing stresses and as a result of production, mainly bacterial impurities. Degradation occurred by hydrolytic action which randomly cleaved the ester linkages, initially weakening the fibres and eventually leading to their physical collapse to fibre fragments and progressivly to the monomer, (See Figs. 4.1, 4.7 & 4.8).

The matrix degradation was characterized by a gradual decrease in the melting point with little change during the stage IV time period, whilst the fusion enthalpy and crystallinity increased to a peak around day 7 and then decreased. Thus, there was an initial degradation of the mainly amorphous regions followed by the crystalline. These trends were generally consistent to those observed for the increased purity polymer sample PHB(FM)IP. However, in this case, the melting point changes were not as great initially, with a more gradual decrease, whilst the enthalpy/crystallinity peak occurred earlier around day 4.

Purifying the PHB removed some of the impurities, solvent residue and primary amorphous regions of the PHB(FM)IP. This increased the matrix stability when compared to the technical grade matrix; PHB(FM)TG, so that a gradual collapse and degradation of the PHB(FM)IP was observed, this then ensured a greater percentage degradation when compared to the PHB(FM)TG. The affects of altering the production solvent on the PHB(FM)IP degradation was also investigated. Degradation was facilitated by the heavily porous nature of those fibres extracted from the methylene chloride solvent, such that the degradation exceeded that of the PHB(FM) from the chloroform. However, the degradation of those fibres extracted from the 50/50 solvent mixture exceeded that of both the other matrices.

Thus, the experiments in this chapter have 'fine tuned' the degradation models and investigated and discussed the degradation of the PHB fibrous matrix in the accelerated degradation model. The surface area to volume ratio of the fibrous matrix during degradation and the constraints imposed by the degradation model were concluded as major factors affecting the degradation and were reflected in the degradation profiles.

The degradation of the PHB(FM)IP acts as a baseline to which the degradation of other samples could be compared. Attempts to alter the PHB(FM)IP degradation by blending it with various polysaccharides and by copolymerizing with poly(β-hydroxyvalerate), (PHV), are investigated in the next chapter.

Chapter Five.

The Effects Of Blending And Copolymerizing On The Degradation Of PHB(FM)IP In The Accelerated Degradation Model.

5.0. General Introduction.

This chapter investigates the effects of blending and copolymerizing on the degradation of the PHB(FM)IP in the accelerated degradation model. Degradation of the samples was monitored by gravimetric and particulate analysis, whilst the PHB degradation was also monitored by monomer analysis. The partially degraded samples were analyzed qualitatively using phase contrast and scanning electron microscopy and characterized utilizing DSC and FTIR-PAS. The degradation of the samples was then compared to the homopolymer degradation discussed in chapter 4.

5.1. The Degradation Of PHB(FM)IP Blended With Various Polysaccharides.

5.1.0. Introduction.

The degradation of PHB(FM)IP samples blended with the following polysaccharides were investigated in the accelerated degradation model utilizing monomer analysis. The degradation profiles obtained were then compared to that obtained for the homopolymer.

1)	Glu-42.	PHB(FM)IP + 42% Glucose.
2)	Suc-42.	" 42% Sucrose.
3)	SA-30.	" 30% Sodium Alginate.
4)	SA-7.	" 7% Sodium Alginate.
5)	SCC-9.	" 9% Sodium Carboxycellulose.

Unfortunately, due to a lack of sample, gravimetric analysis and the subsequent examinations of the partially degraded matrices were not performed.

5.1.1. Degradation Profiles And Their Comparison To The PHB(FM)IP Profile.

Graphs 5.1-5.4 illustrate the degradation profiles for the co-blended samples and their comparisons with the profile obtained for the PHB(FM)IP.

As can be observed from graph 5.1, the degradation to monomer of Glu-42. and PHB(FM)IP were similar, but with two noticeable differences in the profiles; Glu-42. had a slight step stage II with a collapse of fibres at days 6 to 10 and then a comparatively sudden stage IV at day 25, whilst the IP sample was far more gradual in its collapse and degradation. The similarity in the degradation profiles occurred despite the fact that ideally only 58%, by weight, of PHB was initially present in sample Glu-42. compared to the homopolymer sample. This indicated that the blending was most probably a mixture of the PHB and glucose rather than a homogenous blend. However, from the monomer measurements and the sample weight remaining at termination of the experiment on day 36, approximately 27.1% was unaccounted for, therefore a maximum of only 27% glucose could have been initially present. Thus, it was concluded that the blending efficiency was not effective and the proportions of the two components was not as originally claimed.

Sucrose was also blended at a weight value of 42%, but this had a more noticeable effect on the degradation profile when compared to Glu-42. (Graph 5.2). An initial rapid degradation occurred at stage I so that by day 3 approximately 69% of the sample

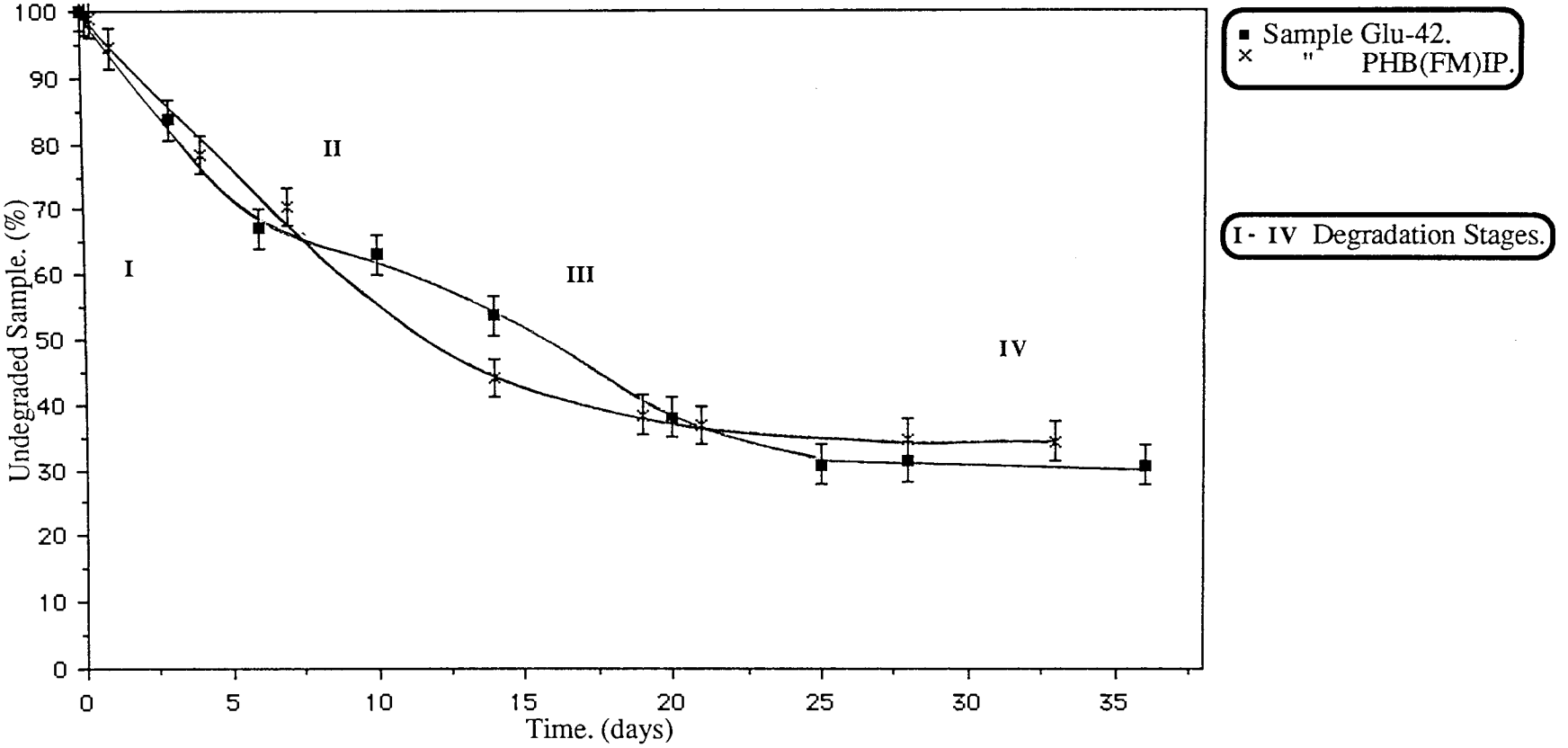

Graph 5.1.

Degradation Profiles Of PHB Component Of Samples Glu-42. And PHB(FM)IP. In The Accelerated Degradation Model. Monitored By Monomer Analysis.

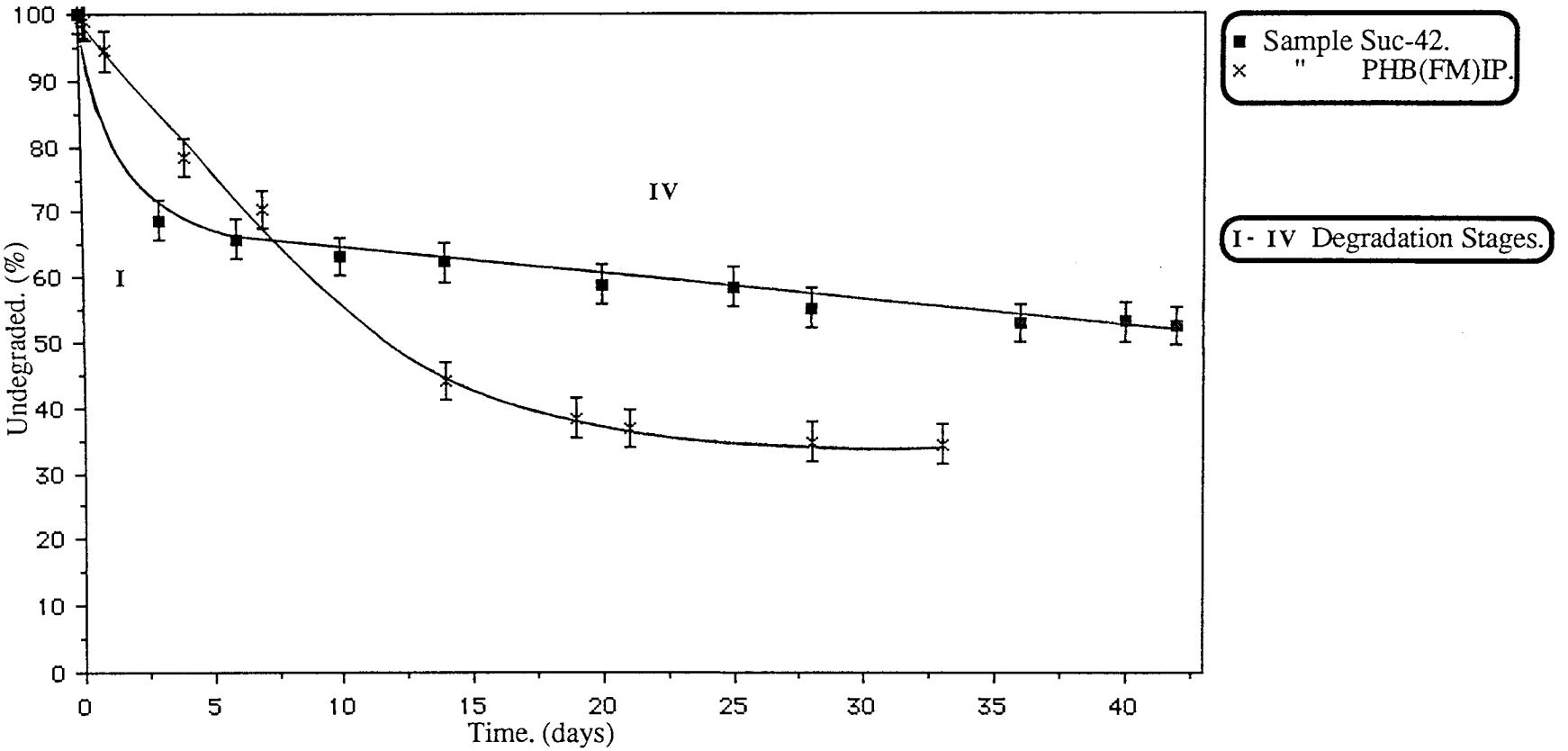

Graph 5.2.

Degradation Profiles Of PHB Component Of Samples Suc-42. And PHB(FM)IP. In The Accelerated Degradation Model, Monitored By Monomer Analysis.

remained 'undegraded'. After day 3 the degradation of Suc-42. was minimal due to the settlement and compaction of the fibre fragments at the phial base. As a result of this, the degradation of the PHB(FM)IP equaled that of Suc-42. around day 8 with a value of approximately 35%. This indicated that the collapse of the matrix readily occurred within the first few days and was due to a proportional lack of polymer in the sample when compared to the IP sample. Settlement and compaction at stage IV readily occurred with a small release of monomer. Nevertheless, a total degradation of around 47% in sample Suc-42.occurred out of a possible 58%, assuming a correct initial loading of 42% Sucrose.

Graph 5.3 illustrates the degradation profile for the PHB(FM)IP blended with 9%, by weight, Sodium Carboxycellulose. Sample SCC-9. exhibited a similar degradation profile to that of Glu-42. with an initial rapid degradation at stage I, followed by a step stage around days 10 to 14 with approximately 50% degradation.

The degradation of the PHB from samples IP and SCC-9. was the same at day 12 with approximately 48%. The IP sample began its gradual terminal stage at day 14, whilst in SCC-9. this did not occur until day 20, so that at the terminal step stage IV the degradation for the IP sample was 65% and 78% for the co-blend, at days 28 and 36 respectively.

The degradation profiles for the PHB(FM)IP blended with 7 and 30% sodium alginate (SA-7. and SA-30.) are illustrated in graph 5.4 and are compared to the IP sample. The initial degradation at stage I was similar for all three samples until about day 6 where the

sodium alginate samples exhibited step stages at days 6 to 10.

The stage III matrix collapse greatly increased the available surface area to volume ratio of the fibre fragments and particulate matter, such that an increase in the degradation was observed. In the case of SA-30., the proportional lack of remaining polymer reduced the amount of monomer produced, whilst for SA-7. the degradation proceeded more quickly and exceeded that of the IP sample.

The terminal step stage IV of the SA-30. sample occurred comparatively suddenly at day 25, whilst for SA-7. a more gradual degradation was observed from day 20 to the stage IV at day 25. However, this gradual degradation was less noticeable than that observed for the IP sample. At day 25, when the step stage IV for all three samples was reached, the degradation was in the order: SA-7.>IP>SA-30., with approximately 79, 64 and 61% degradation respectively.

Weight measurements of the final undegraded samples revealed similar values for SA-7. and SA-30., with 9.7 and 8.8mg. respectively, (Approximately 3.2 and 2.9%). These values were well within a 2% error range. Consequently it was concluded that increasing the percentage loading of the sodium alginate from 7 to 30% (ideally) had little effect on the further degradation of the samples, despite the fact that the initial weight of PHB was considerably reduced.

The increase in monomer formation with SA-7. above that determined for the IP sample, was greater than could be justified by the reduced initial weight of PHB and the effect of

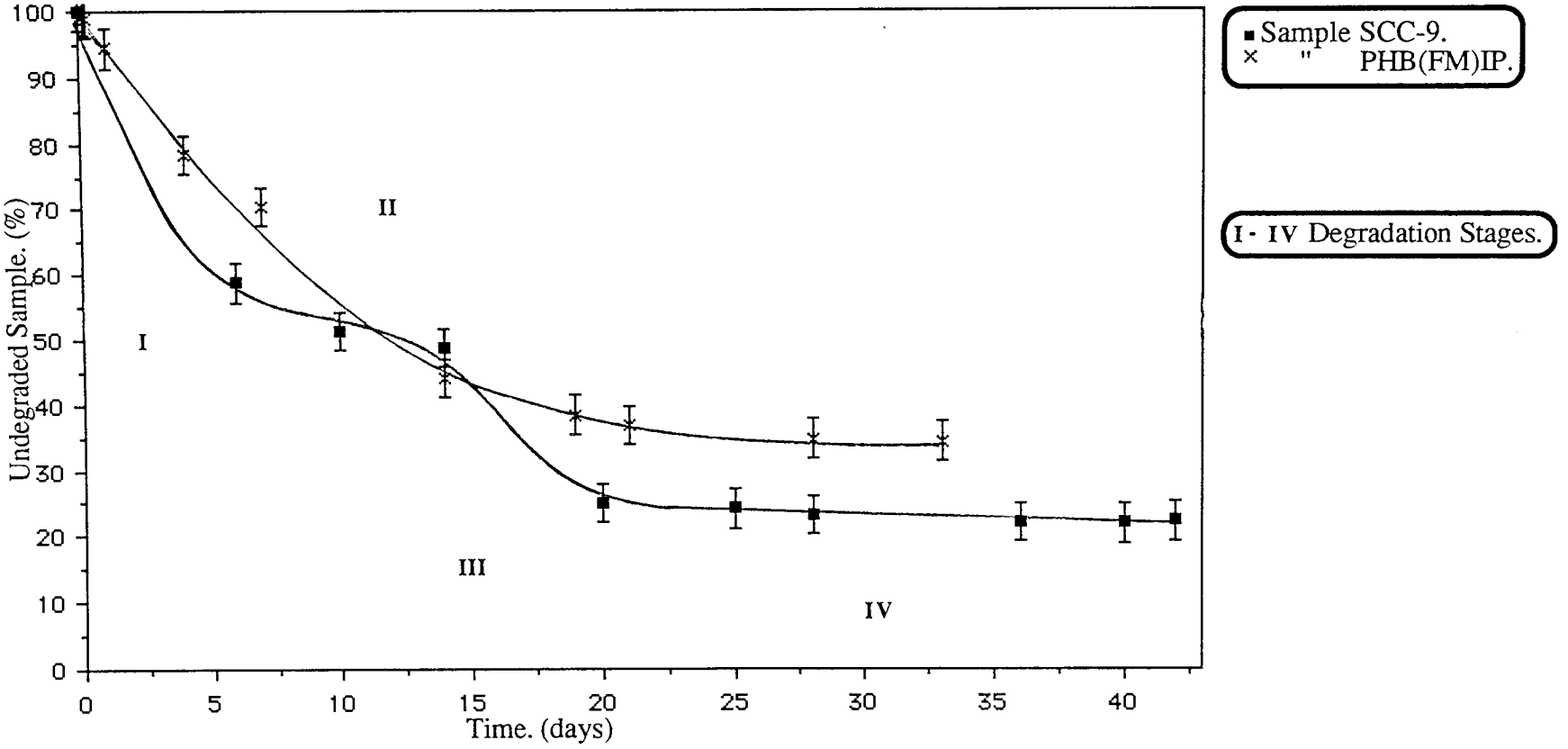

Graph 5.3.

Degradation Profiles Of PHB Component Of Samples SCC-9. And PHB(FM)IP. In The Accelerated Degradation Model. Monitored By Monomer Analysis.

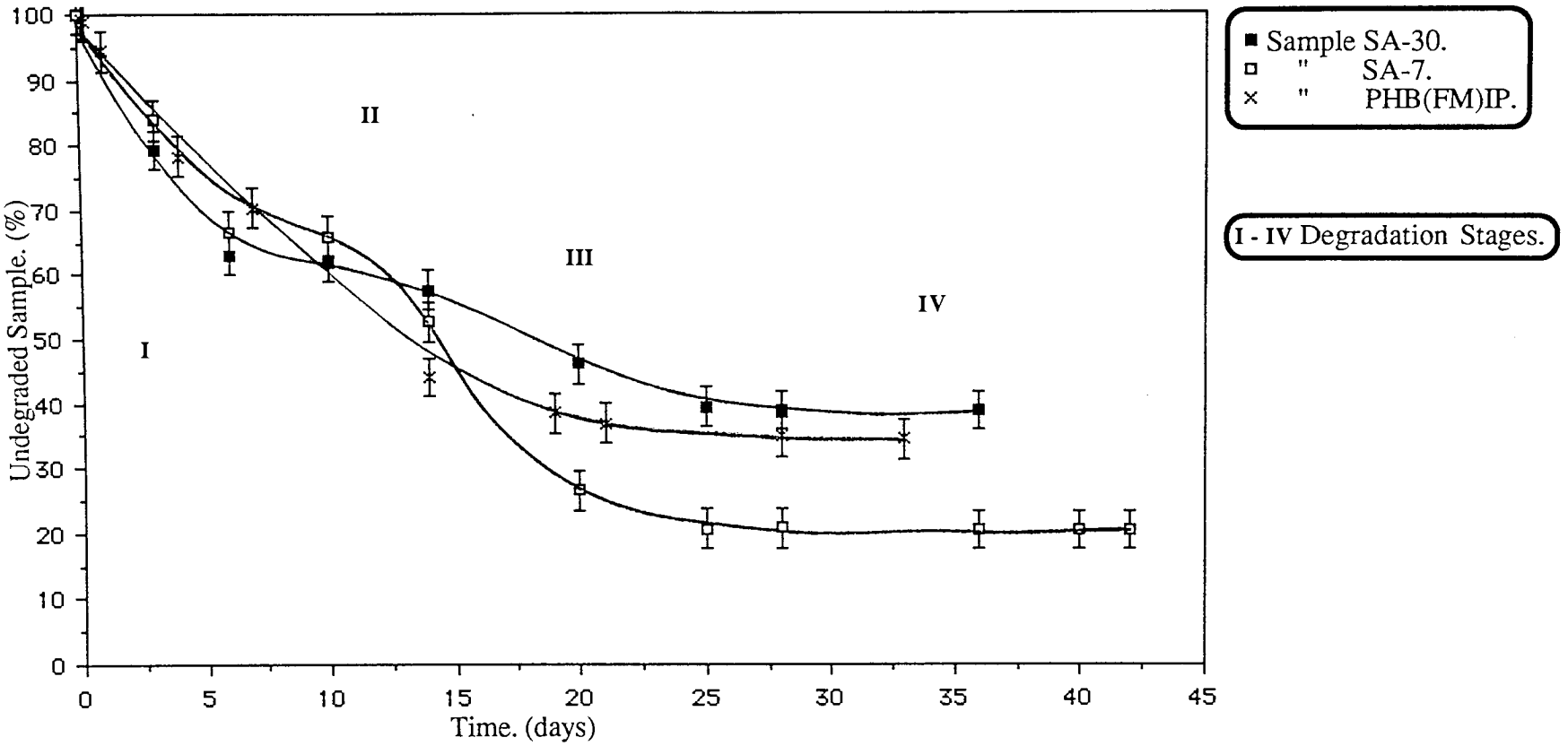

Graph 5.4.

Degradation Profiles Of PHB Component Of Samples SA-30., SA-7. And PHB(FM)IP. In The Accelerated Degradation Model, Monitored By Monomer Analysis.

this on the experimental conditions of phial size etc. Thus, in this instance, blending facilitated the degradation of the matrix and the polymer.

Thus, the co-blend degradation was characterized by an initial period of rapid degradation (Stage I) followed by a step stage period where little degradation of the PHB occurred, (Stage II). After the stage II a further period of comparatively rapid degradation was observed, (Stage III), before the gradual decrease in the degradation rate until the terminal step stage IV was attained, where only small amounts of degradation were measured. This contrasted with the PHB(FM)IP degradation profile which exhibited a gradual degradation from stage I to stage IV, with no noticeable stage II or III.

Therefore, it was concluded that the polysaccharides affected the stability of the matrix. The polysaccharide readily dissolved into the degrading medium and weakened the blended fibres so that a proportion of these collapsed into various sized fragments, this increased the surface area to volume ratio of the PHB available for degradation and thus the rapid degradation at stage I was observed.

The proportion of the collapsing fibres in the stage I was dependent upon the nature and loading of the polysaccharide. In those co-blends with a comparatively low percentage loading the stage I degradation was similar to that of the unblended matrix. This tended to indicate that in these cases the polysaccharide increased the surface area to volume ratio and substantially weakened some of the fibres but did not increase the initial collapse rate, (SA-7. and SCC-9.). Increasing the loading substantially weakened a comparatively greater number of fibres, such that a practically total collpase of the matrix was observed

and the degradation simply progressed into the terminal stage IV almost immediately, as in the case of sample Suc-42.

The degradation, settlement and compaction of the fibre fragments and particulate matter from the stage I reduced the availabe surface area to volume ratio, so that a period of little degradation was observed, this was the step stage II. The time of this step varied, with the majority of the samples exhibiting the stage II between days 6 to 10 approximately, but for sample SCC-9. it was observed around days 10 to 14. During this period the remaining matrix collapsed and this then facilitated an increase in the degradation rate, observed as stage III. The degradation proceeded until the limiting factors of the experimental system, as discussed in chapter 4, caused the terminal step stage IV.

Assuming linearity to the terminal step stage IV, the overall degradation rates were calculated and these were found to occur in the following order:

SCC-9.> SA-7. > IP. > Glu-42. > SA-30. > Suc-42.

3.8	3.2	3.0	2.8	2.4	2.1	$\%dy.^{-1}$: Rate.
9	7	0	<27	30	42	% : Loading.

These rates show that increasing the polysaccharide loading reduced the monomer formation and therefore the degradation rate by reducing the initial amount of polymer present and facilitating the collapse of the matrix. Glu-42. was alleged to have 42% glucose, but from the monomer degradation values and the weight remaining at termination, it was determined that the value was less than 27%.

5.1.2. Conclusions.

It was concluded that blending the PHB(FM)IP with various percentage loadings of different polysaccharides had the effect of altering the degradation profile. The degradation profiles determined were dependent upon the nature of the polysaccharide, its dissolution and loading. The polysaccharides caused the introduction of a step at stage II. Larger percentage loadings facilitated the matrix collapse, settlement and compaction so that a sudden noticeable stage IV occurred, whilst the lower percentage loadings produced a more gradual stage IV, but less so than the IP sample.

The degradation profiles and the overall linear degradation rates illustrated that blending with a small percentage loading noticeably affected the degradation of the matrix and polymer although this was also dependent upon the polysaccharide, whilst further increasing the percentage loading simply reduced the amount of PHB present. Thus, it was concluded that blending between the PHB and the polysaccharides probably occurred to a certain optimum loading, increasing this loading then merely mixed the two constituents and did not appear to affect the further degradation of the PHB. The optimum loading and its affects on the matrix/polymer degradation were dependent upon the polysaccharide utilized.

The degradation of these samples was as anticipated from the observations and examinations of the undegraded samples in chapter 3.

5.2 The structure And Degradation Of PHB(FM)IP Blended With Various Percentage Loadings Of Pectin.

5.2.0. Introduction.

The degradation of the following samples were investigated utilizing gravimetric analysis in the initial stages until day 7, except for sample L.Pec.9. which continued the analysis until termination of the experiment at day 33. The effects on the degradation of the PHB were also investigated utilizing monomer analysis until day 33.

1)	L.Pec.9.	PHB(FM)IP + 9%	Low Mwt.	Pectin.	
2)	L.Pec.15.	"	15%	"	
3)	L.Pec.25.S.	"	25%	"	Start of manufacturing run.
4)	L.Pec.25.E.	"	25%	"	End of manufacturing run.
5)	H.Pec.10.	"	10% High Mwt.	Pectin.	

These experiments were performed in order to investigate the effects on the degradation of the PHB and the matrix by blending the PHB(FM)IP with different loadings and molecular weights of pectin. The results were intended for use in the alteration of the PHB degradation to more favourable time periods depending upon the proposed situation and function of the matrix. The blending efficiency was also determined as part of the degradation investigations.

5.2.1. Comparison Of Degradation Profiles.

5.2.1.1. Comparison Of Gravimetric, Particulate And Monomer Analysis For Sample L.Pec.9.

Graph 5.5 illustrates the degradation profiles for the sample L.Pec.9. utilizing monomer and gravimetric analysis. The former profile shows the degradation of the PHB only, whilst the latter reveals the degradation of the matrix. The two profiles were similar with the first step (stage II) occurring between days 7 and 10 and the second terminal step (stage IV) beginning at approximately day 19 and gradually occurring until completion at day 25.

When the stage IV was attained at day 25, the difference between the monomer and gravimetric analysis profiles was approximately 10.8%, with values of 12.9 and 2.1% undegraded sample remaining respectively, (ie; 87.1 and 97.9% degradation.). This difference between the two systems was due to the degraded particulate matter, the pectin and error. Utilizing the degraded particle measurements in graphs 5.6 and 5.7 a profile of the measured degraded fraction (monomer + measured degraded particulate matter) was also illustrated, (Graph 5.5), the difference between the gravimetric and degraded fraction profiles was then determined as 2.9%. The stability studies in chapter 3 indicated that a proportion of the degraded particulate matter was due not only to the PHB but to the pectin also degrading. Consequently this 2.9% difference between the undegraded and degraded determinations was due to dissolved pectin, contaminants and errors.

As observed from graph 5.5B there was a sudden difference at day 1 between the monomer and particulate analysis profiles, this tended to indicate that the majority of the

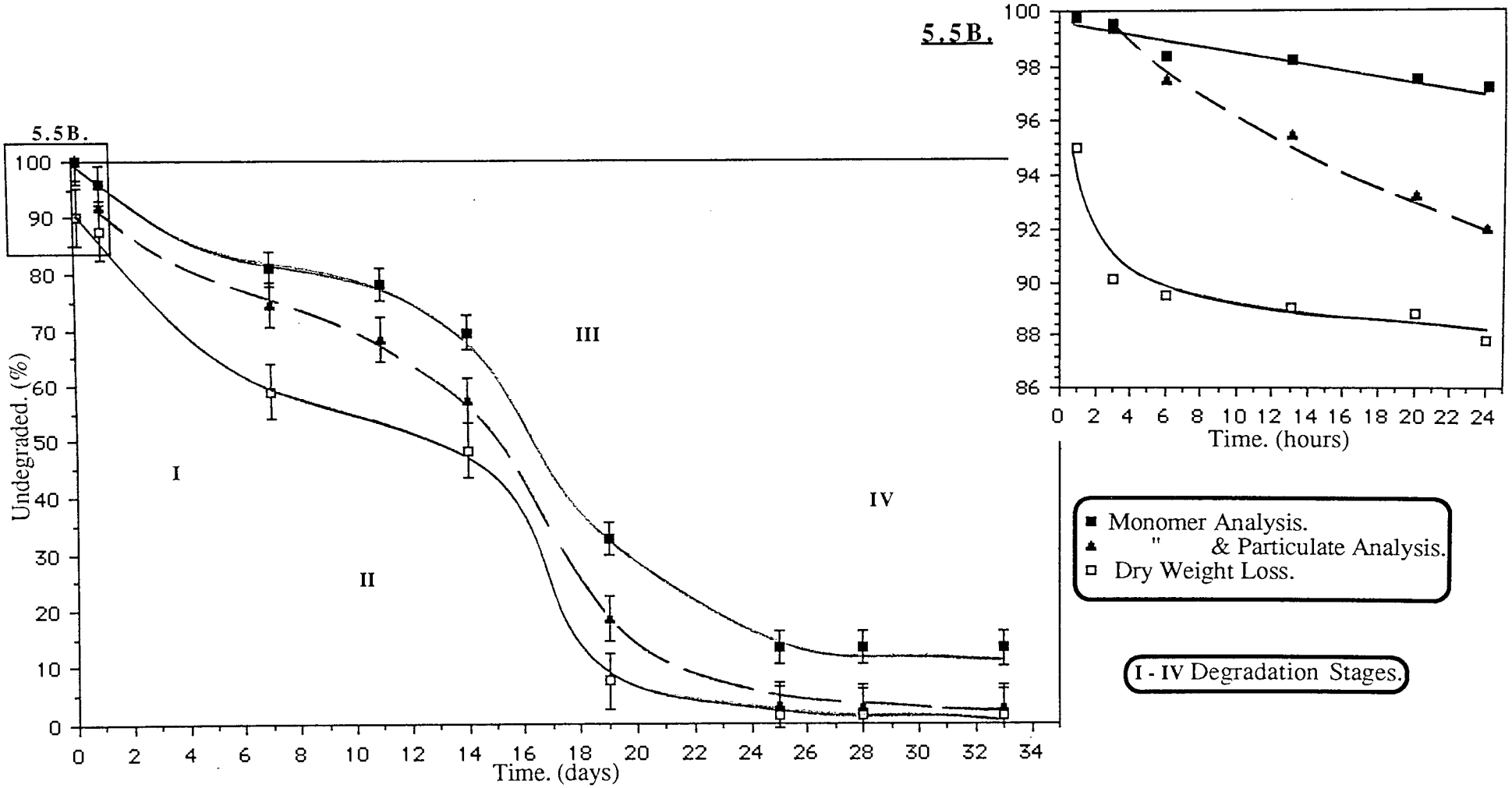

Graph 5.5.

Degradation Profiles Of Sample L.Pec.9. In The Accelerated Degradation Model, Monitored By Monomer And Gravimetric Analysis.

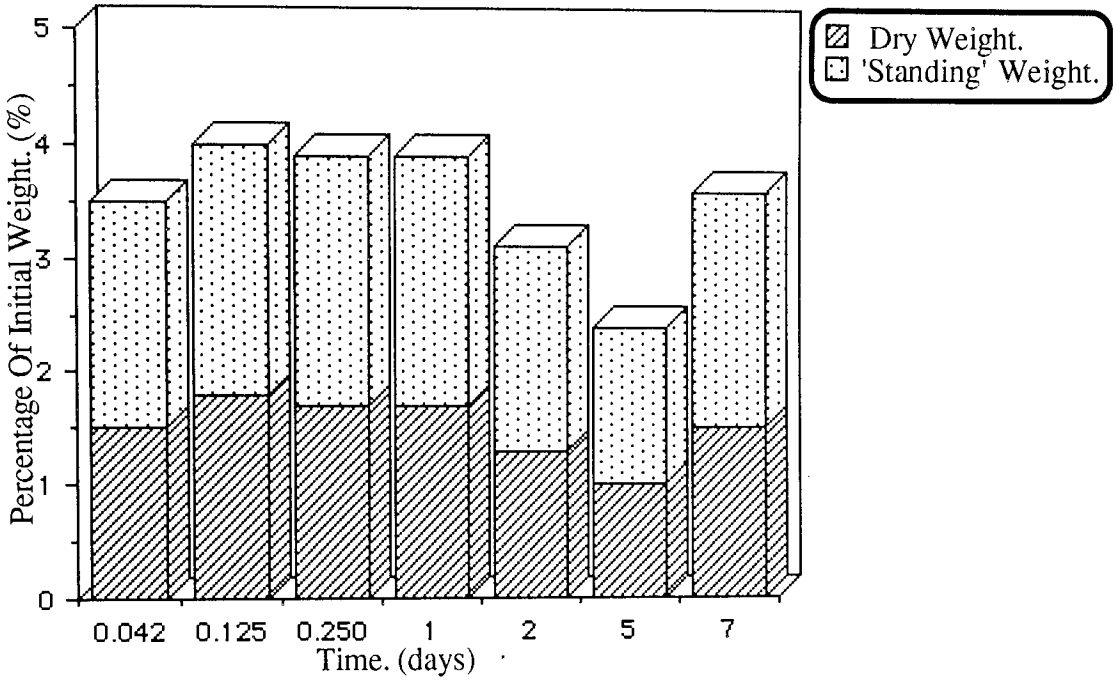

Graph 5.6.

Measured Degraded Particulate Matter For Sample L.Pec.9.

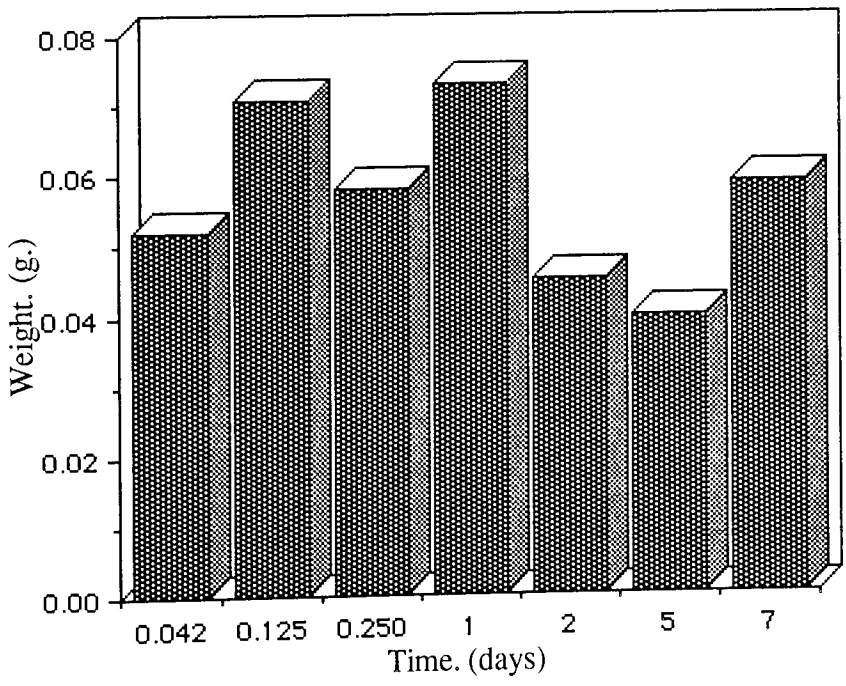

Graph 5.7.

Ideal Total Degraded Particulate Matter For Sample L.Pec.9.

pectin was removed as particulate matter. Similarly, there was an initial weight loss of approximately 9.6% at 3 hours degradation, (Graph 5.5B), this was most probably due to a degradation to particulate matter, dissolution of contaminants and the primary amorphous regions which were comparatively greater than those observed for the IP sample and therefore most probably contained a substantial proportion of the pectin.

The degraded fraction profile (monomer + degraded particulate analysis) mirrored the monomer analysis degradation profile at most stages. However, a difference was observed between the step stages, where the degraded particulate matter caused a less noticeable step than that observed for the monomer analysis profile alone. This indicated that the collapse of the remaining matrix occurred during this stage, which then facilitated an increase in the surface area to volume ratio by the production of large quantities of degraded and undegraded particulate matter this then resulted in a greater monomer analysis degradation rate at stage III, but during stage II was observed as the proportional increase in the amount of degraded particulate matter, so that the step stage II was less pronounced in the degraded fraction profile than that of the monomer analysis profile.

5.2.1.2. Comparison Of L.Pec.9. With PHB(FM)IP.

The monomer analysis degradation profile for L.Pec.9. was compared to that determined for PHB(FM)IP, (Graph 5.8) whilst the degraded fraction profiles (monomer with degraded particulate matter) for both samples were also examined, (Graph 5.9). These illustrate the differences in PHB degradation due to the blending.

It was observed from graph 5.8 that at stage I the initial degradation of the IP sample was

similar to that of the L.Pec.9., this indicated that the pectin did not affect the initial fibre collapse. As the IP sample continued to collapse and degrade, the L.Pec.9. apparently remained relatively stable. The L.Pec.9. degradation to monomer from the fibre fragments and particulate matter of the stage I collapsed fibres was reduced due to a lack of degraded particulate matter (Graphs 5.6 and 5.7) and this was observed as the step stage II. However, the IP sample continued to gradually degrade so that between days 2 and 18, the degradation of the PHB to monomer for the PHB(FM)IP exceeded that of L.Pec.9.

At approximately day 7 the remaining L.Pec.9. matrix collapsed and the fibres readily fragmented to a comparatively greater extent than the gradual fragmentation of the IP sample, thus, the amount of particulate matter increased and the degradation to monomer gradually increased around day 11 (stage III) and then exceeded that of the IP, so that at day 18 the degradation of the L.Pec.9. and the PHB(FM)IP was approximately 60%.

Thus, the degradation to monomer gradually reduced for the IP sample and the terminal step stage IV began at day 14, with approximately 63% degradation by day 25. The terminal step stage for L.Pec.9. also occurred gradually but with a much greater degradation rate and therefore a relatively sudden stage IV occurred at day 25 with about 84% degradation.

Utilizing the initial sample weight versus log linear degradation rate in section 4.1, an approximation for the degradation rate increase due to the initial presence of less PHB in the blend was determined, this was approximately $0.5\%.dy.^{-1}$. This expected change in the degradation rate would ideally account for a further 12.5% degradation to monomer by

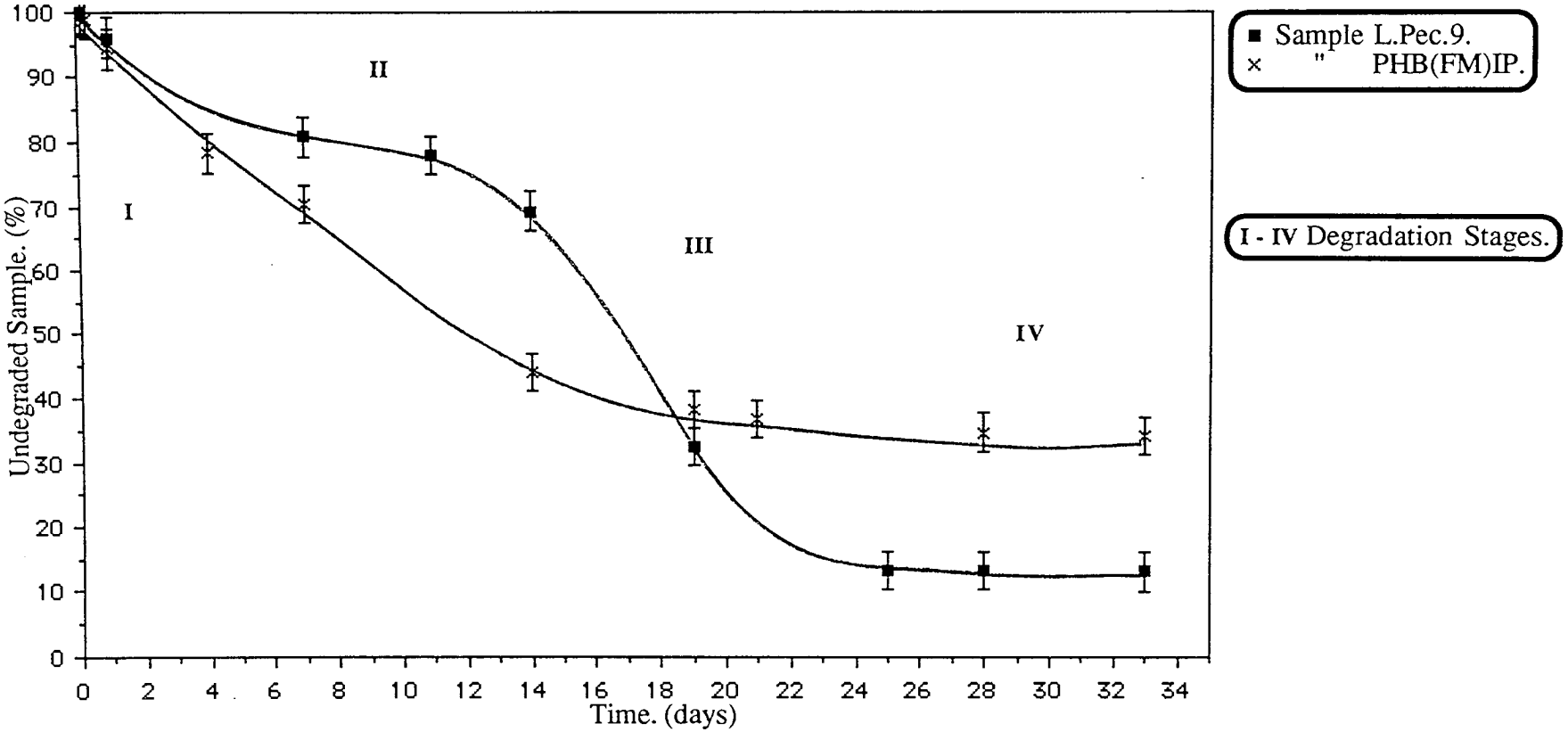

Graph 5.8.

Degradation Profiles Of PHB Component Of Samples L.Pec.9. And PHB(FM)IP. In The Accelerated Degradation Model, Monitored By Monomer Analysis.

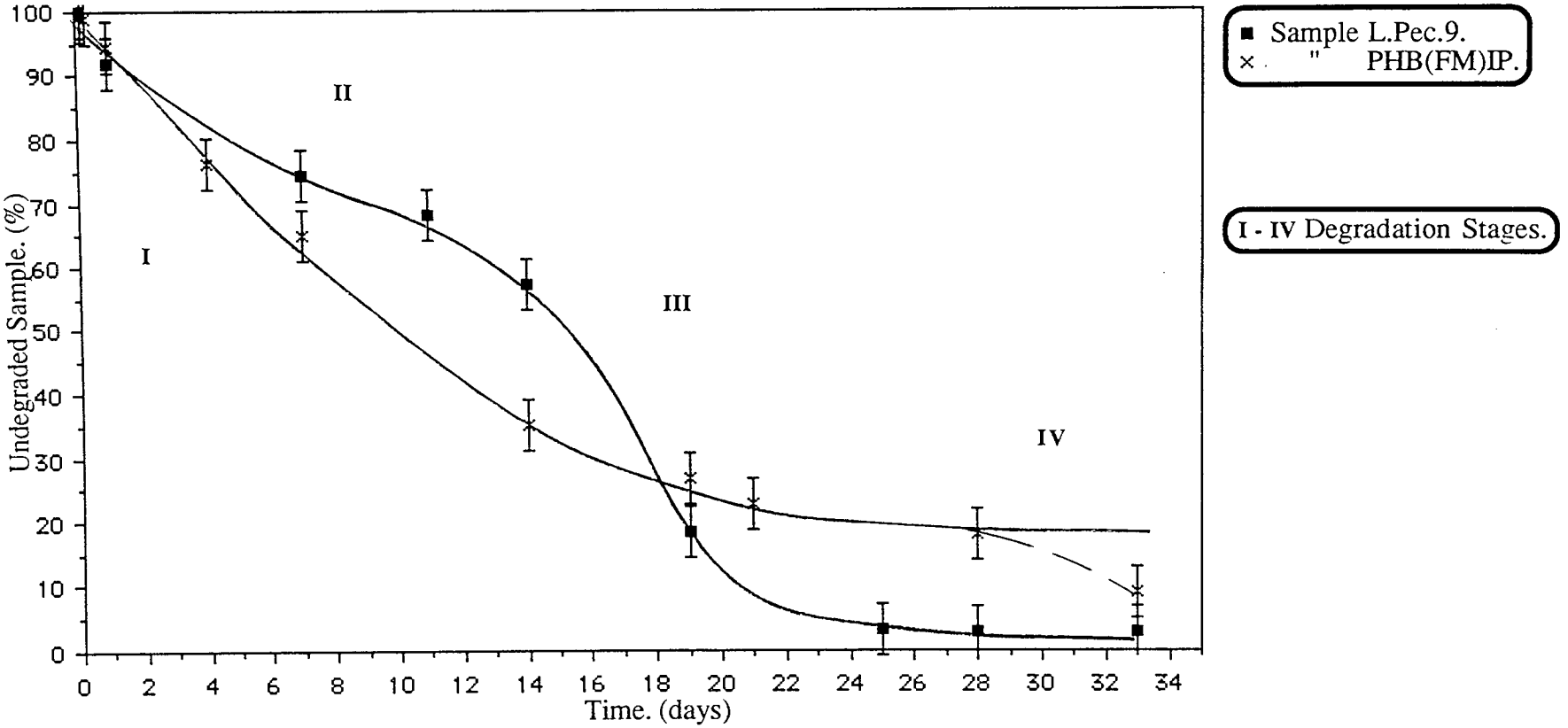

Graph 5.9.

Degradation Profiles Of Samples L.Pec.9. And PHB(FM)IP. In The Accelerated Degradation Model. Monitored By Monomer With Degraded Particulate Analysis.

stage IV at day 25. However, at day 25 the overall linear degradation rates were approximately 2.6%dy.$^{-1}$ for the IP sample and 3.5%dy.$^{-1}$ for the L.Pec.9., such that the actual PHB degradation difference between the two samples was approximately 22.5%.

Thus, the IP sample matrix gradually collapsed and settled throughout the experiment. The addition of 9% low molecular weight pectin increased the initial stability of the matrix but decreased the stability of the fibres, so that extensive weakening occurred in the initial degradation stages. Consequently upon collapse a comparatively rapid degradation was observed, this then increased the degradation to monomer by a further 22.5%. Similar to the samples SA-7. and SCC-9. in section 5.1., this degradation increase could not be explained by the reduction in the initial weight of PHB.

A comparison of the degradation profiles for monomer with particulate analysis (degraded fraction) for L.Pec.9. and the IP sample (Graph 5.9) revealed similar trends as to those observed from the monomer analysis profiles, (Graph 5.8), with the step stage II being less noticeable. The production of degraded particulate matter was basically the same as in stage I until day 25, when more degraded particles were observed from the IP sample.

Therefore, from the monomer, gravimetric and particulate analysis profiles it was concluded that the L.Pec.9. sample retained its matrix integrity for a comparatively longer period than the IP sample. Upon collapse, the limiting factors of the experimental system ensured that no further degradation was observed, whilst the IP sample still continued to degrade slightly. This was due to the fact that at the stage IV the compaction of the remaining matter possessed a greater influence on the degradation to monomer for the IP

sample than it did for L.Pec.9.

At day 33 L.Pec.9. had an undegraded weight fraction of approximately 4% according to the degraded fraction profile, this was similar to the actual weight at termination; 3.2%. This further emphasized the good correlation between the analysis methods of measuring both the undegraded and degraded fractions of a sample.

5.2.1.3. Comparison Of L.Pec.9. With SCC-9.

The monomer analysis degradation curve for L.Pec.9. was compared to that obtained for the co-blend sample SCC-9., which ideally had the same percentage loading but with a different polysaccharide, (Graph 5.10).

As can be observed from graph 5.10 the SCC-9. sample had a lower initial stability and therefore a greater degradation compared to the L.Pec.9. Consequently, 50% degradation to monomer was observed before the primary step stage II at day 10, whilst the L.Pec.9. had only 19% degradation before stage II at day 7. This indicated that the stability of the SCC-9. matrix was much less than that of the L.Pec.9. Collapse and compaction of the fibre fragments for SCC-9. readily occurred at day 20 with 75% degradation, whilst L.Pec.9. showed approximately 87% degradation at day 25.

The degradation differences between the two samples confirmed previous conclusions that the polysaccharide nature affected the ultimate degradation of the PHB polymer, by altering the stability of the matrix and of the fibres themselves.

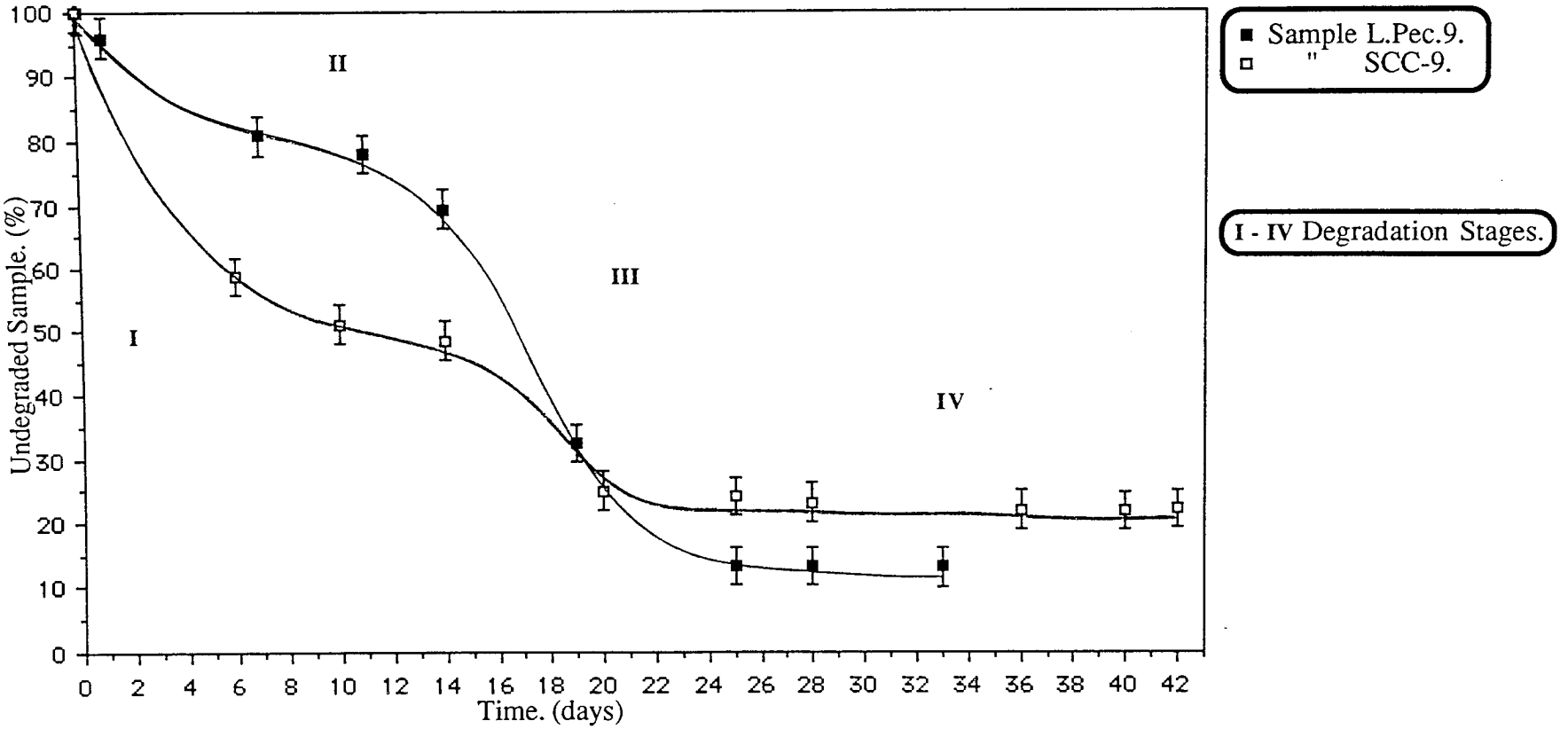

Graph 5.10.

Degradation Profiles Of PHB Component Of Samples L.Pec.9. And SCC-9. In The Accelerated Degradation Model, Monitored By Monomer Analysis.

5.2.1.4. Effect On The Degradation Of Increasing The Filler Loading.

Increasing the percentage loading of the low molecular weight pectin from 9 to 15% produced a similar initial degradation profile as sample L.Pec.9., with the stage II occurring at day 7 and possessing a similar stage III, (Graph 5.11). Stage IV, however, occurred comparatively suddenly at day 19 with a degradation of approximately 79%. The total degradation of the PHB content of L.Pec.15. was reduced by 8.5% compared to that for L.Pec.9. Thus, increasing the percentage of pectin facilitated the increase in the collapse of the matrix and the stage IV formation.

The overall linear degradation rate for L.Pec.15. was 4.1%$dy.^{-1}$, this was a slight increase compared to L.Pec.9., indicating a greater degradation. However, considering the total amount of degradation it was observed that increasing the pectin loading from 0 to 9% increased the PHB degradation by 22.5%, whilst increasing it to 15% reduced this amount of degradation to approximately 14%, a loss of 8.5%. This was due therefore, not only to the lack of PHB initially present, but also the effects on the structure stability.

Similar to L.Pec.9., gravimetric investigations (Graph 5.11B) revealed an initial weight loss of approximately 14% within the first hour of degradation. This was due to the pectin dissolution. Some of this weight loss was observed as degraded particulate matter (Graphs 5.12 & 5.13).

The particulate matter production was similar to that of the L.Pec.9. saample, with a gradual increase in the amount of degraded particulate matter produced until day 1 and then a sudden decrease at day 4, before returning to a greater level at day 7. This time

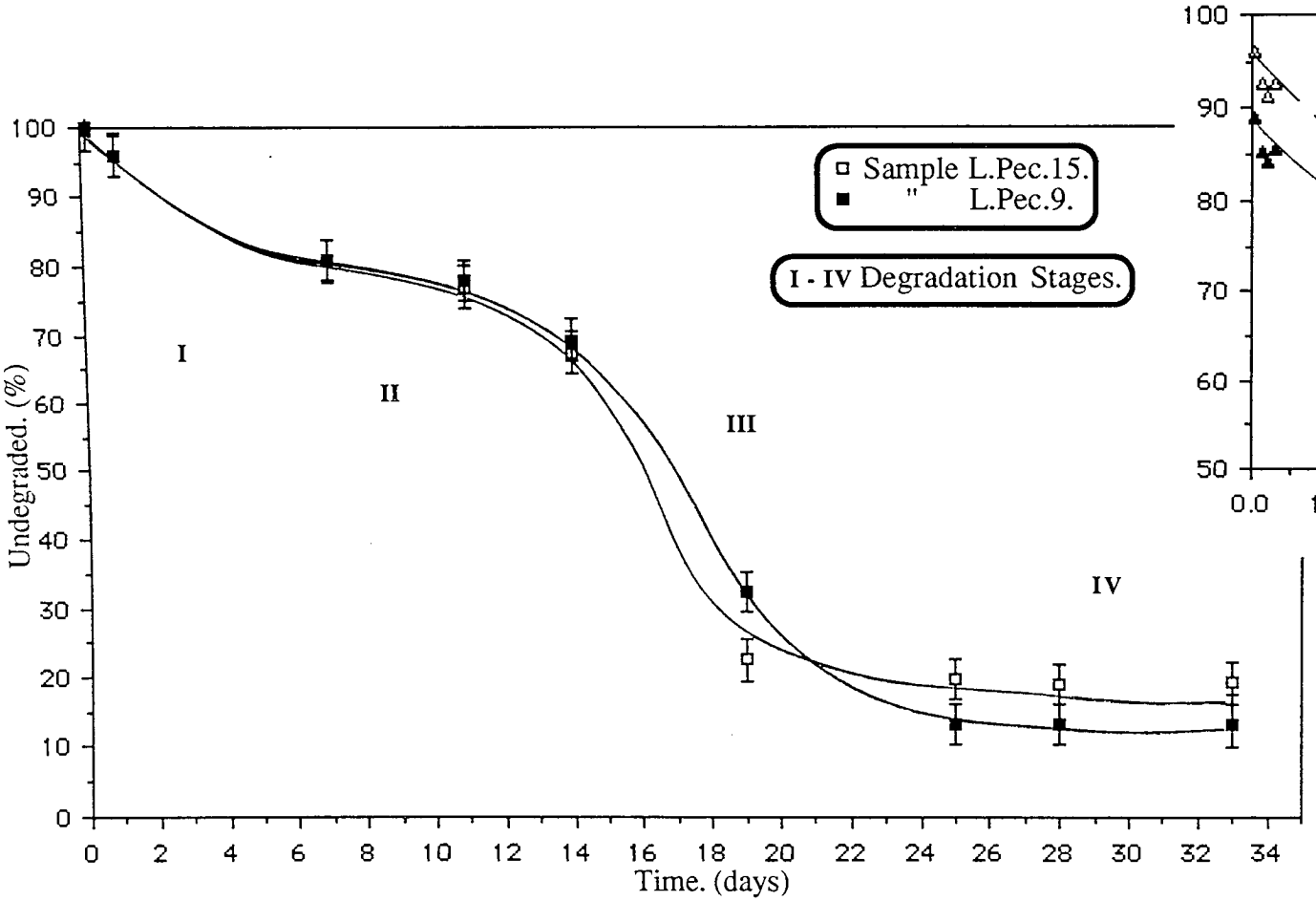

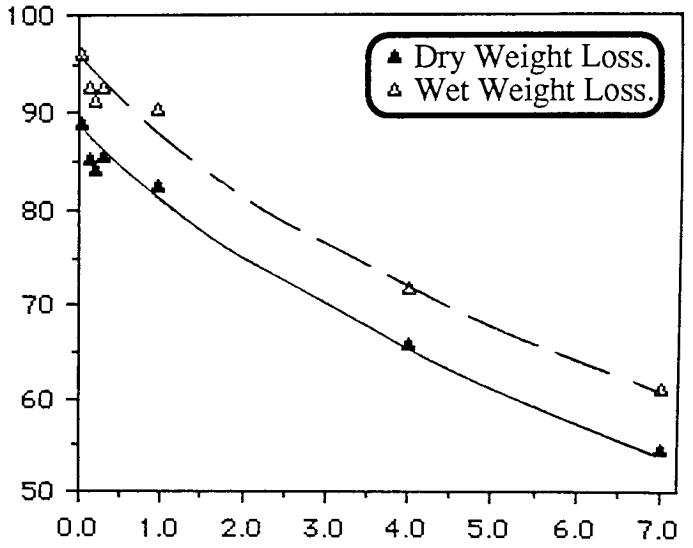

Graph 5.11B.

Degradation Profile Of L.Pec.15. In The Accelerated Degradation Model, Monitored By Gravimetric Analysis.

Graph 5.11.

Degradation Profiles Of PHB Component Of Samples L.Pec.9. And L.Pec.15. In The Accelerated Degradation Model, Monitored By Monomer Analysis.

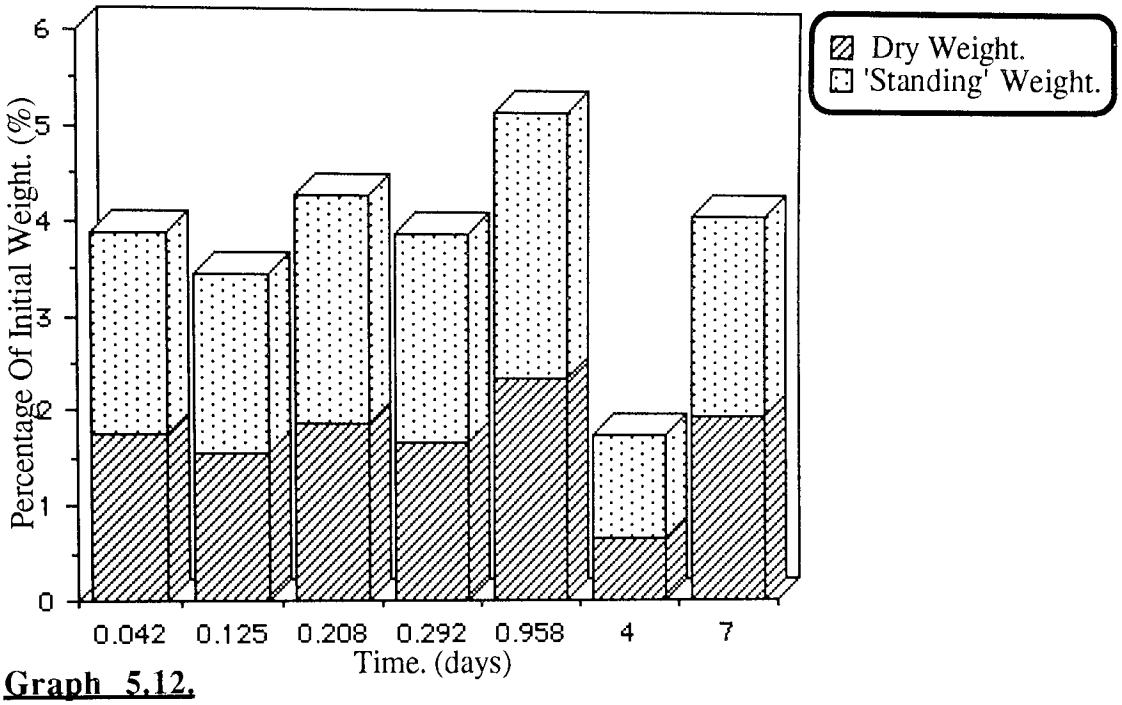

Graph 5.12.

Measured Degraded Particulate Matter For Sample L.Pec.15.

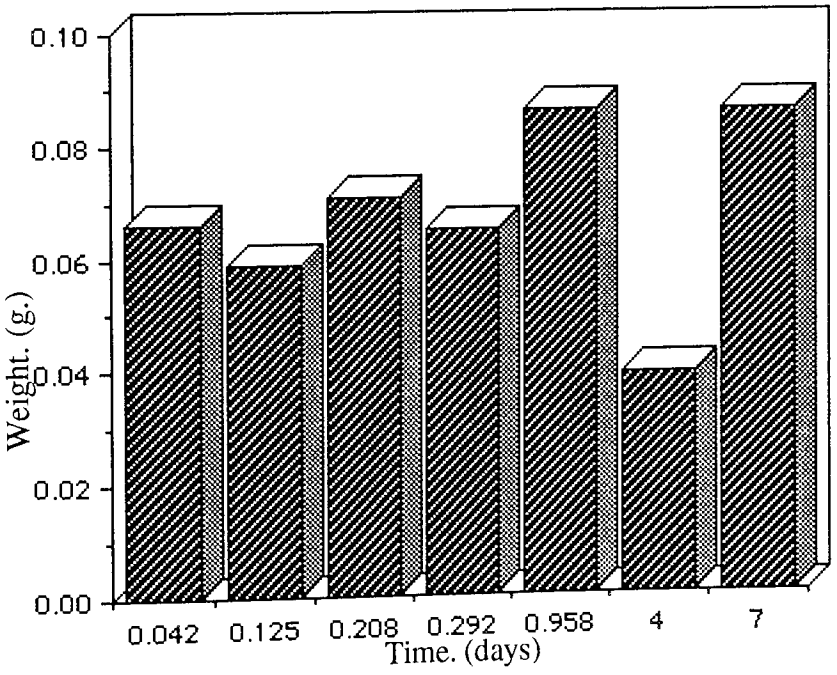

Graph 5.13.

Ideal Total Degraded Particulate Matter For Sample L.Pec.15.

period of days 4 to 7 coincided with the step stage II.

Graph 5.14 illustrates the monomer degradation profiles for the co-blends with ideally 25% pectin sampled at the start and end of the manufacturing run; L.Pec.25.S. and L.Pec.25.E. respectively, and compares them to that obtained for PHB(FM)IP. As can be observed, a difference in the pectin loading occurred which affected the degradation and was reflected in the degradation profiles, (Graphs 5.14 and 5.15). There were indications from the gravimetric graphs 5.5 and 5.11B, that the pectin loaded co-blends L.Pec.9. and L.Pec.15. had approximately the same pectin loading as was originally alleged ie; 9 and 15% respectively. However, the differences in the gravimetric analysis degradation profiles for the samples L.Pec.25.S. and L.Pec.25.E. readily illustrated a difference in the loadings between these two samples with values of approximately 6 and 17% respectively. This loading difference was further emphasized by staining samples of similar weights from each using ruthenium red, a pectin specific dye,[98] (Plate 5.1). As can be observed from plate 5.1, the L.Pec.25.E. had apparently more pectin present than L.Pec.25.S.

The monomer analysis degradation profiles were very similar with the characteristic two step degradation observed, (Graph 5.14). The stage IV was observed around day 21 with approximately 80 and 73% degradation for L.Pec.25.S. and L.Pec.25.E. respectively. The degraded particulate analysis illustrated in graphs 5.16 to 5.19 was similar to those obtained for the other pectin co-blends. The loss of degraded particulate matter at day 4 was also present, indicating the beginning of the step stage II.

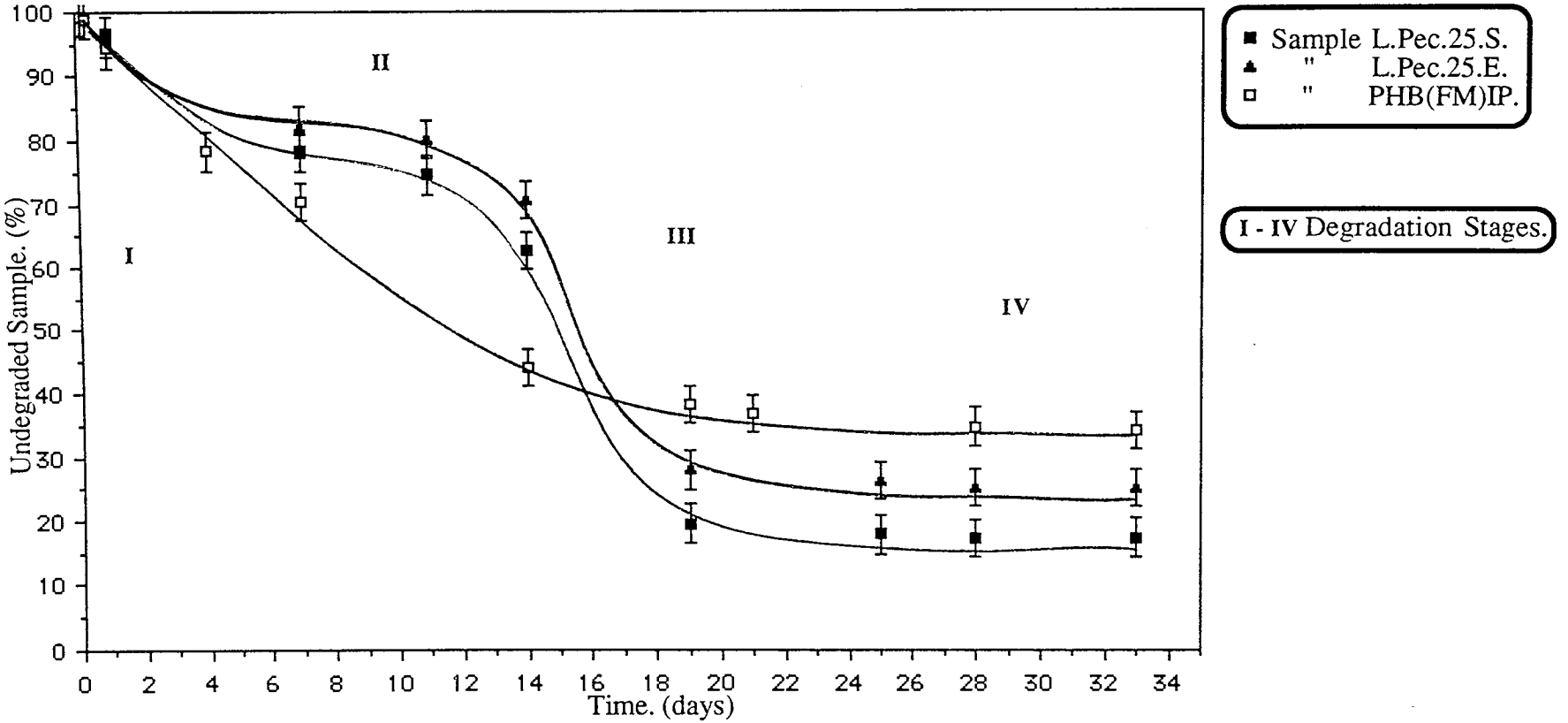

Graph 5.14.

Degradation Profiles Of PHB Component Of Samples L.Pec.25.S., L.Pec.25.E. And PHB(FM)IP In The Accelerated Degradation Model, Monitored By Monomer Analysis.

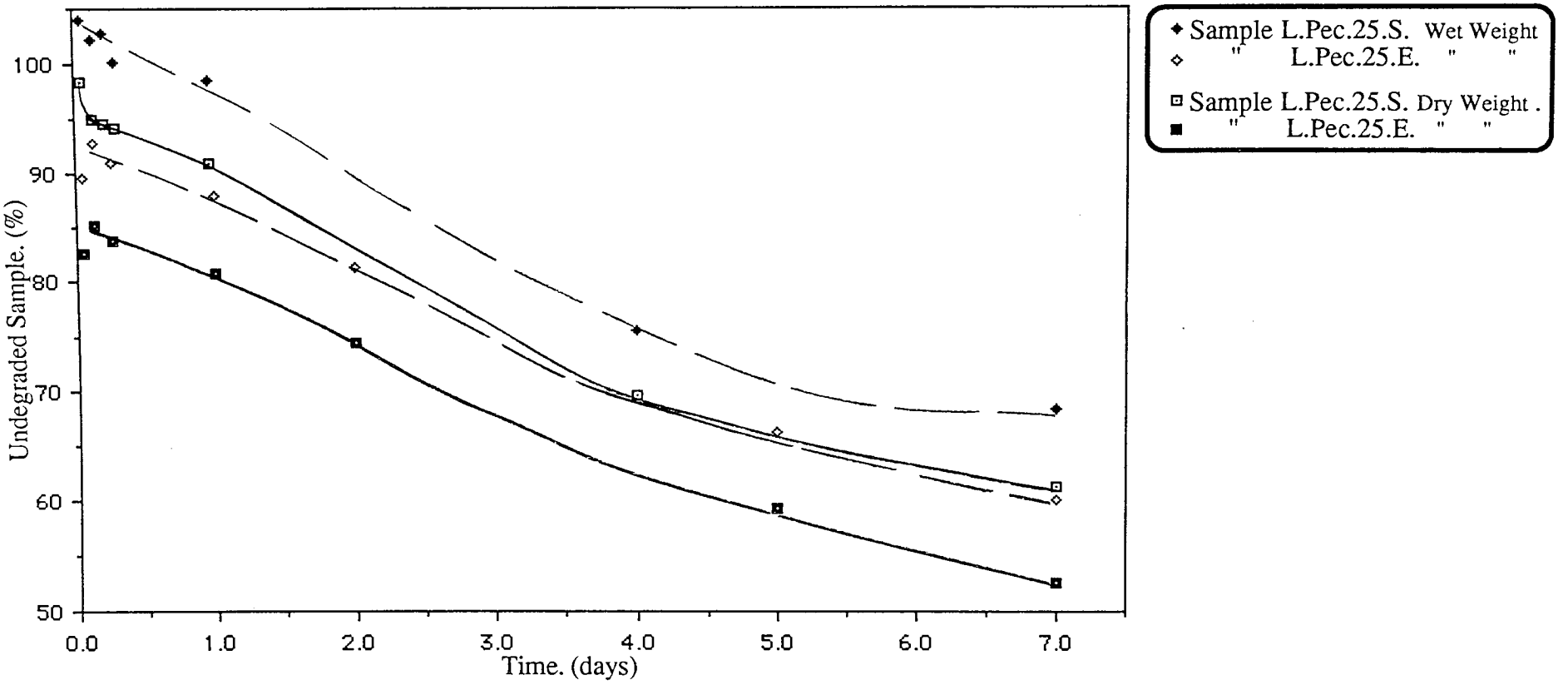

Graph 5.15.

Degradation Profiles Of Samples L.Pec.25.S. And L.Pec.25.E. In The Acclerated Degradation Model, Monitored By Gravimetric Analysis.

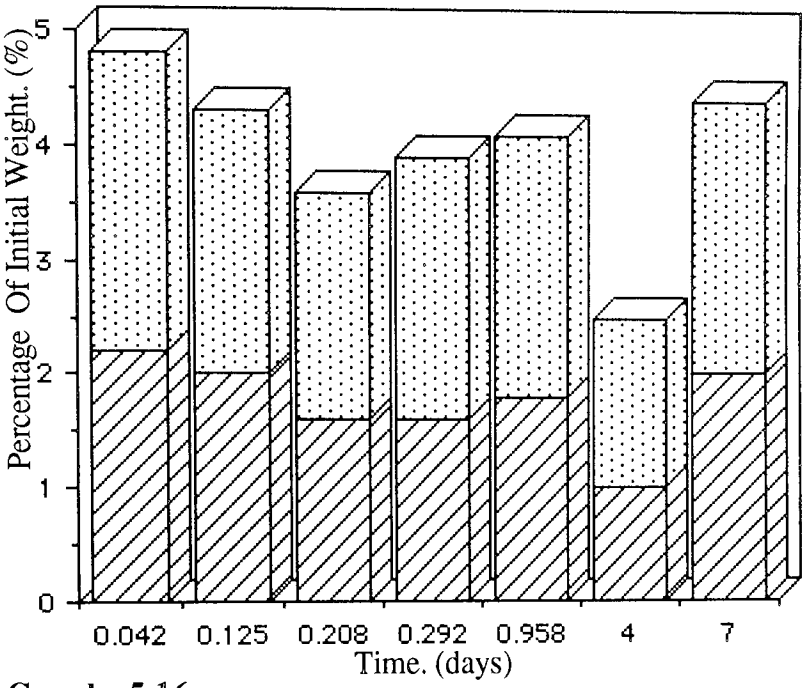

Graph 5.16.

Measured Degraded Particulate Matter For Sample L.Pec.25.S.

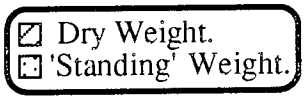

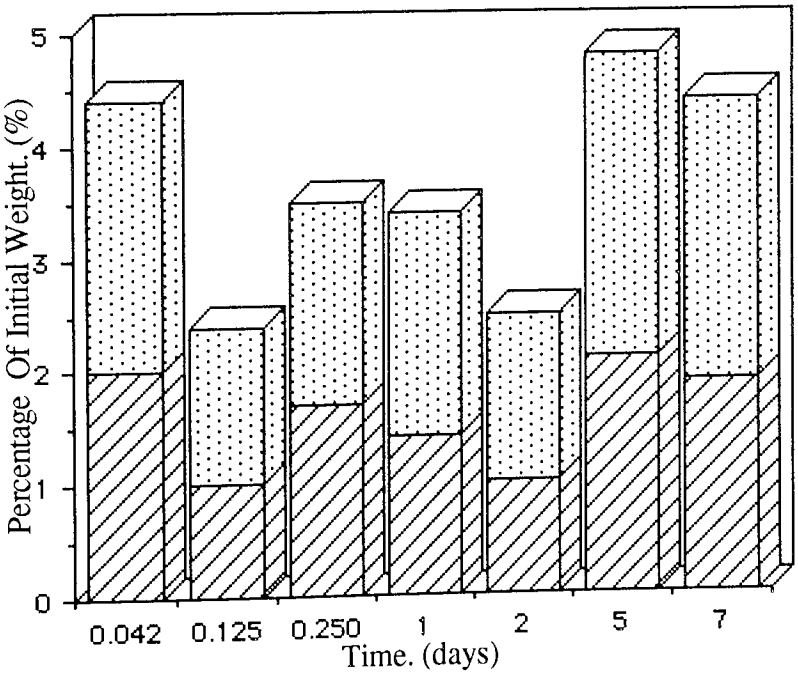

Graph 5.17.

Measured Degraded Particulate Matter For Sample L.Pec.25.E.

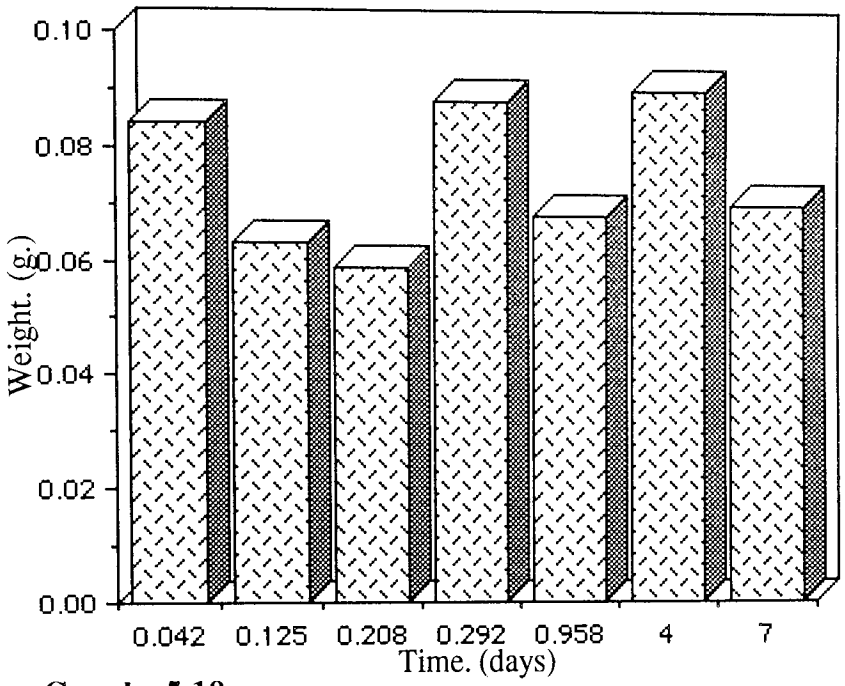

Graph 5.18.

Ideal Total Degraded Particulate Matter For Sample L.Pec.25.S.

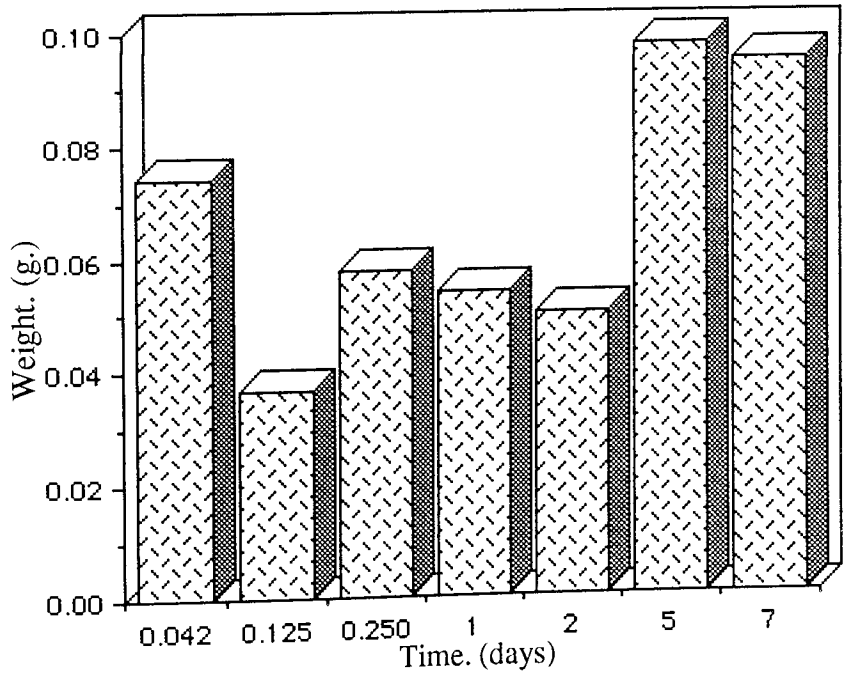

Graph 5.19.

Ideal Total Degraded Particulate Matter For Sample L.Pec.25.E.

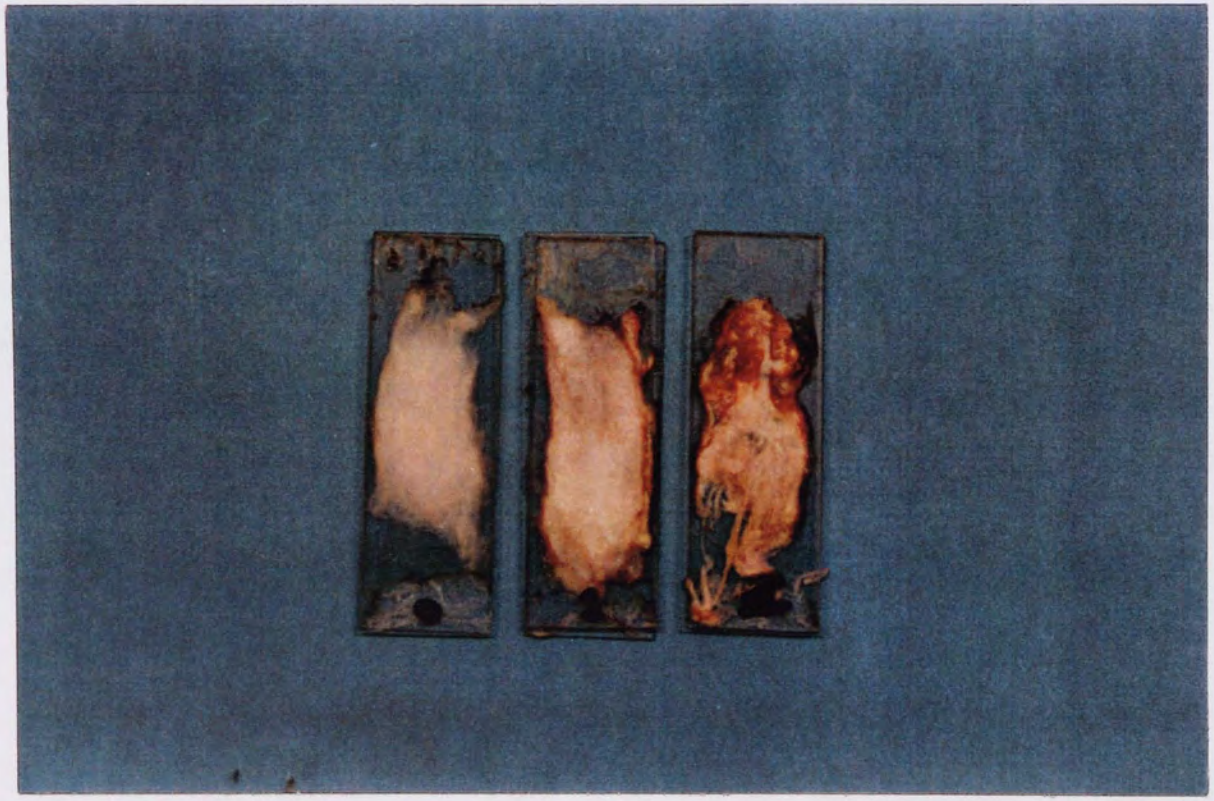

Plate 5.1.

PHB(FM)IP Blended With 25% Low Moleular Weight Pectin Sampled From The Start And End Of The Manufacturing Run. The Dyed Regions Illustrate The Different Pectin Loadings For The Three Samples.

Thus, it was concluded that in the blending procedure a certain percentage of the pectin was initially blended and /or mixed with the PHB, whilst at the end of the manufacturing run the remaining, greater percentage of pectin was present in the matrix. However, the blending was inefficient and there was a pectin loss in the production process.

Graph 5.20 illustrates the relationship between the monomer analysis degradation profiles for all the co-blended samples expressed as a function of the initial sample weight. As can be readily observed, the initial stages were generally the same with only small differences observed in the degradation, whilst the later stages illustrated greater differences but still remained similar. At day 25, when the stage IV was attained, there was approximately 87% degradation for L.Pec.9., allegedly the lowest percentage loading, and 72% for L.Pec.25.E., the highest percentage loading, a difference of approximately 15%.

A comparison of the overall linear degradation rates for the co-blends at day 25 with the anticipated degradation rates obtained from the initial weight loss versus log. linear degradation rate from section 4.1, indicated that the increase in PHB degradation was due to the blending effect on the matrix structure and a reduction in the initial weight of PHB. However, the differences between the actual and anticipated degradation rates were reduced when compared to the rate difference determined for the L.Pec.9. sample. Thus, it was concluded that increasing the percentage loading above an optimum facilitated the degradation due to a reduction in stability, but was not as noticeable as with the lower percentage loaded samples.

Graph 5.21 illustrates the degradation of the PHB content for the co-blends, expressed as

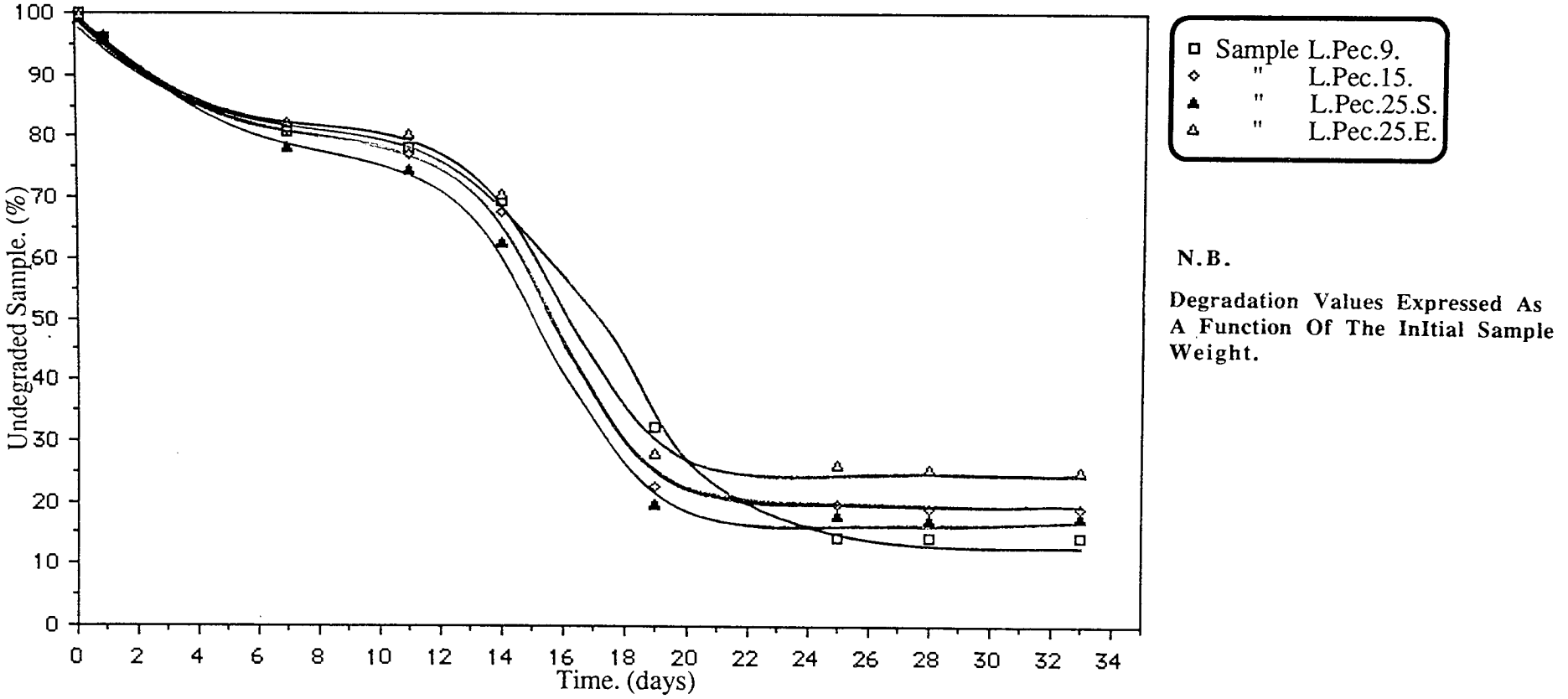

N.B.

Degradation Values Expressed As A Function Of The InItial Sample Weight.

Graph 5.20.

Degradation Profiles Of PHB Component For Pectin Co-blends In The Accelerated Degradation Model, Monitored By Monomer Analysis.

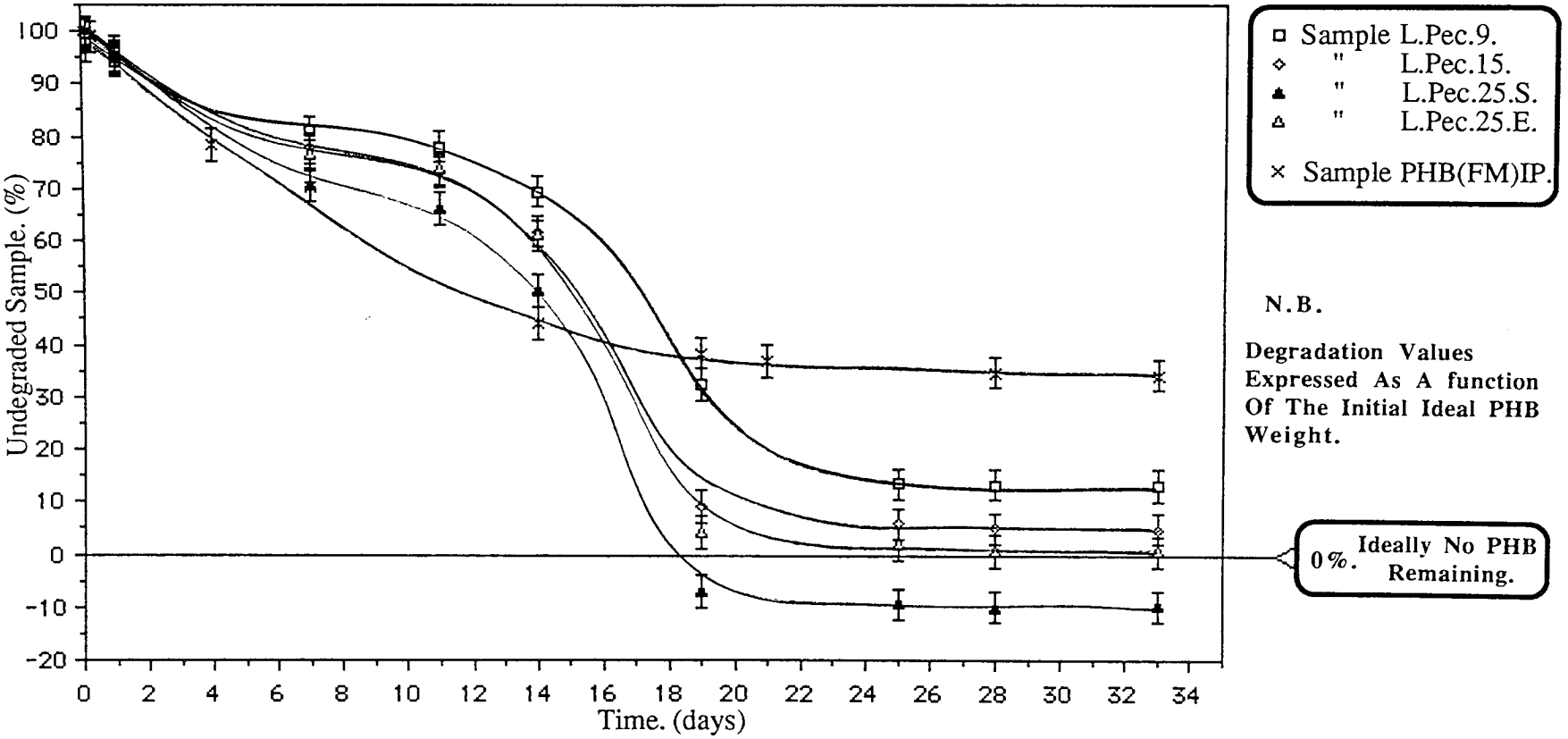

Graph 5.21.

Degradation Profiles Of PHB For Pectin Co-blends In The Accelerated Degradation Model, Monitored By Monomer Analysis.

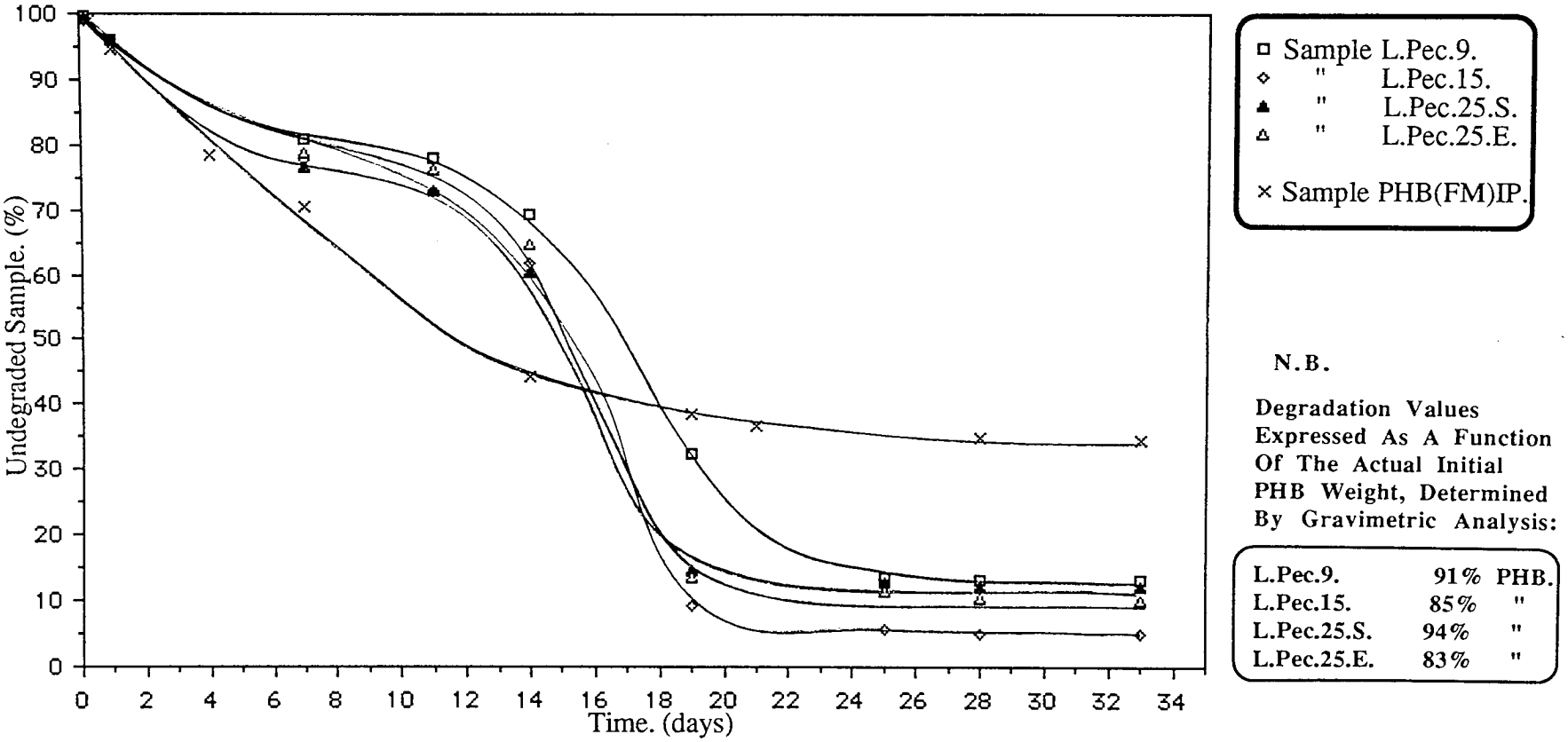

Graph 5.22.

Degradation Profiles Of Actual PHB Component Of Pectin Co-blends In The Accelerated Degradation Model, Monitored By Monomer Analysis.

a function of the initial claimed PHB weight and reveals a poor blending efficiency in those samples with alleged high pectin loadings; L.Pec.25.S. and L.Pec.25.E. However, graph 5.22 illustrates the degradation of the PHB for the co-blends expressed as a function of the initial weight of PHB actually present. As can be observed, the degradation profiles were very similar. The main differences in degradation were observed at the stage III, whilst at the stage IV, day 25, there was little difference between samples L.Pec.9., L.Pec.25.S. and L.Pec.25.E. with approximately 87% degradation, however, sample L.Pec.15. exhibited approximately 93% degradation.

Thus, increasing the pectin loading produced noticeable effects on the collapse of the matrix and the degradation profile, particualarly at stage III, but exhibited a similar PHB degradation to that of L.Pec.9.

5.2.1.5. Effect On Degradation Of Increasing The Molecular Weight Of The Pectin.

Altering the pectin from low molecular weight to high molecular weight had a more noticeable effect on the degradation of the matrix than increasing the low molecular weight loading, (Graph 5.23). This tended to indicate that the high molecular weight pectin was readily blended with the PHB. Graph 5.23 illustrates the degradation profiles by monomer analysis for the H.Pec.10. sample and compares it to that obtained for the PHB(FM)IP. Graph 5.24 shows the initial gravimetric degradation.

The monomer analysis degradation profiles for L.Pec.9. and H.Pec.10. were very similar. However, the dissolution of the pectin in H.Pec.10., in the initial stages of the

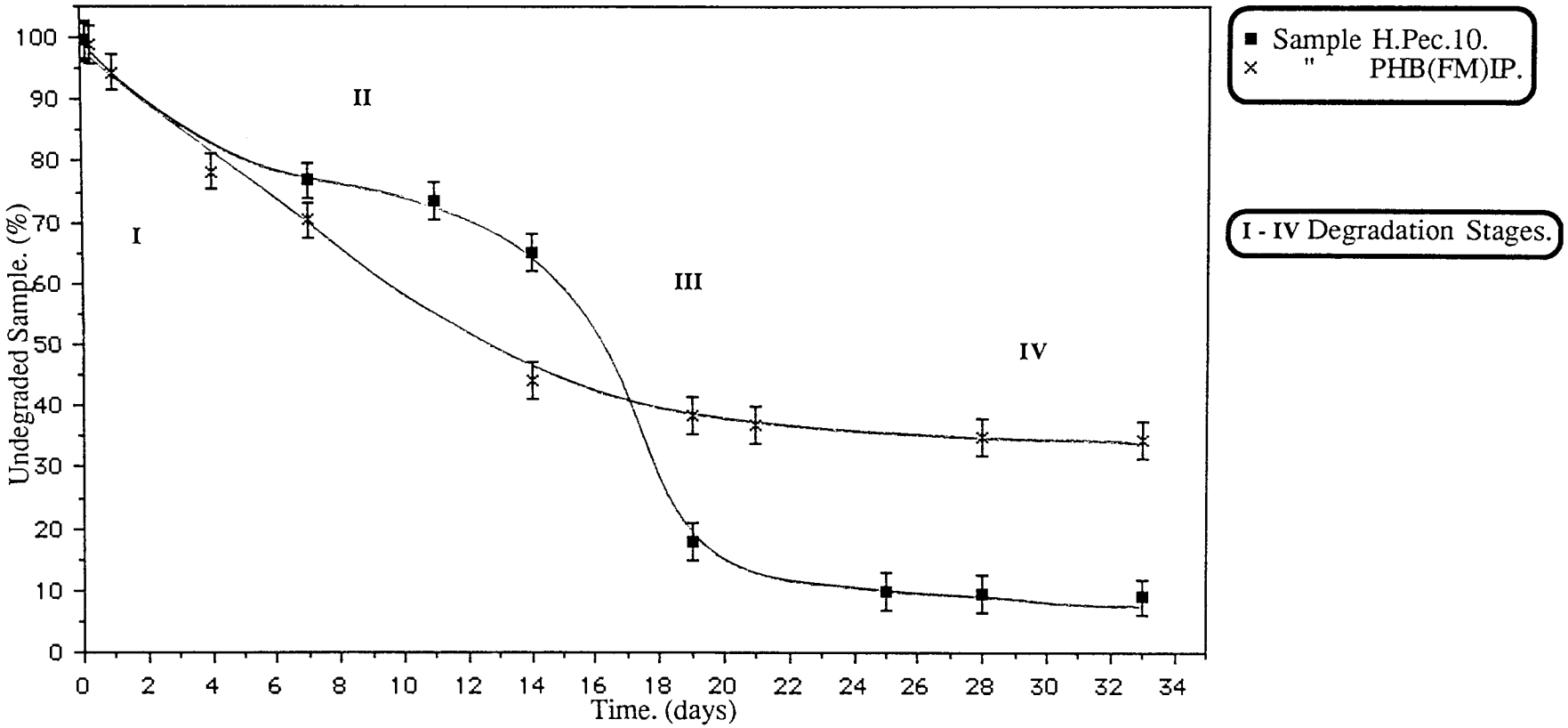

Graph 5.23.

Degradation Profiles Of PHB Component Of Samples H.Pec.10. And PHB(FM)IP. In The Accelerated Degradation Model, Monitored By Monomer Analysis.

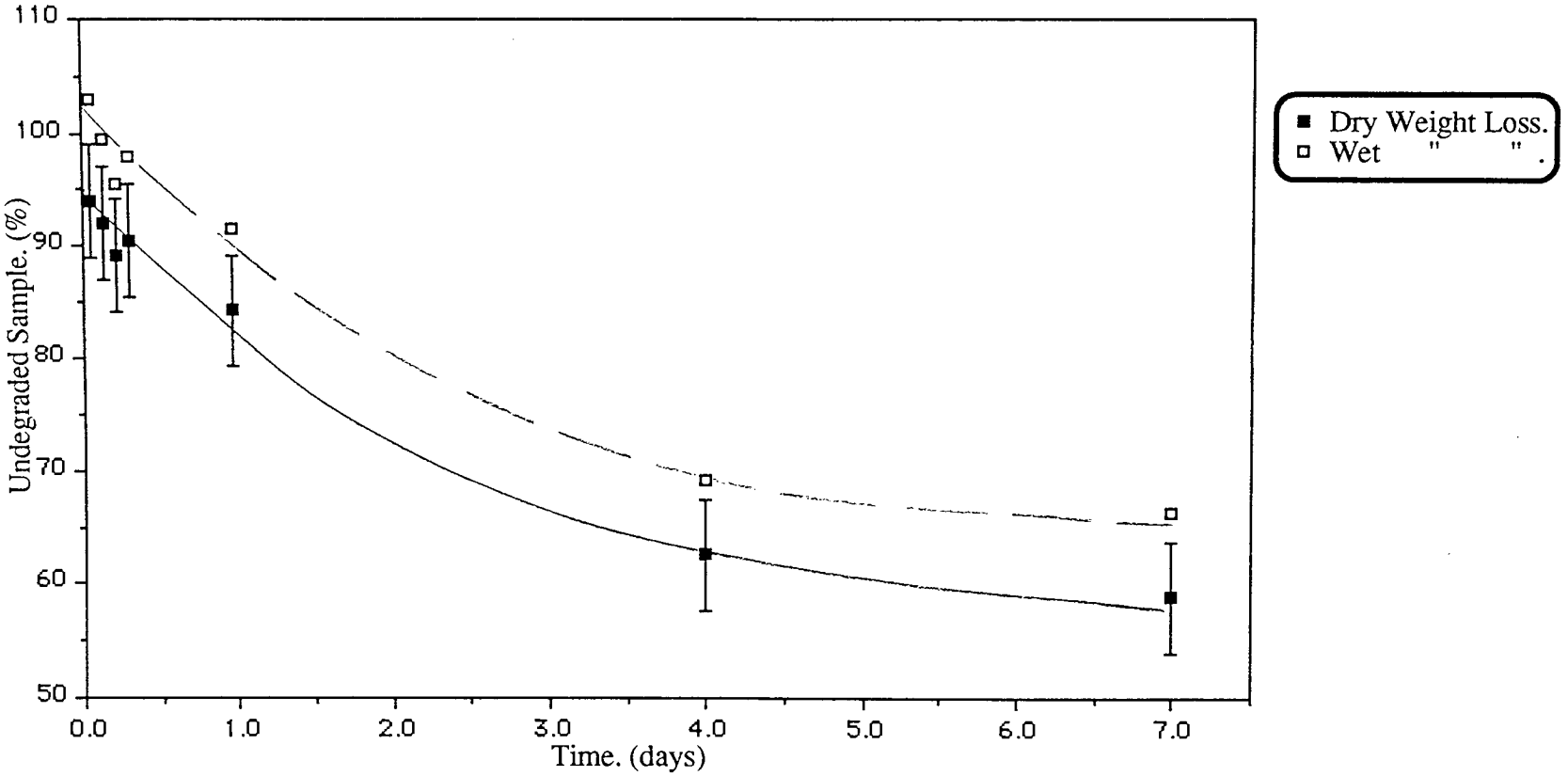

Graph 5.24.

Degradation Profile Of Sample H.Pec.10. In The Acclerated Degradation Model, Monitored By Gravimetric Analysis.

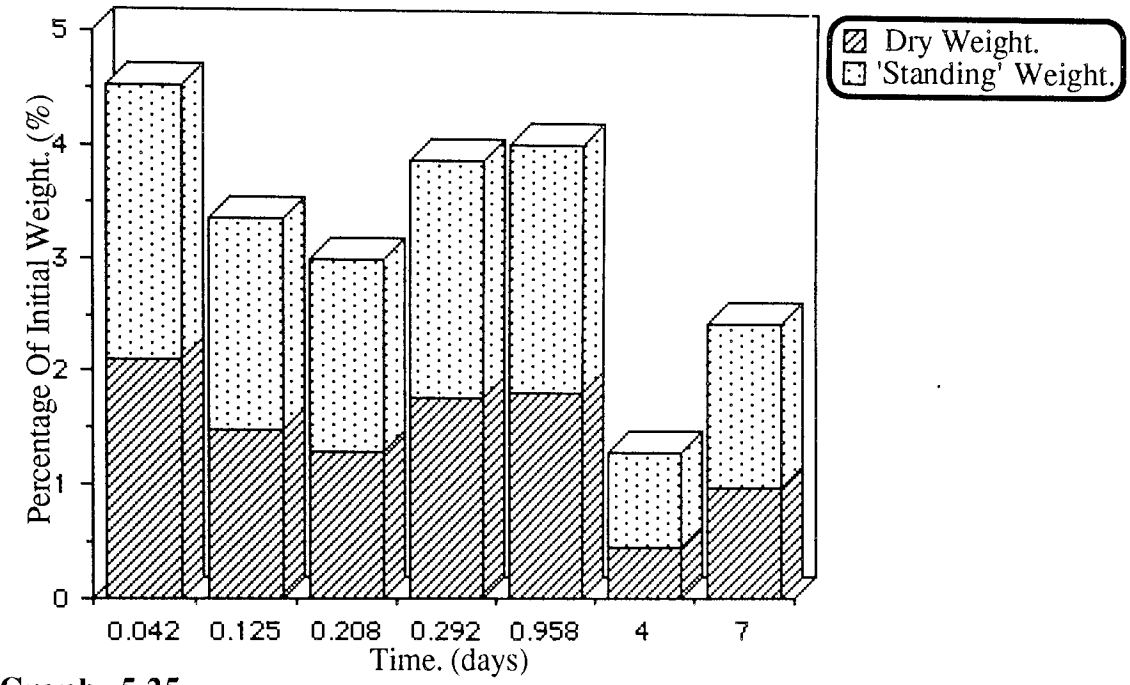

Graph 5.25.

Measured Degraded Particulate Matter For Sample H.Pec.10.

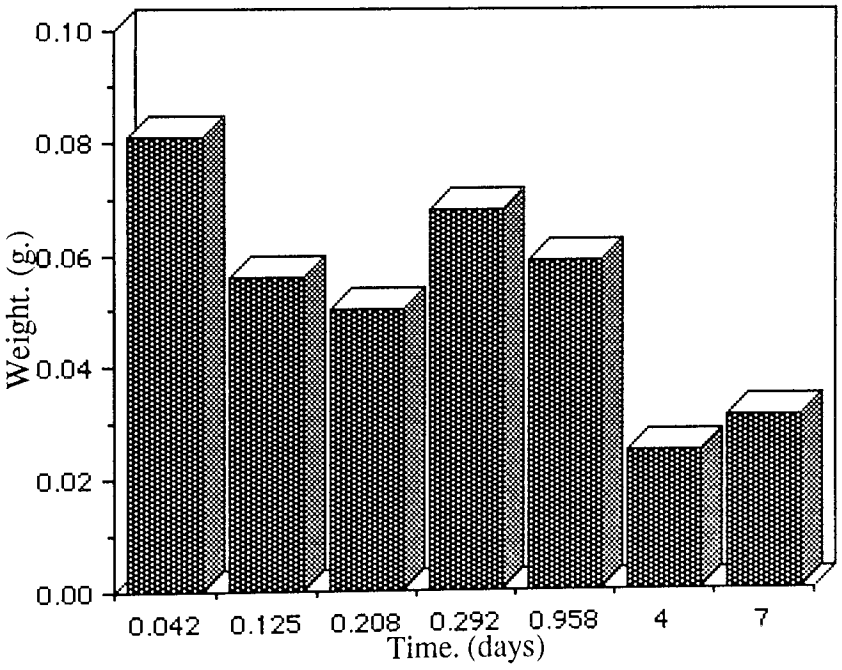

Graph 5.26.

Ideal Total Degraded Particulate Matter For Sample H.Pec.10.

degradation ensured a larger surface area to volume ratio than in sample L.Pec.9. This was due to the increase in blending efficiency of the high molecular weight pectin with the PHB when compared to the low molecular weight pectin in sample L.Pec.9. As a result of this, the step stage II was observed at days 7 to 11 for both H.Pec.10. and L.Pec.9. but with approximately 25 and 20% degradation respectively. Similarly, the stage II for the L.Pec.9. was more pronounced than that of H.Pec.10. which still continued to degrade slightly.

Due to the comparatively greater blending efficiency of the H.Pec.10. sample, the collapse of the remaining matrix and fibre fragments at stage II was greater than that of L.Pec.9., so that a more pronounced stage III, with a greater degradation rate was observed. Thus, at day 19 there was approximately 75 and 67% degradation for samples H.Pec.10. and L.Pec.9. respectively, at day 25, when the terminal stage IV for both samples was reached, these values had increased to approximately 90 and 85%.

Thus increasing the molecular weight of the pectin slightly altered the degradation profile of the matrix when compared to its low molecular weight counterpart. This was due to a greater blending efficiency.

5.2.2. Conclusions.

It was anticipated that blending the PHB with various loadings of pectin would have an effect on the matrix and PHB degradation within the experimental confines of the system, simply by the reduction of the initial weight of PHB. Consequently, these effects would also be reflected in the monomer analysis degradation profiles. However, the changes

observed in these profiles indicated the initial collapse of a large proportion of fibres from the co-blends compared to the homopolymer sample. Thus, although the degradation rates were affected by the initial amount of PHB present, in the lower percentage loadings the difference between the actual and anticipated degradation values was too great to be justified by this alone and was due to blending. Increasing the pectin loading reduced the blending efficiency.

Increases in the molecular weight of the pectin had a comparatively greater effect on the PHB degradation than increases in the percentage loading of the low molecular weight pectin. This was due to a greater blending efficiency, which under degradation conditions provided a greater surface area to volume ratio than that of a low molecular weight counterpart. Therefore, a comparatively greater PHB degradation to monomer was observed before the terminal step stage IV.

It was observed from section 4.5 that agitation of the PHB(FM)IP sample affected the degradation profile with an increase in degradation. There was no reason to suspect that agitation of the co-blended samples would not exhibit similar effects and therefore, although in all samples compaction of the partially degraded matrix was a limiting factor, the stability and degradation characteristics of the co-blends in relation to the IP sample would ideally remain the same.

5.2.3. Observations Of The Partially Degraded Co-blends.

Sample L.Pec.9. had a similar amount of fragmentation within the first hour of degradation as that of the IP sample, (Plates 4.33 & 4.34 Sec.4.3). However, whilst the

IP fibres appeared smooth and comparatively 'clear', the L.Pec.9. fibres were more irregular and appeared to have a number of cavities with the pectin filling readily noticed. Some of these pectin cavities were observed in the larger and medium sized fibres where the pectin had already dissolved into the buffer medium, (Plate 5.2). The majority of the smaller diameter fibres were unaffected and the matrix was readily maintained. Fragmentation was more noticeable after 3 hours degradation, such that a large number of fibre pieces were observed and was comparable to the IP sample, (Plate 4.26).

Plate 5.4 illustrates the irregular nature of the co-blended fibres and an apparently greater fragmentation at day 1 compared to the IP sample. The large number of cavities caused by the degradation of the pectin facilitated the PHB degradation by increasing the available surface area to volume ratio. However, a smaller degree of fracturing was observed when compared to the IP sample. This tended to indicate that these fragments were most likely due to the filtering and mounting procedures.

Plates 5.5 and 5.6 show the fragmentation of the LPec.9. fibres at day 4, the fibre fragments were generally smaller than those observed for the IP sample at the same time. The larger diameter fibres for the co-blended sample had more irregularities to facilitate degradation than their IP counterparts. Plate 5.6 illustrates these cavities and their fracturing irregularities.

After 7 days degradation the degree of fragmentation for the L.Pec.9. fibres was still greater than for the IP fibres, however, the large number of cavities in the medium and large diameter fibres ensured that an uneven mat at the base of the phial occurred. Thus,

Plate 5.2. (x25) 1 Hour Degradation.
L.Pec.9.; PHB(FM)IP Blended With 9% Low Molecular Weight Pectin, Illustrating The Cavities Of Degraded Pectin In The Large And Medium Sized Fibres And The Smooth Small Diameter Fibres.

Plate 5.3. (x15) 3 Hours Degradation.
L.Pec.9.; Matrix And Fibre Fragmentation.

Plate 5.4. (x25) 1 Day Degradation.
L.Pec.9.; Fibre Fragmentation And Irregularities, 'Pectin Cavities'.

Plate 5.5. (x15) 5 Days Degradation.
L.Pec.9.; Mltiple Fragmentation At All The Diameter Sizes After 5 Days Degradation.

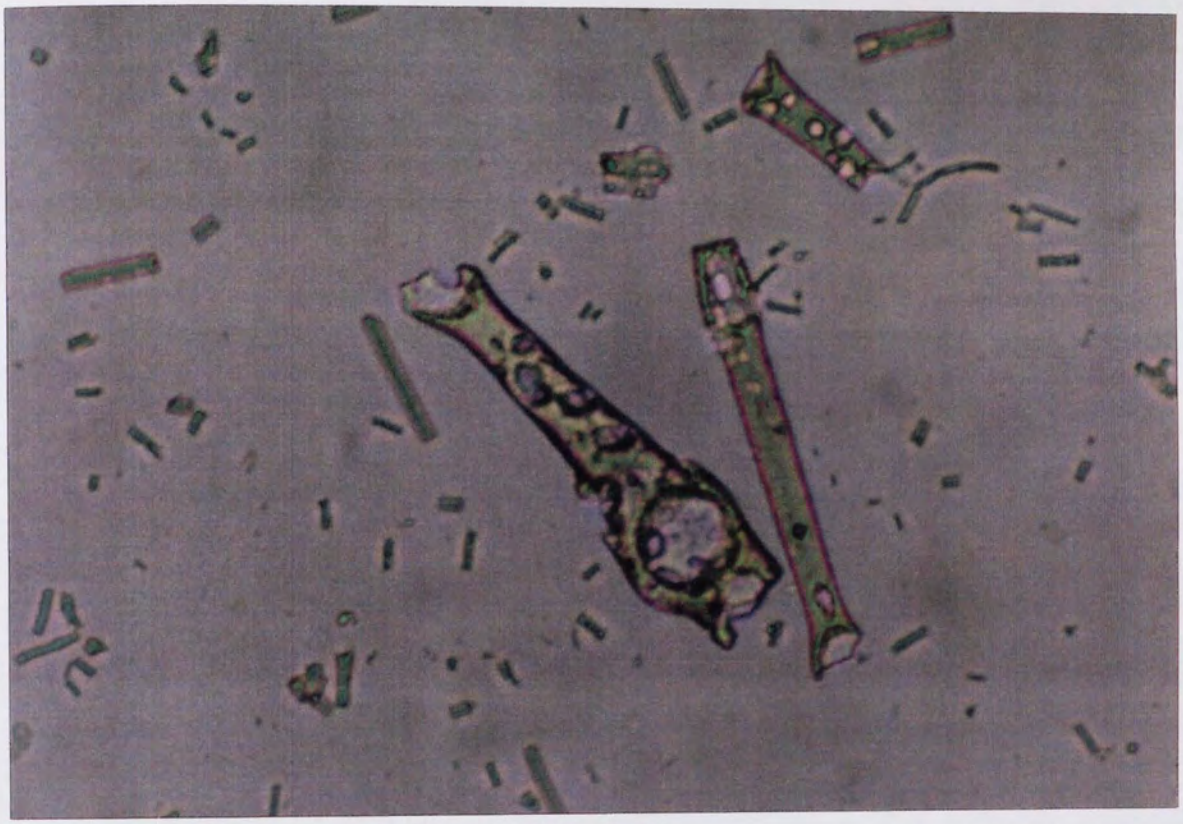

Plate 5.6. (x15) 5 Days Degradation.
L.Pec.9.; Large And Medium Diameter Fibres Exhibiting 'Pectin Cavities' And Irregularities.

Plate 5.7. (x25) 7 Days Degradation.
L.Pec.9.; Readily Noticeable Pectin Cavities In A Large Diameter Fibre.

after collapse, the surface area to volume ratio was maintained at a comparatively higher level than the IP fibres and consequently the surface erosion was greater. This was observed as an increase in the monomer released and the large degradation rate at stage III.

The amount of pectin blended within the smaller diameter fibres was observed to be somewhat less than that in the larger/medium sized fibres. In those small fibres possessing a percentage of blended pectin, the fragmentation and fracturing at these points readily occurred, such that at days 4 and 7 the fractured ends of the IP fibres appeared relatively smooth, whilst those for the L.Pec.9. sample were much more irregular, (Plate 4.38 Sec.4.4. & Plates 5.6 & 5.7).

Thus it was observed that the blending of the IP fibres with 9% low molecular weight pectin effectively occurred in the large and medium sized fibres, so that upon degradation the pectin cavities facilitated the degradation of the PHB by increasing the available surface area to volume ratio. Blending with the smaller diameter fibres also occured but to a comparatively smaller degree. The increased amounts of fragmentation, compared to the PHB(FM)IP, observed in the initial degradation stages were mainly due to handling and thus the fibres were weaker than their IP equivalents. However, some fragmentation, collapse and degradation of the weakest fibres did occur and these were mainly responsible for the stage I degradation.

Increasing the pectin loading to 15% had noticeable effects on the partially degraded fibre structures when compared to the L.Pec.9. sample. After 1 hour degradation the matrix

was still intact and a number of bubbles observed, (Plate 5.8). Some of the larger diameter fibres appeared heavily loaded with the pectin, as observed in plate 5.9, whilst some of these still remained intact after 3 hours degradation, a larger proportion had fragmentated to a similar level as the L.Pec.9. sample, (Plate 5.9). Plate 5.10 illustrates a fibre heavily loaded with pectin, so that whilst some regions of the matrix had degraded within 7 hours other regions had merely fragmented to a similar extent as L.Pec.9. but with fewer pectin cavities observed, (Plate 5.11).

Fragmentation at day 4 appeared much greater than that observed for L.Pec.9. and the IP sample at the same time, (Plate 5.12). There was a noticeable lack of large diameter fibre fragments, whilst a relatively large amount of fracturing was apparent, indicating the comparatively weaker nature of the L.Pec.15. fibres. Plate 5.13 also illustrates a fibre fragment with a large number of pectin cavities that were readily degraded by day 4. It is possible that this was a 'piece' of PHB blended with a comparatively large amount of pectin effectively forming a large particulate mass.

Day 7 observations appeared similar to those of L.Pec.9., with a large amount of fibre fragments observed. These fragments were heavily pitted and eroded due to the pectin loss, but no noticeable differences in the degree of pitting between L.Pec.9. and L.Pec.15. were observed, (Plates 5.14 & 5.15).

Thus, increasing the pectin loading had apparently little effect on the distribution of the pectin cavities within the matrix, but did increase the amount of pectin within some larger diameter fibres, so that the weakening of these fibres was greater than that of L.Pec.9.

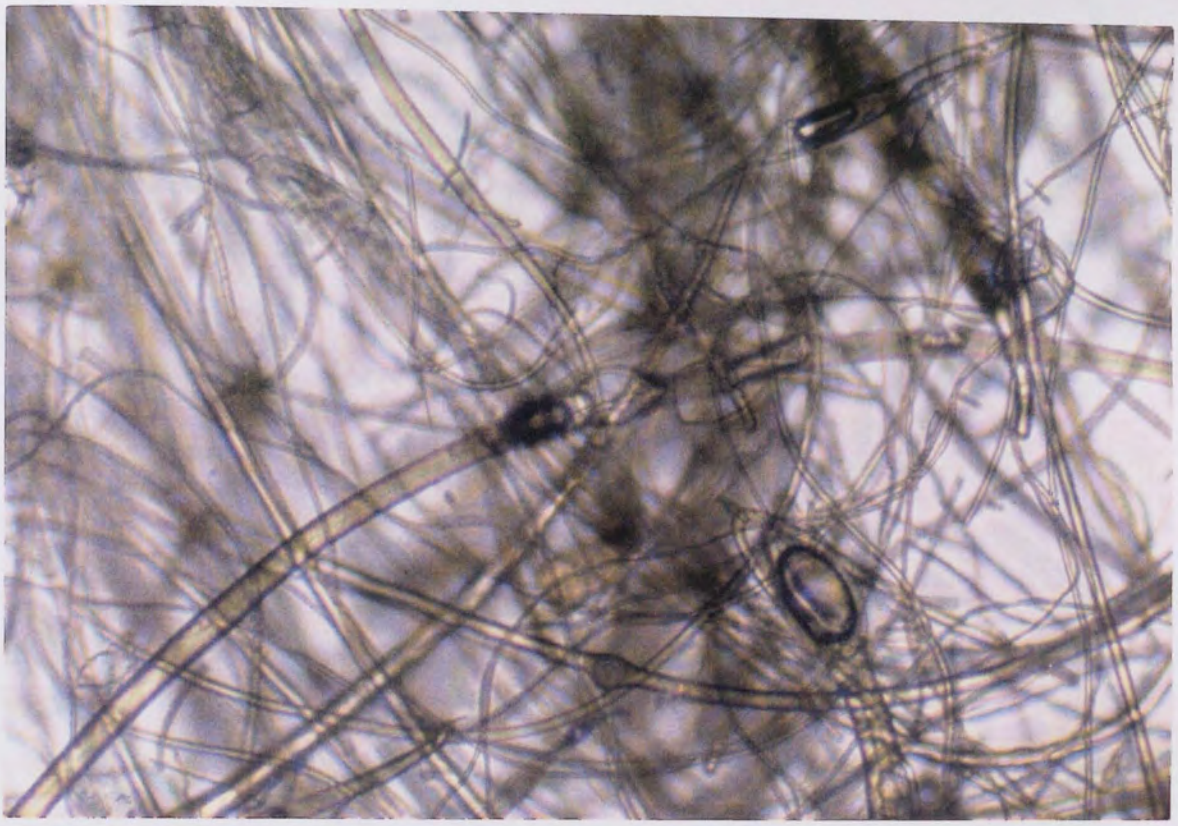

Plate 5.8. (x10) 1 Hour Degradation.
L.Pec.15.; PHB(FM)IP Blended With 15% Low Molecular Weight Pectin, Illustrating The Matrix Integrity After 1 Hours Degradation.

Plate 5.9. (x15) 3 Hours Degradation.
L.Pec.15.; Little Matrix Collapse After 3 Hours Degradation, Heavily Pectin Loaded Large Diameter Fibre.

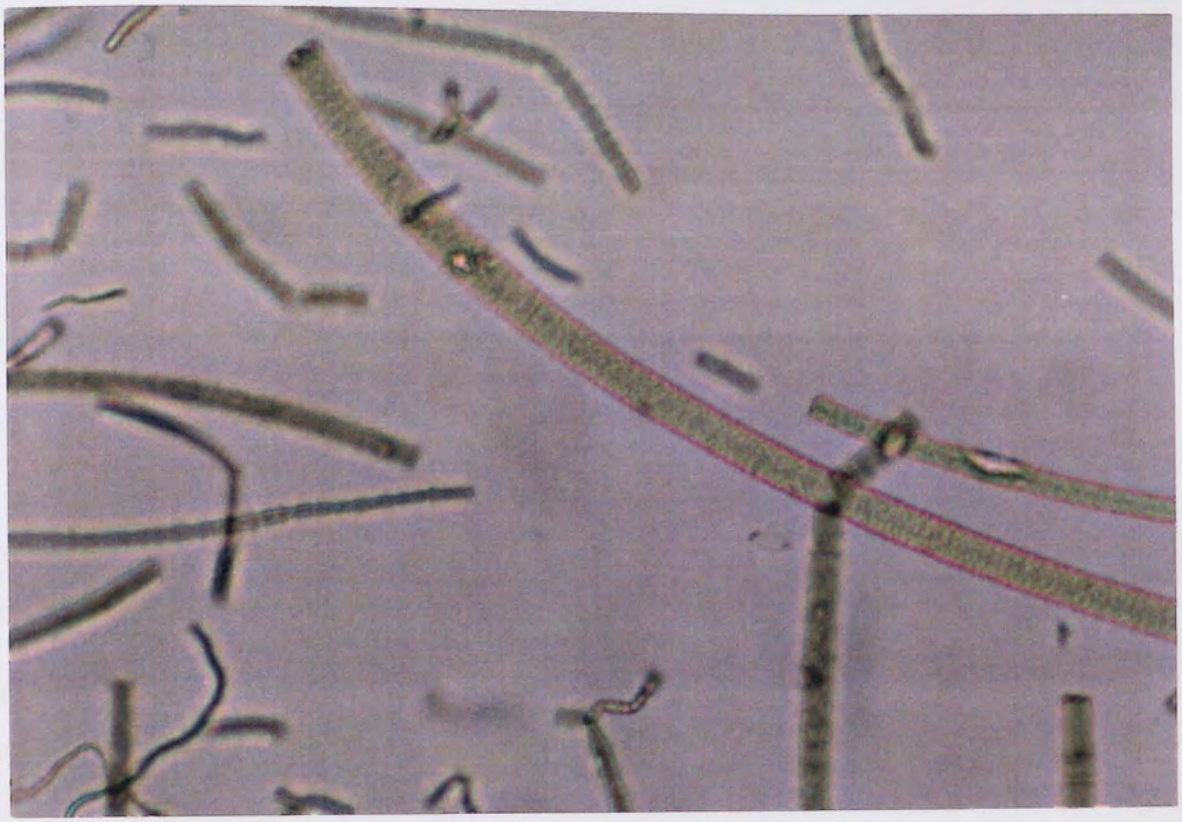

Plate 5.10. (x25) 7 Hours Degradation.
L.Pec.15.; A Medium Sized Fibre With An 'Even' Distribution Of Pectin.

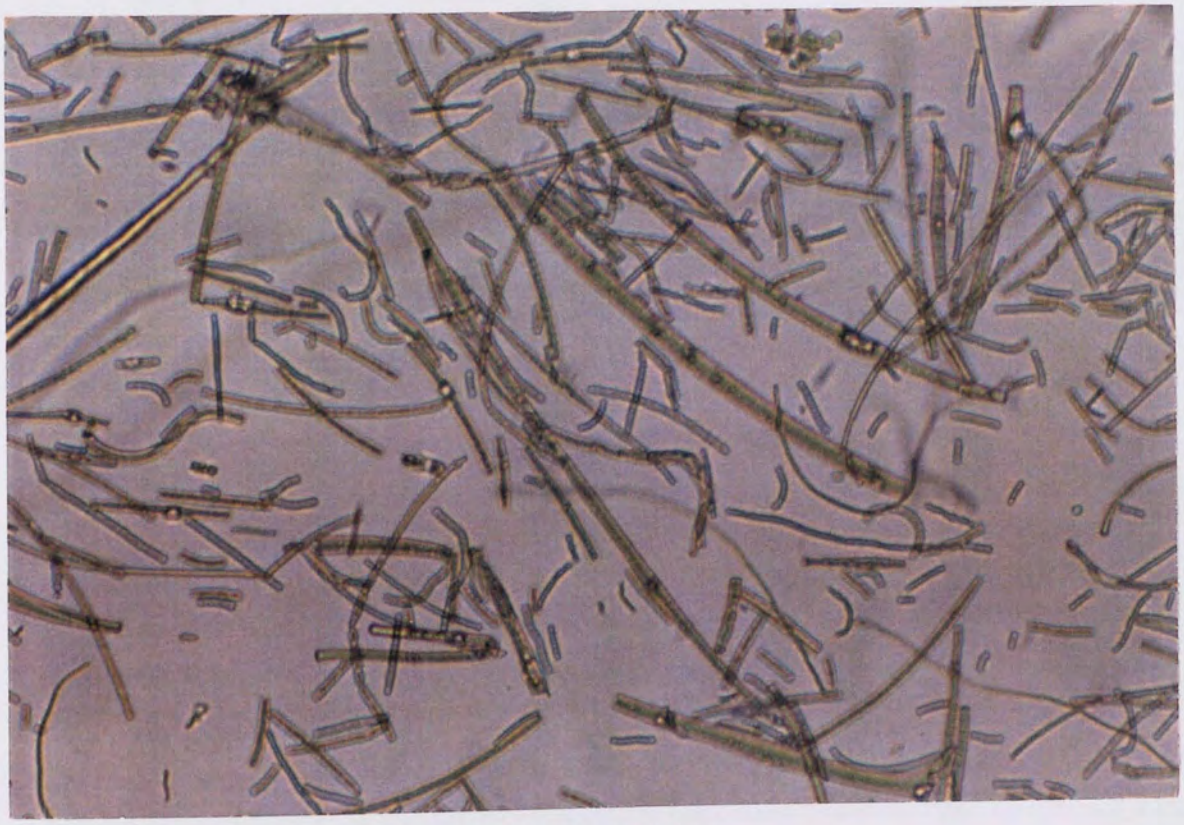

Plate 5.11. (x10) 7 Hours Degradation.
L.Pec.15.; Fragmentation Of Matrix After 7 Hours Degradation.

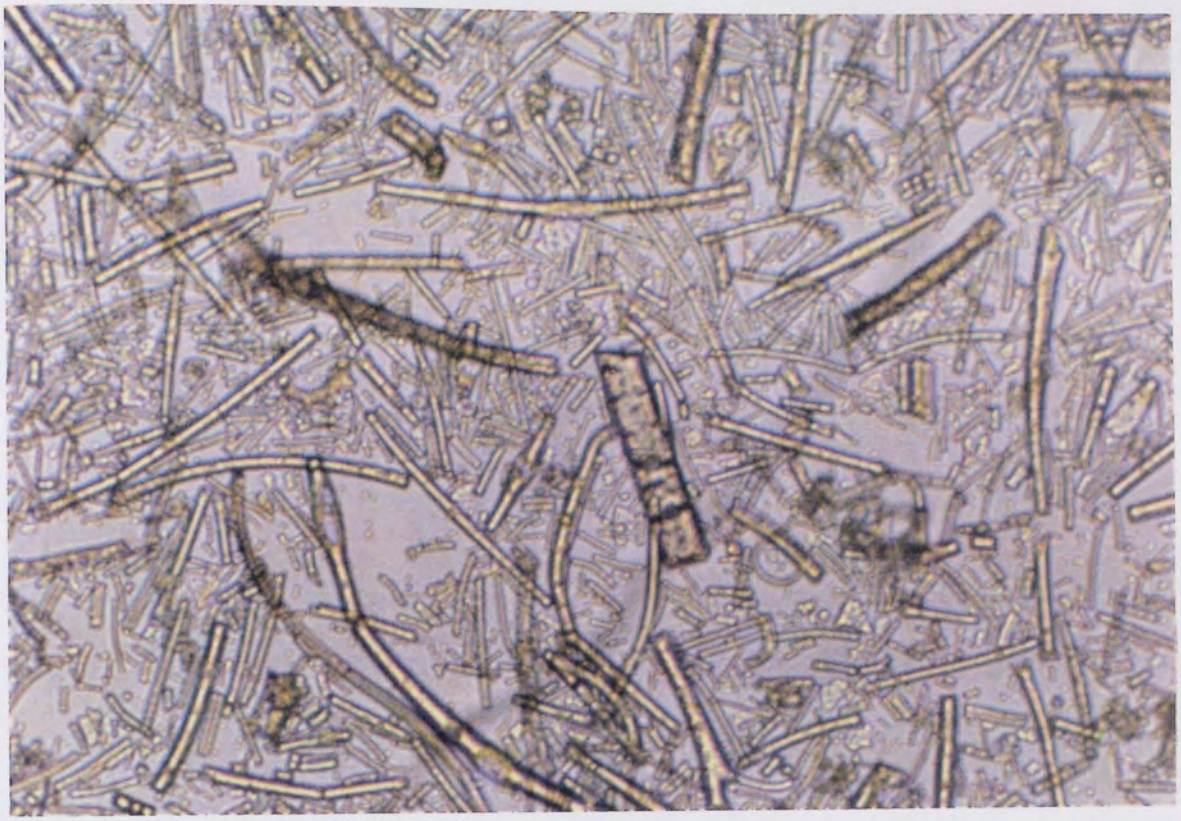

Plate 5.12. (x25) 4 Days Degradation.
L.Pec.15.; Large Degree Of Fragmentation And Fracturing At Day 4, With A Noticeable Lack Of Large Fibre Fragments Compared To L.Pec.9.

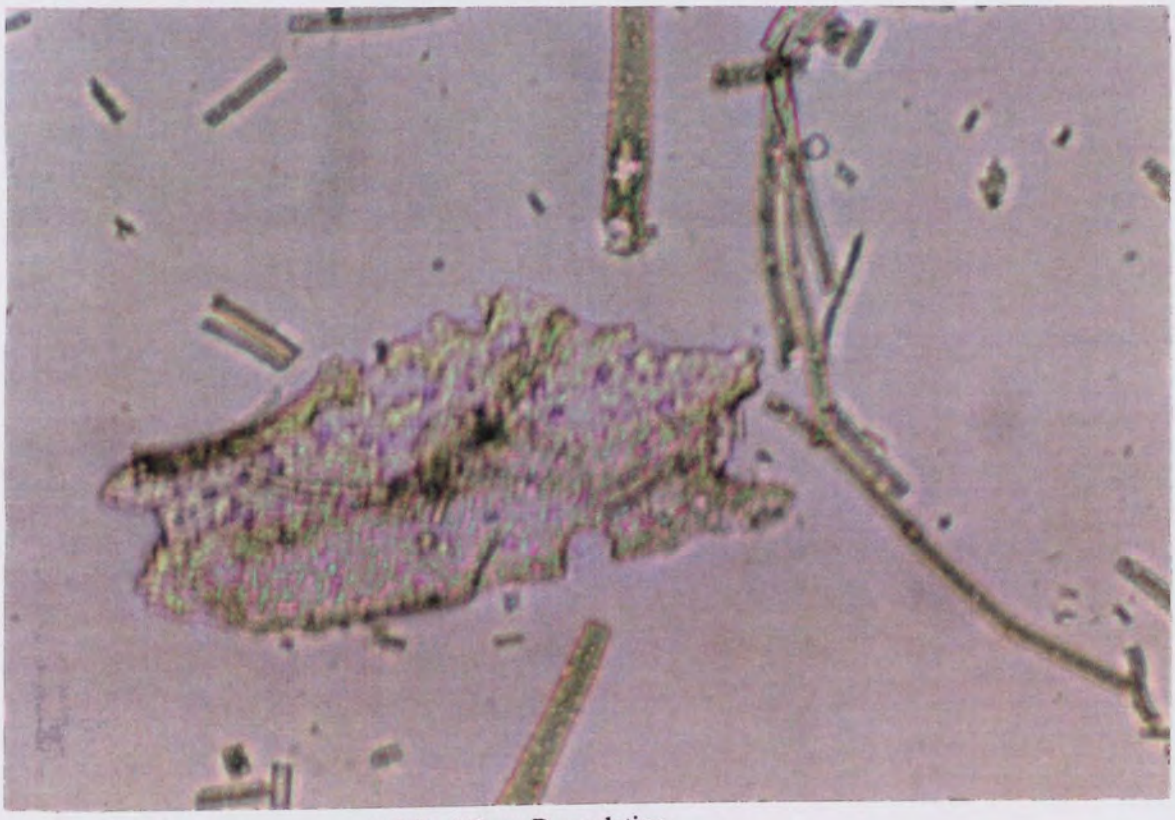

Plate 5.13. (x25) 4 Days Degradation.
L.Pec.15.; Piece Of Particulate Matter With A Large Number Of Pectin Cavities.

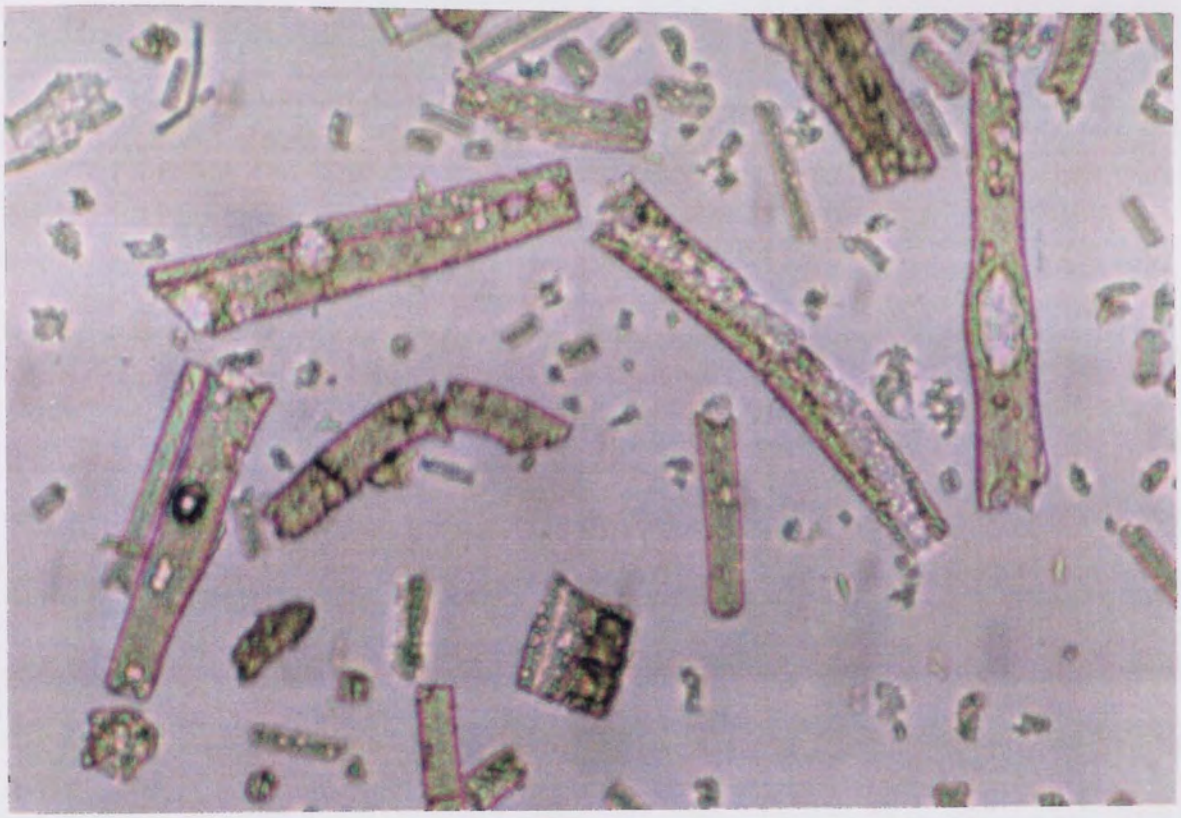

Plate 5.14. (x25) 7 Days Degradation.
L.Pec.15.; Pectin Cavities And A Degree Of Fragmentation Comparable With That Of L.Pec.9. After 7 Days Degradation.

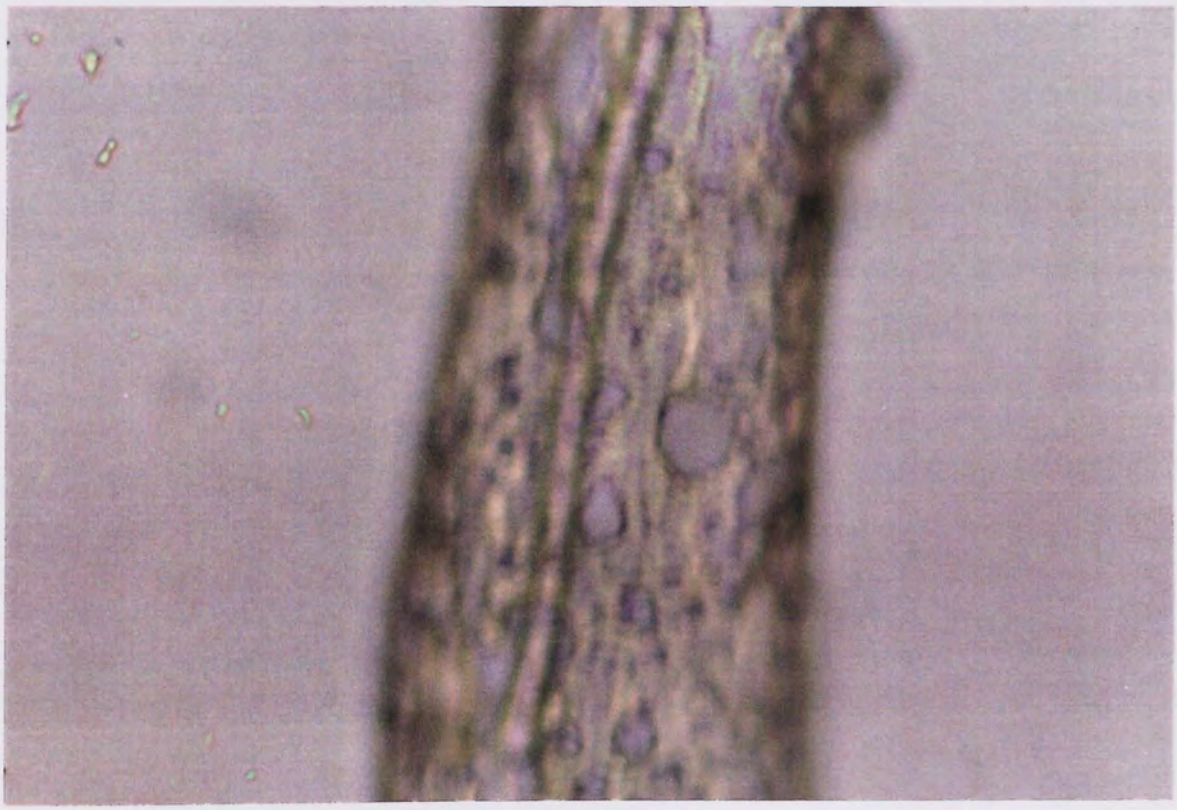

Plate 5.15. (x25) 7 Days Degradation.
L.Pec.15.; Pectin Cavities In A Large Diameter Fibre.

and thus upon collapse at stage II, a relatively rapid stage III degradation rate was observed.

Examination of L.Pec.25.S. and L.Pec.25.E. after 1 hour degradation revealed noticeable differences in the degradation. These were due to a difference in the pectin loading. The observations of L.Pec.25.E. were similar to those of L.Pec.15., with a number of fibres possessing what appeared to be a fairly even distribution of pectin and the matrix integrity still intact. After 3 hours degradation the matrix integrity was still present although a small degree of fracturing and fragmentation had occurred, but to a lesser extent than L.Pec.15. The smaller diameter fibres of L.Pec.25.S. appeared rather irregular, (Plate 5.16), whilst the L.Pec.25.E. fibres exhibited a larger pectin loading and this was noticed in certain fibres which were similar to the L.Pec.15., (Plate 5.17), wheras L.Pec.25.S. was similar to the IP sample.

The matrix integrity for L.Pec.25.S. was reduced for samples 5 and 7 hours, but appeared similar to that of the 3 hour sample with a slightly greater degree of fragmentation. However, the sample taken at the end of the manufacturing run (L.Pec.25.E.) had a number of noticeable differences, with larger amounts of fracturing, fragmentation and pectin cavities being observed, (Plate 5.18). Plate 5.19 illustrates a large piece of particulate matter, this was probably PHB mixed with pectin, similar pieces were quite numerous but not as readily observed in the later degradation stages and consequently they were considered to be heavily loaded with pectin. These pieces were observed in greater numbers for L.Pec.25.E. than L.Pec.15. and in L.Pec.15. than L.Pec.9. Thus, these observations tended to indicate that increasing the pectin loading

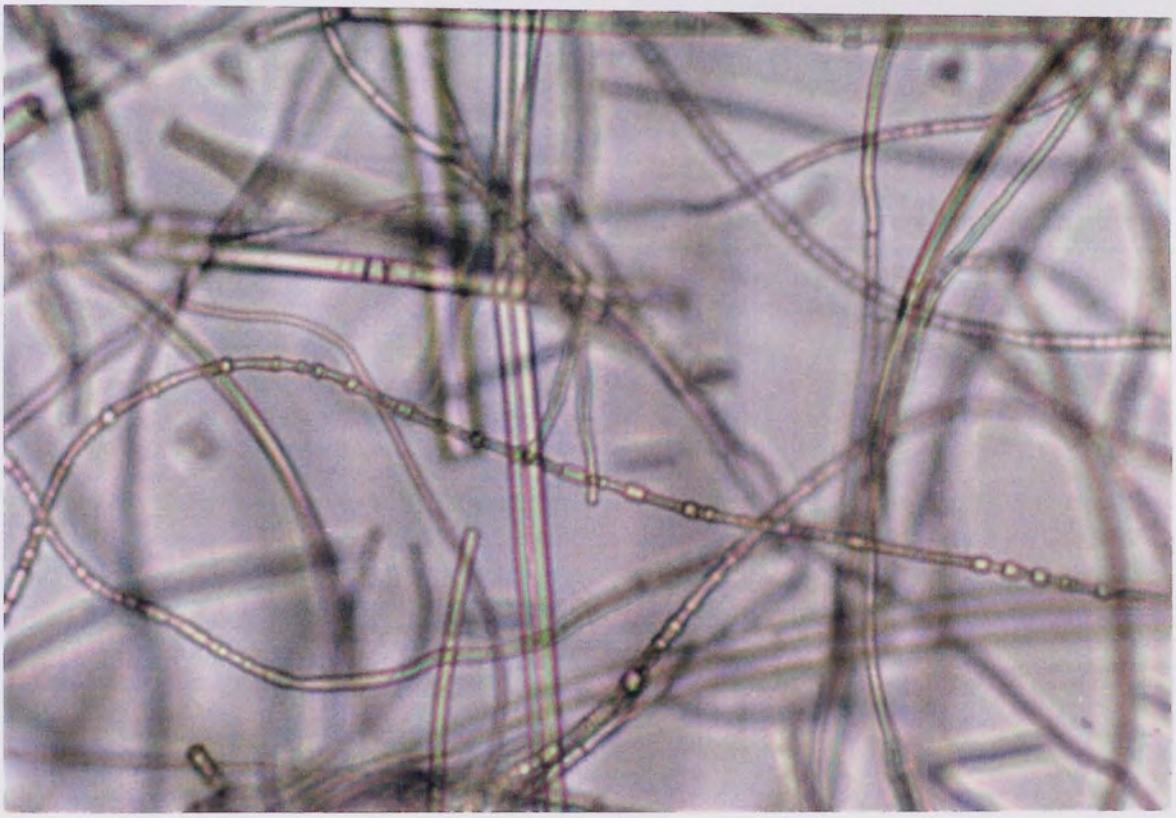

Plate 5.16. (x25) 3 Hours Degradation.
L.Pec.25.S.; PHB(FM)IP Blended With 25% Low Molecular Weight Pectin Sampled At The Start Of The Manufacturing Run, Illustrating An Irregular Small Fibre.

Plate 5.17. (x25) 3 Hours Degradation.
L.Pec.25.E.; PHB(FM)IP Blended With 25% Low Molecular Weight Pectin Sampled From The End Of The Manufacturing Run, Illustrating A Heavily Pectin Loaded Large Fibre.

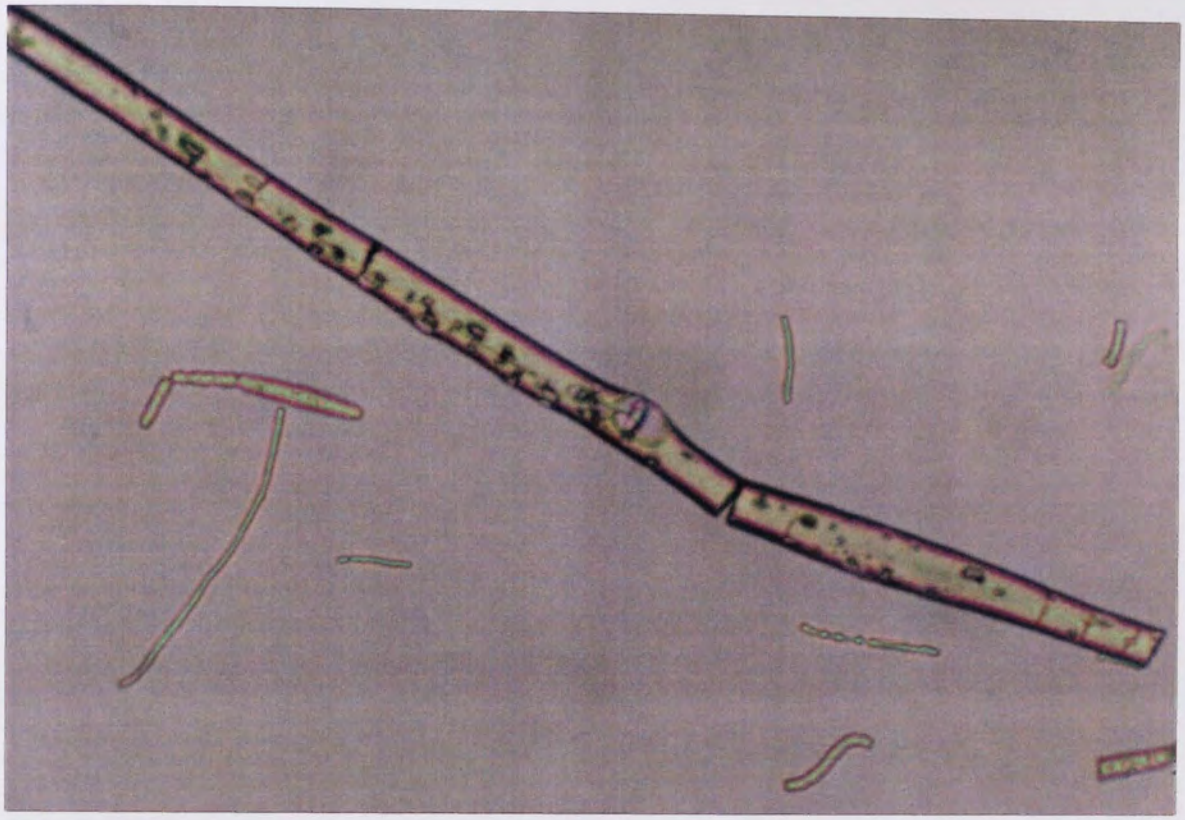

Plate 5.18. (x15) 6 Hours Degradation.
L.Pec.25.E.; Pectin Cavities And Fragmentation Due To Handling In A Medium Sized Fibre

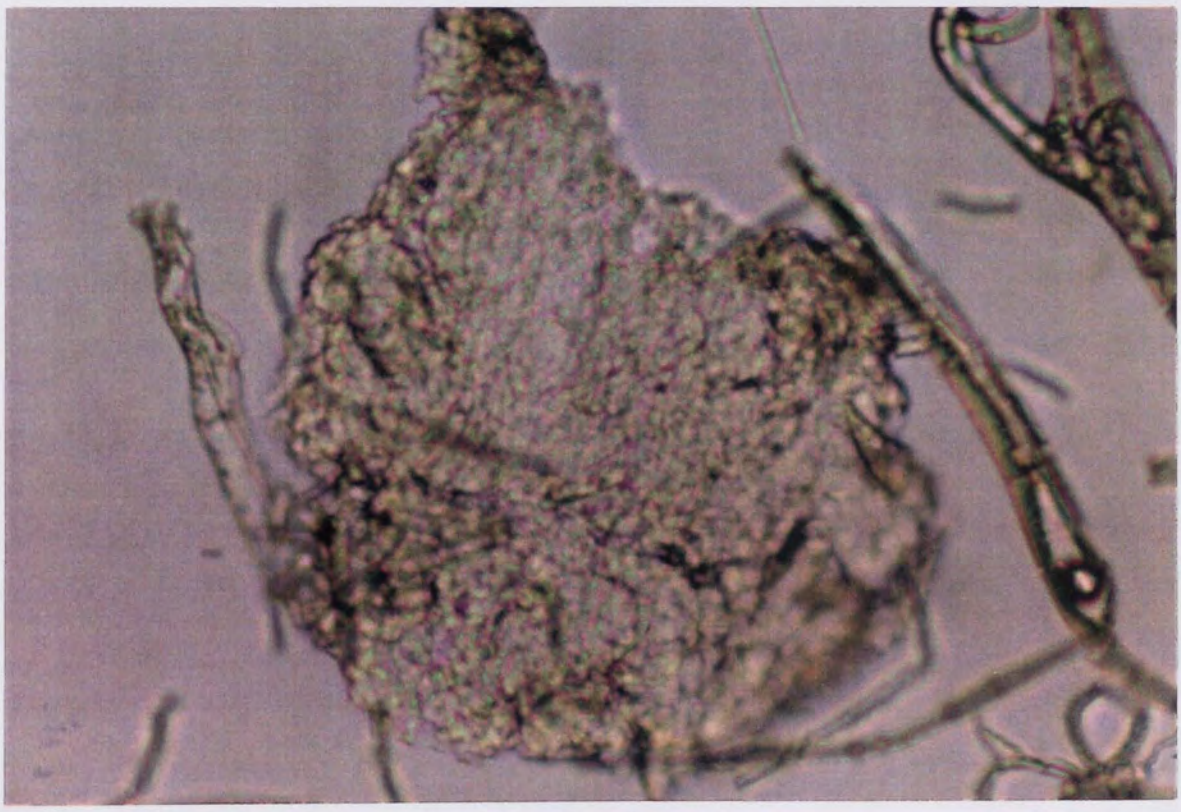

Plate 5.19. (x25) 6 Hours Degradation.
L.Pec.25.E.; Large Particulate Mass Containing A Relatively Large Pectin Loading - 'Mixed Pectin'.

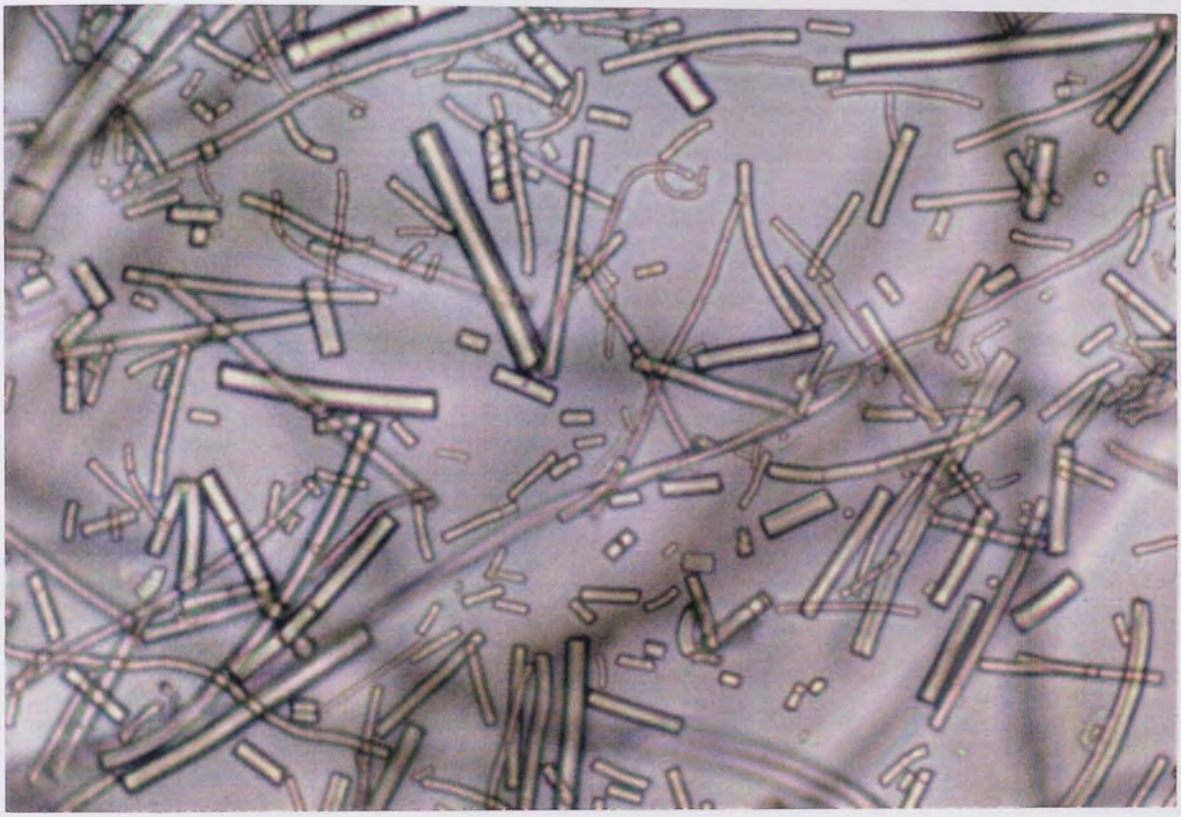

Plate 5.20. (x25) 1 Days Degradation.
L.Pec.25.S.; Smooth Large Fibre Fragments Indicating A Comparatively Lower Pectin Loading Than L.Pec.25.E.

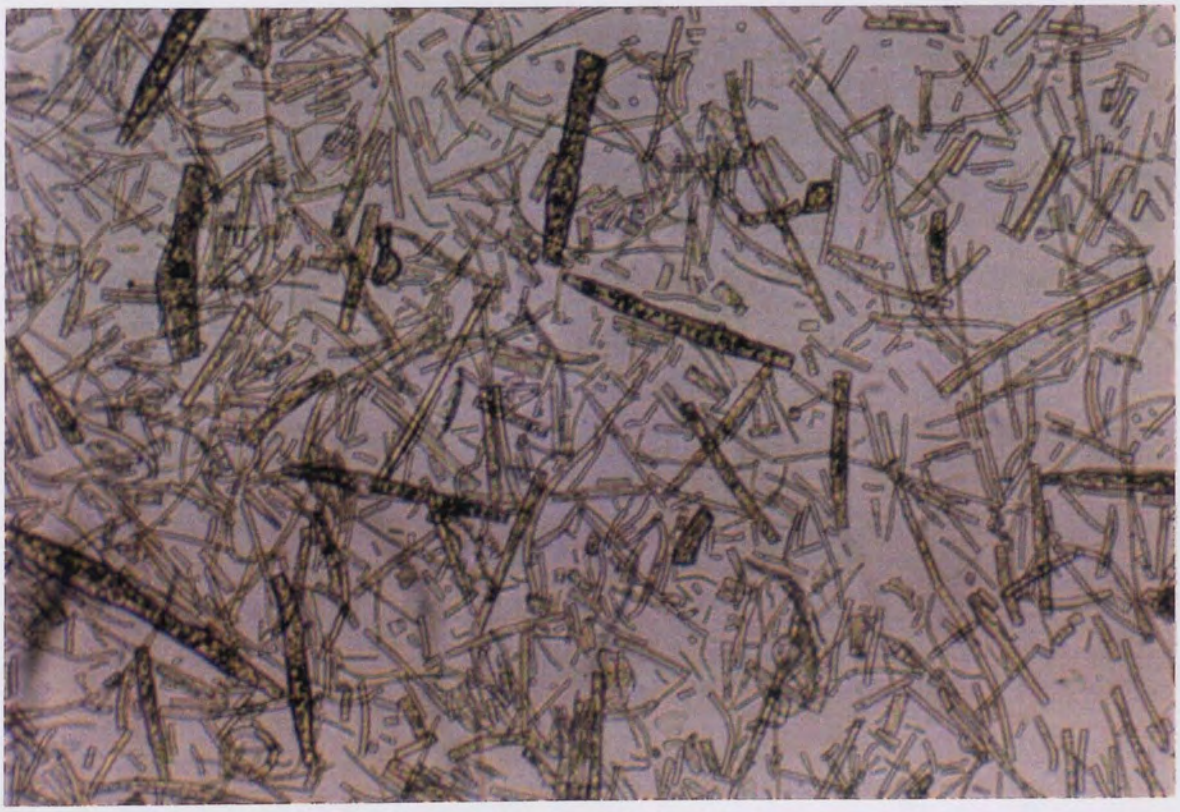

Plate 5.21. (x15) 1 Days Degradation.
L.Pec.25.E.; A Larger Degree Of Fragmentation And Pectin Cavities Than L.Pec.25.S. In Plate 5.20.

Plate 5.22. (x15) 7 Days Degradation.
L.Pec.25.S.; Small Fibre Fragments And Particulate Matter After 7 Days Degradation.

Plate 5.23. (x25) 7 Days Degradation.
L.Pec.25.E.; A Similar Degree Of Fragmentation To L.Pec.25.S. In Plate 5.22 But With More Irregularities And Pectin Cavities.

caused the mixing of the excess unblended pectin with some PHB in these readily degradable particulate forms.

At day 1 L.Pec.25.S. had a similar appearence of matrix breakdown and fragmentation as the IP sample, whilst L.Pec.25.E. was much more fragmented and appeared more like L.Pec.15., with the fibres having a noticeable increase in the number of pectin cavities, (Plates 5.20 & 5.21). L.Pec.25.S. displayed a similar degradation at day 4 as was observed with the IP sample, whilst sample L.Pec.25.E. appeared more degraded. Similar amounts of fragmentation for the two samples were observed at day 7. L.Pec.25.E. displayed much more irregularity in the fibres, thus presenting a larger surface area to volume ratio and consequently a larger amount of degradation was considered to have occurred, when compared to L.Pec.25.S., (Plates 5.22 & 5.23).

Thus, it was concluded that the blending efficiency between the PHB and the low molecular weight pectin was rather poor, so that a greater proportion of loading was produced at the end of the manufacturing run. The degradation observations for L.Pec.25.S. were similar to the IP sample, whilst the L.Pec.25.E. observations were more similar to those of L.Pec.15. Increasing the percentage loading therefore, only increased the blending slightly whilst the remaining pectin was mixed with the PHB in particulate forms and lost in the production process.

Sample H.Pec.10. had noticeable differences when compared to L.Pec.9. Fibres from H.Pec.10. were similar in the initial degradation stages to those of the IP and L.Pec.25.S. samples. Some medium diameter fibres had a similar appearence to those of L.Pec.15.

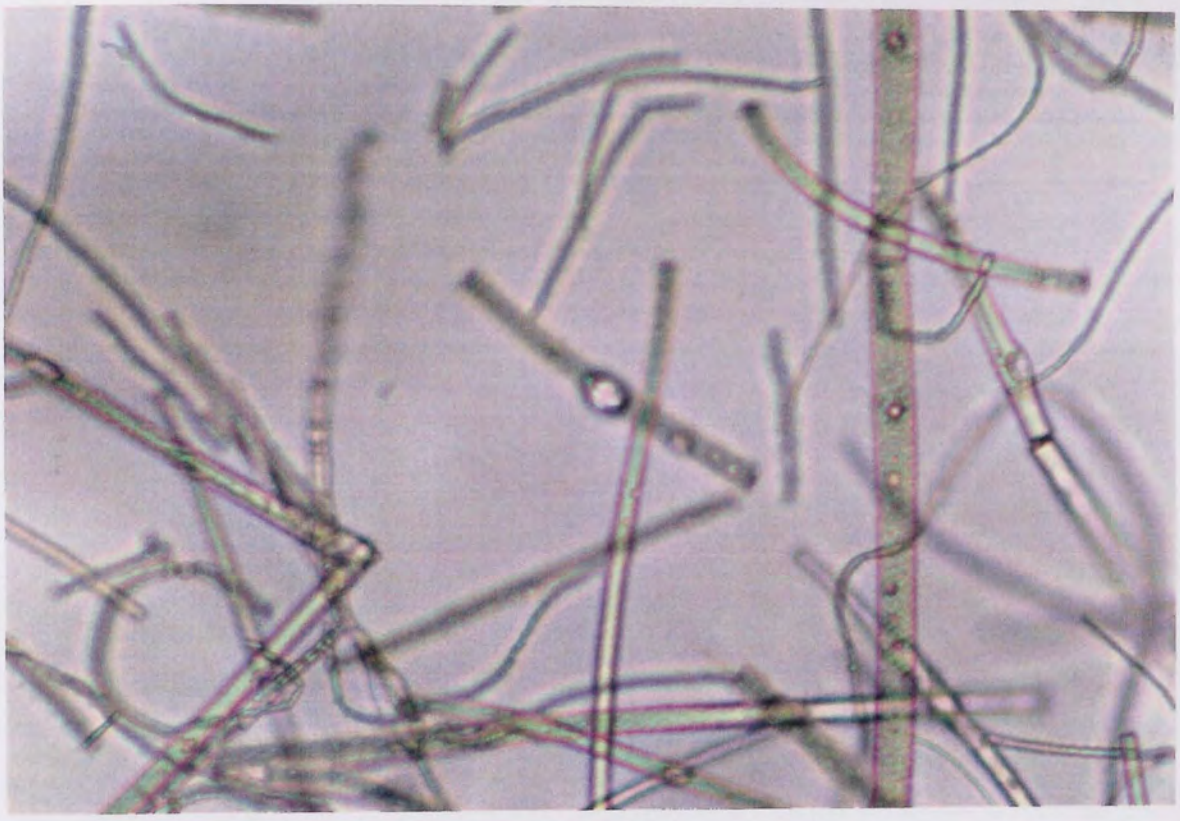

Plate 5.24. (x25) 1 Hour Degradation.
H.Pec.10.; PHB(FM)IP Blended With 10% High Molecular Weight Pectin, Illustrating A Similar Appearance To L.Pec.15. In Plate 5.17.

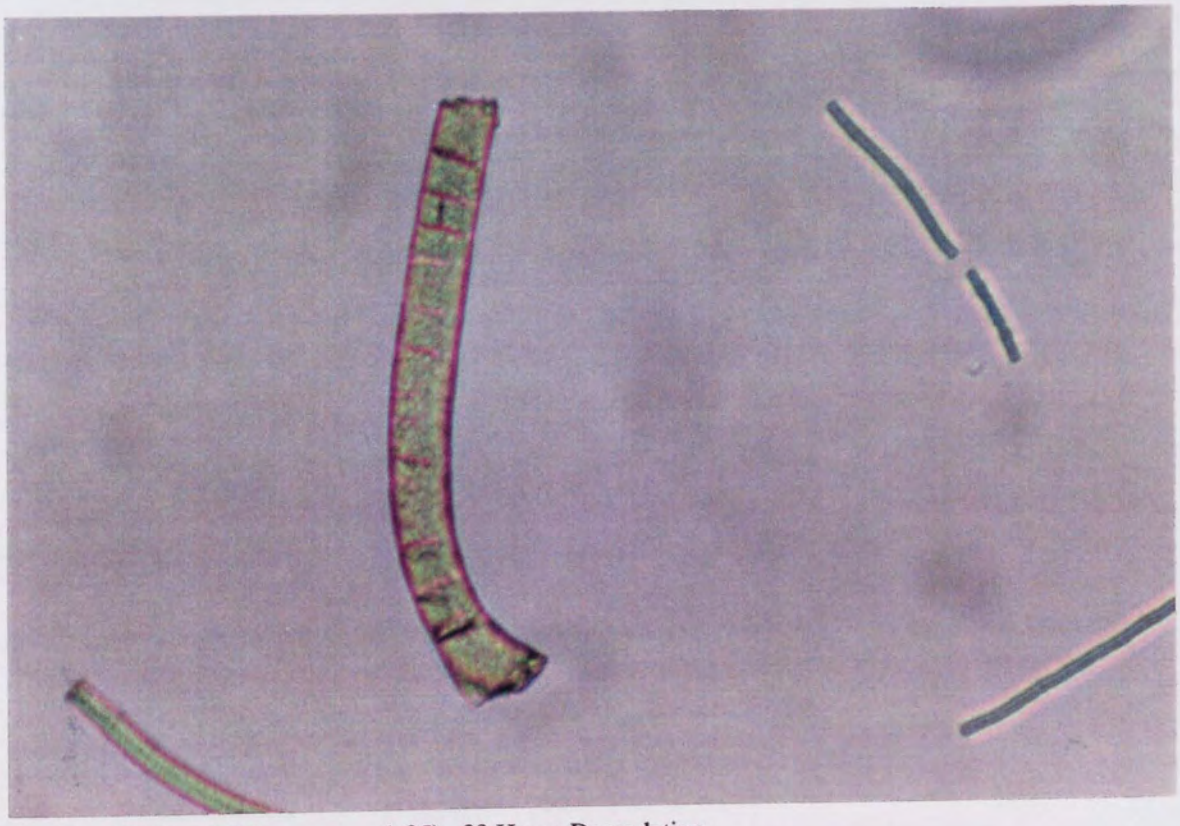

Plate 5.25. (x25) 23 Hours Degradation.
H.Pec.10.; Fragmentation To Fibre Fragments Readily Occurred With Fracturing In All Plains Observed.

Plate 5.26. (x25) 4 Days Degradation.
H.Pec.10.; A Large Degree Of Fragmentation To Small Fibre Fragments And Large Particulate Matter.

Plate 5.27. (x25) 4 Days Degradation.
H.Pec.10.; A Proportion Of Large Diameter Fibres Maintained Integrity But Still Exhibited Surface Erosion.

with a visable pectin loading, (Plates 5.24 & 5.10). No noticeable change in the matrix and fibre structure was observed after 3 and 7 hours degradation. A greater degree of fracturing and fragmentation was noticed in all the fibre sizes after 23 hours, but most of these fractures appeared to be due to mechanical degradation, (Plate 5.25). Although fragmentation had occurred to a similar extent as L.Pec.9., the H.Pec.10. fibres did not appear to have the same shape irregularities as their lower molecular weight counterparts, nor did they exhibit the large pectin cavities. These differences were comparable to those observed between the two L.Pec.25. samples. This tended to indicate that L.Pec.25.S. had a relatively small proportion of pectin which was of a comparatively higher molecular weight when compared to the larger pectin loading in L.Pec.25.E.

At day 4, fragmentation in H.Pec.10. had occurred to a comparatively greater extent in the majority of small and medium sized fibres than in L.Pec.9., whilst some of the larger diameter fibres still maintained their integrity. In most cases surface erosion was readily observed and appeared comparable to the surface erosion of the technical grade (TG) fibres at days 2.29 and 5 (Plates 5.26 & 5.27). Observations of the H.Pec.10. sample after 7 days degradation revealed a similar amount of fragmentation as L.Pec.9., but a lack of surface erosion in some fibres. These fibres had a greater integrity and collapsed at a later stage. A few large pectin cavities were also observed.

Thus, it was concluded that the high molecular weight pectin was blended more homogeneously within the fibres. Upon degradation this increased the surface area to volume ratio to a greater extent than the low molecular weight samples, thus facilitating the degradation of the PHB, whilst still maintaining the initial matrix stability.

Examinations of the partially degraded co-blends at higher magnifications were done using SEM. After 1 hours degradation sample L.Pec.9. apparently exhibited a similar matrix integrity to the homopolymer sample from the same degradation period. The pectin cavities readily observed using phase contrast microscopy were less noticeable using SEM, (Plate 5.28), this was probably due to the handling and mounting procedures which facilitated the further collapse of the fibres at these structurally weak points.

Fragmentation was more noticeable after a days degradation with the pectin cavities and porous nature of the large diameter fibres, in particular, being readily observed, (Plate 5.29). The fragmentation at day 3 was similar to that observed at day 1, with the large diameter fibres having noticeable irregularities, (Plates 5.30 & 5.31). Plates 5.32 to 5.35 illustrate the increasing degree of fragmentation of the L.Pec.9. fibres during degradation, from the large fibre fragments at day 5 (Plates 5.32) to a mass of small fibre fragments and particulate matter at day 14. These small fibre fragments were relatively smooth compared to the particulate matter and this tended to indicate that the pectin loading was greater in the larger sized fibres than in the small. As a result of this, the small sized fibres were comparatively more stable and less degraded at the later stages (Plates 5.34). The hollow nature of many of the larger sized fibres is illustrated in plate 5.35.

The partially degraded L.Pec.15. matrix (Platess 5.36-5.39) exhibited a greater degree of fragmentation at day 4 than that observed for the L.Pec.9. sample, with many small fibre fragments observed, (Plate 5.37). The larger diameter fibres were readily eroded by day 7, so that they possessed a 'honeycombed' appearence, (Plates 5.38 & 5.39). This was due to the pectin mainly blending with the large diameter fibres.

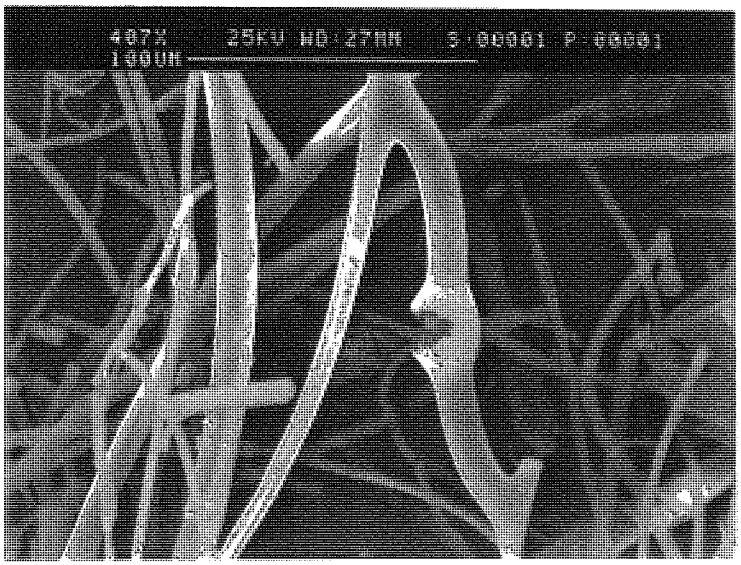

Plate 5.28. (x407) 1 Hours Degradation.
L.Pec.9.; A Similar Matrix Integrity To PHB(FM)IP, Also Illustrating A Fractured Bulbous Region.

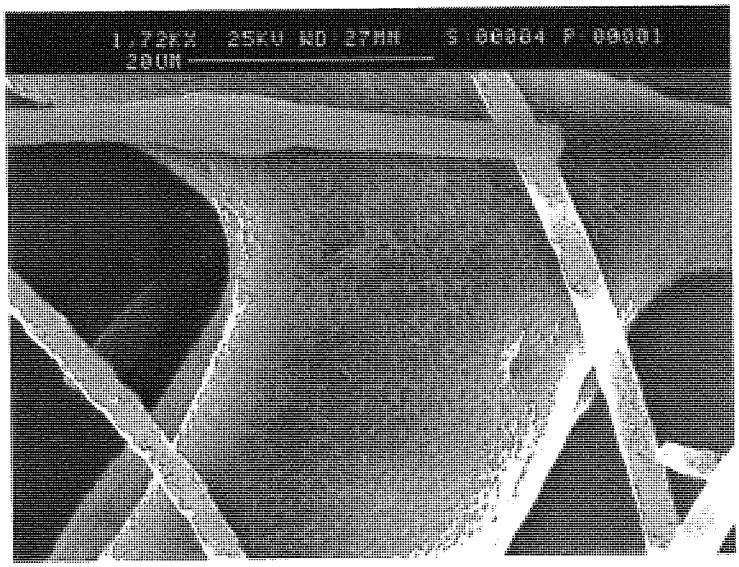

Plate 5.29. (x1.72K) 1 Day Degradation.
L.Pec.9.; A Large Diameter Fibre With A Highly Porous Nature.

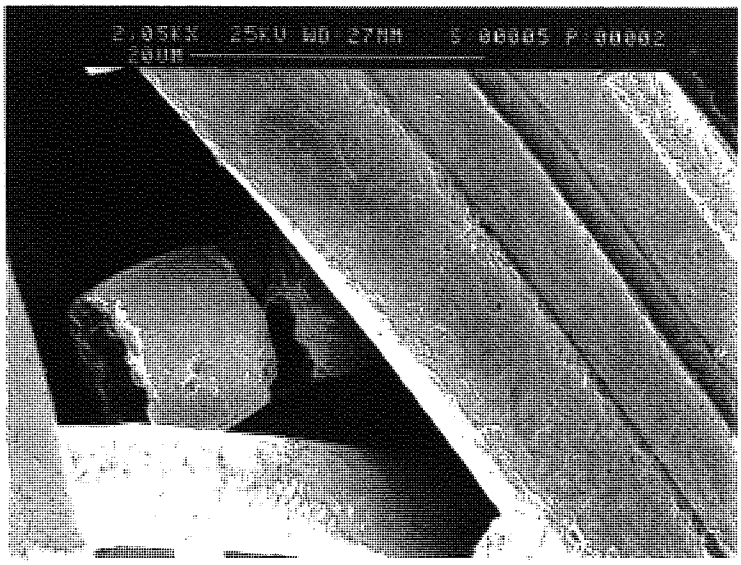

Plate 5.30. (x2.05K) 3 Days Degradation.
L.Pec.9.; Large Porous Agglutinated Fibres And The Hollow Nature Of A Large Fibre Fragment.

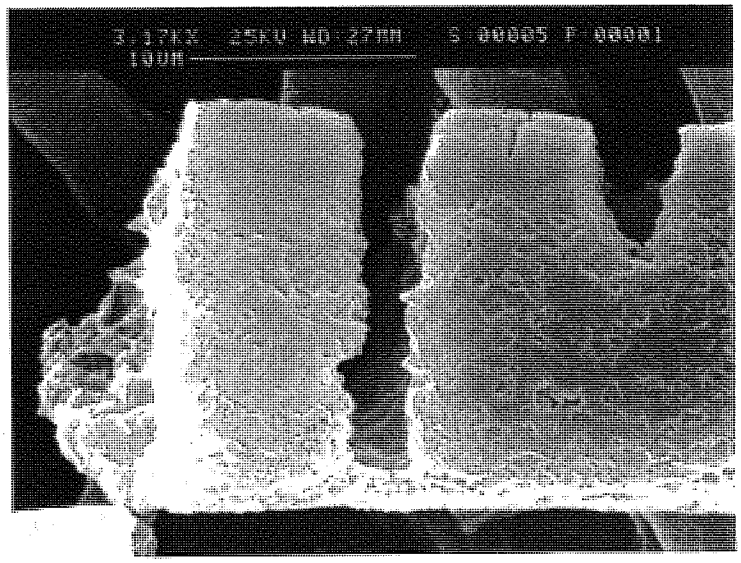

Plate 5.31. (x3.17K) 3 Days Degradation.
L.Pec.9.; Erosion Of Fibre Fragment At The Points Of Fracture - 'Eaten Away'.

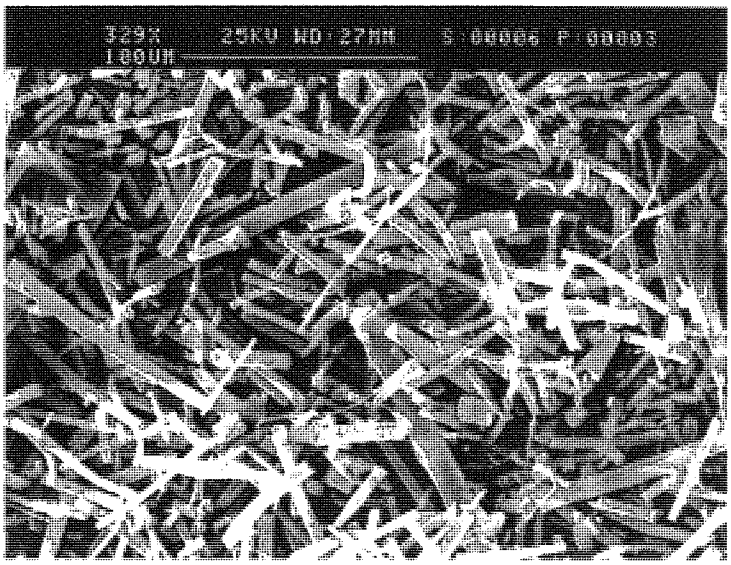

Plate 5.32 (x329) 5 Days Degradation.

L.Pec.9.; Fragmentation To Large Fibre Fragments After 5 Days Degradation.

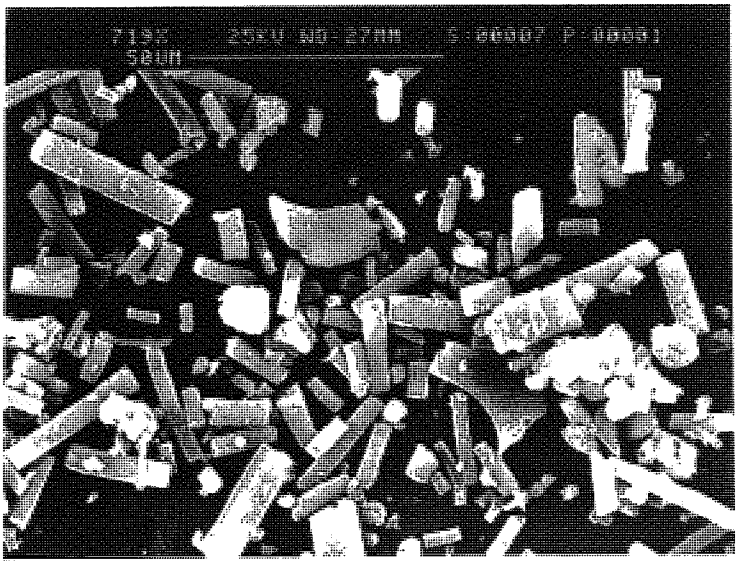

Plate 5.33. (x719) 7 Days Degradation.

L.Pec.9.; Increased Degree Of Fragmentation To After 7 Days Degradation, Smaller Fibre Fragments Compared To Plate 5.32.

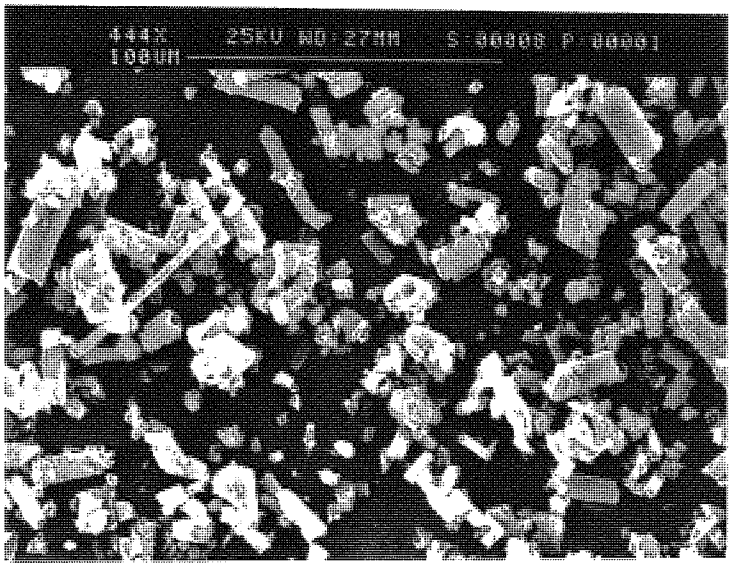

Plate 5.34. (x444) 14 Days Degradation.
L.Pec.9.; Large Degree Of Fragmentation To Small Fibre Fragments And Large Particulate Matter.

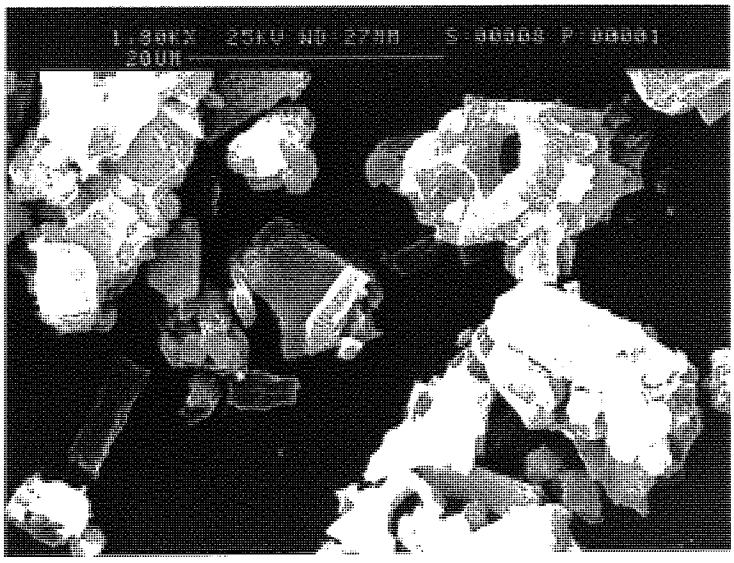

Plate 5.35. (x1.80K) 14 Days Degradation.
L.Pec.9.; Hollow Nature Of Fibre Fragments Increases The Available Surface Area to Volume Ratio.

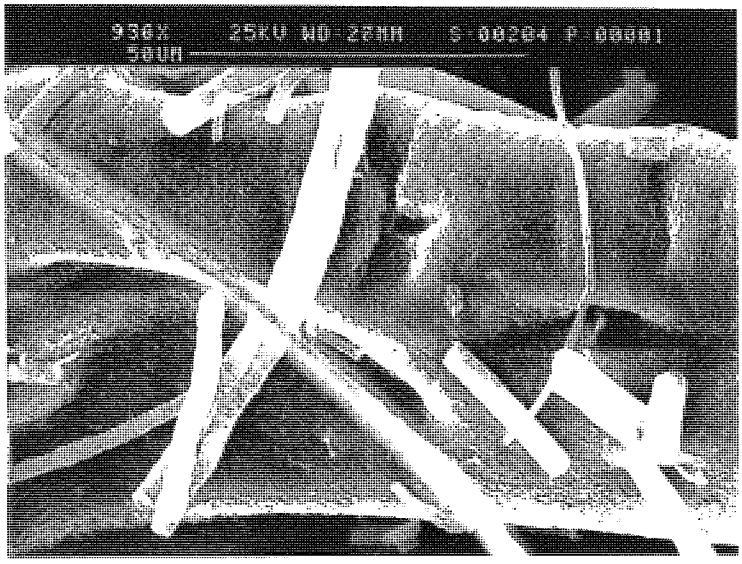

Plate 5.36. (x936) 1 Day Degradation.
L.Pec.15.; Pectin Cavity In A Large Diameter Fibre And Small Diameter Fibre Fragments.

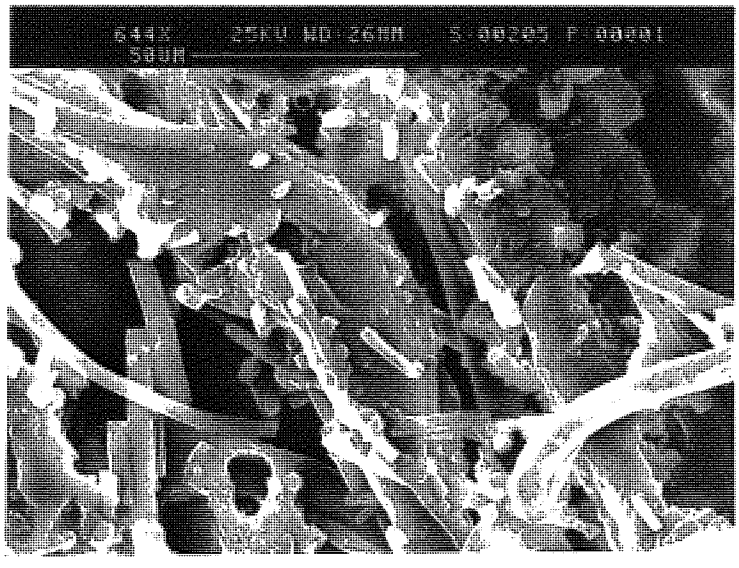

Plate 5.37. (x644) 4 Days Degradation.
L.Pec.15.; Large Degree Of Fragmentation To Small Fibre Fragments And Particulate Matter.

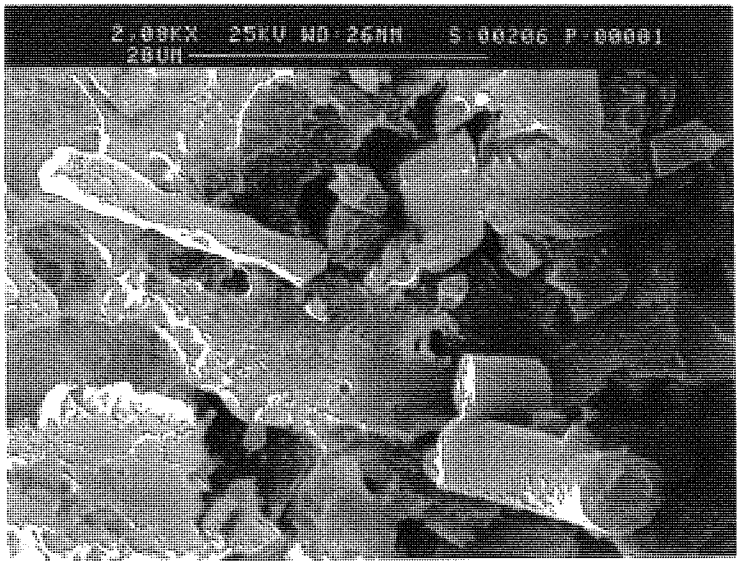

Plate 5.38. (x2.08K) 7 Days Degradation.
L.Pec.15.; Fibre Fragments And Mat Of Particulate Matter.

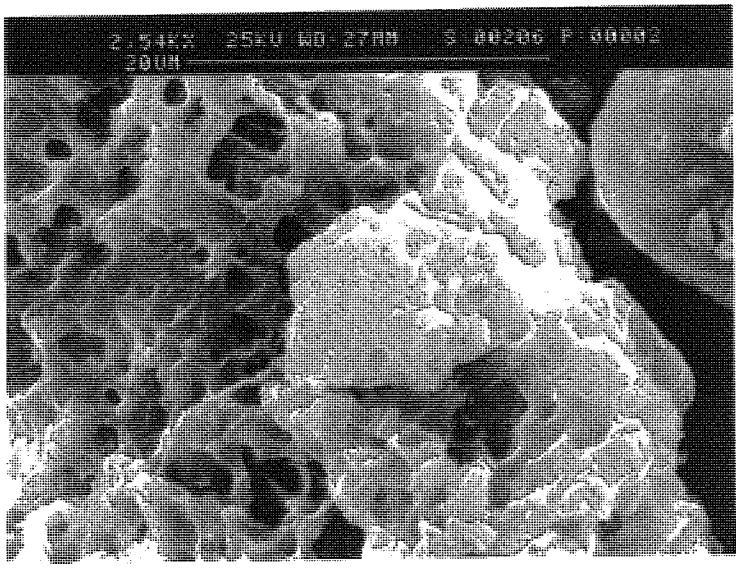

Plate 5.39. (x2.54K) 7 Days Degradation.
L.Pec.15.; The Readily Noticeable Porous Nature Of The Particulate Mat With 'Eroded' Surface.

Sample L.Pec.25.S. was previously concluded as possessing a loading of approximately 6%, (Graph 5.11B), which was of a comparatively higher molecular weight than the other pectin blended samples; L.Pec.9., L.Pec.15. and L.Pec.25.E. This was also indicated from the phase contrast and scanning electron microscopy observations, (Plates 5.40-5.45). The matrix integrity of L.Pec.25.S. gradually decreased until around day 1, where the small diameter fibres readily fragmented to a greater extent than observed for L.Pec.9., whilst after 1 days degradation the large diameter L.Pec.25.S. fibres appeared to be comparatively unaffected, (Plates 5.29 & 5.41). The fragmentation gradually increased, so that by day 4 there were some large fibre fragments, a large number of smaller fibre fragments and a dense mat of particulate matter, (Plates 5.42 & 5.43). Generally the degree of fragmentation at day 4 appeared slightly greater than observed for the L.Pec.9. sample at day 5. At day 7 the fragmentation of the L.Pec.25.S. fibre fragments was greater than at day 3, whilst the larger diameter fibre fragments still retained some integrity and exhibited a large number of comparatively small pores, (Plate 5.44). The L.Pec.25.S. fibres did not exhibit any large irregularities or a honeycombed nature as observed for L.Pec.9. and L.Pec.15. respectively. These observations of the partially degraded L.Pec.25.S. fibres are consistent with previous conclusions about their pectin molecular weight and loading.

L.Pec.25.E. exhibited a considerable degree of fragmentation after only 1 hours degradation, comparable to that observed for sample L.Pec.15. Plates 5.45 and 5.46 illustrate that the fragmentation was mainly limited to the large diameter fibres, which appeared hollow. This was most likely due to a dissolution of pectin acting as a filler, particulate matter and surface irregularities were also readily observed (Plates 5.45 &

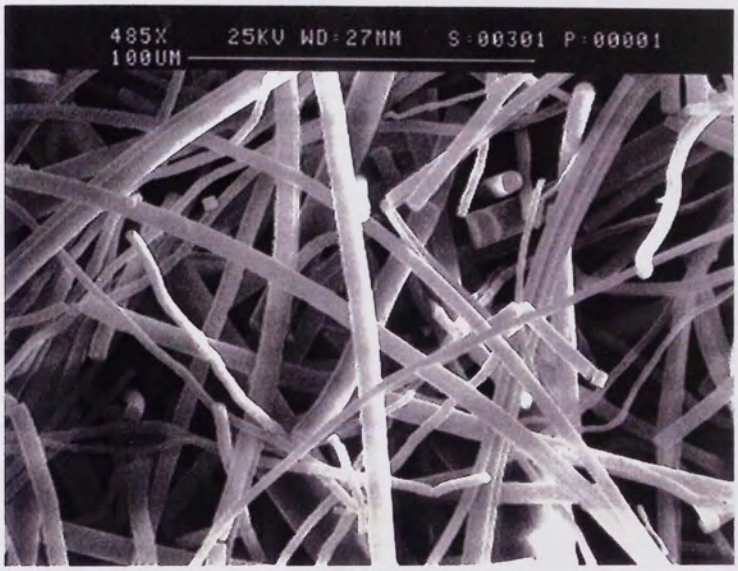

Plate 5.40. (x485) 1 Hour Degradation.
L.Pec.25.S.; Matrix Integrity In The Initial Degradation Stages.

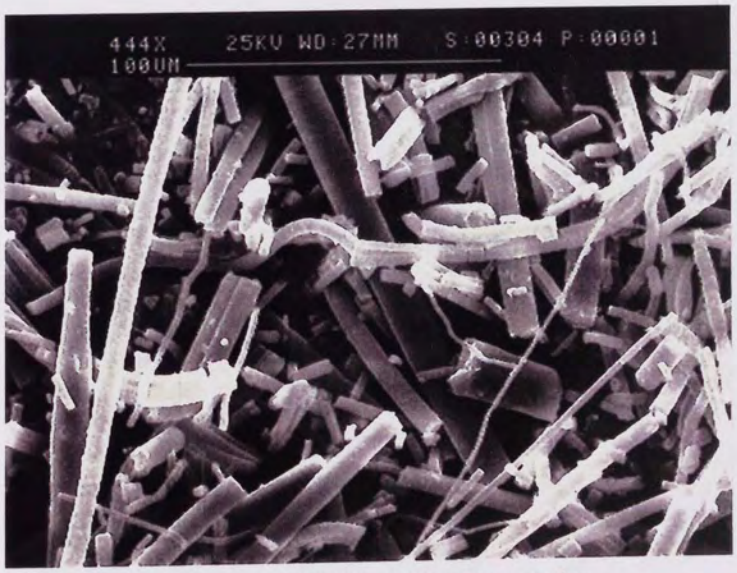

Plate 5.41. (x444K) 1 Day Degradation.
L.Pec.25.S.; Fragmentation Of The Mainly Small Diameter Fibres Readily Occurred After 1 Days Degradation.

Plate 5.42. (x1.59K) 4 Days Degradation.
L.Pec.25.S.; Small Fibre Fragments And Comparatively Intact Large Diameter Fibres.

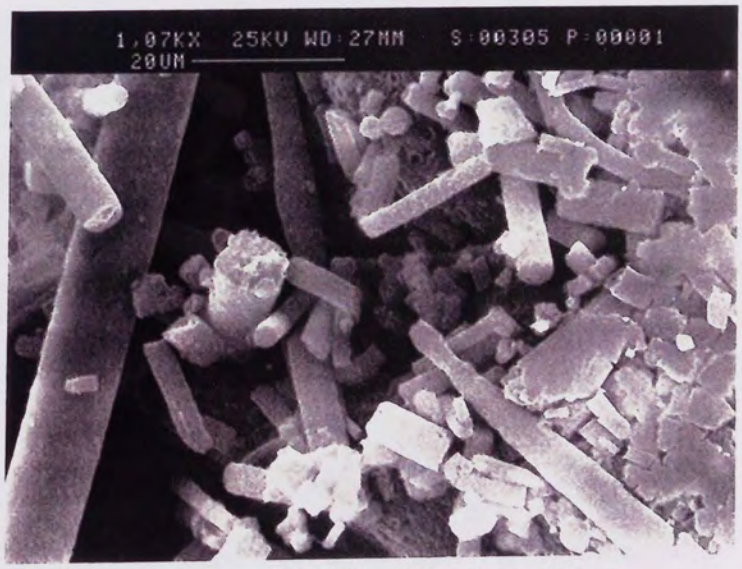

Plate 5.43. (x1.07K) 4 Days Degradation.
L.Pec.25.S.; Fibre Fragments And Mat Of Particulate Matter.

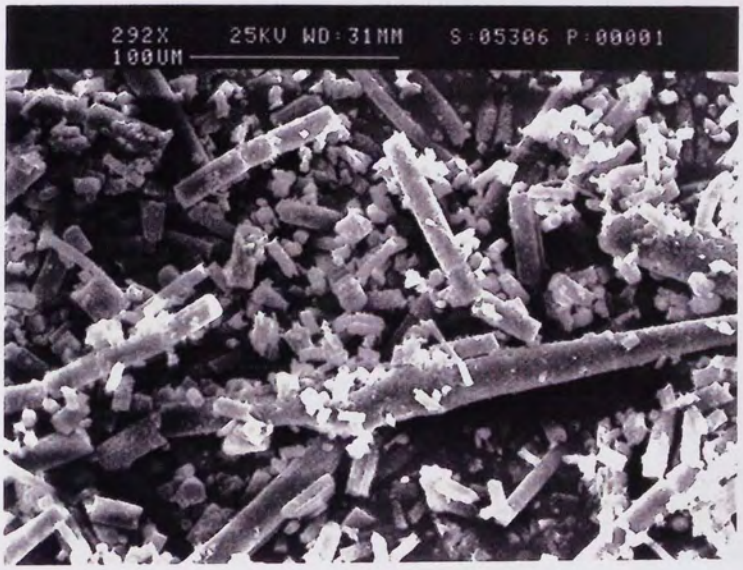

Plate 5.44. (x292) 7 Days Degradation.
L.Pec.25.S.; Large Diameter Fibre Fragments Maintained A Degree Of Integrity After 7 Days Degradation.

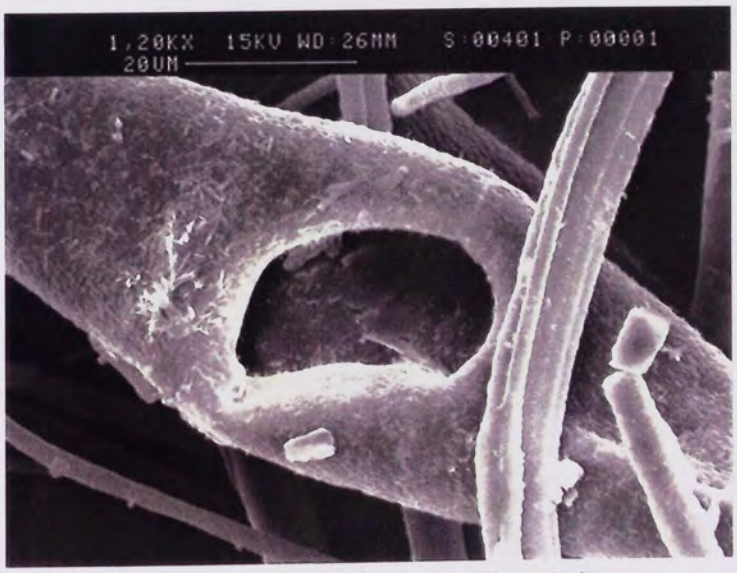

Plate 5.45. (x1.20K) 1 Hour Degradation.
L.Pec.25.E.; Heavily Porous Large Diameter Fibre With A Noticeable Pectin Cavity.

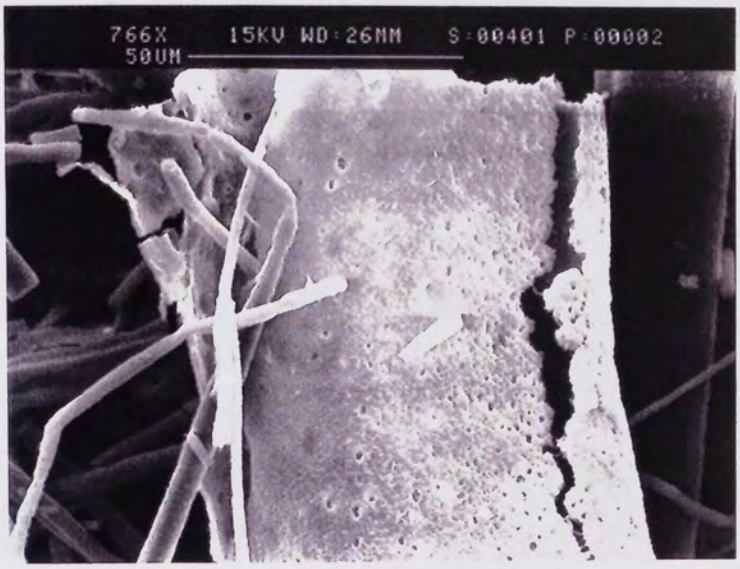

Plate 5.46. (x766) 1 Hour Degradation.
L.Pec.25.E.; Large Diameter Fibre Readily Illustrating The Hollow Nature And Structural Weakness.

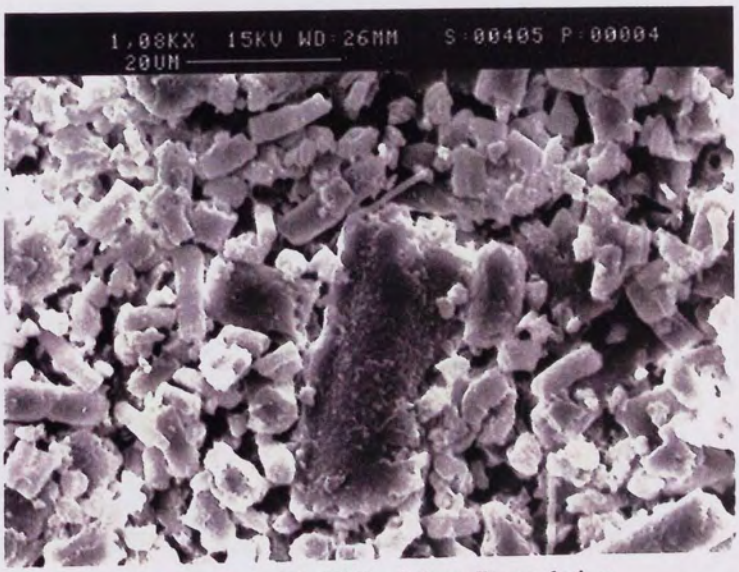

Plate 5.47. (x1.08K) 4 Days Degradation.
L.Pec.25.E.; Matrix Readily Fragmented To Small Fibre Fragments And Particulate Matter After 4 Days Degradation.

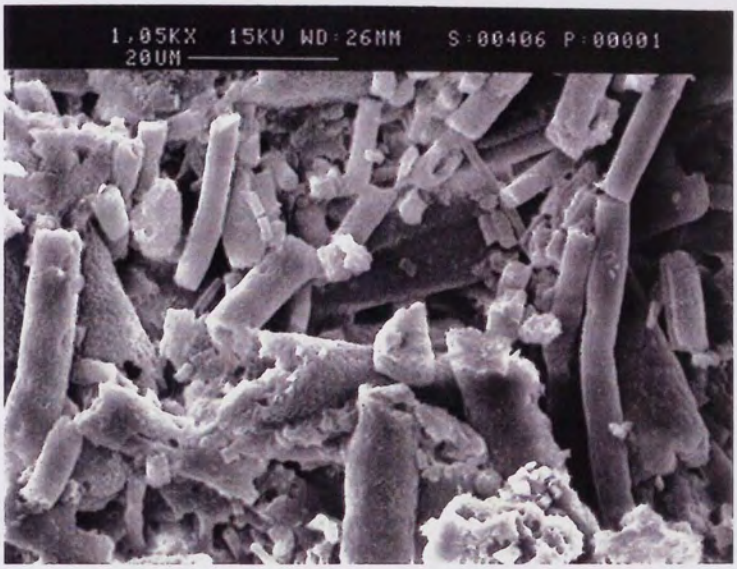

Plate 5.48. (x1.05K) 7 Days Degradation.
L.Pec.25.E.; Degree Of Fragmentation At Day 7 Was Similar To That At Day 4.

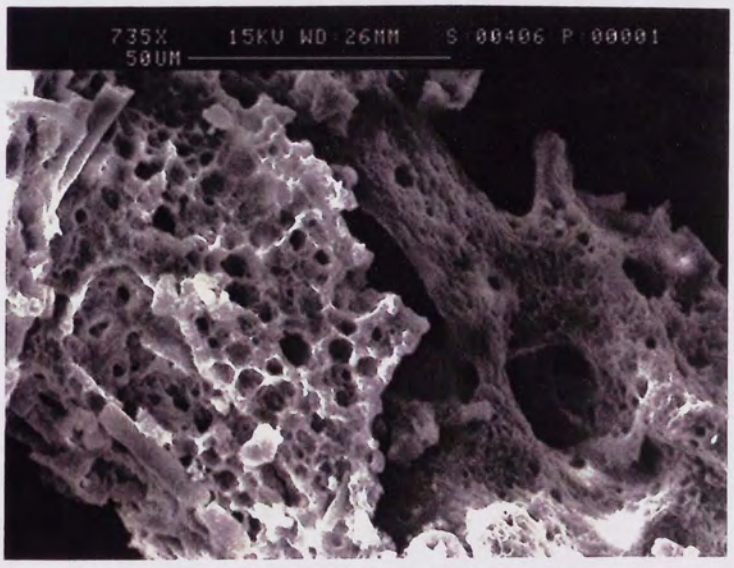

Plate 5.49. (x735) 7 Days Degradation.
L.Pec.25.E.; Large Diameter Fibre Fragment With Readily Noticeable Pectin Cavities And Eroded Regions.

5.46). In contrast to its counterpart; L.Pec.25.S., L.Pec.25.E. exhibited a greater degree of fragmentation for all the fibre diameters, so that a mat of small fibre fragments and particulate matter was observed, (Plate 5.47).. The honeycombed appearence of sample L.Pec.15. at day 7 was also observed for the larger fibre fragments of L.Pec.25.E. together with the porous nature and surface irregularities of the smaller and medium sized fibre fragments, (Plates 5.48-5.50).

Plates 5.51 to 5.54 show the gradual increase in fragmentation for fibres from sample H.Pec.10. The matrix integrity until 23 hours degradation was comparable to that observed for the unblended homopolymer matrix and the fragmentation was considerably less than that observed by the lower molecular weight pectin co-blend. Plate 5.55 illustrates the degradation of a large bulbous region from a H.Pec.10. fibre after 7 hours degradation, as can be observed; the region was a hollow cavity with comparatively thin walls which were a structurally weak point facilitating the fibre collapse and degradation by increasing the available surface area to volume ratio. The fragmentation at day 4 was similar to that of L.Pec.25.S. at day 7, (Plates 5.56 & 5.57), but with the fragmentation of the larger diameter H.Pec.10. fibres being substantially greater.

Thus, the observations of the partially degraded co-blended matrices were consistent with previous conclusions about their degradation. Further information about the matrix degradation and fibre fragmentation was determined by the changes in the fibre diameter distributions.

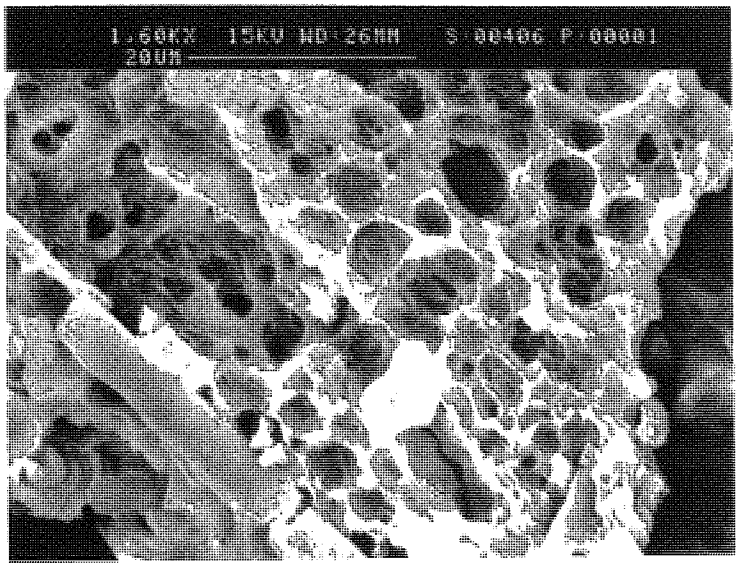

Plate 5.50. (x1.60ZK) 7 Days Degradation.
L.Pec.25.E.; Eroded Large Fibre Fragment.

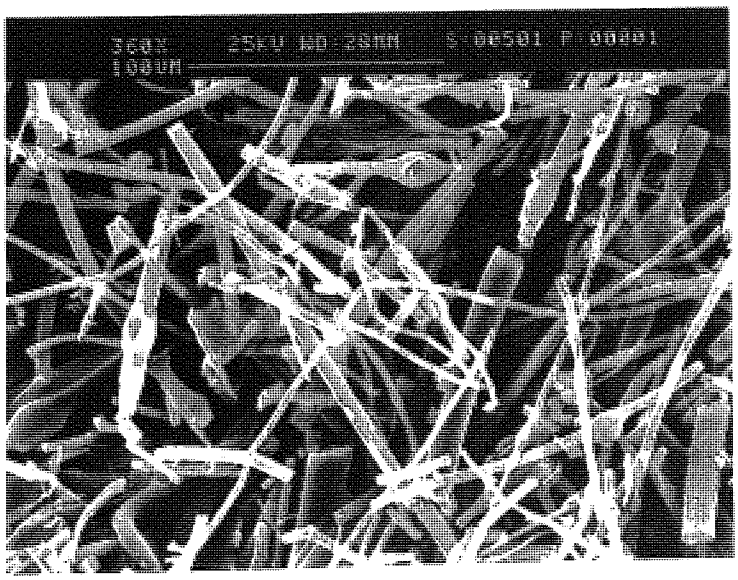

Plate 5.51. (x360) 1 Hour Degradation.
H.Pec.10.; 'Fine' Fibres Of H.Pec.10. Matrix After 1 Hours Degradation.

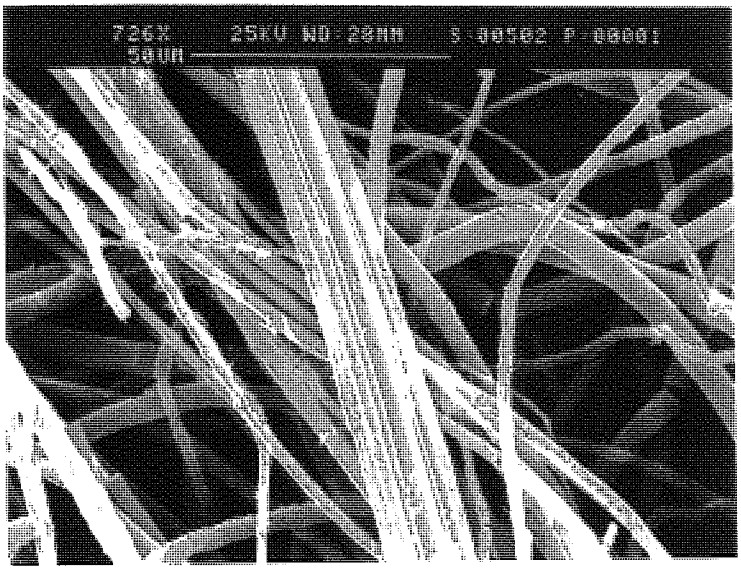

Plate 5.52. (x726) 3 Hours Degradation.
H.Pec.10.; Agglutinated Fibres And Trapped Particulate Matter.

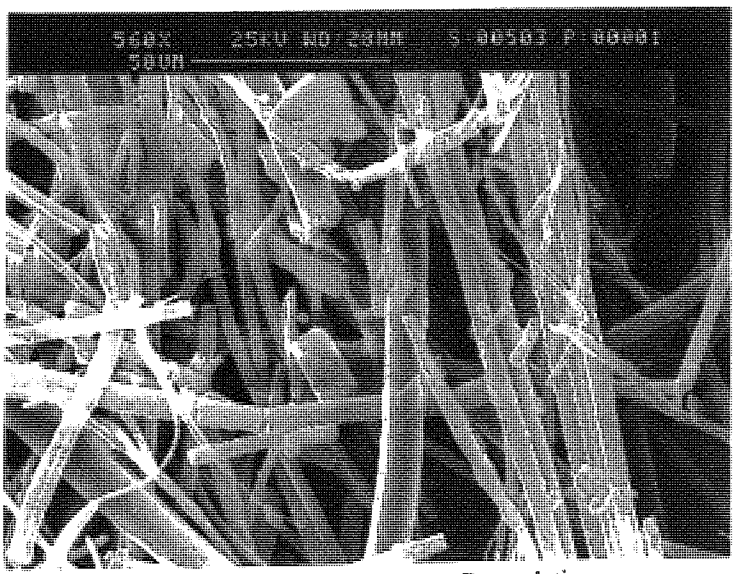

Plate 5.53. (x560) 7 Hours Degradation.
H.Pec.10.; A Small Degree Of Fragmentation, Mainly In The Small Diameter 'Fine' Fibres.

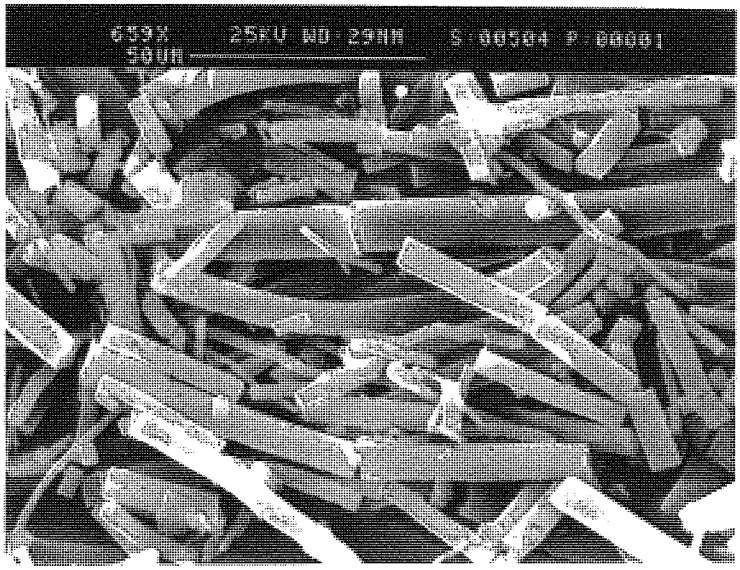

Plate 5.54. (x659) 23 Hours Degradation.
H.Pec.10.; Matrix Fragmentation After 23 Hours Degradation.

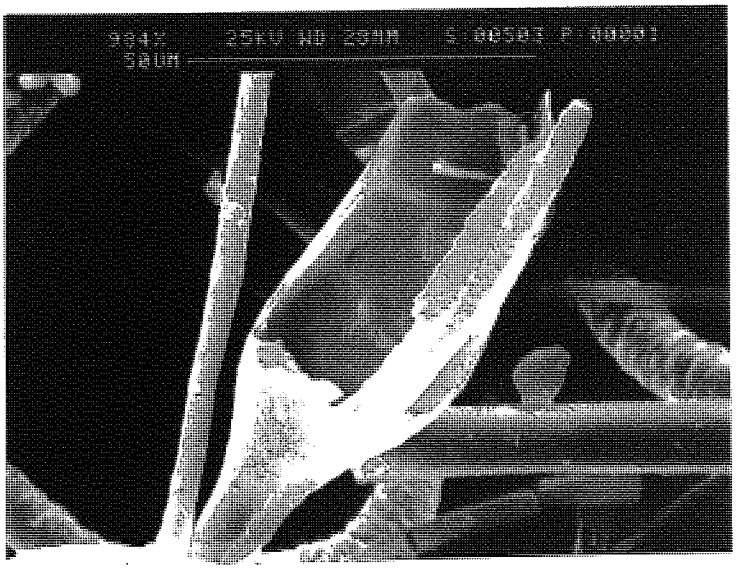

Plate 5.55. (x984) 7 Hours Degradation.
H.Pec.10.; Hollow Nature Of The Bulbous Region Due To An 'Escaped' Bubble, A Structurally Weak Point.

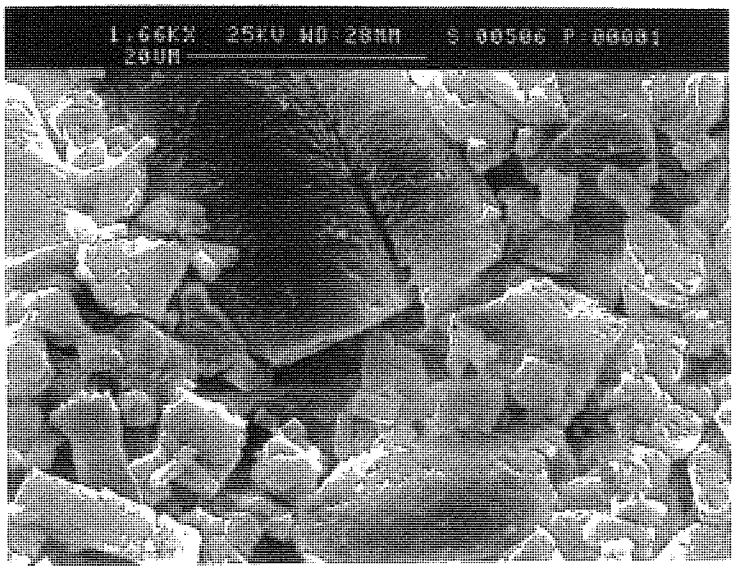

Plate 5.56. (x1.66K) 4 Days Degradation.
H.Pec.10.; Fibre Fragmentation To Small Fibre Fragments With 'Rough' Surfaces But The Absence Of Pectin Cavities.

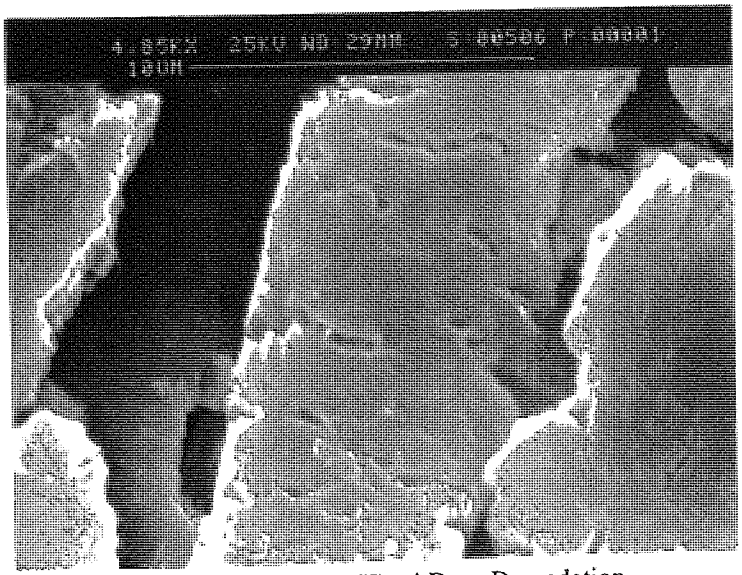

Plate 5.57. (x4.85K) 4 Days Degradation.
H.Pec.10.; Fracturing And Eroded Fibre Fragment.

Graphs 5.27 to 5.32 show the fibre diameter distributions for sample L.Pec.9. during degradation. The frequencies of the fibres at the 0-1 and 1-2um. range was drastically reduced from 12 and 16% in the undegraded sample to 0% after 1 hours degradation. Similarly, the 2-3 micron range was reduced from 20 to 14%. However, the 3-4, 4-5 and 5-6um. ranges increased from 10, 12 and 8% to approximately 18, 12 and 12% respectively. There was also a large frequency increase from 2 to 12% for the medium sized 8-9um. diameter range. The medium sized fibres in the undegraded sample had a range from 6 to 9 microns and 10-11um. In The partially degraded sample this increased from 6 to 13 microns with little change in the frequencies. As a result of these changes, the distribution appeared to shift from the small diameter peak at 0 to 3 microns to two peaks at the larger size ranges of 2 to 6 and 6 to 13 microns. This was due to the fragmentation of the smaller fibres to particulate matter and of the medium sized fibres to the still countable fibre fragments.

After 3 and 7 hours degradation the fibre diameter distributions shifted to the lower diameter ranges with the main peaks being at 2-3 and 3-4um. where frequencies of approximately 22 and 20% after 3 hours degradation and 20% each after 7 hours were observed (Graphs 5.28 & 5.29). These peaks were greatly reduced to 4 and 8% after a days degradation, whilst an increase in the 5-6um. range from 14% after 7 hours degradation to 24% was observed. Fibres were counted at all the diameters except for the 0-1, 11-12 and 13-14um. ranges. After 3 days degradation the L.Pec.9. fibre diameter distribution then shifted to the smaller diameter ranges once again with peaks of 26 and 24% at the 3-4 and 4-5um. diameters. After 5 days the main peaks were observed at 2-3 and 4-5um. with frequencies of approximately 22% each.

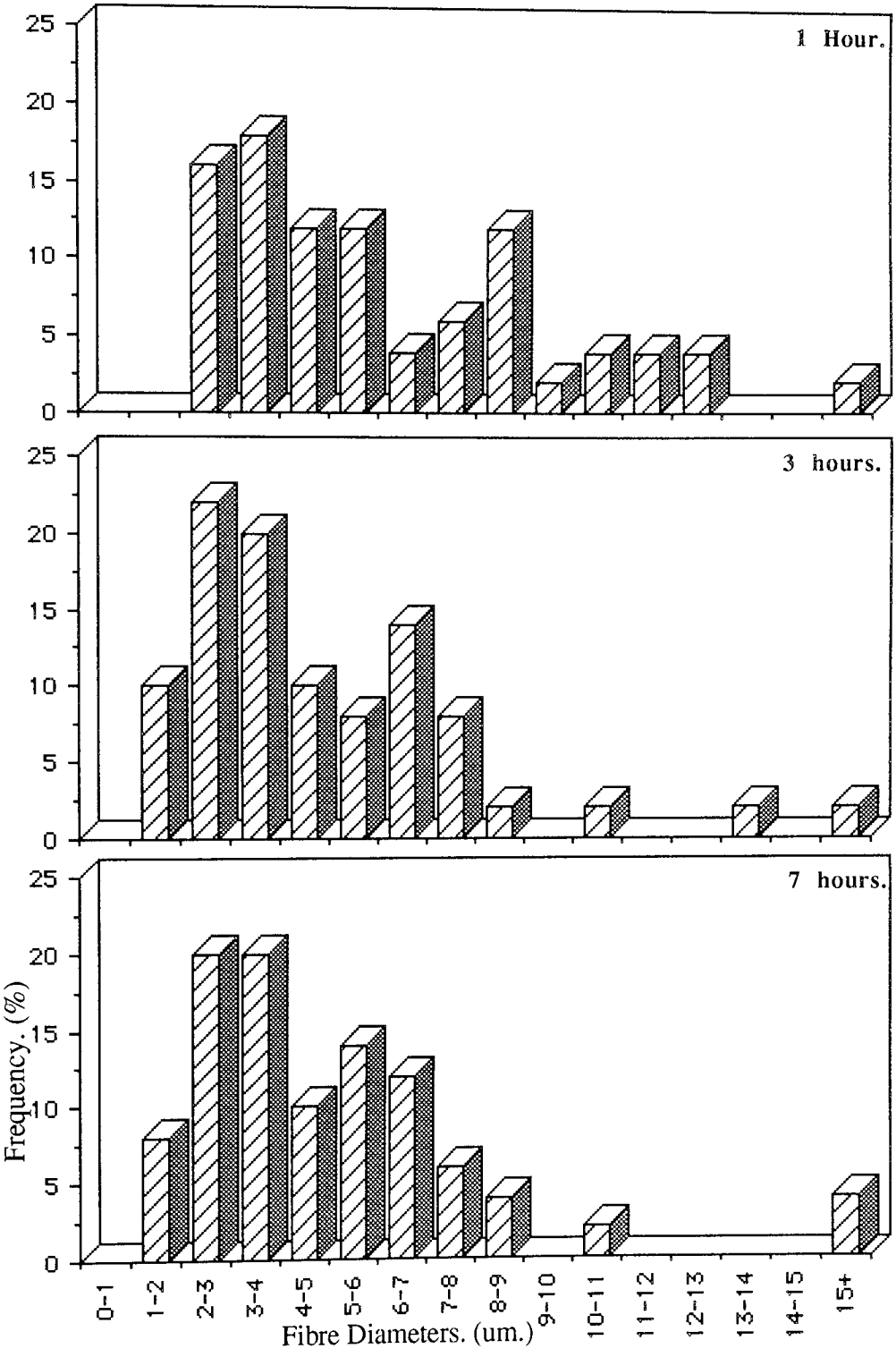

Graphs 5.27 To 5.29.

Fibre Diameter Distributions For Sample L.Pec.9, During Degradation In The Accelerated Degradation Model.

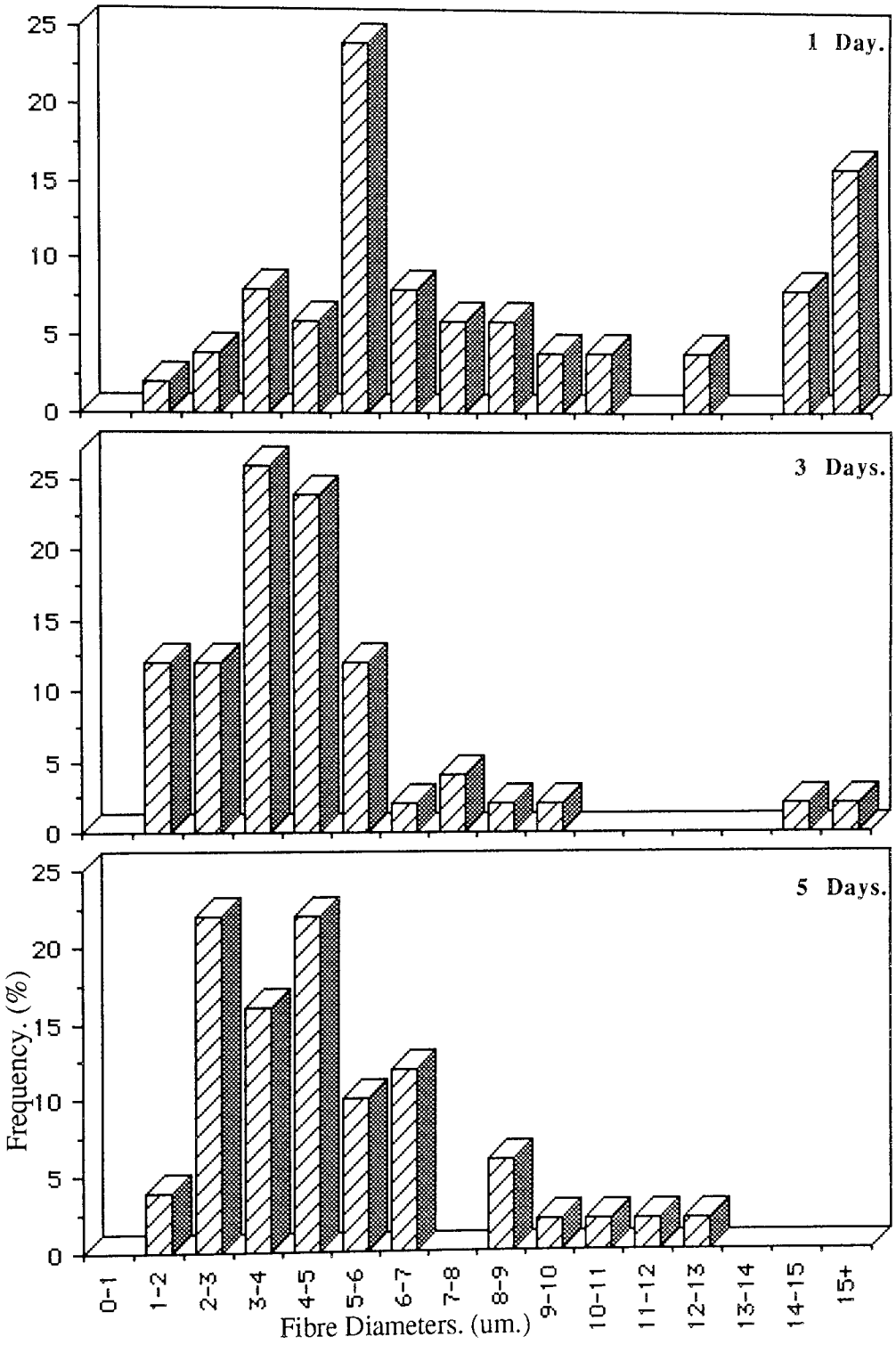

Graphs 5.30 To 5.32.

Fibre Diameter Distributions For Sample L.Pec.9. During Degradation In The Accelerated Degradation Model.

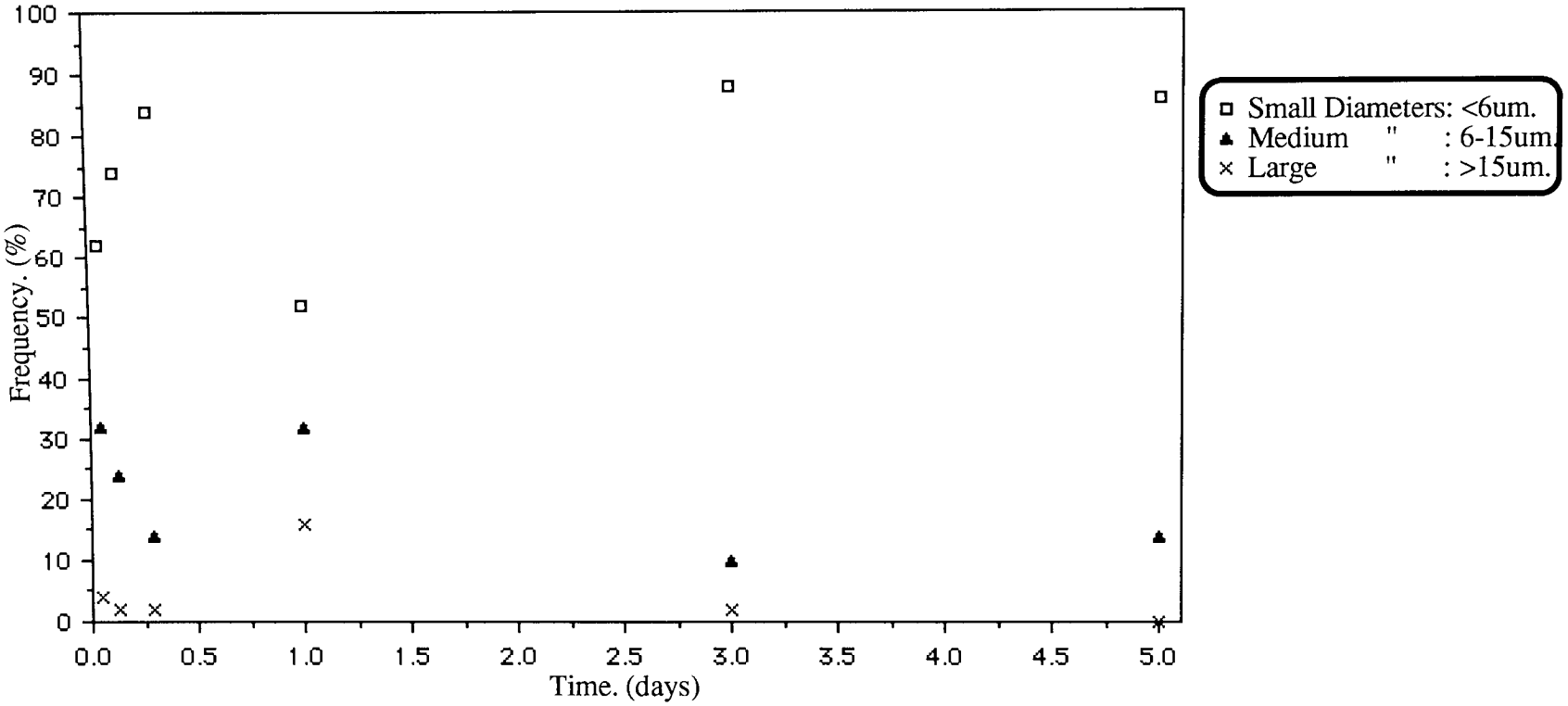

Graph 5.33.

General Fibre Diameter Distributions For Sample L.Pec.9. During Degradation In The Accelerated Degradation Model.

Graph 5.33 illustrates the changes in the L.Pec.9. fibre diameter groups; small, medium and large, during degradation. As can be observed, the small diameter fibre frequency increased from around 61% at 1 hour to approximately 84% after 7 hours and then increased slightly to 87% at days 3 and 5. There was a sharp decrease to approximately 53% at day 1 but this was due to the collapse and fragmentation of the medium and large sized fibres.

Thus, it was concluded that the majority of fibres with a diameter of less than 6 microns readily fragmented within the first few hours and then maintained a similar frequency until day 5, whilst a proportion of the medium and large sized fibres maintained their integrity until day 1 before fragmenting. However, after day 1 the degradation to particulate matter of the medium and large fibres readily occurred, such that by day 5, no large diameter fibres were observed and only a small proportion of the medium sized fibres remained.

The L.Pec.9. distribution was similar to that determined for the PHB(FM)IP, (Graph 4.27). However, the degree of fragmentation for the small diameter fibres appeared to be greater for the L.Pec.9. sample, whilst the PHB(FM)IP medium sized fibres fragmented at a comparatively earlier time of 7 hours. The large diameter fibres remained stable throughout. These comparisons confirmed that the pectin was mainly distributed in the large diameter fibres and a proportion of the medium sized ones.

The fibre diameter distributions for sample L.Pec.15. are illustrated in graphs 5.34 to 5.38. The distributions were generally the same until 7 hours degradation, with the majority of the fibres observed to possess diameters between 1 and 10 microns. This large

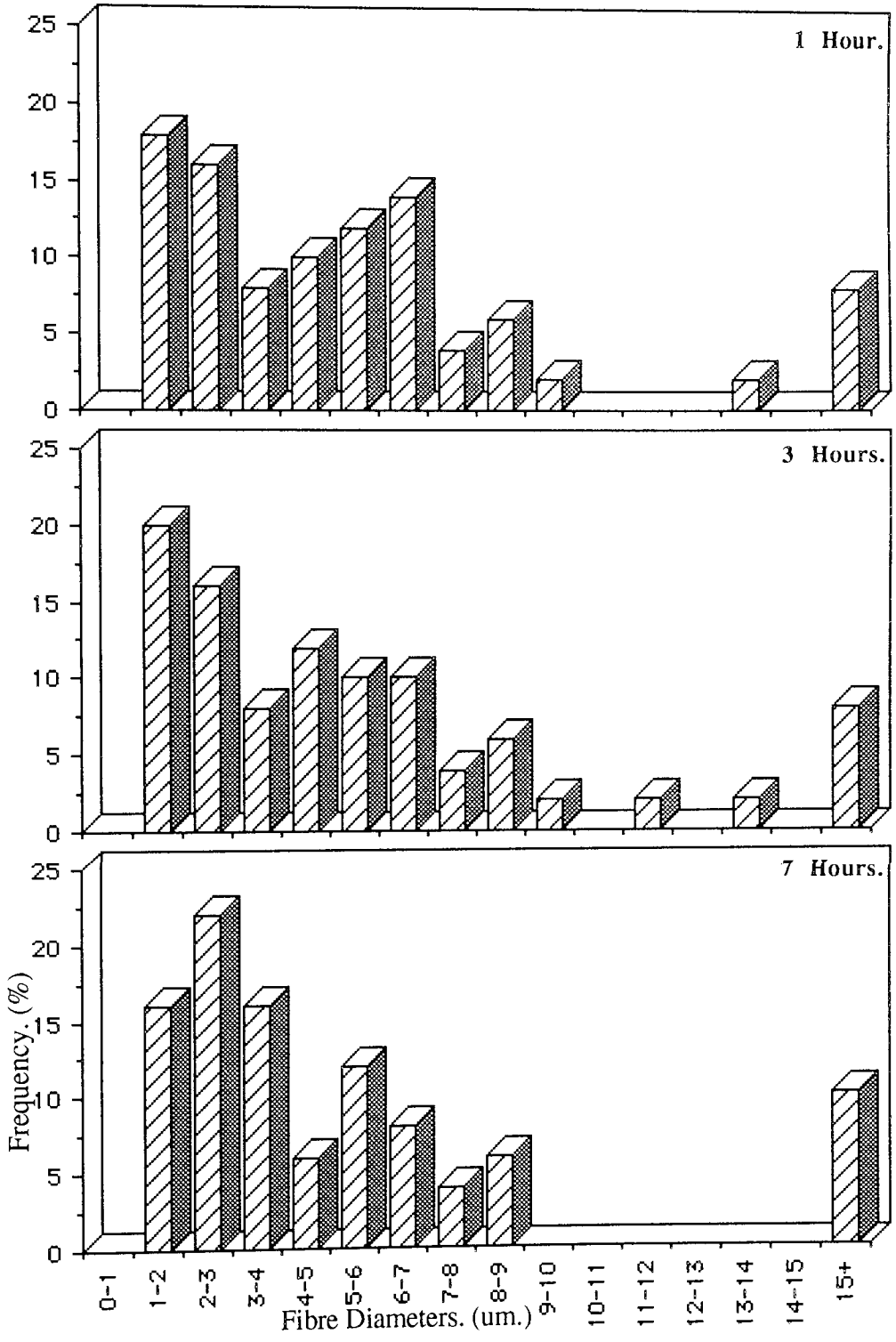

Graphs 5.34 To 5.36.

Fibre Diameter Distributions For Sample L.Pec.15, During Degradation In The Accelerated Degradation Model.

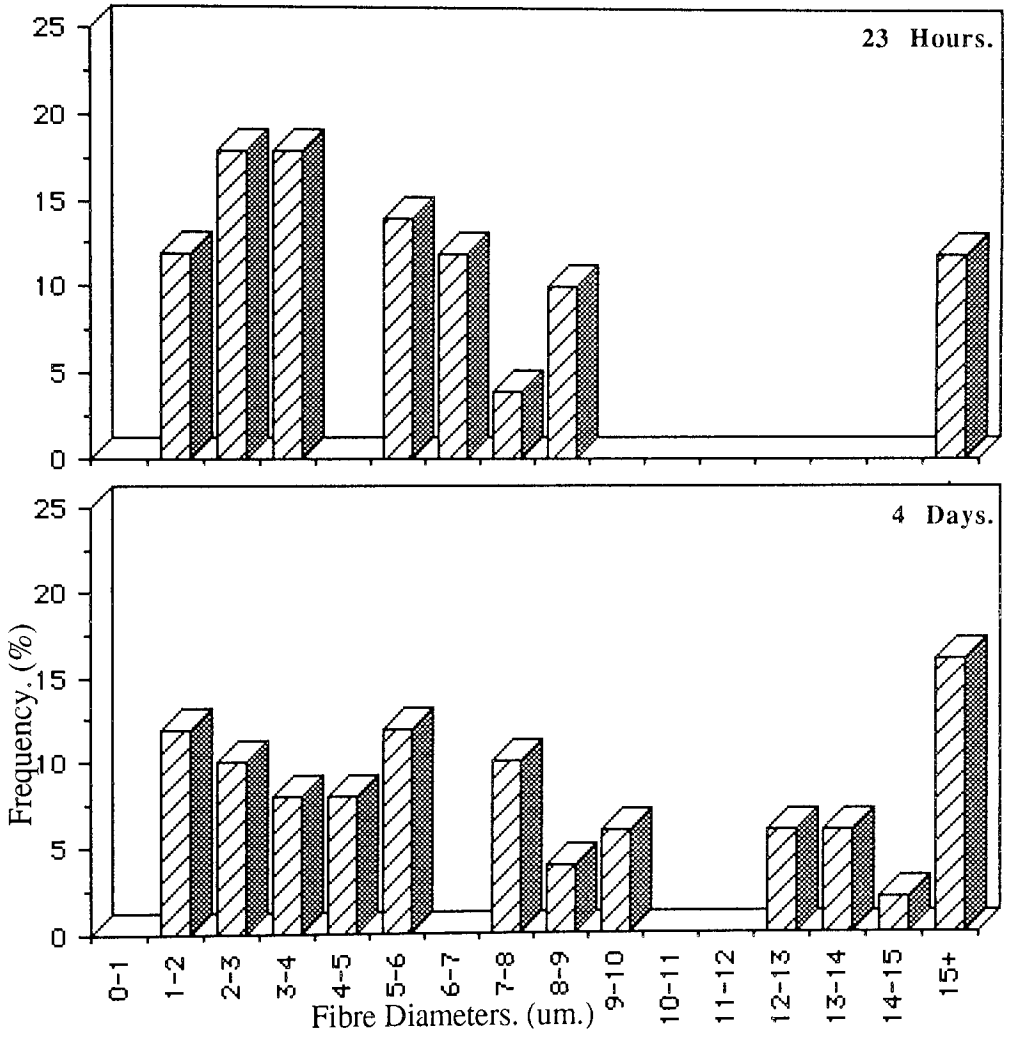

Graphs 5.37 & 5.38.

Fibre Diameter Distributions For Sample L.Pec.15. During Degradation In The Accelerated Degradation Model.

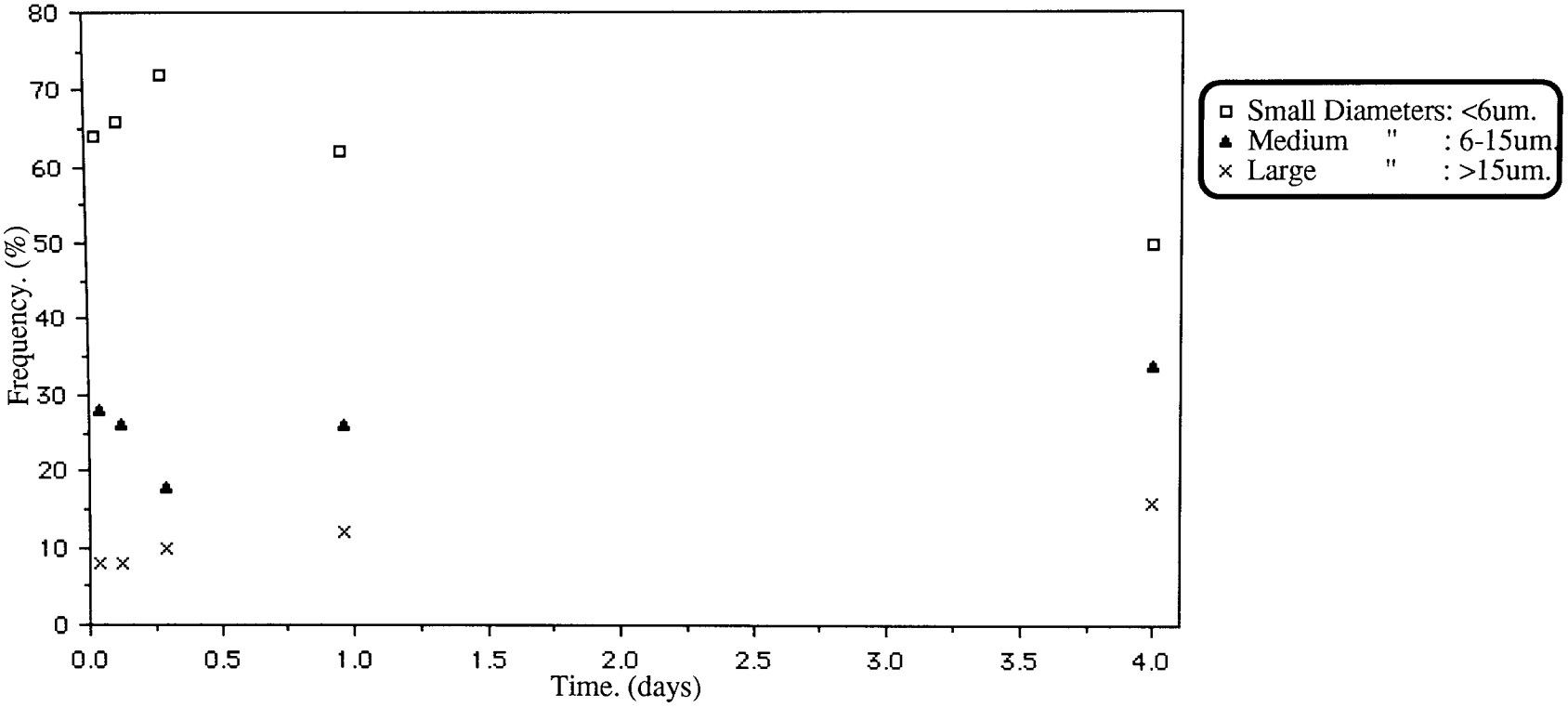

Graph 5.39.

General Fibre Diameter Distributions For Sample L.Pec.15. During Degradation In The Accelerated Degradation Model.

distribution range gradually seperated into two regions of 1 to 4 and 5 to 9 microns at 23 hours, and then to 3 regions with reduced frequencies at day 4; 1 to 6, 7 to 10 and 12 to 15um. The number of fibres possessing a diameter greater than 15um. gradually increased during degradation from 6% in the undegraded sample to approximately 12% at 23 hours and 16% at day 4.

The general distribution of the small, medium and large diameter groups for L.Pec.15. was initially similar to that of sample L.Pec.9. with an increase in the small diameter frequency until 7 hours and a medium and large diameter frequency increase at day 1. However, in contrast to the L.Pec.9. general distribution, the number of fibres possessing diameters in the range of 6 to 15 and >15um., medium and large groups respectively, increased slightly after day 1 from around 26 and 12% to approximately 32 and 16% respectively, whilst the number of small diameter fibres observed gradually decreased after 7 hours degradation from around 63 to 52% at day 4.

These results indicated that the fragmentation of the L.Pec.15. fibres were similar in the initial stages as that determined for the L.Pec.9. sample, this was consistent with the degradation profiles for the two samples which exhibited a similar degradation at stages I and II.

The fibre diameter distributions for the partially degraded L.Pec.25.S. samples were generally similar to those observed for the L.Pec.9. samples but with some noticeable differences, (Graphs 5.40-5.45). There was a main peak of approximately 24% at the 2-3um. range after 1 hours degradation, this decreased after 5 hours to 20% and then to

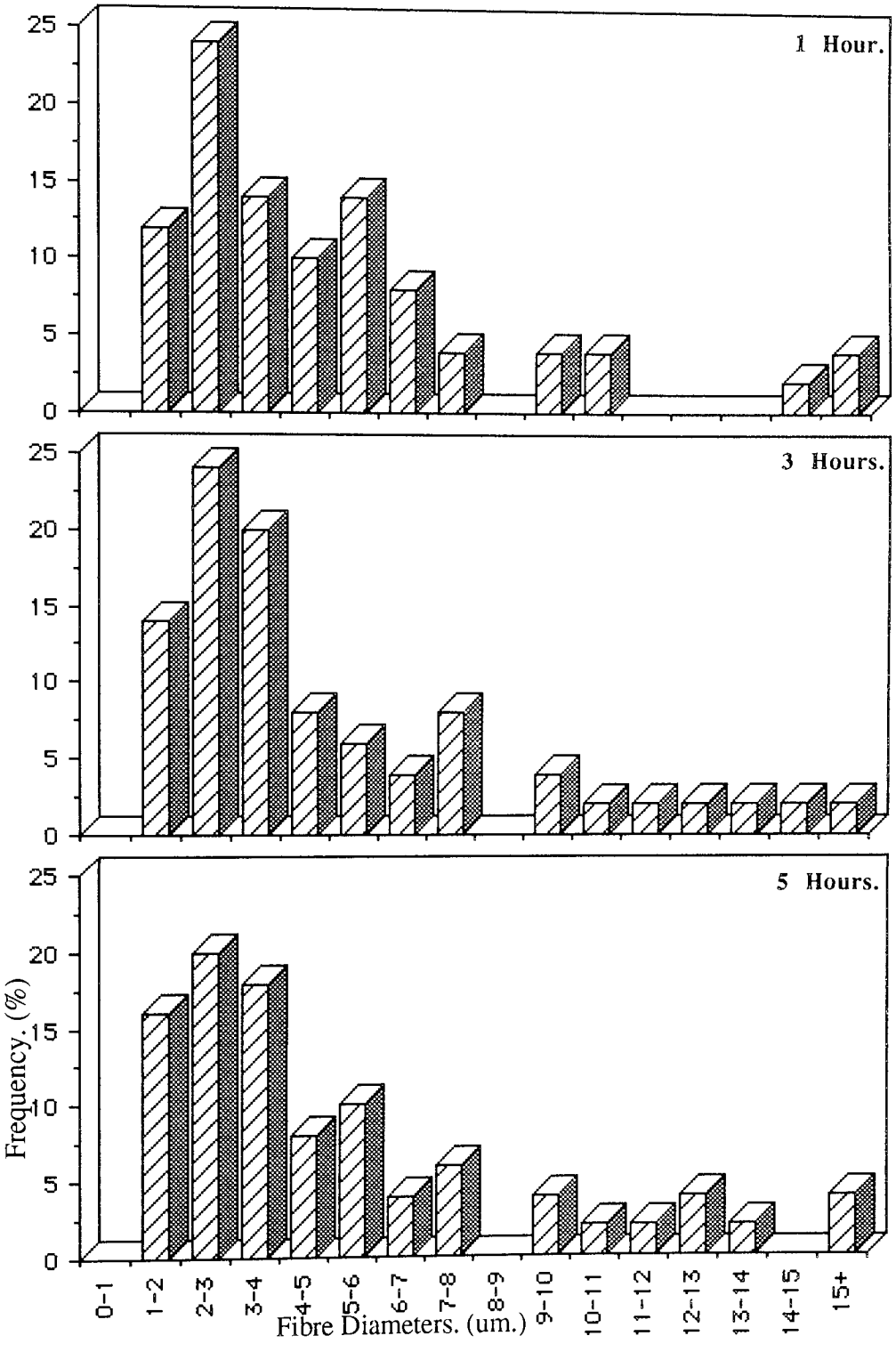

Graphs 5.40. To 5.42.

Fibre Diameter Distributions For Sample L.Pec.25.S. During Degradation In The Accelerated Degradation Model.

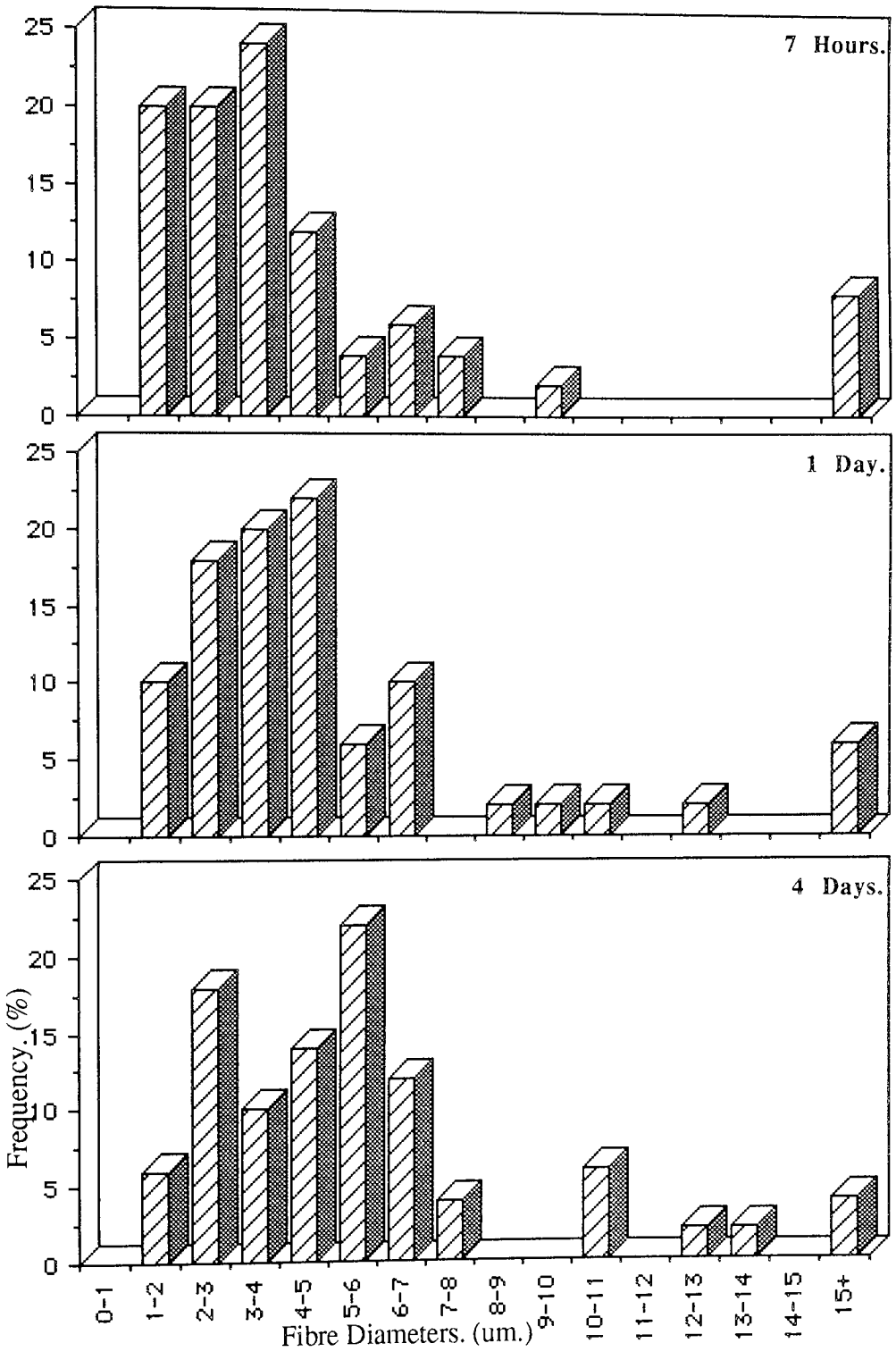

Graphs 5.43. To 5.45.

Fibre Diameter Distributions For L.Pec.25.S. During Degradation In The Accelerated Degradation Model.

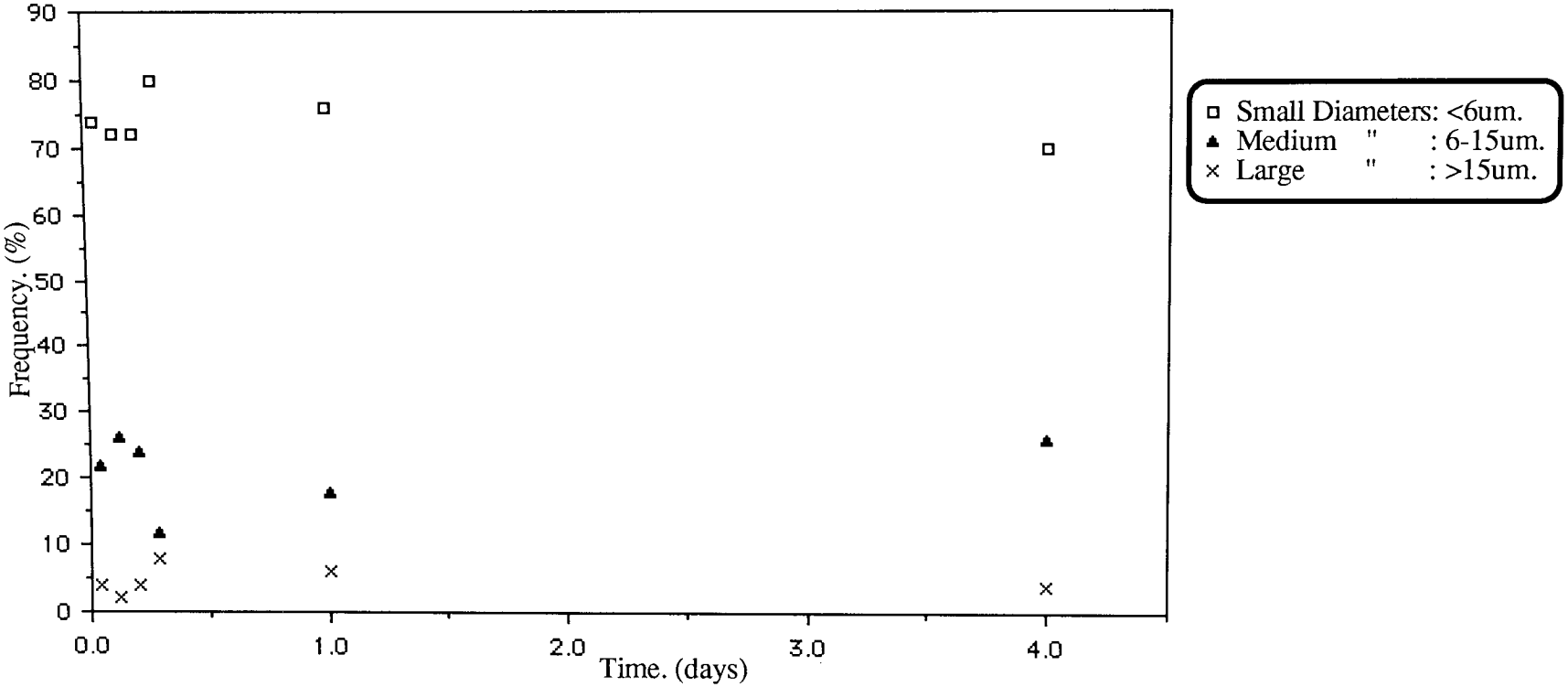

Graph 5.46.

General Fibre Diameter Distribution For Sample L.Pec.25.S. During Degradation In The Accelerated Degradation Model.

18% at day 1, where it remained constant until day 4. The 1-2 and 3-4um. ranges gradually increased until 5 hours, and at 7 hours shifted to a 3-4um. peak of 24%, then to a 4-5um. peak of approximately 22% at day 1, before seperating into two main peaks at 2-3 and 5-6um. with frequencies of around 18 and 22% respectively.

Thus, the fibre diameter distributions gradually changed from a peak at the 2-3um. range after 1 hours degradation to a peak at the 5-6um. range, whilst the 2-3um. diameter fibres remained relatively stable and maintained a similar frequency after 5 hours degradation. Similarly, the L.Pec.9. distribution shifted to the higher diameter ranges with degradation until around day 1, but after this it returned to the smaller diameter ranges. These shifts were also more noticeable than those observed for the L.Pec.15. distributions, which maintained a range of approximately 1 to 8 microns throughout the degradation, in comparison the L.Pec.9. shifts varied from 2 to 13um. at 1 hour degradation to 1 to 9um. at 3 and 7 hours, 1 to 10/11um. at days 1 and 3 and finally to 1 to 7um. after 5 days degradation.

The distribution of the L.Pec.25.S. fibre diameters as small, medium and large groups are illustrated in graph 5.46. The number of fibres with small diameters increased from around 74% after 5 hours degradation to a peak of 80% at 7 hours. This was similar to the large diameter fibre frequency which also increased from 4% to approximately 8% at 7 hours. In both cases the frequencies then gradually decreased until day 4 with values of approximately 71 and 3% for the small and large sized fibres respectively. The medium sized fibres decreased after 7 hours degradation from around 25% to 11%, before gradually returning to approximately 25% frequency at day 4. These results indicated that

both the small and large diameter fibres fragmented within 7 hours in the accelerated degradation model, whilst the medium sized fibres maintained their integrity longer and gradually fragmented during the course of the degradation experiment. These trends exhibited by the medium and small sized fibres were similar to those displayed by the L.Pec.15. sample. However, the large diameter fibre frequency trend was more similar to that of L.Pec.9. These results were due to sample L.Pec.25.S. possessing an initial pectin loading of approximately 6% but of a somewhat higher molecular weight.

Graphs 5.47 to 5.51 illustrate the fibre diameter distributions for the L.Pec.25.E. sample. The distributions for L.Pec.25.E. were noticeably different from its counterpart L.Pec.25.S. After 1 hours degradation a broad distribution of diameters from 1 to 9 microns was observed, with a slight peak of approximately 18% at the 2-3um. range. This distribution remained similar until 6 hours where no noticeable peaks were observed. After 6 hours degradation fibres were counted at all diameters except the 0-1um. range.

There was a noticeable peak of 15% at the 4-5um. range after 1 days degradation with minor peaks at 1-2 and 8-9um. possessing frequencies of 12 and 10% respectively. After 2 days there was a noticeable increase in the frequencies of fibres possessing diameters between 1 and 6um., as a result of this, the distribution shifted to the lower diameter range. No distributions were determined for days 4 and 7 due to the large degree of fragmentation which made an accurate determination impossible.

The frequency distribution of the fibre diameters <6, 6-15 and >15um. (small, medium and large) for the partially degraded L.Pec.25.E. samples is illustrated in graph 5.52. The

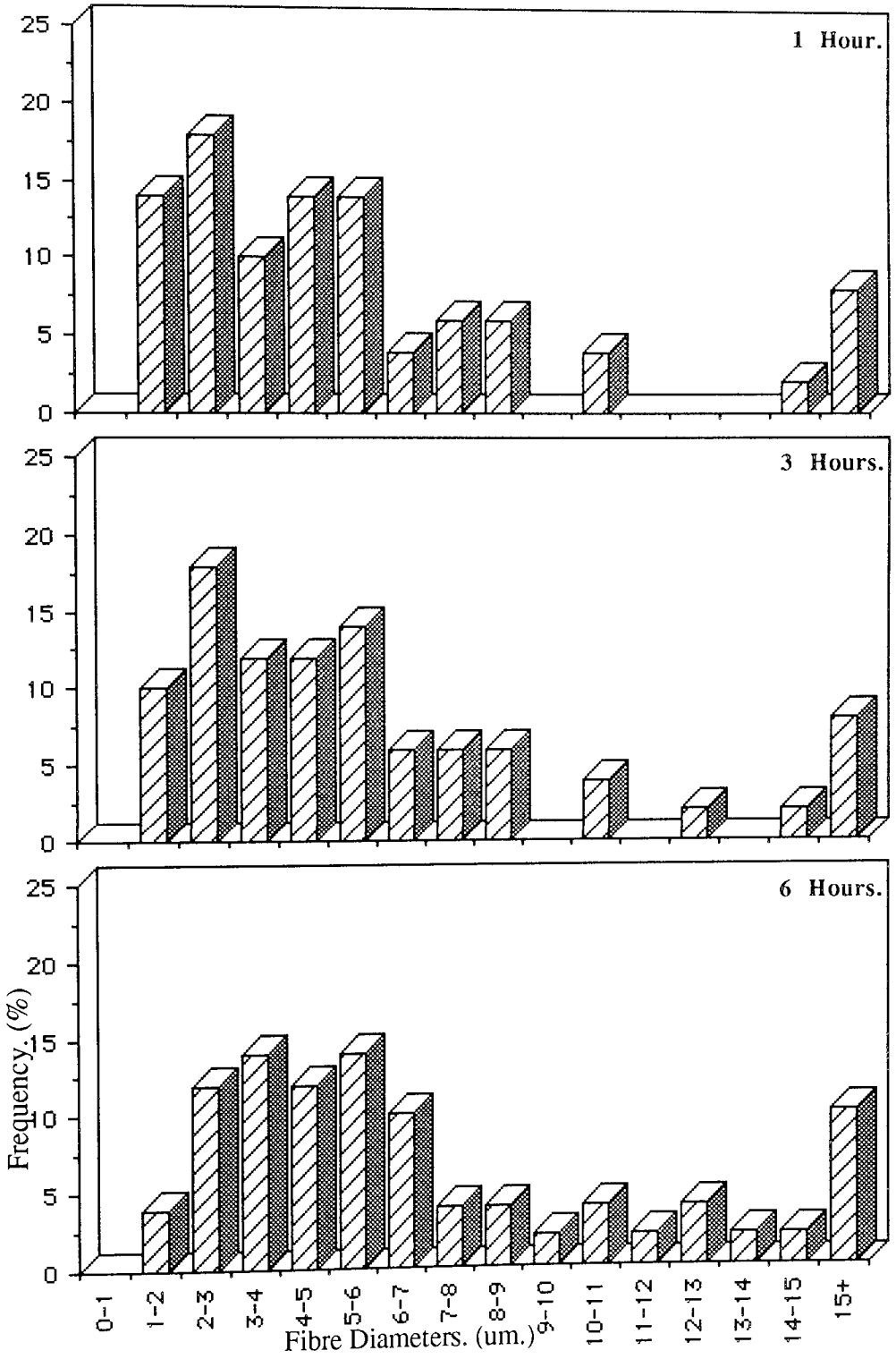

Graphs 5.47. To 5.49.

Fibre Diameter Distributions For L.Pec.25.E. During Degradation In The Accelerated Degradation Model.

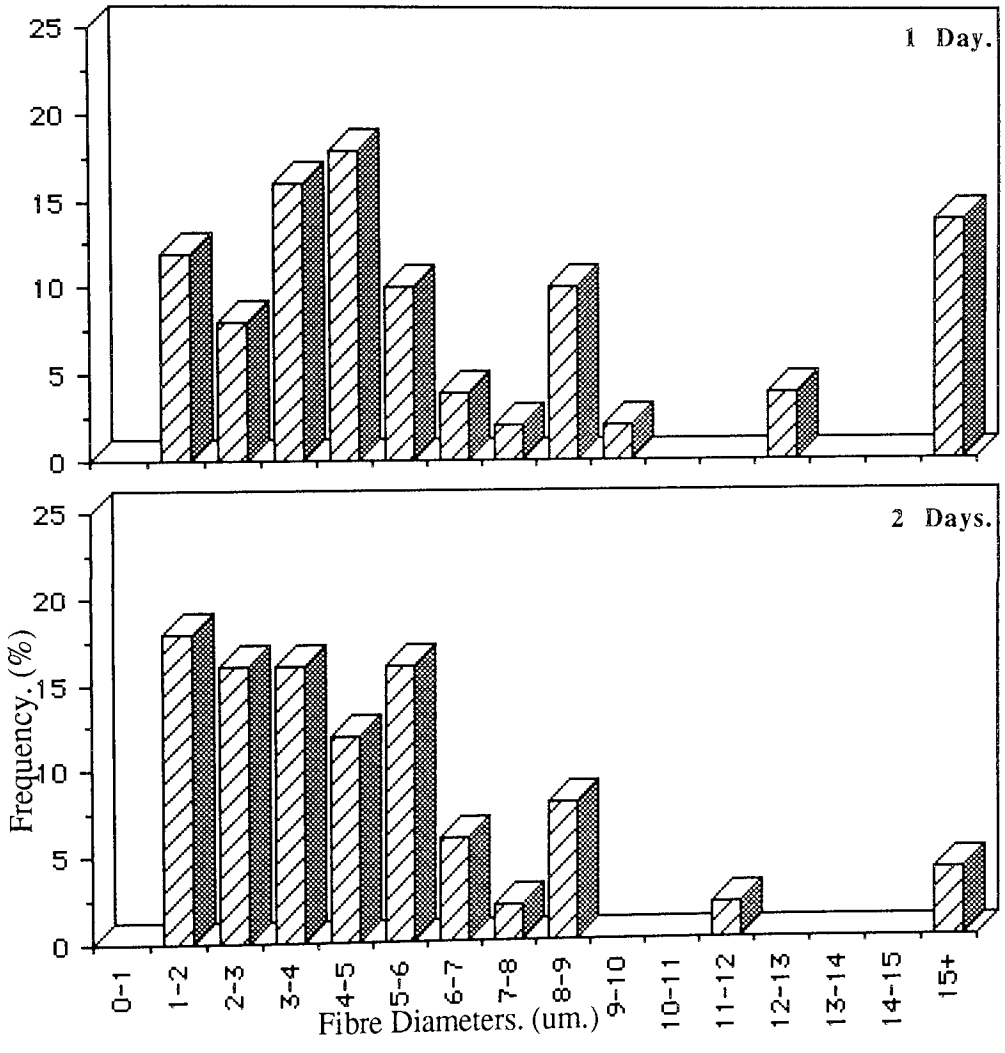

Graphs 5.50. & 5.51.

Fibre Diameter Distributions For L.Pec.25.E. During Degradation In The Accelerated Degradation Model.

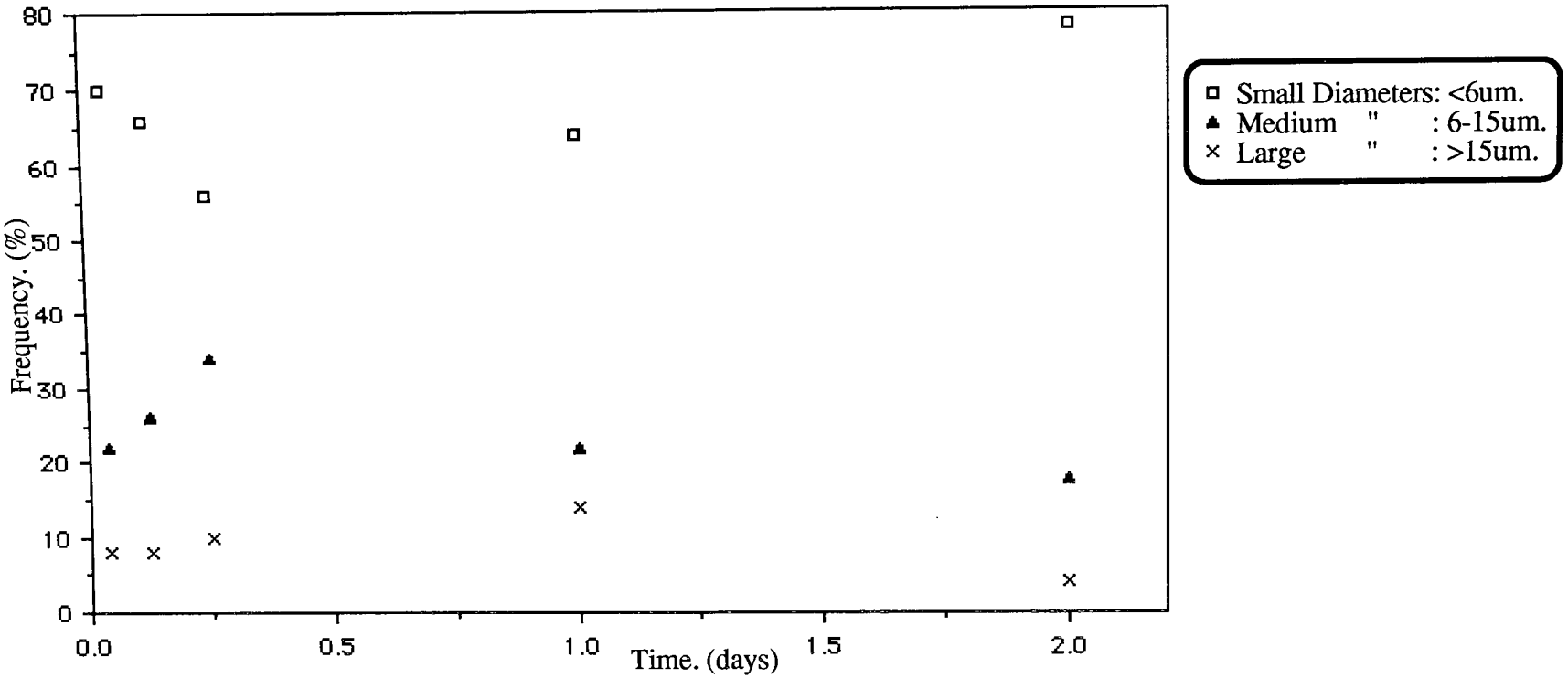

Graph 5.52.

General Fibre Diameter Distribution For Sample L.Pec.25.E. During Degradation In The Accelerated Degradation Model.

small diameter fibre frequency decreased from 70% to approximately 56% at 6 hours degradation, before gradually increasing to about 79% at day 2. This initial decrease was due to a fragmentation of the medium sized fibres, which correspondingly increased from 21% at 1 hour to 34% at 6 hours. This indicated that the small diameters were comparatively more stable until 6 hours degradation, whilst the medium sized fibres readily fragmented. After 6 hours the medium sized fibre frequency gradually decreased to 21 and 18% at days 1 and 2 respectively, this was due to the fragmentation of the small fibres. Similarly, the number of large diameter fibres gradually increased from 8% after 3 hours degradation to a peak of 14% at day 1 before decreasing to 4% at day 2. These results indicate that the comparatively high pectin loading facilitated the pectin blending within both the large, and a substantal proportion of the medium sized fibres, so that both these groups readily collapsed to fibre fragments and particulate matter by day 4. The small diameter fibres however, had a more gradual fragmentation.

The fibre diameter distributions for sample H.Pec.10. were similar to those observed for sample L.Pec.25.S. with the majority of the fibres counted possessing diameters below 6um. ie; the small group range, (Graphs 5.53-5.56). After 1 hours degradation there were fibres counted at all the diameter ranges except at 0-1 and 12 to 14um., the main peak was at 2 to 3 microns with a 30% frequency. This peak shifted slightly during the course of degradation to the 1-2um. range, whilst the total number of fibres possessing diameters below 6um. increased slightly from 70% after 1 hours degradation to 78% after 23 hours, (Graph 5.57).

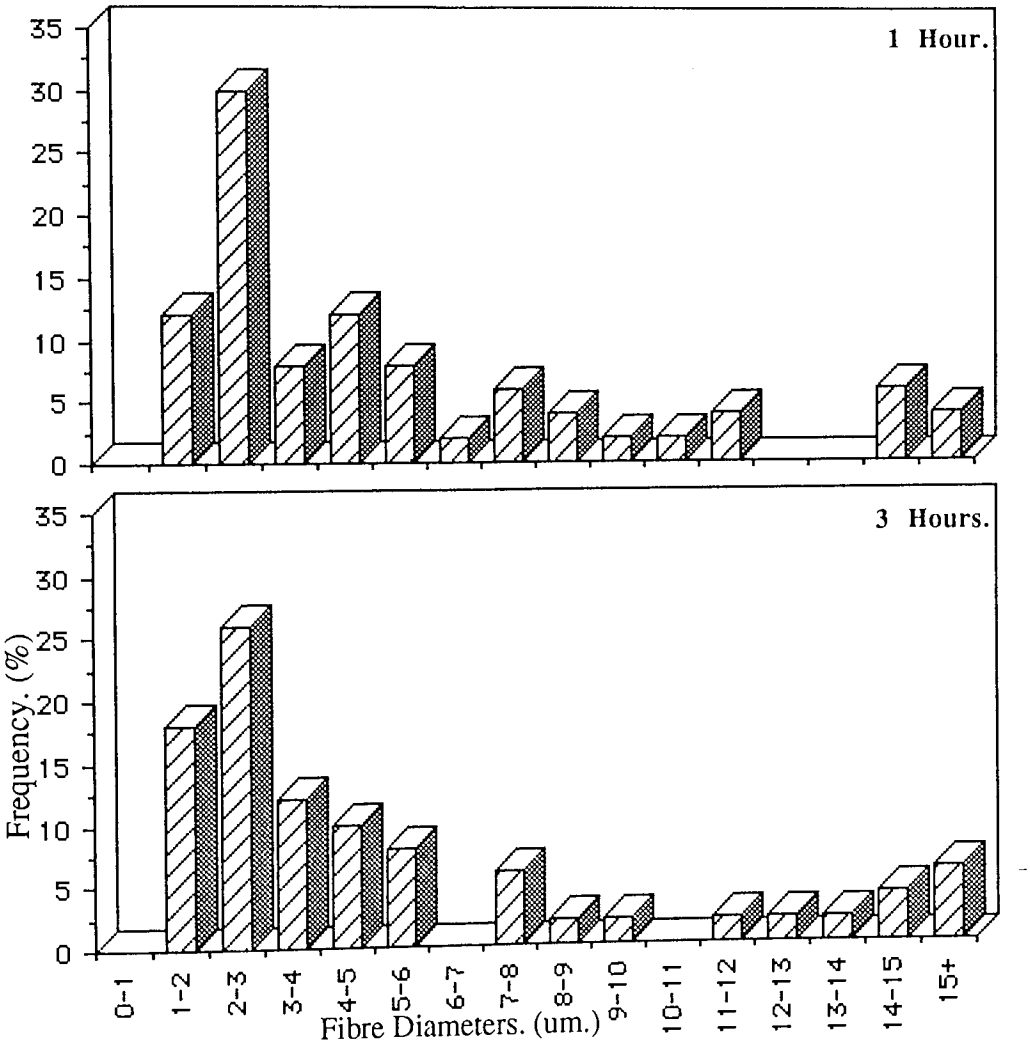

Graphs 5.53. & 5.54.

Fibre Diameter Distributions For Sample H.Pec.10. During Degradation In The Accelerated Degradation Model.

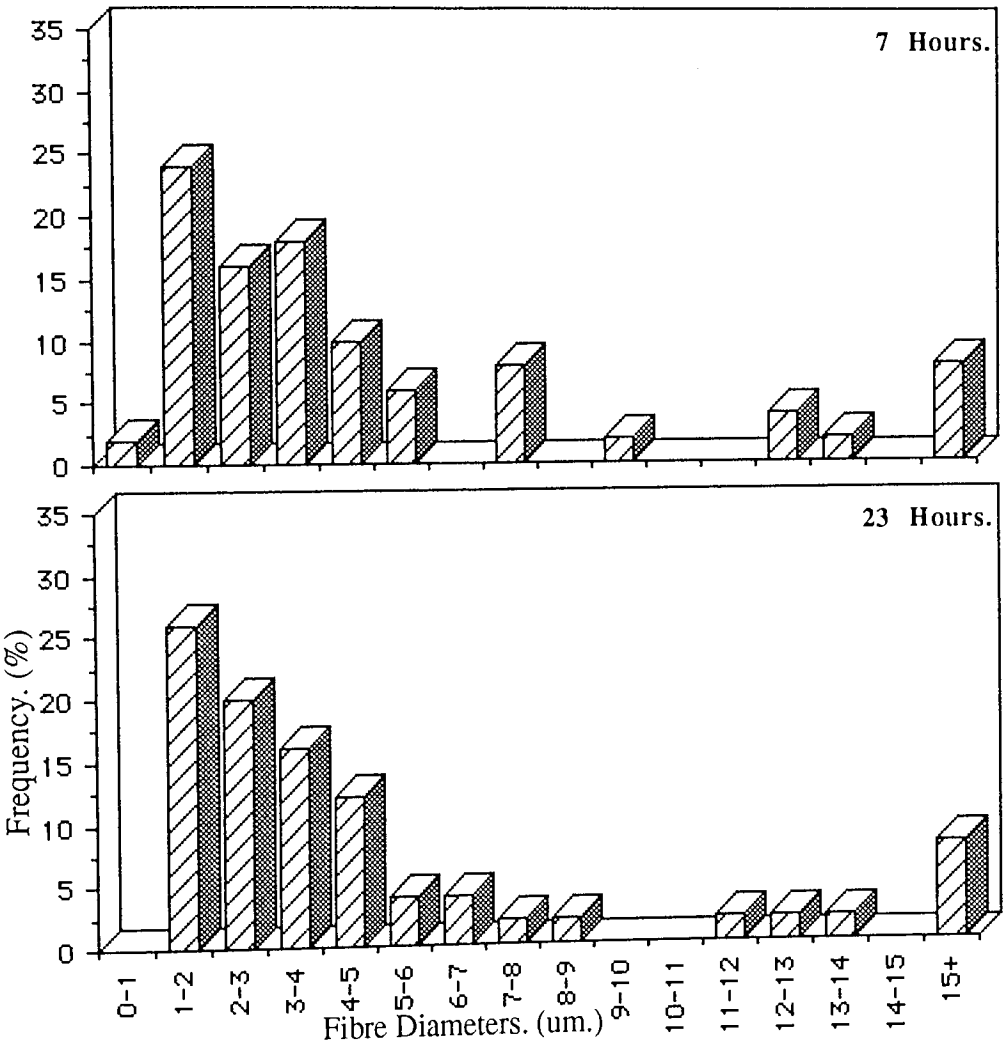

Graphs 5.55. & 5.56.

Fibre Diameter Distributions For Sample H.Pec.10. During Degradation In The Accelerated Degradation Model.

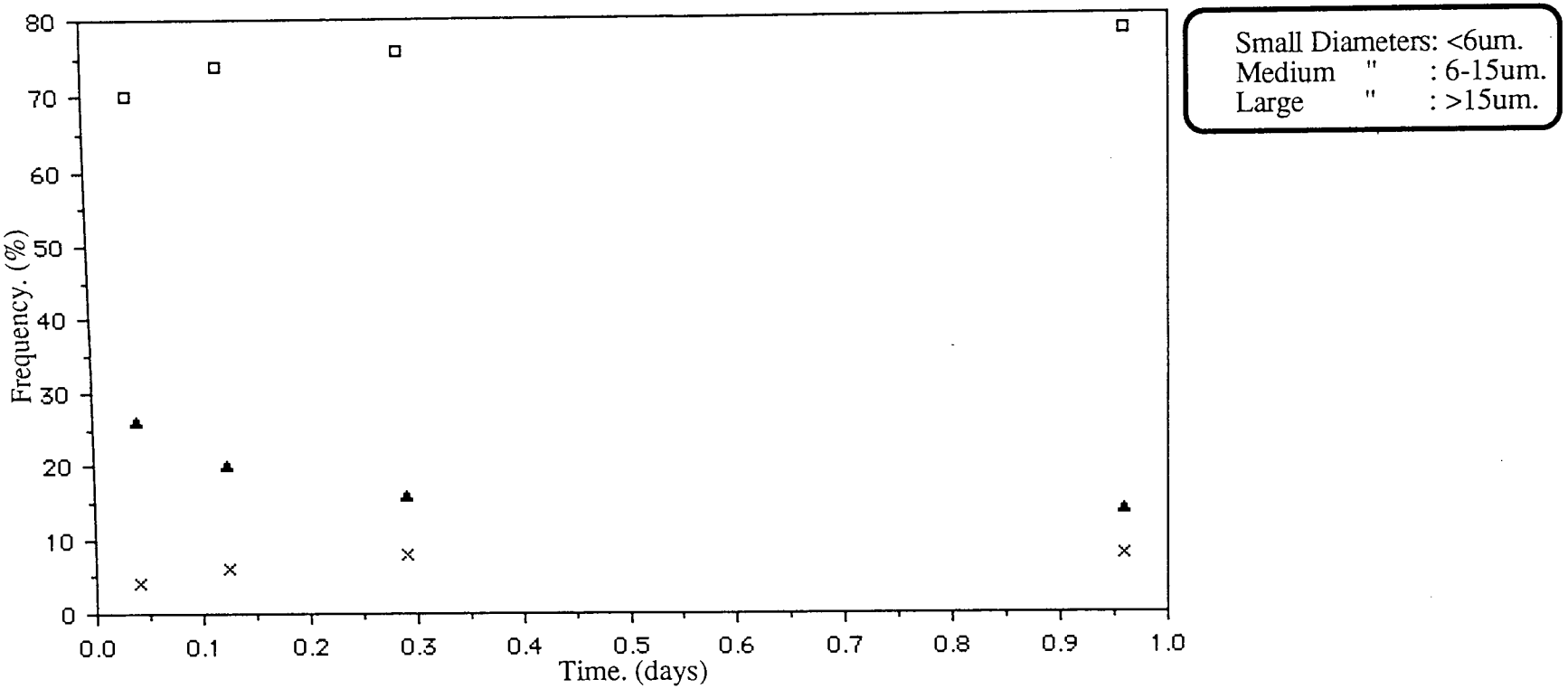

Graph 5.57.

General Fibre Diameter Distribution For Sample H.Pec.10. During Degradation In The Accelerated Degradation Model.

The medium sized fibres; 6-15um., gradually decreased from 26% at 1 hour to 14% at 23 hours, the large diameter fibres; >15um., increased from 4 to 8% by 7 hours degradation and remained at this frequency until 23 hours (Graph 5.57). These results indicated that the small and large diameter fibres gradually fragmented whilst the medium sized ones remained comparatively stable. This was due to the relatively greater homogeneous blending of the high molecular weight pectin with the PHB fibres compared to the low molecular weight samples. This blending affected all the fibres, so that upon the pectin dissolution it facilitated the collapse of the predominantly small diameter fibres whilst the medium sized ones were more resistant to fragmentation. The large diameter fibres also fragmented but to a substantially lesser extent compared to the small sized fibres, this was mainly due to manufacturing sand handling induced structural weaknesses rather than the pectin blending, although this may have contributed to their collapse.

Therefore, the phase contrast and scanning electron microscopy observations revealed substantial increases in the degree of fragmentation and the irregularity of the fibre surfaces for the co-blended samples compared to the unblended homopolymer sample, PHB(FM)IP. The fibre diameter distributions for the samples indicated that the blending between the PHB and the low molecular weight pectin occurred predominantly in the large diameter fibres, increasing the pectin loading facilitated in their fragmentation. Increasing the molecular weight of the pectin increased the homogeneity of the blending, this then facilitated in the small diameter fibre fragmentation, whilst the fragmentation of the large diameter fibres was mainly due to mechanical stresses.

It should be remembered that the filtering, drying and mounting procedures of the partially degraded samples contributed to the degree of fragmentation and therefore, the fibre diameter distributions. As such, these observations are an indication to the comparative structural weaknesses of the matrices and their fibres.

5.2.4 Differential Scanning Calorimetry (DSC) Studies.

5.2.4.0. Introduction.

The partially degraded co-blends from days 0 to 7 were examined utilizing differential scanning calorimetry (DSC) and the melting points, (mp) fusion enthalpies (ΔHm) and glass transition temperatures (Tg) determined. Sample L.Pec.9. was examined from days 0 to 25, day 33 had insufficient sample.

5.2.4.1. Degradation Of L.Pec.9. And Its Comparison With The IP Sample.

Graphs 5.58 to 5.60 illustrate the changes in the melting point, fusion enthalpy and glass transition temperatures of the partially degraded L.Pec.9. samples.

As can be observed from graph 5.58, the melting point decreased slightly within the initial stages of the degradation from approximately 173 to 169°C. by day 1, this was due to the dissolution of the pectin which weakened a proportion of the fibres and reduced the matrix stability. Between days 1 and 4 there was a stability period with little change in the melting point, after day 4 this decreased quite sharply from 169°C. to approximately 159°C., before gradually decreasing to 153°C. at day 25. This melting point profile was similar to that obtained for the IP sample, but the latter did not possess an initial stability period. This indicated the comparatively greater stability of the L.Pec.9. sample.

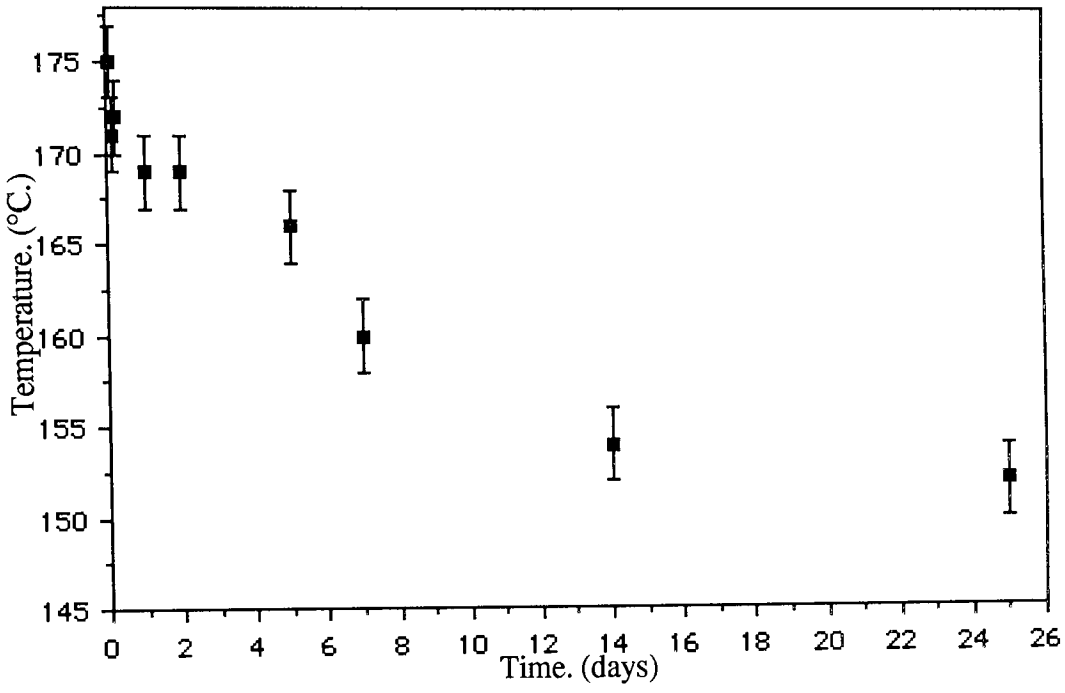

Graph 5.58.

Change In The Melting Point Of Sample L.Pec.9. During Degradation In The Accelerated Degradation Model.

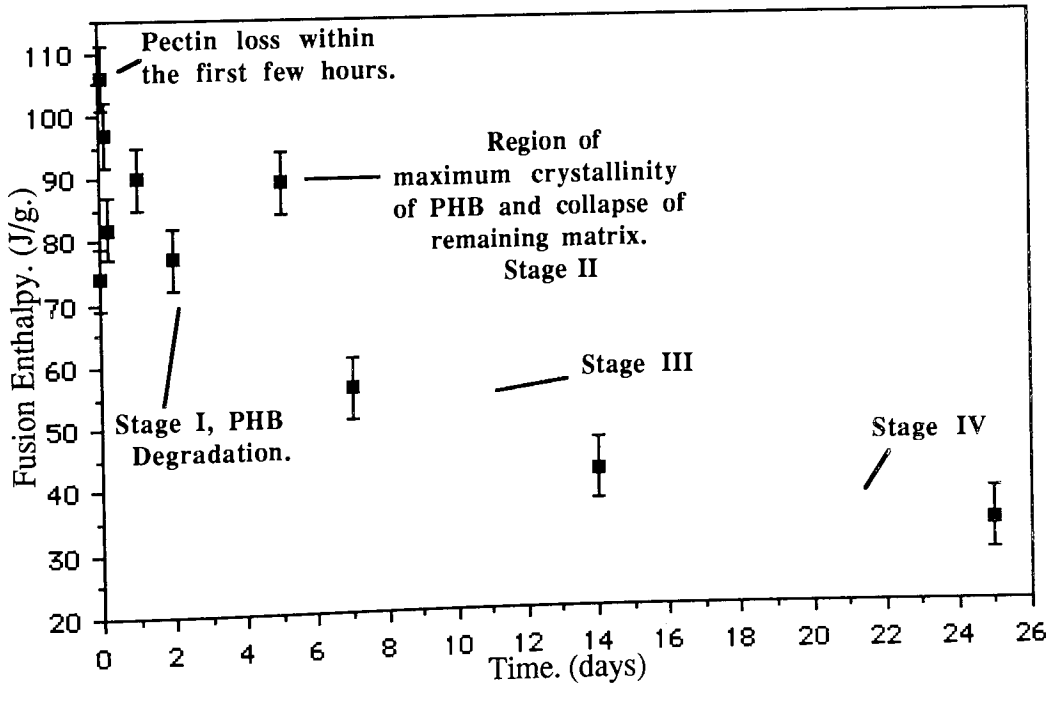

Graph 5.59.

Change In The Fusion Enthalpy Of Sample L.Pec.9. During Degradation In The Accelerated Degradation Model.

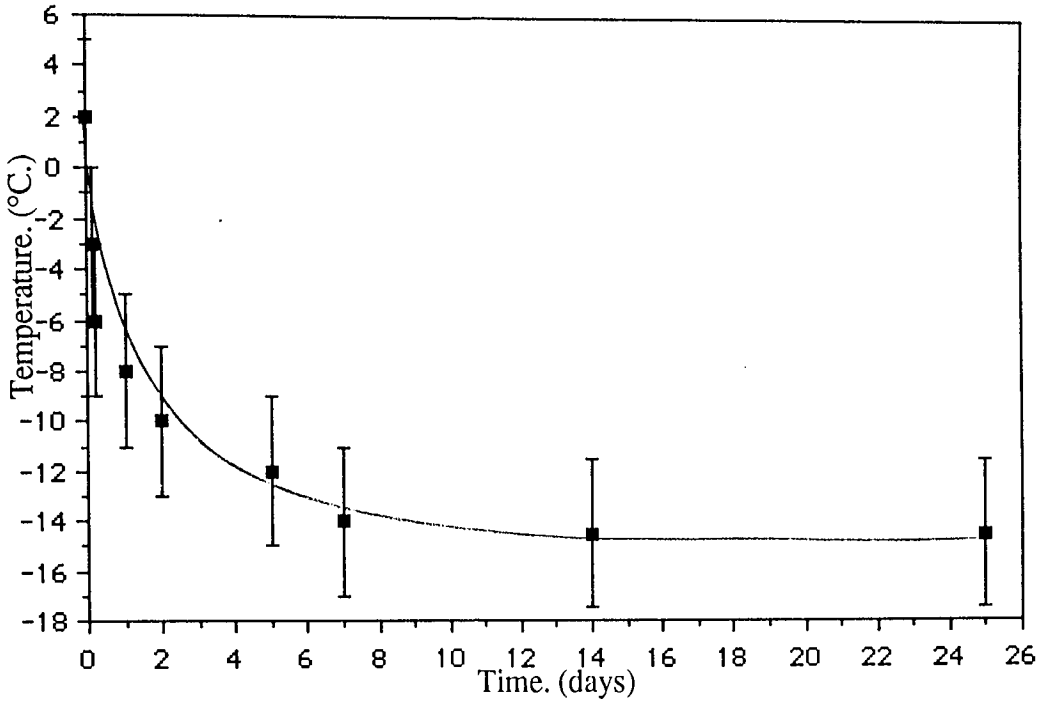

Graph 5.60.

Change In The Glass Transition Temperature Of Sample L.Pec.9, During Degradation In The Accelerated Degradation Model.

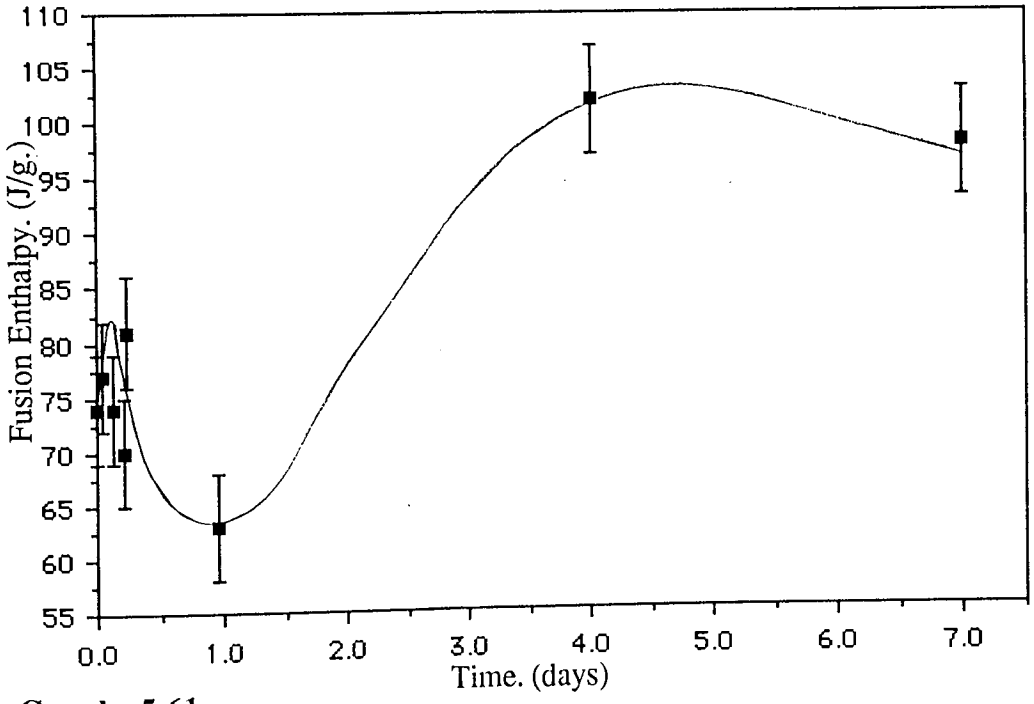

Graph 5.61.

Change In The Fusion Enthalpy Of Sample L.Pec.15, During Degradation In The Accelerated Degradation Model.

The change in the fusion enthalpy of the partially degraded L.Pec.9. samples, as illustrated in graph 5.59, was unusual in that it exhibited a double peak, this was a charateristic of the two step degradation observed in the monomer analysis degradation profile, (Graph 5.5).

The fusion enthalpy increased from approximately 76Jg.$^{-1}$ in the undegraded sample to 106Jg.$^{-1}$ within the first hour of degradation, this was due to the dissolution of the pectin. Since the fusion enthalpy can be utilized as an indication of the crystallinity, this initial enthalpy change would appear to indicate an increase in the crystallinity of the remaining matrix, this was observed because the blending reduced the initial crystallinity of the PHB(FM)IP and therefore, upon the pectin degradation the crystallinity and fusion enthalpy increased.

However, the pectin degradation substantially weakened a proportion of the fibres which collapsed and degraded, this was observed as stage I in the degradation profile, (Graph 5.5). As a result of this, the crystallinity and fusion enthalpy gradually decreased to approximately 76Jg.$^{-1}$ around day 2. The enthalpy then increased to a peak of approximately 90Jg.$^{-1}$ at day 5, this corresponded to the step stage II of the degradation profile and indicated that the relatively small amount of degradation at this stage was mainly due to the amorphous content degradation of the remaining matrix, which gradually increased the crystallinity. Thus, after day 5 the collapse and degradation of the matrix readily occurred. (Stage III) This stage III degradation was then observed as a comparatively rapid decrease in the fusion enthalpy from 90Jg.$^{-1}$ at day 5 to approximately 58Jg.$^{-1}$ at day 7. As the degradation proceeded to the step stage IV there

was little change in the crystallinity of the partially degraded matrix and the enthalpy gradually decreased to approximately 35Jg.$^{-1}$ at day 25.

Therefore, the initial peak was due to the pectin dissolution, whilst the later stages of the enthalpy profile possessed characteristics of the IP degradation. The PHB in L.Pec.9. therefore increased to a crystallinity of approximately 83% at day 4 before reducing to a minimum of around 32% at day 25.

The glass transition temperatures for sample L.Pec.9. were readily noticeable during degradation and, unlike the IP sample, the use of the first order derivative was not neccessary, (Fig. 5.1). An initial sharp drop from 2°C. for the undegraded sample to -6°C. after 3 hours degradation was observed before a gradual decrease to approximately -14°C. at day 7, (Graph 5.60). The Tg. then maintained this level. This indicated the relevently rapid changes in the polymer structure during the initial stages and then the more gradual weakening of the fibres until day 7, where the most unstable form was achieved and degradation of the PHB readily occurred. This period coincided with the step stage II and later produced the relatively rapid degradation at stage III. This trend also confirmed the conclusions determined from the melting point and fusion enthalpy profiles.

Similar to the IP sample, the DSC melting point curves were observed to shift to the lower temperatures and generally occupied a larger temperature range, (Fig. 5.2).

Thus it was concluded that the initial decrease in the melting point, fusion enthalpy and glass transition temperature within the first day were due to the pectin degradation and the

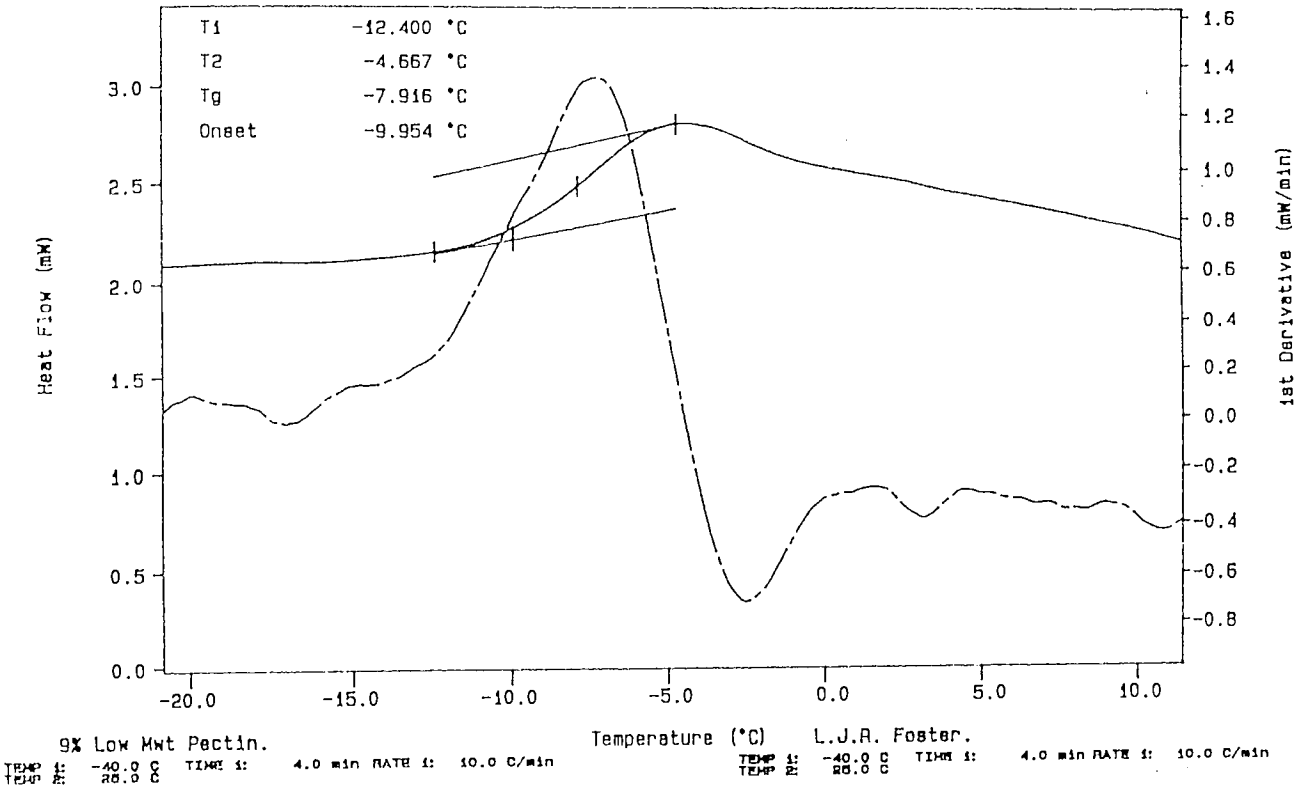

1 Day.

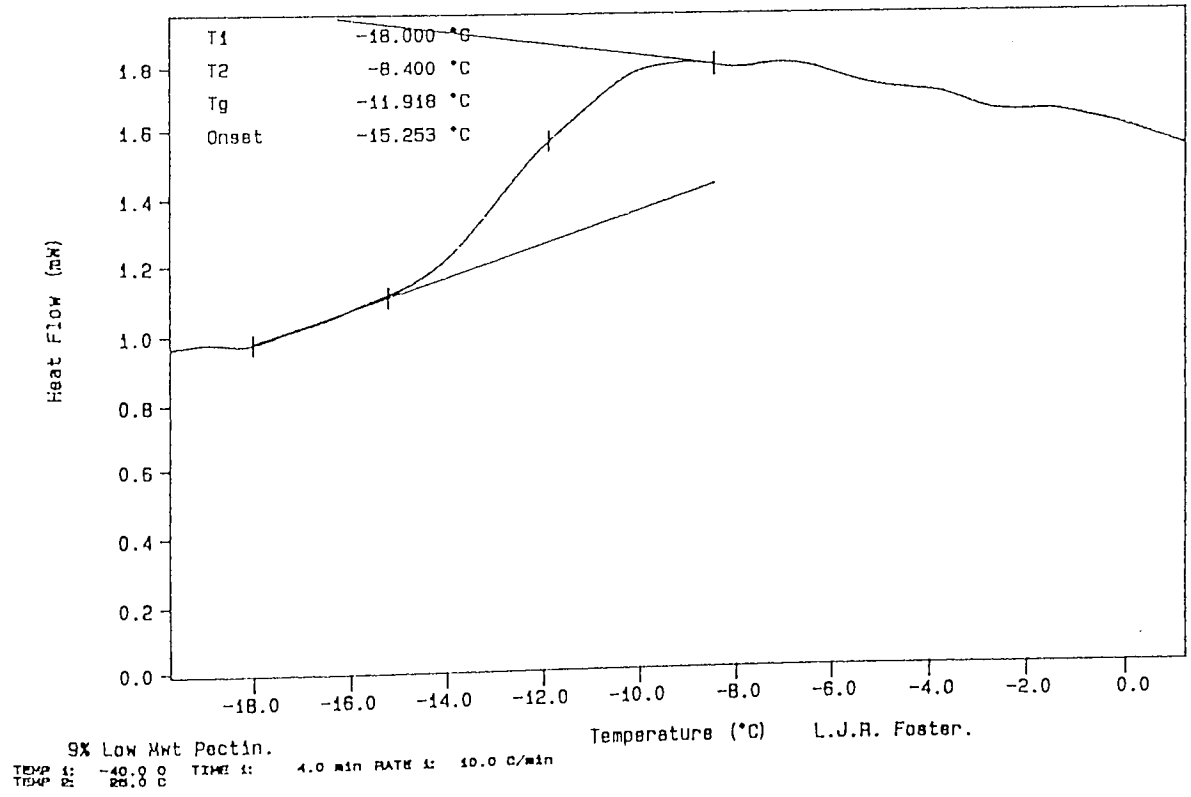

5 Days.

Figure 5.1. Characterization Of L.Pec.9.; DSC Curves For Partially Degraded L.Pec.9. Samples, Illustrating The Glass Transition Points And Their Determination.

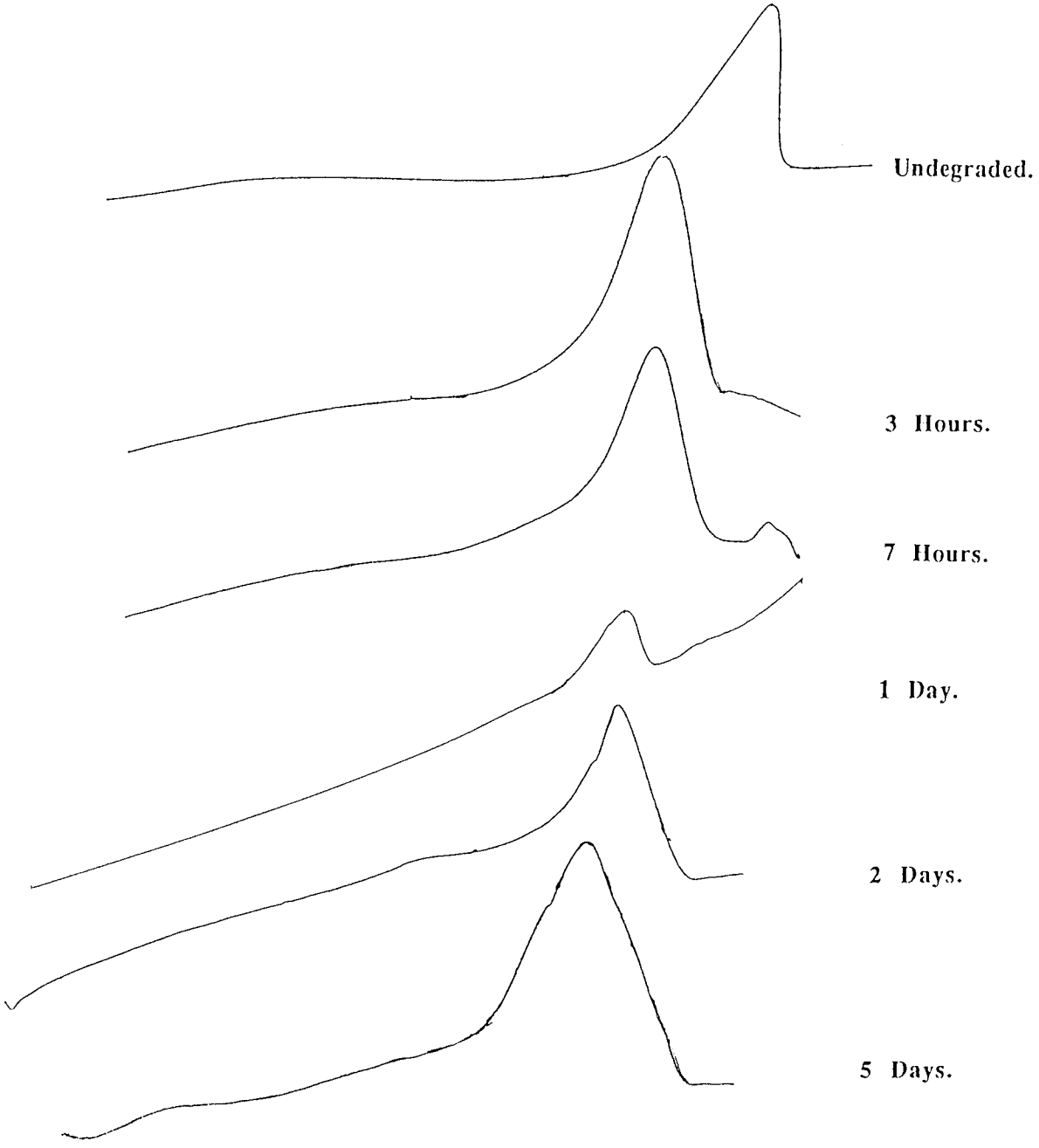

Figure 5.2.

Characterization Of L.Pec.9.; DSC Curves Illustrating The Change In L.Pec.9. Melting Points During Degradation In The Accelerated Model.

subsequent collapse and degradation of a proportion of the matrix. This resulted in a characteristic double peak enthalpy graph, with the first peak a function of the pectin degradation and the second of the PHB. The 9% pectin loading delayed the PHB enthalpy peak from day 4 in the IP sample to day 5.

5.2.4.2. Increasing The Percentage Loading.

The changes in the melting point, glass transition temperature and fusion enthalpy observed for the L.Pec.9. sample during degradation were also observed in the other co-blends, (Graphs 5.61 to 5.69).

The changes in fusion enthalpy for the partially degraded L.Pec.15. samples also exhibited the charateristic double peak observed for L.Pec.9., (Graph 5.61), however, in this case, the first peak did not occur until around 7 hours degradation, with an increase from 74Jg.$^{-1}$ for the undegraded sample to approximately 82Jg.$^{-1}$. This indicated a more gradual degradation of the pectin due to its comparatively greater loading. The second peak then occurred at day 4 with an enthalpy increase from approximately 63Jg.$^{-1}$ at day 1 to 102Jg.$^{-1}$, this indicated a PHB crystallinity of approximately 94%. However, in contrast to the L.Pec.9. enthalpy changes, the second peak was more prolonged with the enthalpy decreasing to only 98Jg.$^{-1}$ by day 7. Thus, the L.Pec.15. matrix collapse occurred slightly earlier than the L.Pec.9., but to a greater extent, such that the degradation of the fibre fragments were reduced due to compaction.

Graph 5.62 illustrates the changes in melting point for L.Pec.15. during degradation. The melting point changes were similar to those observed for the L.Pec.9. sample with a sharp

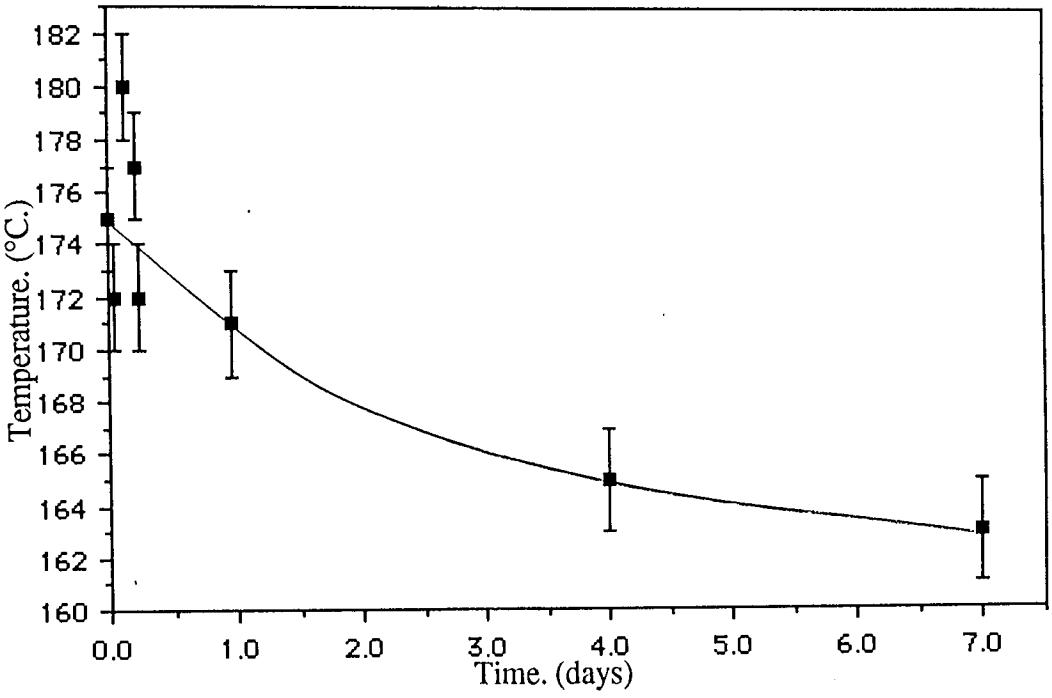

Graph 5.62.

Change In The Melting Point Of Sample L.Pec.15. During Degradation In The Accelerated Degradation Model.

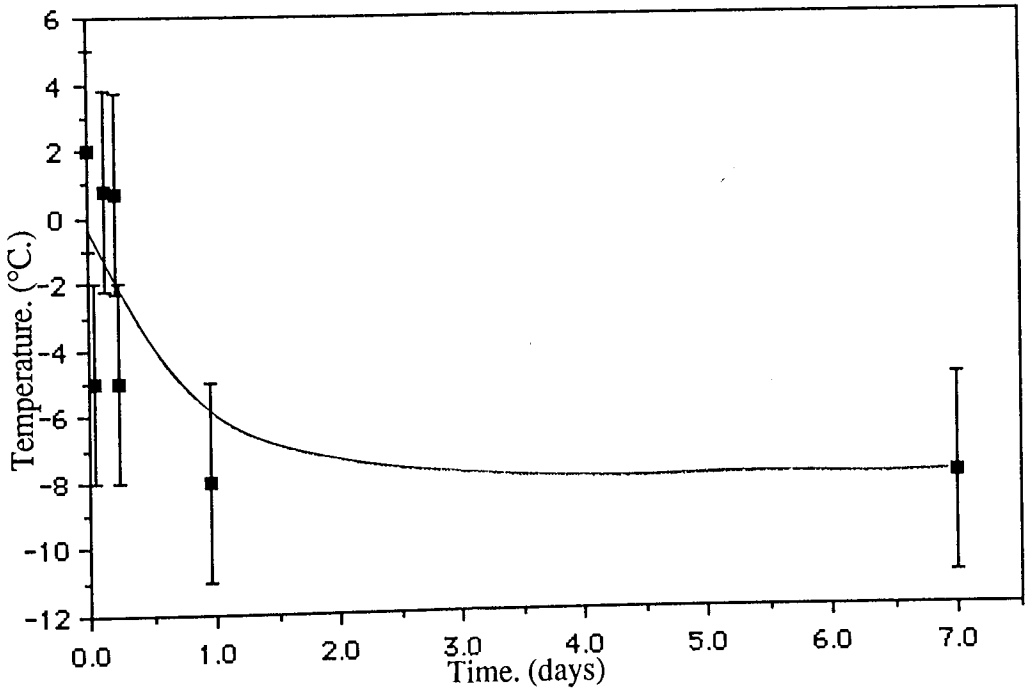

Graph 5.63.

Change In The Glass Transition Temperature Of Sample L.Pec.15. During Degradation In The Accelerated Degradation Model.

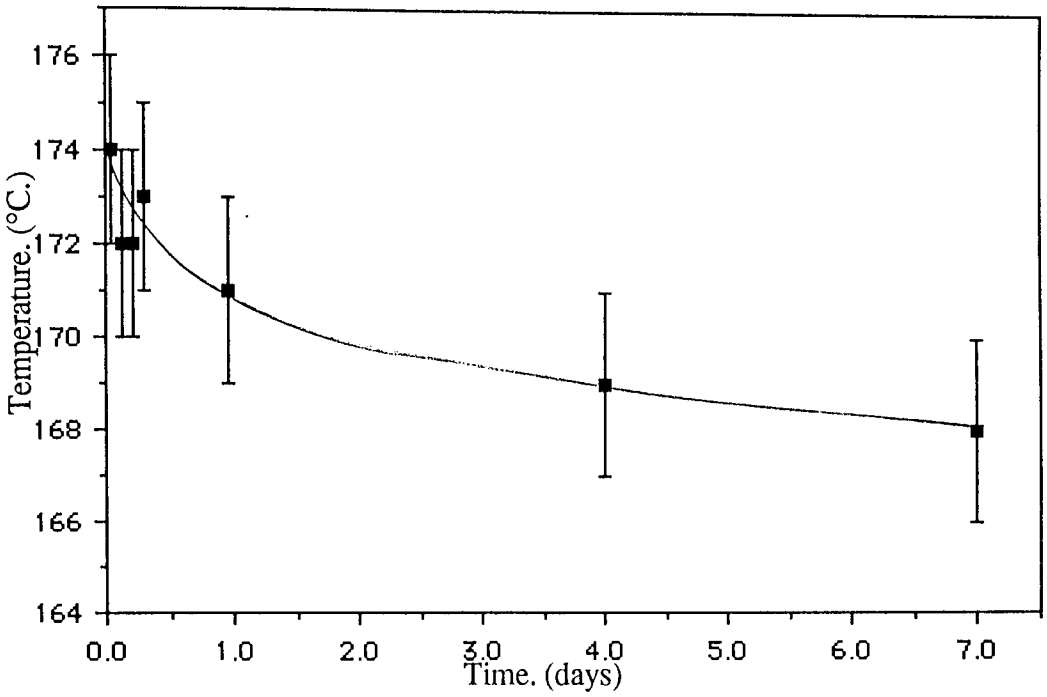

Graph 5.64.

Change In The Melting Point Of Sample L.Pec.25.S. During Degradation In The Accelerated Degradation Model.

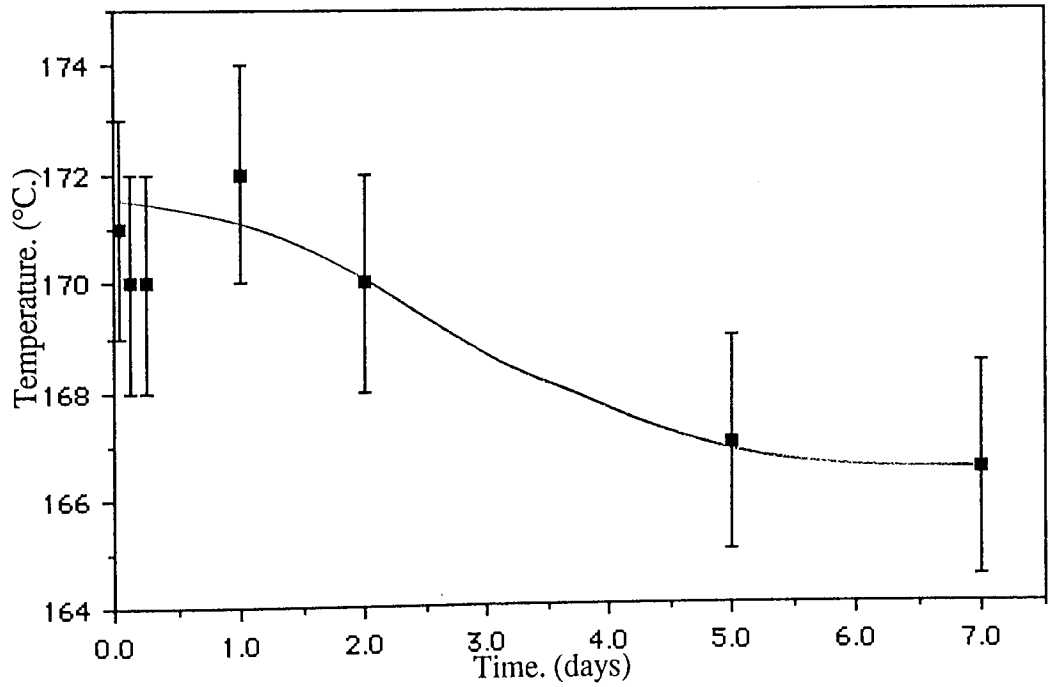

Graph 5.65.

Change In The Melting Point Of Sample L.Pec.25.E. During Degradation In The Accelerated Degradation Model.

decrease from 175°C. for the undegraded sample to approximately 172°C. within 7 hours degradation, this then gradually decreased to 168°C. by day 7. This indicated a more gradual degradation than the L.Pec.9. and was most probably due to a comparatively greater initial matrix collapse as a result of the pectin degradation.

The glass transition temperature graph for L.Pec.15. (Graph 5.63) exhibited a sharp decrease from 1°C. for the undegraded sample to approximately -4°C. at 7 hours degradation, before gradually decreasing to -8°C. at day 7. The initial sharp decrease in Tg. until 7 hours was comparable to the L.Pec.9. Tg. decrease, (Graph 5.60) which occurred for a longer duration until day 2. Thus, the relatively greater pectin loading in the larger diameter L.Pec.15. fibres compared to those of L.Pec.9., reduced the fibre stability such that the matrix collapse and PHB degradation readily occurred. However, due to the subsequent fibre fragment and particulate matter compaction, the degradation of the PHB was reduced and this was illustrated as the little change in the Tg's. in the later stages from 7 hours to day 7.

Sample L.Pec.25.S. exhibited a sharp decrease in the melting point from 176°C. for the undegraded sample to approximately 172°C. after 7 hours degradation before a gradual decrease to approximately 168°C. at day 7. This trend was similar to that determined for the IP sample, whilst the initial melting point drop was similar to that of L.Pec.9. However, L.Pec.25.E. showed an initial decrease from 175°C. to approximately 170°C. after 3 hours degradation and then maintained this value until around day 2, before gradually decreasing to approximately 166°C. at day 7, (Graph 5.65).

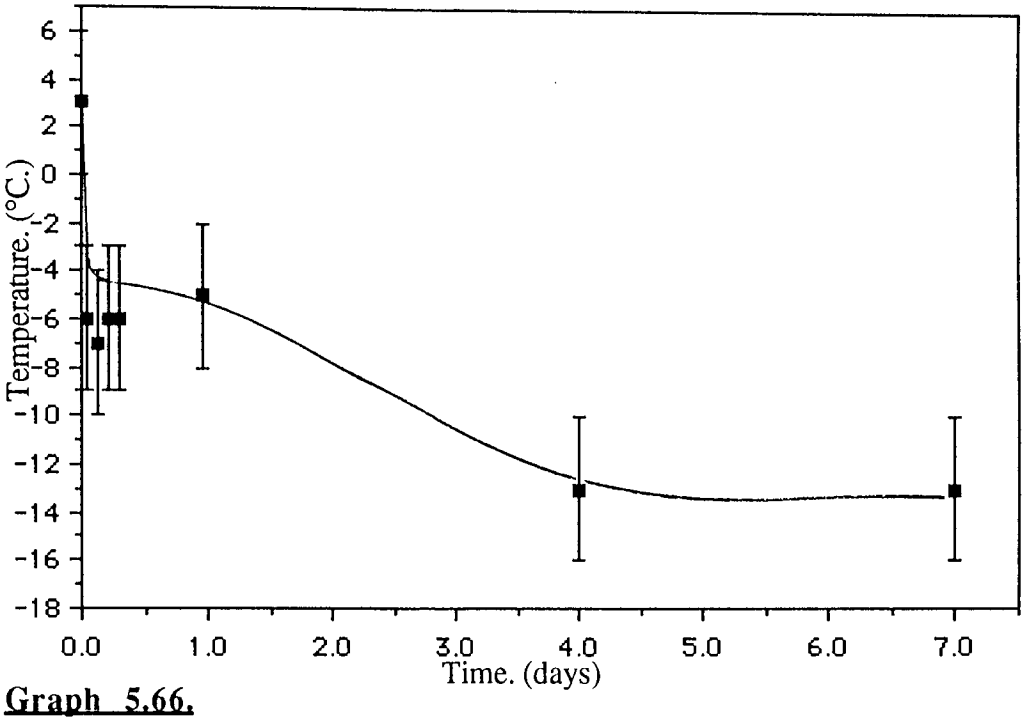

Graph 5.66.

Change In The Glass Transition Temperature Of Sample L.Pec.25.S. During Degradation In The Accelerated Degradation Model.

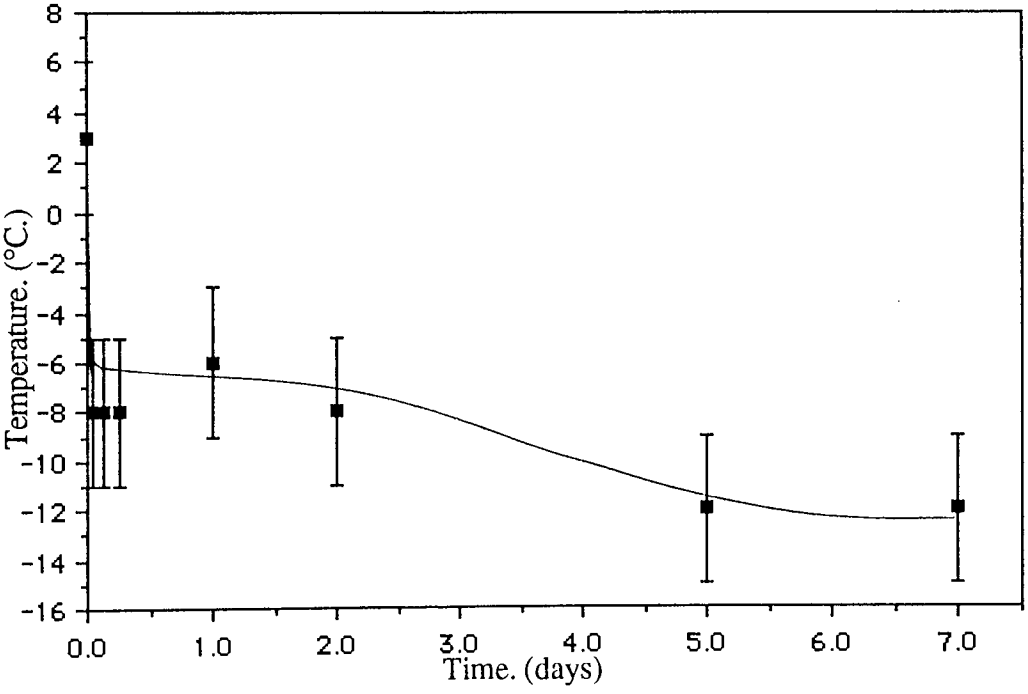

Graph 5.67.

Change In The Glass Transition Temperature Of Sample L.Pec.25.E. During Degradation In The Accelerated Degradation Model.

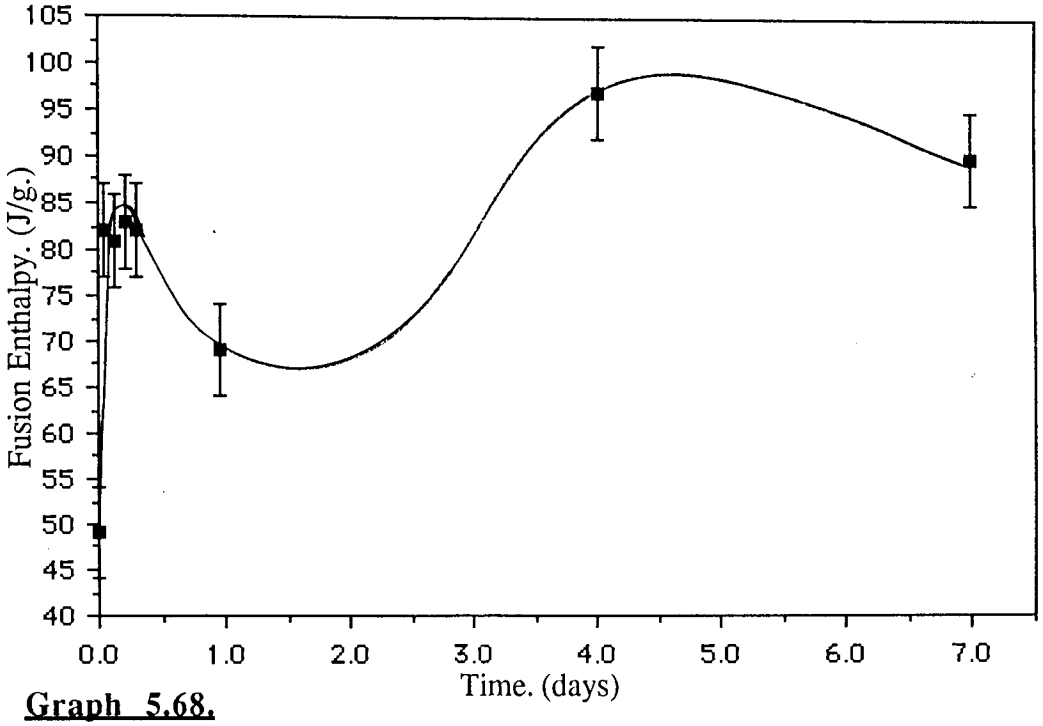

Graph 5.68.

Change In The Fusion Enthalpy Of Sample L.Pec.25.S. During Degradation In The Accelerated Degradation Model.

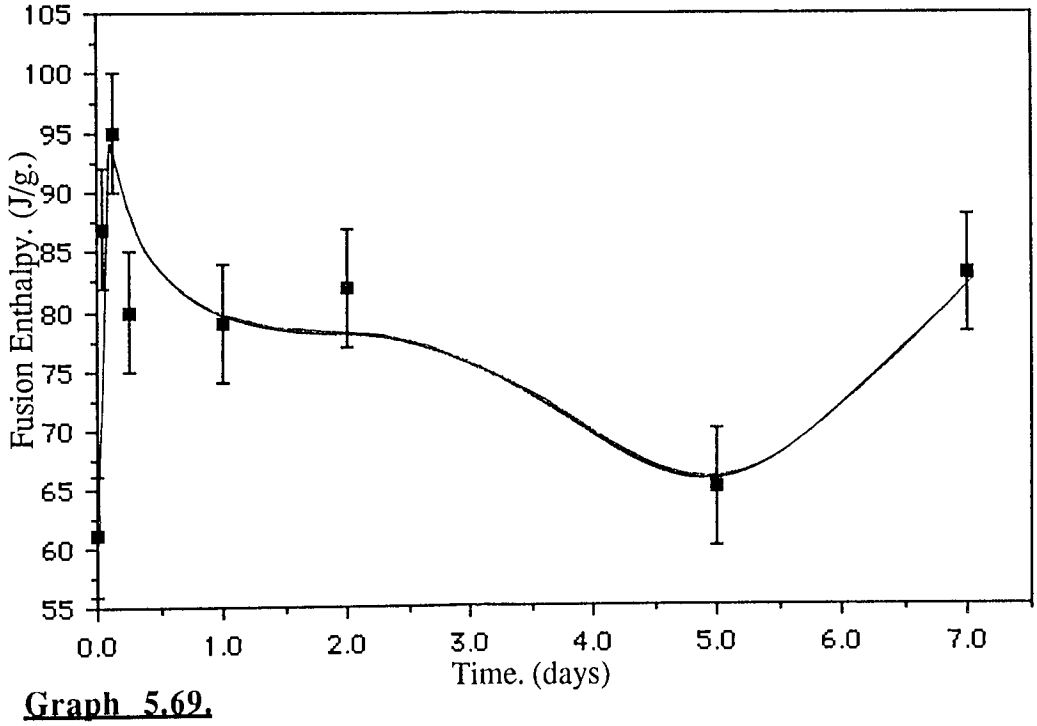

Graph 5.69.

Change In The Fusion Enthalpy Of Sample L.Pec.25.E. During Degradation In The Accelerated Degradation Model.

The changes in glass transition temperatures during degradation for L.Pec.25.S. and L.Pec.25.E. are illustrated in graphs 5.66 and 5.67 respectively and exhibit similar trends to each other and to L.Pec.9. There was an initial sharp decrease from around 3°C. to approximately -6°C. by day 1 for L.Pec.25.S., this drop was slightly greater for L.Pec.25.E. (-8°C.). After day 1 the glass transition temperatures for both samples gradually decreased to -13 and -12°C. for L.Pec.25.S. and L.Pec.25.E. respectively. These trends were very similar to those determined for the L.Pec.9. sample.

The fusion enthalpy profiles in graphs 5.68 and 5.69, illustrate greater differences between L.Pec.25.S. and L.Pec.25.E. than the mp. and Tg. profiles. The enthalpy increased from approximately $49Jg.^{-1}$ for the undegraded L.Pec.25.S.sample to $82Jg.^{-1}$ after 5 hours degradation, it then decreased to approximately $68Jg.^{-1}$ at day 1. This was the 'pectin peak'. The enthalpy then gradually increased to the second peak of $97Jg.^{-1}$ at day 4 with a crystallinity of about 89%. The first peak for L.Pec.25.E. occurred around 3hrs. with an increase from 61 to $95Jg.^{-1}$ before decreasing to approximately $80Jg.^{-1}$ at 7hrs. then gradually to $65Jg.^{-1}$ at day 5. The enthalpy then increased to approximately $85Jg.^{-1}$ at day 7 and this tended to indicate that the second peak was around day 8. The main degradation of the PHB at stage II therefore occurred comparatively sooner for L.Pec.25.S. than for L.Pec.25.E.

The melting point and enthalpy profiles of L.Pec.25.S. are more similar to those observed from L.Pec15. than L.Pec.9., despite the fact that the L.Pec.25.S. pectin loading was determined as approximately 6%. This tended to indicate that besides the loading difference between L.Pec.25.S.and L.Pec.25.E. there was also a difference in the

molecular weight of the blended pectin, with L.Pec.25.S. possessing a comparatively higher molecular weight pectin. This was also suggested from the qualitative examinations.

Thus, it was concluded that increasing the percentage loading of the pectin altered the times and intensities of the first and second enthalpy peaks and slightly altered the melting point and glass transition temperature profiles. These alterations were due to the degradation of the pectin and the effects on the stability and degradation of the remaining matrix. It was also concluded that L.Pec.25.S. possessed pectin of a comparatively higher molecular weight than its counterpart L.Pec.25.E. which had a greater pectin loading.

5.2.4.3. Increasing The Pectin Molecular Weight.

Sample H.Pec.10. showed a similar trend in the mp. changes during degradation as sample L.Pec.9. with an initial decrease from 172°C. for the undegraded sample to 167°C. at 7 hours and a stability period from 7hrs. to day 1, (Graph 5.70). A gradual decrease to approximately 148°C. then occurred until day 7. This indicated that H.Pec.10. exhibited a comparatively earlier loss of stability than L.Pec.9.

No Tg's. were determined for H.Pec.10. even in the initial stages and this tended to indicate that the partially degraded samples were of a high crystallinity.

Graph 5.71 illustrates the changes in the fusion enthalpy with degradation. The enthalpy increased sharply from approximately 67Jg.$^{-1}$ for the undegraded sample to 93Jg.$^{-1}$ at day 1 before a practically linear increase to 107Jg.$^{-1}$ at day 7. This indicated that there was a

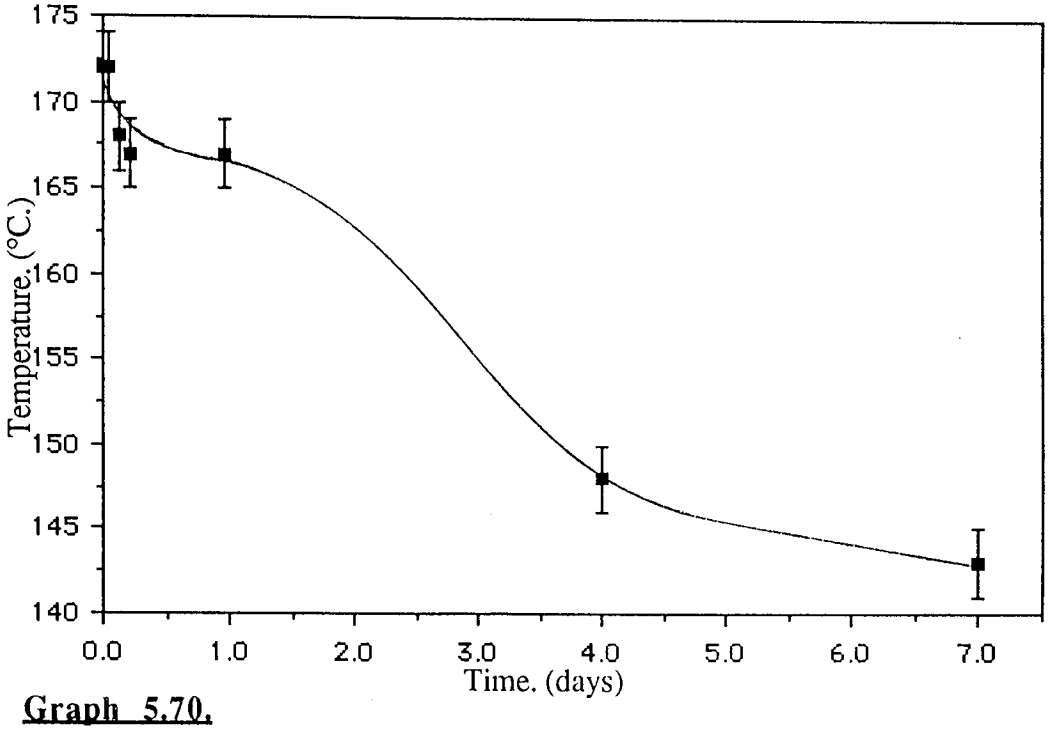

Graph 5.70.

Change In The Melting Point Of Sample H.Pec.10. During Degradation In The Accelerated Degradation Model.

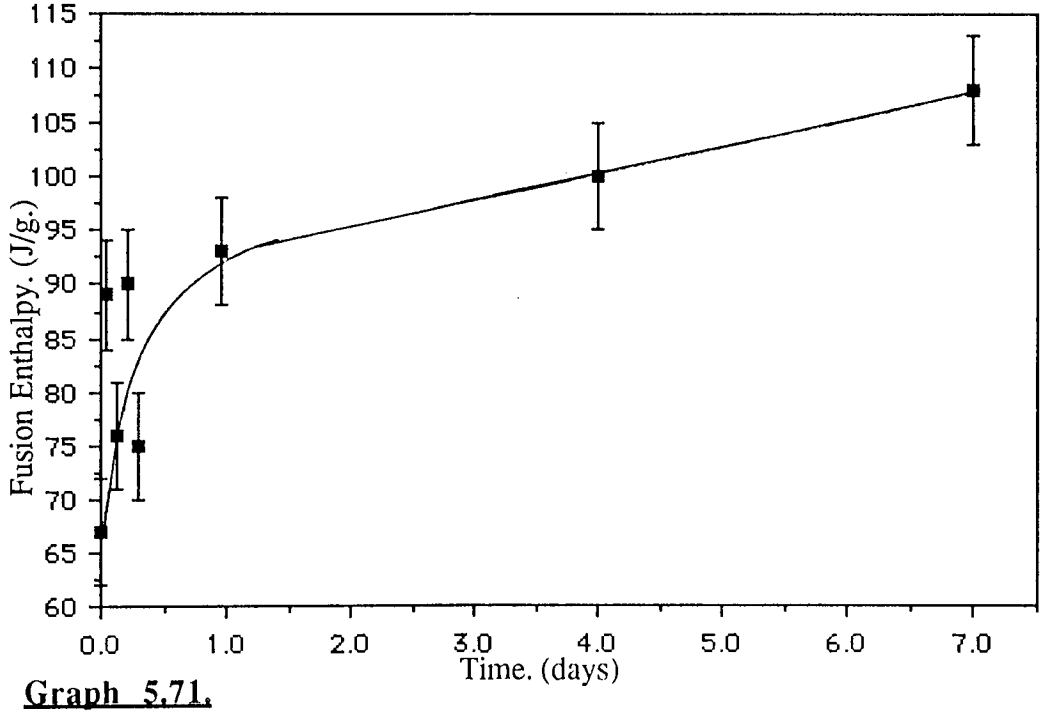

Graph 5.71.

Change In The Fusion Enthalpy Of Sample H.Pec.10. During Degradation In The Accelerated Degradation Model.

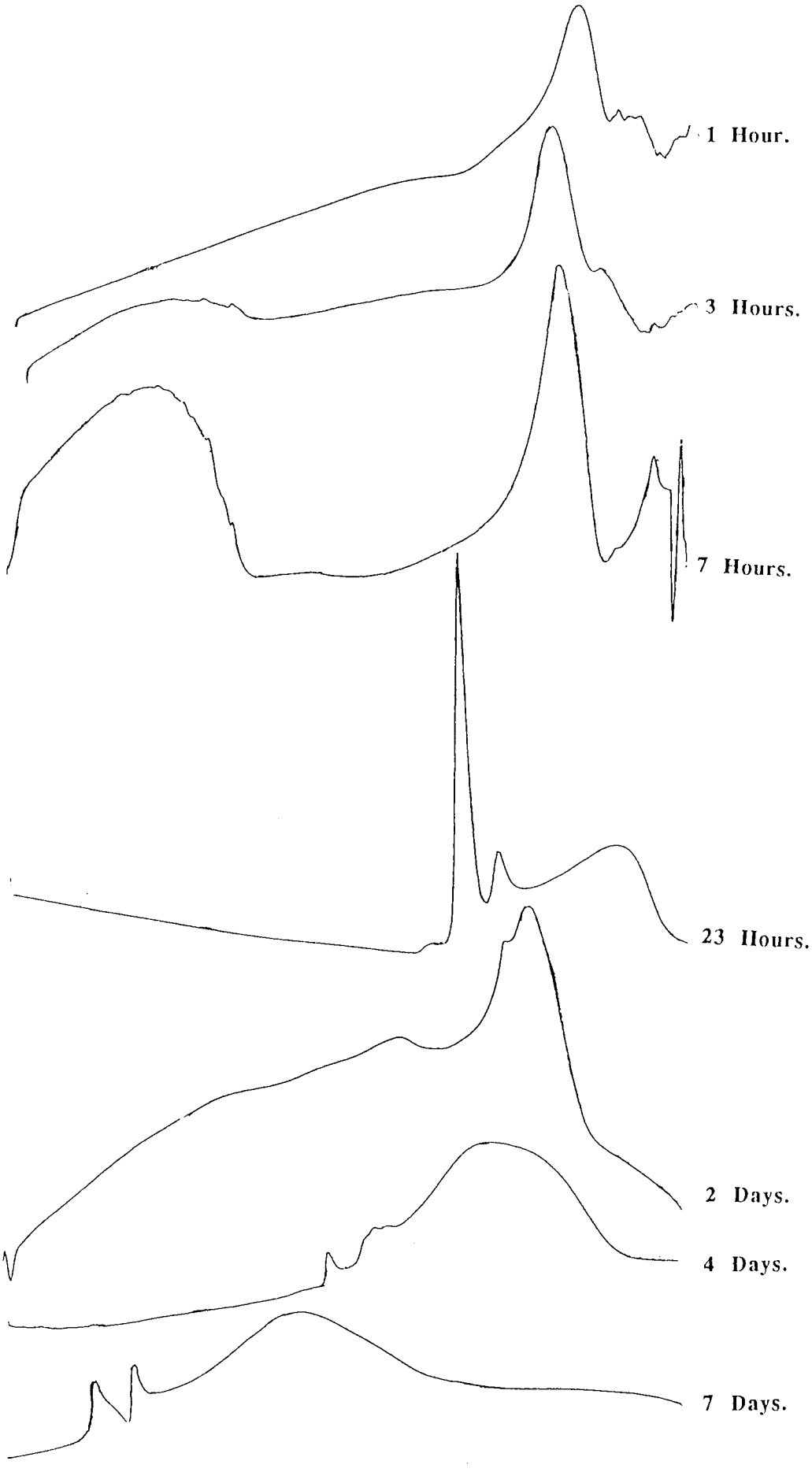

Figure 5.3.

Characterization Of H.Pec.10.; DSC Curves Illustrating The Change In H.Pec.10. Melting Points During Degradation In The Accelerated Model.

gradual degradation of the pectin by day 1, with a relatively rapid crystallinity increase followed by a gradual increase in the crystallinity to day 7. Thus, it was concluded that the high molecular weight pectin was more homogeneously blended than the low molecular weight pectin, so that the matrix collapse was more gradual. This was also noticed in the qualitative observations.

Figure 5.3 illustrates the changes in the mp. curves for H.Pec.10. and as can be readily observed, the original narrow peak gradually moved to the lower temperature regions and became more diverse, similar to L.Pec.9. However, this greater diversity reduced the peak so that it contrasted with the noticeable peaks for the IP and low molecular weight samples.

5.2.4.4. Conclusions.

The DSC results confirmed previous conclusions that increasing the percentage loading of the low molecular weight pectin reduced the efficiency of the blending, such that the initial degradation weakened the fibres excessively and collapse readily occurred. Settlement and compaction was therefore considerably faster in the higher percentage loadings and the degradation of the remaining PHB delayed and reduced. L.Pec.25.S. was confirmed as possessing a higher molecular weight fraction.

The blending between the PHB(FM)IP and 10% high molecular weight pectin was more homogeneous than in a low molecular weight counterpart. This increased the long term stability of the fibres and subsequently reduced the effect of compaction so that the degradation was greater.

5.2.5 Photoacoustic Spectroscopy (PAS) Studies.

The partially degraded samples were investigated utilizing photoacoustic spectroscopy. (PAS) Figure 5.4 illustrates the traces obtained for L.Pec.9. As anticipated, it was observed that the method of degradation was the same as that for the homopolymer. Within 1 hour of degradation a 'shoulder' at the 1568 $cm.^{-1}$ waveband was observed, this increased during degradation and was identified as the carboxylate ion peak. However, this peak emerged earlier than that of the IP sample and this indicated an apparently earlier degradation of the fibres. Similarly, an apparent decrease in the saturated carbon-hydrogen bond energies at region B was more noticeable than that for the IP or TG samples and this may well have been due to a decrease in the proportion of pectin present.

The emergence of the carboxylate ion peak at 1568 $cm.^{-1}$ indicated that the degradation of the PHB occurred earlier for L.Pec.9. compared to the IP sample. Thus, a cleavage of the ester linkages and hence the polymer chains readily occurred. This could have been due to a number of reasons:

1) The blending with pectin. The pectin acted as a random or block copolymer which degraded into the buffer medium and thus, readily broke the ester linkages.

2) The physical presence of the pectin in random regions, which upon degrading merely increased the available surface area to volume ratio and mechanically weakened the remaining PHB fibres, thus facilitating their degradation.

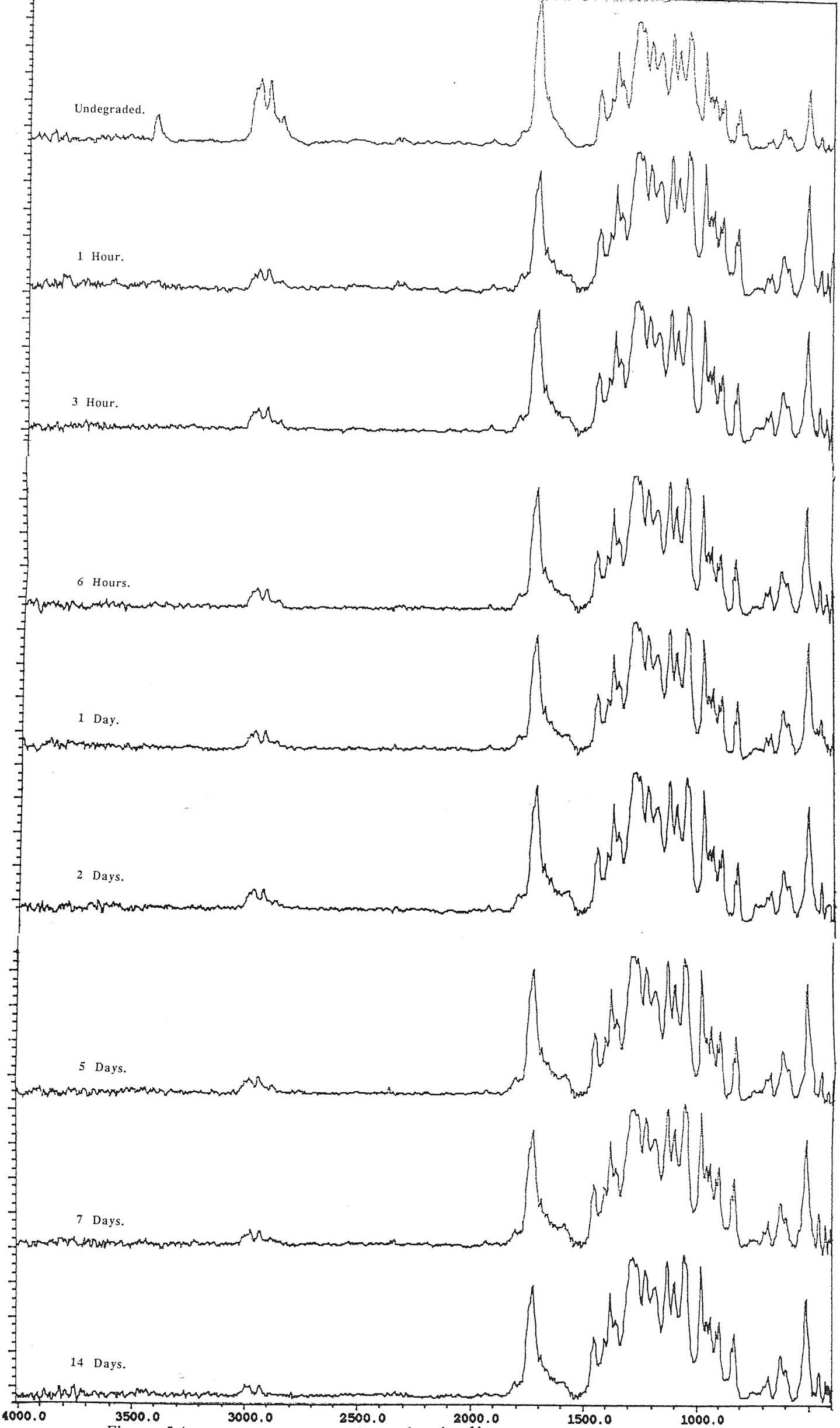

Figure 5.4.

Characterization Of Partially Degraded L.Pec.9: FTIR-PAS Traces Of L.Pec.9. Samples During Degradation In The Accelerated Degradation Model.

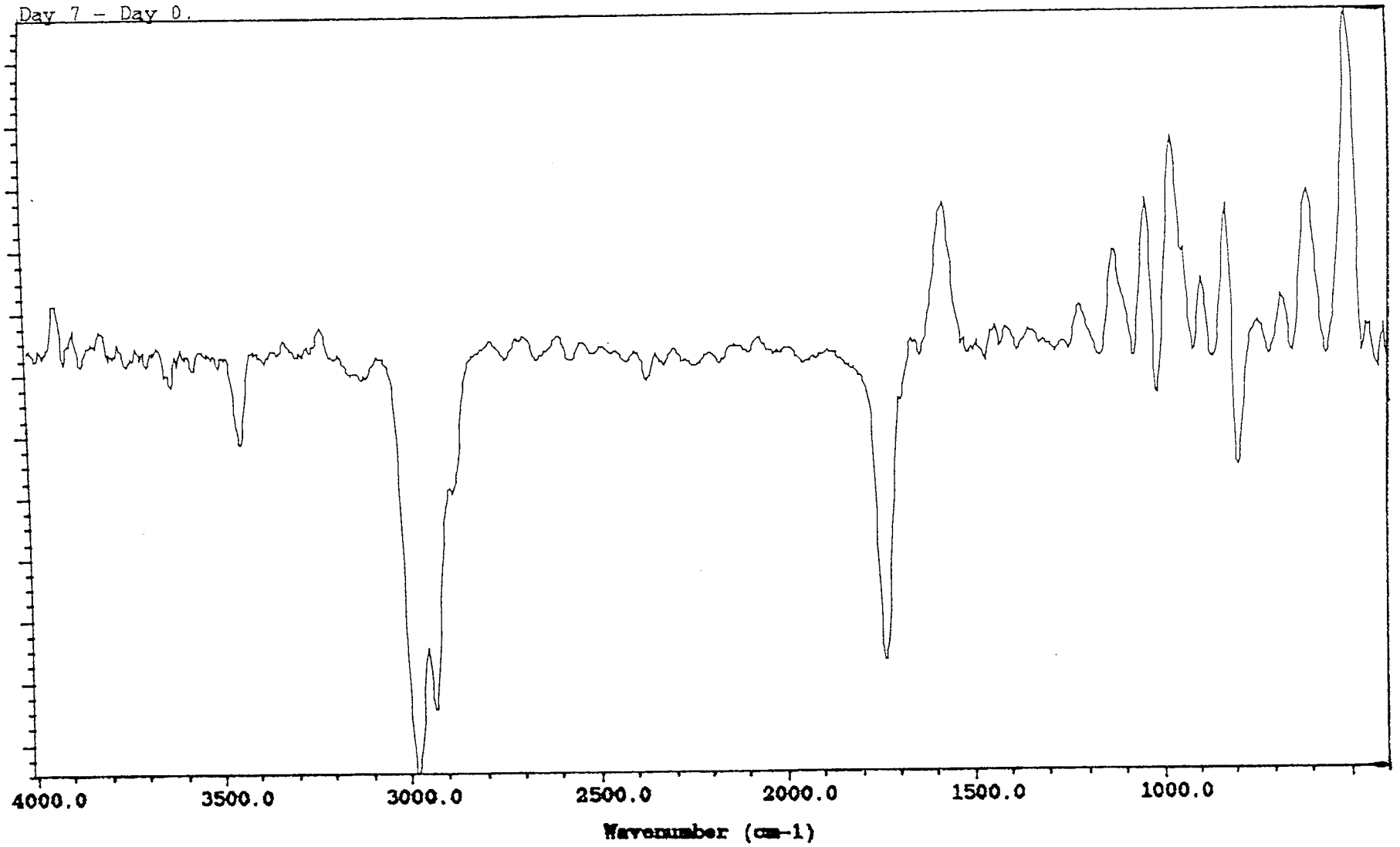

Figure 5.5.

Characterization Of L.Pec.9.; FTIR-PAS Trace Of The Undegraded L.Pec.9. Subtracted From L.Pec.9. After 7 Days Degradation In The Accelerated Degradation Model.

3) A combination of both 1) and 2) occurred to varying extents.

The relatively small changes in the molecular weight data for the undegraded samples compared to the undegraded IP sample tended to indicate that little or no copolymerization occurred. Similarly, the DSC results also indicated no copolymerization. Since the degradation to monomer was initially greater for the IP sample than the co-blends, it could be concluded that the earlier appearence of the ester link breakages and therefore, the polymer chain length reduction for L.Pec.9., did not result in any PHB loss. This confirmed previous suspicions that although some initial fibre collapse was still present, the ester link breakages occurred more randomly, weakening the matrix and the fibres. This was recognized as the fragile and 'brittle' nature of the partially degraded samples after the filtering and drying procedures and was also observed using phase contrast microscopy as the apparently greater amount of fragmentation. The weakened fibres then facilitated the matrix collapse at stage II and increased the degradation rate of the co-blends compared to the IP sample at stage III, this was then observed as the enthalpy decrease between days 7 and 23 (Graph 5.59) and a minimum in the mp. and Tg. profiles, (Graphs 5.58 & 5.60). Thus, reason 2 was considered the most probable.

Subtracting the day 7 trace from the undegraded (Fig. 5.5) revealed the increase in the 1568 $cm.^{-1}$ waveband coupled with the carbonyl shift at 1728 $cm.^{-1}$. Increasing the pectin loading did not appear to affect the traces obtained. However, the subtractions from the undegraded (Figs. 5.6-5.8) illustrated some differences in the relevent peak heights of the carboxylate ion waveband and the carbonyl shift.

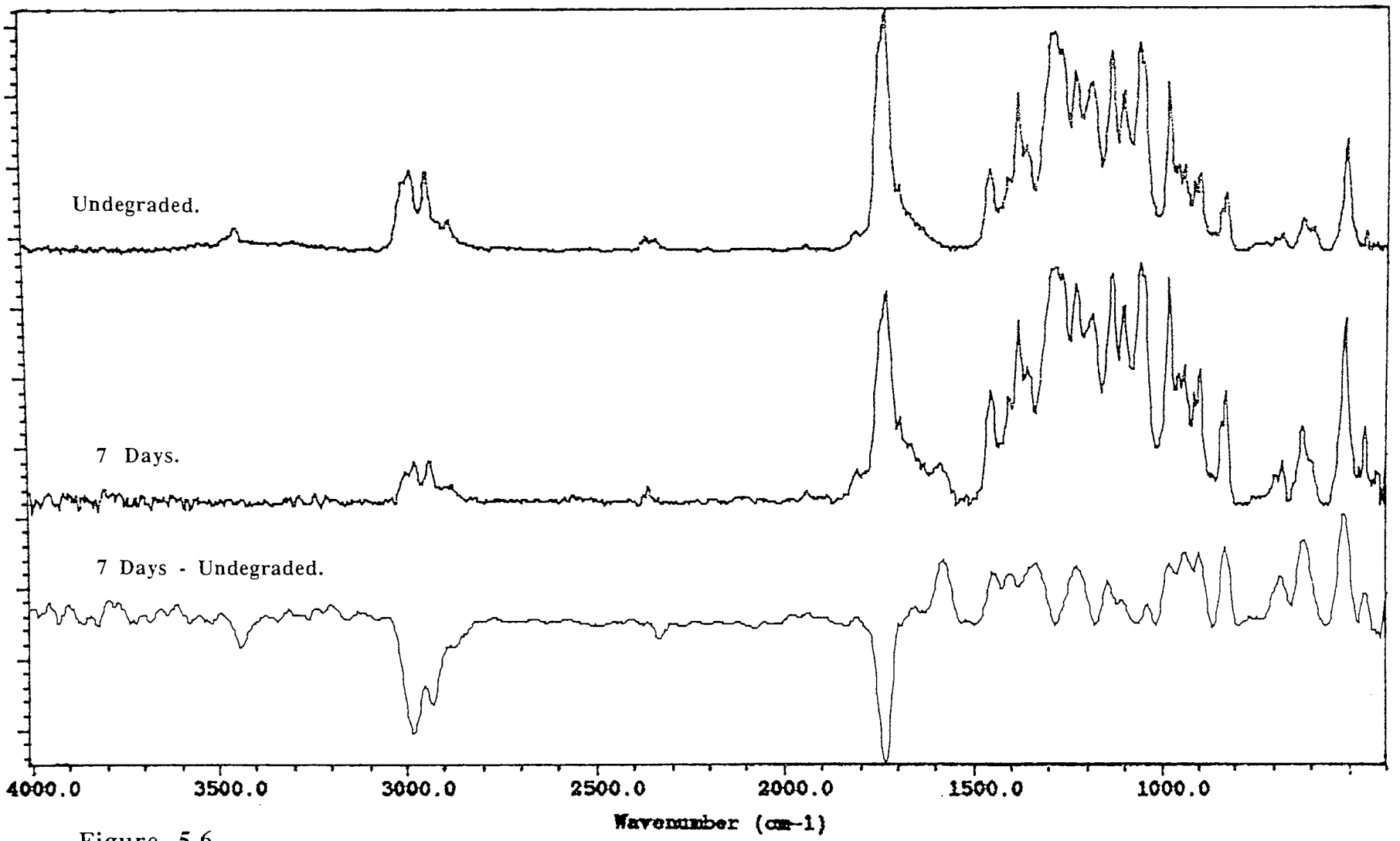

Figure 5.6.

Characterization Of L.Pec.15.; FTIR-PAS Traces Of Undegraded L.Pec.15., After 7 Days Degradation In The Accelerated Degradation Model And Their Difference.

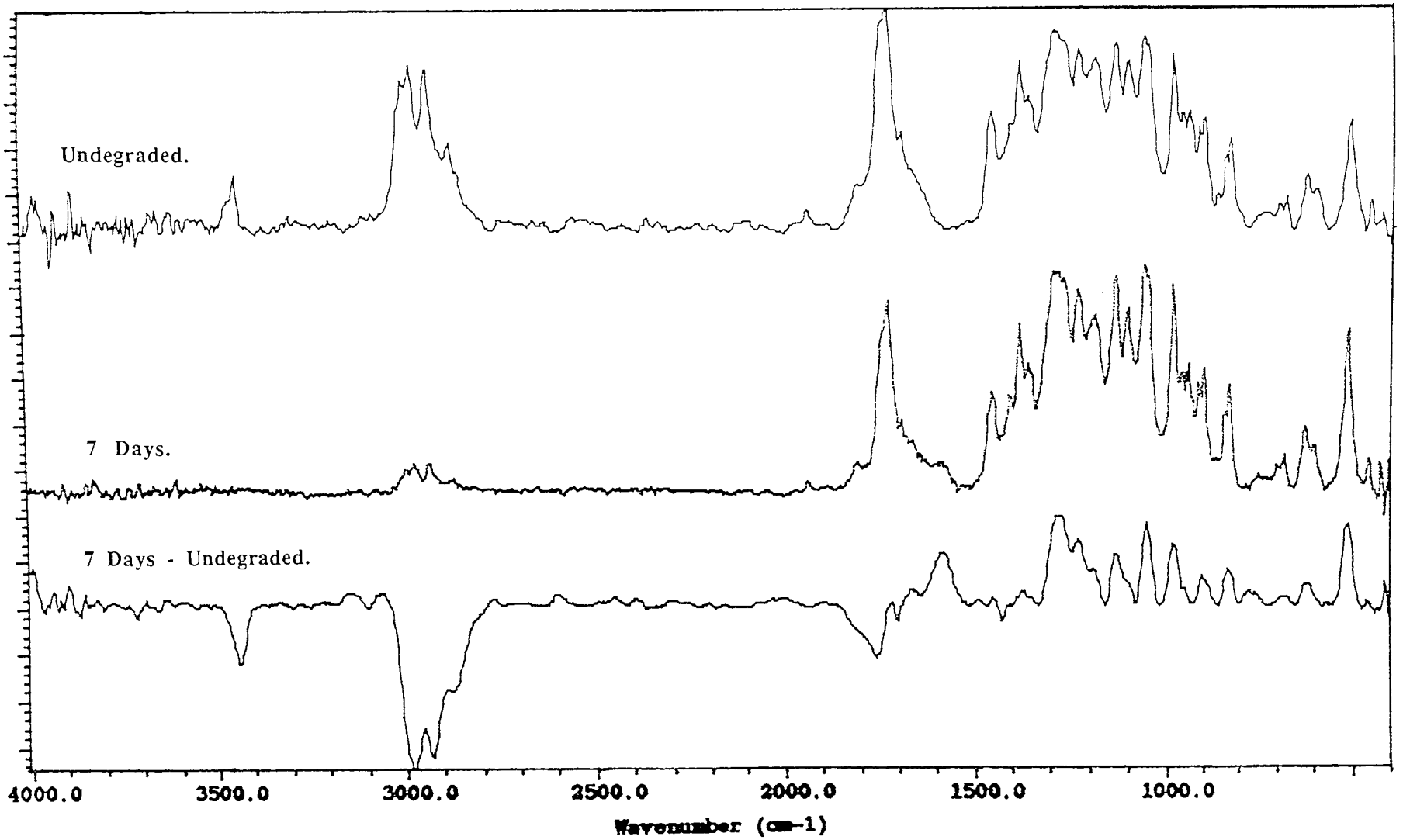

Figure 5.7.

Characterization Of L.Pec.25.S.; FTIR-PAS Traces Of Undegraded L.Pec.25.S., After 7 Days Degradation In The Accelerated Degradation Model And Their Difference.

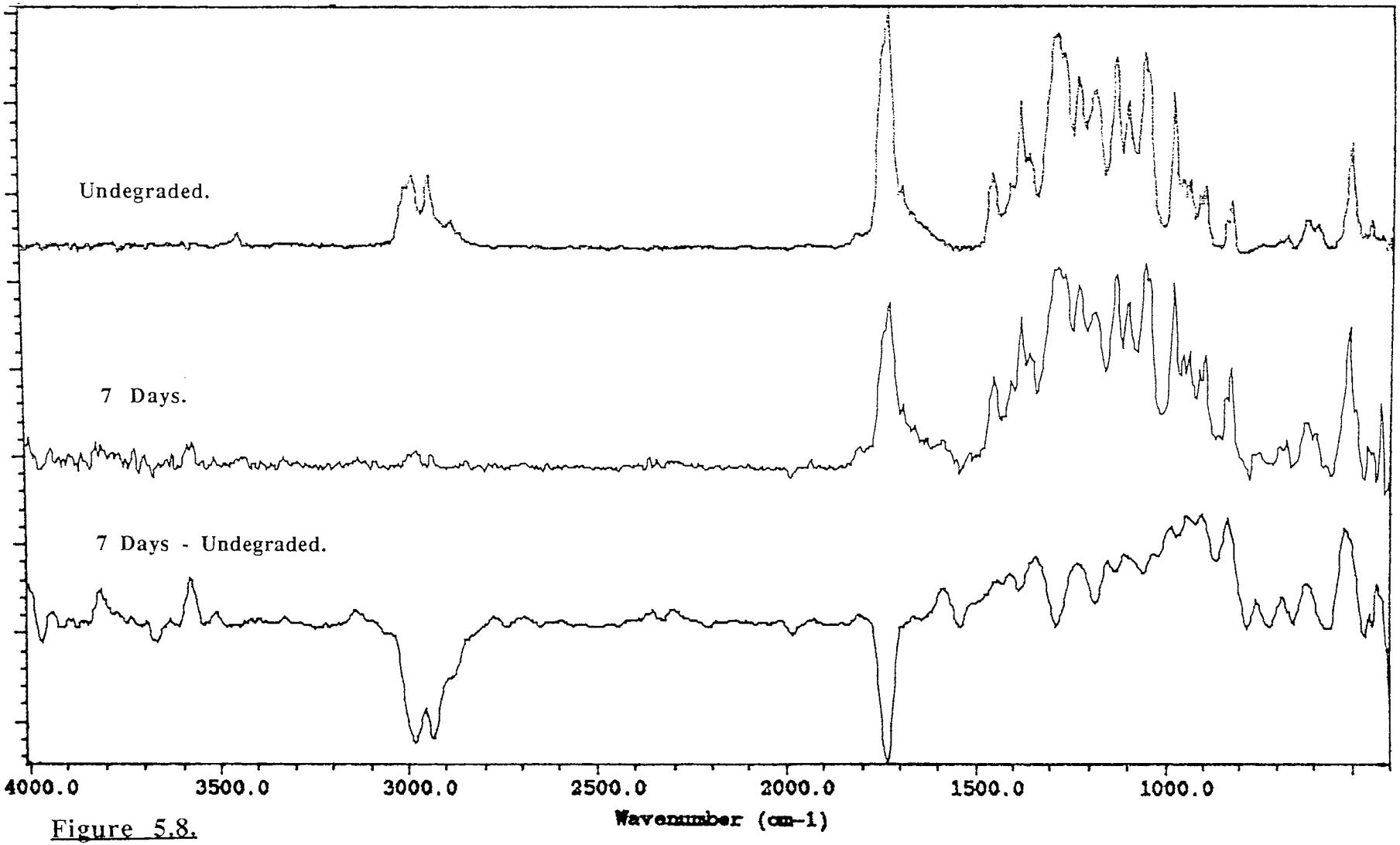

Figure 5.8.

Characterization Of L.Pec.25.E.; FTIR-PAS Traces Of Undegraded L.Pec.25.E., After 7 Days Degradation In The Accelerated Degradation Model And Their Difference.

The examination of the partially degraded samples blended with 10% high molecular weight pectin also revealed little difference from the L.Pec.9. traces, (Fig. 5.9). The carboxylate ion peak did not appear noticeable until after 7 hours degradation and thus the amount of initial degradation and weakening of the matrix appeared to be less. Therefore, it could be concluded that the initial stability of the H.Pec.10. fibres was greater than that of the L.Pec.9.

At day 1, the carboxylate ion peak drastically increased for the H.Pec.10. sample when compared to the L.Pec.9., which was much smaller. This peak then gradually increased until a maximum at day 7. Thus, compared to the L.Pec.9. sample, the 10% high molecular weight readily blended with the PHB and was more homogenous, this was also concluded from the DSC results and qualitative observations.

Figure 5.10 illustrates the difference between the H.Pec.10. day 7 sample and the undegraded. The carboxylate ion peak and the carbonyl shift were very noticeable when compared to the low molecular weight blends.

Therefore, it was concluded that the degradation of the co-blends occurred by an initial weakening of the partially degraded matrix due to ester link cleavage. The pectin did not affect the polymer chain lengths but facilitated their weakening by introducing mechanical stresses.

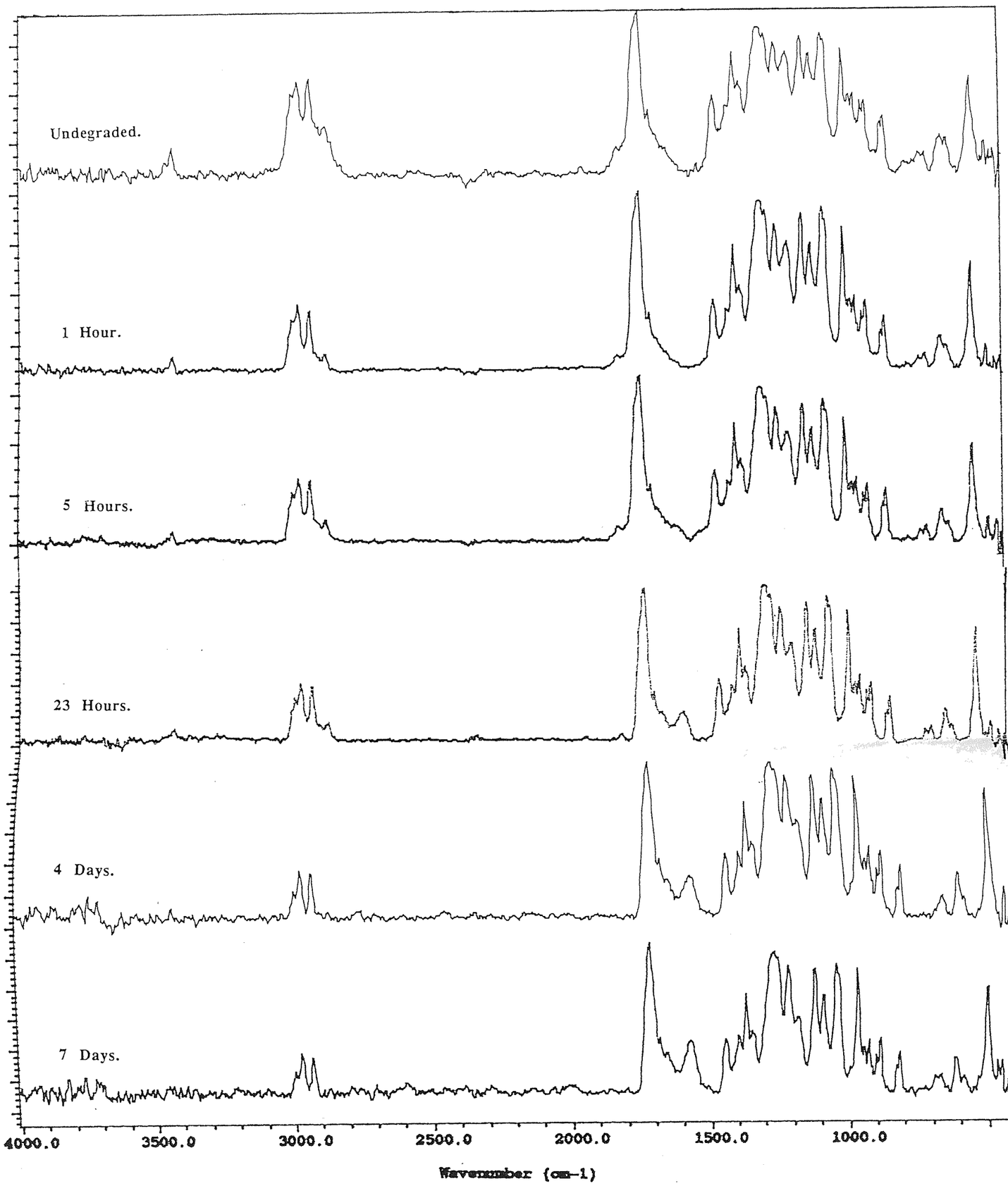

Figure 5.9.

Characterization Of H.Pec.10.; FTIR-PAS Traces Of Partially Degraded H.Pec.10. In The Accelerated Degradation Model.

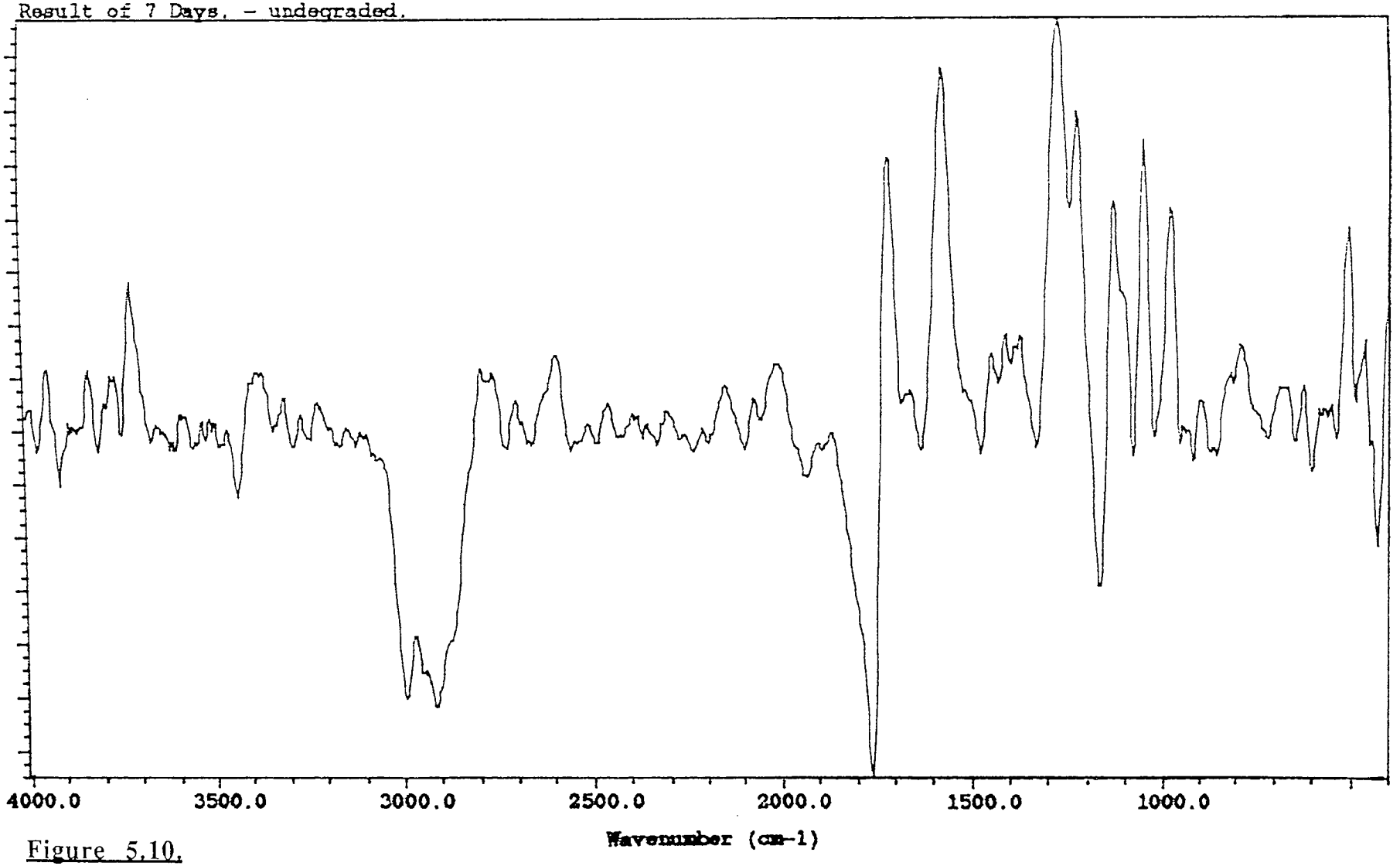

Figure 5.10.

Characterization Of H.Pec.10.: FTIR-PAS Trace Of The Undegraded H.Pec.10 Subtracted From H.Pec.10. After 7 Days Degradation In The Accelerated Degradation Model.

5.2.6 Conclusions.

Blending the PHB(FM)IP with a relatively small percentage loading of pectin affected the initial structure of some of the mainly large diameter fibres. During the first day of degradation the gradual dissolution of the pectin increased the surface area to volume ratio and weakened the fibre/matrix integrity by the introducing mechanical stresses and facilitating the ester bond cleavages, thus reducing the polymer chain lengths. Upon collapse the degradation of the PHB proceeded to a greater extent than in the IP sample, due to these pectin cavities.

Increasing the pectin loading increased the amount of pectin blended within the fibres but reduced the blending efficiency and resulted in a pectin loss during the production process. The increase in pectin cavities reduced the initial stability and ensured a comparatively greater matrix collapse and fragmentation, so that compaction of the fibre fragments possessed a greater influence than for the lower loaded co-blends.

The distribution of the pectin was not homogenous and tended to accumulate in the large and larger medium sized fibres. A considerably smaller proportion of higher molecular weight pectin was present at the start of the manufacturing run than at the end in those samples with a high production loading.

Increasing the molecular weight of the pectin increased the blending efficiency, consequently, after the pectin degradation there was a considerably larger surface area to volume ratio of the remaining PHB fibres than for a low molecular weight counterpart. This increased the fibre stability and ensured a comparatively more gradual and greater

degradation.

Thus, the degradation of the co-blends within the accelerated degradation system was affected by blending, such that the samples degraded to a greater extent than the homopolymer by the simple addition of a small percentage loading.

5.3. The Degradation Of PHB(FM)IP Blended With The Copolymer PHV And Its Comparison To The Homopolymer And Co-blended L.Pec.9. Samples.

5.3.0. Introduction.

The PHB(FM)IP was blended with an equal weight of PHB+10%PHV(FM)IP, such that the final sample ideally possessed 5% PHV. ie; PHB/5V(FM)IP, (Sample PHB/5V). The degradation of the PHB/5V was investigated in the accelerated degradation model and was then compared to that of the IP sample.

PHV has been statistically proven, utilizing nuclear magnetic resonance spectra, to be a random copolymer of PHB.[22] Thus, the effects on the PHB degradation of this known copolymer was also compared to the effects produced by the non-homogenous blending of the PHB(FM)IP with 9% low molecular weight pectin.

5.3.1. Degradation Profiles.

5.3.1.1. Degradation Of PHB/5V.

Graph 5.72 illustrates the degradation profiles of the PHB/5V sample utilizing monomer and monomer with particulate analysis. (Degraded fraction.) The degradation of PHB/5V was characteristic of the co-blend degradation with an initial gradual stage I to around day 10 where the step stage II was observed with a degradation of approximately 16%. At day 14 the degradation rate rapidly increased so that by day 18 45% degradation was observed, (Stage III). However, the degradation then suddenly reduced, so that from day 18 until the termination of the experiment at day 65, there was only a slight increase in degradation from approximately 45% to 51%, this was the step stage IV.

The degradation of approximately 27% to monomer by day 14 was due to the initial presence of particulate PHB and the collapse of a proportion of the weakened fibres. This trend was initially comparable with the degraded fraction profile, (monomer + degraded particulate analysis) which revealed small amounts of degraded particles within the first 3 days, (Graphs 5.73 & 5.74). The initial degradation occurred therefore, due to the monomer formation from the particulate matter already present and produced by initial fibre fragmentation.

The degraded particulate matter increased drastically from 3% at day 3 to approximately 11% at day 5 and continued to gradually increase until day 14, where a value of approximately 14% of the initial mass was noted as degraded particulate matter. Thus, the step stage II for the monomer profile was observed to be reduced when compared to the degraded fraction profile, (monomer + degraded particulate matter) this was due to the

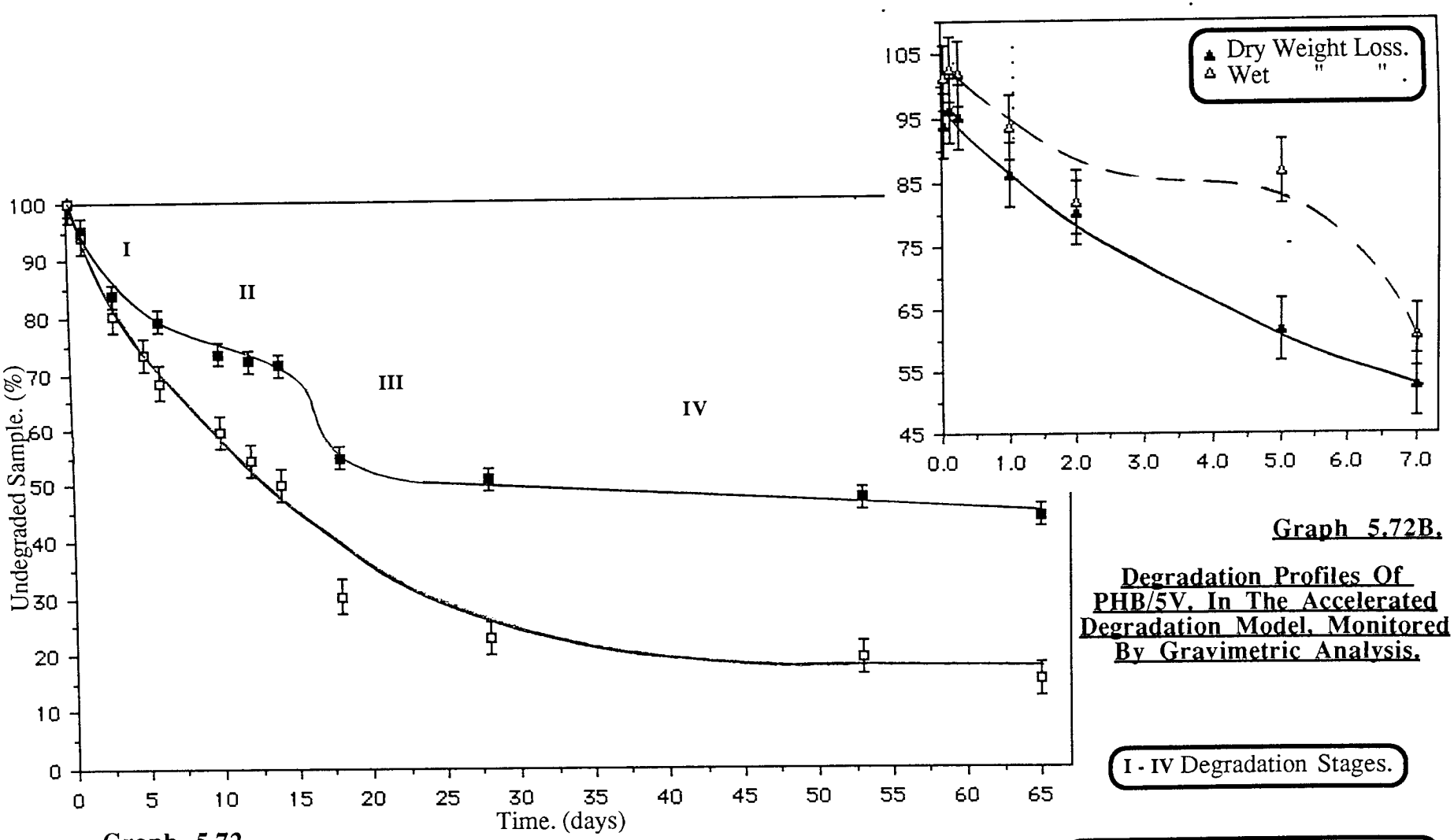

Graph 5.72.

Degradation Profiles Of Sample PHB/5V, In The Accelerated Degradation Model, Monitored By Monomer And Gravimetric Analysis.

Graph 5.72B.

Degradation Profiles Of PHB/5V, In The Accelerated Degradation Model, Monitored By Gravimetric Analysis.

I - IV Degradation Stages.

■ Monomer Analysis.
□ " & Particulate Analysis.

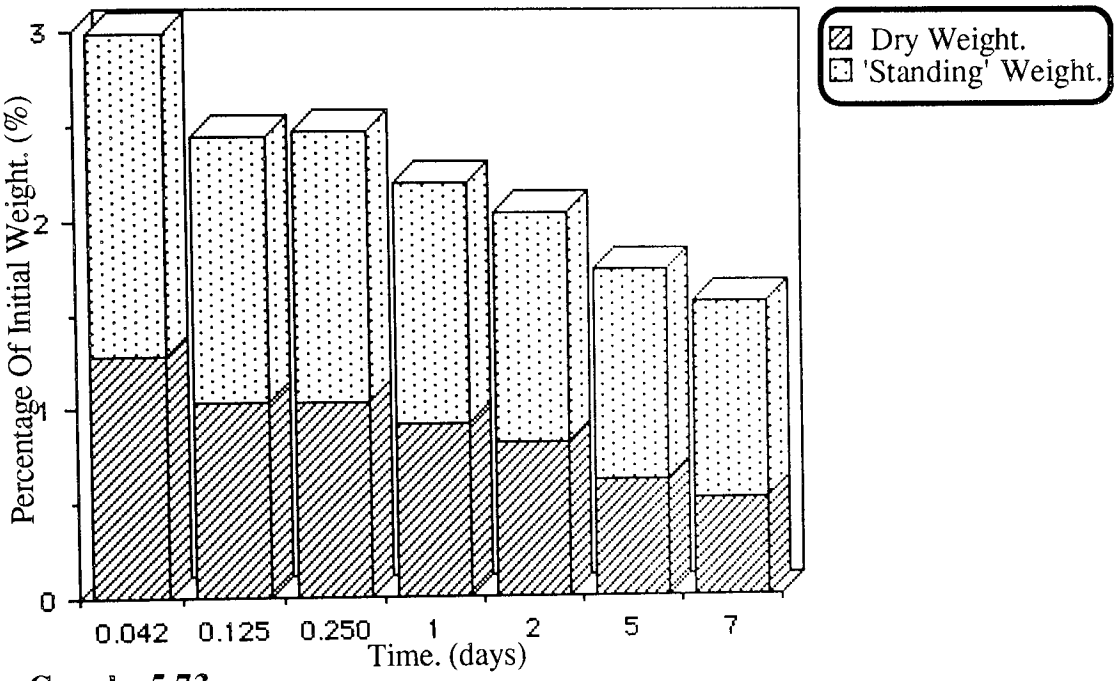

Graph 5.73.

Measured Degraded Particulate Matter For Sample PHB/5V.

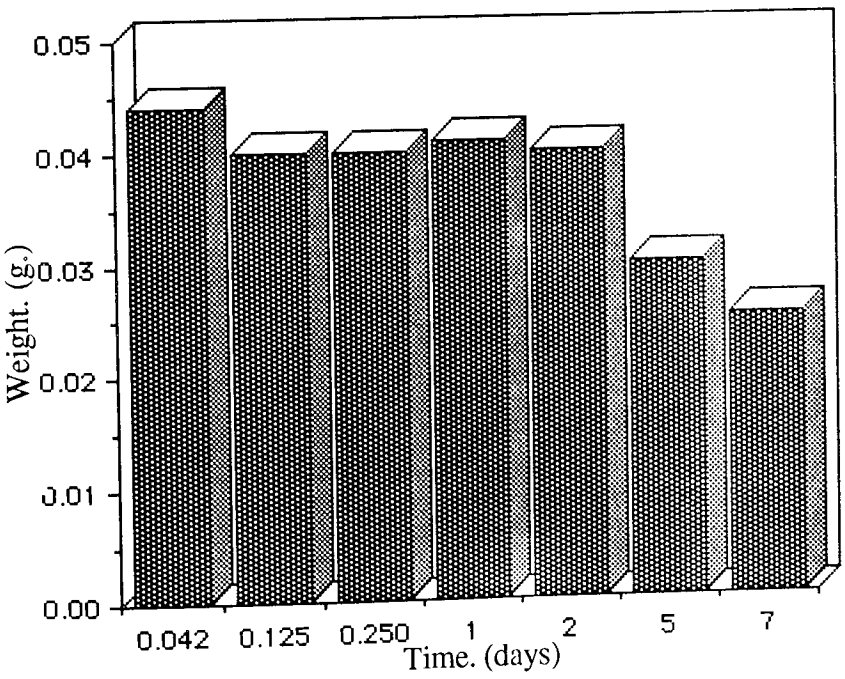

Graph 5.74.

Ideal Total Degraded Particulate Matter For Sample PHB/5V.

collapse of the remaining matrix which released large quantities of particulate matter. This particulate matter then readily degraded to monomer and facilitated in the production of the comparatively large degradation rate at stage III.

At stage IV particulate matter formation was greatly reduced, consequently, the difference between the two profiles was effectively constant. Therefore, at day 65 approximately 52% of the PHB had degraded to monomer, whilst degradation to particulate matter accounted for a further 29%. Thus, a total degradation of 81% appeared to have occurred. However, a proportion of the degraded particulate matter may also have been due to the PHV presence.

Assuming that the 5% copolymerization was accurate and utilizing the initial PHB mass as 95% of the original, the overall linear degradation rate to the start of stage IV at day 18 was determined as 2.6%$dy.^{-1}$. The anticipated linear degradation rate due to the reduction of initial PHB, according to section 4.1, was approximately 5%$dy.^{-1}$. This tended to indicate that the addition of the PHV copolymer reduced the degradation of the PHB. This was due to the comparatively greater matrix collapse and compaction in the later degradation stages.

5.3.1.2. Comparison Of PHB/5V Degradation With PHB(FM)IP. and L.Pec.9.

Graphs 5.75 and 5.76 illustrate the monomer analysis degradation profile of PHB/5V and compares it to those determined for the IP and L.Pec.9. samples. The monomer analysis for the PHB/5V was adjusted assuming the 5% PHV presence. Thus, the profiles in graphs 5.75 and 5.76 illustrate the degradation of the PHB as a function of the initial PHB

weight.

The initial degradation stage I for both the copolymerized and homopolymer samples were very similar, but the PHB/5V degradation rate gradually decreased and exhibited the step stage II between days 11 and 14. The IP sample however, exhibited a gradual degradation until the beginning of the stage IV around day 18. The initial PHB/5V degradation profile trend was due to the collapse of the weakened fibres in stage I, but due to the PHV presence in some of the matrix the proportions of the weaker fibres between the IP and PHB/5V samples were altered, thus, the IP continued to gradually degrade, whilst the PHB/5V sample had proportionally less weaker fibres and the degradation rate was therefore reduced in stage II.

The stage III degradation for the PHB/5V. sample was similar to those determined for the co-blends, however, in this case the stage III only proceeded for a short period from days 14 to 18, before entering the terminal step stage IV. As a result of this there was approximately 51.5 and 69.4% degradation for the PHB/5V and the IP samples respectively, a difference of approximately 18%. Thus, degradation of the IP sample appeared to have occurred sooner and to a greater extent than that of the sample with 5% copolymer.

The degradation profiles for PHB/5V and L.Pec.9. were very similar and exhibited the same two step degradation. However, for the PHB/5V sample the stage III was of a reduced duration compared to the L.Pec.9. and as a result of this, the degradation of the co-blended sample exceeded that of the copolymerized.

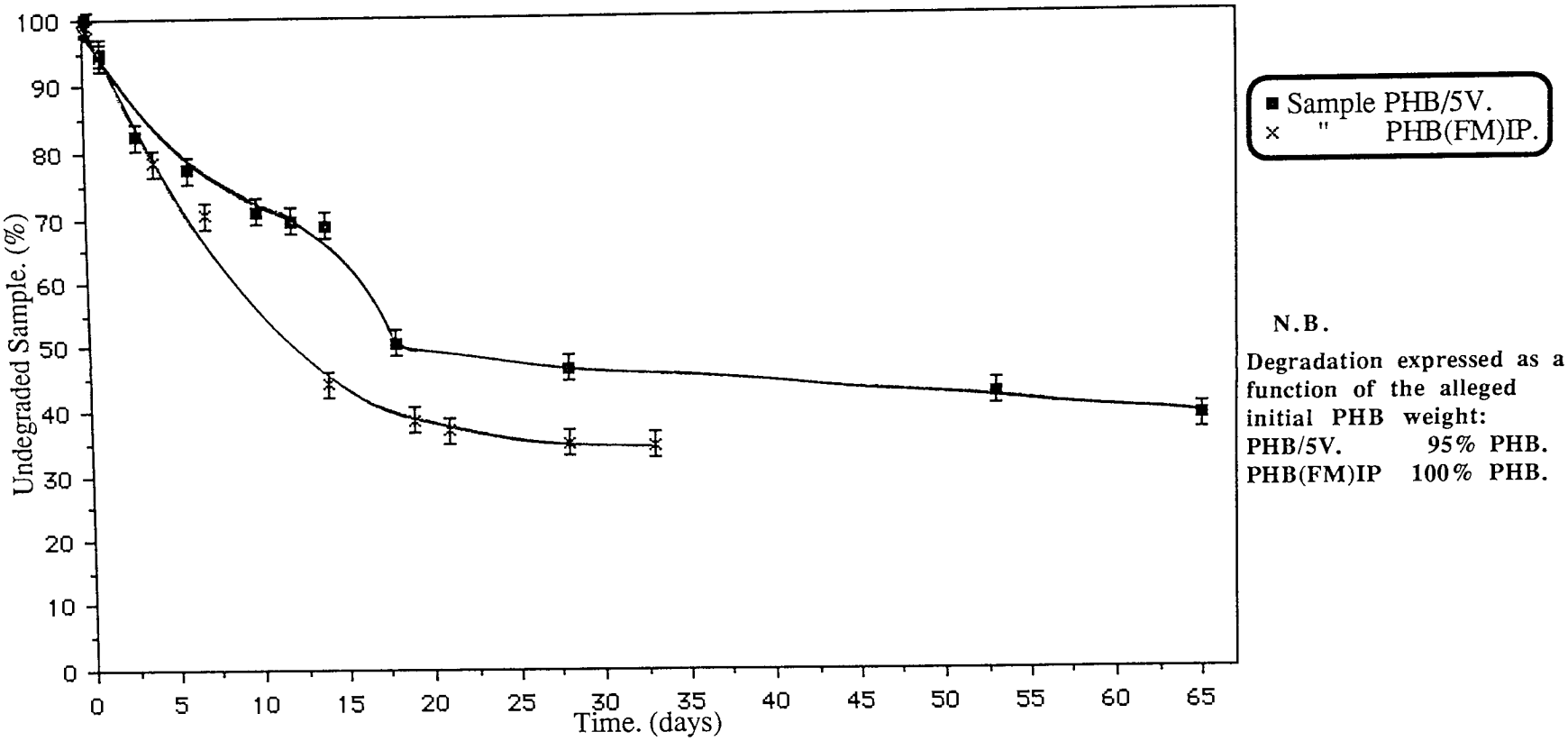

Graph 5.75.

Comparison Of Degradation Profiles Of PHB Component For Samples PHB/5V. And PHB(FM)IP In The Accelerated Degradation Model, Monitored By Monomer Analysis.

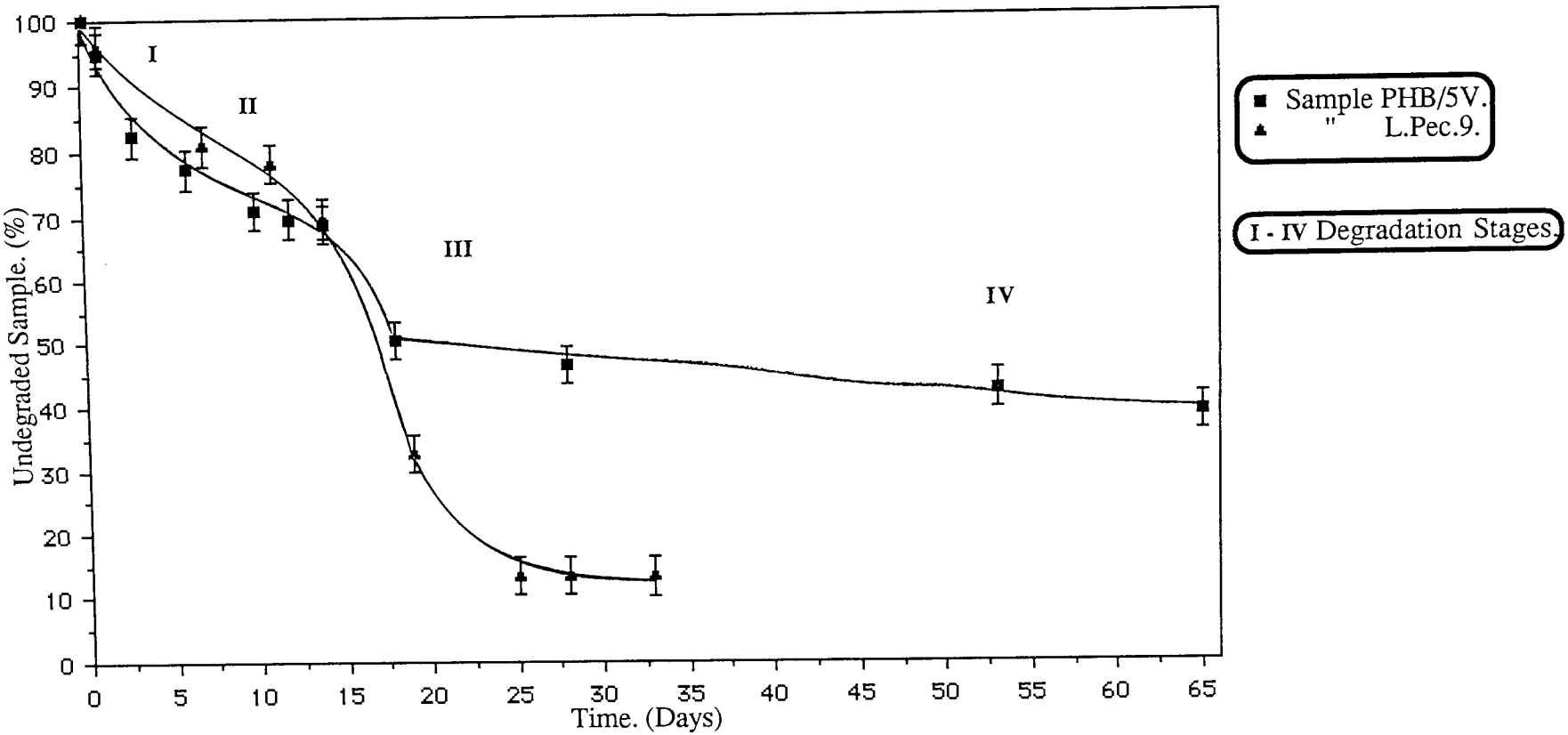

Graph 5.76.

Degradation Profiles Of The PHB Component Of Samples PHB/5V. And L.Pec.9. In The Accelerated Degradation Model, Monitored By Monomer Analysis.

Therefore, copolymerizing the PHB(FM)IP with 5% PHV affected the initial stability of the matrix and fibres, such that a greater proportion of the matrix retained its integrity for a comparatively longer time period when compared to the IP sample. Upon collapsing, compaction of the fibre fragments and particulate matter for the copolymerized sample readily occurred, whilst the compaction for the homopolymer sample was much more gradual. The PHB/5V degradation profile exhibited the same trends as those observed for the co-blends. Therefore, it was concluded that the PHV had apparently the same effect on the PHB degradation as co-blending, however, the PHV was more resistant to degradation than the blending agents and as a result, the stage III degradation was much shorter in comparison.

5.3.2. Observations Of The Partially Degraded PHB/5V Samples And Their Comparison To The IP Sample.

Examinations of the partially degraded PHB/5V samples using phase contrast microscopy revealed little difference in degradation compared to the IP samples. Plates 5.58 and 5.59 show the PHB/5V fibre structure in the initial degradation stage I at 1 hour and day 1 respectively. The irregular shaped, 'banded' fibres of small and medium diameters were readily noticeable, it is most likely the numerous irregularities were points of mechanical stress that facilitated the production of comparatively large quantities of degraded particulate matter. Fragmentation did not appear as great as with the other co-blended samples eg: L.Pec.9. Similarly, the surface area to volume ratio was also comparatively smaller due to a lack of pectin cavities.

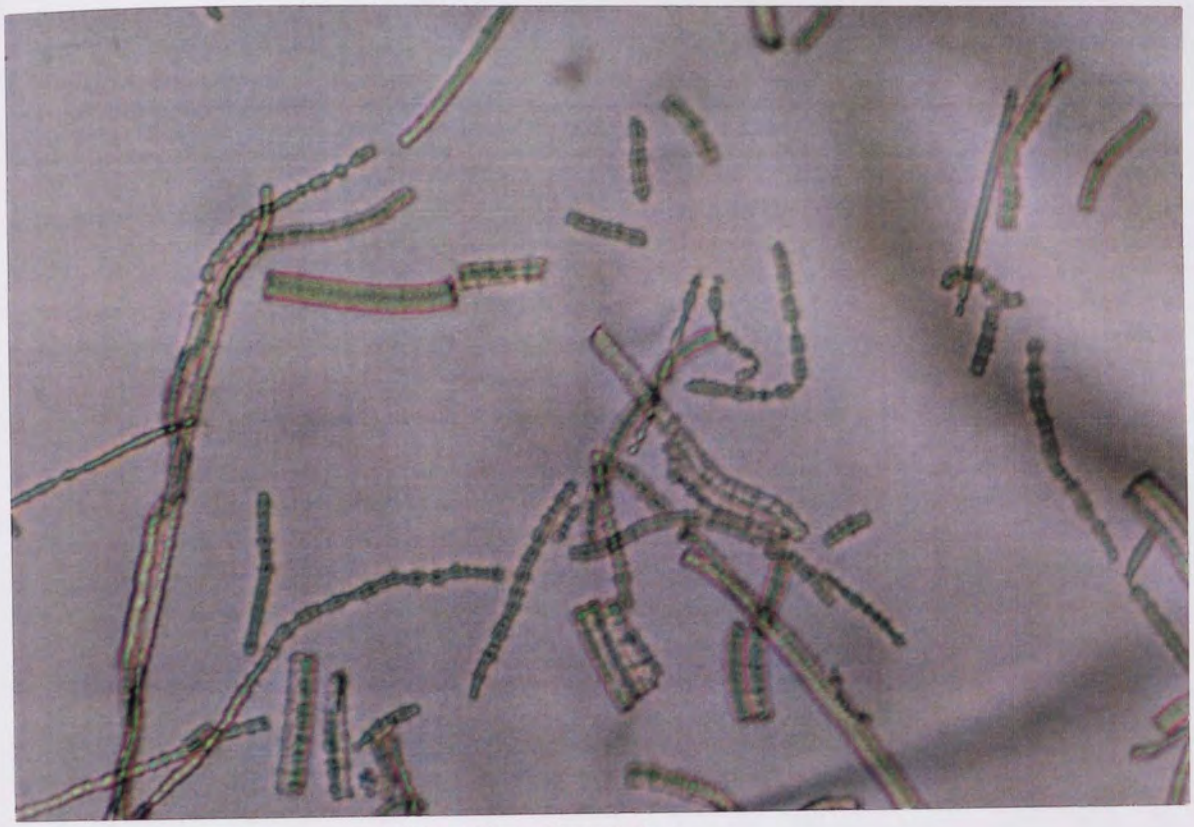

Plate 5.58. (x25) 1 Hour Degradation.
PHB/5V.; PHB(FM)IP Blended With 5% Poly(β-hydroxyvalerate) After 1 Hours Degradation, Illustrating The Irregular 'Banded' Small Diameter Fibres.

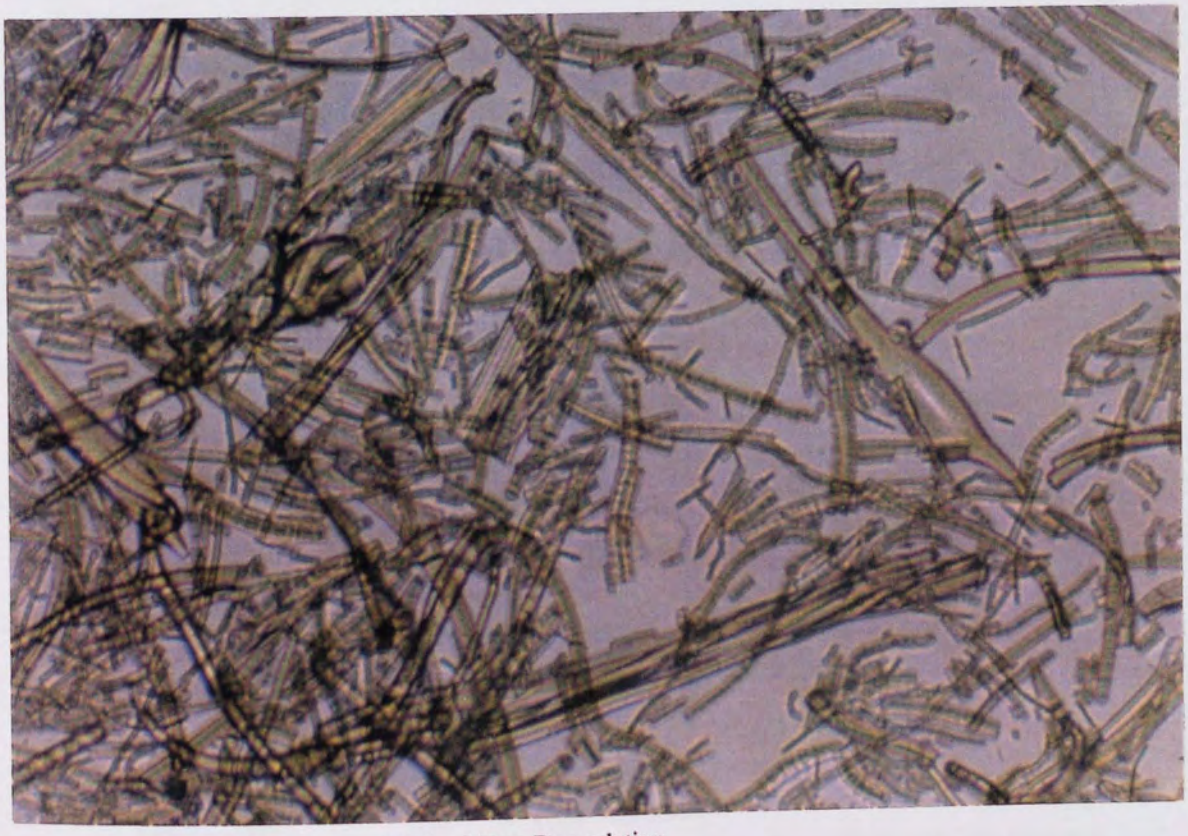

Plate 5.59. (x25) 1 Day Degradation.
PHB/5V.; A Comparatively Large Degree Of Fragmentation Due To Filtering And Drying.

Plate 5.60. (x25) 7 Days Degradation.
PHB/5V.; Large Degree Of Fragmentation And To Fibre Fragments With Some Erosion Observed.

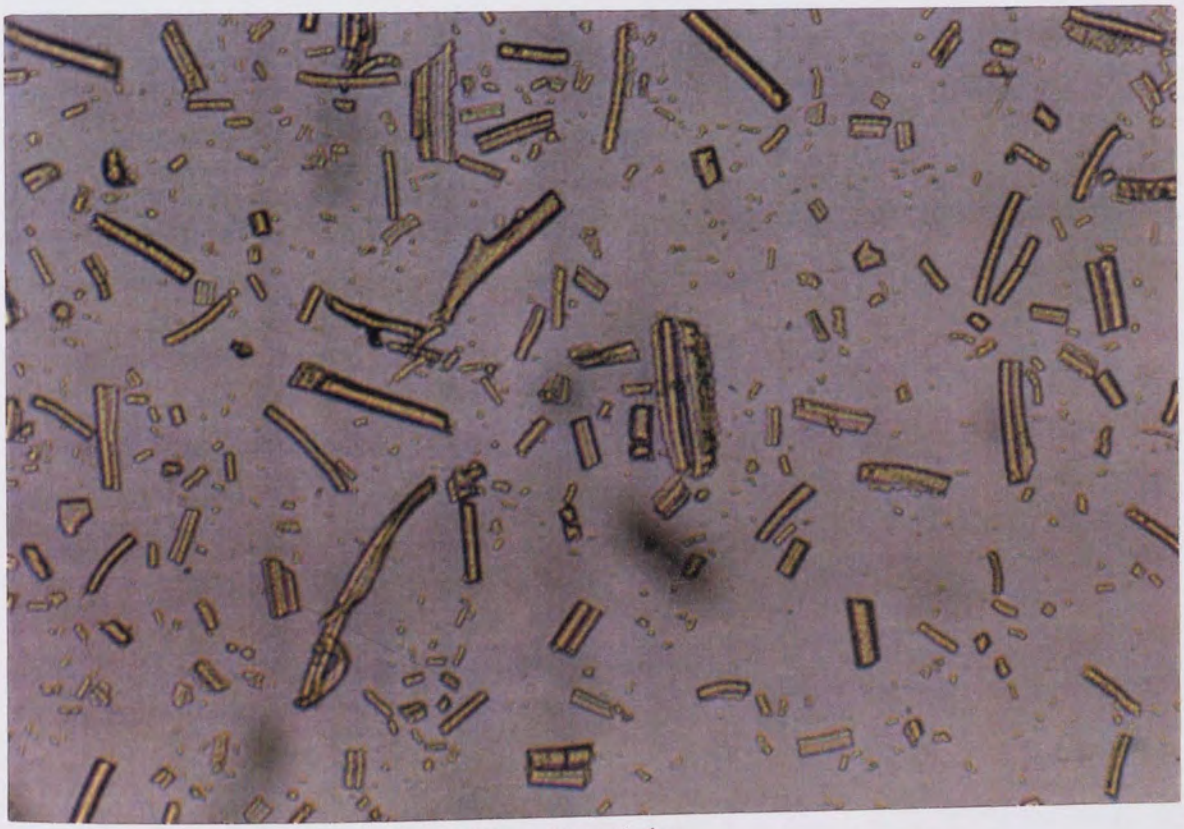

Plate 5.61. (x25) 10 Days Degradation.
PHB/5V.; Small Fibre Fragments And Large Quantities Of Particulate Matter With A Large Degree Of Erosion.

Fragmentation had apparently occurred to a great extent after 7 days degradation and erosion was noticeable, (Plate 5.60). Similarly, at day 10 the erosion was much greater although not as noticeable as in the co-blends, (Plate 5.61). Cavities were not observed in any of the partially degraded samples.

Examinations of the samples at higher magnifications using SEM revealed similar partially degraded fibres to those observed for the IP sample. Day 1 possessed similar amounts of matrix integrity and fragmentation, with the presence of some very large fibres, (Plate 5.62). A closer examination of the matrix revealed a number of medium sized fibres possessing smooth, even surfaces, (Plate 5.63). These fibres were most likely comparatively degradation resistant due to the lower surface area to volume ratio and therefore partly responsible for the maintained matrix integrity.

At day 3 the amount of fragmentation had increased, but similar to other sample observations, this was most probably due to the handling processes of the weakened fibres, as can be observed in plate 5.64, which also illustrates the hollow nature of some of the larger diameter fibres. Those fibres with small and medium diameters appeared to have fragmentated to a much greater extent than the large diameter fibres. A number of large bulbous regions were also observed. These contrasted with the bulbous regions observed for the IP and SCC-9. samples in that they were much more irregular, (Plate 5.65). A closer examination of the large diameter fibres at day 3 revealed a heavily pitted nature which increased the surface area to volume ratio and thus facilitated degradation. A large number of small fragmented fibre pieces were also readily noticed, (Plate 5.66) The more irregular nature of fibres from all the diameter sizes was readily observed after 7

Plate 5.62. (x31) 1 Day Degradation.
PHB/5V.; Fibrous Matrix Still Relatively Intact With The Presence Of Some Large Diameter Fibres, A Similar Appearance To PHB(FM)IP Of The Same Time.

Plate 5.63. (x10.0K) 1 Day Degradation.
PHB/5V.; Smooth Medium Sized Fibre.

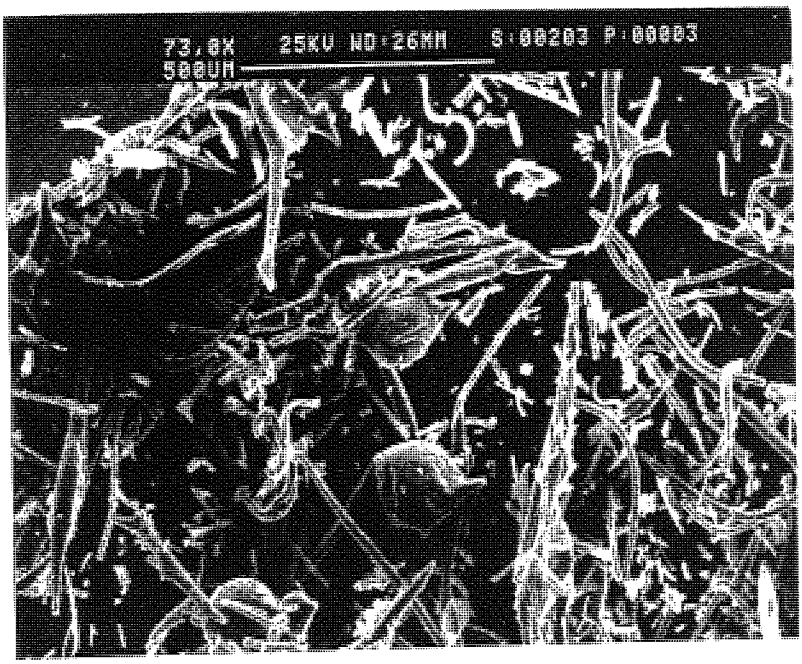

Plate 5.64. (x73) 3 Days Degradation.
PHB/5V.; Large Degree At Day 3 With Irregular Shaped Bulbous Regions.

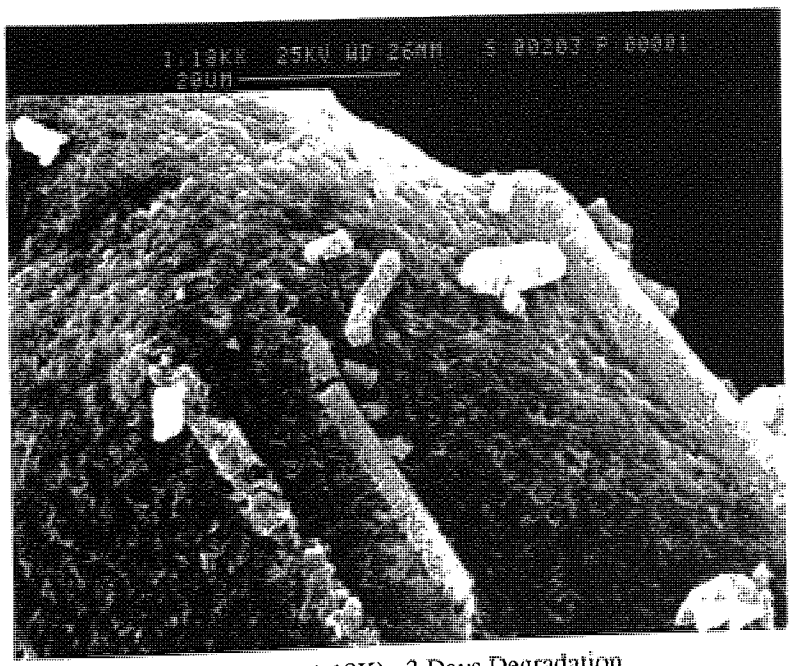

Plate 5.65. (x1.18K) 3 Days Degradation.
PHB/5V.; Large Fibre With A Heavily Pitted Nature And A Large Number Of Small Fibre Fragments.

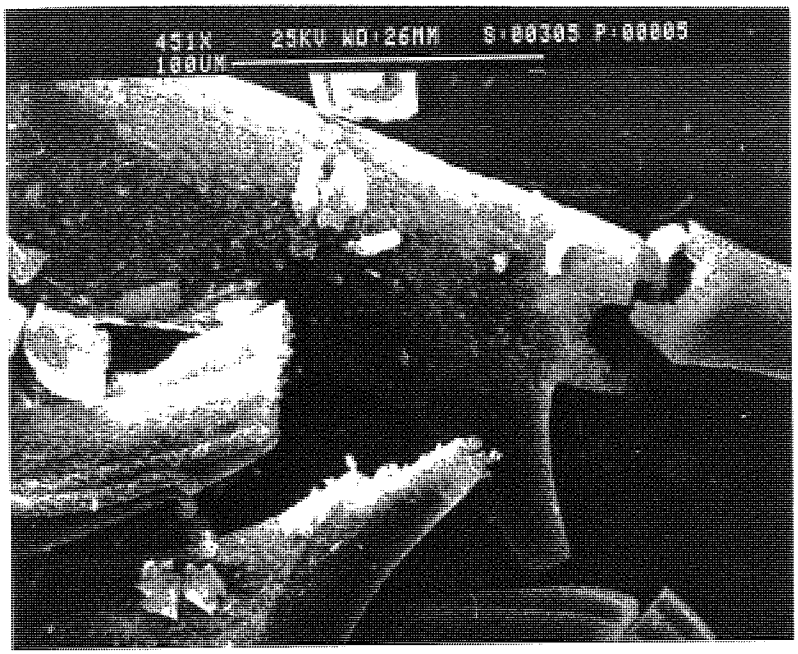

Plate 5.66. (x451) 5 Days Degradation.
PHB/5V.; A Hollow Large Diameter Fibre Fragmentated Due To SEM Preparation.

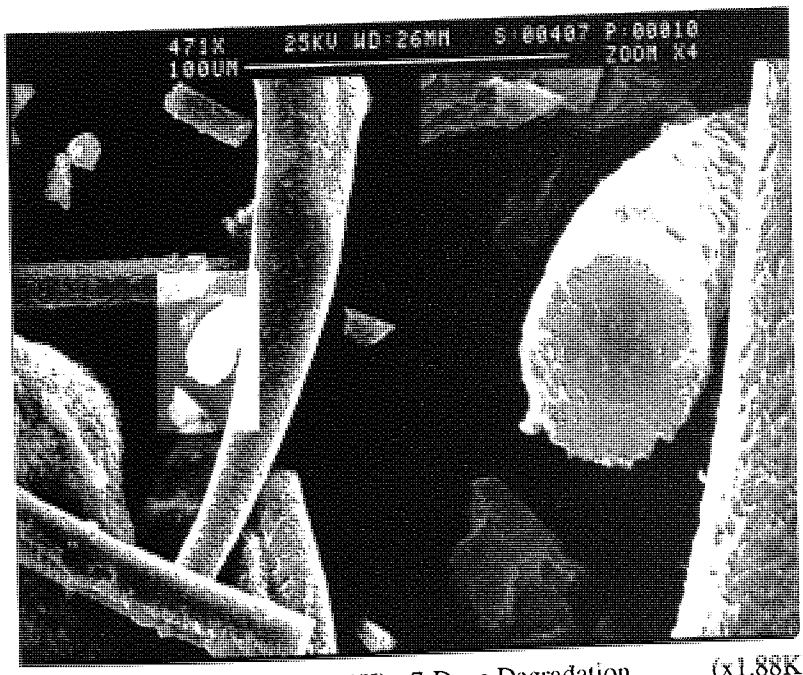

Plate 5.67. (x471K) 7 Days Degradation. (x1.88K)
PHB/5V.; Irregular Surfaces Were Observed For All The Fibre Sizes.

days degradation, (Plate 5.67). This indicated that the initial degradation of the PHB/5V sample until around day 3 was the same as the IP sample and was due to the weaker PHB fibres in both samples.

Utilizing SEM, changes in the fibre diameters of the partially degraded samples were measured. These are illustrated in graphs 5.77 to 5.85.

The initial degradation period revealed a reduction in the small diameter fibres, such that the noticeable peaks at the 0-1 and 1-2 micron diameters in the undegraded sample changed from 8 and 10% respectively, to 2 and 8% after 3 hours degradation. After 6 hours no fibres within the 0-1 micron range were observed. The large diameter (15+ um.) frequency also increased during these initial degradation stages. The other noticeable peaks in the undegraded sample at 5-6 um. (16%) and 8-9um. (12%) also decreased, so that the frequency distribution was more even. Consequently, the distribution appeared to shift to the larger diameter ranges. These results indicated the ready collapse of the very small diameter fibres when compared to the other diameters. Weakening of these fibres therefore resulted in their degradation, so that by 6 hours more fibres were observed at the 0-1 um. range. These fibres were responsible for the initial stage I in the monomer analysis degradation profile, (Graph 5.72). Similarly, the frequency decrease of the 1-2 um. diameter fibres could have been due to this fragmentation and therefore counting procedures, (Graphs 5.77-5.79).

The initial slight increase in the large diameter fibres (15+um.) from 6% in the undegraded sample to 10% at day 1 (Graph 5.81) was probably due to the reduced frequencies of the

other diameter ranges. The large increase from 10% at day 1 to 16% at day 2 was most likely due to the combination of a number of the large diameter fibres fragmenting and the fragmentation of the small diameter fibres, to the point where the latter were considered as particulate matter and not counted, some of these were observed in plate 5.67. At day 2 frequencies at all the fibre diameters, except the 0-1 and 1-2 um. ranges, were observed. (Graph 5.82). This was compared to the initial distribution between day 0 and day 2 where a number of the larger medium sized diameters were not represented; 12-13, 14-15 and 15-16 um.

The distribution at day 3 was similar to that at day 2, (Graph 5.83), however, the frequencies continued to shift slightly to the large diameter ranges so that the main peak was at 8-9 um. and not 3-4 and 5-6 um. as in the day 2 distribution. After 5 days degradation the large diameter frequency had dramatically increased to approximately 50%. This was due to fragmentation and the apparent lack of fibres at the other diameter ranges, of which the greater frequencies of 8 and 12% were for the 7-8 and 14-15 um. ranges respectively. The remaining diameter ranges above 3 microns each had less than a 5% frequency, (Graph 5.84).

At day 7 the distributions altered once again and became far more irregular, the 15+ micron range frequency was reduced to 32% and other peaks emerged at 7-8, 9-10 and 10-11 um. with frequencies of 14, 12 and 10% respectively. The 2-3 um. diameter frequency also increased from 0 to 6%, whilst no frequencies were observed at the 8-9 and 11-12 um. (Graph 5.85).

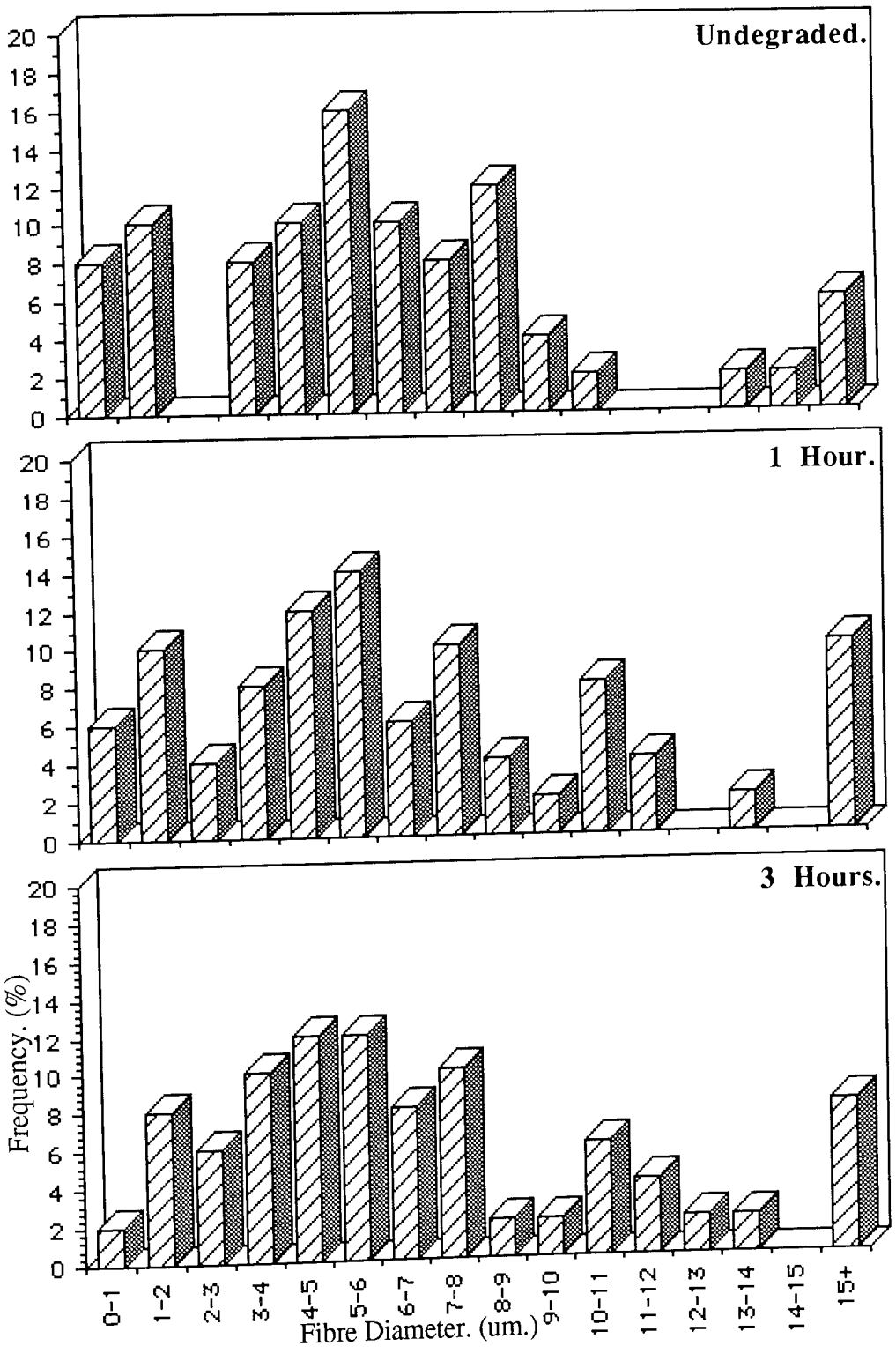

Graphs 5.77 To 5.79.

Fibre Diameter Distributions For Sample PHB/5V, During Degradation In The Accelerated Degradation Model.

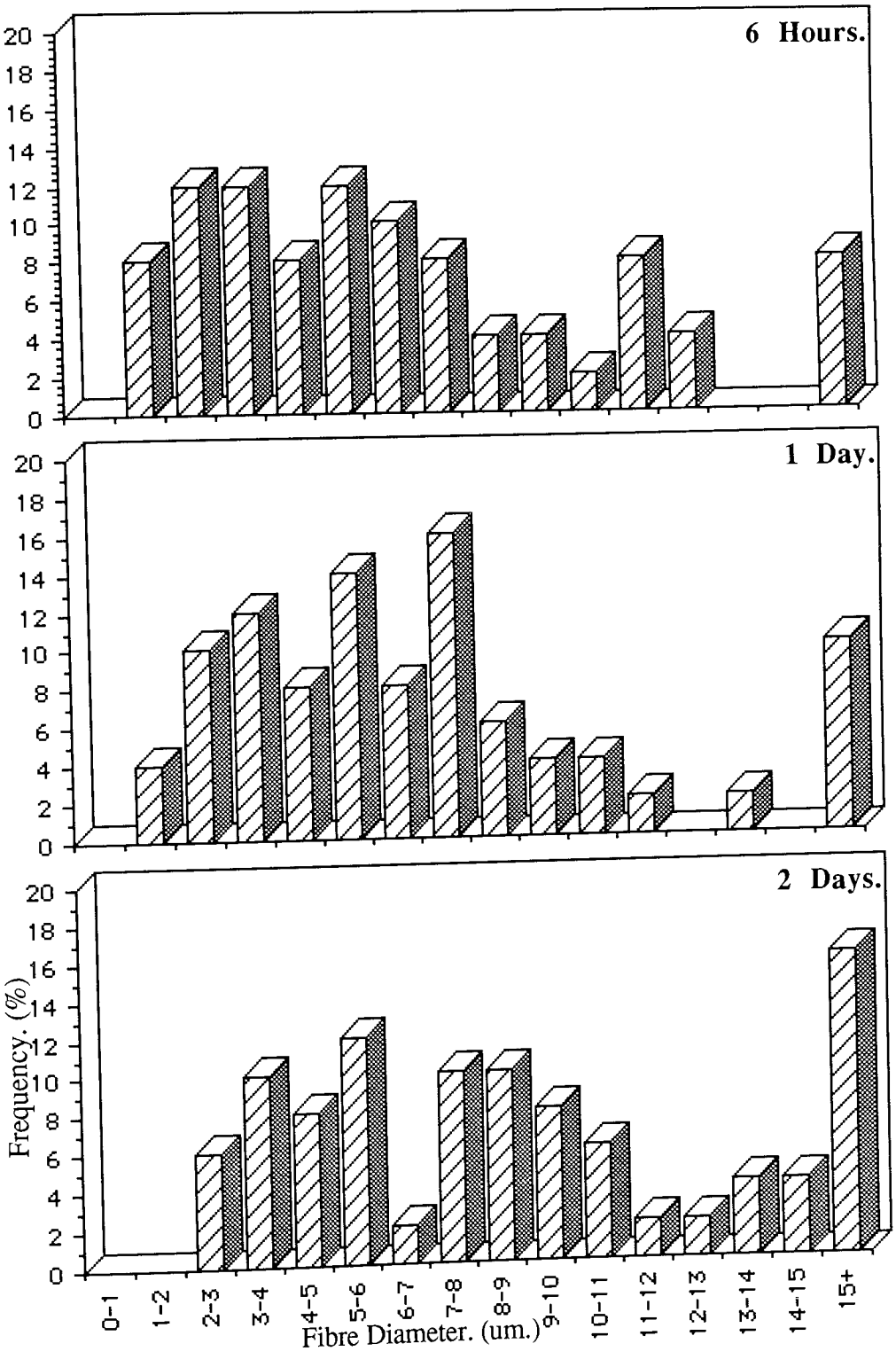

Graphs 5.80 To 5.82.

Fibre Diameter Distributions For Sample PHB/5V, During Degradation In The Accelerated Degradation Model.

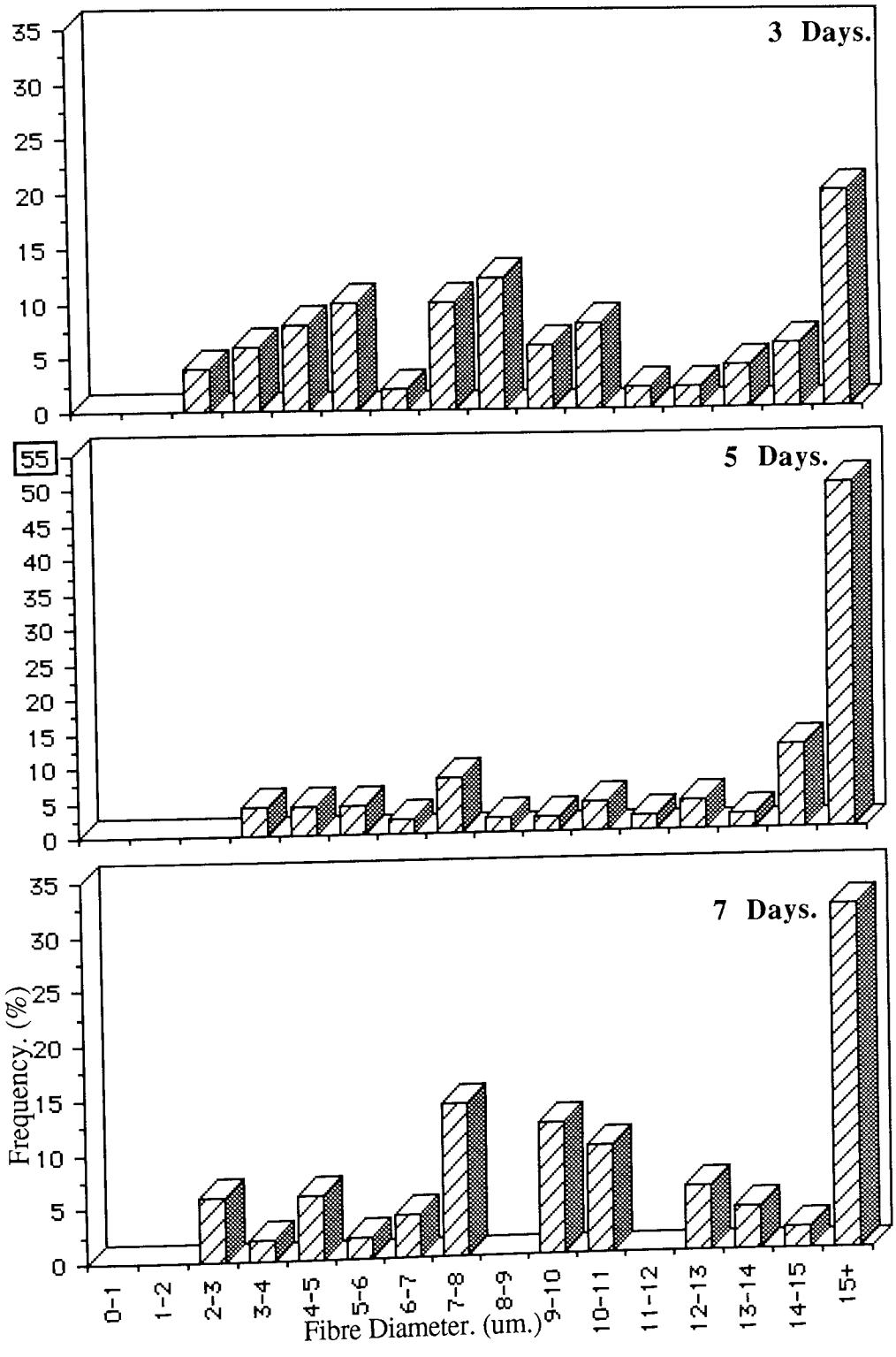

Graphs 5.83 To 5.85.

Fibre Diameter Distributions For Sample PHB/5V, During Degradation In The Accelerated Degradation Model.

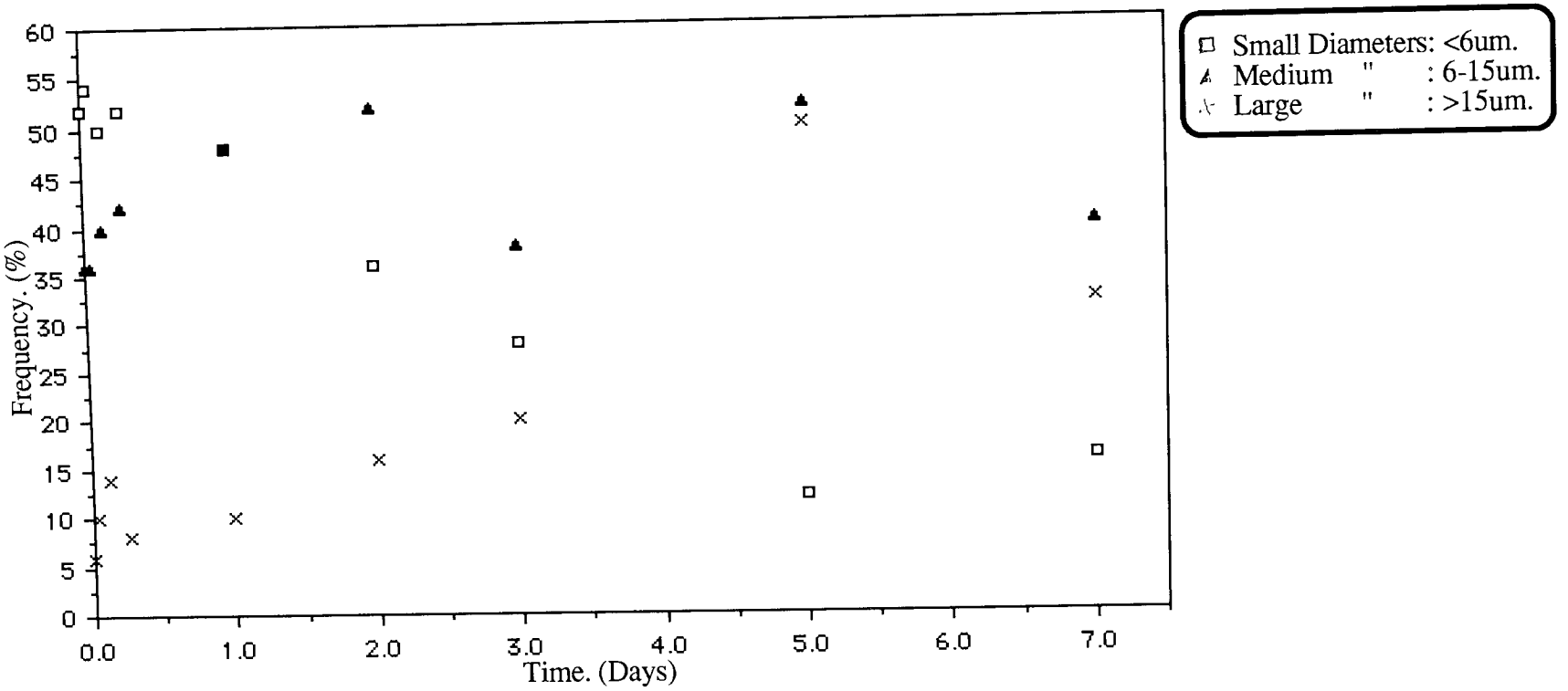

Graph 5.86.

General Fibre Diameter Distribution For Sample PHB/5V, During Degradation In The Accelerated Degradation Model.

Thus, during degradation the distribution of fibre diameters shifted to the larger ranges, such that by day 5 approximately half the fibres sampled possessed diameters greater than 15 microns, this was considered as being due to the fragmentation of these, therefore increasing their frequency, and the smaller diameter fibre fragmentation to uncountable pieces. The medium and larger small sized fibres remained relatively stable. At day 7 the collapse of the weakened fibres and fibre fragments at all the diameters readily occurred and the distribution returned to a more irregular nature.

Considering the changes in fibre diameter distribution as small, medium and large diameter groups for <6, 6-15 and >15um. respectively, a graph of the distributions was plotted and is illustrated in Graph 5.86. As can be observed from Graph 5.86 the large diameter frequency gradually increased from 6% at day 0 until approximately 20% at day 3, before rising sharply to 50% at day 5. Similarly, the number of medium sized fibres also increased until day 2 with a frequency of 50%. A decrease to 36% at day 3 was most likely due to the counting procedures. The increases in the frequencies of the large and medium sized fibres were coupled with the practically linear frequency decrease for the small diameter fibres from 54% in the undegraded matrix to 14% at day 5. After day 5 the degradation of the medium and large diameter fibres reduced their frequencies such that, the number of small diameter fibres appeared to increase slightly.

These trends differed from those observed in the degradation of the IP sample, where the large diameter frequency rarely changed and maintained a value of 8% throughout the degradation, this could have been due to a maximum fragmentation and a stability loss within the first hour of degradation and then a retention of stability. In fact, the frequency

had increased from only 8% in the undegraded to 10% at 3 and 6 hours. Thus, the large diameter fibres were considered as very stable when compared to their copolymerized counterparts. The small diameter fibre frequency gradually increased, due to fragmentation, to a value of 68% at day 4, whilst the medium sized fibre frequency gradually decreased due to their comparatively greater stability, (Graph 4.29). The changes in fibre diameter distribution during degradation for the PHB/5V. sample were very similar to those observed for the TG sample, which exhibited similar trends, (Graph 4.16).

Thus, it was concluded that the large diameter fibres of the IP sample were more stable than those from the copolymerized sample. Weakening of the large fibres in PHB/5V was probably due to the presence of the copolymer, which considerably increased the proportion of the amorphous regions within the matrix, such that upon degradation, collapse and compaction readily occurred. However, observational comparisons between the homopolymer and copolymerized samples indicated that the degradation for the PHB(FM)IP was somewhat greater than that for the PHB/5V.

5.3.3. Characterization Of The Partially Degraded Samples.

5.3.3.1. Differential Scanning Calorimetry (DSC) Studies.

Graph 5.87 illustrates the change in melting point of the partially degraded samples, as can be observed, the mp. decreased linearly from approximately 165°C. in the undegraded sample to 126°C. at day 14, a rate of approximately -2.8°C.dy.$^{-1}$. This illustrated the gradual erosion of the PHB and the consequent reduction in stability of the remaining matrix/fibre mass despite compaction. The mp. of the IP sample also initially decreased

linearly until day 4 with a rate of approximately -1.4C.dy.$^{-1}$. This rate then increased slightly until day 7, where a mp. of 160°C. was observed, this contrasted with the PHB/5V sample which, at day 7, had a much lower mp. of 145°C. These values were then subtracted from their undegraded mp.s to illustrate the comparative decrease in stability; -14°C. for the PHB sample and -20°C. for the PHB/5V sample.

The mp. trends of the copolymerized sample also contrasted with that of the L.Pec.9. DSC observations, where an the initial stability period until day 2 occurred, before a gradual mp. reduction until day 14, such that the mp. decrease was approximately -20°C. at day 14 compared to the PHB/5V mp. reduction of -39°C. at the same time period.

The Tg. profile (Graph 5.88) was similar to the L.Pec.9., with an initial sharp decrease between the undegraded sample at approximately 1°C. and -18°C. at day 1, compared to the L.Pec.9. Tg. reduction from 2°C. at day 0 to -6°C. at 6 hours. The Tg. for the PHB/5V sample then continued to decrease gradually until day 10 to a value of -21°C., before finally decreasing to -30°C. at day 18. The L.Pec.9. sample had a more gradual Tg. decrease after 6 hours before levelling, so that at day 18 a value of approximately -15°C. was noted.

Graph 5.89 illustrates the enthalpy changes during degradation for the PHB/5V sample. The profile was similar to that of the IP sample, with a number of slight differences. The IP sample had a number of initial fluctuations within the first few hours and a slight decrease at day 1, (Graph 4.30). No such decrease was observed for the copolymerized sample where the enthalpy rose steadily to a maximum of 84Jg.$^{-1}$ at day 5 and then

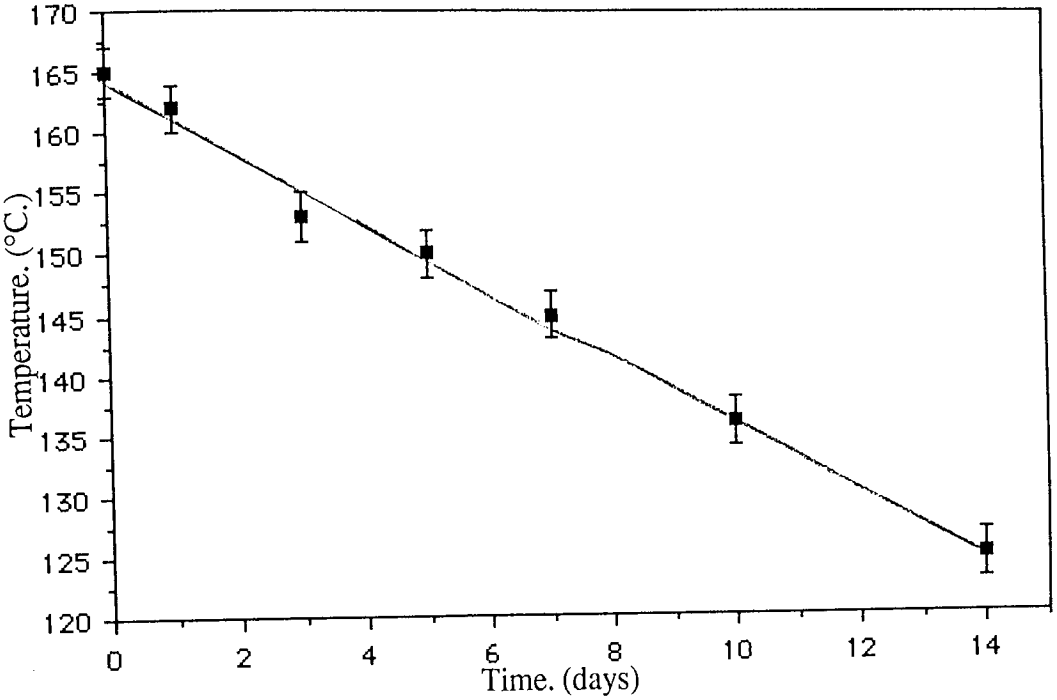

Graph 5.87.

Change In Melting Point Of Sample PHB/5V, During Degradation In The Accelerated Degradation Model.

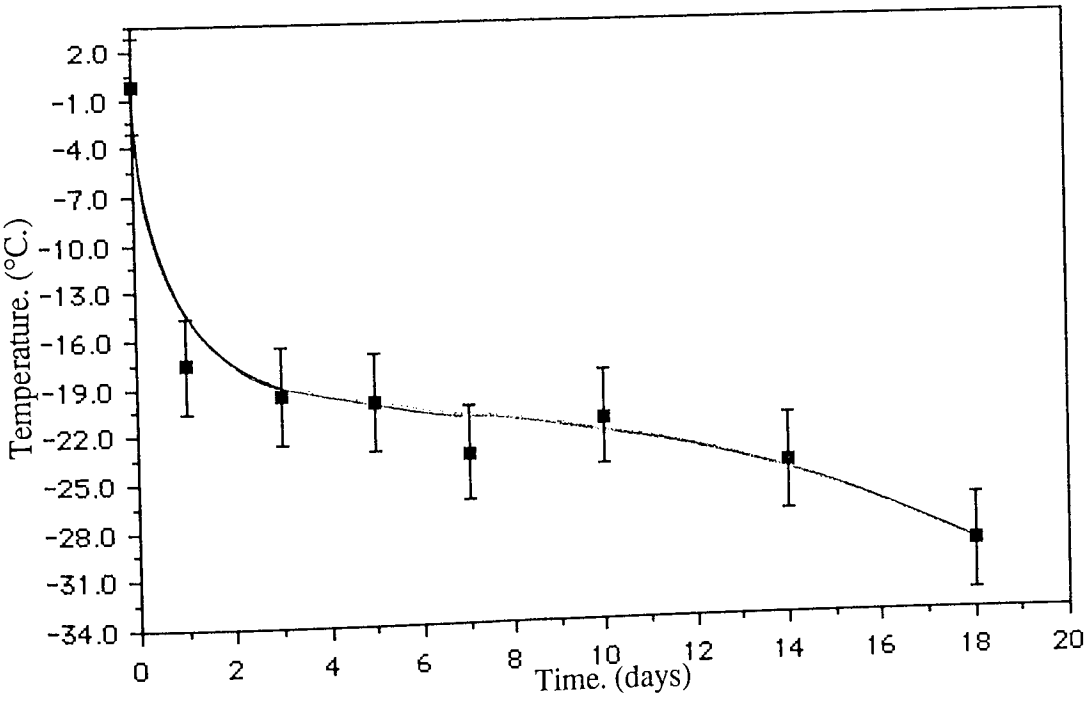

Graph 5.88.

Change In The Glass Transition Temperature Of Sample PHB/5V, During Degradation In The Accelerated Degradation Model.

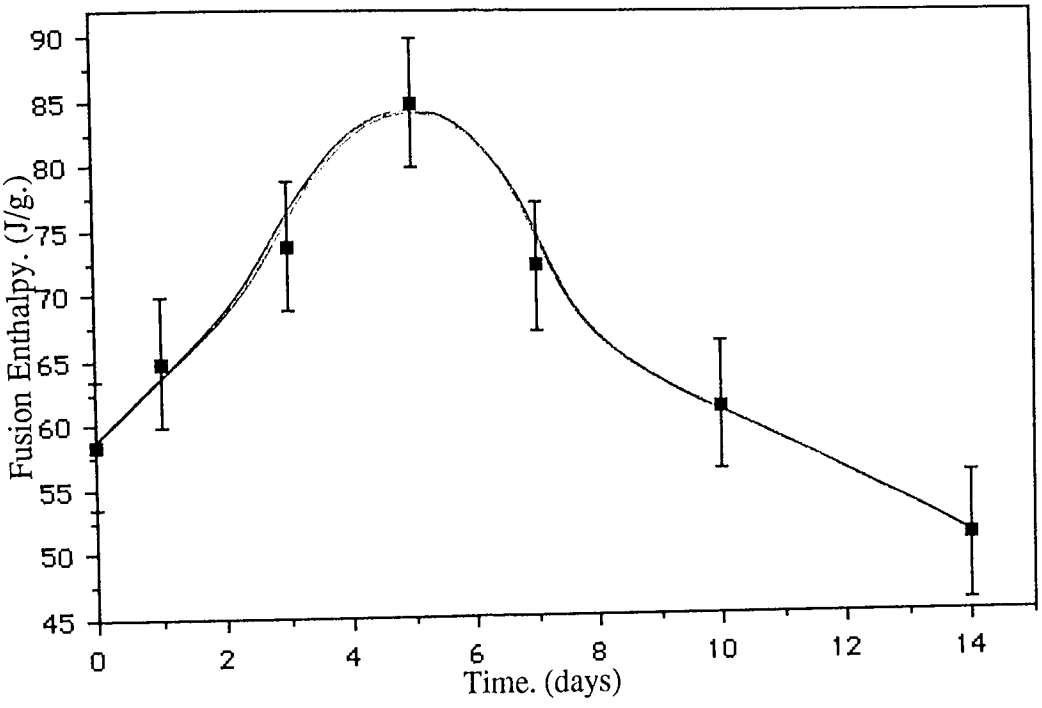

Graph 5.89.

Change In Fusion Enthalpy Of Sample PHB/5V, During Degradation In The Accelerated Degradation Model.

decreased at a similar rate until day 14, so that a comparatively uniform peak was observed. The partially degraded PHB/5V samples therefore attained a maximum crystallinity at day 5. Assuming the gradual degradation of both the PHB and PHV content, such that the relevent proportions remained the same, the crystallinity at day 5 was approximately 66 ±3%. This was considerably less than the 89 ±3% at day 4 for the IP sample. Similarly, if all the PHV had degraded then a crystallinity of 78% for the remaining PHB would have been present. These results indicated that there was a proportionally greater PHV presence which continued to depress the percentage crystallinity. Similarly, the proportional increase in the amount of PHV to PHB in the partially degraded samples depressed the mp. and Tg. results. Thus, it was concluded that the PHV did not degrade at a similar rate as the PHB and was apparently more degradation resistant.

The enthalpy profile for sample L.Pec.9. had an initial peak at day 1, this was due to the co-blend degradation. No such copolymer peak was observed for the PHB/5V sample. This tended to confirm the previous conclusions that the copolymer was relatively degradation resistant.

Unlike the IP samples, the Tg. was very noticeable in all the partially degraded PHB/5V samples, this also indicated the comparatively high amorphous content of the copolymerized sample, (Fig. 5.11). The mp. DSC traces were slightly different from the other samples investigated, with a noticeable 'shoulder' in the initial stages, whilst in the later stages a gradual flattening of the curve into an irregular 'hump' over a large temperature range was observed, (Fig. 5.12) This indicated that the degradation of the

1 Hour.

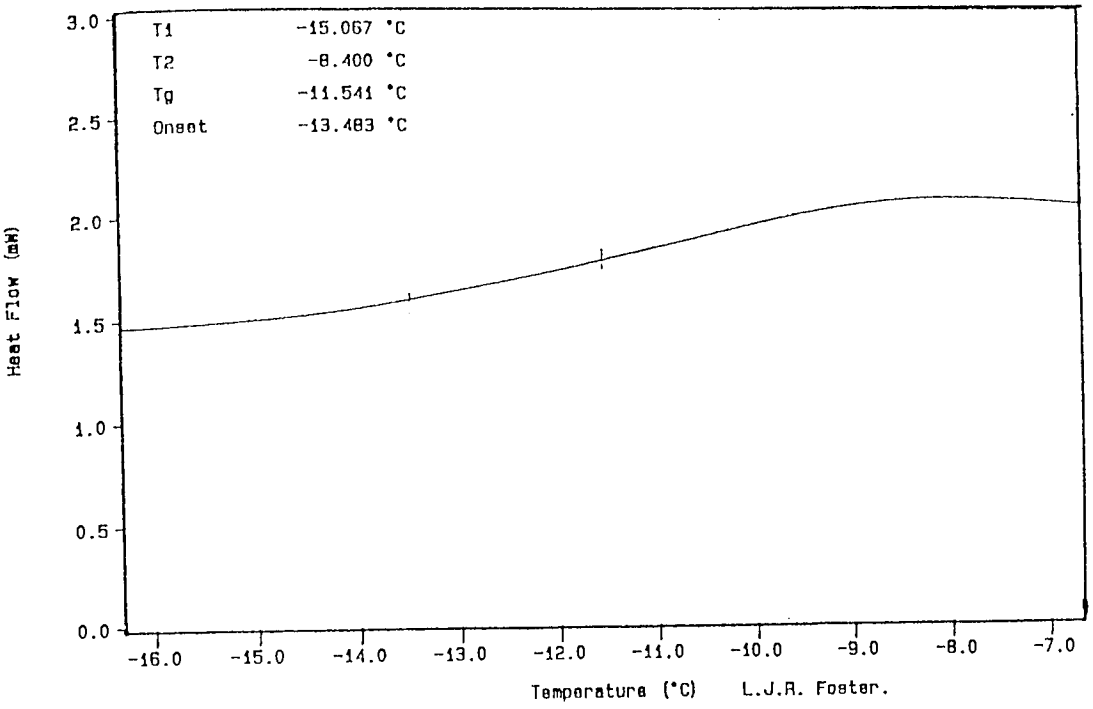

1 Day.

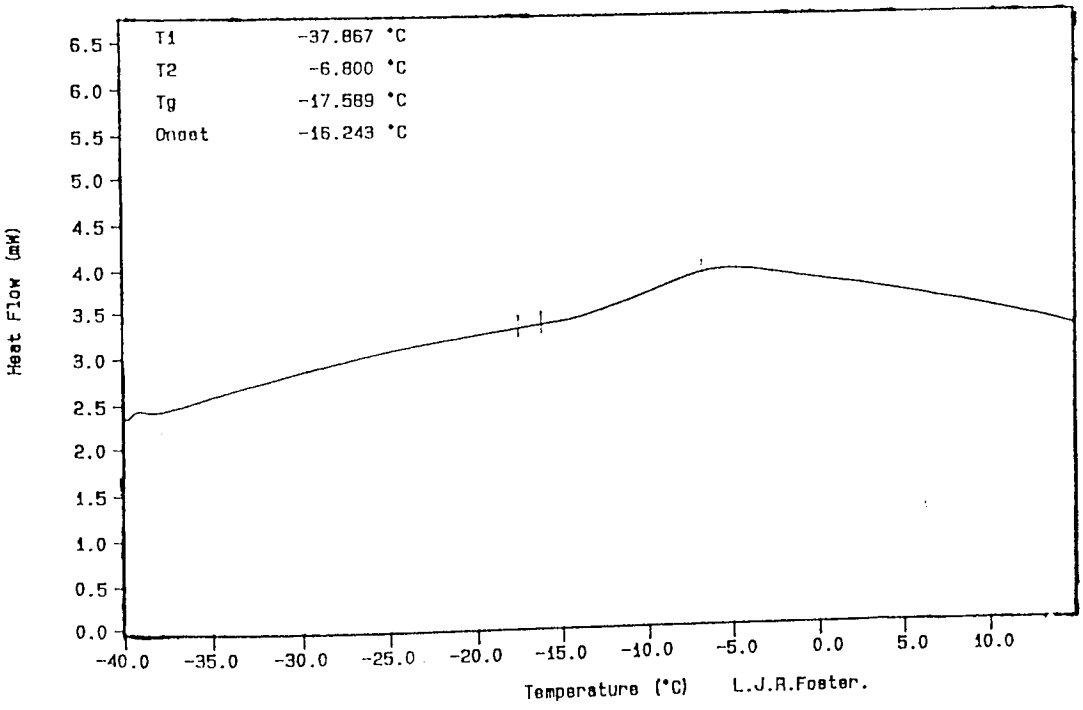

Figure 5.11.

Characterization Of PHB/5V: DSC Curves Illustrating The Determination Of The Glass Transistion Temperatures.

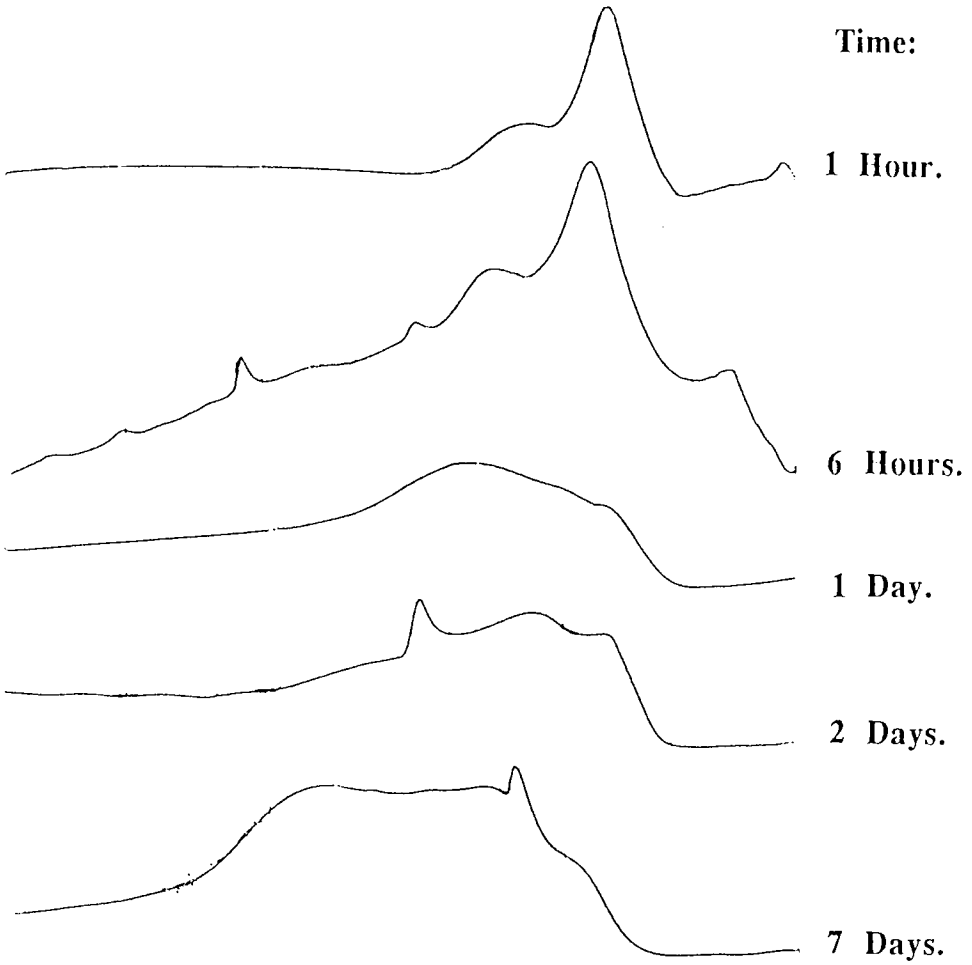

Figure 5.12.

Characterization Of PHB/5V; Change In DSC Curves During Degradation In The Accelerated Degradation Model.

remaining samples was not uniform and consequently some regions of the partially degraded sample were more degraded than others. This was similar to the IP sample, but to a comparatively greater extent.

Thus, it was concluded that the PHV content of the PHB/5V sample increased during degradation due to the degradation of the PHB. This then depressed the melting point, glass transition temperature and fusion enthalpy, such that greater changes were observed when compared to the IP and other co-blended samples.

5.3.3.2. Photoacoustic Spectroscopy (PAS) Studies.

Figure 5.13 illustrates the PAS trace obtained after 7 days degradation from the PHB/5V sample and compares it to the undegraded sample. The trace at day 7 was similar to that obtained for the IP and co-blended samples. A reduction in the amount of saturated carbon-hydrogen bond energies around the 2800 to 3000 $cm.^{-1}$ wavebands was observed, (Region B) such that upon subtraction of the day 7 from the undegraded trace a negative peak was readily noticed.

Similar to the IP sample, a carbonyl shift at the 1772 $cm.^{-1}$ waveband and a carboxylate ion peak at the 1568 $cm.^{-1}$ waveband were observed. However, these were not as noticeable as those for the IP and co-blended samples. This tended to indicate that the degradation of the partially degraded PHB/5V at day 7 was not as great as the IP or co-blended samples.

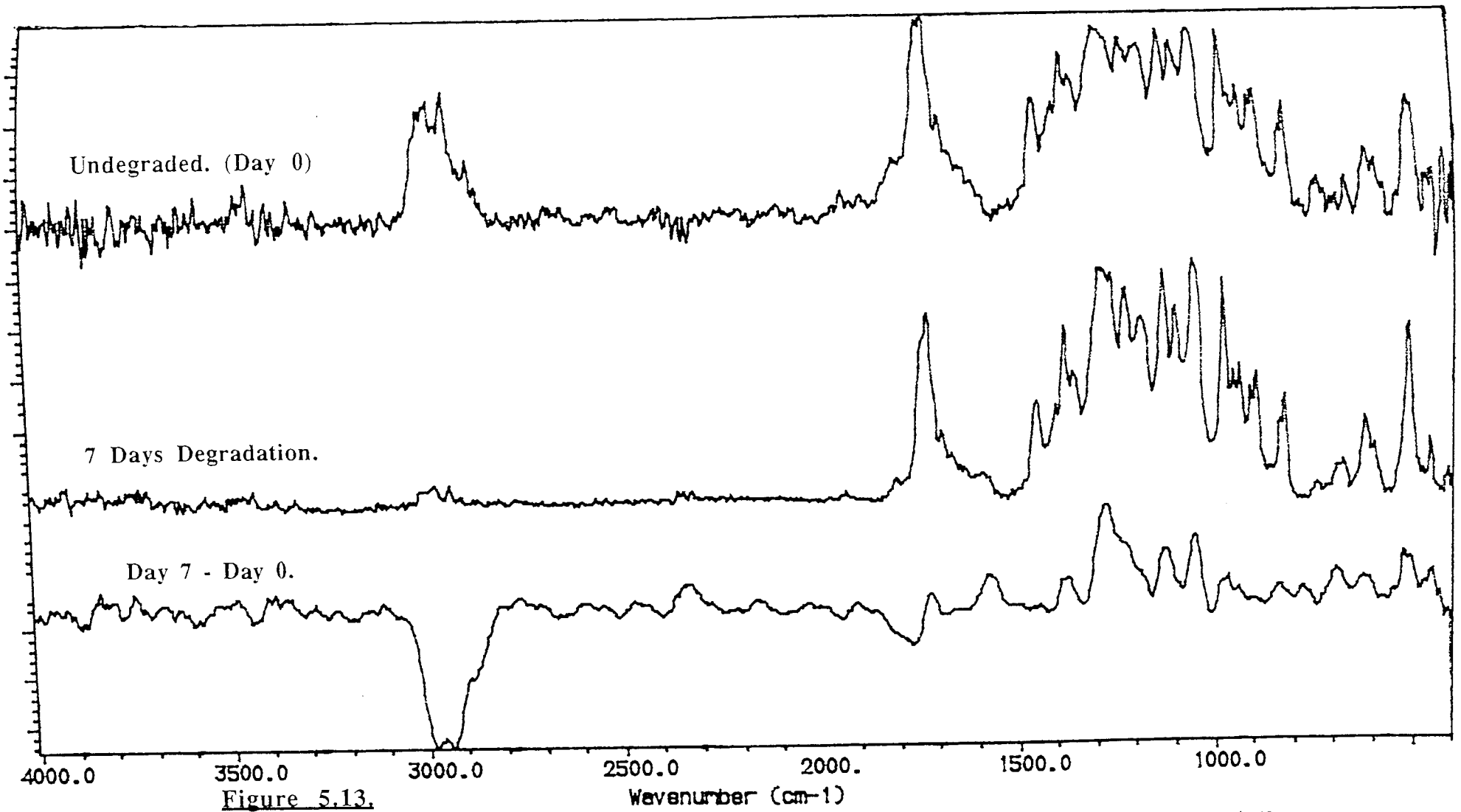

Figure 5.13.

Characterization Of PHB/5V; FTIR-PAS Traces From The Undegraded PHB/5V, Day 7 Degradation In The Accelerated Degradation Model And Their Difference.

5.3.4. Conclusions.

The copolymerized sample exhibited the same two step degradation as the co-blends.

The copolymer was relatively degradation resistant despite its apparent affect of reducing the initial percentage crystallinity in the undegraded sample. The PHV initially increased the stability of a proportion of the matrix fibres, such that the matrix collapse occurred due to a loss of mechanical integrity, compaction then reduced the degradation so that it was comparatively less than the IP sample.

It was concluded that, similar to the co-blends, the PHV presence increased the initial stability of a proportion of the matrix fibres. However, whilst the degradation of the PHB content for the co-blended samples readily occurred due to the dissolution of the blending agents and their subsequent affects on the surface area to volume ratio of the fibres, the copolymerized fibres fragmented and collapsed due to the increased amorphous content and the mechanical degradation of the PHB, similar to the IP sample. Therefore upon collapse the remaining fibre fragments of the co-blended samples were relatively more degraded than that of the copolymerized sample.

5.4. General Conclusions.

This chapter has discussed the degradation of the co-blended and copolymerized PHB(FM)IP samples and related their degradation to the homopolymer. The degradation of the PHB content and the characterization of the samples during their degradation in the accelerated degradation model was also discussed.

It was concluded that the degradation profile of PHB(FM)IP could be altered by blending the matrix with various polysaccharides, the subsequent profiles were dependent upon the polysaccharide nature and loading. Generally, the co-blend degradation exhibited a noticeable step stage II, whilst increasing the polysaccharide loading facilitated the matrix collapse so that the terminal step stage IV was influenced by the settlement/compaction limiting factor to a comparatively greater extent than in the lower loaded samples and, as a result of this, the stage IV was more sudden. Similar to the homopolymer degradation, there was a good correlation between the profiles of the degraded and undegraded fractions, confirming the experimental accuracy.

Blending the PHB(FM)IP with pectin facilitated the matrix and PHB degradation. The blending was non-homogenous and the pectin readily degraded within the first day causing the formation of 'pectin cavities'. These cavities increased the surface area to volume ratio and decreased the stability of the remaining matrix, so that a characteristic two step degradation profile was observed.

Increasing the pectin loading facilitated the matrix collapse by the introduction of mechanical stresses after the pectin degradation. The blending efficiency was reduced in the higher pectin loadings, so that the sample from the start of the manufacturing run was blended with a lower loading of comparatively higher molecular weight pectin than the sample from the end of the run, (L.Pec.25.S. & L.Pec.25.E.). Pectin was also lost in the production process. The blending mainly weakened the small and large diameter fibres (<6 & >15um.), increasing the pectin loading increased the number of large diameter fibres and shifted the diameter distribution towards the larger diameter ranges. As a result

of this, in samples L.Pec.9. and L.Pec.15. there was an initial fragmentation of the small and large diameter fibres, in L.Pec.25.S. a proportion of the medium sized fibres initially fragmented prior to the small and large, whilst for the L.Pec.25.E. sample a comparatively greater proportion of the medium diameter fibres fragmented more readily.

The increase in the PHB degradation for the co-blends compared to the IP sample was greater than could be justified by the reductions in the initial PHB weights and favoured the lower loaded sample L.Pec.9.

The changes in melting point of sample L.Pec.9.during degradation were characterized by an initial decrease and a 'step' stage around days 1 to 3, this was due to a reduction in the pectin component. After 3 days the melting point decreased considerably before levelling off around day 14. This trend was also exhibited by the other pectin co-blends, but with less noticeable step stages. Similarly, the fusion enthalpy changes exhibited a characteristic double peak. The primary peak occurred within the first day and was due to the pectin dissolution, the secondary peak was due to the PHB degradation, (See graph 5.59). The position of this secondary peak varied according to the extent of the PHB degradation and was at days 4/5 for samples L.Pec.9., L.Pec.15. and L.Pec.25.S. and at days 7/8 for sample L.Pec.25.E. In all cases there was a gradual decrease in the glass transition temperatures.

The higher molecular weight pectin blended more homogenously with the PHB (H.Pec.10.) and this increased the long term matrix stability whilst maintaining a comparatively large surface area to volume ratio, this stability subsequently reduced the

effects of compaction so that the sample and PHB degradation was greater than its low molecular weight counterpart. The melting point change for sample H.Pec.10 was similar to that observed for L.Pec.9. with a noticeable step stage, however, the fusion enthalpy change exhibited an initial sharp rise within the first day followed by a gradual increase.

Copolymerizing the PHB with 5% PHV also affected the DSC trends, there was an initial sharp decrease in the glass transition temperature followed by a more gradual decrease, whilst the fusion enthalpy profile exhibited a single peak. The DSC traces illustrated the gradual formation of a broad peak covering a comparatively large temperature range, indicating that the degradation was not uniform for the whole sample.

The copolymerized sample PHB/5V exhibited a similar degradation profile to the co-blends, but with a reduced stage III duration, this was due to the comparatively degradation resistant PHV. Similarly, the surface area to volume ratio of the fibres was reduced when compared to the co-blend fibres which possessed 'pectin cavities'. As a result of this, the PHB/5V degraded less than the co-blended and the homopolymer samples.

Therefore, it was concluded that the matrix and PHB degradation could be altered by blending and copolymerizing, the former of which increased the sample and PHB degradation due to the changes in stability, whilst the latter reduced the degradation. Thus, the degradation of the PHB fibrous matrix could be adjusted to provide various degradation profiles as may be suited for a particular implantation device or wound type/location.

The degradation of the co-blended and copolymerized samples in the accelerated degradation model could then be related to the degradation of the same samples in the physiological degradation model, this would provide a more accurate indication as to the samples biodegradation in a wound site. The degradation of the fibrous matrix in the physiological degradation model is discussed in the next chapter.